Repair of Bridge Deck Fascias

OR22-002

Final Report

09/30/2023

Prepared For:

Michigan Department of Transportation

Research Administration

8885 Ricks Rd.

P.O. Box 30049

Lansing MI 48909

Prepared By:

Furkan Cakmak
Fatmir Menkulasi
Christopher Eamon
Hwai-Chung Wu

Wayne State University

5050 Anthony Wayne Drive

Detroit, MI, 48202

Reinforcement Innovations

3121 Spring Hollow Court,

Ann Arbor, MI, 48105

TECHNICAL REPORT DOCUMENTATION PAGE

1. Report No. SPR-1730	**2. Government Accession No.** N/A	**3. Recipient's Catalog No.**
4. Title and Subtitle Repair of Bridge Deck Fascias		**5. Report Date** 09/30/2023
		6. Performing Organization Code N/A
7. Author(s) Furkan Cakmak, Fatmir Menkulasi, Christopher Eamon, Hwai-Chung Wu		**8. Performing Organization Report No.** N/A
9. Performing Organization Name and Address Wayne State University 5057 Woodward Ave., Suite 13001 Detroit, MI 48202		**10. Work Unit No.** N/A
		11. Contract or Grant No. Contract #2019-0314Z2
12. Sponsoring Agency Name and Address Michigan Department of Transportation (MDOT) Research Administration 8885 Ricks Road P.O. Box 33049 Lansing, Michigan 48909		**13. Type of Report and Period Covered** Final Report, 10/1/2021 - 09/30/2023
		14. Sponsoring Agency Code N/A

15. Supplementary Notes

Conducted in cooperation with the U.S. Department of Transportation, Federal Highway Administration. MDOT research reports are available at www.michigan.gov/mdotresearch.

16. Abstract

The relatively high supply of moisture in bridge deck fascias often causes them to deteriorate more quickly than other portions of the bridge. This causes the fascia concrete to become debonded from the reinforcement and fall, posing a safety hazard to traffic or pedestrians beneath the bridge. A related concern is that the deterioration of the connection between the barrier and deck may significantly degrade the crashworthiness of the barrier, thus undermining its main function. A literature review, nationwide survey, and several examinations of bridges in Michigan that exhibit bridge deck fascia deterioration were conducted with the goal of determining the cause of the deterioration. Alternative repair details were developed. The repair details were divided into two categories: 1) restoration of original geometry and strength, and 2) maintain current geometry and prevent further deterioration. The restoration of original geometry and strength requires drilling and epoxying dowels and using a repair cementitious material. Small-scale and large-scale testing was conducted with the goal of evaluating the proposed repair detail for restoring the original geometry and strength. A computer program called MDOT Barrier was developed to evaluate the crashworthiness of bridge barriers that feature deck fascia deterioration and to determine whether intervention is required. Guidelines for designing and detailing future repair details and new barrier to deck overhang connections were developed. A special provision for the repair of bridge deck fascia and an implementation plan was prepared. It was determined that the main cause of deck fascia deterioration was the excessive amount of moisture which led to reinforcement corrosion and freeze-thaw deterioration. Several alternative details aimed at reducing the moisture content in the deck fascia were developed for new bridges. For cases, when a repair is required, two repair concrete materials combined with epoxy coated dowels, which are drilled and epoxied into the existing deck were proposed: 1) a self-consolidating concrete mix, and 2) a fiber reinforced self-consolidating concrete mix. The proposed repair details were proved viable through small-scale and large-scale testing. Small-scale testing included tests for: 1) material characterization; 2) relative material durability; and 3) strength of the repair concrete host concrete interface to direct shear. The FRSCC was deemed as the most appropriate mixture as it possesses self-consolidating properties, and good initial and sustained tensile strength. The proposed repair detail was evaluated at full scale using barrier deck subassemblies. A total of three tests were conducted. Both selected repair concrete materials were able to provide the equivalent of TL-4 level crashworthiness. It was demonstrated that both hooked and straight rebars in the deck overhang were able to transfer forces form the barrier to the deck during vehicle impact.

17. Key Words: Deck fascia; deterioration mechanism; corrosion; freeze-thaw; repair; barrier; crashworthiness; surface treatment; corrosion resistant reinforcement; field investigation; coring; testing	**18. Distribution Statement** No restrictions. This document is also available to the public through the Michigan Department of Transportation.

19. Security Classif. (of this report) Unclassified	**20. Security Classif. (of this page)** Unclassified	**21. No. of Pages** 479	**22. Price** N/A

ACKNOWLEDGEMENTS

The authors would like to express their gratitude to the Michigan Department of Transportation (MDOT) for sponsoring this research and for providing them the opportunity to work on this project. The authors are especially grateful to Mr. Matthew Beatty (project manager) who was instrumental in the completion of each task and coordinated field investigations, progress meetings, data exchange, and many other tasks. Special thanks also go to Mr. Michael Townley, Mr. Dean Kanitz, Mr. Tim Stallard, Mr. John Belcher, and Mr. Jeff Triezenberg for their valuable comments during the progress meetings, which helped enhance the quality and clarity of this report. The authors would like to thank: 1) ABC Coating for donating and fabricating the epoxy coated reinforcement; 2) Modified Concrete LLC for donating the latex modifying admixture; 3) Lafarge Holcim for donating the Type IL Cement; 3) Edw. C. Levy Co. for donating the fine, intermediate, and coarse aggregates; and 4) Premiere Admixture for donating the admixtures.

Table of Content

List of Figures

List of Tables

Executive Summary

The relatively high supply of moisture in bridge deck fascias often causes them to deteriorate more quickly than other portions of the bridge. This causes the fascia concrete to become debonded from the reinforcement and fall, posing a safety hazard to traffic or pedestrians beneath the bridge. A related concern is that the deterioration of the connection between the barrier and deck may significantly degrade the crashworthiness of the barrier, thus undermining its main function.

A literature review, nationwide survey, and several examinations of bridges in Michigan that exhibit bridge deck fascia deterioration were conducted with the goal of determining the cause of the deterioration. It was determined that the main cause of deck fascia deterioration was the excessive amount of moisture, which led to reinforcement corrosion and freeze-thaw deterioration. The excessive amount of moisture in the deck fascia was exacerbated by the slope of the deck making the fascia on one side of the bridge more vulnerable to deterioration. Inconsistencies in clear cover were identified in some bridges suggesting that the corrosion of reinforcement may have been exacerbated by low clear cover to the reinforcement. The traffic volume on or below the bridge was determined to correlate well with deterioration suggesting more vulnerable deck fascia conditions in bridges with heavy traffic on or below the bridge. Alkali silica reaction was also determined as a likely deterioration mechanism. The above factors combined with what is now considered low grade concrete for bridge decks is believed to have led to the deck fascia deterioration. Several alternative details aimed at reducing the moisture content in the deck fascia were developed for new bridges.

In addition, alternative repair details are presented for existing bridges. The repair details are divided into two categories: 1) restoration of original geometry and strength, and 2) maintain current geometry and prevent further deterioration. The restoration of original geometry and strength requires drilling and epoxying dowels and using a repair cementitious material. Two repair concrete materials combined with epoxy coated dowels, which are drilled and epoxied into the existing deck were proposed: 1) a self-consolidating concrete (SCC) mix, and 2) a fiber reinforced self-consolidating concrete (FRSCC) mix. The proposed repair detail was proved viable through small-scale and large-scale testing. Small-scale testing included tests for: 1) material characterization; 2) relative material durability; and 3) strength of the interface between repair

concrete and host concrete to direct shear. The FRSCC was deemed the most appropriate mixture as it possesses: 1) self-consolidating properties, 2) good initial and sustained tensile strength, and 3) good resilience against weathering as suggested by good stability in mass and dynamic modulus of elasticity obtained through periodic measurements during freeze-thaw testing.

The proposed repair detail was evaluated at full scale using barrier deck subassemblies. A total of three tests were conducted. Both selected repair concrete materials were able to provide the equivalent of TL-4 level crashworthiness. The repair specimen that featured FRSCC exhibited a load versus horizontal displacement relationship that was almost coincidental with the control specimen. The repair specimen that featured FRSCC exhibited a stiffer response than that exhibited by the repair specimen that featured SCC. It was demonstrated that both hooked and straight rebars in the deck overhang were able to transfer forces from the barrier to the deck during vehicle impact.

A computer program called MDOT Barrier was developed to evaluate the crashworthiness of bridge barriers that feature deck fascia deterioration and to determine whether intervention is required. The program requires the analyst to idealize the deteriorated fascia in terms of an average deteriorated width and average deteriorated length. This information is then used to conduct yield line analysis to determine the capacity of the barrier considering the deterioration in the fascia. The barrier to deck connection and the deck overhang are then evaluated in terms of whether they can sustain the forces transferred from the barrier in the event of a vehicle impact.

The insights obtained from this research were used to develop guidelines for designing and detailing future repair details and new barrier to deck overhang connections. A special provision for the repair of bridge deck fascias and an implementation plan was developed.

Chapter 1: Introduction

Chapter 1: Introduction

1.1 Statement of the Problem

The relatively high supply of moisture in bridge deck fascias often causes them to deteriorate more quickly than other portions of the bridge. This causes the fascia concrete to become debonded from the reinforcement and fall, posing a safety hazard to traffic or pedestrians beneath the bridge. An example of a deteriorated bridge deck fascia is shown in Fig. 1.1 which shows signs of corrosion in deck reinforcement. The current Michigan Department of Transportation (MDOT) maintenance strategy is to avoid patching these areas, since overhead patches can later spall off, posing the same safety risk as the original fascia failure. Rather, delaminated concrete is removed to minimize the potential of falling debris. However, this practice leaves the fascia reinforcement exposed, resulting in corrosion and further degradation.

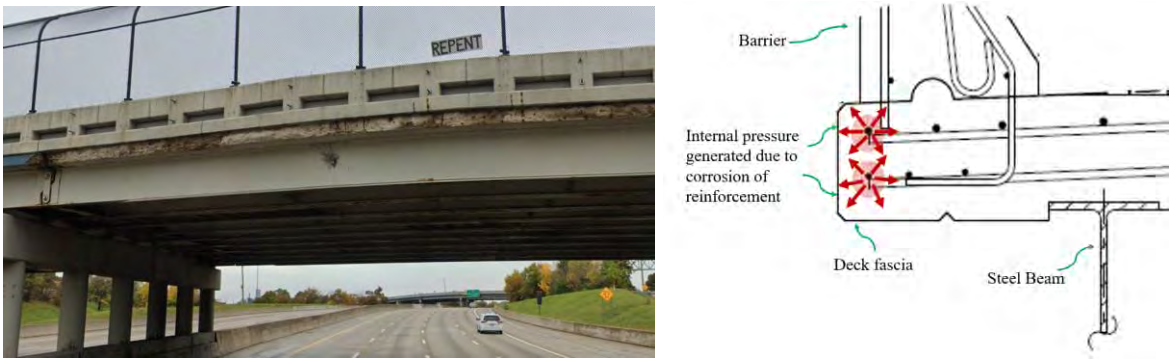

Fig. 1.1 Example of deck fascia deterioration on McGraw Avenue Bridge over I-96 eastbound (detected by PI) and illustration of built-in pressures due to reinforcement corrosion

A related concern is that the deterioration of the connection between the barrier and deck and the repetitive scaling of these areas to remove poorly adhered concrete may significantly degrade the crashworthiness of the barrier, thus undermining its main function. Barriers are designed such that in the event of a crash, the failure mode is to be a yield line mechanism within the barrier. The intent is not to allow the failure mode to extend to the deck, such that major repair after a crash can be limited to the barrier. However, the deterioration of the deck fascia and accompanying reinforcement has the potential to shift the failure location from the barrier to the deck-barrier connection, which may become the weakest link in the event of a crash. Moreover, in extreme cases, repeated scaling of the deck overhang may weaken it to such an extent that the barrier may become unstable even under its self-weight. The goal of this research project is to identify the cause of this deterioration, develop strategies for how to prevent this problem from

reoccurring, and present repair details for existing bridges. The characterization of bridge deck fascia deterioration was conducted through field investigations and evaluation of current construction details. Field investigations were conducted in all regions in the lower peninsula and featured nondestructive testing, concrete core obtention, and collection of broken concrete fragments for further laboratory analysis. A database of 40 bridges exhibiting deteriorated deck fascias was used to identify trends and correlations. A total of four repair cementitious composite materials were investigated through small-scale laboratory testing featuring accelerated weathering techniques. The repair details feature strategies for restoring the original geometry and strength as well as those that maintain current geometry and prevent further deterioration. The most promising repair cementitious composite materials dictated by the results of small-scale laboratory testing were used with epoxy coated reinforcement in larger scale sub-assemblage testing to evaluate the efficiency of the proposed repair detail when subject to horizontal loading that emulates forces during a vehicle impact. Specific research objectives are presented below.

1.2 Research Objectives

1. Identify the main cause of deck fascia deterioration.
2. Develop maintenance alternatives to scaling deck fascias.
3. Identify current design details contributing to fascia deterioration and develop corrective measures.
4. Develop best practices for long-term repair options of deteriorated fascias without removing the traffic barrier.
5. Develop best practices in design, construction, and preventive maintenance to prevent deck fascia deterioration from occurring.

1.3 Significance of Work

Falling concrete from deteriorated bridge deck fascias poses a safety hazard for the public, and a weakened deck overhang undermines the crashworthiness of the barrier, thus compromising its main function. The identification of the cause of this deterioration led to the development of strategies for preventing this problem from reoccurring. The developed repair methods are anticipated to eliminate the safety risks mentioned above, prevent further deterioration, and restore the crashworthiness of the barrier. The implementation of the proposed repairs for existing bridges as well as design details for new deck overhangs are anticipated to reduce the number of existing bridges that manifest this condition as well as lead to more durable bridges in the future.

Chapter 2: Literature Review and Current Practice

Chapter 2: Literature Review and Current Practice

The goal of this chapter is three fold: 1) Provide a brief background on the problem; 2) Present a summary of relevant research on the subject matter; and 3) Present the results of a national survey that summarizes observations by other State Department of Transportation (DOT) staff. The overarching goal was to identify solutions and determine strategies that would further inform the research plan. The literature review pertained to the identification of deterioration mechanisms, identification of methods for removing unsound concrete, types of concrete surface treatments and their efficiency, repair of deteriorated bridge deck facias, potential impact of deck fascia deterioration on the crashworthiness of the barrier, and alternative barrier to deck connection details.

2.1 Background

In general, concrete deck or slab edges exposed to weather are susceptible to deterioration due to the combined effects of reinforcement corrosion and freeze-thaw cycles. The lack of restraint in deck edges makes them vulnerable to spalling since the only resisting mechanism to corrosion-induced expansion is the concrete tensile strength. This situation can be exacerbated in cases when concrete cover is inadequate and concrete is not properly consolidated when placed. Freeze-thaw cycles cause a similar hazard in the sense that the built-in pressure due to the expansion of frozen water is met with little resistance in a saturated deck fascia. This saturation could be due to improper drainage or expected frequent moisture exposure. Frequently critical locations include deck fascia near joints in simply supported multi-span bridges, since these areas serve as unintended drainage points, subjecting them to higher loads of water laden with deicing salts. The research team noted multiple examples of this condition in bridges over I-96 east bound between exits 170 and 190. In other cases, such as that shown in Fig. 1.1, the deterioration extends along the entire length of the fascia. Deck concrete placement practices and workmanship are also a potential concern. During placement, a number of properties that significantly influence long-term durability are established, including pore structure development, air-void system formation, material uniformity, and potential for cracking (ACI 2016).

As a general design strategy, the use of appropriate cementitious materials, corrosion resistant reinforcement and/or bar relocation from susceptible areas, as possible, combined with proper drainage, are expected to reduce the likelihood of deterioration. For repair, the use of

concrete that exhibits sustained tensile strength after the first crack is ideal because it inhibits delaminated sections from separating and falling. Common formulations for this purpose include fiber reinforced concrete (FRC), as well as high performance, and ultra-high-performance concrete (UHPC). The use of the latter in areas of high distress caused by loads or environmental factors has gained popularity in the last decade (Aaleti et al. 2013; Graybeal 2014; Haber et al. 2018; Khodayari et al. 2021). UHPC also possesses excellent flow properties, which is instrumental in ensuring proper consolidation for repairs. However, there appears to be no research in which the implementation of the presented strategies is investigated through physical testing for the purpose of addressing the deterioration of deck fascias.

As a result, a research program was executed in which the deterioration of deck fascias was addressed by controlling the hazard causing the deterioration as well as by increasing the durability of the deck fascia when exposed to the hazard. The primary hazard appears to be excessive moisture, potentially in combination with deicing chemicals, where minimizing exposure can be accomplished by effective drainage. Durability is enhanced by using high performance materials, sound repair strategies, as well as consideration of alternative barrier-to-deck connection details.

2.2 Literature Review

The literature review on the subject matter revealed that there is virtually no research on the topic of deterioration of bridge deck fascias. Research on other relevant topics include studies conducted on the deterioration of balconies in building structures, bridge barriers, bridge fascia beams, and bridge decks.

Some studies appear to have addressed balcony deterioration in building structures (Svensson et al. 1980; Lahdensivu 2012; Lahdensivu et al. 2013). However, these studies are relevant to this research, as the nature and causes of deterioration are similar to those of deck fascias. Svensson et al. (1980) investigated the durability of different repair systems by conducting laboratory and field studies, and concluded it was very doubtful that any repair system could protect a low-grade concrete slab (i.e. with no air entrainment and highwater-cement ratio) from further damage, suggesting the need for higher performance materials in areas of high distress. Repairs that featured highly frost resistant cement mortar were found to perform better. Marusin (1985) presented a case study of repairs in concrete columns, spandrels, and balconies on a high-rise housing complex in Chicago. The cause of concrete spalling was believed to be corrosion of

steel reinforcement combined with freeze-thaw effects. Inspections of implemented repairs suggested that repairs made with acrylic modified concrete and epoxy mortar, including the application of a 100% acrylic paint, remained sound.

Other relevant research on the subject matter appears to be related to the deterioration of bridge barriers. Several studies were conducted on this topic and include those presented by Shahriari et al. (2021), Miller et al. (2020), Miller et al. (2017), Bazzo et al. (2013), Kalabon (2013), Bush (2008), Staton and Knauff. (2007), Kamaitis (2006), Aktan et al. (2004). These studies were sponsored by various state DOTs in the United States such as those in Wisconsin (one study), Ohio (four studies), Oregon (one study), and Michigan (two studies). The subject of bridge barrier deterioration has also been investigated in other countries such as the study conducted by Kamaitis (2006) in Lithuania.

There is a plethora of research regarding the deterioration of bridge decks and other members (Howell et al. 2015; Grace and Jensen 2012). However, these studies have not been included in this literature review, since the focus of it were studies that feature the deterioration of elements directly in the vicinity of the deck fascia, such as barriers, and those that featured similar characteristics (similar geometry), such as balconies in building structures.

The impact of the deterioration of bridge deck fascias on the crashworthiness of the barrier is also discussed. Several studies that investigated the crashworthiness of the barrier are presented, although none appears to have addressed the case of a deteriorated deck fascia or a repaired one. It appears that these studies were motivated by the consideration of alternative details for bridge barriers such as corrosion resistant reinforcement in the barrier or deck overhang.

The subject of concrete surface treatment options appears to be well researched. There are several studies that considered various surface treatment options for decks and barriers. Here, only those that were considered for barriers or other vertical surfaces are discussed because the application on horizontal surfaces is assisted by gravity and successful performance in horizontal surfaces may not imply successful performance on vertical surfaces such as deck fascias.

This literature review is organized based on various themes that are relevant to the deterioration and repair of bridge deck fascias and includes:

1) Deterioration mechanisms;
2) Concrete removal;
3) Concrete surface treatment;

4) Repair of deteriorated bridge deck fascias;
5) Impact of deck fascia deterioration on crashworthiness of the barrier;
6) Alternative construction details;
7) Quality of deck concrete;
8) Corrosion resistant reinforcement; and
9) Construction practices

2.2.1 Deterioration Mechanism

Emmons (1993), Delatte (2009), and Kosmatka and Wilson (2016) provide an overview of various deterioration mechanisms in concrete structures. The discussion of deterioration mechanisms herein is limited to those that are believed to cause the deterioration of bridge deck fascias. The following deterioration mechanisms are discussed: 1) reinforcement corrosion, 2) shrinkage and temperature induced cracking, 3) freeze-thaw deterioration, 4) alkali-silica reaction, and 5) exposure to deicers and anti-icers.

Reinforcement Corrosion

Reinforcement corrosion appears to be the single most prevalent cause of deterioration in concrete structures. The kinematics of corrosion are explained in several references (Vaysburd et al. 2000) and are not repeated here for brevity. Corrosion of steel reinforcement can be promoted by the presence of moisture and chloride combined with insufficient cover, large crack widths, poor quality concrete that exhibits high permeability, and carbonation. Bridge deck fascias are exposed concrete elements, therefore, the presence of moisture on the surface of concrete cannot be eliminated. Similarly, the use of deicing and anti-icing chemicals on bridge decks appears to represent the current state of practice for either melting ice or preventing freezing. Therefore, their presence can also be considered as an unavoidable hazard. The presence of excessive moisture and chlorides, can however, be avoided by using proper drainage systems and ensuring their functionality. For example, Kamaitis (2006) concluded that one of the reasons for the deterioration of various bridge elements was improper drainage. An extensively deteriorated deck fascia was provided as an example of the ramifications of improper deck drainage. Assuming that some amount of moisture and chloride will always be present in the surface of bridge deck fascias, current practices focus on providing sufficient reinforcement cover, controlling the depth of

penetration of moisture and chloride, and considering corrosion resistant reinforcement. Visible reinforcement corrosion in bridge barriers due to insufficient cover was reported in several bridges in Ohio (Miller et al. 2017). Similarly, the deterioration of many balconies in Finland was attributed partly to insufficient cover. Guidance for appropriate reinforcement cover exists, however, many studies have reported that the actual cover deviated from the specified cover. This can be corrected by ensuring good quality control during construction. Miller et al. (2017) report that in some bridges, reinforcement corrosion was reported despite appropriate cover. It was speculated that since appropriate cover combined with good quality concrete should prevent the corrosion of reinforcement simply by permeation, the cause of deterioration must have been another deterioration mechanism. Possible causes presented include corrosion after cracking and spalling of concrete due to freeze-thaw deterioration or alkali-silica reaction.

Strategies that can be used to reduce the likelihood or eliminate corrosion include the use of good quality concrete with low permeability, use of corrosion resistant reinforcement, electrochemical chloride extraction, and cathodic protection systems. The case of corrosion inhibitors is discussed below.

Corrosion Inhibitors

Some studies evaluated the effectiveness of various corrosion inhibitors. Mixed results are reported. For example, Islam (2003) evaluated the long-term performance of two corrosion inhibiting admixtures when used to repair various concrete bridge elements such as decks and piers. The two systems featured spray on applications of a calcium nitrite-based inorganic inhibitor, and an amine-based organic inhibitor. Several analyses and visual inspections such as half-cell potential tests, corrosion rate measurements, total chloride ion content measurements and delamination surveys were performed. It was concluded that neither of the corrosion inhibitors used provided any corrosion-inhibiting benefit. Similarly, Sohanghpurwala et al. (2002) conducted a study on the repair and rehabilitation of bridge components containing epoxy coated reinforcement. Several combinations of epoxy injection materials and corrosion inhibitors were evaluated as corrosion mitigation strategies for corrosion and non-corrosion induced cracks. Two types of corrosion inhibitors were considered. None of these strategies exhibited any ability to provide protection against corrosion in the areas of interest. Other repair strategies were considered to address delaminations and spalls. It was concluded that “no benefit was discernable from the

use of admixed and migrating corrosion inhibitors in repair areas and/or areas adjacent to the repair and that the best response from a corrosion protection standpoint was demonstrated by a high resistance, low permeability silica fume modified patch material and an epoxy rebar coating compatible with ECR in the repair area". Although, "the water based alkaline coating with corrosion inhibitor showed promise in providing protection in the repair area".

Conversely, Virmani et al. (1998) report that the utilization of corrosion inhibiting admixtures such as calcium nitrite serves as a very good corrosion protection system. Similarly, for repaired concrete elements, Vaysburd et al. (2000) concluded that the use of good quality, crack resistant repair materials with the addition of corrosion inhibitors is critical for proper and durable repairs.

Zhang et al. (2012) investigated the effectiveness of surface applied corrosion inhibitors and concluded that the inhibitors were less effective for higher w/c ratios where pores are larger. El-Hacha et al. (2011) investigated the effectiveness of inhibitors in cracked and uncracked concrete specimens and concluded that they were effective in both although the width of cracks was limited to hairline type cracks.

Shrinkage and Temperature Induced Cracking

Shrinkage (or rather restrained/differential shrinkage) and temperature induced cracking has been reported as a common phenomenon in bridge barriers (Bazzo et al. 2013; Shahriari et al. 2021). In general, it was concluded that shrinkage and temperature induced cracking in the barriers, not controlled by the saw cut joints, leads to corrosion of the reinforcement and the deterioration of barriers resulting in spalled concrete. Such cracking may also promote other deterioration mechanisms such as concrete spalling due to freezing and thawing. Shrinkage and temperature induced cracking in bridge barriers is exhibited in the form of vertical cracks such as those observed in the field by Shahriari et al. (2021).

A similar deterioration may be present in bridge deck fascias since the edge of the deck is more vulnerable to shrinkage than the rest of the deck due to the higher deck surface exposed to drying. The edge of the deck is exposed to drying on three surfaces, whereas the rest of the deck only on two surfaces. This leads to differential shrinkage within the deck itself. The presence of the barrier adds another level of restraint on the top surface thus increasing the likelihood of restrained shrinkage induced cracking. The presence of differential shrinkage in bridge deck

fascias may also be exacerbated by construction practices. A field visit conducted by the research team during deck placement for a bridge rehabilitation project near Bay City, MI, revealed that while concrete is pumped in the majority of the deck surface, the region near deck fascia receives concrete through free flow facilitated by the use of vibrators. The reinforcement configuration at the deck barrier connection can be dense and may create a situation in which only the paste of the cementitious matrix travels to the deck fascia, thus resulting in increased moisture content, enhanced vulnerability of differential shrinkage, and differential shrinkage induced cracking.

For bridge barriers, Bazzo et al. (2013) report that premature cracking of bridge barrier due to restrained shrinkage could be controlled by increasing the number of barrier joints (i.e. reducing the member length, and therefore, the magnitude of the restrained shrinkage strain) and discontinuing the longitudinal reinforcement at the vertical joints to further reduce the level of restraint to the free shrinkage of the barrier. While effective for bridge barriers, these techniques may not be applied for bridge deck fascias.

Freeze-thaw Deterioration

Freeze-thaw deterioration is another common deterioration mechanism for all concrete structures exposed to aggressive environment. It is precipitated by the presence of moisture in concrete and the lack of an internal structure to relieve internal pressures created due to the freezing of penetrated water. Good moisture control, crack control, and the specification of air entrained concrete are the first line of defense against this deterioration mechanism. Moisture control in deck fascias can be facilitated by effective water stops at the deck to barrier connection and an effective drainage system. Crack control can be facilitated by low shrinkage concrete, and adequately sized and spaced corrosion resistant reinforcement. The method of creating water-stops in Michigan at the barrier to deck connection was revisited since the current method required the manual creation of the water-stop using fresh concrete with the only access provided through the space between the vertical barrier reinforcement. Deterioration due to freezing and thawing was reported in balconies in Finland by Lahdensivu et al. (2013), and in bridge barriers in Oregon and Michigan by Bush (2008), and Staton and Knauff (2007), respectively.

Alkali-silica Reaction

Alkali-silica reaction is another type of deterioration mechanism that is exhibited in the form of map cracking or a network of cracks, cracks with straining or exuding gel, closed or spalled joints, relative displacements of different parts of a structure, or fragments breaking out of the surface of concrete (Kosmatka and Wilson 2016). Alkali-silica reaction was speculated as a potential reason for observed map cracking in several bridge barriers in Ohio by Miller et al. (2017), although, this was not verified. Similarly, map cracking was also observed in several bridge barriers in Wisconsin by Shahriari et al. (2021), although laboratory studies revealed that no alkali-silica reaction was present.

Exposure to Deicers and Anti-icers

Deicers are solid or liquid chemicals that are applied to the surface of concrete to facilitate the melting of ice or snow; whereas anti-icers are liquids that are applied before a precipitation event to prevent the water from freezing or refreezing (Kostmatka and Wilson 2016). The hygroscopic (moisture absorbing) properties of deicing salts result in a saturation of concrete and in an increase in the likelihood of freeze-thaw deterioration. Bridge deck fascias, while not directly subject to deicing or anti-icing chemicals may be especially vulnerable to these chemicals indirectly. For example, a dysfunctional water stop between the deck and barrier may allow the deicing and anti-icing chemical to migrate horizontally through the deck barrier interface thus reaching the deck fascia. When the snow is cleared during winter months, the interior of the barrier and the nearby deck regions are subject to accumulated snow and deicing or anti-icing chemicals. A good quality air entrained concrete may prevent the built up of osmotic and hydraulic pressures past the critical point, and withstand the effects of such chemicals for many years (Kostmatka and Wilson 2016).

2.2.2 Concrete Removal

The current method in Michigan to address the deterioration of bridge deck fascias is to remove the unsound concrete. With respect to the method used to remove unsound concrete, the most common method is the impact method, informally known as jackhammering (ACI 2004; Fay 2015). A similar method is used in Ohio and many other states. However, this method presents the following problems (Miller et al 2020):

1. Due to a lack of precision in terms of identifying the demarcation between sound and unsound concrete, the operator may remove sound concrete. This problem has been reported by ACI 546R-04 (ACI 2004), Bertolini et al. (2013), and Fay (2015), where it is noted that this method tends to damage sound concrete by causing microfractures, thus creating potential future failure or fall-off in the case of deck fascias. Recommendations regarding the size of pneumatic hammers as well as the type of bits are available. For example, both ACI 546R-04 (ACI 2004) and Fay (2015) recommend the use of 15-30 pound hammers, and sharp pointed bits in lieu of the spade bits. It is recommended that spade bits be used near saw cuts.
2. The use of such pneumatic tools for a prolonged period may result in musculoskeletal problems.
3. This method may also damage reinforcement.
4. The dust generated from removing concrete in this fashion, may be a health hazard. For example, in 2017, the Occupational Health and Safety Administration (OSHA) instituted new rules for the protection of workers against silica duct, which are likely to increase the cost of repairs conducted in this manner.

Other methods to remove unsound concrete exist, such as high-water pressure methods (water jet hand lances and hydroblast/hydrodemolition), and abrasive removal (sandblasting and shotblasting). However, Miller et al. (2020) report that these methods are typically used for concrete on flat surfaces and are not intended for applications that involve vertical surfaces such as bridge barriers or deck fascias. For examples, Fay (2015) reports that shot blasting is effective in removing less than ½ in. of concrete in flat surfaces, as it is reported (Miller et al. 2020) that the equipment is made to operate on flat surfaces, making the method impractical for vertical surface applications. ACI 546R-04 (ACI 2004) reports that sand blasting may be used if the removal depth is contained to ¼ in. and precautions are taken to contain the sand.

It is reported (Miller et al. 2017) that hydro demolition is an effective method of removing unsound concrete in large areas and it avoids damaging sound concrete or reinforcement. For small areas pneumatic hammers may be used. While most hydro demolition equipment is made for horizontal surfaces, options for vertical surface applications do exist and include the use of robotic equipment. Hand-held devices are available such as lances, however, they are not as effective as

robotic machines, and are appropriate for small areas. One limitation of the hand-held devices is the amount of force that the operator can tolerate, which can be up to 250 N (56 lbs), whereas robots can sustain forces up to 1000 to 4000 N (225 lbs to 900 lbs). Another ramification is the containment, treatment and appropriate disposal of waste water.

Miller et al. (2017; 2020) investigated the use of hydro demolition through the deployment of a robot capable of working in vertical surfaces as an alternative to using pneumatic hammers. A total of three robotic machines were considered, all of which had the capability to reach over the side of the bridge using a flexible arm if no vandal fence is present. In cases when a vandal fence is present, the machine can be modified with a boom that has a reach about 22 feet, so that the deck fascia can be accessed from below. One of the robotic machines (CONJET 327) is reported to be small enough to be placed in a scissor lift platform to extend the vertical reach. One of the robotic machines operates on diesel or electricity, whereas the other two operate based on electricity. The robotic machines are remote controlled and require a power unit to operate. The size of the unit is reported to be similar to a 20-foot shipping container, and includes the generator and water pumping units. As noted earlier, one challenge is the containment of the water, which in Ohio appears to be considered hazardous waste based on the Ohio Environmental Protection Agency. In Ohio, the waste water must be collected so that it does not drain into streams or waterways, and the Ohio requires the water to be treated, or allows land application with proper permits (Miller et al. 2017). Another challenge related to the use of robotic machines is their cost. The machine identified by Miller et al. (2017) costs about $350,000. Renting the equipment is an option with one rental location being in Ann Arbor, Michigan.

Determination of the Depth of Removal

Since many repair guides require the removal of unsound and contaminated concrete, the determination of the depth of removal is of interest. Unsound concrete is considered to be concrete that is cracked and/or debonded (Miller et al. 2017). Since the transition between sound and unsound concrete is a gradual one, rather than a distinctive one, the determination of the demarcation between sound and unsound concrete is a challenging task. Qualitative methods exist, such as the use of metal hammers followed by an examination of the type of sound. It is reported that unsound concrete creates a hollow sound followed by a low rebound, whereas good quality

concrete creates a distinct ring followed by a high rebound. Rebound hammers may also be used to distinguish between sound and unsound concrete by examining the rebound readings.

The identification of contaminated concrete is a more challenging task compared to that of identifying unsound concrete. The corrosion of reinforcement is typically precipitated by the carbonation and chloride intrusion. Both of these mechanisms are well addressed in the literature.

Carbonation caused by the carbon dioxide in the air reduces the alkalinity of concrete thus comprising the effectiveness of the passive layer around the reinforcement. Simple tests for identifying carbonation exist, in which an alcohol-based solution is sprayed on the concrete. A pink color suggests the presence of non-carbonated concrete, whereas areas that do not change color are suspected to be subject to carbonation.

The identification of chloride contamination is more difficult because of a lack of an established threshold that is related to this phenomenon. Even if a threshold were to be established, and contaminated concrete were to be removed, the corrosion of reinforcement may continue. In a bridge rehabilitation project, it may be possible to remove contaminated concrete, and corroded reinforcement and replace it with sound materials. However, for maintenance activities, the prospect of further corrosion in reinforcement is a phenomenon that may have to be accepted (Miller et al. 2017).

2.2.3 Concrete Surface Treatment

While the first line of defense against various deterioration mechanisms is the use of good quality concrete with low permeability, the use of protective treatments is another approach that may be used to enhance the service life of concrete structures. The protective treatments prevent aggressive substances from coming into direct contact with concrete. Kerkhoff (2007) discusses the effects of several chemicals on concrete and provides treatment options.

In general, two types of waterproofing systems are available: permanent sheet systems and spray-on coatings. Permanent sheet systems are commonly used for bridge deck protection and are usually applied in several layers, including a waterproofing membrane, protection board, tack coating, and then an asphaltic layer to be used as a wearing surface. Various commercial products exist (Iko, Vibraflex, GeoTac, etc.), and since the 1970s, various National Cooperative Highway Research Program (NCHRP) Synthesis reports investigated these systems, including NCHRP 57 (Transportation Research Board 1979), 220 (Manning 1995), 333 (Russell 2004), and most

recently, 425 (Russell 2012). Although meant for bridge deck traffic, these coatings can be highly durable, and a modified version, such as with removal of the wearing surface layer, may be useful for protection of the fascia region. However, drawbacks include application cost and time, as well as that its presence inhibits inspection of the concrete surface.

Spray-on systems include polymer-based waterproofing membranes that adhere to the concrete surface, and penetrative sealants. Polymer membrane systems are commonly made of acrylic or polyurethane, and are applied in 1 or 2 coats with a tack coat to enhance bond. Such products have become more widely used in recent years and many commercial options exist (BDM, Deckguard, etc). The least expensive but least durable option is a penetrative sealant.

The effectiveness and durability of these various types of protective systems have been thoroughly studied in previous research. Illinois DOT, for example, evaluated over twenty different sealants, membrane, and laminate products applied to over 60 bridges (Morse 2009). From a cost-benefit perspective, it was found that periodic application of sealants offered relatively effective durability enhancement. Moreover, a significant amount of research knowledge exists with regard to the performance of different penetrative sealants (Attanayaka et al. 2002; Johnson et al. 2009; Shearer et al. 2015; ElBatanouny et al. 2017; Tan 2019). For example, Attanayaka et al. (2002) found that silane and siloxane treatments can be applied in new decks, while existing deck treatment is a function of crack width. It was determined that if the crack width is less than 0.002 inches, silane sealers were adequate, whereas for cracks widths between 0.002-0.08 in., silane and high molecular weight methacrylate (HMWM) were deemed suitable options provided that an adequate drying period is maintained between silane and HMWM applications. Tan (2019) investigated the long-term bond strength and chloride resistance of epoxy and concrete overlays and concluded that while the initial bond strength of both types of overlays is good, the long-term bond strength of the thin epoxy overlay decreases sharply after 300 freeze-thaw cycles, whereas the bond performance of the low slump dense concrete (LSDC) overlay remained unchanged. It was further found that the chloride resistance of the epoxy overlay is much better than the LSDC overlay and the percentage of air voids in the substrate concrete was found to have an effect on initial performance of the overlays.

One current challenge in Michigan is that the silane treatment that is applied to the inside of the deck and barrier for protection against weathering, is not applied to the deck facia since this region is painted for aesthetic purposes. The paint prevents proper adhesion between the silane

treatment and the concrete substrate. The order of application can be reversed thus providing some enhanced initial durability to the deck fascia. However, since the silane treatment needs to be reapplied periodically, the initial level of protection may not be maintained in the long term. In addition, it is unclear whether the application of the silane treatment on the deck fascia undermines the bond between the aesthetic paint and concrete deck. Provided that the aesthetic paint can be applied after the silane treatment on the deck fascia, options for future preventive maintenance include removing the paint and reapplying it after the deck fascia has been retreated with silane. Alternatively, using colored options for the silane treatment that provide protection while maintaining the aesthetics of the bridge could be another solution.

Some of the abovementioned studies and others that dealt with the evaluation of the performance of various concrete surface treatment options are summarized below in greater detail in reverse chronological order.

Safiuddin (2017) reports that a proper selection of sealer or coating products, surface treatment before application, and use of less aggressive deicing and anti-icing chemicals helps increase the performance of concrete sealer and coating systems in field conditions.

ElBatanouny et al. (2017) conducted an extensive study about the utilization of polymer overlays and sealers in bridge decks. It was concluded that multi-layer epoxies and premixed polyester concrete were the best-performing polymer overlays, whereas the silanes and siloxanes were the most widely used sealer products as penetrating deck sealers. The service life models and life cycle cost analysis results indicated that it was best to install polymer overlays on new bridge decks, with reapplication at the end of the overlay's service life, approximately every 25 years or less. Hybrid preventative maintenance was also recommended, by applying the sealer immediately after construction, and installing the polymer overlay within the first 5 years. It was stated that this application would double the service life of the bridge decks.

Liang et al. (2014) conducted a study about the performance of deck sealers on highway bridges in the state of Colorado. Based on previously conducted research on deck sealers by various state DOTs, four sealer products, high molecular weight methacrylate (HMWM), two epoxies and a silane were selected for evaluation. The performance of such products was assessed for their skid resistance, and ability to prevent or slow down the moisture and chloride ion penetration into concrete bridge decks. The selected products were applied on the bridge deck surfaces, and performance was monitored by examining the variation of temperature, humidity

fluctuation, chloride penetration profile and skid resistance. The four sealers were ranked based on abovementioned metrics. It was concluded that all four sealer products tested were effective in terms of blocking water penetration in concrete. HMWM was found to be the most durable in terms of providing resistance against chloride ions, and was selected as the best sealer among the four.

Oman et al. (2014) evaluated the long-term performance of 12 sealant products in bridges over a three-year period. Field permeability tests, visual observations, and petrographic examinations were performed to assess performance. Visual observations indicated that the effectiveness of sealant products diminished significantly after two winters due to major loss of sealant and surface sand materials. Some cores were extracted two winters after sealants were applied. Based on the petrographic test results, it was stated that the sealant penetration was highly variable and was likely dependent on the presence of debris within the crack, crack width, and deck temperature during application. The failure mode of the sealants was observed as the detachment from the crack face, and lack of completely bridging the cracks. Four epoxy and three methacrylate products were recommended. The surface preparation and application method conditions were emphasized as important factors for the performance of sealants.

Wenzlick (2007) investigated the performance of four penetrating sealers in laboratory environment as an alternative to linseed oil, which at the time was used by Missouri DOT. The motivation for consideration of alternatives was the relatively low performance of skin resistance of linseed oil when used in excess, and its high curing time. It was claimed that cracks smaller than 0.007 in. (0.18 mm) did not let chloride agents penetrate concrete and therefore, did not need to be sealed. The use of linseed oil was deemed appropriate to prevent scaling for areas that featured few cracks even if the size of cracks was larger than 0.007 in. However, for multiple cracks larger than 0.007 in., the use of a penetrating sealer was recommended. It was concluded that none of the penetrating sealers were effective at sealing the large cracks. Therefore, for large cracks, the use of crack filler/sealer was deemed more appropriate. One of the considered concrete crack sealers, acrylic-based Star Macro-Deck, exhibited good performance and had lower cost, thus was suggested for use to seal large cracks as preventative maintenance.

Palle and Hopwood (2006) evaluated the performance of various coatings on bridge barriers using laboratory and field testing. It was concluded that some coatings did not provide any protection in terms of preventing chloride penetration, while some showed good performance.

Attanayake et al. (2006) evaluated the performance of silane and siloxane on concrete bridge decks. It was determined that the major parameter controlling the effectiveness of the penetrating sealants was the depth of penetration. Moisture content within the first 6 mm (0.24 in.) depth of the concrete was also determined to be an important factor for the penetration of sealant.

Pincheira and Dorshorst (2005) evaluated the performance of ten crack sealants and 13 deck sealants under laboratory conditions. Out of the thirteen deck sealants, two of them, Sonneborn Penetrating Sealer 40 VOC and Hydrozo Silane 40 VOC exhibited the best performance, and met the WisDOT acceptance criteria. Out of ten crack sealants, sealant Sikadur 55 SLV and Dural 335 showed excellent performance.

Attanayaka et al. (2002) evaluated the durability of penetrating sealants on concrete bridge decks. It was determined that the depth of penetration was one of the most critical factors for the effectiveness of penetrating sealants. Surface preparation, application procedures, and water conditions were determined to affect the depth of sealant penetration. In addition, it was emphasized that a successful application of sealant required close attention to detail such as deck cleaning, crack sealing, and repetition of this process in regular preventative maintenance cycles. It was concluded that penetrating sealants are effective for protecting concrete bridge decks. The sealants had an effective service life of four to five years. It was suggested that while silane and siloxane penetrating sealants could be used on new decks, high-molecular-weight methacrylate, HMWM, in conjunction with silane sealers could be used for cracked decks. Suggestions about the penetrating sealants were provided depending on the crack widths. If the crack width is smaller than 0.002 inches, silane sealers was more suitable. On the other hand, if the crack width is in the range of 0.002 inches to 0.08 inches, silane and HMWM products could be utilized.

King (1993) investigated the performance of various waterproofing sealers for concrete bridge decks using laboratory and field tests. It was concluded that silane and siloxane were the most effective sealers to prevent intrusion of chloride and moisture into concrete.

Smith (1986) studied the performance of silanes composed of alkyltrialkoxysilane chemical products in bridges. Previously conducted laboratory studies showed that two particular silane products significantly reduce the moisture and chloride penetration into concrete, hence prevent corrosion of steel reinforcement. A field test conducted in 1977 also proved that bridge decks treated with silane products exhibited excellent performance for moisture penetration. Later, eight more silane treated bridges were investigated to evaluate the performance of silane agents

since 1977. The metrics for the evaluation were the amount of corrosion, concrete delamination, scaling and spalling. It was concluded that all applied silane products showed very good performance in terms of preventing moisture and chloride penetration into concrete, and corrosion rate in the reinforcement. It was also determined that surface friction did not affect the performance of silane treatment. It was suggested that before applying a silane product, the surface should be dry for a successful application, and after the silane has penetrated into the concrete, a water treatment on the silane treated surface should be applied to assure that sufficient moisture is provided to facilitate the chemical reaction between silane and concrete.

Pfeifer and Scali (1981) conducted an NCHRP sponsored study on the performance of various concrete sealers as a means to provide protection for bridge structures. The investigation considered all bridge surfaces except the top surface of the bridge deck, which is subjected to tire abrasion. A wide range of generic types of chemicals were evaluated under laboratory conditions. It was concluded that many of the chemical materials were found to be ineffective in reducing water and chloride intrusion into concrete. In addition to this, it was emphasized that significant variation in performance within a given generic type of chemical was observed. On the other hand, it was reported that some materials showed excellent performance in terms of reducing the intrusion of chloride by 80 to 99 % when compared to uncoated concrete. Some materials were applied to cracked concrete, and it was determined that certain materials offered added corrosion protection to embedded reinforcement. The tested chemical materials could be sprayed, roller-applied or brush-applied.

Further discussions on various types of concrete surface treatment options are provided below:

Penetrating Sealers

Penetrating sealers usually come in two forms: 1) pore liners, and 2) pore blockers, both of which repel water by their hydrophobic nature. The main function of the pore liners is to coat the inside of pores in concrete using small water repellant molecules (such as silane) with the purpose of preventing water penetration into the concrete material. Conversely, the function of pore blockers is to seal the pores against water penetration. However, they are incapable of sealing cracks that are larger than 0.002 in. Therefore, their primary function is to protect new concrete surfaces or extent the life or existing concretes with little to no damage (Miller et al. 2017).

The use of silanes as a treatment option of bridge barriers was not recommended by Miller et al. (2017) since they have no ability to bridge cracks and may prevent proper bonding of future surface treatments to the concrete surface. Epoxy was considered to be a better, cost effective option for bridge barriers (Miller et al. 2017). Penetrating sealers as a material are relatively inexpensive, $0.10 to $0.40 per square foot (Morse 2009). Miller et al. (2017) reports that installed prices range from $1.00-$2.00 per square foot when installed by Ohio Department of Transportation (ODOT) crews. They can be applied easily with a sprayer, brush or roller, and provide a breathable surface, thus allowing interior moisture vapor to escape. One challenge is that the concrete surface needs to be cleaned and completely dried before the application of the sealant (Fay 2015). Miller et al. (2017) report that while there is no long-term durability data on penetrating sealers on bridge barriers, a study by Christodoulou et al. (2013) investigated pier caps coated with silane approximately 20 years earlier and reported that the silane was still effective, however, since there was no baseline for comparison, the researchers could not determine how effective the material was.

Acrylics, Epoxies, Polyurethanes, HMWM, and Polyureas

Acrylics provide a thin protective coat on concrete surfaces. Miller et al. (2017) report that no studies were found in which acrylic coatings were tested for bridge deck applications, and since they have the tendency to wear faster than other coatings, they were not considered suitable for bridge barrier applications.

Miller et al. (2017) concluded that epoxies were more effective than silane in bridging small cracks in bridge barriers. In addition, silanes prevent the bonding of future surface treatments. However, epoxies are able to penetrate only 1/16 in. of the concrete surface. Large cracks need to be filled with other materials prior to the application of epoxy. In addition, epoxies have limited ability to seal cracks that are created after their application due to their limited extensibility and cracks can be expected. As a result, Miller et al. (2017) recommend that after a year when most of the shrinkage in the barrier has taken place, cracked areas should be resealed. It is recommended (Miller et al. 2017) that this be done during cooler temperatures when the cracks are wider. HMWM may also be used to seal the cracks. However, studies have shown that while HMWM penetrate deeper, epoxy bonds better and is compatible with the previous epoxy coating in addition to being easy to apply. Studies conducted by Morse (2009) and Knight and Hudleson

(2016) suggest that the price of epoxies appears to be similar to that of penetrating sealers. In addition, Miller et al. (2017) report that not all epoxy coatings are freeze-thaw resistant and recommend that they be qualified as such. It was also recommended that barriers be recoated periodically with estimated periods varying from 5-20 years.

Among the many options available for protective sealant, the study by Miller et al. (2017) identified polyureas as a promising option especially for barriers that exhibit excessive cracking, spalling or deterioration, but not to the degree that requires replacement. It was reported that the material in addition to sealing concrete surfaces, also acts as a reinforcing barrier retaining broken fragments of concrete with some studies likening them to carbon fiber reinforcement. Polyureas are described as (Miller et al. 2017) a two-component material that develops into a polymer compound by mixing a resin with a catalyst. There are generally two types: aromatic and aliphatic with the difference between the two being in the shape of the molecule. They need to be sprayed on using special equipment, and the material sets fast (i.e. there is a limited time window to conduct the installation). The application requires skilled workers and appropriate protective equipment. Although polyaspartic polyureas are formulated to have a longer setting time allowing more flexibility for installation and making it possible for them to be sprayed, rolled, or brushed onto a surface. The aromatic options are easier to apply, while the aliphatic ones are deemed more appropriate for concrete surfaces due to their durability against ultraviolet light (UV). Some manufactures suggest a combination of both, with the aromatic option serving as a base coat, and the aliphatic layer providing UV resistance. While typically coating range in 0.02 to 0.1 in. in thickness, they can be as thick as ½ in. The study by Miller et al. (2017) distinguished polyureas from the rest of protective sealants due to their ability to provide:

1) Abrasion resistance
2) Good bond to concrete and steel
3) Good resistance to many chemicals including chloride as well as to changes in humidity and temperature
4) Good sealing capability including cracks up to 1/8 in. due to their high level of elasticity
5) Reinforcement capabilities with some manufactures providing blast resistant formulas (Davidson et al. 2004; 2005)
6) A repairable material
7) Freeze-thaw and salt fogging resistance

8) A flexible repair option, which can be applied over a wide range of temperatures (-30ºF to 140ºF)
9) Colored as well as clear options

The drawbacks appear to be the relatively higher cost of the installed material, which ranges from $3-$7.5 per square foot, compared to $1-$2 per square foot for epoxies (Miller et al. 2017). For many polyureas special equipment is required for application, and for the spray on option training is required for the workers. The training is available by the manufacturers and lasts 10 days. For spray on polyureas, special equipment includes a high-pressure machine with high volume and high heating capabilities. The cost for such machines varies from $20,000-$40,000 (Miller et al. 2017). Lower cost options exist and include cold spray and joint fill equipment utilizing static mixers, which operate at lower output pressures. The pricing for this varies from $5,000-$15,000 (Miller et al. 2017). Miller et al. (2017) recommend that polyaspartic polyureas be explored first since they are easier to apply, with the sprayed-on option as a second alternative due to the more complex application procedure.

2.2.4 Repair of Deteriorated Deck Fascias

While the removal of unsound concrete prevents fall-off, it does not restore the original structural integrity of the barrier to deck connection. This may be accomplished if the geometry of the deteriorated deck fascia is restored with repair concrete and that the corrosion of reinforcement is addressed such that the phenomenon does not re-appear. Studies on the topic of repairing concrete areas with corroded reinforcement include those conducted by FHWA (1998; 2001), which concluded that patching concrete over corroded reinforcement is not effective due to the differential shrinkage between the two materials. This differential shrinkage leads to the formation of cracks at the interface, which allow chloride contaminated water to reach the reinforcement and further exacerbate the corrosion process. The differential shrinkage induced cracking and subsequent deterioration is confirmed by other studies that address the corrosion of reinforcement (Bertolini et al. 2013, Vaysburd and Emmons 2000; 2004, and Fay 2015). These studies also note that the electrochemical incompatibility between the existing and new concrete may provide a path for electrochemical corrosion especially if the bar is partially embedded in both materials, and if water and chlorides penetrate the perimeter of the patch (Miller et al. 2017).

To address the repair of concrete areas that feature corroded reinforcement, Vaysburd and Emmons (2000; 2004) provide different options:

1. The bar may be cleaned and the area patched. However, this method is subject to the problems discussed above.
2. The reinforcement may be cleaned, coated with epoxy and the area patched. This requires a two-stage application as the epoxy needs to be applied first and allowed to cure prior to patching. In addition, the epoxy coating may compromise bond strength, and this needs to be considered.
3. The reinforcement may be cleaned and coated with cement mortar. The use of cement mortar in lieu of epoxy promotes good bond with the repair concrete material and provides a layer of protection against corrosion that features high alkalinity. Although this layer and the repair concrete material is still permeable to chlorides.
4. The reinforcement may be cleaned and the surface coated with a zinc primer that may provide cathodic protection. However, the effectiveness of this method is unknown (Miller et al. 2017).
5. The reinforcement may be cleaned and the geometry of the deteriorated area restored using a repair concrete material that contains corrosion inhibitors. The effectiveness of corrosion inhibitors was previously discussed as being controversial and a study by FHWA (2001) found this approach to be ineffective due to the shrinkage of the repair concrete material. The use of low shrinkage concrete may make the method effective.

The abovementioned options may be adopted and modified to repair deteriorated deck fascias. Other options for deck fascia repair include:

1. The installation of corrosion resistant dowels and the use of repair concrete material that exhibits sustained tensile strength in deck fascias that feature severe deterioration. Options for the repair concrete material and corrosion resistant reinforcement are discussed further below.
2. The use of polyureas on new deck fascias or existing ones that feature low to moderate deterioration.

Repair Concrete Material

Cracking-induced spalling is fundamentally an issue of insufficient tensile strength. The ability of the concrete mix used for repair to exhibit sustained tensile strength after the first crack is instrumental. This is especially the case for deck fascias because if cracks were to occur, the sustained tensile strength, typically realized through fiber bridging action (such as that present in fiber reinforced concrete) or a laminate type reinforcement layer (such as polyurea), may prevent concrete from falling and may facilitate stress redistribution. Similarly, low permeability for the repair concrete material is essential in reducing the penetration of water and deicing chemicals in concrete. This reduction in permeability controls the magnitude of expansive forces within concrete that occur due to freeze-thaw cycles. In addition, concrete with low permeability controls the continuation of corrosion in steel reinforcement protruding from the deck fascia. Finally, flowability is important if the repair is desired to be implemented without removing the barrier.

One option for the repair concrete material is to use an ultra high-performance concrete (UHPC) mix, which possesses low permeability, high sustained tensile strength, high resistance to freeze-thaw cycles, excellent flowability and overall excellent durability (Russel and Graybeal 2013). The idea of using UHPC in highly distressed areas is not new and has been implemented by various states in joints between precast deck panels (Graybeal 2014), deck overlays (Haber et al. 2018), and steel beam ends as a repair material (Zmetra et al. 2017; Mcullen and Zaghi 2020) to reinstitute the original strength. To date, in the United States, nearly 200 bridges in 27 states and the District of Columbia have been constructed using UHPC materials, and 93% of these projects used UHPC for prefabricated bridge element connections (Haber and Graybeal 2019). Various nonproprietary mixes for UHPC exist including one developed for MDOT (El-Tawil et al. 2020).

However, if this option is deemed too costly, another repair material is fiber reinforced concrete (FRC), which does not meet the definition for UHPC (which includes a minimum limit on compressive strength) but still possesses a high sustained tensile strength which can be maintained after the first crack through fiber bridging action. FRC does not have equivalent permeability, tensile strength and flowability with UHPC but may provide sustained tensile strength after cracking. Mix formulations for fiber reinforced concrete are available in the literature (ACI 2008).

The use of fiber reinforced high performance concrete can be also an option for new construction, in which a construction joint is established between the deck fascia and the rest of the deck. In this scenario the deck fascia may feature fiber reinforced ultra/high performance concrete, and the rest of the deck may feature normal strength concrete. This may create an avenue for differential shrinkage and crack opening along the joint, therefore, sufficient time needs to be allowed after the placement of the main deck before the UHPC is placed for the deck fascia. A similar approach appears to be the current state of practices for continuous bridges, in which the deck concrete in the positive moment regions of the spans is placed first, followed by a second placement at the negative moment regions to reduce differential shrinkage induced cracking. An extension of this approach may include the barrier, which is another element that is subject to high concentrations of moisture and deicing chemical during the winter as the snow is cleared from the roads (i.e. the barrier and the deck fascia may feature HPFRC/UHPC and the rest of the deck normal strength concrete.

A third option is high strength self-consolidating concrete. A drawback of this material is its inability to provide sustained tensile strength after the first crack. While this is an important capability to lose, the relatively higher tensile strength than existing low-grade deck concrete, high flowability, combined with corrosion resistant reinforcing (addressed next) may make it a suitable option.

Repair Reinforcement

In deck fascia repair applications, the ability of the repair concrete material to bond and act in unison with the newly installed anchor reinforcement is critical as this determines the ability of the repair region to transfer axial force, shear force, and bending moments due to vehicle impact and barrier self-weight. This bond depends not only on the topography of the surface of the reinforcement but also on the repair concrete material.

Moen and Sharp (2016) investigated bond properties between concrete and various corrosion resistant reinforcing steels, including solid and cladded stainless-steel, and epoxy coated bars. It was found that stainless steel had a lower pullout bond stiffness when compared to black steel, and the epoxy coating decreased the adhesion strength but did not appreciably affect mechanical load-slip response or peak bond strength.

2.2.5 Impact of Deck Fascia Deterioration on the Crashworthiness of the Barrier

The importance of a sound deck-to-barrier connection to maintain the crashworthiness of the barrier has been recognized by several researchers (Maheu and Bakht 1994; Trejo et al. 2001; Deitz et al. 2004; Matta and Nanni 2009), although this topic has received limited attention. These efforts have generally investigated the use of corrosion resisting reinforcement in the barrier and barrier-to-deck overhang connection. Maheu and Bakht (1994) developed a hybrid steel and glass fiber reinforced polymer (GFRP) reinforced concrete barrier in Ontario. In this application, carbon FRP grids were used as flexural reinforcement in the deck and barrier wall, along with stainless steel double headed bars to provide sufficient anchorage. Similarly, the performance of connections between a steel reinforced concrete barrier and a deck overhang reinforced with GFRP bars was investigated through pendulum impact tests on full scale subassemblies (Trejo et al. 2001). In another experimental study (Deitz et al. 2004), GFRP, steel, and hybrid (i.e. having GFRP and steel bars in the top and bottom mats, respectively) reinforced concrete deck overhang subassemblies cast with a steel reinforced concrete barrier were subject to transverse static loading, where it was verified that the connections met the AASHTO Standard Specifications Criteria (2002) for barrier loads. Later, Matta and Nanni (2009) investigated the connection of a concrete railing post and bridge deck constructed with internal fiber reinforced polymer (FRP) reinforcement, and conducted full-scale static tests to verify compliance with AASHTO (2002) strength criteria for vehicle impact. The crashworthiness of the barriers that feature a repaired deck fascia appears to be currently unexamined.

2.2.6 Barrier to Deck Connection and Edge Details that Reduce Moisture Content in Deck Fascia

A review of barrier to deck connection and fascia edge details used by various states in the Midwest was conducted with the purpose of identifying details that inhibit or reduce moisture content in the deck fascia, especially moisture that travels through the deck-to-barrier connection by horizontal migration. A particular focus was placed on connections that feature effective water stops, as the current semicircular water stop detail featured in typical MDOT bridge barrier details has proved difficult to construct. This difficulty is due to the presence of barrier reinforcement, which prevents proper access to construct the desired water stop. Other states in the Midwest (Iowa and North Dakota – See Appendix C) use details that feature a shear key in the barrier to deck connection. This shear key may serve as a water stop. Alternative solutions include commercially available

corrosion resistant strips (such as plastic), which can be inserted into the wet deck concrete to serve as water stops after barrier placement. However, an insertion point needs to be identified for this strip and installation methods need to be explored such that the strip can be installed along the entire length of the barrier.

In addition, the overall configuration of the deck to barrier connection was examined in terms of deck drainage. For example, in some states in the Midwest (Wisconsin and Illinois – see Appendix C), the slope of the top of the deck in the vicinity of the barrier is such that it directs water away from the deck fascia and toward the toe of the barrier. This prevents gravity promoted moisture migration from the inside of the deck into the fascia. With respect to the slope of the bottom of the deck overhang near the barrier, some states in the Midwest have adopted a mixture of approaches depending on the application and type of barrier. Some details promote moisture movement away from the deck fascia (Minnesota, Iowa, Wisconsin), while other details promote moisture concentration at the bottom corner of the deck fascia (Iowa), Wisconsin, Indiana – Appendix C). Current MDOT details feature a deck overhang with no slope at the bottom. Conceptually, the detail used by Illinois DOT appears promising as it promotes moisture movement away from the deck fascia but also away from the fascia girder, creating a low point for drainage that lies between the beam and deck edge. Perhaps more applicable for open-railing barriers, some states (Wisconsin, and Ohio – Appendix C) have applied metal drip edges to the fascia edge to prevent water from contacting the vertical fascia surface.

2.2.7 Alternative reinforcement configurations

As an alternative or in addition to changing the type of deck fascia material, corrosion-prone bars may have the potential to be relocated or removed completely, limiting the exposure of the steel reinforcement to moisture. In particular, the possibility of increasing bar side cover and/or removing or consolidating bars should be considered. For example, the location and need for the first set of bars on the edge of the deck that are parallel to traffic should be reviewed, since the corrosion of these bars may lead to spalling across the entire length of the fascia. However, the placement of the longitudinal bars near the edge of the beam may help retain cracked concrete that is ready to spall by serving as an anchor for it. Therefore, if the cause of concrete spalling in deck fascias is due to a mechanism other than reinforcement corrosion, then the proximity of these bars to the edge is helpful. However, as will be shown in Chapter 3, there is clear evidence that one of

the deterioration mechanisms is corrosion of deck reinforcement, especially for bridges that were constructed prior to the 1980 mandate in Michigan (Boatman 2010) for epoxy coated reinforcement in all superstructure components.

In addition, the position of the top transverse bars in the deck, currently situated below the top longitudinal bars in some typical barrier details (MDOT 2020a), should also be reviewed in terms of structural efficiency for the deck design and not necessarily from the perspective of deck fascia deterioration. In the current MDOT Bridge Design Guide Section (MDOT 2019) 6.41.01 – Standard Bridge Slabs – Load Factor Design (MDOT 2019), the top transverse bars are placed below the top longitudinal bars. In section 6.41.02 – Standard Bridge Slab – Empirical Design, the transverse top and bottom bars are placed at the extreme layers. This placement is logical from a structural efficiency perspective as it increases the moment arm in the transverse direction. It is not clear why, in 6.41.01 the top transverse bars are placed below the top longitudinal bars. If this is done for durability reasons, then greater protection can always be provided by increasing the minimum cover, which currently appears to comply with AASHTO LRFD (2020) and ACI 318-19 (ACI 2019).

2.2.8 Quality of Deck Concrete

ACI 318-19 (ACI 2019) provides guidance for the type of concrete used as a function of various exposure categories. For example, to protect against freezing and thawing, for exposure categories that are considered to be very severe (F3), and in which concrete is exposed to freezing and thawing cycles, and will be in continuous contact with moisture and exposure to deicing chemicals or seawater, it is recommended that the water to cementitious materials ratio, w/cm, is limited to 0.4, and that the minimum design compressive strength is 5000 psi. Identical requirements are specified to provide protection against corrosion for severe exposure categories in which concrete is exposed to moisture and an external source of chlorides in service (C2). Typical mix designs used by MDOT for bridge decks were reviewed and the following observations are presented:

Compressive Strength

Currently, the MDOT Bridge Design Guide (MDOT 2019) (6.41.01 – Standard Bridge Slabs – Load Factor Design) refers to a deck concrete with a specified compressive strength f_c' = 4000 psi, while the reinforcement conforms to ASTM A615 (ASTM 2020). The 2020 MDOT Construction

Specifications (MDOT 2020b) for concrete grade 4500HP, which is used for decks and barriers in all regions, except the superior region, require that the minimum compressive strength at 28 days is 4,500 psi. As will be discussed further in Chapter 3, compared to previous MDOT practice, in which the minimum compressive strength for deck concrete was 3000 psi, this is a significant improvement. However, the compressive strength of 4,500 psi is still 500 psi lower than what ACI 318-19 (ACI 2019) requires for severe environments.

Water to Cementitious Materials Ratio

In addition, the maximum water to cementitious materials ratio, w/cm, according to ACI 318-19 (ACI 2019) for exposure class F3 and C2, as defined above, is 0.40. A review of a mix design for a 4500 psi grade concrete (i.e. 4500HP) revealed that the target w/cm ratio when considering the net water content is 0.44, which is above the 0.4 maximum limit. When considering the total water content, the w/cm ratio is 0.5. AASHTO LRFD Construction Specifications (2017) Article 8.2.2 – Normal Weight (-Density) Concrete indicates that for concrete exposed to deicing chemicals the maximum water to cement ratio shall be 0.45. However, the water content when calculating the water to cement ratio is required to be the total free water in the mix which includes the mixing water, the water in any admixture solutions, and any water in aggregates in excess of that needed to reach the saturated surface dry condition (Article 8.4.2). Based on both, ACI 318-19 (ACI 2019) and AASHTO LRFD Construction Specifications (2017), it appears that mix design used for the deck may need some adjustments to produce concrete that conforms with the minimum requirements for severe exposure.

Air Content

According to Table 19.3.3.1 of ACI 318-19 (ACI 2019) the target air content for exposure F3 for nominal maximum aggregate size of 1 in. is 6%. The target air content (design air) in the mix design that was provided by MDOT for concrete grade 4500HP is 7%. The specified aggregate type in the mix design was 6AA, which according to Table 902-1 in 2020 MDOT Standard Specifications for Construction (MDOT 2020b) translates to a 1 in. nominal maximum aggregate size.

Supplementary Cementitious Materials

The percentage of cementitious materials (Class F Fly Ash) in the mix design submitted by MDOT is 25%, which is compliance with Table 26.4.2.3(b) of ACI 318-19 (ACI 2019).

Slump

According to AASHTO LRFD Construction Specifications (2017) Table 8.4.2-1, for sections 12 in. thick or less, the nominal slump is 1-4 in., while the maximum slump is 5 in. Although, when Type F or G water-reducing admixture are used the slump may be exceeded as permitted by the engineer. In the mix submitted by MDOT, Type D and Type MR water reducing admixtures were used. The design maximum slump was 6 in., whereas the measured slump during the trial batches varied from 3.5 in. to 5 in., which are within the 5 in. limit and certainly within the MDOT specified 6 in. limit when Type MR water reducing admixtures are used (2020 MDOT Construction Specifications Table 1004-1, MDOT 2020b).

2.2.9 Corrosion Resistant Reinforcement

Since there is clear evidence that one of the deterioration mechanisms in bridge deck fascias is reinforcement corrosion, it is important to identify the type of reinforcement that has corroded and to consider alternative options in the future. Boatman (2010) reports that MDOT has been designing bridges dating back to the 1900s, with original designs featuring uncoated reinforcement informally referred to as “black rebar”. The first use of epoxy coated reinforcement in bridge decks appears to be around 1975 (Boatman 2010) with a mandate issued in 1980 requiring that all bridge deck construction starting in December of 1980 features epoxy coated reinforcement.

There is concern that the epoxy coating may be damaged during the construction process and the reinforcement may lose its corrosion resistant properties. Another concern with epoxy coated bars used for doweling is pull-out strength and its ability to properly bond and anchor to the newly placed concrete material when considered in a repair application. The deck fascia experiences high tensile forces and bending moments transferred from the barrier in the event of a vehicle impact, and implicit in the design philosophy for the barrier is that the failure mode is contained within the barrier. Even in new construction the embedment length and development lengths for epoxy coated bars are larger than those for uncoated bars. It appears that MDOT is currently considering high chromium steel as an alternative to epoxy coated reinforcement. This

addresses concerns regarding damage to the coating during construction and provides smaller embedment and development lengths. Although the full strength of the high strength steel may not be fully mobilized due to limits in reinforcement spacings to provide satisfactory performance in service in terms of controlling cracks widths.

Several options exist for corrosion resisting reinforcement, including galvanized, solid stainless steel, stainless steel clad, and fiber reinforced polymer (FRP) reinforcement. Although current MDOT policy is that all superstructure reinforcement is to be epoxy coated, stainless-clad and solid stainless-steel reinforcement are currently permitted to be used in deck construction when the additional cost is justified by the expected enhancement in durability (MDOT 2020). Since the prevailing cause of deterioration as reported in the literature appears to be reinforcement corrosion, there is strong incentive to use alternative types of corrosion resistant reinforcement in the deck fascia region. The MDOT Bridge Design Manual (MDOT 2020a) (7.04.02) states that "dissimilar metals contact, whether with epoxy coated reinforcement, uncoated reinforcement, or galvanized steel, is not considered detrimental when embedded in concrete. The standard cover requirement of three inches can be reduced to two inches."

2.2.10 Construction Practices

Since the presence of moisture is a common denominator for many of the deterioration mechanisms discussed above, a control of moisture content through proper and functional drainage as well as an understanding of the distribution of moisture in fresh concrete is important in helping identify the underlying cause of deck fascia deterioration. A field visit during deck placement for a bridge rehabilitation project near Bay City, MI, revealed that while concrete is pumped in the majority of the deck surface, the region near deck fascia receives concrete through free flow facilitated by the use of vibrators. The reinforcement configuration at the deck-to-barrier connection can be dense and may create a situation in which only the paste of the cementitious matrix travels to the deck fascia thus resulting in increased moisture content, enhanced vulnerability to differential shrinkage and differential shrinkage induced cracking.

2.2.11 Summary of the Literature Review

The deterioration of bridge deck fascias appears to be largely unexamined. In general, moisture reduction, good quality concrete, corrosion resistant reinforcement, and appropriate construction

practices appear to be the first line of defense for all concrete elements subject to severe environmental effects. For the deck fascia deterioration to take place two factors must be present: 1) moisture, and 2) low grade materials. The negation of either addresses the problem.

Moisture Reduction

- Alternative deck configurations that utilize gravity to keep water laden with deicing and anti-icing chemicals from flowing from the deck to the deck fascia is an alternative worthy of consideration. In addition, as will be discussed further in Chapter 3, a large number of bridges in Michigan that exhibited deteriorated deck fascias featured fencing, open barriers, and sidewalks. The presence of fencing increases the amount of moisture that travels down to the deck fascia. Open barrier and sidewalks also lead to increased moisture content. The use of closed barriers, and alternative fencing configurations are options worth considering.

Higher Performing Materials

- There appears to be a strong incentive to use higher performing concrete in the deck fascia region or in the entire deck to enhance the durability of this element. The reduction of the likelihood of freeze-thaw damage would require the consideration of higher performing air entrained concrete. The retainment of broken concrete fragments in the future in new bridges requires the consideration of concrete that exhibits sustained tensile strength such as fiber reinforced concrete. Alternatively, for existing bridges as well as for new construction, the use of polyurea as a coating on the deck fascia appears promising.
- In Michigan, there have been significant improvements in terms of pursuing higher grade materials for the deck. As will be discussed in Chapter 3, the majority of the bridges that feature deteriorated deck fascias, consist of low-grade concrete for the deck featuring an f_c'=3000 psi at 28 days. The current specifications require a deck concrete with an f_c'=4,500 psi. While this is 500 psi lower than the ACI 318-19 (ACI 2019) requirements for severe environments, it is an improvement compared to the f_c'= 3000 psi mix used in the past.
- Similarly, the use of alternative corrosion resistant reinforcement that is not prone to damage during construction appears to be a viable option for eliminating corrosion as a potential deterioration mechanism. In Michigan, epoxy coated reinforcement appears to have performed well since the 1980 mandate to use corrosion resistant reinforcement. Only

a few of the bridges that were identified as having deteriorated deck fascias were constructed after the 1980s.

Repair

- The use of hydro-demolition via a robot as a means to remove unsound concrete was proved effective and viable by Miller et al. (2017; 2020) for large repair areas compared to the traditional approach of damaged concrete removal using pneumatic hammers, which was deemed appropriate for small repair areas. Chapter 4 presents a repair detail for deteriorated deck fascias, which was proved effective through small-scale and large-scale testing.

2.3 Survey State DOTs

A survey was created and submitted to the state DOTs to determine the extent of deck fascia deterioration in other states, and to identify associated practices for design, construction, maintenance, and long-term repair. The results of this survey are provided in Appendices A-B. None of the states have sponsored research that deals with the deterioration of bridge deck fascias. The general focus appears to be with the overall performance and durability of the deck.

Fig. 2.1 provides a summary of the reported cause of deterioration (Fig. 2.1a), type of reinforcement at the barrier to deck connection (Fig. 2.1b), methods used to remove unsound concrete (Fig. 2.1c), and type of protectants or sealants used as a means to prevent the deterioration of deck fascias or prevent its exacerbation (Fig. 2.1d). When responding to the survey, some states provided more than one answer. For example, when stating the cause of deterioration, some states indicated that it is due to poor construction practices, corrosion, and freeze-thaw. The histograms were prepared accordingly, therefore, the summation of the states providing a given response may not equal the total number of respondents.

According to Fig. 2.1a, six states reported that the cause of bridge deck fascia deterioration is poor drainage, five attributed it to poor construction practices, three attributed it to corrosion, three to chemical intrusion such as deicing chemicals, and one state to freezing and thawing. The DOT representatives from Minnesota reported that the deterioration of deck fascias is common in bridges with sidewalks and fencing that allow chlorides to drain over the coping – such as in a chain link fence. Similarly, some states reported that the deterioration of deck fascias is generally

common in older bridges with open rail bridge barriers, or those that originally featured a curb and the deck was later paved on to the point that the efficiency of the curb was reduced. The reported poor construction practices include deviation from the specified cover and poor consolidation. Kansas for example has added an inch of cover to exterior soffit of girder bridges, and has increased bottom cover to 1.5 in. on all bridges.

According to Fig. 2.1b, 14 out of 18 states reported that they use epoxy coated reinforcement at the deck to barrier connection, five use uncoated reinforcement, and three use other types of reinforcement, such as carbon chromium steel, stainless steel, and corrosion resistant high chromium steel. These results reflect current practice. In the past, many of the states that currently use a type of corrosion resistant reinforcement have used uncoated reinforcement. It was reported that it is primarily the bridges, which feature such uncoated reinforcement that generally exhibit deck fascias deterioration. This observation was confirmed by the research team for bridges in Michigan. North Carolina uses a combination of epoxy coated reinforcement for the top mat, and uncoated steel for the bottom mat. This practice appears to have been used in Oklahoma in the past, however, it was reported as problematic for their state and corrosion was reported in the bottom deck reinforcement due to the slower melting of the snow near the parapet region. In Oklahoma, epoxy coated bars are used in On-System bridges, and uncoated reinforcement in Off-System bridges. It was reported by many states that the bridges that primarily exhibit deteriorated deck fascias are older bridges constructed with uncoated reinforcement, suggesting that the use of any type of corrosion resistant reinforcement improves the condition. The use of stainless steel in some states is reserved for critical bridges.

In terms of unsound concrete removal, Fig. 2.1c suggests that 13 out of 18 states use a mechanical method such as: impact hammers and saw cutting; two states use abrasive blasting; one state water blasting; one state epoxy injection; and one state other methods such as a Hoe-Ram. However, some states reported that the method for removing concrete is typically left to the discretion of the contractor as it falls under means and methods of construction. Many respondents stated that the method to distinguish between sound and unsound concrete is the sounding of the area of concern.

Fig. 2.1d shows that the type of protectants or sealants used as a means to prevent the deterioration of deck fascias or prevent its exacerbation varies greatly. Seven states currently do not use any surface treatments for the deck fascias; three states did not state their current practice,

and the rest of the states used a variety of concrete surface treatments as illustrated in Fig. 2.1d. Wisconsin uses varies types of concrete surface treatments.

Reported repair techniques varied as a function of the degree of deterioration. Patching was reported as an option when the deterioration was not extensive. Prior to patching, typical repair techniques that include cleaning and coating of existing reinforcement appear to be specified. Deck overhang and barrier replacement were reported as options in cases of severe deterioration. Shotcrete was reported as an option for repair followed by smoothing of the surface to supply the desired geometry.

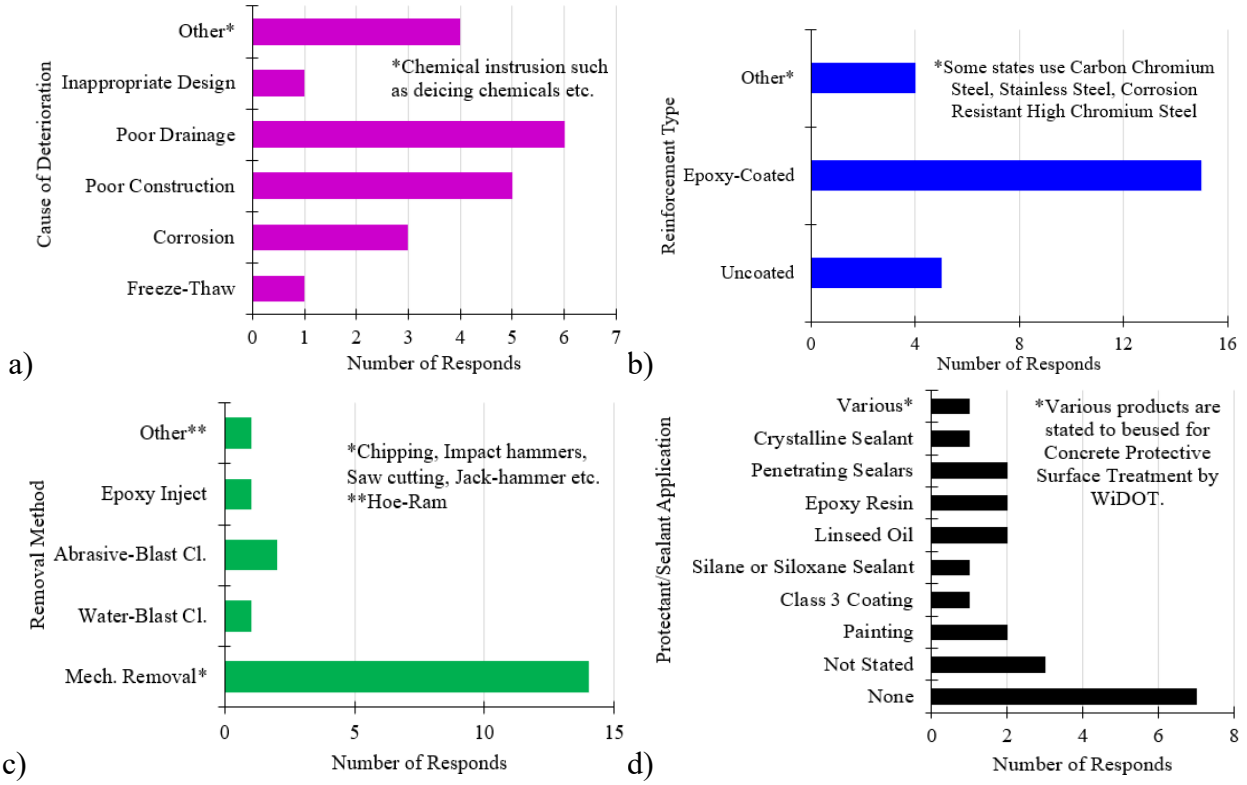

Fig. 2.1 Summary of survey results – histograms for: a) cause of deterioration of bridge deck fascias; b) type of reinforcement at the barrier-to-deck connection; c) methods to remove unsound concrete, and d) type of protectants or sealants used as a means to prevent the deterioration of deck fascias or prevent its exacerbation

Fig. 2.2 shows the frequency of deck fascia deterioration in each state based on the survey results. States that feature similar climates with Michigan indicated that the deck fascia deterioration is common in older bridges, but not common in new bridges. These states are reported as having a high frequency of deck fascia deterioration and are indicated with a dark red color in

the map. Minnesota, Wisconsin, Michigan, and Pennsylvania fall in this category. Montana and Louisiana indicated that they have no deck fascia deterioration in their bridges. Nine states reported that they have a low frequency of deck fascia deterioration (i.e. the phenomenon is present but not common). The representatives of Alaska DOT reported to have only one freeze-thaw cycle suggesting that deterioration due to freezing and thawing is not an issue. They also reported that their steel bridges typically feature precast deck panels and concrete bridges feature decked bulb tees. This provides a higher quality concrete for the deck and may be the reason why the deterioration of deck fascias is not common. Many of the states that indicated to have a low frequency of deck fascia deterioration are in the southeast. However, some are located in other regions, such as: Massachusetts, Kansas, West Virginia, Alaska, and Washington.

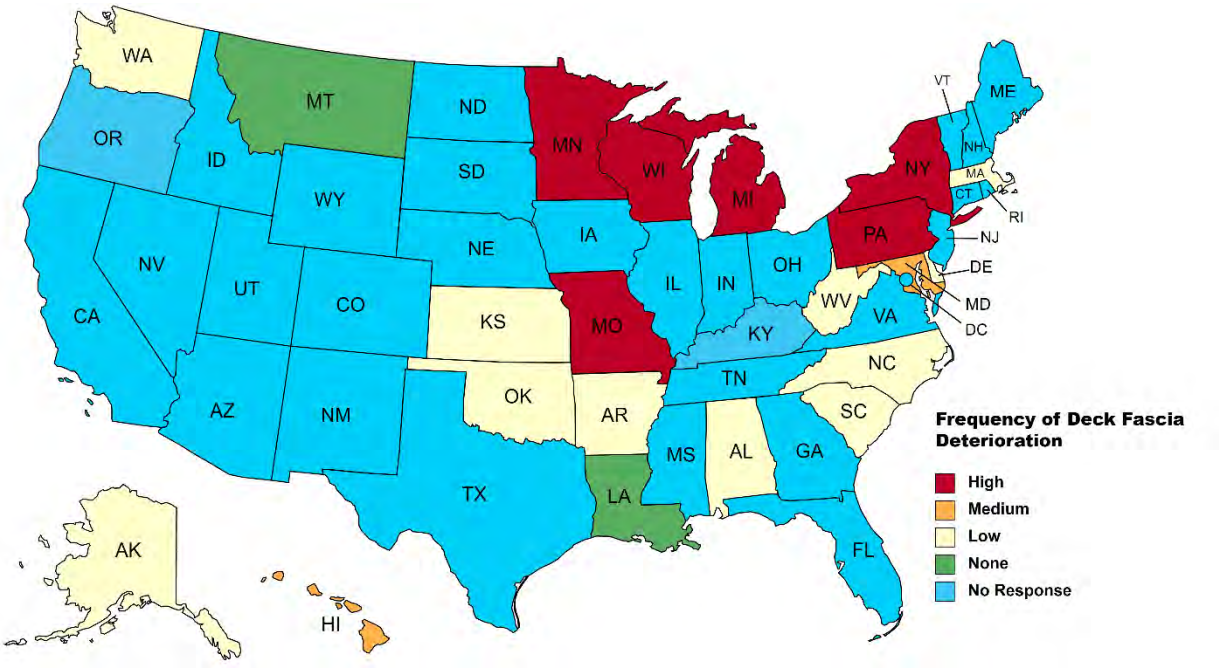

Fig. 2.2 Frequency of deck fascia deterioration in each state based on survey results

As previously noted, the current MDOT maintenance strategy for bridges that exhibit deck fascia deterioration is to avoid patching deteriorated regions, since overhead patches can later spall off, posing the same safety risk as the original fascia failure. Rather, delaminated concrete is removed to minimize the potential of falling debris. However, this practice leaves the fascia reinforcement exposed, resulting in corrosion and further degradation. Over time, repeatedly

scaling of these areas to remove poorly adhered concrete can cause the barrier to become undermined. In addition, one current challenge in Michigan, is that the silane treatment that is applied to the barrier for protection against weathering, is not applied to the deck facia since this region is painted for aesthetic purposes. The paint prevents proper adhesion between the silane treatment and the concrete substrate. The order of application can be reversed thus providing some enhanced initial durability to the deck fascia. However, since the silane treatment needs to be reapplied periodically, the initial level of protection may not be maintained in the long term. Alternative options include removing the paint prior to the application of the silane treatment and reapplying it, or using colored options for the silane treatment that provide protection while maintaining the aesthetics of the bridge. The special provision for silane treatment for bridge concrete prevents its application on traffic surfaces. The treatment includes the application of spray-applied penetrating silane, including the preparation and cleaning of the concrete. Suggested locations include: barriers, deck fascias, piers, abutments, retaining walls, beams, etc. Although deck fascias are a suggested location, for the application of silane, it appears that this region is typically not specified for reasons mentioned above. The painting of the deck fascia appears to be a practice common in other states as well, with some states indicating that the aesthetic coating used has some silane properties and provides some protection against chloride permeability.

Chapter 3: Bridges with Deteriorated Deck Fascias

Chapter 3: Bridges with Deteriorated Deck Fascias

3.1 Identify Bridges with Deteriorated Deck Fascias

A total of 40 bridges that feature deteriorated deck fascias were identified. The location of these bridges is shown in Fig. 3.1 and their characteristics are summarized in Table 3.1. The first set of 20 bridges were identified by MDOT and the second set was identified by the research team. The bridges included in the first set feature geographic locations that are spread out in the lower peninsula. The 20 bridges identified by the research team are located in the Detroit Metropolitan area. Figures illustrating the deteriorated deck fascias in the selected bridges are provided in Appendix D.

The characteristics of the identified bridges were obtained from the MiBridge database. The degree of deterioration was determined by the research team on a scale of 0-10 with 0 representing no deterioration and 10 representing severe deterioration. This determination was based on photographic evidence. This rating was used to conduct certain observations and establish correlations between deck fascia deterioration and various parameters.

For each bridge shown in Table 3.1, the original construction year is shown followed by the year when some type of intervention was reported, such as barrier or deck repair or replacement. The year of the intervention is provided in parentheses. For some of the bridges shown in Table 3.1 (such as Struct. ID 21) two numbers are shown for the deck overhang thickness, t_d. In these cases, the original deck overhang had a certain thickness (represented by the first number), and when the deck was repaired or replaced it featured another thickness (second number). A similar approach was used to characterize all other properties in the original and repaired or replaced structure. In some cases, the thickness of the deck overhang was specified to be greater than a certain number (i.e. the exact thickness was not specified). When certain information was not available in the documents provided in the MiBridge database this was indicated with “NA” (not available).

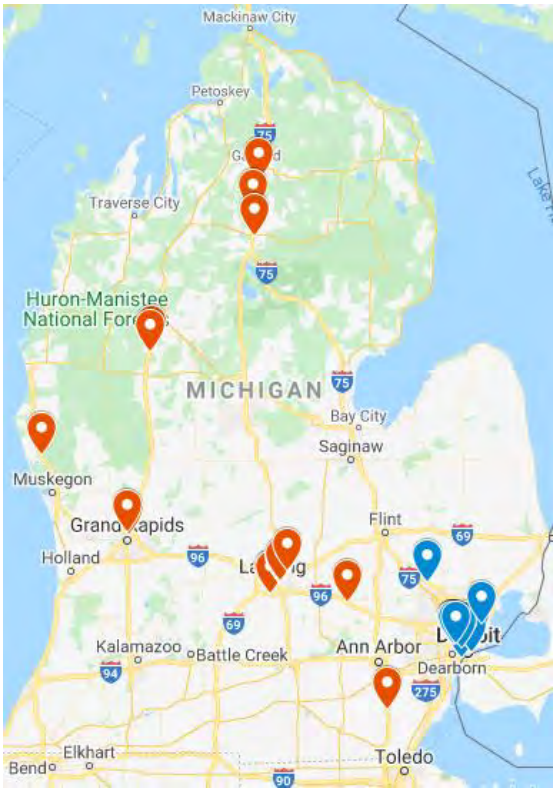

Map Link

Fig. 3.1 Map of bridges with deteriorated deck fascias identified by MDOT (red icons) and research team (blue icons)

Table 3.1 Database for deteriorated bridges

Struct. (ID) No.	Location	Cons. Year/ Mod.	Beams	No. of spans	Deg. of det. (out of 10)	Superel. (%)	Drain. dir.	t_d (in.)	Reinf.		Conc. strength, f'_c (ksi)		Barrier type	Fig. No. (App. D.)
									Deck	Barrier	Deck	Barrier		
Bridges Identified by MDOT														
(1) 3802	I-96 EB over M-99	1962 (1981)	S-PH	4	10	NA	NA	10.0	UC	EC (in Type 3)	3	3	Parap. rail. with thrieb. Type 3 (mod.) (1981)	D.1
(2) 3761	I-496 WB Ramp over CSX Railroad	1963	S	4	9.5	NA	NA	NA	UC	UC	3	3	Parap. rail. with thrieb.	D.2
(3) 2033	I-75 NB over Lake State Railroad	1961 (1991)	S	3	9	1.5	TW	11.1	EC	EC	3	3	Parap. rail. with thrieb. Type 4 (1991)	D.3
(4) 7607	US-31 SB US-31 Business Route	1965	S	4	8.5	NA	NA	NA	UC	UC	3	3	Parap. rail. with thrieb.	D.4
(5) 3851	M-43 WB (Grand River) over US-127	1970	S-PH	2	8.5	NA	NA	NA	UC	UC	3	3	Parap. rail. with thrieb.	D.5
(6) 1850	Webster Rd. over I-69	1985	S-B	2	8	1.5	TW	12.9	EC	EC	4	4	Type 4	D.6
(7) 2047	County Rd 612 over I-75 SB	1961 (1979)	S	3	7.5	NA	TW	9.8	UC	UC	3	3	Parap. rail. with thrieb. Type 3 (mod.) (1979)	D.7
(8) 3852	US-127 NB over Kalamazoo St.	1970	S-PH	3	7.5	NA	TW	10.0	UC	UC	3	3	Parap. rail. with thrieb.	D.8
(9) 3758	I-496 WB over CSX Railroad & Trowbridge Ramp	1963 (2000)	S	3	7	NA	NA	NA	UC	UC	3	3	Parap. rail. with thrieb./Type 4 (2000)	D.9
(10) 8546	Luther Rd over US-131	1985	S-PH	3	7	1.5	TW	12.4	EC	EC	4	4	Type 4	D.10
(11) 5779	M-59 / I-96 BL over I-96	1962 (1976)	S	4	6.5	NA	TW	12.3	UC	UC	3	3	Parap. rail. with thrieb. Type 1 (mod.) (1976)	D.11
(12) 7083	Milwaukee Rd over US-23	1961 (1976)	S	4	6	NA	NA	10.0	UC	EC	3	3	Parap. rail. with thrieb./ Type 3 (mod.) (1976)	D.12
(13) 3757	I-496 EB over CSX Railroad & Trowbridge Ramp	1963	S	4	6	NA	NA	NA	UC	UC	NA	NA	Parap. rail.with thrieb./Type 4	D.13
(14) 4761	I-296 WB connector over I-96 EB	1962 (1976) (1988)	S-PH	3	6	NA	NA	NA	UC-EC	UC-EC	NA	NA	Parap. rail. with thrieb./Type 1 (1976)/ Type 4 (mod.) (1988)	D.14

Struct. (ID) No.	Location	Cons. Year/ Mod.	Beams	No. of spans	Deg. of det. (out of 10)	Superel. (%)	Drain. dir.	t_d (in.)	Reinf.		Conc. strength, f'_c (ksi)		Barrier type	Fig. No. (App. D.)
									Deck	Barrier	Deck	Barrier		
(15) 3803	I-96 WB over M-99	1962	S-PH	3	5	Varies	OW	11.5	UC-EC	EC	NA	NA	Parap. rail. with thrieb./ Type 3 (mod.)	D.15
(16) 8675	I-75 NB over Charles Brink	1961 (1979)	PC	3	4	Varies	OW	9.5	UC-EC	EC	3 - 4	3 - 4	Parap. rail. with thrieb./ Type 4 (mod.) (1979)	D.16
(17) 3786	I-496 WB over US-127 SB Ramp	1970	S-PH	3	3	Varies	TW	10.3	UC	UC	3	3	Parap. rail. with thrieb.	D.17
(18) 3846	US-127 SB over Kalamazoo St.	1970 (1998)	S-PH	3	2	2	TW	11.8	EC	EC	3 - 4.5	3 - 4.5	Parap. rail. with thrieb./ Type 4 (1998)	D.18
(19) 4980	I-296WB/US-131 over Ann St.	1962	S	3	1	Varies	M	NA	UC	UC	3	3	Parap. rail. with thrieb.	D.19
(20) 8547	Leroy Rd over US-131	1985	S-B	3	0	1.5	TW	12.4	EC	EC	4	4	Type 4	D.20
Bridges Identified by WSU														
(21) 11586	McGraw Ave. over I-96 in Detroit	1971	S-PH	4	10	NA	TW	10-12	UC-EC	UC-EC	3 - 4	3 - 4	Open parapet w/ fence	D.21
(22) 11782	Brush St. over I-75	1970	S-PH	3	10	NA	TW	7	UC	UC	3	3	Open parapet w/ fence	D.22
(23) 11392	Larned St. over I-375	1960	S	4	10	NA	TW	7	UC	EC	3	3	Solid parapet w/ fence	D.23
(24) 11739	Junction Ave. over I-75	1968 (2017)	S-B	2	9	NA	TW	10.3	UC	UC	3	3	Temp. conc. bar. (2017) - open parapet w/fence	D.24
(25) 11750	Dragoon St. over I-75	1967	S-PH&B	4	9	NA	TW	10	UC	UC	3	3	Open parapet w/ fence	D.25
(26) 11222	McClellan Ave. over I-94	1957	S-PH	4	8.5	NA	TW	9	UC	UC	3	3	Solid parapet w/ fence	D.26
(27) 11845	Holbrook Ave. over I-75	1969	S-B	2	7.5	NA	TW	11.6	UC	UC	3	3	Open parapet w/ fence	D.27
(28) 11761	Rosa Parks Blvd. over I-75	1970 (1998)	S-PH&B	6	7	Varies	M	NA	UC-EC	UC-EC	3-NA	3-NA	Open parapet w/ fence – Type 5 (mod.) (1998)	D.28
(29) 11561	Fullerton Ave over I -96	1970	S-PH	4	7	NA	TW	11.5	UC	UC	3	3	Solid parapet w/ fence	D.29
(30) 11562	Schaefer Rd. over I-96	1971	S-PH	4	7	NA	TW	11	UC	UC	3	3	Solid parapet w/ fence	D.30

Struct. (ID) No.	Location	Cons. Year/ Mod.	Beams	No. of spans	Deg. of det. (out of 10)	Superel. (%)	Drain. dir.	t_d (in.)	Reinf.		Conc. strength, f'_c (ksi)		Barrier type	Fig. No. (App. D.)
									Deck	Barrier	Deck	Barrier		
(31) 11736	Green Ave. over I-75	1967	S-PH&B	4	7	NA	TW	NA	UC	UC	3	3	Open parapet w/ fence	D.31
(32) 11393	E Jefferson Ave. over I-375	1962	S	2	7	NA	TW	>8.5	UC	UC	3	3	Open parapet w/ fence	D.32
(33) 11565	Meyers Rd. over I-96	1971	S-PH	4	6.5	1.5	TW	10.5	UC	UC	3	3	Solid parapet w/ fence	D.33
(34) 11394	Chrysler Dr. over I-375	1962	S	2	6	NA	NA	NA	UC	UC	3	3	Open parapet w/ fence	D.34
(35) 11560	Hubbell Ave. over I-96	1970	S-PH	4	6	NA	TW	11	UC	UC	3	3	Solid parapet w/ fence	D.35
(36) 8018	Waldon Rd. over I-75	1962 (1983)	S-PH&B	4	5	2	TW	9	UC-EC	EC	3-4	3-4	Type 4 (mod.) (1983)	D.36
(37) 11598	Scotten Ave. over I-96	1972	S	2	4	NA	TW	11	UC	UC	3	3	Solid Parapet w/ fence	D.37
(38) 6124	Belanger Ave. over I-696	1972	S-B	2	3.5	NA	TW	10.3	UC	UC	3	3	Solid Parapet w/ fence	D.38
(39) 11564	M-5 Grand River Ave, over I-96	1971 (2005)	S-PH	4	3	2	TW	12.3	EC	EC	NA	NA	Curb with alum. Railing/ Aesthetic parapet tube (mod.) Type A (2005)	D.39
(40) 11566	Wyoming Ave. over I-96	1971 (2005)	S-PH&B	4	2.5	NA	TW	>10.3	UC	UC	3	3	Solid parapet w/ fence & thrieb. retrofit (2005)	D.40

S: Steel; S-PH: Steel – Pin-hanger connection; S-B: Steel – Bolted connection; PC: Prestressed concrete; TW: Two-way; OW: One-way; M:Multiple; UC: Uncoated; EC: Epoxy coated; t_d: deck thickness near deck fascia; NA: Not available

3.2 Evaluate Extent of Deterioration and Identify Trends and Correlations

The characterization of the bridge database is illustrated in Fig. 3.2 in terms of the number of bridges with a particular characteristic. The compressive strength of the barrier could not be determined from the information provided in the MiBridge database. Based on conversations with the MDOT project manager, it was assumed that the barrier and deck concrete have the same specified compressive strength. Figures illustrating the deteriorated deck fascias for all 40 bridges are provided in Appendix D. While the selected set of 40 bridges with deteriorated deck fascias is not an exhaustive list, the following observations were made.

Out of the 40 bridges, 30 were constructed before 1971, 7 were constructed between 1971 and 1975, and 3 were constructed in 1985 (Fig. 3.2a). The construction year is an important parameter in terms of identifying the type of reinforcement used in the deck. Fig. 3.2e shows that 27 out of 40 bridges featured uncoated reinforcement in the bridge deck, 6 featured epoxy coated reinforcement, 6 featured a combination of uncoated and coated reinforcement (i.e. a portion of the deck was replaced with epoxy coated reinforcement), and in 1 bridge the type of reinforcement used in the deck could not be determined based on the information provided in the MiBridge database. For bridges constructed prior to the 1980 mandate for epoxy coated reinforcement, where the type of reinforcement used could not be identified based on the information that was available in the MiBridge database, it was assumed that the reinforcement was uncoated. The presence of deck fascia deterioration in bridges with epoxy coated reinforcement in the deck suggests that reinforcement corrosion may not be the only deterioration mechanism. For example, an examination of Fig. D.6, Fig. D.10, and Fig. D.20, all of which illustrate deck fascia deterioration in bridges constructed in 1985, suggests that corrosion of reinforcement is not apparent despite the fact that the reinforcement is exposed. It is possible that the concrete spalled as a result of freeze-thaw cycles and the falling of the concrete removed the epoxy coating and left the reinforcement exposed and vulnerable to subsequent corrosion.

In terms of the number of spans, 1 out of 40 bridges featured 6 spans, 18 featured 4 spans, 13 featured 3 spans, and 8 featured 2 spans. (Fig. 3.2b). Only one bridge was a prestressed concrete girder bridge, while the rest were steel bridges, (Fig. 3.2c). Out of the 39 steel bridges, only 5 featured a bolted connection between the steel girders; 16 featured a pin-hanger connection, 13 were simply supported, and 5 featured both pin-hanger and bolted connections (Fig. 3.2d). Fig.

3.2f suggests that 24 out of 40 bridges featured barriers with uncoated reinforcement, 12 with epoxy coated reinforcement, and 3 with an unspecified type of reinforcement.

The type of barriers used in the 40 bridges is as shown in Fig. 3.2g. Most of the bridges featured in the database were constructed prior to 1980s (mostly in the 1960s) as shown in Fig. 3.2a. In these bridges, the original barrier types were generally curbs with aluminum railings. Most of these barriers were replaced with Type I, Type III and Type IV barriers. For the bridges with replaced barriers, both types of barriers are indicated in Table 3.1 under the column labeled "barrier type". The year when the barrier was replaced is also indicated. In some cases, the abbreviation "mod." is used to indicate that the exiting barrier was modified. In these cases, only a portion of the existing curb or barrier was removed, and the new barrier was attached to the remaining curb or barrier. If the entire barrier was replaced, then the abbreviation "mod." is not used. Generally, bridges that featured an open type of barrier either had their barriers replaced at some point, or currently feature deterioration in the deck. Therefore, the open type barrier appears to be contributing to the deterioration of the deck fascia. However, the deterioration is not only limited to open type barriers, as some bridges with solid barriers also featured deterioration (Fig. D.6)

The compressive strength of deck varied from 3-4.5 ksi with 33 out of 40 bridges featuring a design compressive strength of 3 ksi. This suggests that low grade concrete in combination with an aggressive environment such as that present in Michigan, may have led to the deterioration of the deck fascias. There was only 1 bridge, which featured a deck compressive strength of 4.5 ksi, which did not exhibit any concrete spalling in the deck fascia, but only cracking (map cracking) and signs of saturated concrete.

The super elevation varied as shown in Fig. 3.2i. One strong correlation that was observed in the photographs for the 20 bridges was the direction of drainage. For example, in bridges in which the drainage system was such that one side of the deck was elevated with respect to the other side, almost always, the lower side of the deck featured a much more deteriorated deck fascia compared to the higher side. In some cases, the higher side of the deck featured almost no deterioration. This suggests that the relatively higher supply of moisture laden with deicing and anti-icing chemicals, combined with an ineffective water stop are some of the reasons for the deterioration of deck fascias. A clear illustration of the higher moisture present near the barrier and deck fascia is shown in Fig. 3.3 for the bridge located on I-96 WB over M-99.

One bridge (Fig. D.9) featured two different barrier types; a solid barrier on the lower side, and an open barrier on the higher side. In this bridge the deterioration appears to be more severe on the higher side. However, this may be due to the fact that the open type barrier on the lower side was replaced with a solid side barrier.

In terms of traffic volume, many of the bridges were either located on or over interstate highways or state routes. None of the bridges were located on secondary routes suggesting a correlation between traffic volume and deck fascia deterioration. The higher amount of deicing and anti-icing chemicals used in roads with high traffic volume may have exacerbated the deterioration of deck fascias in identified bridges.

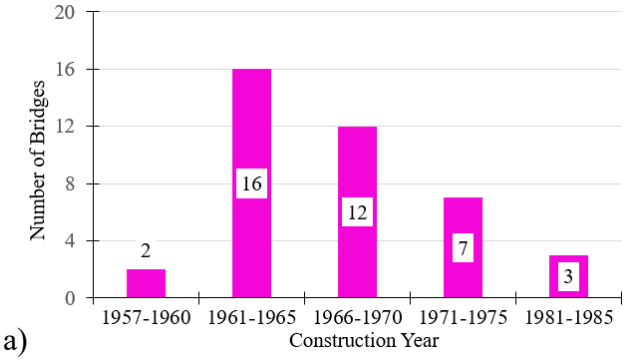

a)

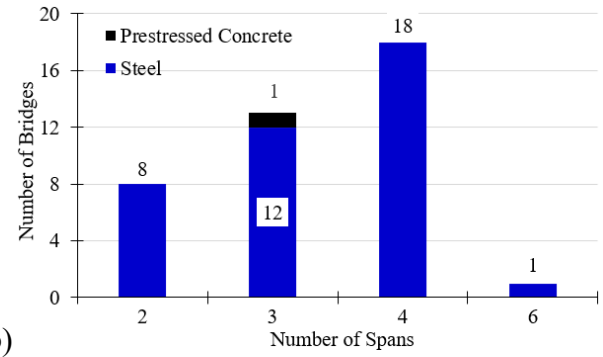

b)

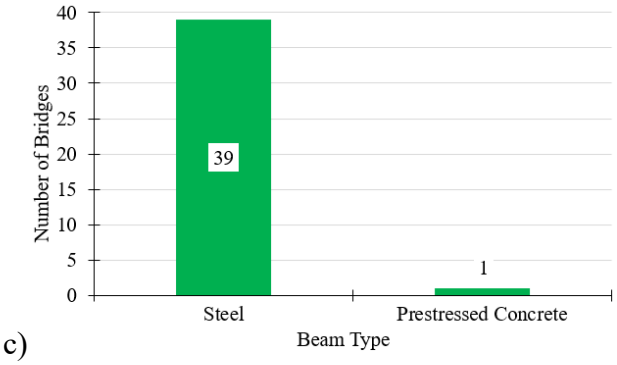

c)

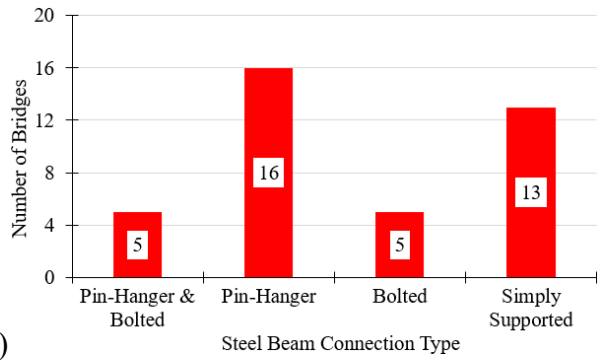

d)

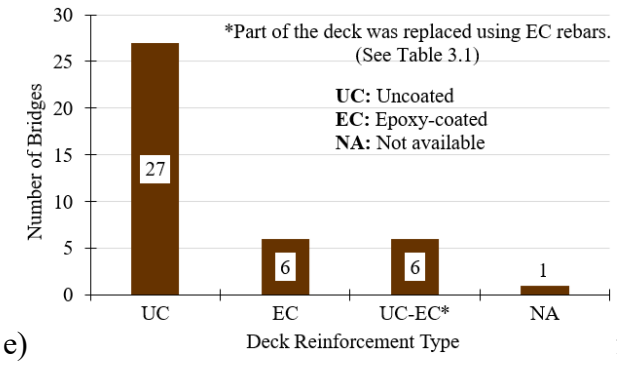

e)

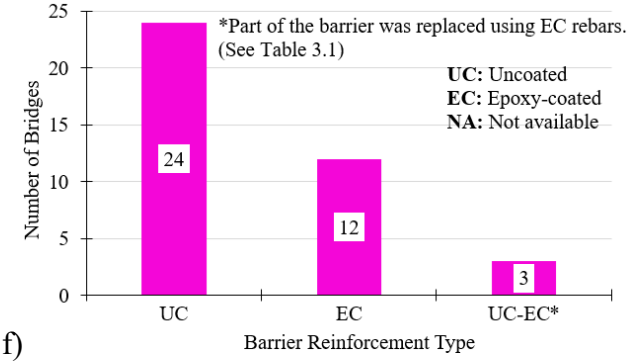

f)

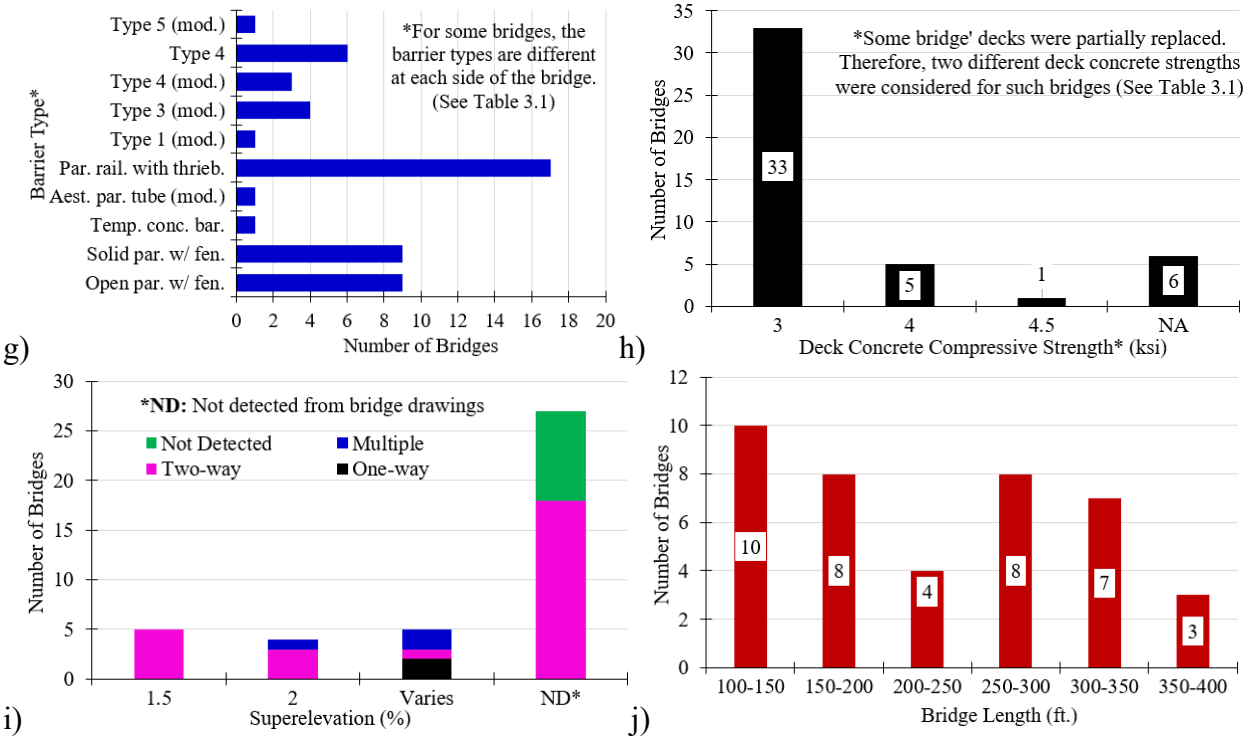

Fig. 3.2 Database characterization in terms of: a) Constuction year; b) Total number of spans; c) Beam type; d) Connection type in steel bridges; e) Type of reinforcements used in bridge decks; f) Type of reinforcements used in bridge barriers; g) Type of barriers used in bridges; h) Deck concrete compressive strength; i) Superelevation and drainage directions; and j) Bridge length

Fig. 3.3 Illustration of the higher moisture near the barrier and deck fascia (image obtained from Google Maps)

Summary of Observations:

1. The slope of the deck is a contributing factor to the deterioration of deck fascias. The lower side of the deck features typically higher deterioration.
2. Reinforcement corrosion is a contributing cause especially for those bridges which were built prior to the 1980 mandate to use epoxy coated reinforcement.

3. The type of barrier is a contributing factor. Open railings appear to promote deck fascia deterioration.
4. The grade of concrete also is a contributing factor. Most bridges in the database featured decks with compressive strengths of 3 ksi.
5. Traffic volume on or below the bridge appears to be related to deck fascia deterioration (i.e. the higher the traffic the higher the deterioration).

3.3 Collect Field Data to Further Characterize the Deterioration

Multiple nondestructive tests were conducted in the field to further characterize the deterioration in the deck fascia in bridges located in different regions in the lower peninsula. The purpose of these tests was to:

1) Validate the observations and conclusions drawn from the evaluation of 40 bridges with deteriorated deck fascias;
2) Establish benchmark values for when to stop accelerated weathering tests in the laboratory;
3) Identify additional causes of deck fascia deterioration.

There are a total of six regions in the lower peninsula: 1) Metro Region, 2) Bay Region, 3) University Region, 4) Grand Region, 5) Southwest Region, and 6) North Region. One bridge was identified for investigation in each region. In each bridge the following types of nondestructive evaluation and testing was conducted. The goal of each test and investigation is briefly described in parentheses:

1) Visual Inspection (Goal: Characterize overall deck fascia condition)
2) Core Obtention (Bay Region Only) (Goal: 1) Establish benchmark compressive strength values, and relative dynamic modulus, for when to terminate accelerated freeze-thaw testing, and 2) conduct ASR testing)
3) Clear Cover Determination (Goal: Identify inconsistencies in clear cover)
4) Relative Stiffness Determination Using Rebound Hammer (Goal: 1) Identify potential trends in relative surface hardness, 2) Establish benchmark values for when to terminate accelerated freeze-thaw testing)
5) Moisture Content Determination: (Goal: Identify relative moisture content in the vicinity of deck fascia)

6) Half-Cell Potential Measurements: (Goal: Identify areas of active corrosion)
7) Reinforcement Section Loss (where possible) (Goal: Establish benchmark values for when to terminate accelerated corrosion testing)
8) ASR Detection (where possible) (Goal: Determine whether ASR is a potential deterioration mechanism)

The selected bridges are further described below:

1) Bay Region: I-69 over Fenton Road. The bridge features steel girders with pin-hanger connections and has 6 spans. In addition, the bridge consists of open parapet barriers with aluminum railings and features a thriebeam retrofit. The EB and WB of the bridge are separated using median barriers (i.e. there is no gap between the EB and WB bridges). According to MDOT inspection reports, the expansion joints and the barrier and deck overhang for WB were replaced in 2021. Since the barrier, deck overhang, and expansion joints were in the process of being demolished, the bridge was closed to traffic, therefore, no traffic control was necessary. The measurements were taken at a location identified as control in Fig. 3.4a. This location was chosen such that the measurements could be taken without interfering with deck fascia demolition preparation activities. The measurements were taken on the top of the deck using the grid shown in Fig. 3.4b.

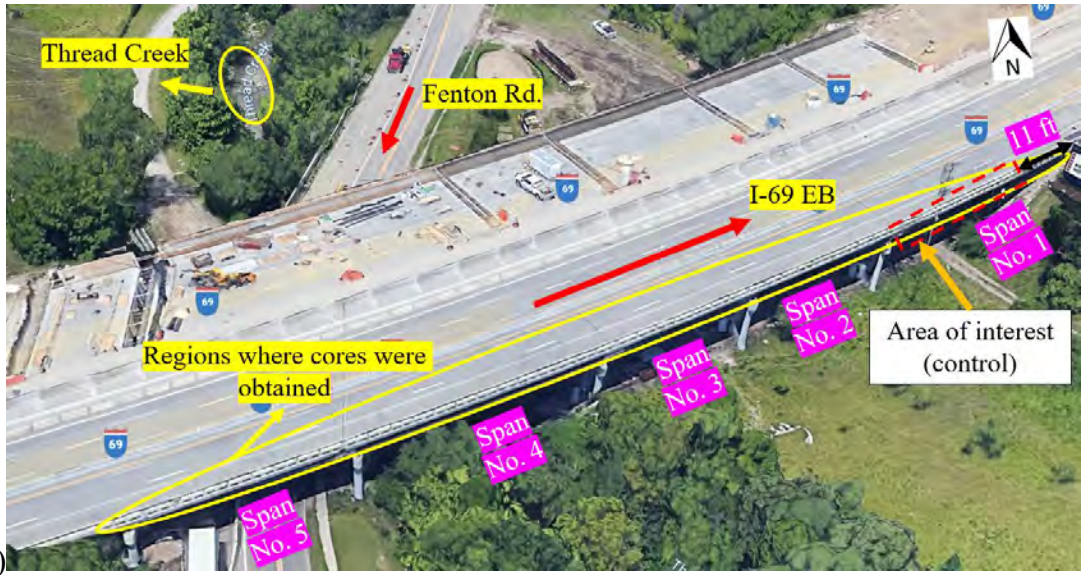

a)

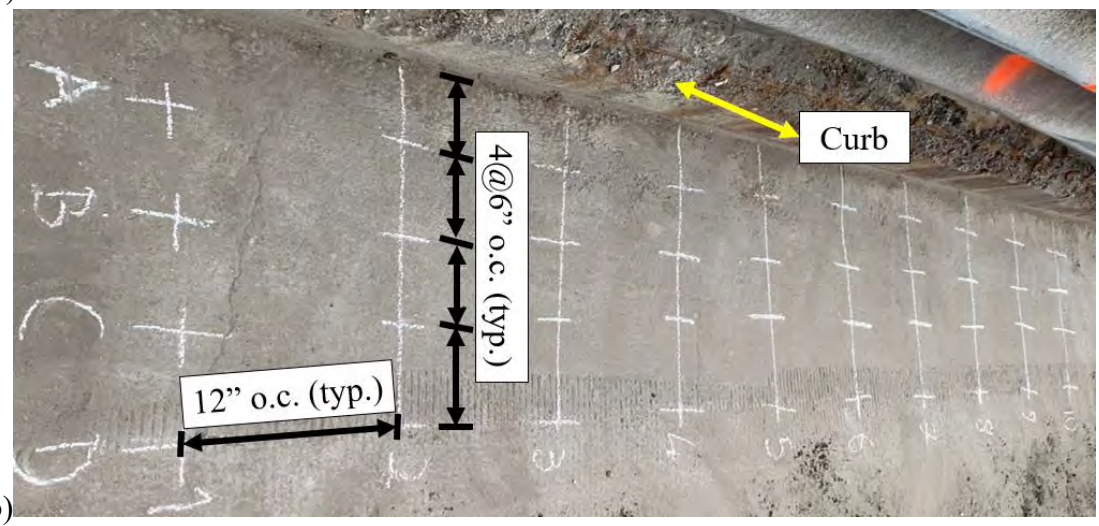

b)

Fig. 3.4 a) Region where cores were obtained, and location of the measurements; and b) the grid prepared for obtaining the measurements

2) University Region: I-69 over M-99. MDOT assisted with traffic control and lane closures on I-96 WB and M-99. The closed lanes are illustrated in Fig. 3.5a. The measurements were taken in the second span from the west in the region illustrated in Figs. 3.5b-c. A bucket truck provided by MDOT was used to access the deck fascia and conduct the nondestructive testing. The measurements taken on the deck fascia are presented by gridline F whereas those taken on the deck surface are represented by gridlines A-E with A being the closest gridline to the barrier. Heavy deterioration as well as map cracking was observed on the barrier (Fig. 3.5d). The deck fascia on I-96 EB on the right side of the bridge exhibited heavy deterioration as illustrated in Fig. 3.5e. However, the presence of a steel barrier adjacent to the concrete barrier on the top of the deck at

this location did not allow the research team to take measurements in the vicinity of the barrier on the top of the deck surface. As a result, measurements were taken on I-96 WB on the right shoulder. The condition of the barrier at this location is shown in Fig. 3.13f and is much better than that on I-96 EB but still shows some signs of deterioration in the form of map cracking and efflorescence. Broken concrete fragments from the barrier were obtained to conduct laboratory testing with the purpose of determining the likelihood of alkali aggregate reaction since map cracking was observed. To be able to conduct the half-cell potential testing, an electrical connection between the electrode and the existing reinforcing steel is required. The research team identified an exposed steel bar in the barrier and connected one of the electrodes to this bar as shown in Fig. 3.13g.

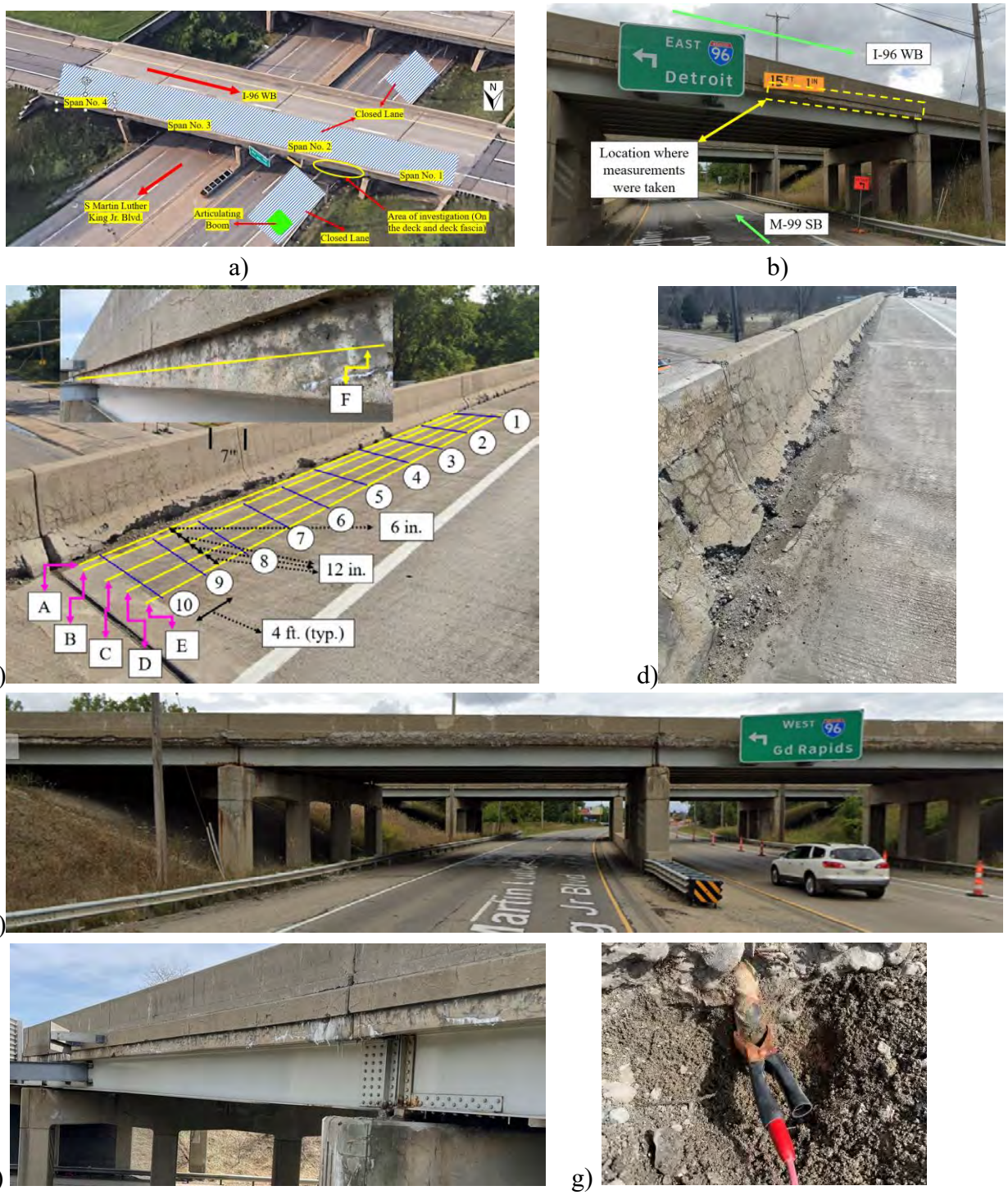

Fig. 3.5 a) Closed lanes on I-96 WB and M-99 to facilitate nondestructive testing on the deck surface and deck fascia, b-c) region where measurements were taken on the deck fascia and deck surface, respectively, d) severe barrier deterioration, e) deck fascia deterioration on I-96 EB, f) deck fascia deterioration on I-96 WB, g) connection of electrode to exposed steel in the barrier

3) North Region: County Road over I-75. Fig. 3.6a shows the closed lanes and the location of the bucket truck. Fig. 3.6b shows the higher moisture content near the deck fascia after a precipitation event the previous day. Fig. 3.6c-g illustrate the deteriorated condition of the deck fascia. Tests were conducted on the deck surface. Due to roughness of the deteriorated fascia region, rebound hammer tests, and moisture content tests were not conducted along the deck fascia. Similarly, due to exposed rebars along the deck fascia, clear cover determination tests and half-cell potential tests were not conducted. The exposed rebars on the deck fascia were used to connect the electrode to conduct half-cell potential testing. Broken concrete fragments from the deck fascia were obtained to conduct ASR detection testing.

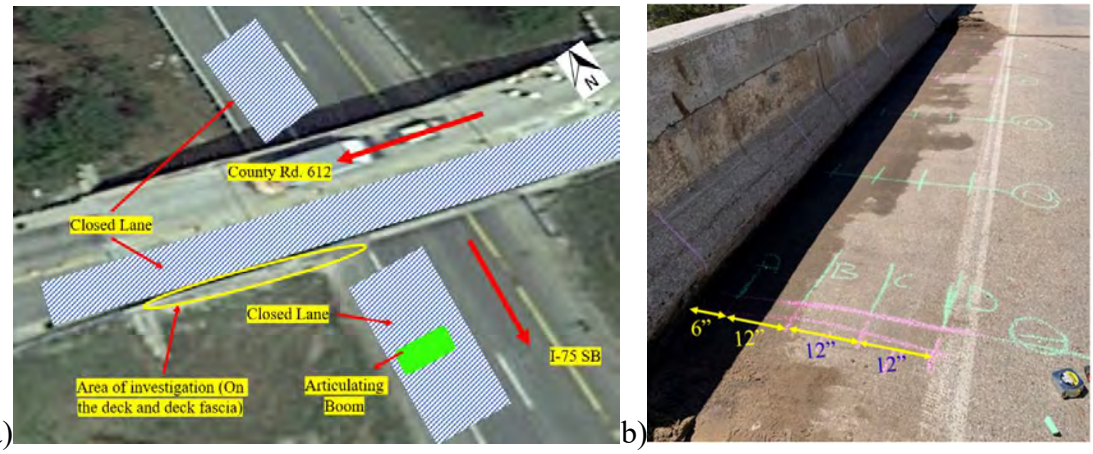

Fig. 3.6 a) Closed lanes and location of bucket truck, b) higher moisture content for the deck, c-g) deteriorated fascia

4) Metro Region: Waldon Road over I-75. Fig. 3.7 shows the location of the bridge, area of investigation and other relevant figures. The bridge is a skewed bridge with deteriorated fascia, corroded bars, and exacerbated conditions near the expansion joint and the abutment. Fig. 3.7a shows the closed lanes and location of bucket truck. Fig. 3.7b-c show the location where measurements were taken and illustration of deteriorated deck fascia near the expansion joint. Tests were conducted on the deck surface. Due to roughness of the deteriorated fascia region, rebound hammer tests, and moisture content tests were not conducted along the deck fascia. Similarly, due to exposed rebars along the deck fascia, clear cover determination tests and half-cell potential tests were not conducted. Fig. 3.7d-e illustrate the deteriorated deck fascia near the abutment. Broken concrete fragments from the deck fascia were obtained to conduct ASR detection testing. Fig. 3.7f shows the location where the electrode was connected to existing bars to close the electrical circuit for half-cell potential measurements. Fig. 3.7g further illustrates deck fascia deterioration near the expansion joint and abutment. The top two photographs in Fig. 3.7g illustrate the condition at the 2nd span near the expansion joint, and the bottom two figures represent the condition at 1st span near the abutment.

Fig. 3.7 Bridge on Waldon Road over I-75: a) closed lanes and location of bucket truck, b-c) location where measurements were taken and illustration of deteriorated deck fascia near the expansion joint, d-e) illustration of deteriorated deck fascia near the abutment, f) location where electrode was connected to existing bars for half-cell potential measurements, g) further illustration of deck fascia deterioration near the expansion joint and abutment

5) Grand Region: US 131 Ramp over W River Dr. NW. The bridge features a deteriorated deck fascia and corroded bars along the deck fascia. Fig. 3.8a shows the general location of the bridge. Fig. 3.8b shows the closed ramp and lanes and position of bucket truck. Fig. 3.8c-d show the locations where measurements were taken on deck and fascia. Fig. 3.8e-f show the deteriorated fascia. Signs of efflorescence were observed, which is typically an indication of moisture presence in the deck fascia. Map cracking was also observed, which is typically an indication of an expansive deterioration mechanism (such as ASR, freeze-thaw, etc.). Deteriorated fascia concrete was ready to fall off. Concrete fragments from the fascia were easily obtained with one steel hammer hit. Such sudden falls of deteriorated concrete may be prevented by using fiber reinforced concrete as the repair cementitious material.

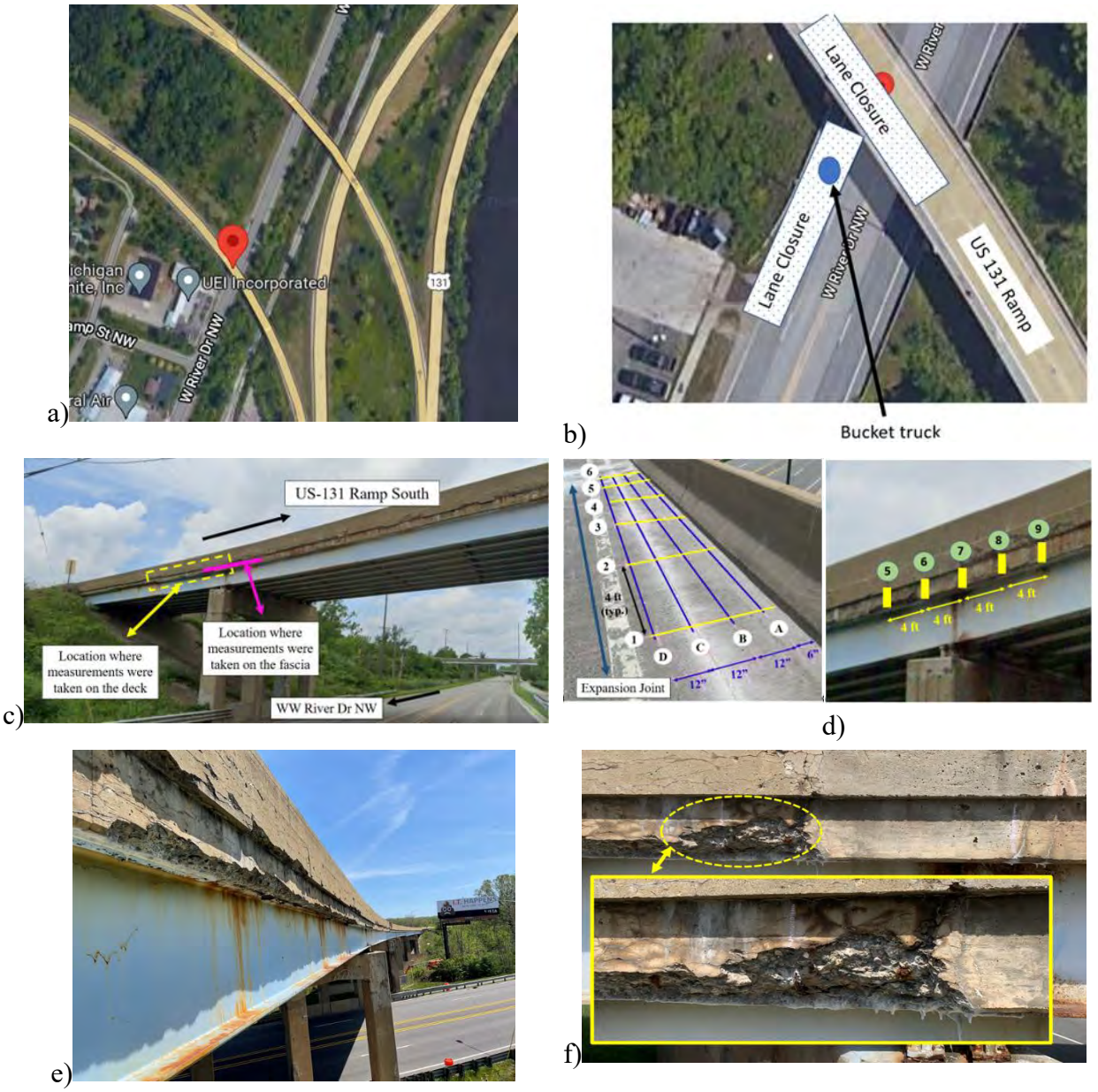

Fig. 3.8 Bridge on US 131 Ramp South over W River Drive NW: a) general location of the bridge, b) closed ramp and lanes and position of bucket truck, c-d) locations where measurements were taken on deck and fascia, e-f) deteriorated fascia

6) Southwest Region: I-94 EB over Red Arrow Highway North. The bridge featured a deteriorated deck fascia. Fig. 3.9a shows the location of the bridge, the area where the investigation was conducted, the location of the bucket truck, which was used to take measurements along the deck fascia, and the lanes that were closed to conduct the investigation. Fig. 3.9b shows the deteriorated deck fascia. Fig. 3.9c shows the location where the measurements were taken along the deck fascia, as well as two close-up photographs illustrating deterioration and corrosion of reinforcement. Fig. 3.9d shows additional close-up photographs illustrating deterioration, the presence of efflorescence, and reinforcement corrosion. Fig. 3.9e shows the location where the electrode was connected to the reinforcement to conduct half-cell potential measurements. Finally, Fig. 3.9f shows the location of the grid that was used to take measurements on the deck surface.

a)

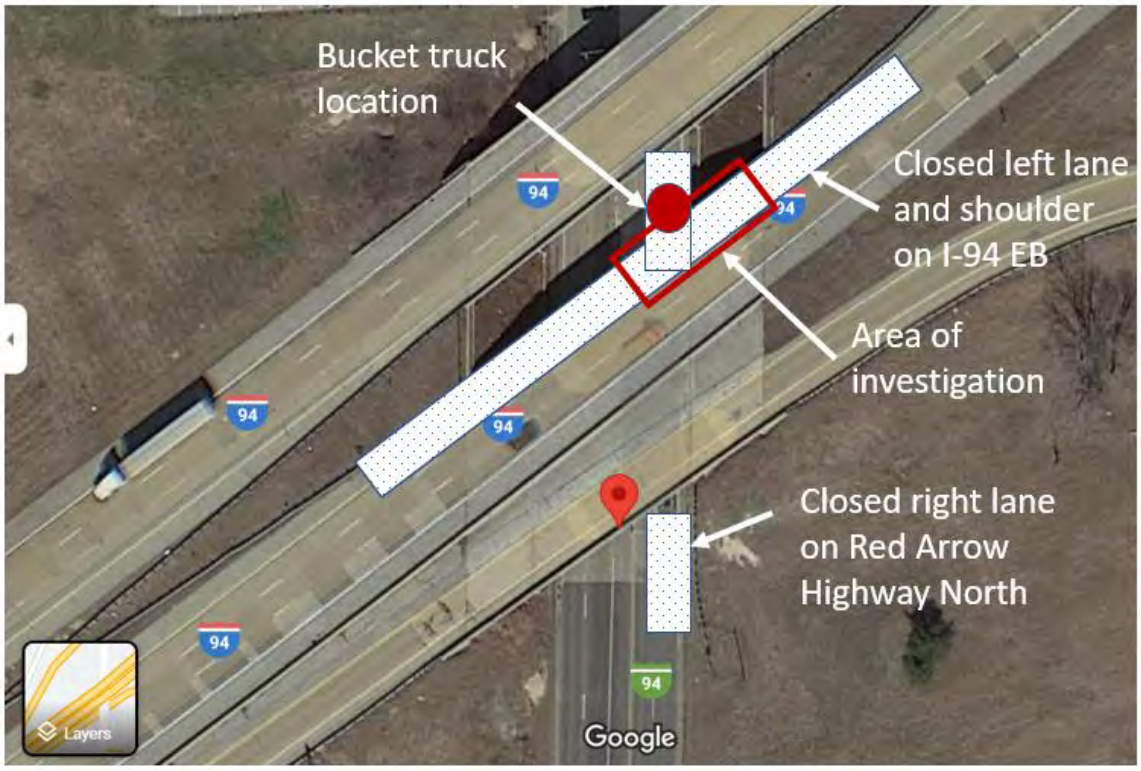
Bucket truck location
Closed left lane and shoulder on I-94 EB
Area of investigation
Closed right lane on Red Arrow Highway North
94
Layers
Google

b)

c)

d)

e)

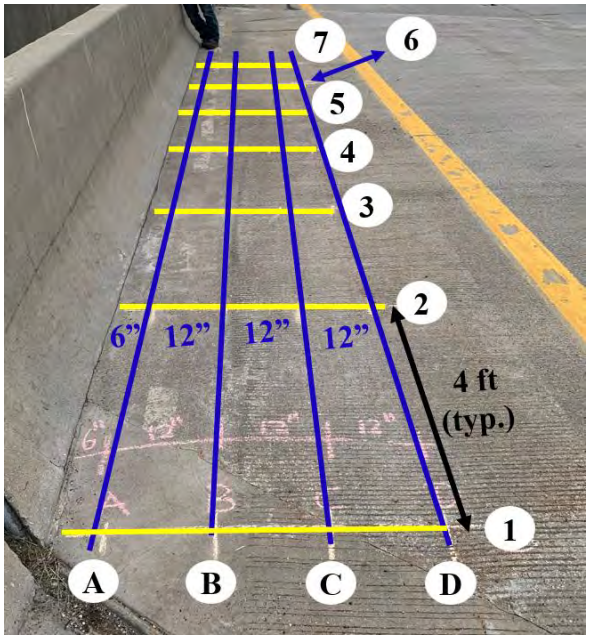

f)

Fig. 3.9 Bridge on I-94 EB over Red Arrow Highway North: a) location of bridge, b) view of deck fascia, c) location where measurements were taken along the fascia, d) photographs of various deck fascia regions, e) connection of electrode to exposed reinforcement at the bottom of deck fascia, f) grid where measurements were taken on the deck surface

Visual Inspection Notes

The following notes were made for each bridge after the visual inspection was completed.

Bridge on I-69 over Fenton Road in Bay Region: The following was noted:

1) Corrosion of reinforcement was observed (see this slide and next slide).
2) Signs of efflorescence were observed, which indicates presence of moisture in the deck fascia.
3) Map cracking was observed – Potential sign of an expansive deterioration mechanism (ASR, freeze-thaw, etc.)

Bridge on I-96 over M-99 in University Region: The following was noted:

1) Deck fascia severely deteriorated on I-96 EB
2) Corrosion of bars noted in the deck fascia
3) Presence of efflorescence noted
4) Map cracking observed
5) Deteriorated barrier and fascia, good examples of what happens to low grade concrete

Bridge on County Road over I-75: The following was noted:

1) Deteriorated deck fascia
2) Clear evidence of higher moisture content along the deck fascia
3) Highly corroded bars.
4) Signs of efflorescence observed
5) Map cracking

Bridge on Waldon Road over I-75: The following was noted:

1) Skewed bridge
2) Deteriorated deck fascia
3) Corroded bars
4) Exacerbated conditions near the expansion joint

Bridge on US 131 Ramp over W River Dr. NW: The following was noted:

1) Deteriorated deck fascia
2) Rebar corrosion along the deck fascia
3) Signs of efflorescence observed
4) Map cracking

5) Deteriorated fascia concrete ready to fall off. Concrete fragments from the fascia were easily obtained with one steel hammer hit.

Bridge on I-94 EB Over Red Arrow Highway North in Southwest Region: The following was noted:

1) Deteriorated deck fascia
2) Corrosion of bars in the deck fascia
3) Presence of efflorescence

Core Obtention and Testing

Several concrete cores were obtained from the bridge on I-69 over Fenton Road to establish benchmarks for accelerated weathering tests, conduct ASR testing, and determine the in-situ compressive strength of concrete. Cores were obtained by Detroit Diamond Drilling. The goal was to obtain cores that represent different levels of deterioration in bridge deck fascias. The levels of deterioration considered include: high, medium, low, and control. The following criteria were used when classifying the level of deterioration:

1) A bridge deck fascia region is considered to have a high level of deterioration if significant and clear spalling of concrete has occurred, and the presence of deterioration mechanisms such as corrosion of reinforcement or other is evident and extensive.
2) A bridge deck fascia region is considered to have a medium level of deterioration if some spalling of concrete is observed together, with some corrosion activity. The reinforcements may or may not be exposed. The length of deterioration and the visible extent of corrosion is smaller than that considered for a high level of deterioration.
3) A bridge deck fascia region is considered to have a low level of deterioration if there is minor or no spalling of concrete together with some or no visible exposed reinforcement. The length of the deterioration and the visible extent of corrosion is smaller than that considered for a medium level of deterioration.
4) A bridge deck fascia region is considered to represent the control (benchmark) case if there is no concrete spalling, and no visible exposed reinforcements along the span. Some map cracking may be present.

Two plans were considered for coring: Plan A and Plan B. In Plan A, concrete cores are obtained directly at the deck fascia region where the deterioration has occurred. This requires

drilling and obtaining cores in horizontal direction. In Plan B, concrete cores are obtained vertically on the top of the bridge deck near the barrier. In this plan, the cores are obtained as close to the inside face of the barrier as drilling equipment allows. Plan A was pursued first. The location of the reinforcement was determined using a profometer capable of detecting location, cover, and size of reinforcement. The location of reinforcement was marked on the deck fascias. However, the profometer is capable of detecting only reinforcement that is parallel with the surface of the deck fascia and not reinforcement that is perpendicular to it. Because of this limitation and because of the density of the reinforcement in the deck fascia region, the coring contractor encountered reinforcement perpendicular to the deck fascia in the first two trials and the cores were breaking at lengths shorter than desired when being extracted. Because of these challenges, the rest of the cores were obtained from the top of the deck in the vicinity of the barrier (i.e. Plan B was pursued).

Number of Cores

Two different options were considered for the determination of total number of cores. In option 1, for each deterioration level, i.e. control, low, medium, and high, a total of 9 cores were to be obtained (6 unreinforced and 3 reinforced). From the 6 unreinforced cores, 3 were to be used to determine the compressive strength, and resonance frequency; and 3 were to be used to determine the tensile strength. The reinforced cores were to be broken to obtain the reinforcing steel and measure any section loss due to corrosion. In option 2, the obtention of 3 reinforced cores for each deterioration level is eliminated and section loss in the reinforcement is measured onsite at the vicinity of the deck fascia. This reduces the total number of cores to 24. Option 2 was pursued for this bridge.

Core size and orientation

The targeted size of the cores was 4 in. in diameter and 8 in. in length. The orientation of the cores was such that the axis of the hole is perpendicular to the deck fascia in Plan A and perpendicular to the surface of the deck in Plan B. As noted earlier Plan B was pursued to obtain the cores. Even though the goal was to obtain 8 in. deep cores, during the coring process some of the cores fractured prematurely and featured lengths that were smaller than 8 in. In addition, to bring the cores to a testable condition, the ends were saw cut. The saw cutting shortened the lengths of the cores further. The number of usable cores after the saw cutting process was completed is shown in Table

3.2 for each level of deterioration. Fig. 3.10 illustrates the cores obtained for each level of deterioration. The dimensions of the cores are summarized in Table 3.3. ASTM C42 (ASTM 2020) requires that the diameter of the cores be at least equal to 3.70 in. All of the cores listed in Table 3.3 satisfy this requirement. In addition, a usable core is considered to be a core that has at least a length to diameter ratio of 1.0 according to ASTM C42 (ASTM 2020). All of the cores listed in Table 3.3 satisfy this requirement as the L/D ratio varies from 1.03 to 1.57. Table 3.3 also shows strength correction factors obtained using the values provides in ASTM C42 (ASTM 2020) and linear interpolation.

Table 3.2 Number of usable cores

Number of usable cores			
Control	Low	Medium	High
6	3	2	2

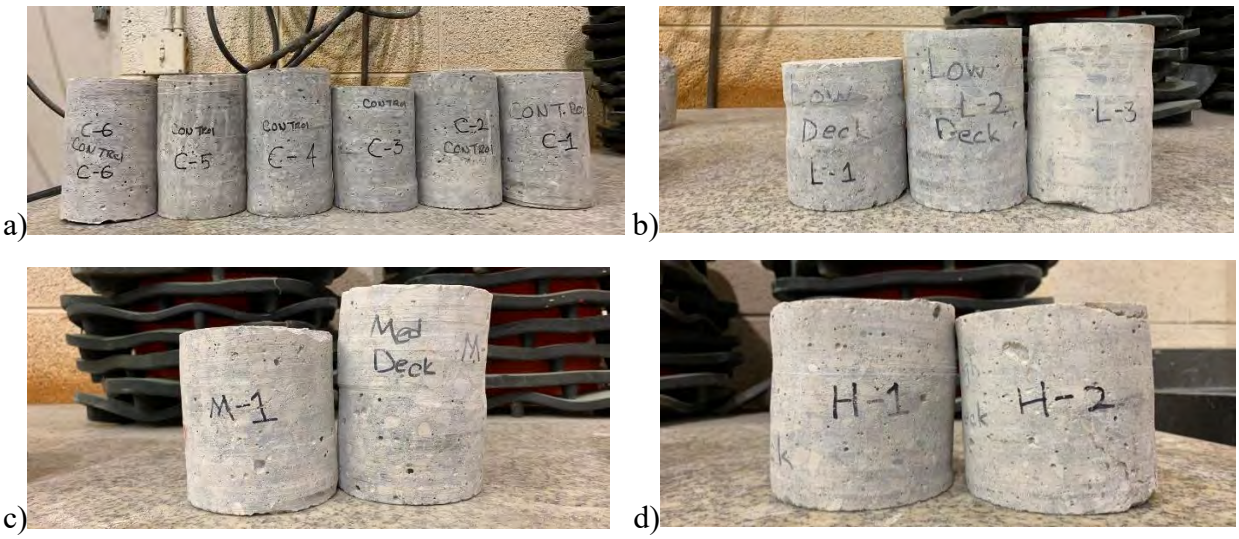

Fig. 3.10 Illustration of usable cores obtained from I-69 EB over Fenton Road for each deterioration level: a) control, b) low, c) medium, and d) high

Table 3.3 Dimensions for the extracted cores from I-69 EB bridge over Fenton Rd.

Specimen ID*	Diameter (in.)	Height (in.)	Ratio = Height/Diameter	Strength Correction Factor (ASTM C42 2020)
C-1	3.75	5.75	1.53	0.96
C-2	3.75	5.75	1.53	0.96
C-3	3.75	5.125	1.37	0.94
C-4	3.75	5.875	1.57	0.97
C-5	3.75	5.75	1.53	0.96
C-6	3.75	5.5	1.47	0.96
L-1ξ	3.75	4.75	1.27	0.93
L-2	3.75	5.625	1.50	0.96
L-3	3.75	5.75	1.53	0.96
M-1	3.75	4.125	1.10	0.89
M-2ξ	3.75	4.875	1.30	0.94
H-1	3.75	4.125	1.10	0.89
H-2	3.75	3.875	1.03	0.88

*C = Control level; L = Low deterioration level; M = Medium deterioration level; H = High deterioration level.
ξIncludes rebar pieces inside the core specimen.

Coring location

Record drawings were used to identify the arrangement of reinforcement in the deck fascia region so that the coring locations could be determined accordingly. Fig. 3.11 shows a typical reinforcement layout in the deck in the 1st span. The layout of reinforcement in the deck fascia is shown in Fig. 3.12. Information about the longitudinal and transverse rebars in the deck such as rebar size and spacing was obtained from Fig. 3.11. It was determined that transverse bar size and spacing was No. 6 bars at 6.5 in. on center top and bottom (a rather dense spacing). The size and spacing of the reinforcement in the longitudinal direction at the top and bottom of the deck is No. 4 at 18 in. on center and No. 6 at 12 in. on center, respectively. The thickness of the deck fascia is 11 in. The thickness of the deck outside of the fascia region is 8 in (Fig. 3.13). The anticipated arrangement of reinforcement is outlined in Fig. 3.14. The location where the cores were attempted to be obtained horizontally is shown in Fig. 3.15a. Since reinforcement parallel with the coring direction was encountered, cores could not be extracted. Therefore, cores were obtained from the top of the deck at the locations shown in Fig. 3.16 for control, low, medium and high levels of deterioration. The core obtention process is illustrated in Fig. 3.15b and samples of obtained cores are shown in Fig. 3.15c.

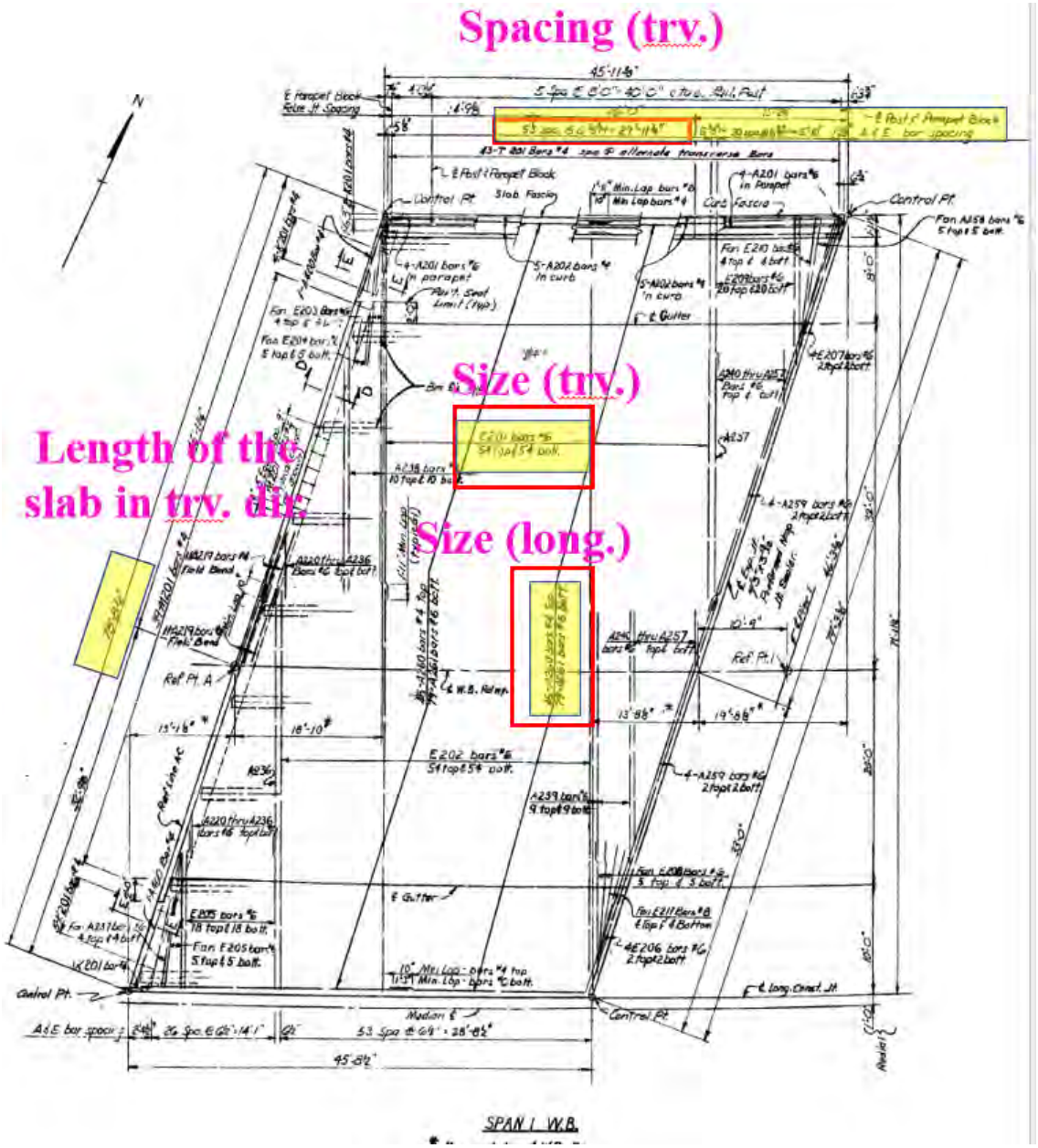

Fig. 3.11 Reinforcement layout for the slab in both longitudinal and transverse directions

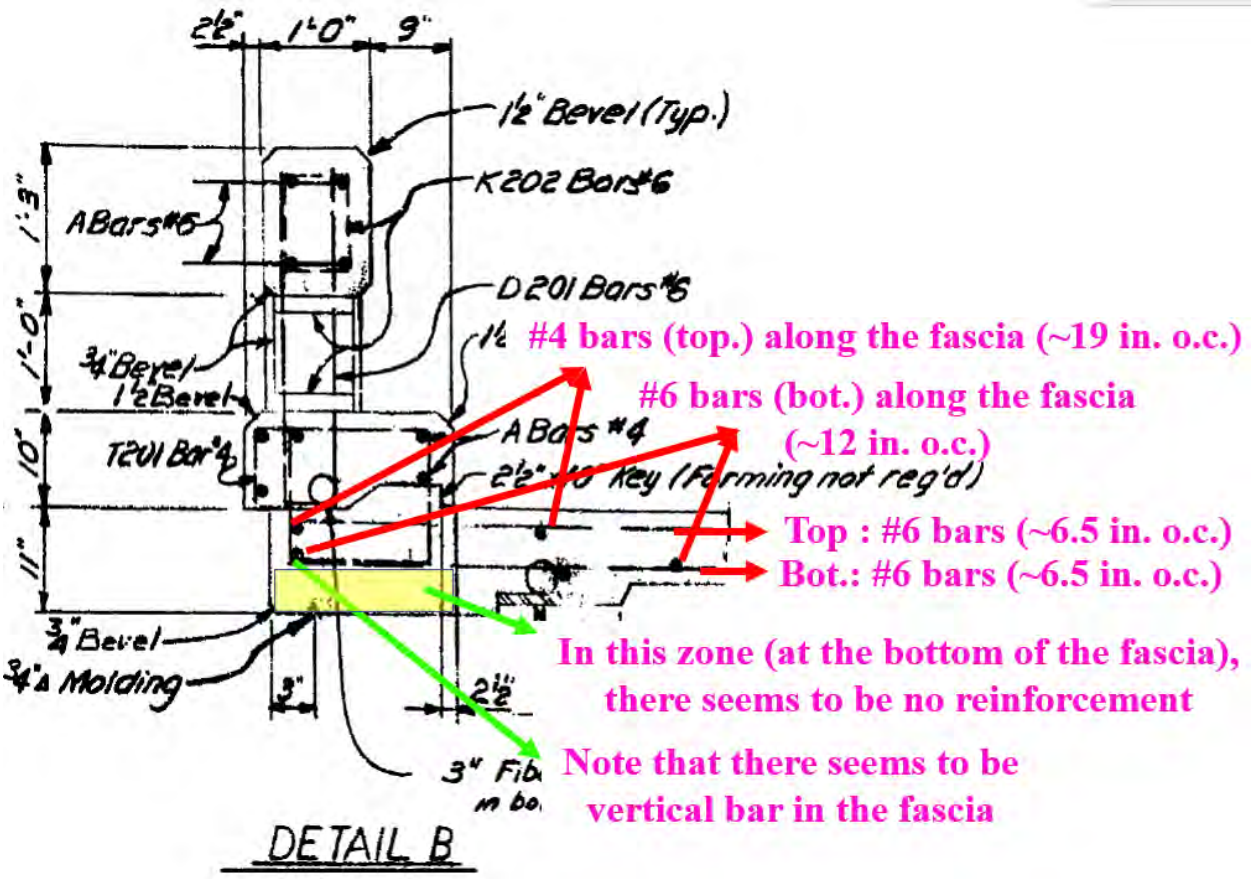

Fig. 3.12 Deck-barrier connection detail

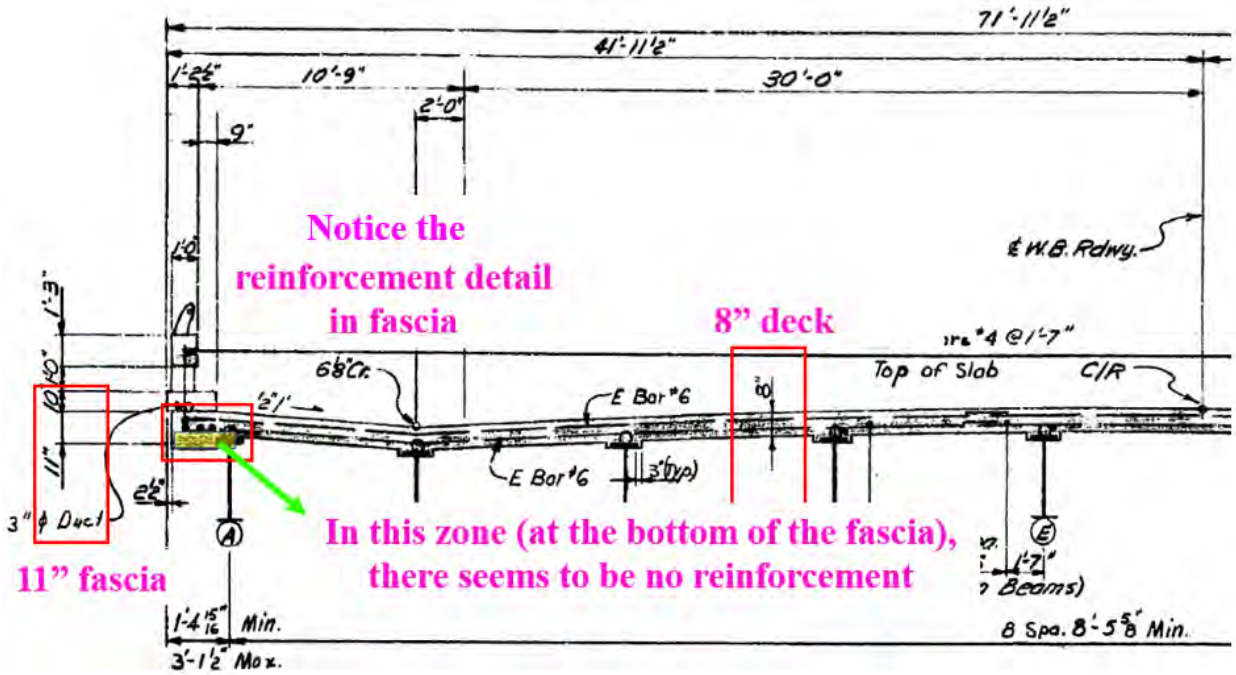

Fig. 3.13 Side view for the deck including the deck fascia

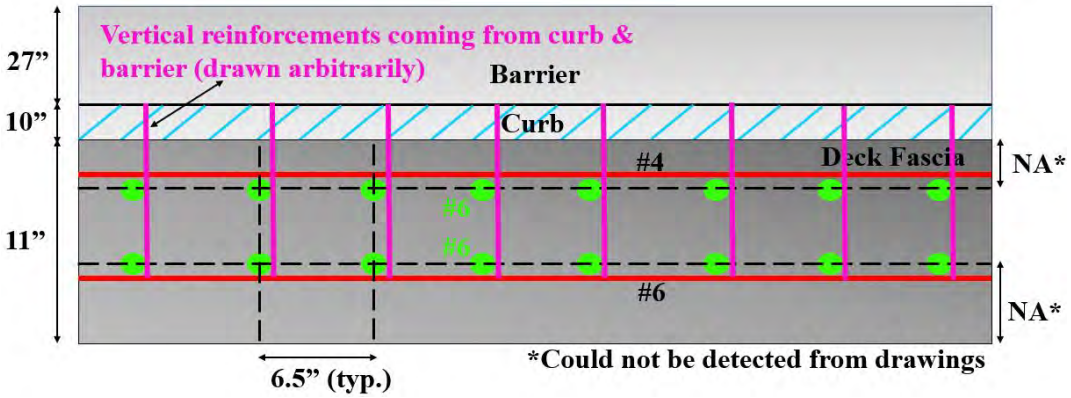

Fig. 3.14 Detailed fascia reinforcement detail (not to scale)

Fig. 3.15 a) First attempt to obtain cores at the deck fascia, b) core obtention on the deck surface, c) cores featuring different heights

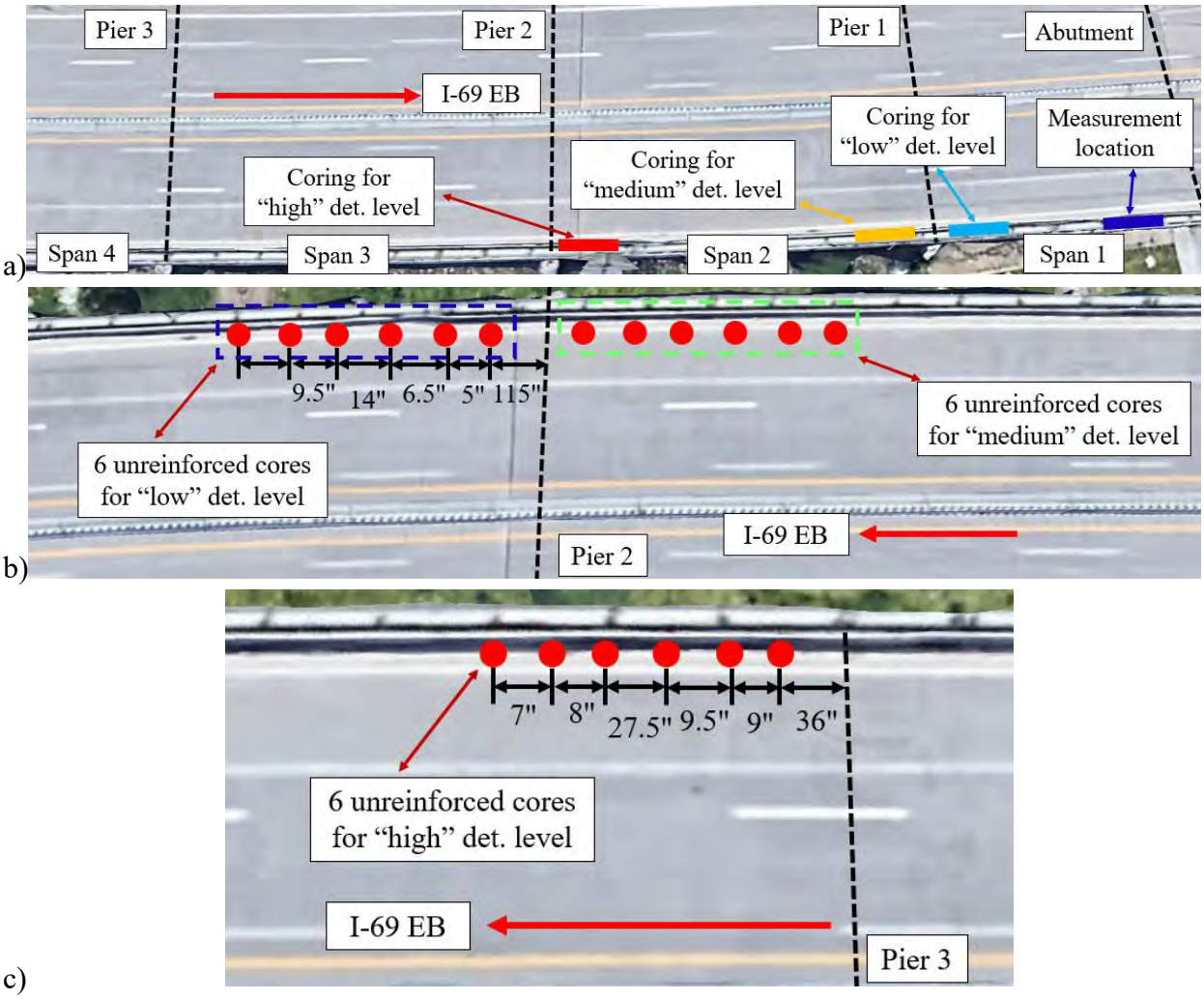

Fig. 3.16 a) Location of cores on the deck, b) detailed view of low and medium deterioration level coring; and c) detailed view of high deterioration level coring

Compressive Strength Testing

The compressive strength testing of cores was conducted in accordance with ASTM C39 (ASTM 2021). The ends of the specimens were sulfur capped. The conditions of the cores before and after testing are shown in Fig. 3.17. Compressive strength test results are shown in Table 3.4 as well as in Fig. 3.18. Measured compressive strengths were adjusted to account for core size based on ASTM C42 (ASTM 2020). The average compressive strengths for control, low, medium and high deterioration levels are 6.0, 6.9, 7.7 and 8.0 ksi with COVs 9.0%, 23.8%, 29.0% and 1.6%, respectively. The average compressive strength for all cores is 6.8 ksi with 19.4% COV. According to the MiBridge Database, the deck concrete compressive strength for I-69 over Fenton Road bridge is specified as 3 ksi. Therefore, the measured core compressive strength was well above the

specified value. The results suggest that there is no correlation between the measured compressive strength and the observed level of deterioration at the deck fascia. This is explained by the fact that the cores were obtained near the toe of the barrier rather than along the edge of the deck fascia due to difficulties encountered with horizontal core obtention. These results suggest that the deterioration of the deck is limited to the deck fascia and does not extend to the deck region in the vicinity of the toe of the barrier – at least from a concrete compressive strength perspective.

In some specimens, such as M-2, it appears that there are two layers of concrete because the colors at the top and bottom regions of the specimen appear to be different. Based on the information provided in the MiBridge database it appears that an overlay was installed in the bridge deck in 2003 thus explaining the presence of two layers. Since the two layers are connected in series the compressive strength test represents the strength of the weaker material.

Fig. 3.17 Core specimens before and after testing: a) Control; b) Low; c) Medium; and d) High

Table 3.4 Compressive test results for the obtained cores from I-69 over Fenton Road bridge's deck

Specimen ID*	Diameter (in.)	Height (in.)	Ratio = Height/Diameter	Strength Correction Factor (ASTM C42 2020)	f'_{cm} (ksi)	f'_c (ksi)
Control Level						
C-1	3.75	5.75	1.53	0.96	7.1	6.8
C-2	3.75	5.75	1.53	0.96	6.3	6.0
C-3	3.75	5.125	1.37	0.94	6.0	5.7
C-4	3.75	5.875	1.57	0.97	6.4	6.2
C-5	3.75	5.75	1.53	0.96	6.1	5.9
C-6	3.75	5.5	1.47	0.96	5.4	5.2
					Avg.	6.0
					St. Dev.	0.5
					COV (%)	9.0
Low Deterioration Level						
L-1$^{\xi}$	3.75	4.75	1.27	0.93	9.5	8.8
L-2	3.75	5.625	1.5	0.96	6.0	5.8
L-3	3.75	5.75	1.53	0.96	6.4	6.2
					Avg.	6.9
					St. Dev.	1.7
					COV (%)	23.8
Medium Deterioration Level						
M-1	3.75	4.125	1.1	0.89	10.5	9.3
M-2$^{\xi}$	3.75	4.875	1.3	0.94	6.5	6.1
					Avg.	7.7
					St. Dev.	2.2
					COV (%)	29.0
High Deterioration Level						
H-1	3.75	4.125	1.1	0.89	8.9	7.9
H-2	3.75	3.875	1.03	0.88	9.2	8.1
					Avg.	8.0
					St. Dev.	0.1
					COV (%)	1.6
					Overall	
					Avg.	6.8
					St. Dev.	1.3
					COV (%)	19.4

*C = Control level; L = Low deterioration level; M = Medium deterioration level; H = High deterioration level. $^{\xi}$Includes rebar pieces inside the core specimen.
f'_{cm}: Apparent compressive strength without considering the size effect; f'_c: Actual compressive strength with the consideration of size effect per ASTM C42 (ASTM 2020).

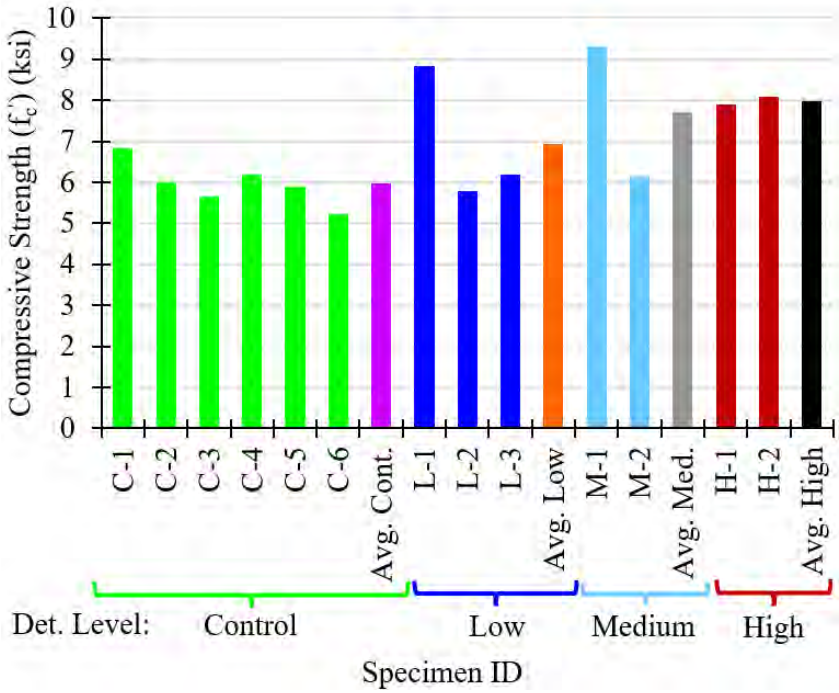

Fig. 3.18 Compressive test results for the deck cores obtained from the Fenton Road bridge

Dynamic Modulus Testing

The test setup used for dynamic modulus testing is shown in Fig. 3.19. Three test setups are shown: one for fundamental longitudinal resonant frequency, one for fundamental transverse resonance frequency, and one for fundamental torsional resonant frequency. First, the fundamental longitudinal resonant frequency was measured. This frequency was used to calculate the dynamic modulus of elasticity. Two test methods may be used to obtain the dynamic modulus: 1) Forced Resonance, and 2) Impact Resonance. The impact resonance testing was selected. Variable size impactors were evaluated to conduct the impact resonance testing. These are summarized in Table 3.5 together with the maximum possible resonant frequency. The selected impactor is shown in bold green. The impactor shown in bold dark red was not appropriate because one of the readings exceeded the maximum possible resonant frequency. The Emodumeter shown in Fig. 3.19 has the capability to calculate the dynamic modulus based on the provided information such as mass, length, diameter. However, the results provided by Emodumeter were confirmed by the research team using the formula shown below and given in ASTM C215 (ASTM 2019), where E_{dyn} is the dynamic Young's modulus of elasticity (in pascals); D is the factor which depends on length, L (meter), and diameter of the sample, d (meter), for the cylindrical specimen; M is the mass of the specimen (kg); and n' is the fundamental longitudinal resonant frequency (Hz).

$$E_{dyn} = DM(n')^2 \quad \text{Eq. 3.1}$$

$$D = 5.093(L/d^2) \quad \text{Eq. 3.2}$$

The results of dynamic modulus testing are shown in Table 3.6 and Fig. 3.20. Fig. 3.20 suggests that there is a general trend of lower dynamic moduli for higher levels of deterioration. The dynamic moduli are generally higher than the static modulus. The calculated static modulus based on AASHTO LRFD (2020) is 3639 ksi. Recall that the goal of the dynamic modulus testing was to establish benchmark values for when to terminate accelerated weathering tests.

Testing was also conducted to determine the fundamental transverse resonant frequency as well as fundamental torsional resonant frequency. However, two problems were encountered during these tests. Firstly, during most of the measurements consistent readings could not be obtained for transverse and torsional resonant frequencies. This could be due to the short *L/D* ratios (see ASTM C215 (ASTM 2019) section 7.3). Secondly, even in cases when consistent measurements could be taken the results were illogical, that is, the results for the dynamic modulus of rigidity, G_{dyna}, and dynamic modulus of elasticity, E_{dyna}, were quite large. Therefore, these results were disregarded.

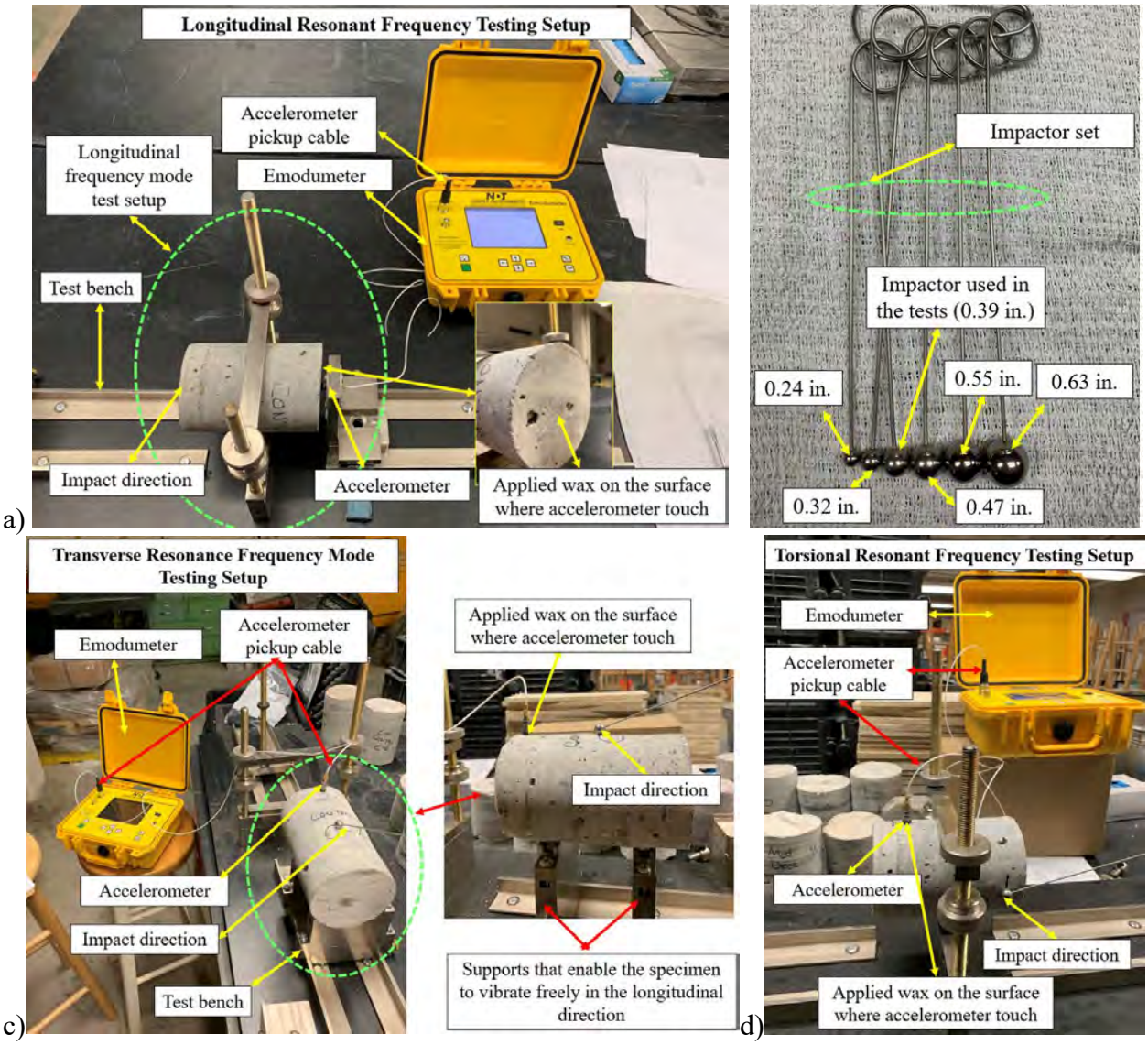

Fig. 3.19 Test setups prepared for measuring: a) fundamental longitudinal resonant frequency (left), impactor set (right); b) fundamental transverse resonance frequency; and c) fundamental torsional resonant frequency

Table 3.5 Maximum possible fundamental resonant frequency that can be generated by available impactors

Impactor Size (in. (mm))	Maximum Possible Resonant Frequency (kHz)
0.24 (6)	48.5
0.32 (8)	36.4
0.39 (10)	**29.1**
0.47 (12)	24.3
0.55 (14)	20.8
0.63 (16)	**18.2**

Table 3.6 Dynamic Modulus Results

Specimen ID	Diameter (in.)	Length (in.)	Mass (lb.)	Fundamental Long. Res. Freq., n', (Hz)[1]	D[2]	Dynamic Modulus, E_{dyn}[3] (ksi)
C-1	3.75	5.75	4.91	14219	82.0	5347
C-2	3.75	5.75	5.02	13508	82.0	4934
C-3	3.75	5.125	4.50	15560	73.1	5231
C-4	3.75	5.875	5.14	13145	83.8	4888
C-5	3.75	5.75	5.06	13704	82.0	5119
C-6	3.75	5.5	4.81	14180	78.4	4983
L-1	3.75	4.75	4.54	16875	67.7	5753
L-2	3.75	5.625	5.22	13418	80.2	4952
L-3	3.75	5.75	5.29	12940	82.0	4771
M-1[4]	3.75	4.125	3.57	NA	NA	NA
M-2	3.75	4.875	4.67	14479	69.5	4471
H-1	3.75	4.125	3.64	18001	58.8	4558
H-2	3.75	3.875	3.50	18568	55.3	4380

[1]Average of three fundamental longitudinal resonant frequency values is provided.
[2]$D = 5.093(L/d^2)\ m^{-1}$ based on ASTM C215 (ASTM 2019) section 10.2.
[3]$E_{dyn} = DM(n')^2$ where M is the mass of the specimen in kg.
[4]Consistent fundamental longitudinal frequency measurements could not be obtained from Emodumeter for this specimen.

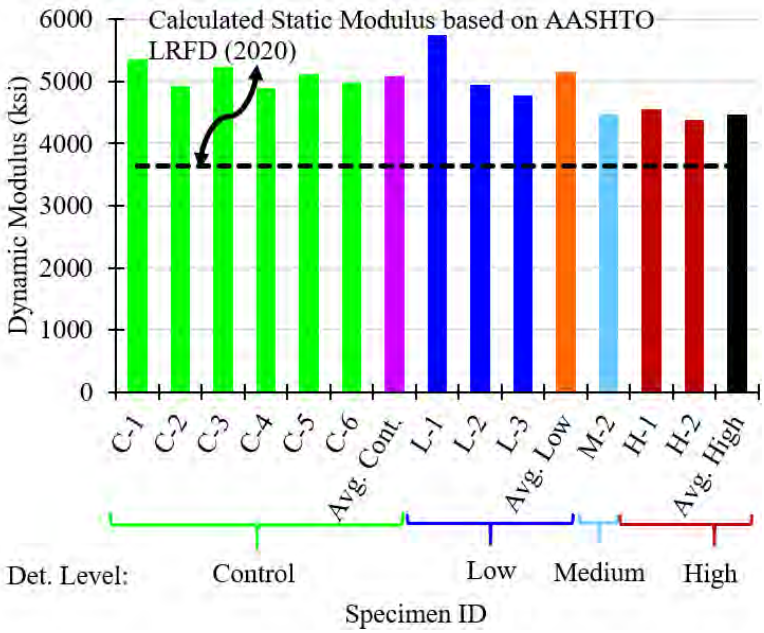

Fig. 3.20 Dynamic modulus test results based on the cores obtained at different deterioration levels

Sulfur Capping of Concrete Cores

The concrete cores were sulfur capped prior to testing them in compression. Fig. 3.21 shows the equipment used for the sulfur capping process; the laboratory setup used for sulfur capping; and the cylinders before and after sulfur capping.

a)

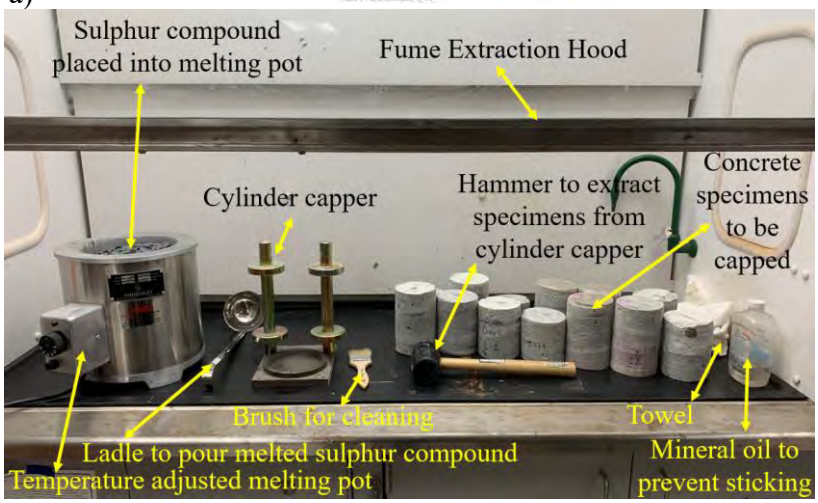

b)

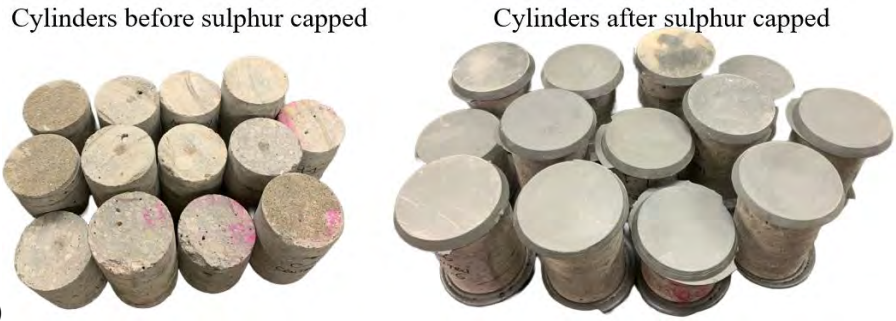

c)

Fig. 3.21 a) Equipment used for the sulfur capping process; b) laboratory setup used for sulfur capping; and c) cylinders before and after sulfur capping

Clear Cover Determination

Methodology: A battery-operated device called a Profoscope – Rebar Detector and Cover Meter (generically known as covermeter) was used to determine clear cover (Fig. 3.22a). Measurements were taken at the intersection of grids as shown in Fig. 3.22b. There are typically two types of cover meters: 1) those that operate based on principle of magnetic reluctance, and 2) those that operate based on the eddy current principle (ACI 2013). The measurement principle as outlined in the manual of the Profoscope is as follows: "The Profoscope uses electromagnetic pulse induction technology to detect rebars. Coils in the probe are periodically charged by current pulses and thus generate a magnetic field. On the surface of any electrically conductive material, which is in the magnetic field, eddy currents are produced. They induce a magnetic field in the opposite direction. The resulting change in voltage can be utilized for the measurement."

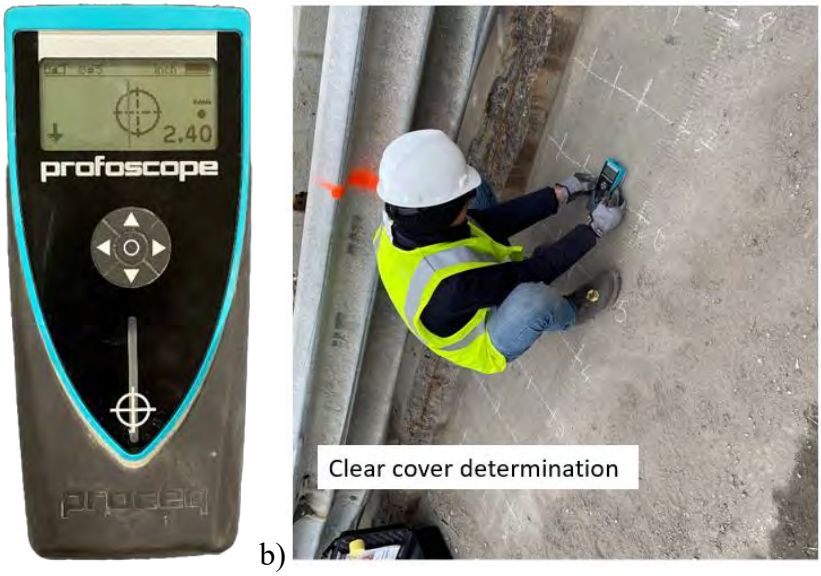

a) b)

Fig. 3.22 a) Profoscope+ (cover meter), b) Clear cover determination setup

Results: The clear cover measurements for each bridge are illustrated in Fig. 3.23.

Bridge on I-69 over Fenton Road in Bay Region: For the bridge on I-69 over Fenton Road in Bay Region, the clear cover varied from 2.5 in. to 4.0 in. with the regions near the deck fascia exhibiting lower cover. This indicates a lower level of protection against corrosion at the deck fascia region. The variation in clear cover readings shows a lack of consistency and varying levels of protection in the selected region.

Bridge on I-96 over M-99 in University Region:

The same observation was made for the bridge on I-96 over M-99 in University Region. The clear cover varied from 2.2 in. to 4.2 in. and was smallest in the regions on the deck fascia or near the deck fascia.

Bridge on County road over I-75:

For the bridge in the North Region (County Road over I-75) clear cover varied from 1.5 in. to 4.0 in. However, with the exception of the expansion joint region, clear cover was consistently above 3.0 in. and between 3.0-4.0 in. The readings near the expansion joint are believed to be affected by the exposed metal at the expansion joint. Therefore, the readings along gridline 6 should be disregarded. Concrete clear cover was generally consistent and met minimum requirements specified in AASHTO LRFD (2020).

Bridge on Waldon road over I-75 Metro Region:

For the bridge in the Metro Region (Waldon Road over I-75) clear cover varied from 3.0 in. to 5.0 in. Clear cover is inconsistent. Minimum requirements specified in AASHTO LRFD (2020) are met. Although, excessive cover, such as 5.0 in. is not necessarily good, because it reduces flexural capacity and creates large crack widths. There appears to be a general trend towards lower cover near the fascia.

Bridge on US 131 Ramp over W River Dr. NW:

For the bridge on US 131 Ramp over W River Dr. NW clear cover on the deck surface varied from 2.0 in. to 4.5 in. Clear cover along the deck fascia varied from 0.98 to 2.9 in. Clear cover was inconsistent. Minimum requirements specified in AASHTO LRFD (2020) were not met. There is a clear trend towards lower cover near the fascia in the deck region. Clear cover along the deck fascia was even smaller.

Bridge on I-94 EB over Red Arrow Highway:

For the Bridge on I-94 EB over Red Arrow Highway, the clear cover measurements did not show a clear trend and varied from 2.6-4.4 in. The measurements taken along the deck fascia were lower

than those measured on the deck surface. Generally, clear cover measurements were larger than 3.0 in. The maximum measured clear cover was 4.33 in.

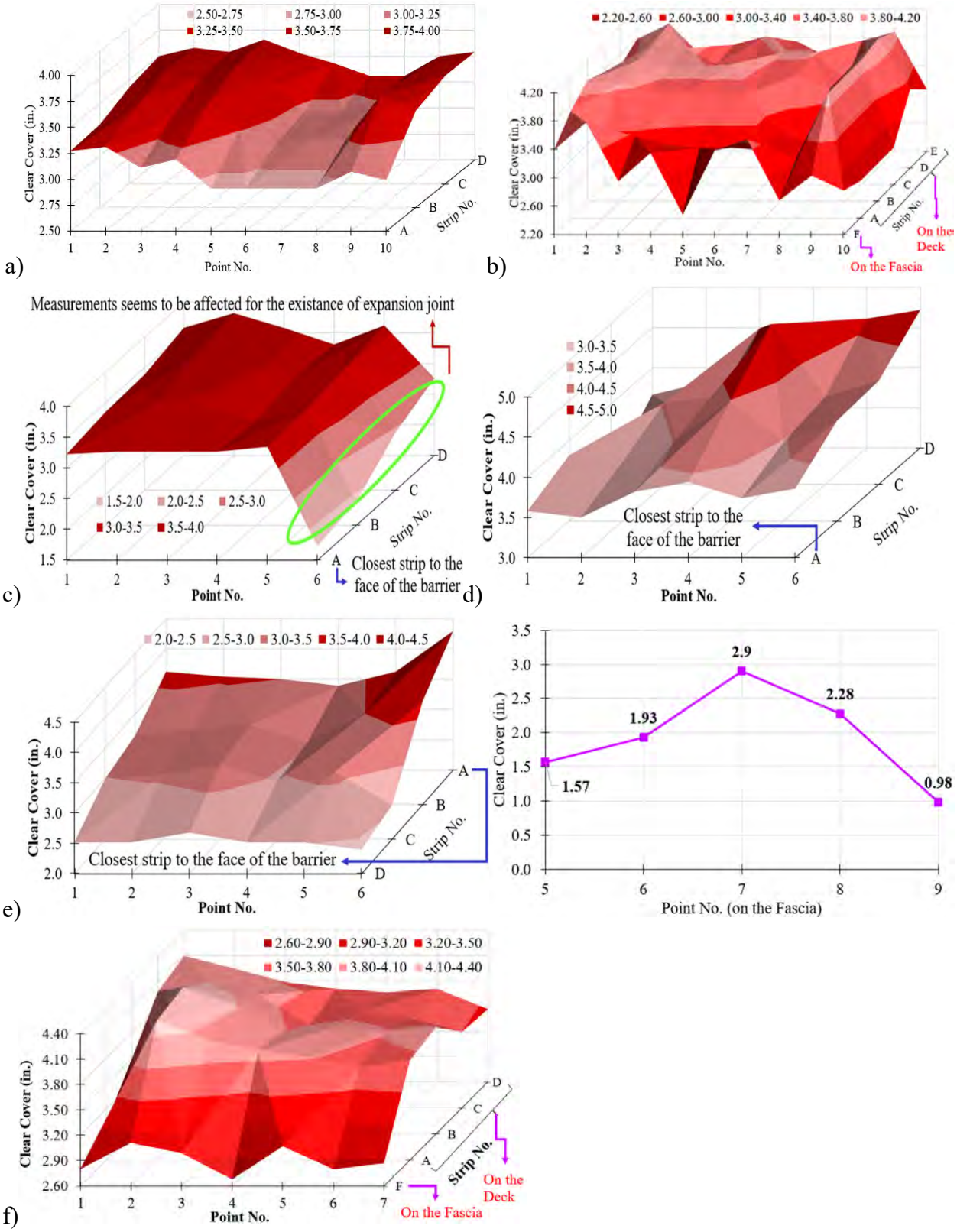

Fig. 3.23 Clear cover for: a) clear cover for the I-69 over Fenton Road bridge in Bay Region, b) clear cover for the I-96 WB over M-99 bridge in Bay Region, c) County road over I-75, d) Waldon road over I-75, e) US 131 Ramp over W River Dr. NW, f) I-94 EB over Red Arrow HW

Surface Hardness Determination Using Rebound Hammer

Methodology: Surface hardness testing was conducted using a Humboldt Concrete Rebound Hammer (H-2987H) (Fig. 3.24a). Rebound hammer readings were collected at the intersection of grids shown in Fig. 3.24b in general compliance with ASTM C805 (ASTM 2018), Standard Test Method for Rebound Number of Hardened Concrete. This test is used to determine the surface hardness and serves as a practical method to determine the uniformity of concrete. It measures the rebound of a spring-loaded mass after it has struck a steel rod in contact with a smooth concrete surface (Kosmatka and Wilson 2016). The rebound numbers are typically used to provide an indication of the relative compressive strength and modulus of elasticity. Although, two different concrete elements featuring the same compressive strength but different moduli of elasticity will give different rebound readings. The rebound hammer was gradually pressed against the deck surface until the hammer impacted the surface. The rebound number was displayed on a mechanical sliding scale and was recorded to the nearest whole number. One reading was collected for each point. The impressions of the impact hammer on the surface of the deck were examined to exclude any readings which corresponded with crushes or breaks. No such locations were determined.

a)

b)

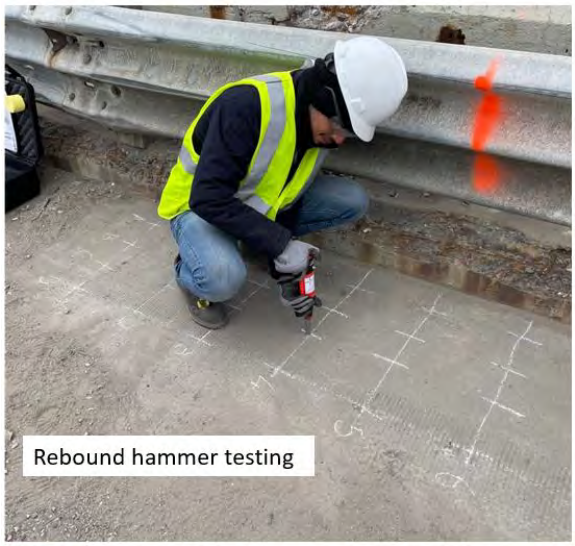

Fig. 3.24 a) Isometric view of rebound hammer and its interior, b) rebound hammer test setup

Results: Rebound hammer measurements are illustrated in Fig. 3.25.

Bridge on I-69 over Fenton Road in Bay Region:

For the bridge located on I-69 over Fenton Road in Bay Region, the rebound hammer readings varied from 30-55 and no specific trend was observed.

Bridge on I-96 over M-99 in University Region:

Similarly, for the bridge located on I-96 over M-99 the rebound hammer readings varied from 20-60 without exhibiting any particular trend.

Bridge on County road over I-75 North Region:

For the bridge on County road over I-75 there was no strong trend in surface hardness in the investigated region. Although there appears to be a tendency towards lower rebound numbers along the gridline closet to the deck fascia. The readings varied from 15-45.

Bridge on Waldon road over I-75:

For the bridge on Waldon Road over I-75 there was no strong trend in surface hardness in the investigated region. Although there appears to be a tendency towards lower rebound numbers along the gridline closest to the deck fascia. The readings varied from 10-50.

Bridge on US 131 Ramp over W River Dr. NW:

For the bridge located on US 131 Ramp over W River Dr. NW, there was no strong trend in surface hardness in the investigated region. The readings varied from 25-55.

Bridge on I-94 EB over Red Arrow HW:

For the bridge located on I-94 EB over Red Arrow HW the rebound hammer readings varied from 24 to 57. No trends in surface hardness was observed.

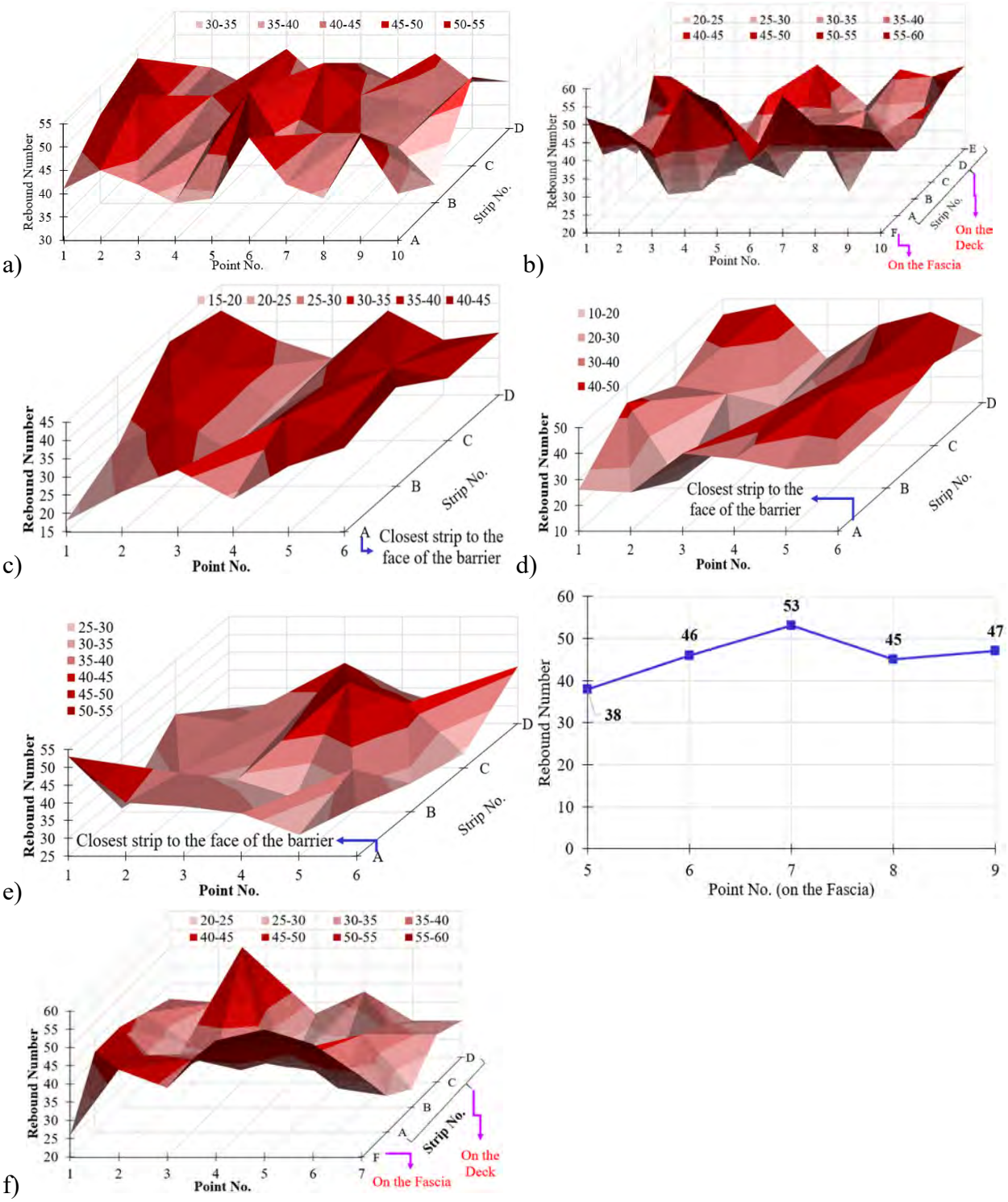

Fig. 3.25 Rebound numbers for: a) the bridge on I-69 over Fenton Road in Bay Region, b) the bridge on I-96 WB over M-99 in University Region, c) County road over I-75, d) Waldon road over I-75, e) US 131 Ramp over W River Dr. NW, f) I-94 EB over Red Arrow HW

Moisture Content Determination

Methodology: It was determined that the most relevant ASTM Standard for determining the moisture content in the deck was ASTM F2659 (ASTM 2023), Standard Guide for Preliminary Evaluation of Comparative Moisture Condition of Concrete, Gypsum Cement and Other Floor Slabs and Screeds Using a Non-destructive Electronic Moisture Meter. The moisture content was measured using a hand-held electronic moisture meter called Concrete Encounter for Moisture Testing supplied by Humboldt (HC-2990). The operating principle of a typical non-destructive electronic moisture meter for concrete is shown in Fig. 3.26. The device uses non-destructive impedance measurement to determine moisture levels in concrete. The electrical impedance of material varies in proportion to its comparative moisture condition. The electrical impedance of the deck underneath the footprint of the device is measured by creating an alternating electric field that penetrates the material under the test. The alternating current flowing through the field is inversely proportional to the impedance of the material. The instrument determines the current's amplitude and thus derives the moisture value (ASTM F2659 2023). It provides instant readings of moisture content up to 6% in the upper 0.5 in. stratum of concrete. The measurements are read directly from an analog meter. Coplanar electrodes with spring loaded contacts enhance signal depth and sensitivity to a depth of 0.5 in. Therefore, the device can be used to determine comparative moisture content up to a depth of 0.5 in. at different locations on the surface. It cannot be used to determine moisture content at a deeper level. It was ensured that the area where the moisture readings were taken had no visible water in liquid form at the time the testing procedure was carried out. In addition, it was ensured that the test area was clean and free of any covering, coatings, adhesive residue, finishes, dirt, curing compounds, or other substances. The moisture content of the deck is expressed as a percentage calculated using Eq. 3.3. The battery operated hand-held electronic moisture meter used is shown in Fig. 3.27a. A snapshot of moisture content measurement process is shown in Fig. 3.27b.

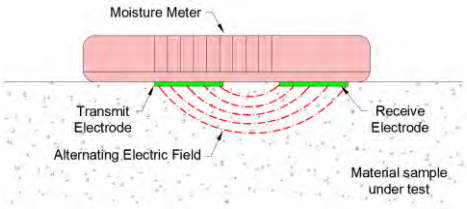

Fig. 3.26 Operating principle of typical non-destructive electronic moisture meter for concrete (reproduced from ASTM F2659, 2023)

$$Moisture\ Content, \% = \frac{Wet\ weight - Dry\ Weight}{Dry\ Weight} * 100 \quad \text{(Eq. 3.3)}$$

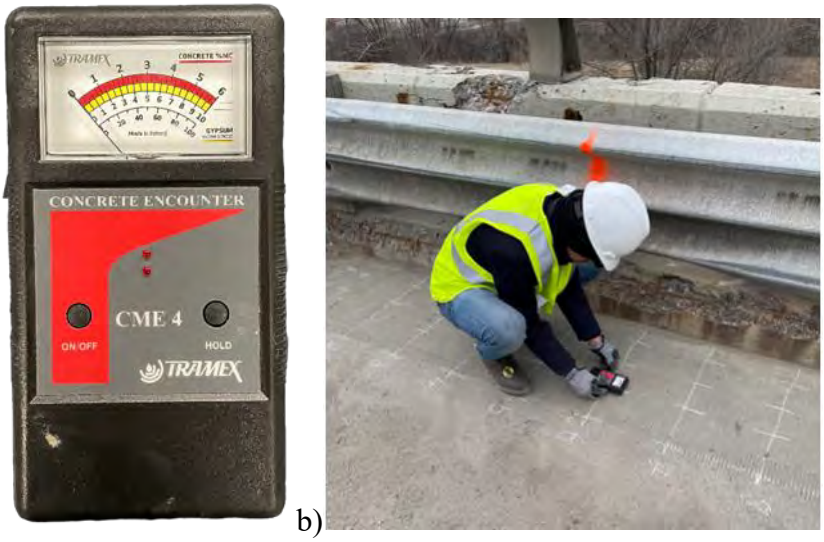

a) b)

Fig. 3.27 a) Concrete Encounter for Moisture Testing (Moisture meter), b) Moisture content test

Results: Moisture content measurements are illustrated in Fig. 3.28

Bridge on I-69 over Fenton Road in Bay Region:

The collected data is shown in Fig. 3.28a. For the bridge on I-69 over Fenton Road in Bay Region, moisture content varies from 2.5 to 4.0 without exhibiting any specific trend at the time of the test.

Bridge on I-96 over M-99 in University Region:

For the bridge on I-96 over M-99 in University Region, moisture content varied from 2.5-6% with moisture content near and on the deck fascia generally being higher than the test of the locations. As shown earlier in Fig. 3.3, there is clear evidence of higher moisture content in the vicinity of the barrier and deck fascia due to improper or incomplete drainage for the bridge on I-96 over M-99 in University Region.

Bridge on County road over I-75 in North Region:

For the bridge on County road over I-75 in North Region both visual inspections and moisture meter readings demonstrate the higher moisture content near the deck fascia. Moisture meter readings varied from 2.5->6% and were consistently higher near the deck fascia.

Bridge on Waldon road over I-75:

For the bridge on Waldon road over I-75, moisture meter readings varied from 1.5-4%. No specific trend was observed.

Bridge on US 131 Ramp over W River Dr. NW:

For the bridge on US 131 Ramp over W River Dr. NW., moisture meter readings varied from 1.5-3.5% on the deck surface. Along the deck fascia they were higher than 3.8%. This is a clear indication of higher surface moisture content along the fascia.

Bridge on I-94 EB over Red Arrow HW:

For the bridge located on I-94 EB over Red Arrow HW the moisture content varied from 2.2% to 4.6%. There was a clear trend towards higher moisture content along the deck fascia.

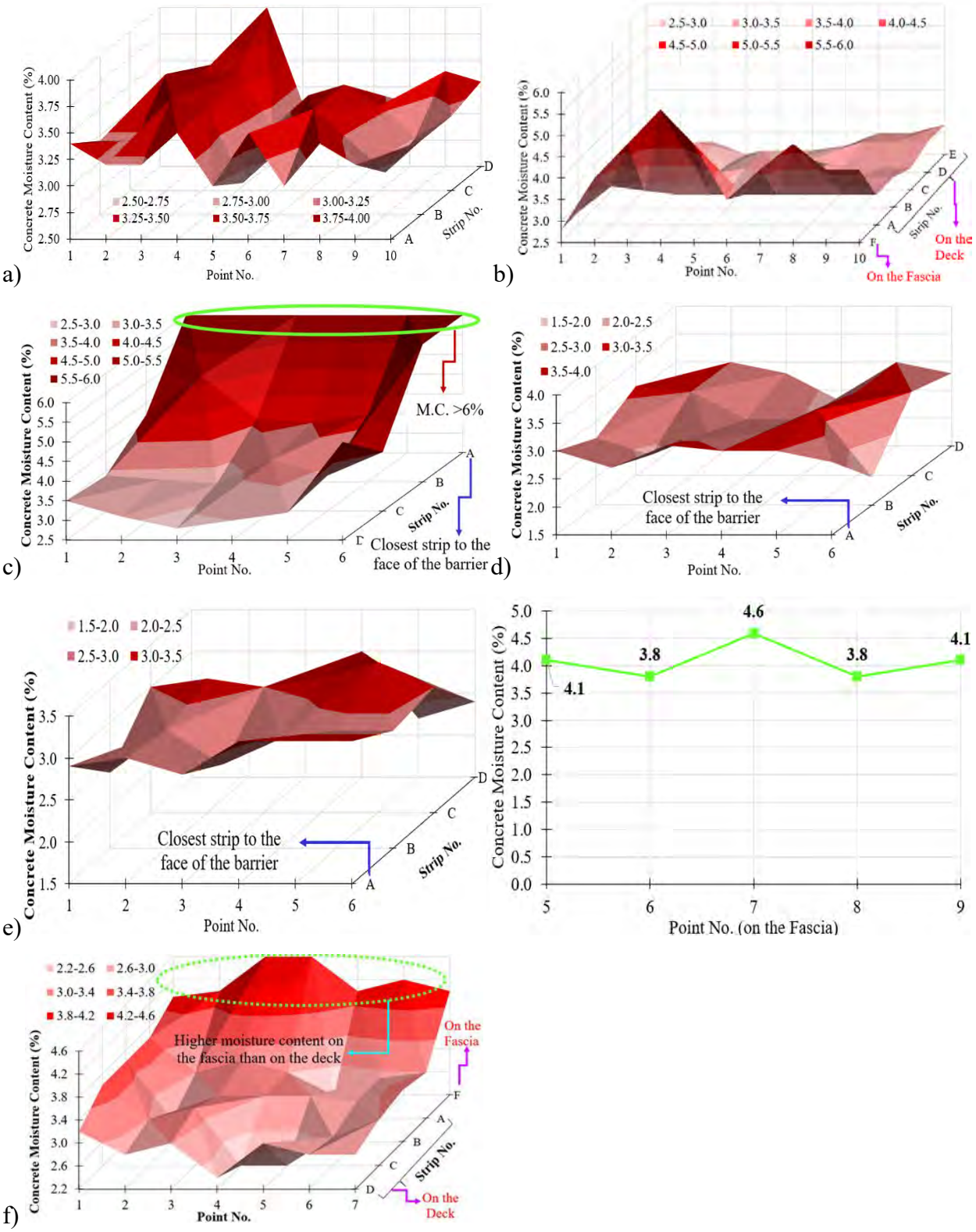

Fig. 3.28 Concrete moisture content for: a) the bridge on I-69 over Fenton Road in Bay Region, b) the bridge on I-96 over M-99 in University Region; c) County road over I-75, d) Waldon road over I-75, e) US 131 Ramp over W River Dr. NW, f) I-94 EB over Red Arrow HW

Corrosion Potential Determination

Methodology: Half-cell potential tests were conducted in accordance with ASTM C876 (ASTM 2022), Standard Test Method for Corrosion Potentials of Uncoated Reinforcing Steel in Concrete. The bridges selected for field investigation feature uncoated steel reinforcement, which renders the half-cell potential measurements appropriate. The operating principle of half-cell potential measurements is illustrated in Fig. 3.29a in which a positive connection is made to the steel reinforcement in concrete, and a negative connection is made to the copper head in the reference electrode. A sectional view of the copper-copper sulfate reference electrode is provided in Fig. 3.29b. The apparatus used was a CorMap Rebar Corrosion Mapping System supplied by Humboldt as shown in Fig. 3.29c. A high impedance battery operated digital voltmeter measures the potential difference between metal in the reference electrode and the steel reinforcement in concrete. A direct connection to the reinforcing steel was established in both bridges. The photographs shown in Fig. 3.30a-d were taken from the bridge on I-69 over Fenton Road. To ensure a low electrical resistance connection, the reinforcing bar was scraped with a wire brush (Fig. 3.30a). The overall half-cell potential measurement setup used in the field is shown in Fig. 3.30b. The direct connection to the steel reinforcement for the bridge on I-69 over Fenton Road is shown in Fig. 3.30c. The reference electrode was touched down on the deck surface at the intersecting grid points to measure the potential difference (Fig. 3.30d). The deck surface where the measurements were taken was cleaned with a brush or broom prior to taking measurements. An electrical junction device (sponge) was wetted using electrical contact solution (soapy water: 100 mL household detergent mixed with 19L water). The deck surface was pre-wetted with abovementioned solution using Method B for Pre-Wetting Concrete Surfaces as described in ASTM C876 (ASTM 2022). The sponge (electrical junction device) was saturated with the abovementioned solution and was placed at the grid locations shown earlier. The sponge was left for a period of time necessary to obtain values that do not fluctuate with time. The measurements were reported to the nearest 10 mV and corrected for temperature. Corrosion potentials were interpreted using the Numeric Magnitude Technique described in ASTM C876 (ASTM 2022).

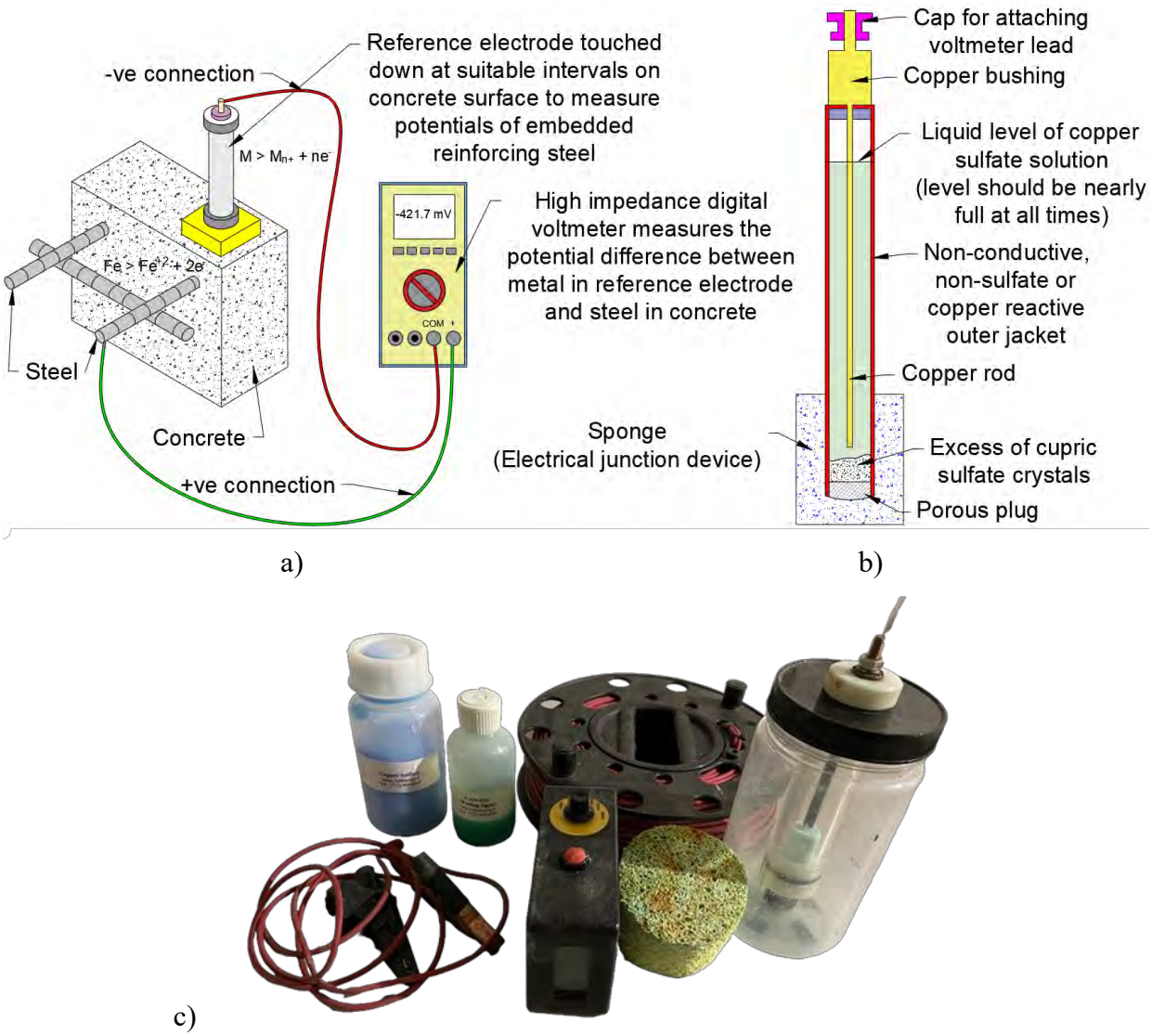

Fig. 3.29 a)-b) Principle of half-cell potential measurements (reproduced from ASTM C876, 2022): a) reference electrode circuitry, b) sectional view of a copper-copper sulfate reference electrode, c) CorMap Rebar Corrosion Mapping System (used for Half-cell Potential Measurements)

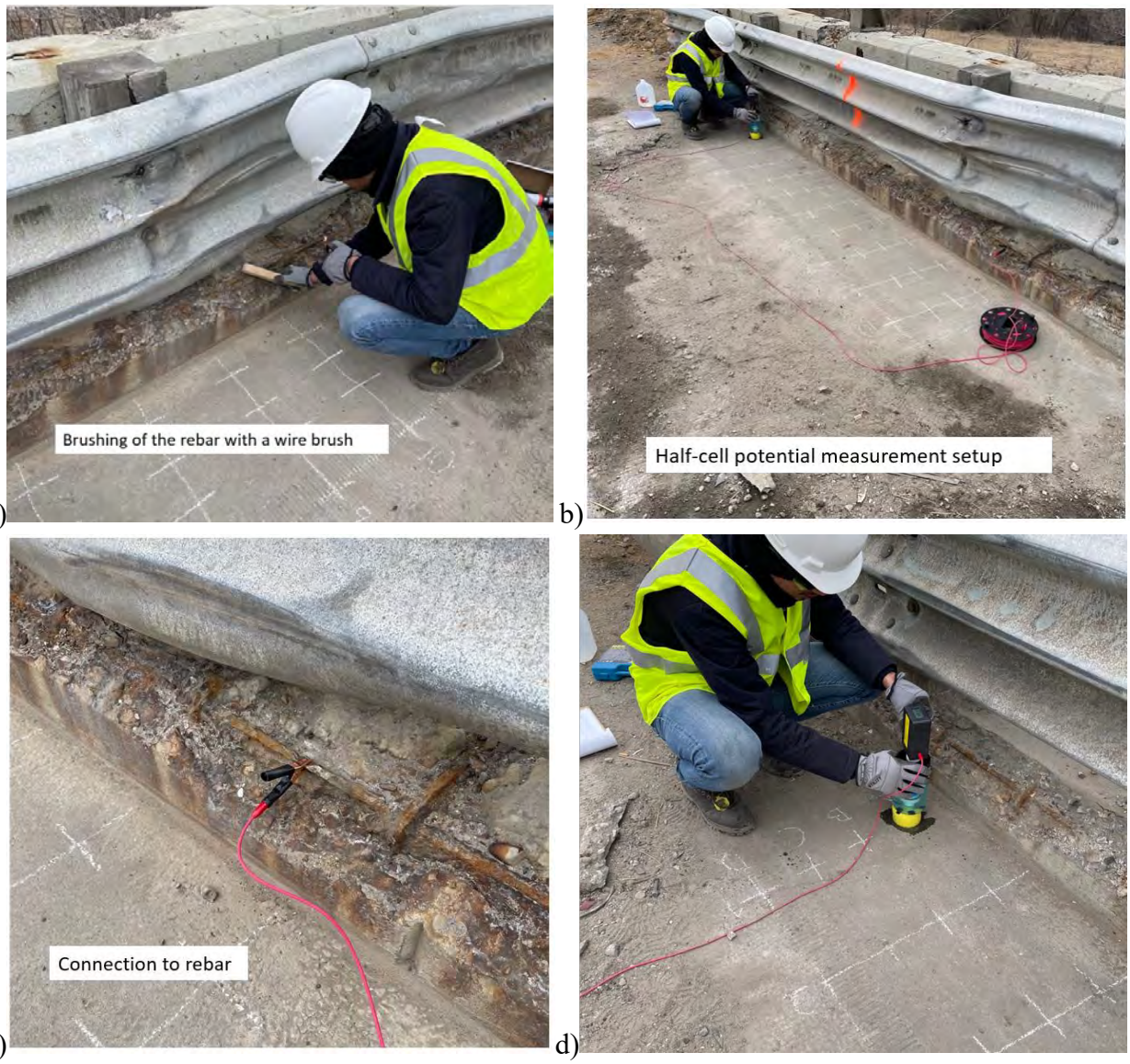

Fig. 3.30 Half-cell potential testing (photographs in a-d were taken from the bridge on I-69 over Fenton Road): a) brushing of the rebar with a wire brush, b) overall setup, c) connection to rebar, d) corrosion potential measurements,

Results: Fig. 3.31 illusrates the results of half-cell potential tests.

Bridge on I-69 over Fenton Road in Bay Region:

For the bridge on I-96 over Fenton Road, generally, higher high-cell potential measurements were recorded in the vicinity of the deck fascia. The results are shown in Fig. 3.31a. Potentials greater than -200Mv generally indicate 90% or higher probability of no corrosion taking place at the time of measurement. For both bridges there are only a few points that fall in this category. Potentials in the range of -200 to -350mV are inconclusive. Potentials less than -350mV generally indicate

90% or higher probability of active corrosion in the area in question at the time of testing. For the bridge on I-69 over Fenton Road there were several points in which the readings were less than -350 mV, including areas in the vicinity of the deck fascia confirming active corrosion activity. As can be seen in, Fig. 3.31a there is active corrosion activity in the curb near the barrier. The half-cell potential readings suggest that such corrosion extends into the deck in the vicinity of the deck fascia.

Bridge on I-96 over M-99 in University Region:

Similar observations were made for the bridge on I-96 over M-99, except that in this case the highest corrosion potentials were recorded near the expansion joint, suggesting a higher probability of active corrosion in this area (Fig. 3.31b). As noted earlier, there is visible corrosion and severe deck fascia deterioration on the deck fascia on I-96 EB. Since the measurements were taken on I-96 WB due to the presence of a steel barrier on I-96 EB, corrosion potentials were not as high as one might have expected for I-96 EB.

Bridge on County Road over I-75 in North Region:

For the bridge located on County Road over I-75 half-cell potential readings varied from -200 to -600 mV, with most readings being above -350 mV. This is a clear indication of high corrosion activity not only along the deck fascia as noted by visual inspections, but also in the deck region where the measurements were taken. Highest half-cell potentials were recorded near the expansion joint.

Bridge on Waldon road over I-75:

For the bridge located on Waldon road over I-75, readings varied from -250 to -600 mV with most readings being above -350 mV. This is a clear indication of high corrosion activity not only along the deck fascia as noted by visual inspections, but also in the deck region where the measurements were taken.

Bridge on US 131 Ramp over W River Dr. NW:

For the bridge located on US 131 Ramp over W River Dr. NW readings varied from -150 to -600 mV. The reading along the deck fascia were all lower than -350 mV. High half-cell potential readings were noted near the expansion joint. This is a clear indication of high corrosion activity not only along the deck fascia, but also in the deck region.

Bridge on I-94 EB over Red Arrow HW:

For the bridge located on I-94 EB over Red Arrow HW half-cell potential measurements varied from 0 to -600 mV. There is a clear trend towards lower readings towards the deck fascia. The average reading along the deck fascia was -560 mV. The average reading on the deck surface was -142 mV. There is a high probability of corrosion along the deck fascia, which was confirmed by visual inspections in certain areas. According to the readings on the deck surface, there is a 90% or higher probability that there is no corrosion on the deck surface, with the exception of the readings that were collected for the gridline closet to the expansion joint. For this gridline, the readings suggested a 90% or higher probability of corrosion. The lower negative values recorded on the rest of the deck surface may have been affected by a latex modified concrete overlay, which was installed in 1993. This overlay may have protected the reinforcement within the deck from reaching notable levels of corrosion activity. In summary, the lower clear cover recorded along the deck fascia, the higher moisture content, and the high level of corrosion activity explain why the fascia in this bridge is deteriorating.

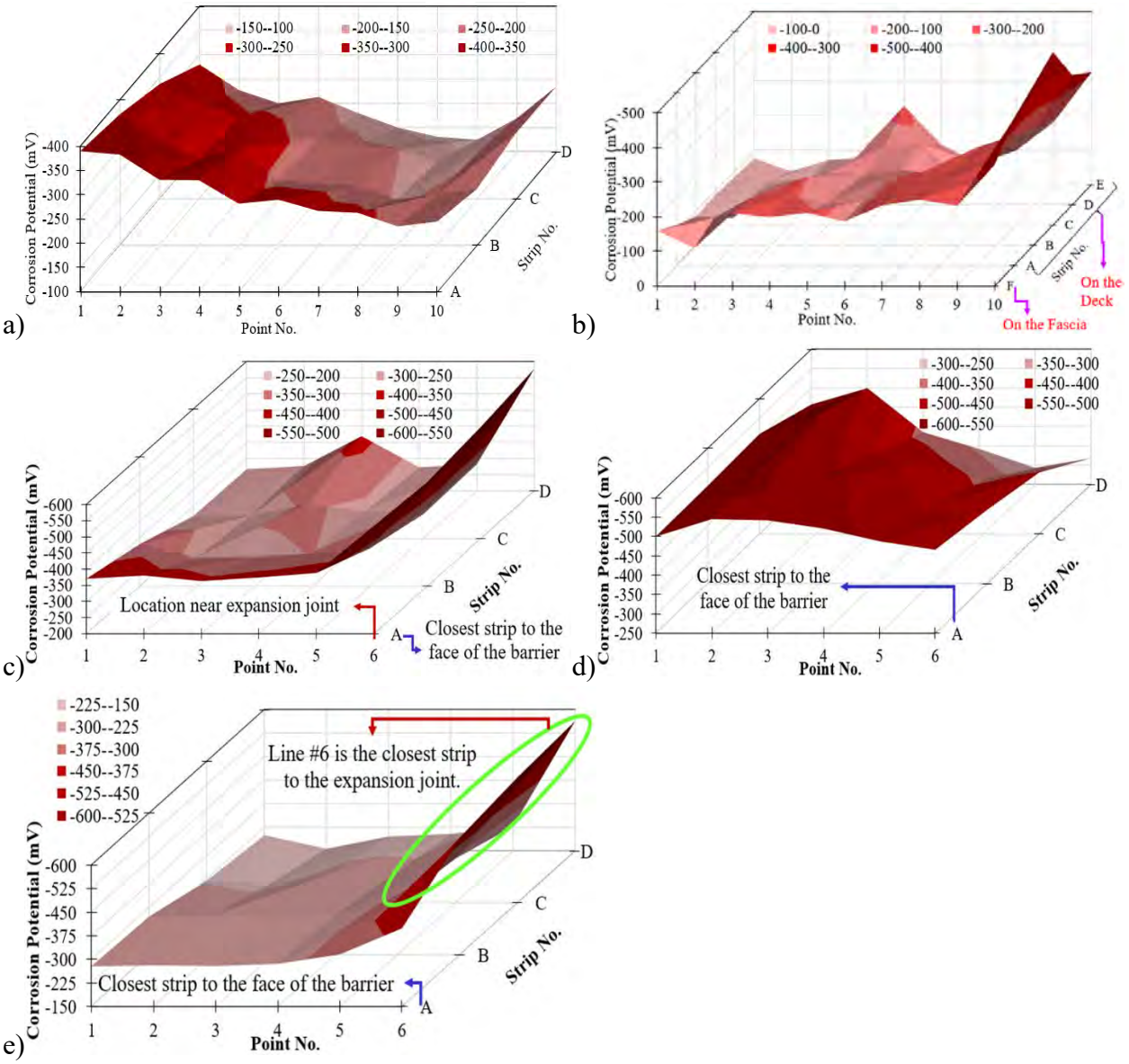

Fig. 3.31 Half-cell potentials for: a) the I-69 bridge over Fenton Road in Bay Region, b) the I-96 bridge over M-99 in University Region, c) County road over I-75, d) Waldon road over I-75, e) US 131 Ramp over W River Dr. HW

Reinforcement Section Loss Measurements

Methodology: Reinforcement section loss due to corrosion was measured in two bridges: 1) I-69 over Fenton Road, and 2) Waldon Road over I-75 using a caliper.

Results: Fig. 3.32 illustrates reinforcement section loss measurements.

Bridge on I-69 over Fenton Road in Bay Region:

In the bridge located on I-69 over Fenton Road, the diameter of corroded reinforcement in the vicinity of the deck fascia (curb) was measured on a No. 4 bar. Various measurements were taken to document various levels of corrosion. The collected data is illustrated in Fig. 3.32a. The measured diameters varied from 0.33 in. to 0.51 in. Up to a 34% section loss was observed at the highly deteriorated areas of rebar.

Bridge on Waldon Road over I-75 in Metro Region:

Similarly, section loss was measured in exposed corroded bars in the bridge located on Waldon Road over I-75. The collected data is illustrated in Fig. 3.32b. Measurements were taken on longitudinal bars along the fascia as well as U-shaped bars (herein denoted as stirrups) in the transverse direction. The size of the bars used was No. 4 and No. 6 (i.e. the uncorroded diameter is 0.5 in. and 0.75 in., respectively). Up to a 15% section loss was observed at the highly deteriorated areas of rebar.

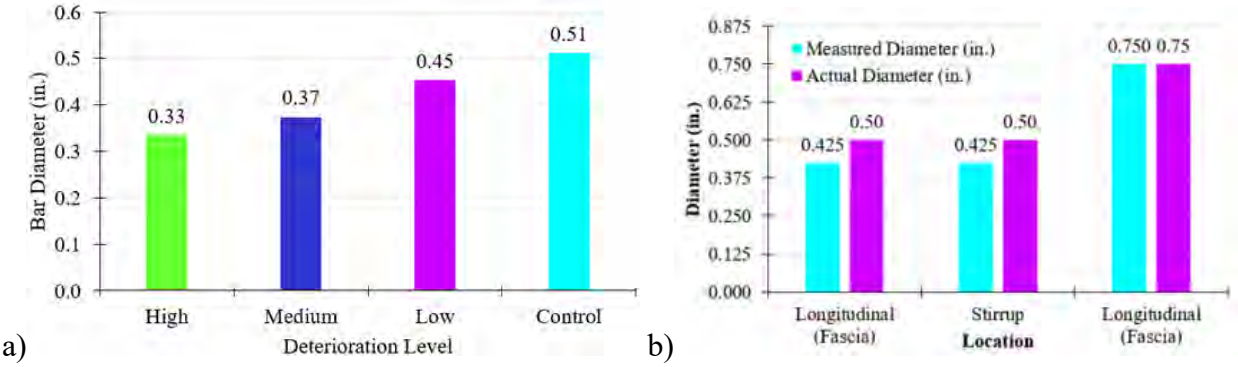

Fig. 3.32 Section loss in corroded bars: a) bridge on I-69 over Fenton Road, and b) bridge on Waldon Road over I-75

ASR Detection

Methodology: An ASR detection kit developed by researchers (Guthrie and Carey 1999) at Los Alamos National Laboratory was used to detect ASR. The kit is based on a geochemical method for staining various products of the alkali-silica reaction. The method is based on both the composition of alkali-silica-reaction (ASR) gel and one of its properties (the ability to exchange cations (a positively charged ion) with a fluid). One stain (sodium cobalt-initrite) reacts with exchangeable potassium in the gel to form a bright yellow precipitate on the gel surface. The other stain (a rhodamine compound) reacts with calcium-rich portions of the gel to form a pink-stained gel. The significance of the pink stained gel is twofold:

1) First, it can provide a high contrast to the yellow stained gel, making them easier to observe
2) Second, some rhodamine compounds react predominately with Ca-rich ASR gels.

A positive diagnosis of ASR is indicated by the presence of yellow/pink stained gel: 1) within the aggregate, 2) at the aggregate paste interface, 3) along fractures, and 4) in air voids. The technique can be used as a rapid field screening method or as a useful aid for detailed petrographic examinations. A shortened and simplified version of the procedure is provided below:

- Wet the surface of the specimen with distilled water and dry with paper towel
- Apply the yellow reagent
- Wash off the yellow reagent with distilled water and dry surface off with a towel
- Observe the surface of the specimen. Bright yellow indicates the presence of ASR
- Apply the pink reagent
- Wash off the pink reagent with distilled water and dry surface off with a towel
- Observe the surface of the specimen. Bright pink with the yellow indicates the presence of advanced ASR
- If there is no yellow or pink stain after wash off the specimen is considered to be ASR free

Results: The results of ASR testing are presented in Fig. 3.33 through Fig. 3.38.

Notes on the Bridge on I-69 over Fenton Road:

- The ASR testing was conducted on the cores obtained from the deck. The testing was conducted on the cross-section of the cores as well as along the height of the cores after

they were subject to compressive strength testing for the control and high deterioration specimens.

- Some yellow stains were observed indicating presence of ASR.
- Pink stains were observed although not necessarily with yellow stains.
- Presence of ASR is likely.

Notes on the Bridge on I-96WB over M-99:

- The ASR testing was conducted on broken concrete fragments obtained from the deteriorated barrier.
- It is assumed that barrier concrete and deck concrete are the same. Records in MiBridge database indicate that both the deck and the barrier have an f_c' = 3 ksi.
- Some yellow stains are observed at the aggregate paste interface indicating presence of ASR.
- Pink stains were observed although not necessarily with yellow stains.
- Presence of ASR is likely.

Notes on Bridge on County Road over I-75:

- The ASR testing was conducted on broken concrete fragments obtained from the deck fascia.
- No visible difference.
- Pink stains were observed although not necessarily with yellow stains.
- Presence of ASR is likely.

Notes on the Bridge on Waldon Road on I-75:

- The ASR testing was conducted on broken concrete fragments obtained from the deck fascia.
- No visible difference.
- Pink stains were observed although not necessarily with yellow stains.
- Presence of ASR is likely.

Notes on the Bridge on US 131 Ramp over W River Dr. NW:

- The ASR testing was conducted on broken concrete fragments obtained from the deck fascia.
- Some yellow stains are present.
- Pink stains were observed in general, and in some locations with yellow stains.
- Presence of ASR is likely.

Notes on the Bridge on I-94 EB over Red Arrow HW:

- The ASR testing was conducted on broken concrete fragments obtained from the deck fascia.
- There is no yellow residue after rinse off
- There is some pink residue after rinse off although this residue appears to be concentrated within the surface of the aggregate and not around the boundaries between the aggregates and paste.
- Presence of ASR does not appear likely.

a)

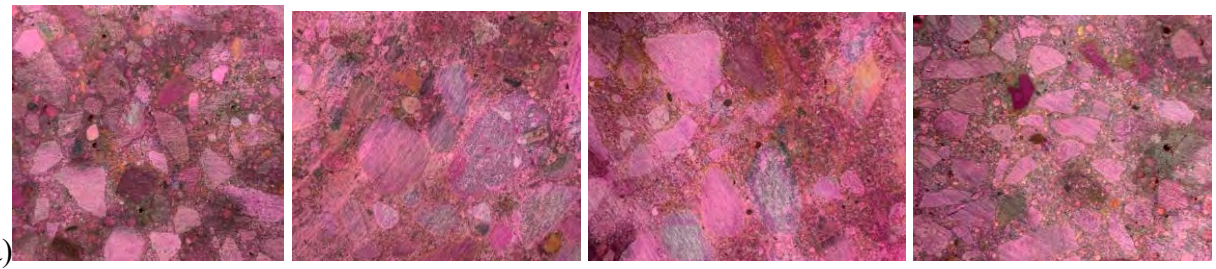

b)

Fig. 3.33 ASR test results for the cores obtained from the bridge located in Bay Region on I-69 over Fenton Road: a) at the cross-section of the cores; b) along the height of the cores after compressive strength testing

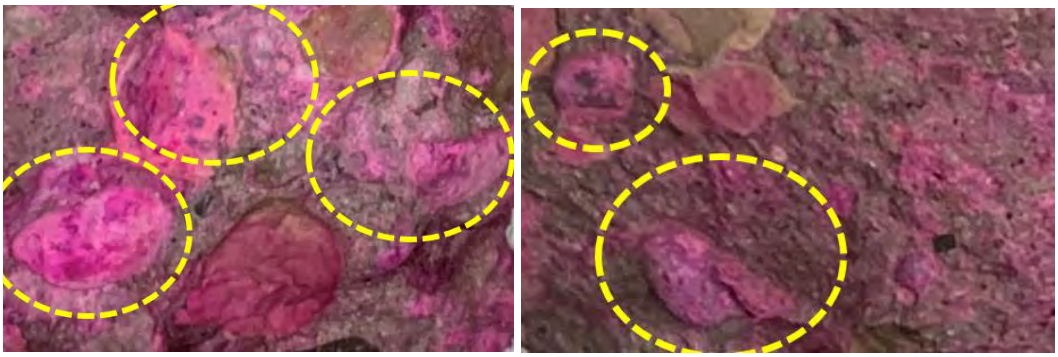

Fig. 3.34 ASR test results for the cores obtained from the bridge located in University Region on I-96 WB over M-99

Fig. 3.35 ASR test results for the cores obtained from the bridge located in North Region on County Road over I-75

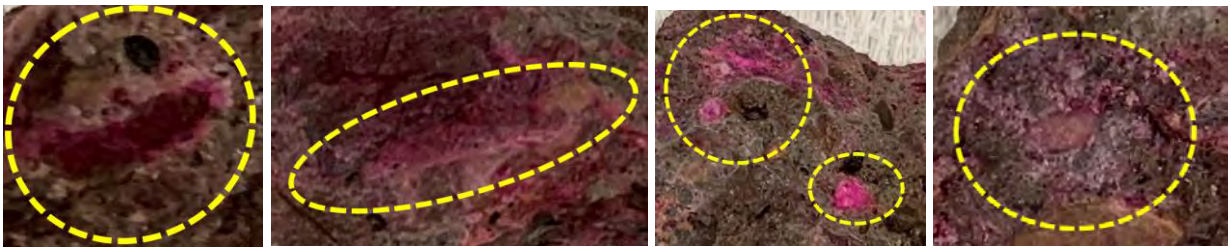

Fig. 3.36 ASR test results for the cores obtained from the bridge located in Metro Region on Waldon Road over I-75

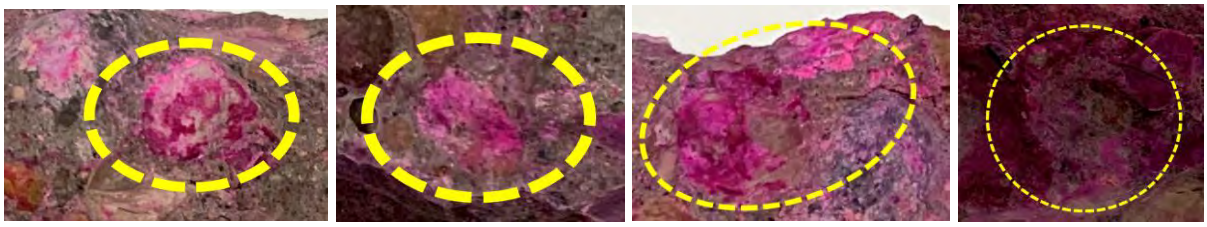

Fig. 3.37 ASR test results for the cores obtained from the bridge located in Grand Region on US 131 Ramp over W River Drive. NW

a)

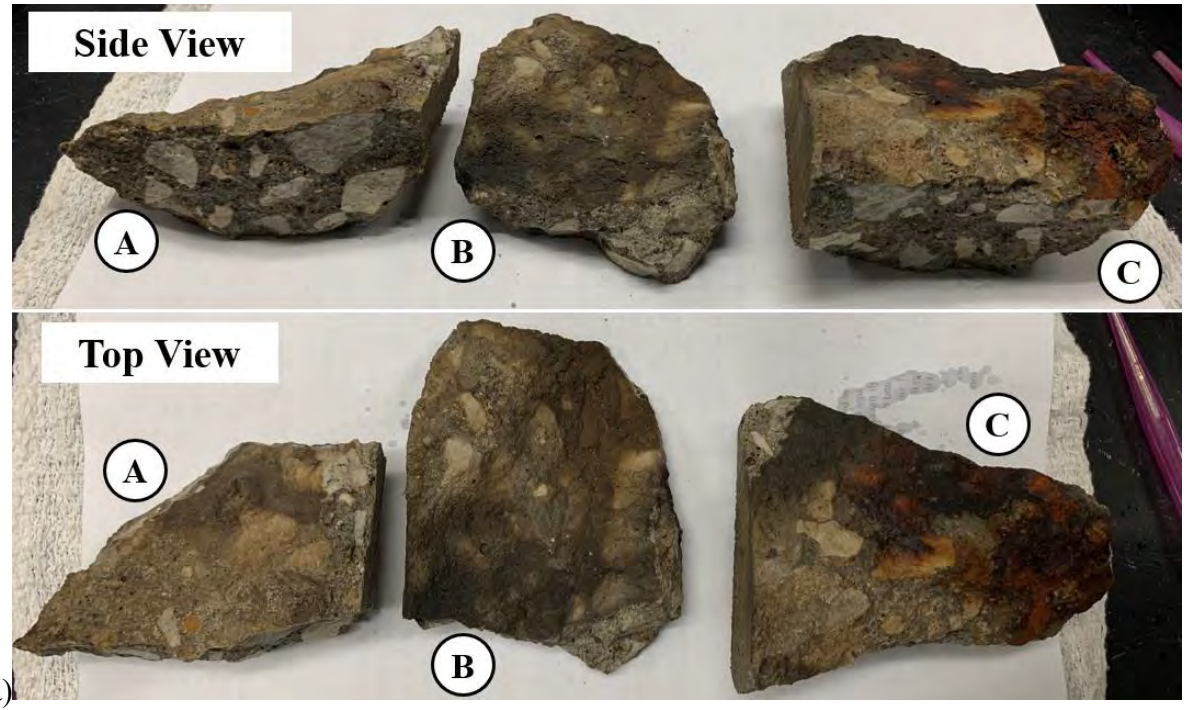

b)

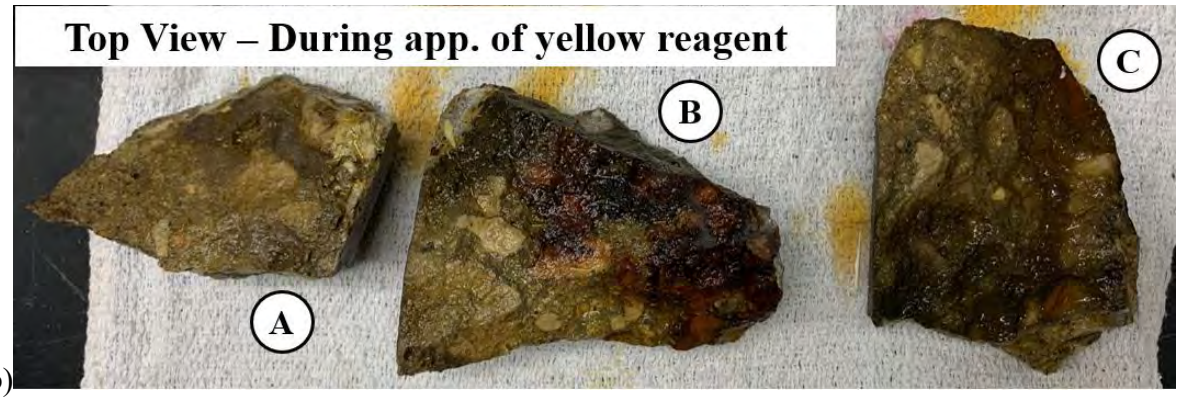
Top View – During app. of yellow reagent
A
B
C

c)

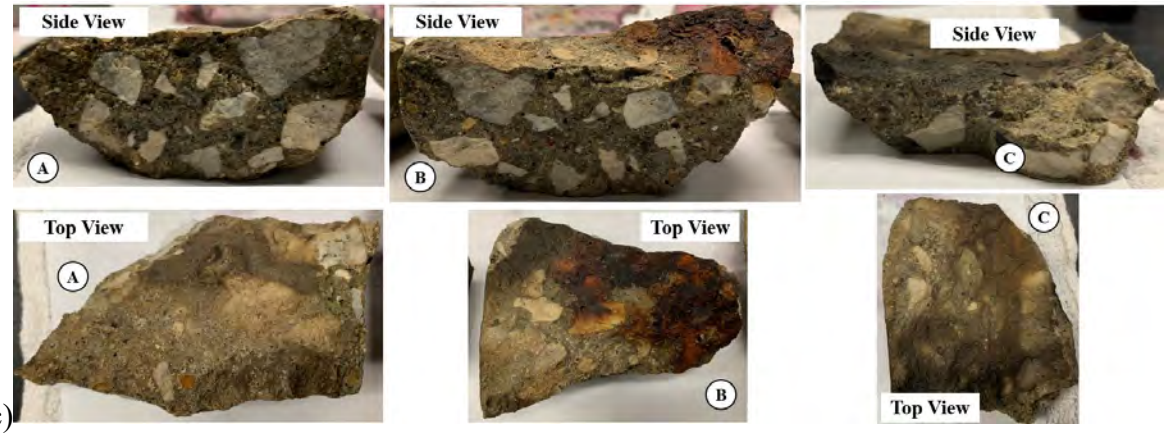
Side View
A
Side View
B
Side View
C
Top View
A
Top View
B
C
Top View

d)

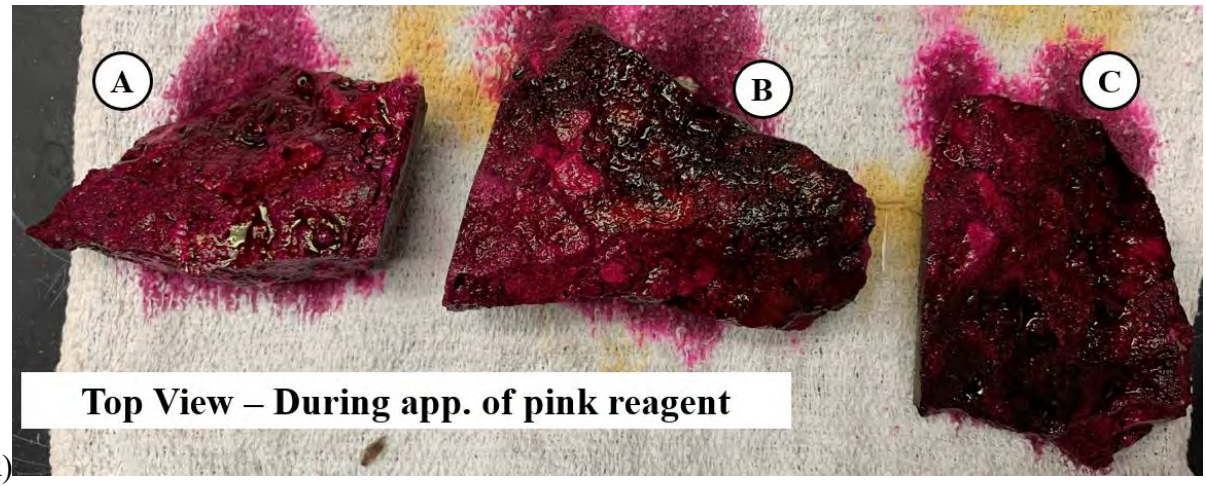
A
B
C
Top View – During app. of pink reagent

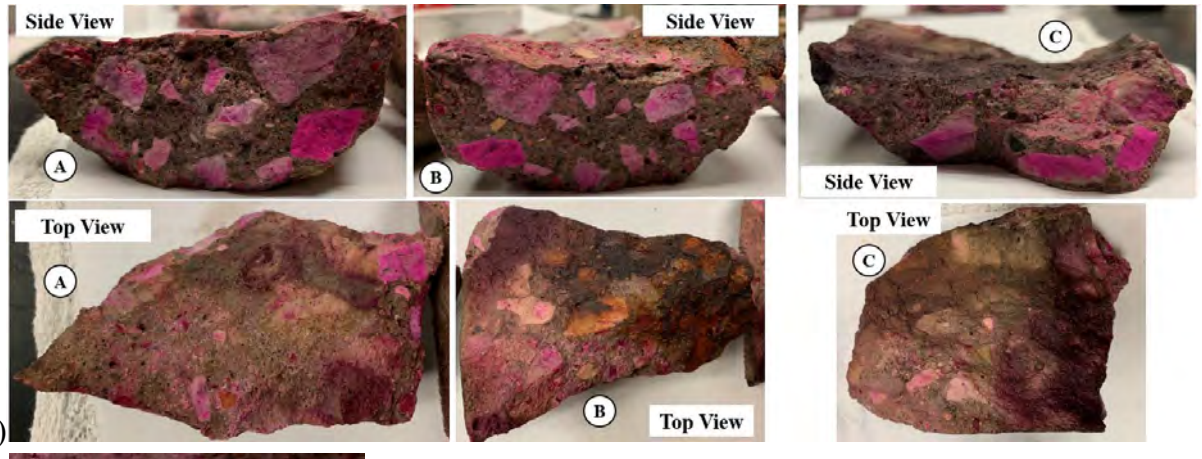

e)

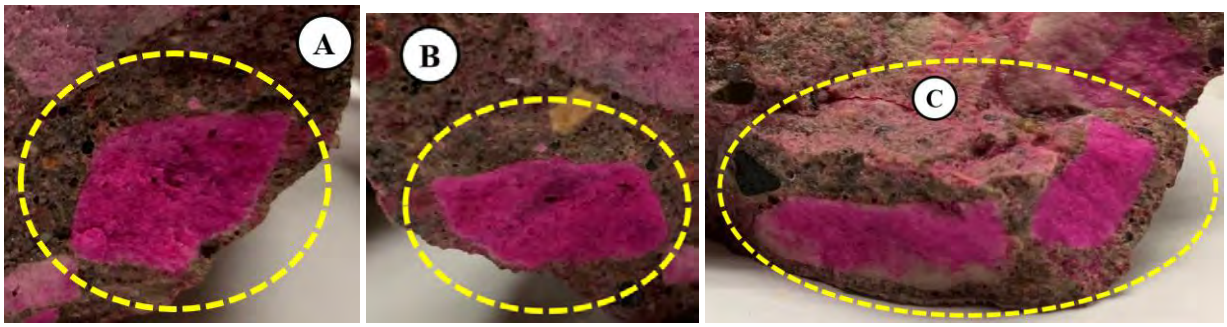

f)

Fig. 3.38 Application of ASR test kit on the concrete fragments obtained from the bridge located in I-94 EB over Red Arrow Highway (S.N. 818 & C.S. S17-11015): a) views before application of reagents; b) views during application of yellow reagent; c) views just after rinsing off the yellow reagent; d) views during application of pink reagent; and e-f) views just after rinsing off the pink reagent

3.4 Summary of Observations

The causes of deck fascia deterioration as determined by the examination of bridges that exhibited this phenomenon are summarized below:

1) Low Grade Concrete: The majority of the bridges that featured deteriorated deck fascias consisted of low-grade deck concrete with an f_c'=3000 psi at 28 days. This is below the ACI 318-19 (ACI 2019) requirements for concrete used in severe environments which refer to a concrete with an f_c'= 5000 psi or greater. The current specification in Michigan, regarding deck concrete refer to a high performing mix with an f_c'= 4,500 psi. This is a significant improvement from past practice. However, it is still 500 psi lower than that required by ACI 318-19 (ACI 2019). Since none of the investigated bridges contained deck concrete with f_c' = 4,500 psi, it is not clear whether this 500 psi difference is another cause for the deterioration of deck fascias. Naturally, a higher performing mix will lead to better future performance and longevity in terms of better durability

against freeze-thaw deterioration since permeability is reduced, and better resistance to corrosion induced spalling since the tensile strength of concrete is higher.

2) Increased Moisture Content: It was observed that a large number of bridges that featured deck fascia deterioration contained fencing, open barriers, and sidewalks. The presence of fencing results in an increased moisture content in the deck fascia due to precipitation induced moisture traveling down the deck fascia from the fencing. The open barriers and elevated sidewalks also lead to increased moisture content in the deck fascia. There was clear evidence of standing water near the barrier, or higher moisture content after a precipitation event for many of the bridges investigated in the field. Moisture content recorded during many of the field investigations was higher along the deck fascia compared to the rest of the deck surface. Efflorescence was noted in many of the field investigations, providing further evidence for higher moisture content along the deck fascia. Improved drainage is one option for reducing the moisture content along the deck fascia. Several approaches for how to reduce moisture content in the deck fascia are presented in the next chapter.

3) Corrosion of reinforcement: Almost all identified bridges with deteriorated deck fascias featured uncoated corroded deck reinforcement, and were built prior to the 1980 mandate to use corrosion resistant reinforcement. The 1980 mandate appears to have addressed the corrosion issue since only a few bridges with deteriorated facias contained corrosion resistant steel. For the investigated bridges, active corrosion was found through visual inspection, reinforcement section loss, and half-cell potential tests along the fascia as well as in the deck near the fascia region. It is recommended that the practice of using epoxy coated reinforcement or other types of corrosion resistant reinforcement be continued.

4) Inconsistencies in concrete clear cover: For the investigated bridges, inconsistencies in clear cover were observed. Measured clear cover was in some locations smaller than what is recommended for concrete exposed to deicing salts in AASHTO LRFD (2020). In addition, for many of the investigated bridges, the recorded clear cover along the deck fascia was lower than that recorded on the deck surface and lower than minimum specified in AASHTO LRFD (2020).

This can be resolved by enforcing the implementation of current details in the field through thorough inspections.

5) Alkali-Silica-Reaction (ASR): The presence of ASR is considered likely based on field data. This issue appears to have been addressed in terms of controlling ASR in new construction. In approximately 2012, MDOT implemented specifications to avoid ASR. Examples include:

- Special Provision for Alkali Silica Reactivity of Fine Aggregate Used in Portland Cement Concrete
- Special Provision for Quality Control and Acceptance of Portland Cement Concrete (For Local Agency Projects Only)
- Construction Specifications: Section 1003. Quality Assurance (Acceptance) for Concrete
- Construction Specifications: Section 902. Aggregates

The bridges exhibiting deck fascia deterioration and considered as part of this research were mostly constructed prior to 1980s.

6) Slope of the Deck: The slope of the deck is a contributing factor to the deterioration of deck fascias. The lower side of the deck features typically higher deterioration.

7) Traffic Volume: Traffic volume on or below the bridge appears to be related to deck fascia deterioration (i.e. the higher the traffic the higher the deterioration). Most bridges with deteriorated fascias were located on or above an interstate/state highway.

Chapter 4: Development of Preliminary Alternative Repair Details and New Construction Details

Chapter 4: Development of Preliminary Alternative Repair Details and New Construction Details

The observations presented in the first three chapters suggest that the relatively higher moisture content present in the deck fascias and the corrosion of reinforcement have led to their deterioration. The introduction of epoxy coated steel has addressed the corrosion aspect of such deterioration. A repair detail is presented for addressing existing bridges in which the intervention is limited to the repair of the deck fascia without any removal of the existing elements. For cases with deck fascias that feature a low level of deterioration, the application of polyurea is suggested based on research conducted by Miller et al. (2017; 2020). Additional information on the use of polyurea on bridge barriers is presented by Miller et al. (2017; 2020).

Several approaches are presented to reduce moisture content in the deck fascia region in new bridges and in those in which the entire deck overhang is replaced. The overview of the proposed approach for the evaluation of existing bridges with deteriorated deck fascias is presented in Fig. 4.1. The evaluation starts with a visual inspection. Then the characterization of the deterioration of the deck fascia is conducted in terms of deteriorated length (longitudinal direction) and width (transverse direction). The deterioration is then idealized in terms of an average deteriorated length and width. This information is entered into the MDOT Barrier Program, which is capable of evaluating the capacity of the barrier and deck overhang. If the crashworthiness of the barrier is undermined the deck fascia should be repaired. Alternatively, the deck overhang and barrier may be replaced. If the crashworthiness of the barrier has not been undermined, the deck fascia may be scaled to avoid the falling off broken fragments of concrete. Alternatively, polyurea may be applied after the scaling process has been completed to avoid further deterioration. Information regarding the efficiency of polyurea as a protective coating on bridge barriers is provided by Miller et al. (2017; 2020). Additionally, information regarding the application of polyurea is provided by various manufacturers. Should this option be chosen, appropriate training and resources should be pursued by contacting the manufacturer.

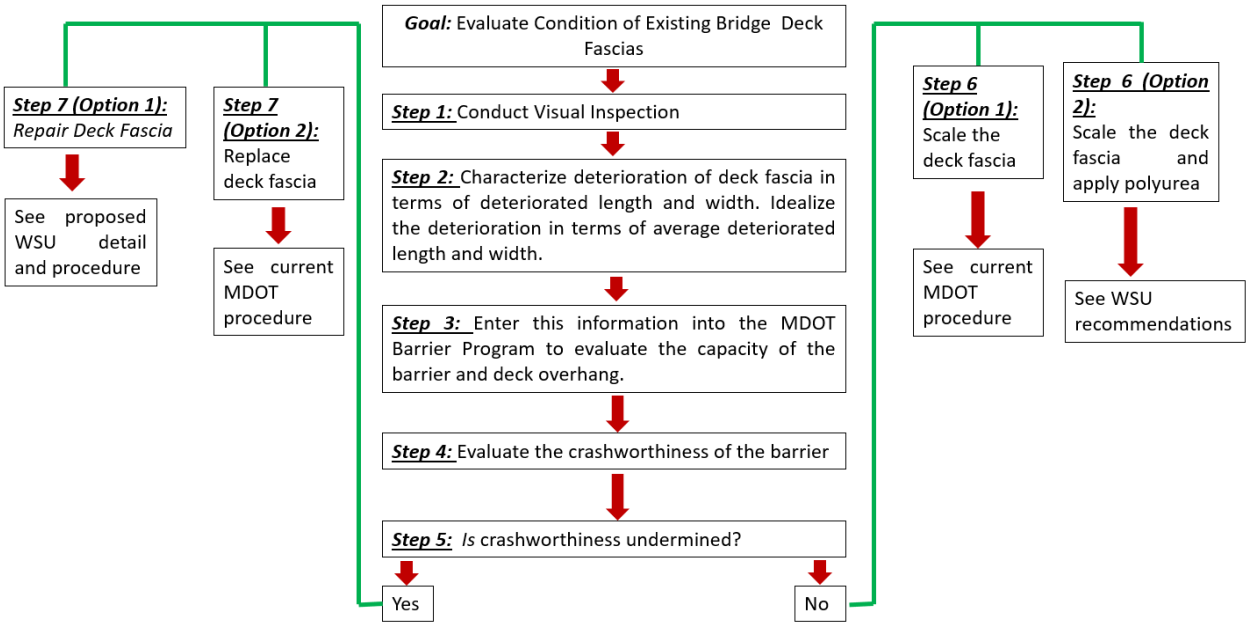

Fig. 4.1 Overview of the proposed approach for the evaluation of existing bridges with deteriorated deck fascia

4.1 Restoration of Original Geometry and Strength - Proposed Repair Detail

The proposed repair detail is shown in Fig. 4.2 and features a repair cementitious composite, and corrosion resistant reinforcement, which is drilled and epoxied in the existing deteriorated deck fascia. The goal of this repair is to restore the original geometry and strength of the deck to barrier connection. This repair detail is appropriate in cases of medium to severe deck fascia deterioration. The intervention is limited to the repair of the deck fascia without any removal of the existing elements. In addition, the repair detail is appropriate for cases where the crashworthiness of the barrier is compromised. This repair detail requires the installation of formwork similar to that used when constructing the deck overhang. Depending on the flowability of the selected repair concrete material, the width of the ledge can be selected such that it is greater than or equal to the value shown in Fig. 4.2 and that the repair concrete material is placed through discrete inclined pockets, the spacing of which can be determined based on the flowability of the mix. Alternatively, the width of the ledge can be increased so that the repair concrete material is placed along the length of repair region. The increase in the width of the ledge is beneficial because it provides sufficient space for the dowels to develop their yield stress especially when considering the reduction in development length due to the presence of epoxy coating. The forces that will be present in the repaired region will be those stemming from the self-weight of the barrier and vehicle impact.

Vehicle impact will create shear and moment at the barrier to deck connection. The moment can be resolved into a compressive and tensile force. The repaired region will be subjected to the compressive force, which will induce shear at the interface. The capacity of the repair interface can be checked using shear friction theory, which is founded on the idea that as the two interfaces try to separate (or shear off) the dowels provide a clamping action (i.e. a normal force), which together with an assumed coefficient of friction result in the shear resistance of the interface. It is therefore important that the dowels be developed on both sides of the interface.

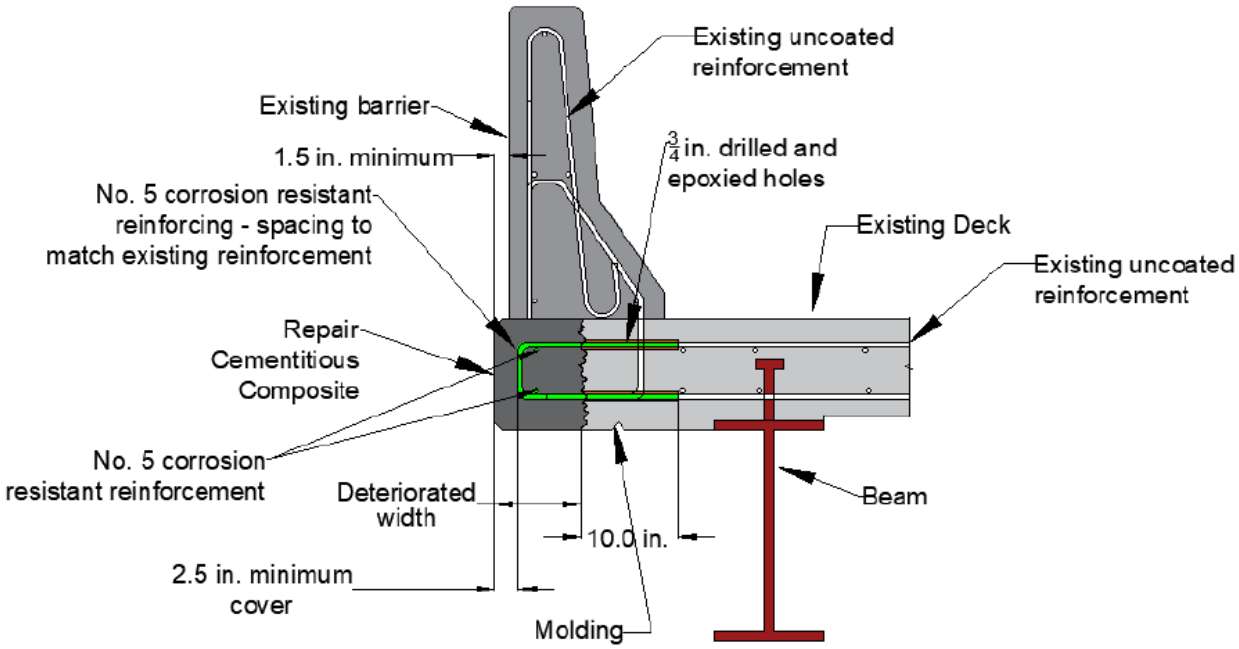

Fig. 4.2 Proposed repair detail for deck fascias with medium to sever deterioration

4.1.1 Repair Cementitious Material Selection

Several options were considered for the repair cementitious composite. Since cracking-induced spalling is fundamentally an issue of insufficient tensile strength, the ability of the cementitious mix to exhibit sustained tensile strength after the first crack is considered instrumental. If a fiber reinforced cementitious composite is used, such sustained tensile strength can be realized through fiber bridging action, which prevents concrete from falling and facilitates stress redistribution. Similarly, low permeability is essential to reduce the penetration of water and the creation of expansive forces due to freeze-thaw cycles as well as potential continued corrosion of dowels protruding from the deck fascia. Finally, flowability is important since the repair is desired to be implemented without removing the barrier. Several options for the repair concrete material were

discussed with MDOT during the first progress meeting. It was pointed out that one option is to select a repair concrete material that is not necessarily indestructible or provides the best performance but one that provides reasonable performance and is more economical. The presented rationale for this is that there will be other areas of the bridge superstructure such as the barriers, expansion joints, and perhaps the deck region near the fascia that will require eventual replacement of these elements. Therefore, in some cases there may be little motivation to select the best performing and perhaps the most expensive repair material, if these regions will soon be replaced. On the other hand, if no replacement of the deck overhang and barrier is anticipated in the foreseeable future, it would be helpful for the repair detail to perform well for a relatively long period of time. Considering these contrasting views, multiple options were considered, so that the appropriate concrete repair material may be chosen for a specific application. The considered materials include: 1) Ultra High Performance Concrete (UHPC), 2) Fiber Reinforced Concrete (FRC), 3) Self-Consolidating Concrete (SCC), and 4) Latex Modified Concrete (LMC). Each are discussed below.

1.0 Ultra High Performance Concrete (UHPC)

One option is to use an ultra high-performance concrete (UHPC) mix, which possesses low permeability, high sustained tensile strength, high resistance to freeze-thaw cycles, excellent flowability and overall excellent durability (Russel and Graybeal 2013). The idea of using UHPC in highly distressed areas is not new and has been implemented by various states in joints between precast deck panels (Graybeal 2014), deck overlays (Haber et al. 2018), and steel beam ends as a repair material (Zmetra et al. 2017; Mcullen and Zaghi 2020) to reinstitute the original strength. To date, in the United States, nearly 200 bridges in 27 states and the District of Columbia have been constructed using UHPC materials, and 93% of these projects used UHPC for prefabricated bridge element connections (Haber and Graybeal 2019).

UHPC Mix Design

Various nonproprietary mixes for UHPC exist including formulations developed for MDOT (El-Tawil et al. 2020) as shown in Table 4.1. The cost of nonproprietary UHPC varied from \$567-\$697/yd^3 in 2019 (El-Tawil et al. 2020). When the fibers were domestically sourced, the cost of the mix including fibers ranged from \$726 to \$856/yd^3 in 2019. When a direct cost comparison

between UHPC and normal strength concrete (NSC) is made, which herein is assumed to cost $120/yd^3, the cost of UHPC materials is about 6 times higher. However, material cost is only a fraction of the total cost of a construction project, which includes mobilization, formwork installation (reported to be 40% of the total cost in CIP concrete applications), placement of reinforcement, transportation, overhead, etc. In addition, the benefit of UHPC is in the long-term maintenance where UHPC exhibits superior performance compared to NSC. In any case, the potential for cost benefits when using UHPC has been demonstrated by various studies and decisions about the use of this material should not be based solely on a direct material cost comparison.

Table 4.1 Various UHPC Mix Designs (El-Tawil et al. 2020)

Ingredients	Mixture* and Ingredient Amount (lbs/yd^3)			
	A	B	C	D
Ordinary Portland Cement Type I	653			
Slag cement	653			
Fine sand[a]	398	396	395	394
Coarse sand[b]	1590	1586	1582	1577
Silica fume	327			
Water	276	272	268	264
HRWRA[c,d]	20	26	33	39
Steel fibers[e]	265			
w/cm	0.17	0.17	0.16	0.16

*Mixtures A, B, C, and D have HRWRA dosages of 1.5, 2, 2.5, and 3%, respectively.
[a]Grain sizes 80 to 200 microns.
[b]Grain sizes 400 to 800 microns.
[c]Polycarboxylate ether-based HRWRA.
[d]HRWRA dosage rates can be adjusted to meet the paste flowability requirements. Dosages vary with the type of silica fume and range from 1.5 to 3.0% by weight of the cement.
[e]Steel fibers are 2% by volume.

UHPC Production

UHPC can be produced using grout mixers onsite or using ready mix trucks. It appears that MDOT has experience with using UHPC using ready mix trucks, which should further simplify UHPC production, delivery and placement.

UHPC Placement

It is envisioned that the proposed repair details will require the installation of formwork on the bottom and side of the deck fascia. The construction and installation of such formwork is similar to that used for deck overhang construction in new bridges. To successfully place UHPC such that the original geometry of the fascias is restored and that no air voids are created, two options can be pursued. In Option 1, a large enough ledge is created at the top of the deck fascia so that UHPC can be placed anywhere along the length of the bridge. This helps with fully developing the yield strength of the drilled and epoxied dowels because the width of the ledge (see Fig. 4.2) can be determined such that this is accomplished. In Option 2, the width of the ledge is kept small, and the inclined pockets are installed at a certain spacing to facilitate the placement of UHPC. In this option, UHPC would spread longitudinally using its self-consolidating properties. The width of the ledge can still be used to confirm a successful UHPC placement.

From discussions, during progress meetings, it was determined that because of the cost of UHPC there was little interest in pursuing it as a repair material for bridge deck fascias.

2.0 Fiber Reinforced Concrete (FRC)

Another repair material that was considered is fiber reinforced concrete (FRC), which does not meet the definition for UHPC (which includes a minimum limit on compressive strength) but still possesses a high sustained tensile strength, which can be maintained after the first crack through fiber bridging action. FRC does not have equivalent permeability, tensile strength and flowability with UHPC. but it provides sustained tensile strength.

FRC Mix Design

Mix formulations for fiber reinforced concrete are available in the literature (ACI 2008). Table 4.2 shows four such mix designs.

The first mix was used by Kassimi et al. (2014) and is a steel fiber self-consolidating concrete mix with 0.5% by volume fiber content.

The second was also used by Kassimi et al. (2014) and is a steel fiber self-consolidating mortar with 1.4% fiber content. These mixes were selected because of their self-consolidating nature, which is an important characteristic given the tight space that the repair material needs to

flow through. The combination of fibers and the self-consolidating nature of the concrete mixtures makes them suitable for this application. The compressive strength at 28 days varies between 7.4-7.5 ksi, which makes them a more affordable option compared to UHPC. The self-consolidating property is facilitated by the use of high range water reducing admixtures (HRWRA) and viscosity modifying admixtures (VMA). The mixtures feature splitting tensile strength in the range of 0.86-0.97 ksi, which is a desired property for such repairs since it helps with containing any broken concrete fragments. In addition, these two mixes were used for repair applications. Mix B features a high drying shrinkage and is not considered appropriate. Therefore, Mix A is proposed for inclusion with certain modifications outlined in the subsequent sections.

The third mix is obtained from Banthia and Bindiganavile (2001). This mix features a compressive strength at 28 days of 6.5 ksi. It meets the ACI 318-19 (ACI 2019) requirements for severe environments, which requires the compressive strength to be at least 5 ksi. The mix features macro as well as micro fibers. This mix was considered appropriate since it was intended for repair applications. However, the mix features a slump of 3 in., which is too stiff for the repair of bridge deck fascias.

The fourth is a mix provided by the MDOT Research Administration Panel (RAP) and features a design strength of 3500 psi. One common conclusion drawn from the literature review is that one of the reasons why deck fascias are deteriorating is the exposure to high levels of moisture and the inability of low-grade concrete to provide the necessary durability against freeze-thaw cycles and corrosion. Since ACI 318-19 (ACI 2019) requires at least a concrete with f_c'=5000 psi for severe environments, this mix is not considered appropriate as is and is proposed for inclusion with certain modifications as outlined in the subsequent sections.

Table 4.2 FRC Mix Design

Ingredient	Amount (lbs/yd^3 – unless otherwise noted)			
	Mix A – Kassimi et al. (2014) S-SCC-0.5	Mix B - Kassimi et al. (2014) S-SCM-1.4	Mix C – Banthia and Bindiganavile (2001)	Mix D - MDOT
Portland Cement (PC)	Type I - 561	Type I - 786	548	Type I - 395
Fly Ash	-	-	103	-
Silica Fume	40	56	27	-
GBFS	200	281	-	-
Slag Cement	-	-	-	169
Fine Sand	1371	1912	1104	1264
Intermediate aggregate	-	-	-	1737 < 1/2 in.
Coarse Aggregate	1256 < 0.39 in.	-	<14 mm (0.5 in.) 1931	-
Water	337	472	246	254
HRWRA	4.19 L/m^3	4.68 L/m^3	2.53	
WRA	-	-	-	13.0 oz/100wgt
VMA	128 mL/m^3	128 mL/m^3		
Air Entraining Ad.	25 mL/m^3	25 mL/m^3	-	0.65 oz/100wgt
Steel Fibers	0.5% by volume	1.4% by volume	65 - (Macrosteel) (0.5% by volume) 65 - (Microsteel) (0.5% by volume)	45 -Helix Uncoated
w/cm	0.42	0.42	0.36	0.45
Properties				
f'_c (ksi)	7.4	7.5	6.5	Design – 3.5
f_{ct} (ksi)	-	-	-	-
f_{tu} (ksi)	0.86	0.97	-	-
E (ksi)	3843	2973	-	-
Slump (in.)	-	-	3 in.	Design < 7
Air Content %	6.4	8.5	6	Design - 6.5
Drying Shrinkage ($\mu\varepsilon$)	645	1260	-	-

3.0 Self-Consolidating Concrete (SCC)

A third option was high strength self-consolidating concrete without fibers. A drawback of this material is its inability to provide sustained tensile strength after the first crack. While this is an important capability to lose, the relatively higher tensile strength than existing low-grade deck concrete, high flowability, combined with corrosion resistant reinforcement may make it a suitable option.

SCC Mix Design

Various SCC mix designs are shown in Table 4.3. These mix designs were obtained from ACI 237R-07 (ACI 2007) and were used on various projects. The compressive strengths at 28 days vary from 6000 psi to 9000 psi, which makes them a suitable option for the repair because they represent high strength and yet affordable formulations compared to UHPC. The self-consolidating nature is facilitated through the use of high range water reducing admixtures (HRWRA), water reducing admixtures (WRA), and viscosity modifying admixtures (VMA).

It is recommended that either Mix B or Mix E be pursued for testing of the repair detail since they feature smaller size coarse aggregates, which is desired because of the limited space to place the repair concrete material.

Table 4.3 Mix designs for SCC (ACI 2007)

Ingredients	Mixture and Ingredient Amount (lbs/yd^3)				
	Mix A[a]	Mix B[b]	Mix C[c]	Mix D[d]	Mix E[e]
Cement (lbs/yd^3)	530	390	639	750	880
GGBFS/Fly ash (lbs/yd^3)	120	260	113	-	-
Coarse Aggregates (lbs/yd^3)	(No. 57 < 1 in.) 1152 (No. 89 < 3/8 in.) 542	(No. 67<3/4 in.) NA	(No.57< 1 in.) NA	(No.57<1 in.) 1000 (No. 8<3/8 in.) 500	-
Fine Aggregate (lbs/yd^3)	1277	-	-	1500	Crushed aggregate (5-10 mm)
Water	279.5	305.5	300.8	300	369.6
HRWRA (fl oz/cwt)	15	8	9	12	4.4
WRA (fl oz/cwt)	1.5	-	-	-	2
Set accelerator (fl oz/cwt)	-	-	12	-	-
VMA (fl oz/cwt)	3.0	-	4 gal./yd^3	1.5	9.2
w/cm	0.43	0.47	0.4	0.4	0.42
Properties					
Slump flow (in.)	28	24	22	26	25
Compressive strength (psi):	24 hours -1800 30 hours - 2500 28 days -7460	28 days - 6000	13 hrs – 4000 28 days > 7200	3 days – 6600 28 days - 9000	24 hrs-870 7 days – 3700 28 days - 6100
Unit weight (lb/ft^3)	-	148	148	-	-
Air Content (%)	-	6.0	5.5	-	1

[a]Project location: Pedestrian Overpass (I-4), Seminole Country, Orlando, Fla.
[b]National Museum of the American Indian, Washington, D.C.
[c]Double-Tee Production, Nitterhouse Concrete Products Inc., Chambersburg, Pa.
[d]Rosenthal Center for Contemporary Arts, Cincinnati, Ohio
[e]University of Sherbrook Strong Wall

4.0 Latex Modified Mix

A latex modified mix was proposed for consideration by the Research Administration Panel (RAP). This mixture is typically used for patching structures where the depth of the patch is greater than 1.5 in.

Latex Modified Mix Design

The mix design for the proposed latex modified mix is provided in Table 4.4. The coarse aggregate size is smaller than ¾ in., which is considered appropriate for the limited space of the repair.

Table 4.4 Latex Modified Concrete Mix Design (Denoted C-L in Table 1006-1 MDOT 2020 Construction Specifications MDOT 2020b)

Ingredients	Amount (lbs/yd^3)
Type I Cement	658
Coarse Aggregate	1458 < 3/4 in.
Fine Aggregate	1348
Net Water	169
Latex Admixture	143
w/cm	0.25
Properties	
Air Content %	4.5+/-1.5

5.0 Proposed Cementitious Composite Mixes

The four mixes proposed for the repair cementitious material as well as the host material representing deck concrete are provided in Table 4.5. Specimens created using these mixes were subjected small-scale tests as described in the next chapter to characterize material response, durability, and reinforced shear strength. The criteria for repair mix selection was as follows:

1) The repair material had to be stronger than the host material and feature a minimum compressive strength of 5 ksi at 28 days to be consistent with ACI 318-19 (ACI 2019) requirements for concrete used in severe environment;

2) The repair material had to feature a w/cm smaller than 0.5 to be consistent with ACI 318-19 (ACI 2019) requirement for concrete used in severe environment;

3) The repair material had to feature a maximum aggregate size smaller than 3/8 in. to facilitate placement in tight spaces;

4) The repair material had to feature good flowability to facilitate placement.

The criteria specified above was met by making the following general and specific modifications to the mixes presented in the previous sections. To simplify mix design, all mixes feature fly ash as the supplementary cementitious material. The maximum aggregate size for all mixes is smaller than 3/8 in.

The mix design for the host material representing deck concrete in the repair specimens was provided by MDOT. Portland Cement Type IL was used to reflect current trends in the concrete industry as well as current practices in some MDOT projects. The fine, intermediate, and coarse aggregates were obtained from prequalified MDOT aggregate suppliers.

FRC (MDOT) Modified

The fiber reinforced concrete (FRC) mix provided by MDOT was modified such that the cement content was increased to yield a higher compressive strength to meet criteria No. 1. The water content was also slightly increased to maintain workability by maintaining a water to cementitious materials ratio of 0.40. In addition, the maximum aggregate size was decreased from ½ in. to 3/8 in. The original mix design featured a design compressive strength of 3.5 ksi.

FRSCC (Kassimi et al. (2014) S-SCC-0.5 Modified)

The fiber reinforced self-consolidating concrete (FRSCC) mix tested by Kassimi et al. (2014) S-SCC-0.5 and labeled as SCC-0.5 was modified such that the supplementary cementitious material features fly ash. The maximum coarse aggregate size was limited to 3/8 in., and the volumetric fiber content was increased to 1.0%, from 0.5%, to provide enhanced sustained tensile strength. The amount of high range water reducing admixtures and viscosity modifying admixtures were adjusted based on trial and error to supply a mix that represented FRSCC and with the desired plastic properties.

SCC (ACI 2007) Mix A - Modified

This mix was primarily based on the SCC (ACI 2007) Mix A presented in the previous section. The only modification is that in the proposed mix, the maximum size of the coarse aggregate is smaller than 3/8 in., whereas in the original mix there were two types of coarse aggregates (No. 57 and No. 89).

Latex Modified Concrete (MDOT) Modified

The only change in the Latex Modified Concrete mix provided by MDOT was that the maximum coarse aggregate size was limited to 3/8 in. rather than ¾ in. The latex material is Trinseo Modifier A/NA latex.

Table 4.5 Selected cementitious composite mixes for use in small-scale laboratory testing

Ingredient	Amount (lbs/yd^3 – unless otherwise noted)				
	Host Material	Repair Material			
		FRC	FRSCC	SCC	LMC
Portland Cement (PC) (Type IL)[a]	500	523	610	543	710
Fly Ash (Class F)[b]	180	175	254	178	-
Fine Agg. (Type 2NS)[c1]	1290	1344	1367	1254	1400
Int. Agg. (26A mod.)[c2]	295	-	-	-	-
Coarse Agg. (6AA/29A)[c2]	1390	1644	1252	1672	1500
Water	300	275	354	296	185
HRWRA (UltarFlo 2000)[d]	-	3.74 oz/cwt	14.78 oz/cwt	21.51 oz/cwt	-
MRWRA (Optiflo Plus)[d]	3.68 oz/cwt	-	-	-	-
WRA (Optiflo 500)[d]	2.57 oz/cwt	16.81 oz/cwt	-	4.33 fl oz/cwt	-
VMA[d]	-	-	0.40 oz/cwt	2.84 fl oz/cwt	-
Air Ent. Ad. (Eucon AEA-92)[d]	1.10 oz/cwt	0.64 oz/cwt	0.08 oz/cwt	-	-
Latex Ad. (Trinseo Mod. A/NA)[e]	-	-	-	-	150
Steel Fibers[f]	-	65.7 (0.5% by volume)	131.1 (1 % by volume)	-	-
w/cm	0.44	0.39	0.41	0.41	0.26/0.47[g]

[a]Type IL Cement was donated by Lafarge Holcim located in Detroit, MI.
[b]Supplied by Diversified Minerals Inc.
[c1]Fine aggregates denoted as 2NS were donated by TRP Sand & Gravel, which is a pre-qualified MDOT aggregate supplier. Fine aggregates were in a bulk-dry condition.
[c2]Intermediate, and coarse aggregates denoted as 26A (mod.) (≤1/2 in.) and 6AA (≤1 in.)/ 29A (≤3/8 in.) were donated by EDWC Levy located in Dearborn, MI, which is a pre-qualified MDOT aggregate supplier. Intermediate and coarse aggregates were in a saturated surface dry condition.
[d]Donated by Premiere Admixtures
[e]Donated by Modified Concrete Suppliers, LLC
[f]Supplied by HiPer Fiber (0.2 mm diameter and 13 mm long brass coated steel fibers)
[g]w/cm is given without and with latex admixture, respectively.

4.1.2 Repair Reinforcement Material Selection

In terms of the repair reinforcement material (dowels) it was recommended by the RAP to consider using epoxy coated reinforcement since that is the default reinforcement type for bridge decks. It was also recommended to limit the dowel size to No. 3 and No. 4 bars to reduce the likelihood of cracking during the drilling process.

4.1.3 Surface Preparation

The proposed general surface preparation procedure is based on the recommendation presented by Emmons (1993) and cover the following five steps:

Step 1: Identify the extent of deck fascia to be repaired. Hammer soundings can be used to identify delamination and determine the extent of concrete removal in the transverse direction. In the direction of the deck thickness, it is recommended that the entire deck fascia concrete is removed in areas identified for repair (i.e. a full depth removal). If corroded reinforcement is encountered, any heavily corroded reinforcement should be fully exposed by additional concrete removal. If it is determined that heavily corroded reinforcement surpasses the footprint of the barrier, deck overhang and barrier replacement should be considered. Simplify the layout of the repair region as the deterioration of concrete surfaces is typically not uniform. The removal layout should be designed to minimize boundary edge length as excessive or complex edge conditions result in differentia shrinkage stress concentrations and cracking. The overall stability of the barrier should be investigated prior to deck fascia concrete removal, and if needed, a temporary support system should be installed.

Step 2: Remove deteriorated concrete using acceptable methods. Such methods include: a) pneumatic chipping hammers, and b) hydrodemolition. The 15# to 30# class chipping hammers are the most common removal tools for surface repair. To facilitate the use of chipping hammers, a temporary supporting structure or an articulating boom should be provided to offer a safe working platform for the operator. The 15# hammer is light enough for use on vertical surfaces such as the deck fascia. Chipping hammers heavier than 30# have the potential to damage reinforcing steel and should be avoided. Electric and hydraulic chippers are also available. If hydro demolition is used, provisions to contain the slurry and water should be made to comply with

applicable environmental laws. Robot operated hydro demolition machines were identified as a promising method in the literature review chapter.

Step 3: Prepare surface repair boundaries to prevent feathered edged conditions.

Step 4: Clean the surface of the exposed reinforcing steel and concrete to remove corrosion and other bond-inhibiting materials with the goal of promoting a good bond between the repair concrete material and existing surface and reinforcement. Heavy oxides or other bond inhibiting materials must be removed by any acceptable cleaning method (Emmons 1993). Bars damaged during concrete removal operations or with significant section loss should be cut. Although protective rebar coatings are available for use, generally, quality concrete is all that is needed to protect embedded reinforcing steel (Emmons 1993).

Step 5: If the substrate is excessively dry, pre-wet the surface to achieve a saturated surface dry condition. An excessively dry surface may absorb too much water from the repair material and result in excessive restrained shrinkage induced cracking. On the other hand, excessive moisture in the substrate may clog the pores and prevent absorption of the repair material. An ideal surface condition is a saturated surface dry.

4.1.4 Reinforcing Steel Cleaning, Repair and Protection

Step 4 in the previous section addressed the cleaning of the surface of exposed reinforcing steel prior to the installation of repair materials. Removal of oxide built up is critical for the long-term success of the repairs, as many repairs have failed within a few years of completion because of insufficient cleaning (Emmons 1993). Various methods exist for cleaning reinforcing steel such as: 1) needle scalers, 2) high pressure water cleaning, 3) abrasive blast cleaning, and 4) power wire brushing. In Step 4 in the previous section it was recommended that bars damaged during concrete removal may require corrective action to facilitate load transfer. The approach for doing this can be as follows. In the proposed repair detail, the repair drilled and epoxied epoxy coated dowels lap with existing reinforcement on both sides of the interface. If protruding existing bars have lost more than 25% of their cross-section, then force transfer should be facilitated only through the drilled and epoxied lap length. If this lap length is found to be insufficient based on code provisions

for development length and the test data provided in this report, then the spacing of the dowels can be decreased to reduce the stress that is supposed to be transferred through each dowel.

In Step 4 in the previous section, it was mentioned that although good quality concrete is generally sufficient in terms of providing alkaline protection, various methods exist to protect the surface of corroded reinforcement after it has been cleaned. These methods fall under the following three themes: 1) Alkaline Protection, 2) Cathodic Protection, and 3) Electrical Insulation. As an alternative to the natural protection by alkaline environment created by the repair cement matrix, alkaline slurry coating may be used to enhance the alkaline environment around the bar. Cathodic protection can be accomplished by applying a sacrificial layer of zinc either directly on the rebar surface or on the concrete surface after the repair is complete. Zinc acts as a sacrificial metal, and sacrifices itself to protect the reinforcing steel. Another method of cathodic protection includes reversing the electrical current flow through the installation of an anode on the concrete surface, which is connected to the reinforcing steel. Electrical current is introduced in the circuit thereby protecting the bars. Impressed current must be balanced with the environment on a continual basis to provide protection (Emmons 1993). The final approach to protecting reinforcing steel bars includes electrical insulation. This is accomplished by installing a layer of epoxy around the bars, which is claimed to electrically insulate the bar. The epoxy resin can be sprayed or brushed onto the bars. It may be difficult to encapsulate the entire surface of the bar in the field due to lack of access. Encapsulation works well when the entire surface of the rebar is protected. In cases when some surfaces are not encapsulated accelerated corrosion may take place since the electrical current may become concentrated in the unprotected areas.

4.1.5 Bonding Repair Materials to Existing Concrete

An ideal repair surface is one which is sound, clean, free of bond inhibiting materials, has adequate compressive strength, is free of any defects, and with aggregate bonded to the cement matrix. After the initial removal of deteriorated concrete, the repair surface should be sounded for delamination and voids, and any area that are found to be unsound should be subject to additional concrete removal. The repair surface must have an open structure. This allows the repair material to bond well with the host surface. If the pore structure is clogged with dust, slurry or water, the absorption process of the repair material will be hindered, and bond strength reduced (Emmons 1993). Abrasive blasting or hydro blasting may be used to achieve a porous structure. The provision of

an open pore structure is important in terms of creating capillary suction of the repair material into the substrate. The repair material should contain a sufficient amount of fluid paste for absorption into the open pore structure of the substrate (Emmons 1993). In some cases, a bond agent is used, although for the repair of bridge deck fascias this will be a challenge considering the presence of protruding existing deck reinforcement and the presence of formwork. Therefore, the application of a bonding agent is not considered essential for a successful repair. The focus should be on proper surface preparation. The repair concrete material should be installed in such a way that creates intimate contact with the host material. This can be accomplished by using a self-consolidating mix, or internal and external vibration depending on which repair material is pursued.

4.1.6 Placement Methods

A variety of methods exist to place the repair concrete material and complete the repair. These include: 1) Dry packing, 2) Form and Cast-in-place, 3) Grouted Preplaced Aggregate, 4) Form and Pump, 5) Dry or Wet Shotcrete, and 6) Hand Applied Methods. The method that is recommended for the repair of bridge deck fascias is the form and cast-in-place method. One of the goals during placement is to ensure proper consolidation. This can be accomplished by: 1) selecting a repair material that is formulated to be extremely flowable and self-consolidating; or 2) using internal and external vibration to ensure proper consolidation. It is highly recommended that a mix with self-consolidating properties is used for the repair and that mixes with low slump are avoided. As noted in the cementitious material selection method, the placement of the repair concrete material can be accomplished by using discrete inclined pockets at a certain spacing in which the repair concrete material is placed and allowed to flow in the longitudinal direction. This is appropriate if a self-consolidating mix is selected. If the selected mix is stiff, then the width of the ledge illustrated in the proposed repair detail must be determined such that the repair concrete may be placed anywhere along the length of the repair. In this case, internal and external vibration must be used to ensure proper consolidation.

4.2 Maintain Current Geometry and Prevent Further Deterioration - Proposed Repair Detail

For bridge deck fascias that exhibit low levels of deterioration one promising repair technique identified during the literature review to prevent further deterioration is the use of Polyurea. In this case, the deck fascia exhibits some deterioration but not to the degree that the crashworthiness of

the barrier is undermined. The goal in this case is to prevent further deterioration. The current deteriorated geometry and aesthetics are considered acceptable.

Polyurea acts as a reinforcement layer to retain broken fragments of concrete. There are two types of polyurea, which are a function of the shape of the molecule: 1) Aromatic polyureas, and 2) Aliphatic polyureas. The aromatic option is easier to apply, while the aliphatic option is more durable against ultraviolet light (Miller et al. 2017). A combination of both is certainly possible. The polyureas set relatively fast. According to the study conducted by Miller et al. (2017) on bridge barriers, the installed material cost varies from $3-$7.5 per square foot, compared to $1-$2 per square foot for epoxies. Special equipment is needed for installation and the cost of the machine for the spray on option may vary from $20,000-$40,000. If the material is installed using a cold spray approach and joint filling equipment utilizing static mixers, then the cost of equipment may vary from $5,000-$15,000. Skilled labor is required for installation, and a 10-day training is provided by the manufacturer. Protective equipment is required during installation. The material can be sprayed on, brushed on, or rolled on a surface. The typical thickness of the coat may vary from 0.02-0.1 in., although it can be as thick as ½ in. The study conducted by Miller et al. (2017) distinguished polyureas from the rest of protective sealants due to their ability to provide:

1) Abrasion resistance
2) Good bond to concrete and steel
3) Good resistance to many chemicals including chloride as well as to changes in humidity and temperature
4) Good sealing capability including cracks up to 1/8 in. due to their high level of elasticity
5) Reinforcement capabilities with some manufactures providing blast resistant formulas (Davidson et al. 2004; 2005)
6) A repairable material
7) Freeze-thaw and salt fogging resistance
8) A flexible repair option, which can be applied over a wide range of temperatures (-30ºF to 140ºF)
10) Colored as well as clear options

Miller et al. (2020) evaluated various polyurea products supplied by various manufacturers: 1) Citadel Floor Finishing Systems, 2) Creative Material Technologies, Ltd., 3) Mirabel Coatings

and 4) VersaFlex, Inc. The types of tests conducted include field testing and laboratory testing. The field testing included V-notch tests, and impact tests. Laboratory testing included pull-off testing, flexural testing, and rapid freeze-thaw testing. All evaluated products were deemed acceptable for the purpose of sealing the surface and restraining small concrete fragments from falling of the surface.

4.3 Barrier to Deck Connection and Edge Details that Reduce Moisture Content in Deck Fascia – Proposed Detail for New Construction

As noted in the literature review section, alternative barrier to deck connection details that were considered to be more effective compared to the current detail used by MDOT were identified. These include: 1) sloped top deck surface connections, 2) suppressed shear key connections, 3) elevated shear key connections, 4) extended barrier and covered deck fascia connection, and 5) a combination of some of the above. Each of these details is discussed below. DOT staff from the states that use the identified promising details were contacted to collect additional information about these details in terms of how they are constructed and how they have performed. This information is provided in Appendix B.

1) Sloped Top Deck Surface Connections

Fig. 4.3a shows the barrier to deck connection used by Illinois DOT. In this detail the top of the deck underneath the barrier is sloped such that gravity is used to direct water away from the deck fascia. This can be achieved by using a relatively low slump concrete for the deck to allow the construction of this slope while the concrete is still plastic. While the bottom of the deck fascia is sloped similarly, this may create potential deterioration problems for the fascia girder unless an effective drip strip is installed. One potential approach is to slope the top of the deck fascia as shown in this detail and keep the bottom of the deck fascia flat as shown in the current MDOT details to avoid promoting moisture movement towards the fascia girder.

A similar detail was identified in technical literature posted by the Delaware DOT. Although communications with Delaware DOT staff revealed that the sloped top deck surface connection detail is currently not used and rather a shear key connection as illustrated later is specified. No account of previous use of this detail could be obtained. Regardless, the concept remains the same. In this detail, the top of the deck underneath the barrier is sloped to promote moisture movement away from the deck fascia, whereas the bottom of the deck is sloped to prevent

moisture movement away from the fascia girder. In addition, the size and location of the drip notch are specified. In both details, there appears to be a V-notch at the deck to barrier joint. Delaware DOT reported a low frequency of deck fascia deterioration.

One of the details used by Minnesota DOT is similar to the one used by Illinois DOT in the sense that both, the top and bottom surfaces of the deck are sloped away from the deck fascia. It should be noted that Minnesota uses various barrier to deck connection details and the one that features the sloped top deck surface is only one of them. Minnesota DOT reported a high frequency of deck fascia deterioration. However, no association was made between a particular detail and the observed deterioration. Minnesota DOT staff acknowledged that the detail can help with moisture content control and seepage prevention and noted that it has not been difficult to implement. The roughened surface was noted to be created inherently by not specifically flat finishing the deck concrete underneath the footprint of the barrier. No specific low slump is used to create the sloped surface and the typical specified slump of 2-5 in. for the deck concrete was reported to be sufficient to create the slope. The slope is created by hand after the placement of deck concrete. No constructability issues were reported for this detail from Minnesota DOT staff. In general, Minnesota DOT staff reported that deck fascia deterioration has not been an issue in solid barrier bridges, but rather in those that feature open barriers (referred to as “One Line” Type barriers in Appendix B) or open barriers that were later retrofit with solid type barriers. This reporting is interesting because it suggests that pre-existing corrosion may play a role in deck fascia deterioration. The hypotheses being that prolonged exposure to increased moisture content in the deck fascias in the open barrier causes reinforcement corrosion and any reduction in moisture content by retrofitting the barrier does not prevent subsequent deck fascia deterioration due to the continuation of the corrosion process. The fact that in solid barriers the deck fascia deterioration is not an issue suggests that in such barriers the moisture content in the deck fascia is not sufficient to precipitate corrosion or freeze-thaw deterioration.

Tennessee DOT uses an interesting detail in which the top surface of the deck is slightly sloped similar to the previously discussed details, and an inclined polyvinyl chloride water stop is specified in the vicinity of the sloped reinforcement for the barrier. This detail provides double protection against moisture travel from the deck surface to the deck fascia assuming that the water stop is installed and functions as intended. The elevated top surface provides an elevation of 1 ¼ in. over one foot.

The detail used by the Wisconsin DOT is similar in concept with the one currently used by MDOT except that the water stop (i.e. the curved region of deck concrete underneath the barrier) is spread through the entire footprint of the barrier. A similar approach to that used by Minnesota DOT and MDOT was reported in the sense that this region is not finished like the rest of the deck thus providing a natural roughness. In addition, efforts are put forth to provide some amplitude in this roughened area. Similar to other observations presented in this report, a correlation between open barrier and deck fascia deterioration was noted by Wisconsin DOT staff suggesting that the use of solid barriers do not typically lead to deck fascia deterioration. For the open barriers, one approach that has been taken by Wisconsin DOT staff is the use of a metal flashing element during the original construction of the bridge with the goal of reducing moisture content in the deck fascia. However, it was acknowledged that this approach introduces yet another element that has to be installed and maintained over the life of the bridge.

It is interesting to note how NY DOT uses a combination of themes in their deck to barrier connections. For example, one detail uses an elevated shear key on a flat deck surface located mid-way in the footprint of the barrier. Two other details feature and elevated shear key located at the edge of the deck combined with a sloped deck surface that promotes moistures movement away from the deck fascia. This detail has the potential to provide double protection in terms of keeping moisture coming from the deck surface away from the deck fascia through the utilization of the elevated shear key and the sloped top deck surface. NYSDOT staff indicated that there are details where the elevated shear key has been used without sloping the top deck surface with satisfactory performance. NY DOT also reported a high frequency of deck fascia deterioration although no association was made between a particular detail and the observed deterioration.

Illinois (IL) DOT

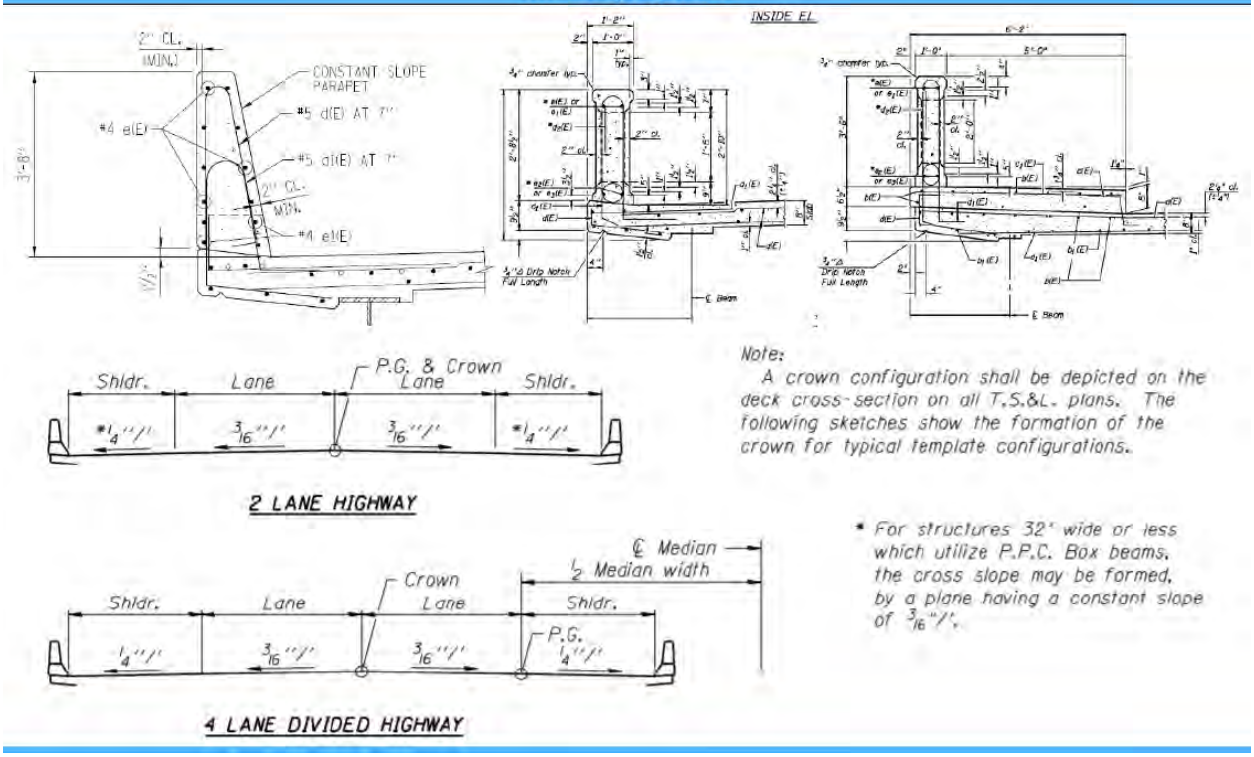

a)

Delaware (DE) DOT

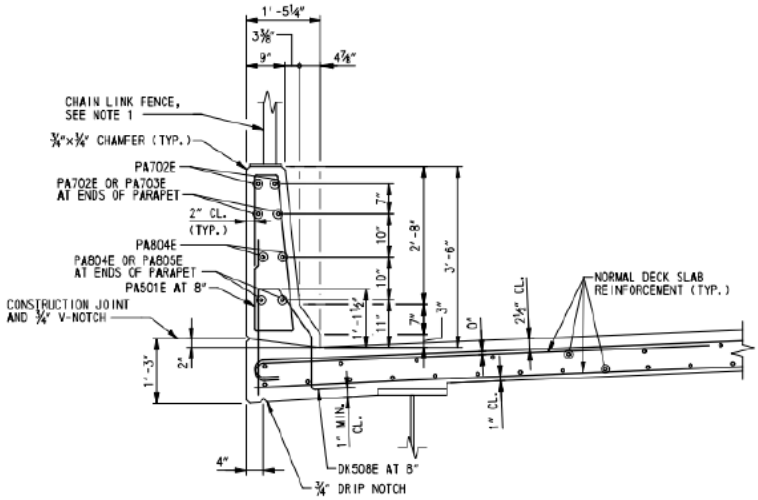

42" F-SHAPE PARAPET REINFORCEMENT TYPICAL SECTION

b)

Minnesota (MN) DOT

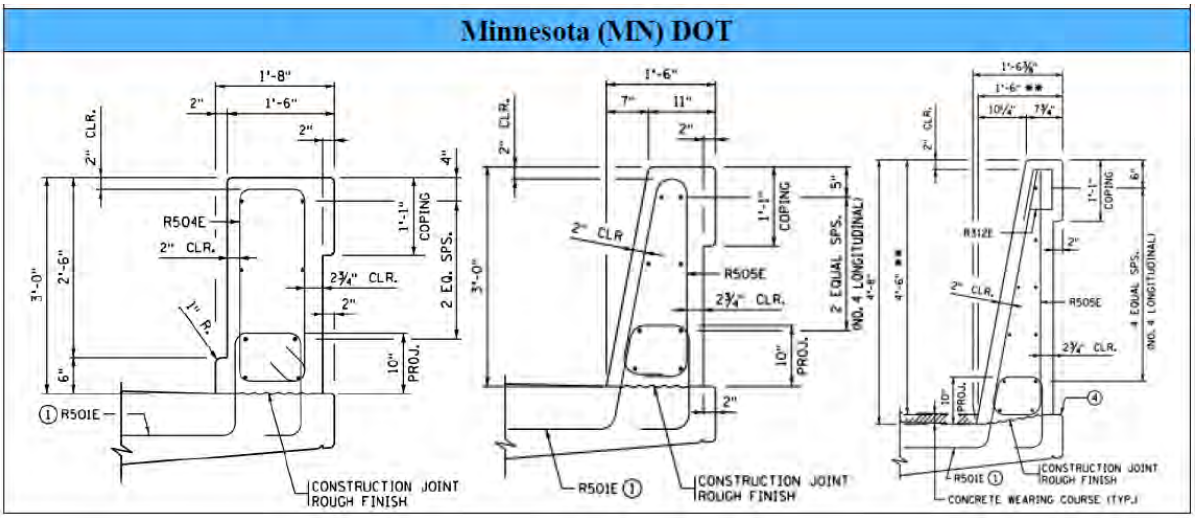

c)

Tennessee (TN) DOT

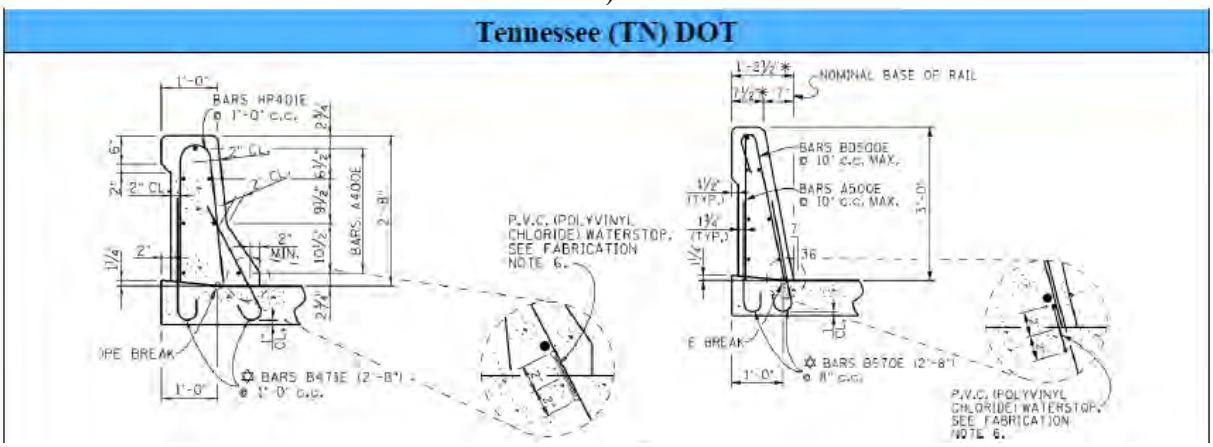

d)

Wisconsin (WI) DOT

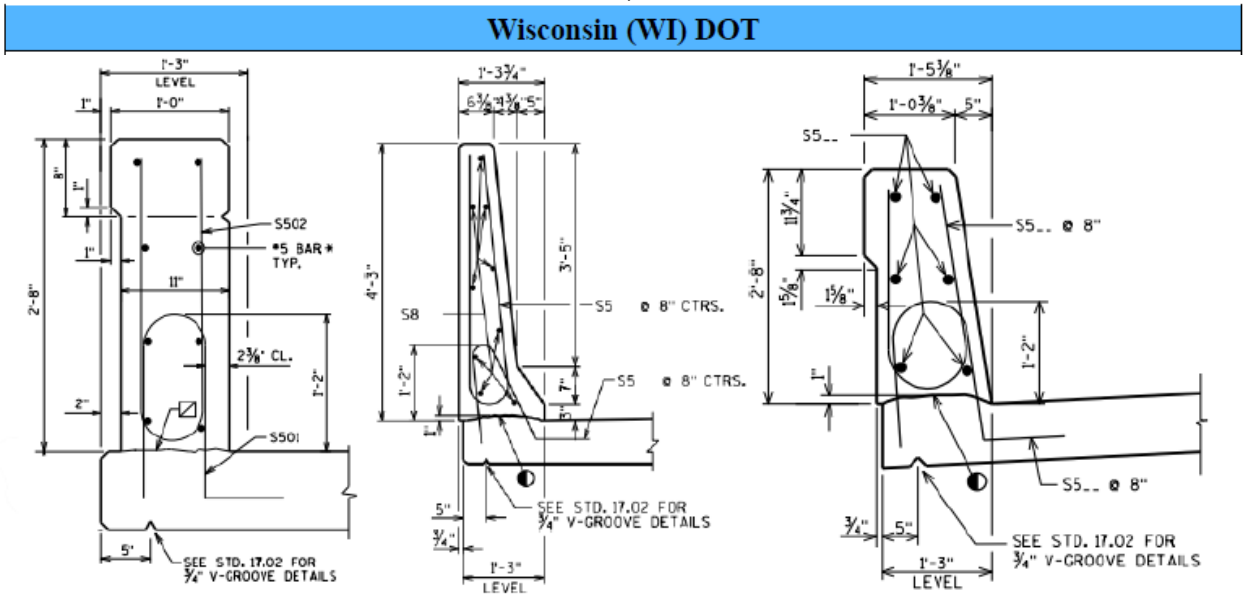

e)

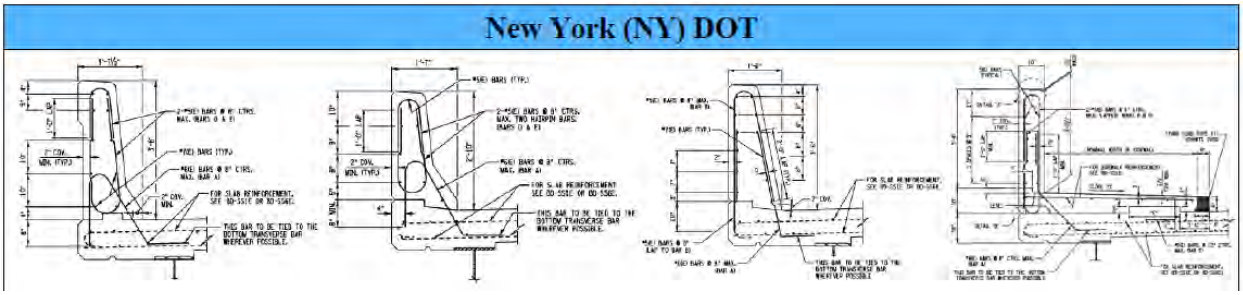

f)

Fig. 4.3 Sloped Top Deck Surface Connection – a) Barrier to deck connection detail used by Illinois DOT, b) Barrier to deck connection detail used by Delaware DOT, c) Minnesota DOT, d) Tennessee DOT, e) Wisconsin DOT, f) New York DOT (figures are reproduced from published state DOT literature)

2) Suppressed Shear Key Connections

Iowa, North Dakota, Delaware, Maryland, Oklahoma, and Rhode Island DOTs use barrier to deck connection details that feature a formed and suppressed shear key in the deck fascia. This may behave as a better water stop compared to the semicircular water stop shown in the current MDOT detail, which is typically hand-formed in the field while the concrete is still wet. The Delaware DOT detail appears to cover the limits of the acrylic protective coating, which covers the barrier and the deck fascia until the edge of the fascia girder. The sealer for the deck appears to be HMWM. When asked whether any correlation was observed between the specified acrylic coating and deck fascia deterioration, Delaware DOT staff indicated that such correlation is difficult to establish since the specification for an acrylic coating became a requirement in the last 25-30 years only. In addition, for the past 30-35 years Delaware DOT has also been using epoxy coated bars, which make the establishment of a positive effect between acrylic coating and a reduction in deck fascia deterioration difficult because the epoxy coated bars could have played a role. Another factor that creates a challenge between establishing a correlation is that Delaware DOT staff has reduced the specification of open scuppers, which were reported to cause deterioration in older bridges (35-65 years old). In summary, Delaware DOT staff indicated general satisfaction with the suppressed shear key detail and suggested a correlation between deterioration and problematic drainage details, lack of drainage maintenance, or failing expansion joints. Delaware and Oklahoma DOT reported a low frequency of deck fascia deterioration, whereas Maryland DOT reported a medium frequency of deck fascia deterioration. The size of the shear key used by Maryland DOT is 2 in. deep and 6 in. wide. Although from the responses provided in Appendix B it was reported that a wooden stud with 2 in. by 4 in. nominal dimensions is used to create the

shear key. A similar response was provided by Delaware DOT staff who indicated that a wooden stud with 2 in. by 4 in. nominal dimensions is pressed against plastic concrete to create the shear key after the Bidwell has passed. Another method is the use of a square channel tool to create the shear key by hand following the Bidwell. Pictures of such a suppressed shear key are provided in Appendix B. Maryland DOT staff reported that while the suppressed shear key appears to slow process of water infiltration, moisture still makes its way through the joint. It was noted that an elevated shear key as discussed next could potentially slow the moisture infiltration further. The slope of the top deck surface appears to be always towards the deck fascia. Maryland DOT appears to be using various details for the bottom surface of the deck fascia, featuring bottom deck surfaces that slope towards the fascia girder, and those that slope away from it.

Iowa (IA) DOT

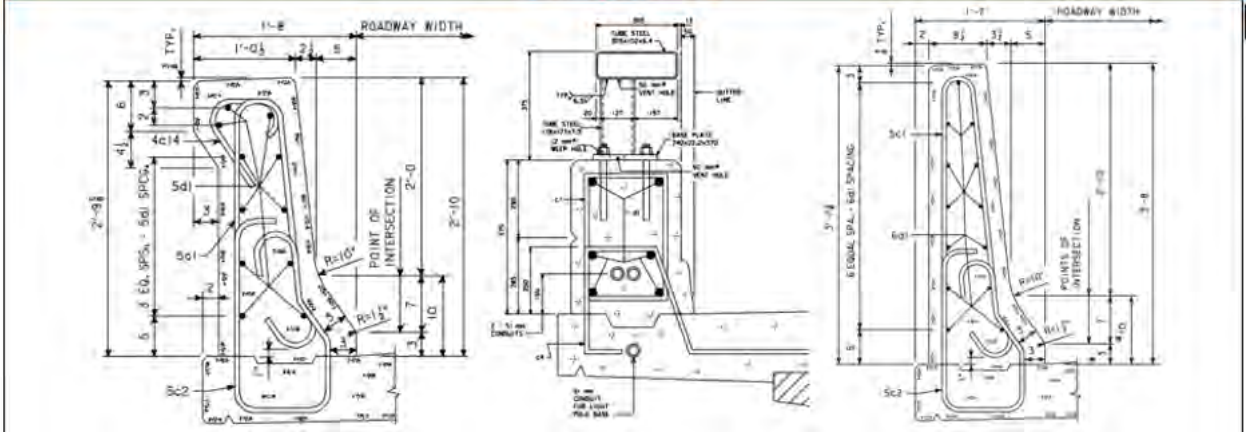

a)

North Dakota (ND) DOT

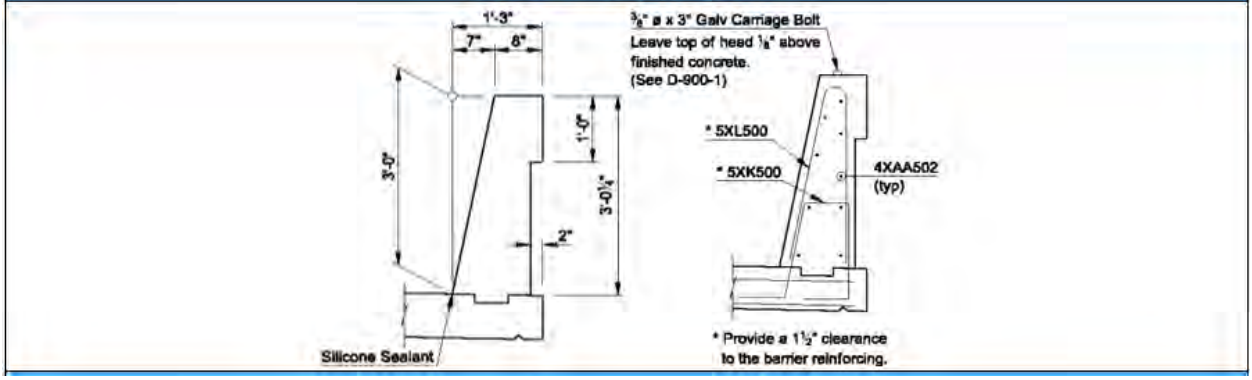

b)

Delaware (DE) DOT

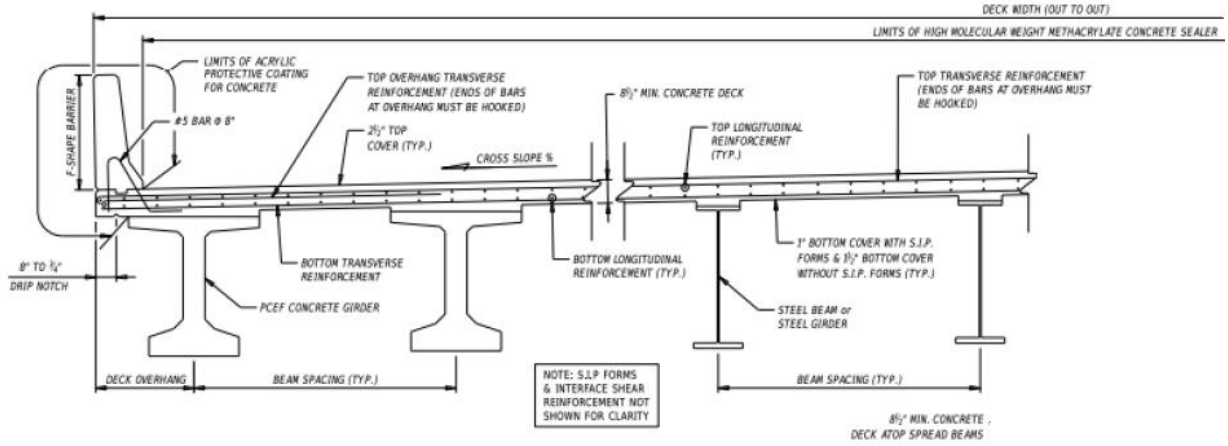

c)

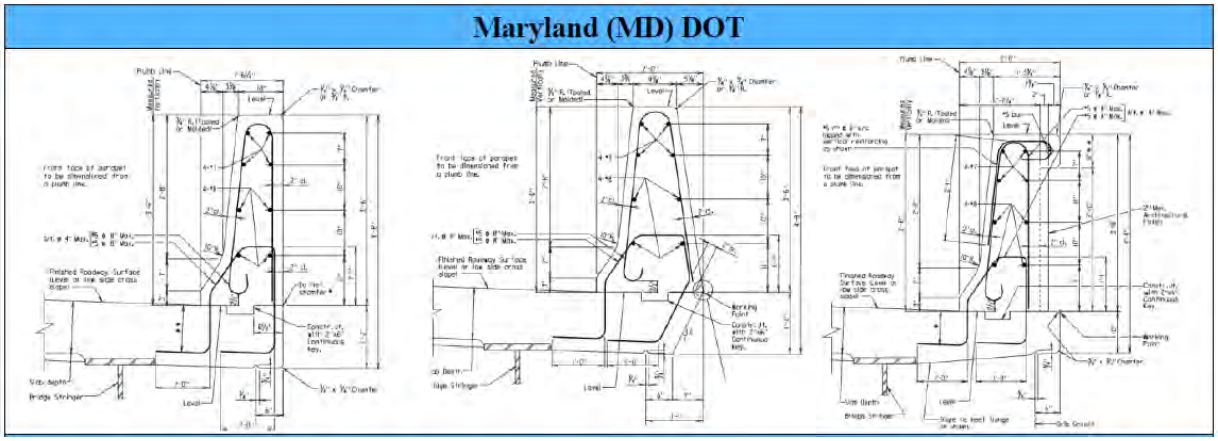

d)

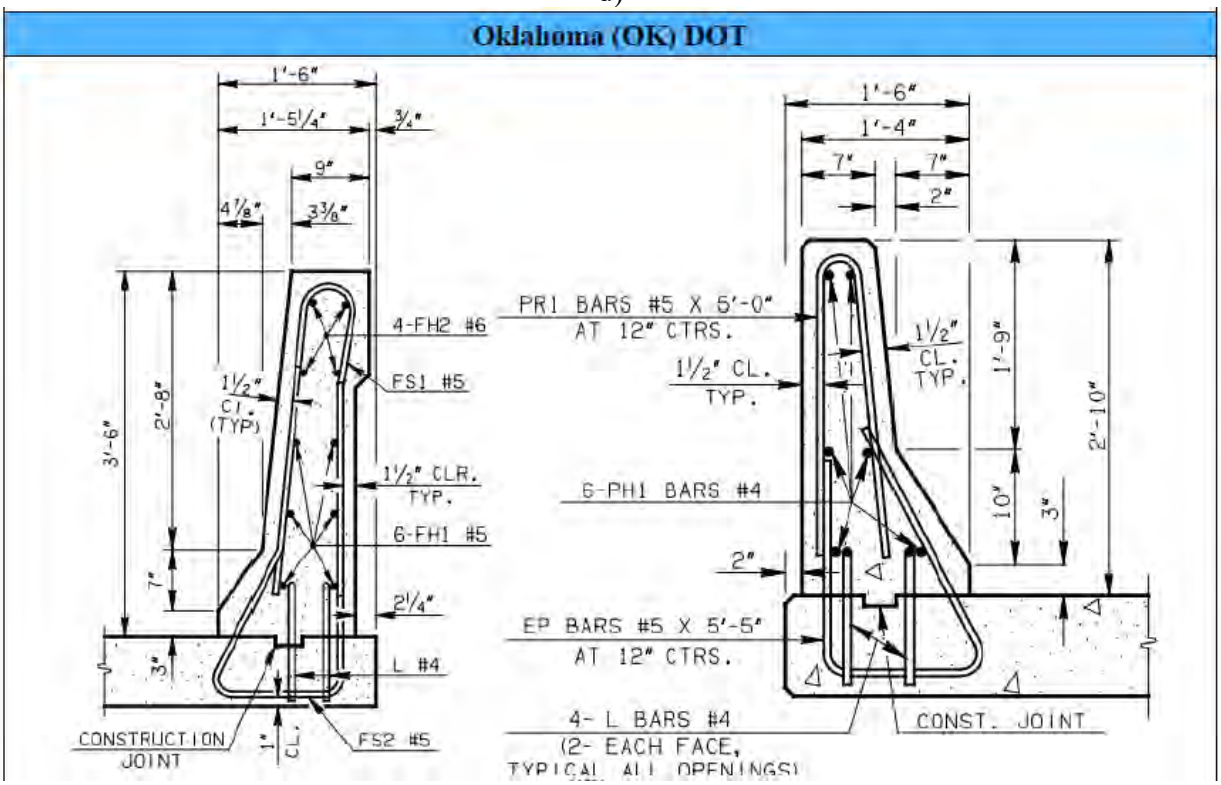

e)

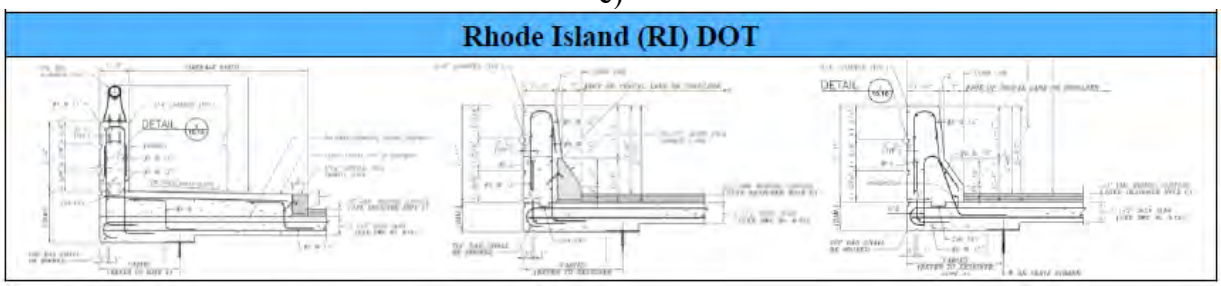

f)

Fig. 4.4 Suppressed Shear Key Connection - Barrier to deck connection details used by: a) Iowa DOT, b) North Dakota DOT, c) Delaware DOT, d) Maryland DOT, e) Oklahoma DOT, f) Rhode Island DOT

3) Elevated Shear Key Connections

Maine DOT appears to be using an elevated shear connection, which may help stop moisture movement from the deck surface to the deck fascia. Maine DOT reported a low frequency of deck fascia deterioration. In terms of deck protection, it appears common practice in Maine to use a waterproofing membrane covered by hot mix asphalt. The elevated shear key connection is also specified by NYSDOT as noted above. A wooden stud placed flat is used to form the elevated shear key. This wooden stud suppresses the portion of concrete underneath the barrier so it remains at the same elevation as the deck, and allows the remaining portion closer to the fascia to be placed higher thus creating the elevated shear key.

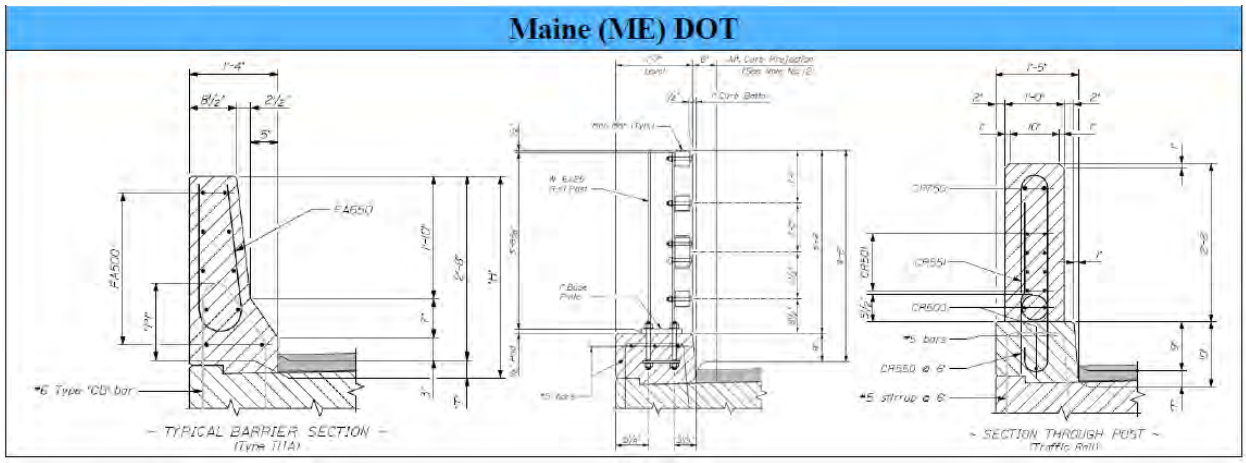

Fig. 4.5 Elevated Shear Key Connection - Barrier to deck connection details used by Maine DOT

4) Extended Barrier and Covered Deck Fascia Connection

Nebraska and Washington DOTs featured barrier to deck connection details in which a portion on the exterior side of the barrier was extended to cover the deck fascia. In this scenario, the vertical surface of the deck fascia is shielded from the environment and the vulnerable element becomes the edge the extended portion of the barrier. If the barrier concrete is more durable then deck concrete, this detail may offer a viable solution because it essentially provides higher grade concrete where the deck fascia would normally be. This detail may also be pursued from an aesthetics perspective because the construction joint between the top of the deck and barrier is not visible. Washington reported a low frequency of deck fascia deterioration. The width of the barrier concrete that covers the deck fascia appears to be relatively thin. Therefore, if this detail is pursued proper consolidation should be ensured.

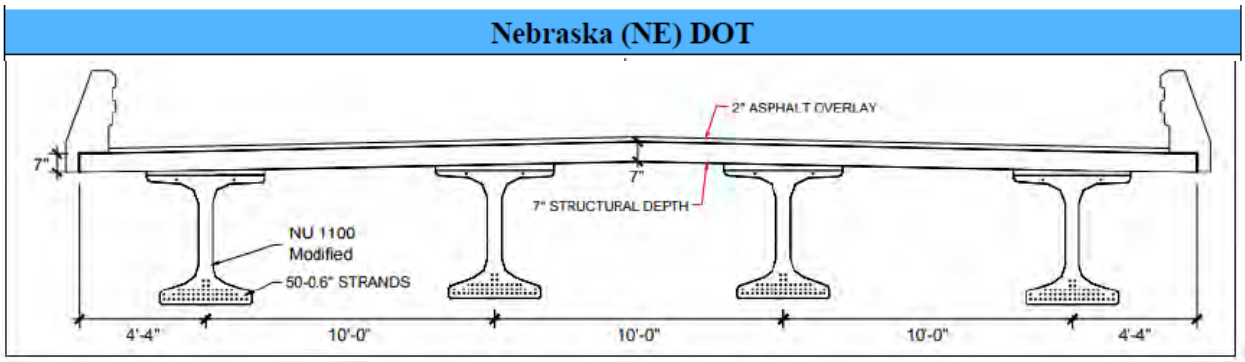

a)

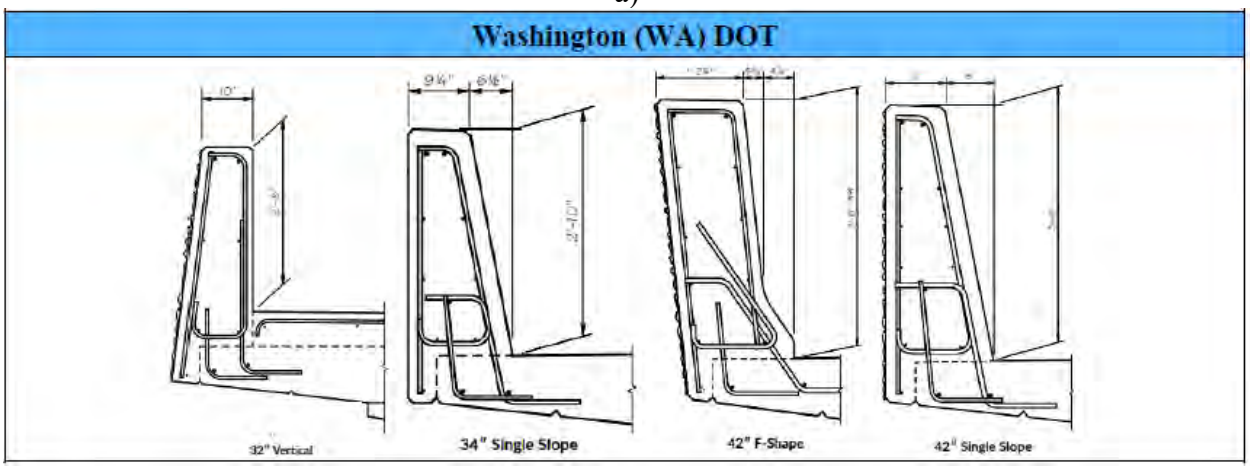

b)

Fig. 4.6 Extended Barrier and Covered Deck Fascia Connection - Barrier to deck connection details used by: a) Nebraska, and b) Washington DOTs

Chapter 5: Small-scale Testing to Identify Most Promising Repair Details

Chapter 5: Small-scale Testing to Identify Most Promising Repair Details

The purpose of the research presented in this chapter is to identify the most promising repair details using accelerated weathering and mechanical testing. The evaluation of the proposed repair details is conducted using the following metrics: 1) material characterization, 2) relative durability, 3) un-weathered reinforced interface shear strength, and 5) weathered reinforced interface shear strength.

5.1 Methodology

5.1.1 Fabrication of Specimens

General Procedure

Small-scale testing featured a variety of test specimens. These include: 1) 30 cylindrical concrete specimens constructed using with deck mixture (host mix – 6 cylinders) as well as four repair concrete mixtures (6 cylinders for each repair mixture total of 24) to characterize compressive strength, splitting tensile strength, and modulus of elasticity at 28 days; 2) 15 prismatic specimens (3 for each mixture) to characterize shrinkage behavior; 3) 5 prismatic specimens to characterize the relative durability of each concrete mixture when subject to freezing and thawing, 4) 5 reinforced prisms to characterize the un-weathered direct shear strength of the interface; and 5) 5 reinforced prisms to characterize the weathered direct shear strength of the interface. Test matrices for material characterization, relative durability testing, un-weathered reinforced interface shear testing, and weathered reinforced interface shear testing are provided in Table 5.1, Table 5.2, Table 5.3, and Table 5.4, respectively. Reinforcement details for un-weathered and weathered reinforced specimens subject to direct shear strength testing are provided in Fig. 5.1 and Fig. 5.2, respectively. The repaired specimens were fabricated in several stages. In the first stage, the host material that represents deck concrete was cast. The specimens were then covered with a plastic sheet and demolded one day after casting. The demolded specimens were moist cured as outlined in the subsequent sections. Dowels were installed in the repair specimens and the repair concrete material was cast afterwards. The subsequent sections provide detailed information about each stage of specimen fabrication.

Table 5.1 Test matrix for material characterization

Mix ID	Hardened Properties				Plastic Properties
	Number of 4x8 cylinders			Number of 3x3x11 in. prisms	
	Concrete age – 28 days				
	f_c'	f_t	E_c	Shrinkage	
Host – Current Deck Mix	3	3	No additional	3	Slump, air content, temperature, unit weight
Repair 1 - FRC	3	3	No additional	3	
Repair 2 - Latex Mod.	3	3	No additional	3	
Repair 3 - SCC	3	3	No additional	3	
Repair 4 - FRC-SCC	3	3	No additional	3	

Table 5.2 Test matrix for determining the *relative durability* of various repair cementitious composite mixtures

Group No.	Specimen No.	Material	Shape	Weathering	Metrics	Testing period
1	1	Control	Unreinforced Prism (in.) (4x4x15.5)	Freeze-thaw	Dynamic modulus, weight, rebound hammer readings	Periodic
2	1	FRC				
3	1	Latex Mod.				
4	1	SCC				
5	1	FRC-SCC				

Table 5.3 Test matrix for determining the reinforced interface shear strength

Group No.	Specimen No.	Concrete Material	Reinforcement material	Shape	Metrics
1	1	Control – Monolithic – U-shaped bars	Uncoated	Reinforced Prism (in.) (5x5x14)	Failure load
2	1	Control FRC - Control	Uncoated - Epoxy		
3	1	Latex Mod. - Control	Uncoated - Epoxy		
4	1	SCC - Control	Uncoated - Epoxy		
5	1	FRC-SCC - Control	Uncoated - Epoxy		

Table 5.4 Test matrix for determining the *Reinforced Interface – Shear Strength –Corrosion*

Group No.	Specimen No.	Concrete Material	Reinforcement material	Shape	Weathering	Metrics	Testing period
1	1	Control – Monolithic – U-shaped bars	Uncoated	Reinforced Prism (in.) (5x5x14)	Corrosion	Failure load at end of weathering	End
2	1	Control FRC - Control	Uncoated - Epoxy				
3	1	Latex Mod. - Control	Uncoated - Epoxy				
4	1	SCC - Control	Uncoated - Epoxy				
5	1	FRC-SCC - Control	Uncoated - Epoxy				

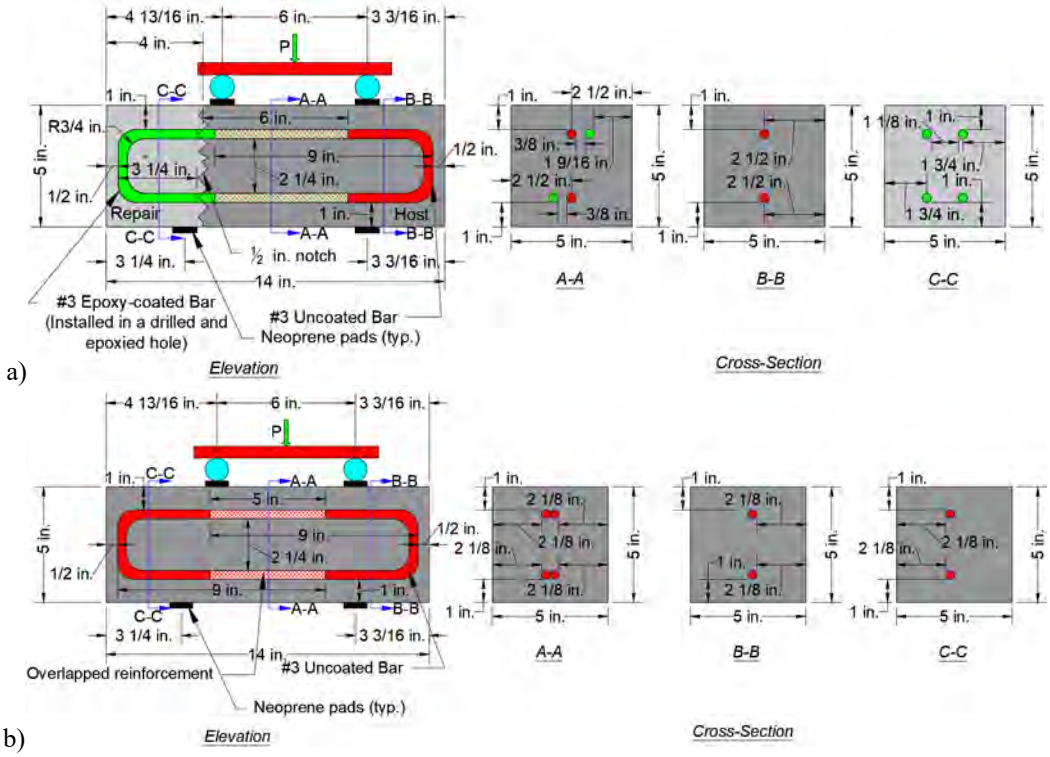

Fig. 5.1 Test setup and specimen details for direct shear testing of reinforced concrete prisms: a) repaired specimen; b) control specimen

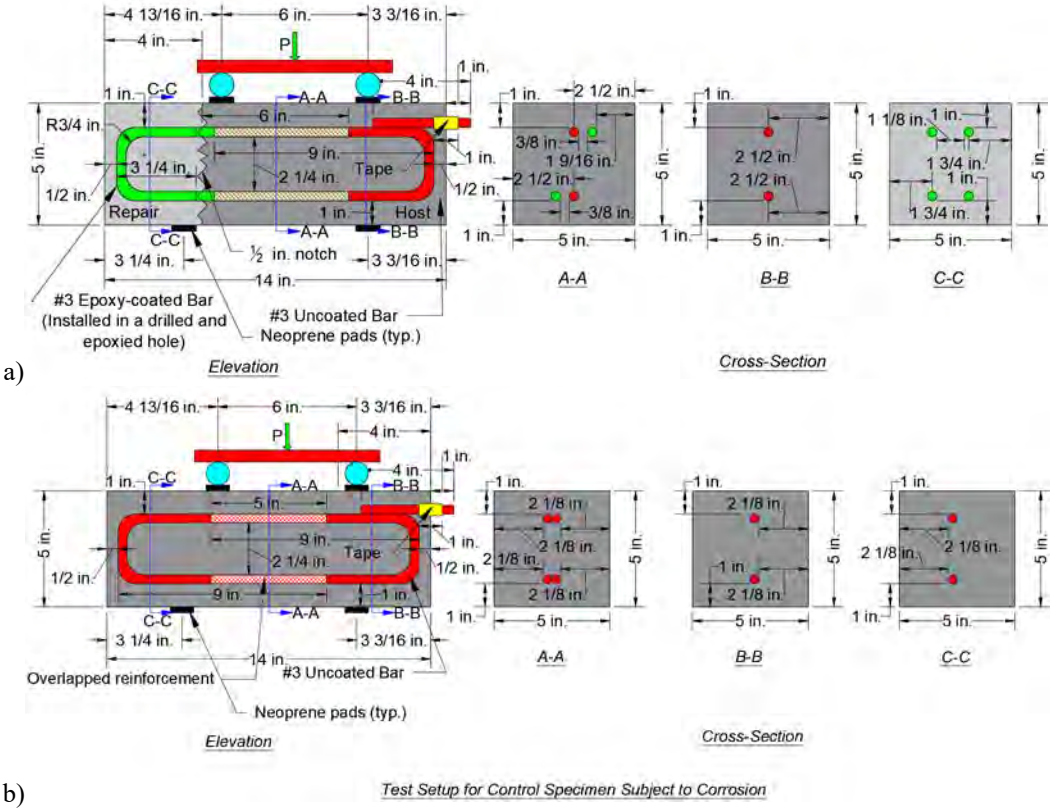

Fig. 5.2 Test setup and specimen details for direct shear testing of weathered reinforced concrete prisms: a) repaired specimen; b) control specimen

Formwork Preparation and Reinforcement Installation

Various types of forms were used to fabricate the small-scale specimens described above. The cylinders used for material characterization were fabricated using 4 in. by 8 in. plastic molds. Shrinkage specimens were fabricated using 3 in. by 3 in. by 11 in. metallic molds. The prismatic specimens used to relative durability testing were fabricated using 4 in. by 4 in. by 15.5 in. plastic molds. Since the specimens targeted for testing the reinforced shear strength of the interface featured unique dimensions, prefabricated 6 in. by 6 in. by 21 in. plastic forms were modified to create specimens with the desired dimensions. For example, ½ in. plywood forms were inserted on the sides and one end of the reinforced specimen. This plywood fillers were secured with C-clamps to the prefabricated plastic molds as shown in Fig. 5.3a-d. A 3D printed plastic template was fabricated to create a consistent roughened interface between the host material and repair concrete material so that any differences in behavior and capacity during direct shear testing could be attributed to the repair mix-host material interaction. The 3D printed template was secured to the ½ in. plywood filler forms as shown in Fig. 5.3a-d. Fig. 5.4a shows the ends of the repair specimens as well as the end of the control specimen. Fig. 5.4b shows the end of the shrinkage specimens. Since one of the goals of the small-scale specimen testing was to characterize the shear strength of the reinforced interface, a weakened plane was created at the interface by installing wooden strips with a 0.25 in. square cross-section. These are illustrated in Fig. 5.3b-c. The purpose of the wooden strips was to induce failure in direct shear at the interface rather than somewhere else along the span of the specimens.

For the reinforced specimens intended for accelerated corrosion testing, 2 layers of tape were installed on the rebar that protruded past the end of the specimens to minimize corrosion effects in the end region. This rebar protrusion was created by lapping a straight rebar to the U-shaped No. 3 rebar as shown in Fig. 5.3c. The rebar protrusion was provided so that a connection between the protruded rebar and the power supply could be established to conduct the accelerated corrosion testing. The reinforced specimens featured U-shaped No. 3 bars with the U-shape being near the end the specimens and the straight legs being near the interface of the repair specimens. For the control monolithic specimen, two U-shaped No. 3 rebars were used and lapped to create a similar condition to that created at the interface of the repaired specimens.

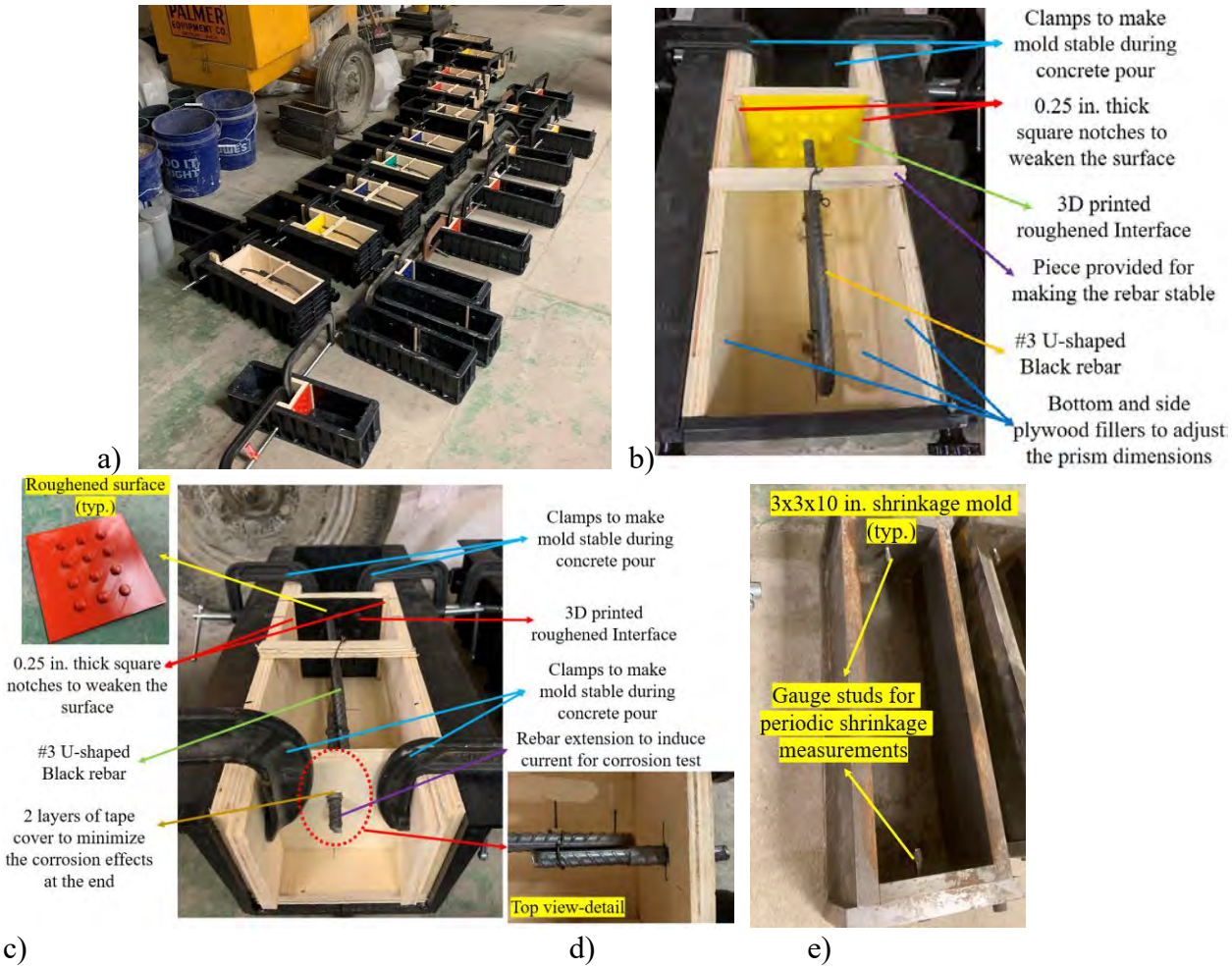

Fig. 5.3 Mold preparation for the small-scale tests: a) overall view for the prepared molds; b) typical mold prepared for the reinforced prisms targeted for unweathered direct shear testing of the interface; c) typical mold prepared for the reinforced prisms targeted for weathered direct shear testing of the interface; d) rebar extension to induce current for corrosion test; and e) typical mold for the shrinkage specimens

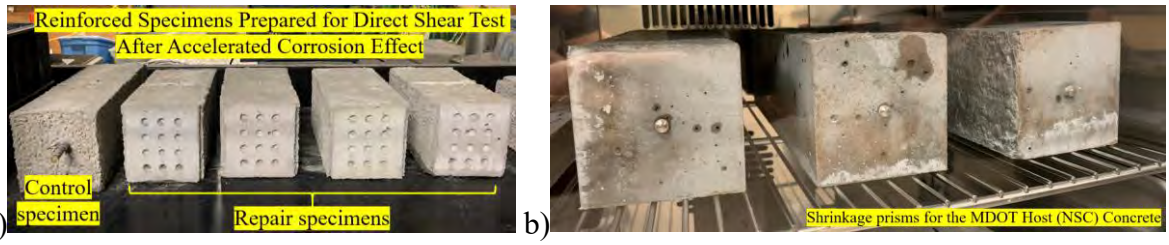

Fig. 5.4 a) Reinforced specimens prepared for direct shear test after accelerated corrosion effect; and b) specimens prepared for periodic shrinkage measurements

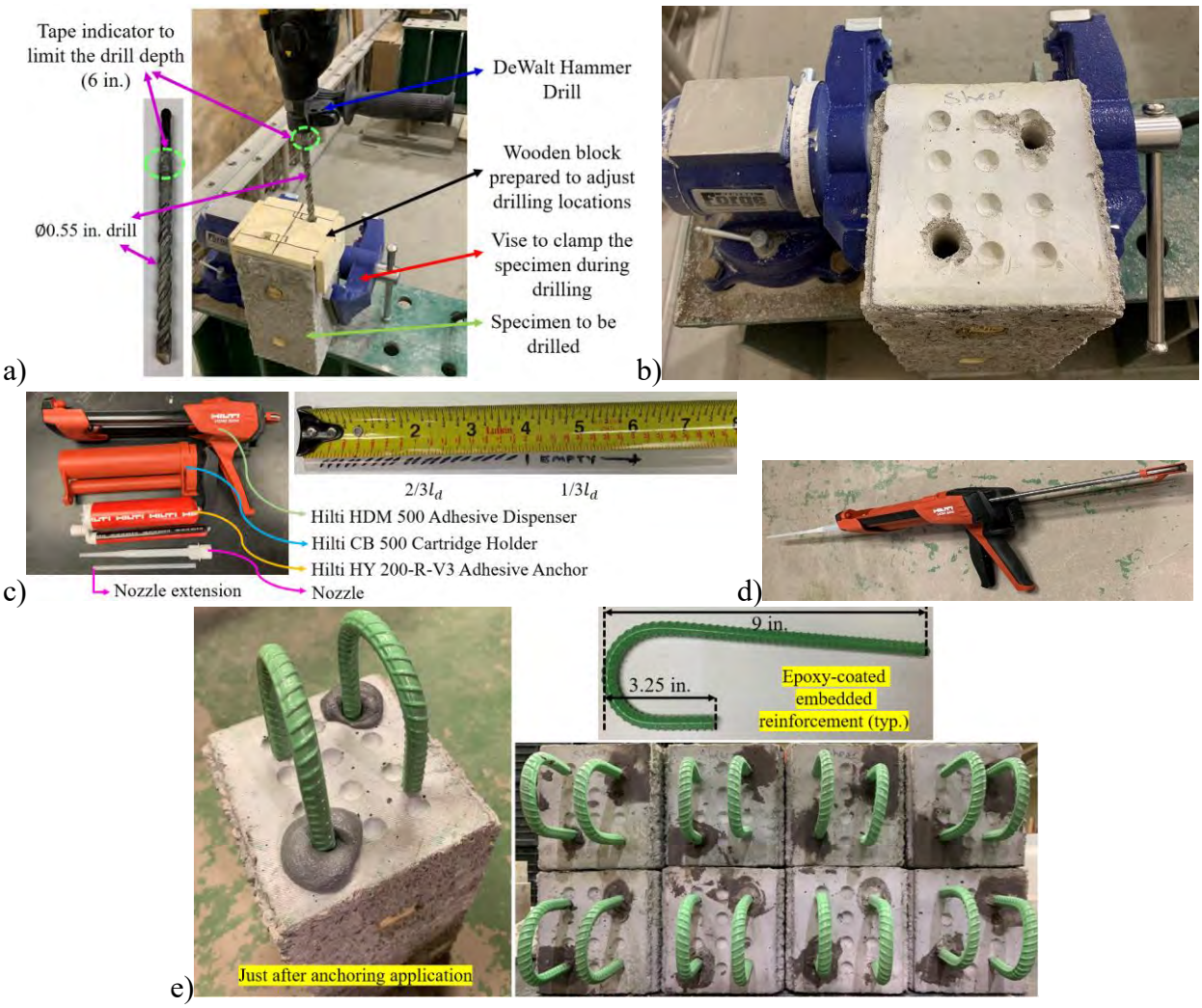

Fig. 5.5 Illustration of the process for embedding reinforcement into the host concrete – a) drilling process; b) top of specimen after drilling is completed; c) tools used for epoxy injection; d) assembled view of the dispenser; and e) magnified view of the top of specimen just after the installation of dowels (left) and an overall view of all reinforced interfaces (right)

Fig. 5.6 Remolding of reinforced prism specimens to receive the repair concrete material

Casting Small-scale Concrete Specimens

Deck Concrete (Host Material)

The small-scale test specimens that were intended to receive the repair material were fabricated first. This included cylinders for material characterization, prisms for shrinkage testing, prisms for relative durability testing, and reinforced prisms for direct shear strength testing. The mixing of concrete and preparation of laboratory specimens was based on ASTM C192 (ASTM 2019) for all concrete mixtures unless otherwise noted in the subsequent sections. The mixing procedure is described below:

1. All of coarse and intermediate aggregate, ¾ of the total water, and all admixtures were added to the mixer.
2. The mixer was started and as the mixer was operating the fine aggregate, cement, fly ash, and the remaining water were added into the mixer.
3. The mixer was operated for 3 minutes, followed by a 3 min rest. The mixer was then operated for an additional of 2 minutes.

Air content was determined in accordance with ASTM C231 (ASTM 2022) 1 using a Type B meter. Concrete temperature was measured using a thermometer based on ASTM C1064 (ASTM 2017).

Installation of Dowels

The dowel installation process is illustrated in Fig. 5.5. After a seven-day moist curing period, the specimens labeled as repaired reinforced specimens were secured in a vice for dowel installation (Fig. 5.5a). A wooden template was used to mark the location where the holes were installed. Dowels consisted of No. 3 bars (Fig. 5.5b). Two holes with a diameter of 0.55 in. were created to install the dowels. Manufacturer's recommendations were followed during the installation of the dowels. The adhesive used was Hilti HIT-HY 200R V3 adhesive (Fig. 5.5c-d). Before the adhesive was applied, the drilled holes were cleaned of any present dust to promote a good bond between the adhesive and the existing concrete. The inside of the holes was cleaned to remove dust. The effective embedment length range specified by Hilti is between 2-3/8 in. to 7-1/2 in. The selected embedment length for the dowels is 6 in., which is within this range. After the drilling operation was completed the specimens were inspected for any potential cracking and no cracking was observed. The epoxy material was prepared and injected inside the holes. The working time for

the application of the epoxy was given as 9 minutes with the application temperature being between 69 °F and 86 °F. The curing time was specified as 1 hour. Based on manufacturer's recommendations, 2/3 of the hole were filled with the epoxy. The nozzle extension was marked to stop epoxy injection when 2/3 of the holes were filled with the adhesive. A blowing time of 40 seconds was used for the 6 in. embedment base on manufacturer's recommendations. The dowels were subsequently installed (Fig. 5.5e). The number of specimens for which dowels could be installed in this manner was determined such that the installation process could be completed within the working time specified above. The procedure was repeated for other sets of specimens as necessary. Two separate dowels as opposed to a single U-shaped dowel with equal legs were used to facilitate installation. The shape and dimensions of the dowels is as shown in Fig. 5.5e. After the dowels were installed, any excess epoxy that came out of the holes was removed. The repair specimens were then re-inserted into the molds to receive the repair cementitious material as shown in Fig. 5.6.

LMC

Latex modified concrete was cast in several specimens. These included cylinders for material characterization, prisms for shrinkage testing, unreinforced prisms for relative durability testing, and the portion of the reinforced prisms that represented the repaired deck fascia for direct shear testing. The mixing procedure was based on FHWA-RD-78-35 (Clear and Chollar 1978) report and is outlined below:

1. Add the coarse aggregate and latex admixture and mix for 30 seconds;
2. Add the sand and cement and mix for an additional 1 minute.
3. Add water and mix for 2 more minutes.

Slump was measured immediately after mixing and 4 minutes after mixing based on the recommendation in FHWA-RD-78-35 (Clear and Chollar 1978) report.

SCC

SCC was cast in several specimens. These included cylinders for material characterization, prisms for shrinkage testing, unreinforced prisms for relative durability testing, and the portion of the reinforced prisms that represented the repaired deck fascia for direct shear testing. The mixing

procedure for SCC was based on Khayat et al. (2014), who provide mixing guidance for fiber reinforced self-consolidating concrete. This mixing procedure was deemed appropriate for the SCC mixture and followed with some modifications as described below:

1. Add sand, coarse aggregate, and 50% of the water into the mixer, and operate the mixer for 3 minutes.
2. Add the cement and fly-ash and mix for 30 seconds.
3. Add the HRWRA and other admixtures with the exception of VMA, and the remaining 50% of the water into the mixer and mix for 1 minute.
4. Add the VMA and mix 2 more minutes.
5. Stop the mixer for 2 minutes.
6. Remix for 2 more minutes.

The filling ability test (slump flow), T_{50}, and Visual Stability Index were determined based on ASTM C1611 (ASTM 2021). A 36 in. square base plate was used with predetermined circles of various radii. Procedure A was followed in which the smaller cone opening was placed on the base plate and the cone was filled form the larger opening. All SCC was placed in one layer without any rodding or compaction. The top surface of the cone was struck off to remove excess concrete. A timer was used for the T_{50} test, and the timer was started when the cone was lifted off the base plate. The cone was lifted within 2-4 seconds. The timer was stopped when the outer edge of the concrete reached the 20 in. diameter circle in the base plate. Once the concrete stopped flowing, the largest diameter was measured in two orthogonal directions and the average of these measurements was calculated and recorded.

FRSCC

FRSCC was cast in several specimens. These included cylinders for material characterization, prisms for shrinkage testing, unreinforced prisms for relative durability testing, and the portion of the reinforced prisms that represented the repaired deck fascia for direct shear testing. The mixing procedure for FRSCC specimens was based on the study conducted by Liao et al. (2006) and is outlined below:

1. Prior to starting the mixing, prepare the premix liquid (Water+HRWRA+WR+VMA+AEA).

2. Dry-mix the cement, fly-ash, and sand for 30 seconds.
3. Pour 50% of the premix liquid into the mixer and mix for 1 minute.
4. Pour 25% of the remaining fluid and mix for 1 minute,
5. Pour 12.5% of liquid and mix for 1 minute,
6. Pour 6.25% of liquid and mix for 1 minute,
7. Pour all remaining liquid and mix for 1 minute,
8. Add all coarse aggregates in the mixer and mix for 2 minutes,
9. Slowly add all steel fibers in the mixer while the mixer is operating and mix for about 3 minutes after all the fibers have been added.
10. Check if the fibers are dispersed thoroughly and remix if necessary.

Laboratory specimens were prepared without the use of rodding or vibration.

FRC

FRC was cast in several specimens. These included cylinders for material characterization, prisms for shrinkage testing, unreinforced prisms for relative durability testing, and the portion of the reinforced prisms that represented the repaired deck fascia for direct shear testing. The mixing procedure for FRC specimens was based on Susetyo (2009) and is outlined below:

1. Add the cement and fly-ash, and the aggregate into the mixer and mix for 3 minutes.
2. Add water reducers and 50% of the required water, and mix for 1 minute.
3. Add 25% of the required water, and mix for another 1 minute.
4. Rest for 1 minute.
5. Add the remaining 25% water and mix for another 1 minute.
6. Include the fibers gradually as the mixer is operating. Keep the mixer operating until it is observed that all fibers have been uniformly dispersed in the concrete mix.

A sieve was used at the top of the mixer to prevent dry balling of fibers and to ensure that they were properly dispersed into the mix.

Curing Concrete Specimens

All specimens with the exception of the ones used for relative durability testing were moist cured for 7 days. Specimens targeted for relative durability testing were moist cured for 14 days based on ASTM C666 (ASTM 2015). After concrete was cast, specimens were covered with a plastic sheet to control moisture loss and to facilitate self-curing. The day after casting the forms were removed and the specimens were inserted in a large water tank in the laboratory. The curing period includes the first day in which the specimens were covered with a plastic sheet as well as the rest of the days in which the specimens were inserted in the water tank.

5.1.2 Material Characterization

Since the repair cementitious materials feature modifications of previously used mixes, a series of tests was conducted to characterize their behavior in terms of plastic and hardened properties. These tests are summarized in Table 5.1. Tests to characterize hardened properties include compressive strength, splitting tensile strength, and modulus of elasticity at 28 days, as well as shrinkage tests. Plastic properties for each mix were characterized in terms of slump, air content, temperature, and unit weight. Fig. 5.7 shows the test setups for concrete mechanical property characterization, and Fig. 5.8 shows the equipment and test setup for concrete shrinkage testing. Compressive strength, splitting tensile strength, and modulus of elasticity testing were conducted in accordance with ASTM C39 (ASTM 2021), ASTM C496 (ASTM 2017), and ASTM C469 (ASTM 2022), respectively. Shrinkage testing was conducted in accordance with ASTM C157 (ASTM 2017) with the exception that the prisms were moist cured for 7 days to mimic field curing conditions. Shrinkage specimens were stored in a Memmert HPP110eco - Peltier Constant Climate Chamber. Shrinkage measurements were taken using a Global Gilson length comparator with a digital dial indicator (Model HM-250D). Since the proposed repair detail features drilled and epoxied epoxy coated dowels and a repair concrete material, the characterization of free shrinkage exhibited by the repair concrete material helps determine the proclivity of the repaired deck fascia towards restrained shrinkage cracking. This is due to the fact the shrinkage in the existing deck concrete has already taken place, and the newly placed concrete will tend to shrink. This shrinkage will be restrained by the interface between the two concretes precipitating restrained shrinkage induced tensile stresses in the longitudinal direction of the bridge. This could potentially cause cracks along the depth of the deck fascia. Ideally, the repair concrete material should exhibit low

shrinkage. However, this goal should not be considered in isolation, as the ability of the material to resist and sustain tensile stresses is perhaps more important than its ability to exhibit low shrinkage. Nonetheless, the shrinkage behavior of the repair concrete materials was of interest and was characterized as described above. The determination of slump, air content, temperature, and unit weight were determined based on ASTM C143 (ASTM 2020), ASTM C231 (ASTM 2022), ASTM C1064 (ASTM 2017), and ASTM C138 (ASTM 2023), respectively.

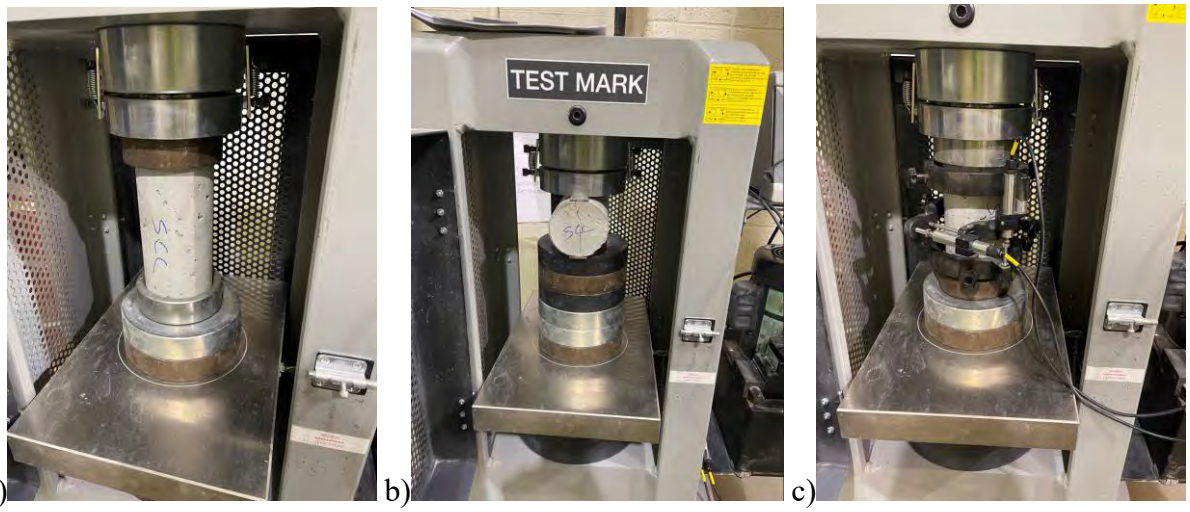

Fig. 5.7 Test setups for concrete mechanical property characterization: a) compressive strength, b) splitting tensile strength, c) modulus of elasticity

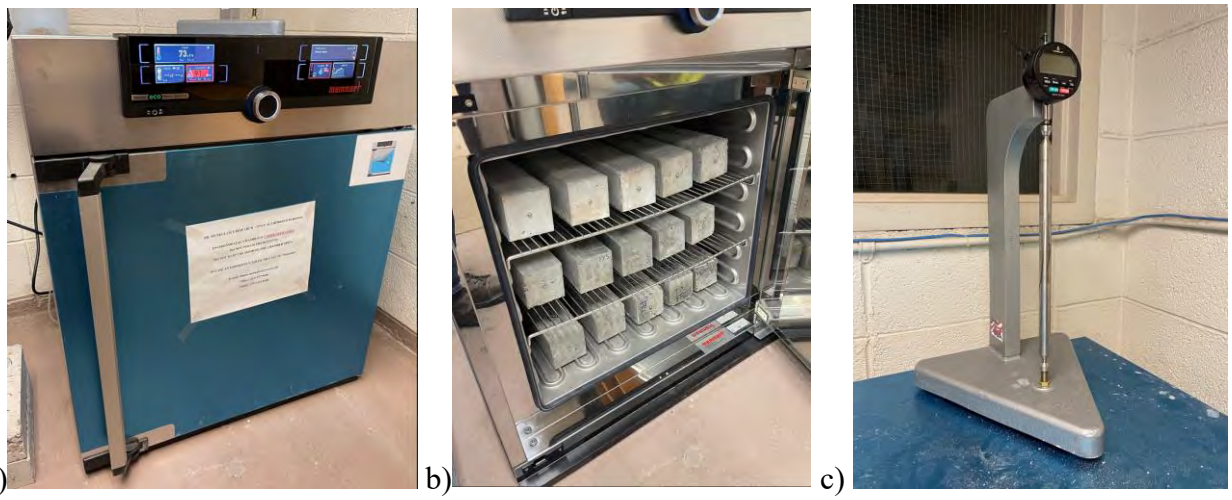

Fig. 5.8 Test setups for concrete shrinkage testing: a) climate chamber, b) storage of shrinkage prisms within the climate chamber, c) length comparator

5.1.3 Relative Durability

The purpose of this series of tests was to determine the relative durability of one host and four repair concrete mixtures when subject to freezing and thawing cycles. The test matrix for determining the relative durability of the abovementioned concrete mixtures is provided in Table 5.2. Concrete prisms (4 in. x 4 in. x 12 in.) made with each proposed repair concrete material and the traditional deck concrete were subject to freeze-thaw testing according to ASTM C666 (ASTM 2015) Procedure A rapid freezing and thawing in water to determine the relative durability of each mix. The metrics that were used to distinguish the relative durability of each concrete mixture include periodic measurements of dynamic modulus of elasticity, weight of specimens, and rebound hammer readings to quantify surface hardness. One unreinforced concrete prism representing each concrete mixture was fabricated and moist cured for a period of 14 days.

Initial Measurements

Once the 14-day moist curing period was completed, the specimens were removed from the water tank and prepared for initial measurements of the dynamic modulus of elasticity, weight of specimens, and rebound hammer readings to quantify surface hardness. Any free-standing water on the surface of the specimens was removed using a clean fabric towel prior to testing.

To calculate the dynamic modulus, the fundamental transverse resonance frequency was measured using the procedure described in ASTM C215 (ASTM 2019). The test setup for the determination of the fundamental transverse resonant frequency is shown in Fig. 5.9. The prismatic specimen is supported at $0.224L$ (3.5 in.) away from the ends, where L (15.5 in.) is the specimen length. This distance in this case is 15.5 in. Rubber cushions were placed at the location where the prism bears on the metal supports to eliminate possible restrictions in vibration in the transverse direction. The research team selected the 2nd largest impactor, whose diameter is 14 mm, to conduct fundamental transverse resonance frequency testing. This impactor creates a maximum fundamental transverse resonant frequency of 20.8 kHz, which is within the operational frequency range of the equipment. The sample size was selected as 2048 points as stated in ASTM C215 (ASTM 2019). The sampling rate was selected as 10 kHz. The amplifier gain was adjusted by a trial-and-error process until a proper gain was obtained. Based on these trials, the value of 50 was found to be appropriate for the gain. The gain allows to control the amplitude of the received signal. The appropriate gain is the one where the waveform is horizontally centered in the graph

and the features of the waveform can be easily seen on the Emodumeter screen. An example of a time domain signal obtained with a proper gain value is shown in Fig. 5.10a. Fig. 5.10b illustrates the results obtained from Emodumeter once the received signal is processed. Having adjusted all of above selections, the dynamic modulus test was performed three times. If the mass and dimensions of the specimens are provided as an input in the Emodumeter, the Emodumeter is able to calculate the dynamic modulus of elasticity, E_{dyna}, however the research team relied on their own calculations to obtain this parameter using the formulations provided in ASTM C215 (ASTM 2019). The results obtained from the Emodumeter were identical. For the control specimen, the fundamental transverse resonant frequency was measured as 2114 Hz, and the mass of specimen was measured as 19.8 lb. According to these values, the dynamic modulus of the specimen was calculated as 4491 ksi using a Poisson's ratio of 0.17. The Poisson's ratio was obtained from the static modulus of elasticity testing conducted later as part of the material characterization study. The AASHTO LRFD (2020) prediction for the static modulus of elasticity assuming an f_c' = 4.5 ksi concrete with a unit weight of 145 pcf is 4453 ksi.

The rebound hammer measurements were obtained at three locations: 1) at the left support; 2) at midspan; and 3) at the right report. These are illustrated in Fig. 5.9b as well as Fig. 5.12a. The average of these 3 values was reported for each specimen. When taking rebound hammer readings, the specimens were placed in a fixed position to ensure consistency between the measurements. The weight of the specimens was measured using the scale shown in Fig. 5.9a.

Prior to inserting specimens in the environmental chamber, they were placed in plastic molds as shown in Fig. 5.12b. Saturated plywood strips were inserted such that the specimen was completely surrounded by not less than 1/32 in. and not more than 1/8 in. of water at all times while being subjected to freezing and thawing cycles based on procedure A rapid freezing and thawing in water as indicated in section 4.1.2 of ASTM C666 (ASTM 2015). This is essential in terms of controlling the amount of water that surrounds the specimens and consequently the freezing and thawing time provided that one freeze-thaw cycle should be completed within 5 hours. A neoprene strip was used to secure the plywood pieces and prevent them from floatation. The environmental chamber could accommodate six prismatic specimens at a time while allowing sufficient space for their periodic removal and insertion.

Once the initial measurements were taken the specimens were inserted in the environmental chamber for freeze-thaw testing. Fig. 5.11a shows the environmental chamber that

was used to conduct the freezing and thawing experiments and Fig. 5.11b shows the duration of a freezing and thawing cycle. Freeze-thaw testing was conducted using a Tenney temperature and humidity chamber (environmental chamber) (Model No. T-20RC) with Versa Tenn III digital controller. The chamber was programmed to maintain a temperature of 40°F for 1 hour and 50 min, transition to a temperature of 0°F within 5 minutes, maintain that temperature for 2 hours and 30 minutes, and transition back to 40°F within 5 minutes, thus completing the cycle in 4 hours and 30 min, which is within the 5 hour limit specified in ASTM C666 (ASTM 2015). Several trial runs were conducted to ensure that this was indeed the case.

The dynamic modulus, weight, and rebound hammer readings were recorded every 36 cycles (once every week). The water inside the molds was replaced with clean water every 36 cycles (once every week). As specified in ASTM C666 (ASTM 2015), the duration of the freeze-thaw tests was determined such that testing was terminated when the specimens were subject to 300 cycles, the relative dynamic modulus of elasticity reaches 60% of the initial modulus (indicative of severe damage), or that corresponding to a severe case of deterioration measured in the field, whichever comes first. For the tests in questions, the attainment of 300 freeze-thaw cycles controlled.

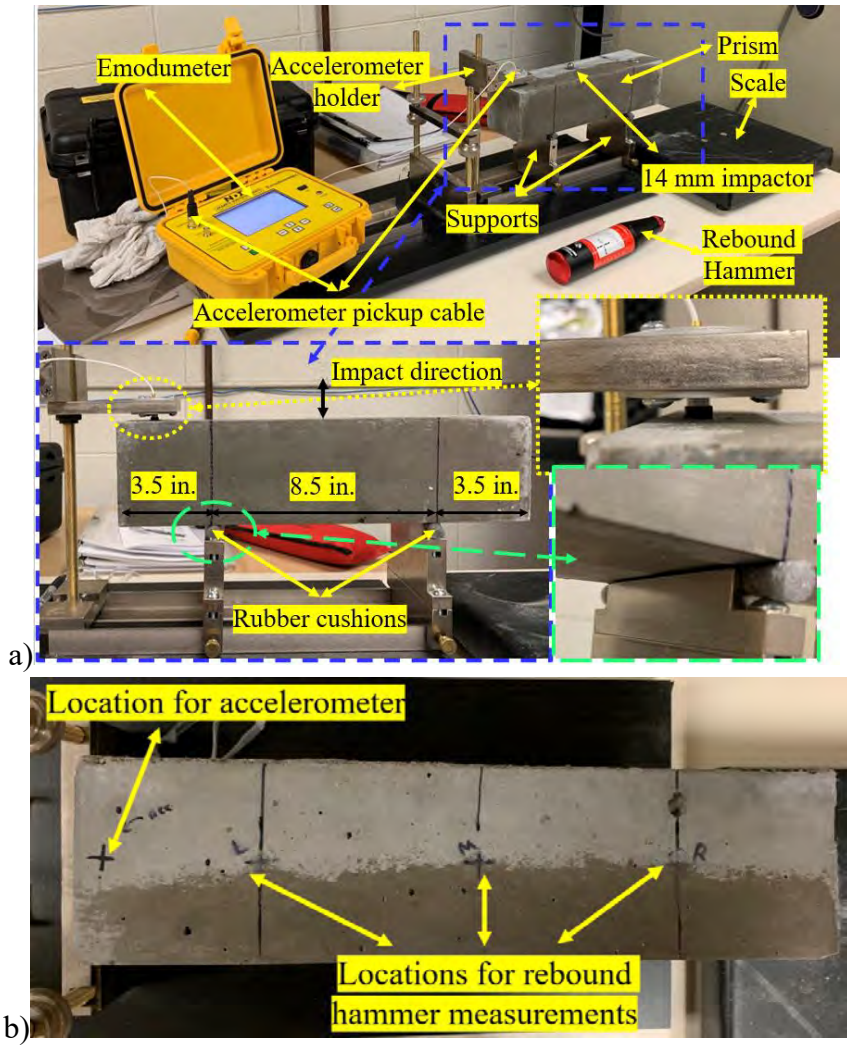

Fig. 5.9 a) Setup prepared for periodic fundamental transverse resonant frequency, mass and rebound hammer measurements; and b) illustration of locations for accelerometer and rebound hammer measurements

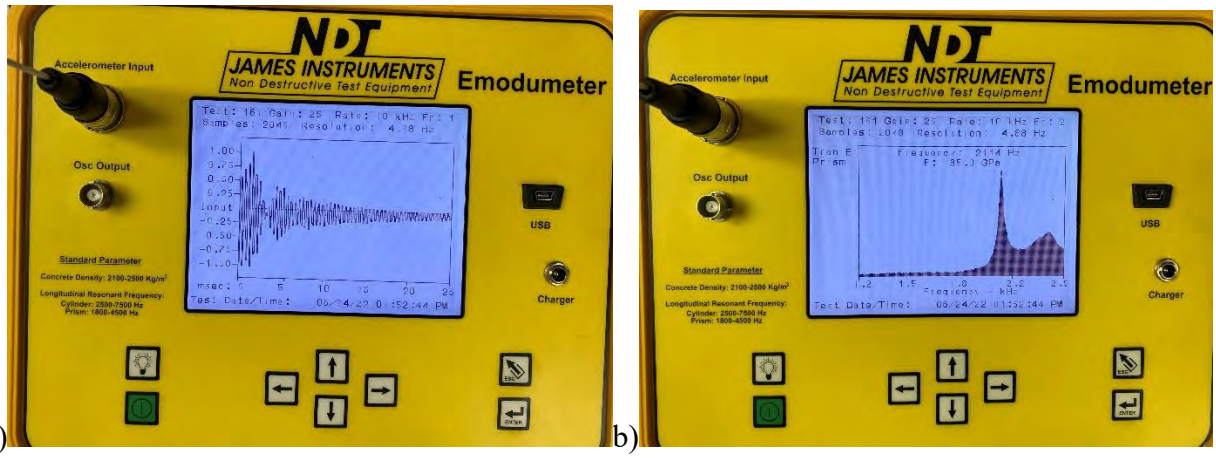

Fig. 5.10 a) Time domain signal obtained with the proper gain value; and b) an illustration of the results obtained from Emodumeter

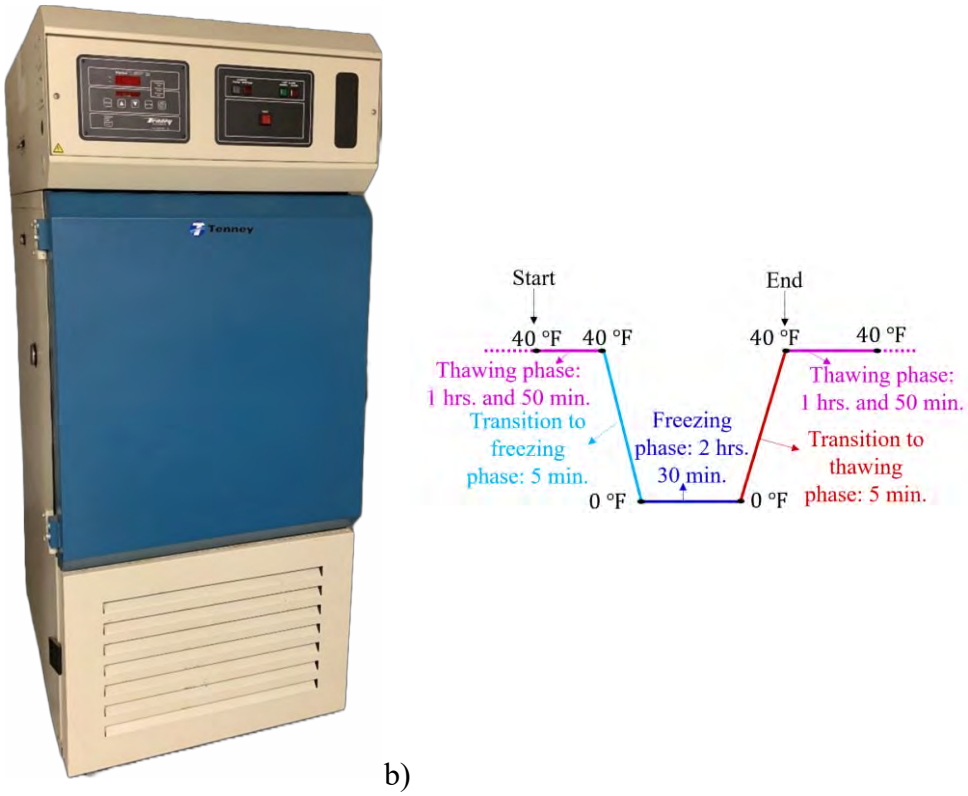

Fig. 5.11 a) Tenney T-20RC environmental chamber with VersaTenn III controller used for freezing and thawing experiment; b) temperature diagram used during freezing and thawing cycles

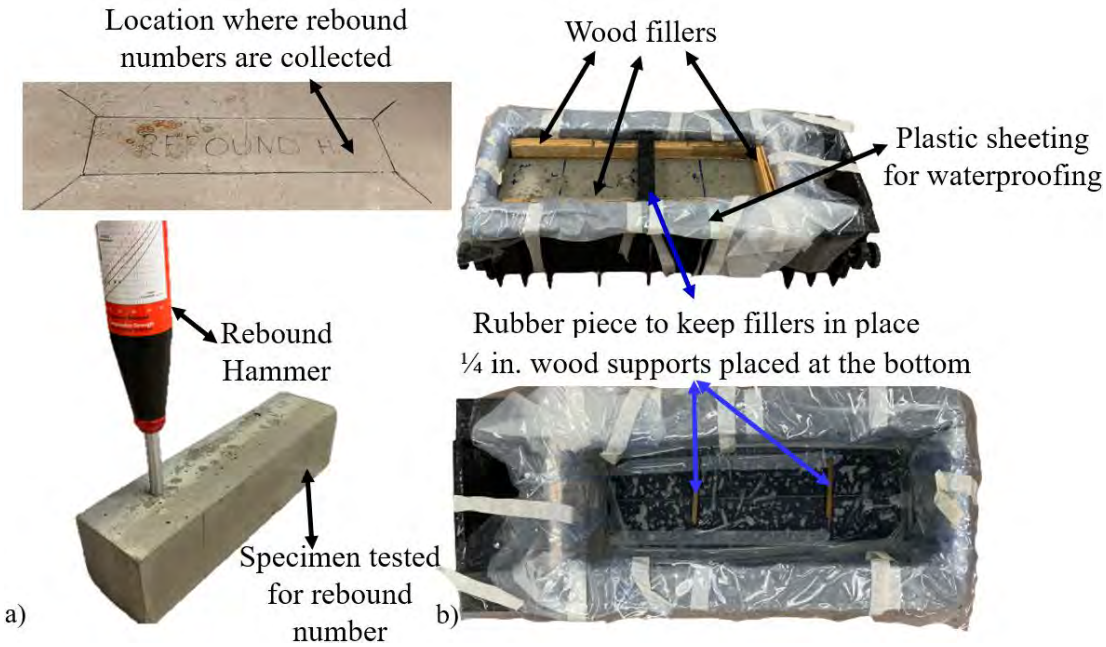

Fig. 5.12 a) Illustration of obtaining periodic rebound measurements on relative durability prisms; and b) prepared mold for freezing and thawing cycles for the relative durability prisms

5.1.4 Reinforced Interface Shear Strength

Reinforced concrete prisms were subjected to direct shear testing as shown in the test setups in Fig. 5.1, Fig. 5.2, and Fig. 5.13 to quantify the direct shear strength of the reinforced interface. This is important because either the self-weight of the barrier or impact forces will create shear forces at the repaired interface (Fig. 5.14). Impact forces generate a moment at the base of the barrier. This moment is resolved into a compression and tension couple at the base of the barrier. The compression force from the barrier causes shear at the repaired interface.

The direct shear test setups illustrated in Fig. 5.1 and Fig. 5.2 are similar to those described in JSCE-SF6 (1990) standard and have been used by Mirsayah and Banthia (2002) and Araujo et al. (2014). Recall that an ½ in. wide groove was created on the sides of the specimens to weaken the interface such that the shear failure would occur along the interface and not elsewhere. The location of the neoprene bearing pads was adjusted such that the edge of each neoprene bearing pad aligned with the corresponding edges of the groove. This provided a total offset of 0.5 in. (13 mm) between the edges of bearing in the neoprene nearing pads. Different approaches have been taken with respect to the magnitude of the offset between the edges bearing. Mirsayah and Banthia (2002) specified an offset of 0.25 mm, although it is not clear what instruments were used to ensure this level of precision in the offset. Araujo et al. (2014) specified a 5 mm offset. Mirsayah and Banthia (2002) report that when the test setup was performed according to JSCE-SF6 (1990) the failure plane deviated from the intended location. This was addressed by the introduction of the groove which weakened the plane at the desired location. The selected offset of 13 mm was chosen to ensure the induction of shear stresses at the interface and to avoid their elimination through unintended alignments of stress fields in the vertical direction during testing. On the right-hand side, the supports were aligned to eliminate shear and the potential of a shear failure since the interface of interest was on the left-hand side where the repair was made. In addition, the research team had concerns about a possible bond failure on the right-hand side and the alignment of load and reaction was intended to reduce the likelihood of such bond failure at this location. The load on top on the right-hand side could have been eliminated without changing the stress field on the left hand side, however, the research team was concerned about possible excessive rotations at the right support and influence of flexural stresses on specimen behavior. Such rotations were limited by aligning the top and bottom supports thus providing partial rotational fixity.

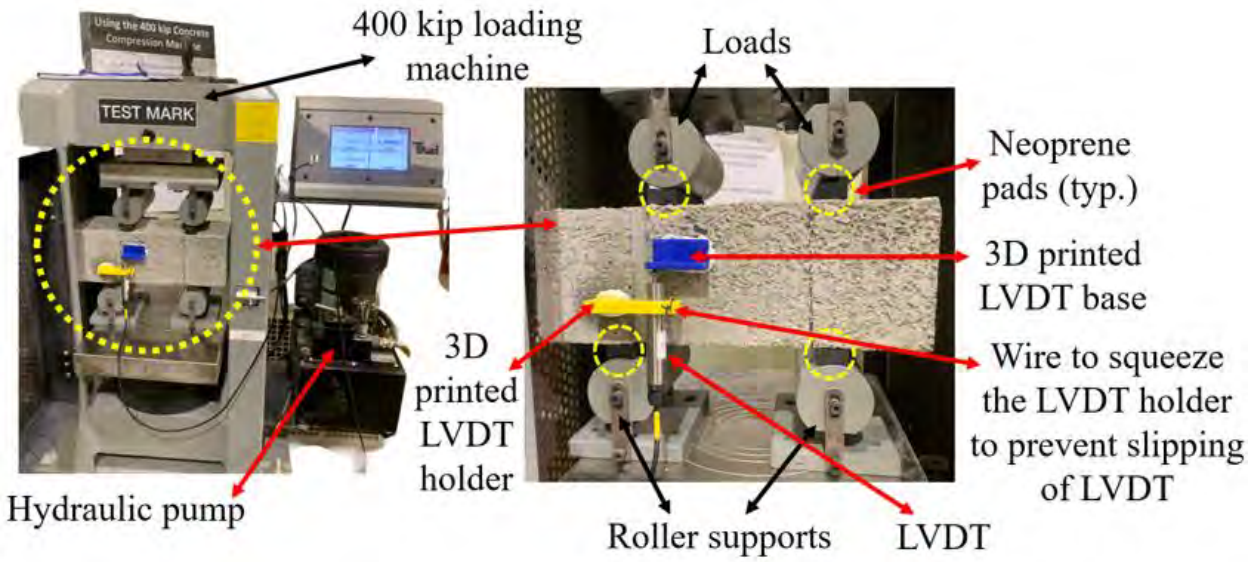

Fig. 5.13 Photograph of test setup for direct shear testing

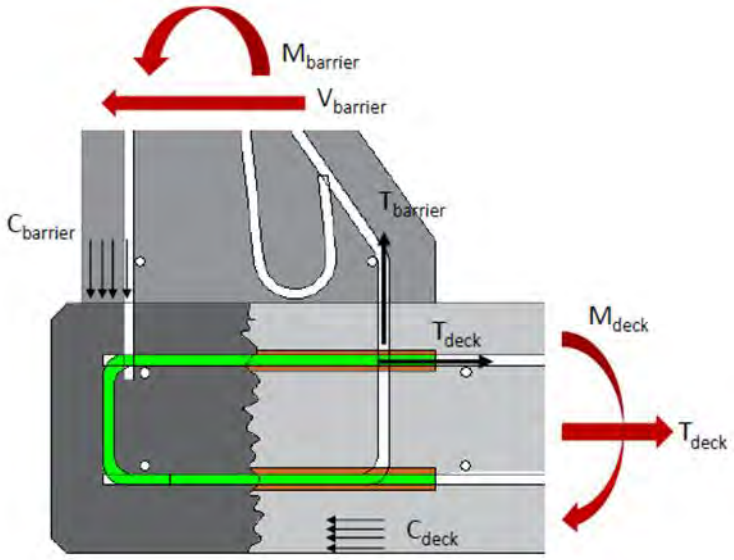

Fig. 5.14 Generation of shear forces at the existing and deck concrete interface

The measured data includes the applied load and the slip at the repair interface. The tests were conducted using a TEST MARK compression machine. The applied load was measured through the built-in load cell and the slip was measured using a linear variable differential transducer (LVDT). Goals of the test include a documentation of the load versus slip relationship for each repaired specimen and the control specimen; and examination of the energy versus slip relationship to characterize the ductility of the connection; and failure mode. The LVDTs were

secured using 3D printed fixtures on each side of the interface (Fig. 5.15 and Fig. 5.17). The sides of concrete specimens where the 3D printed fixtures were installed were grinded to provide a smooth surface for the connection (Fig. 5.16).

Fig. 5.15 3D printed fixtures and glue used to secure the fixtures on the concrete specimens

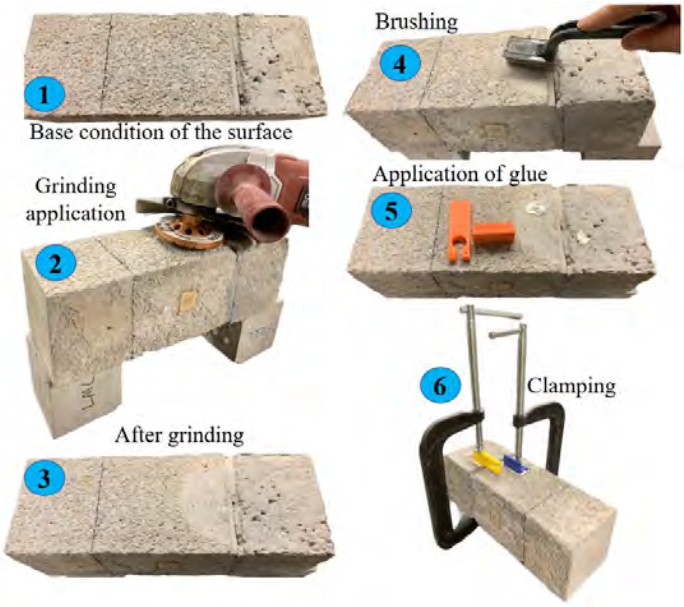

Fig. 5.16 Grinding of the concrete specimens to provide a smooth surface for LVDT fixture installation

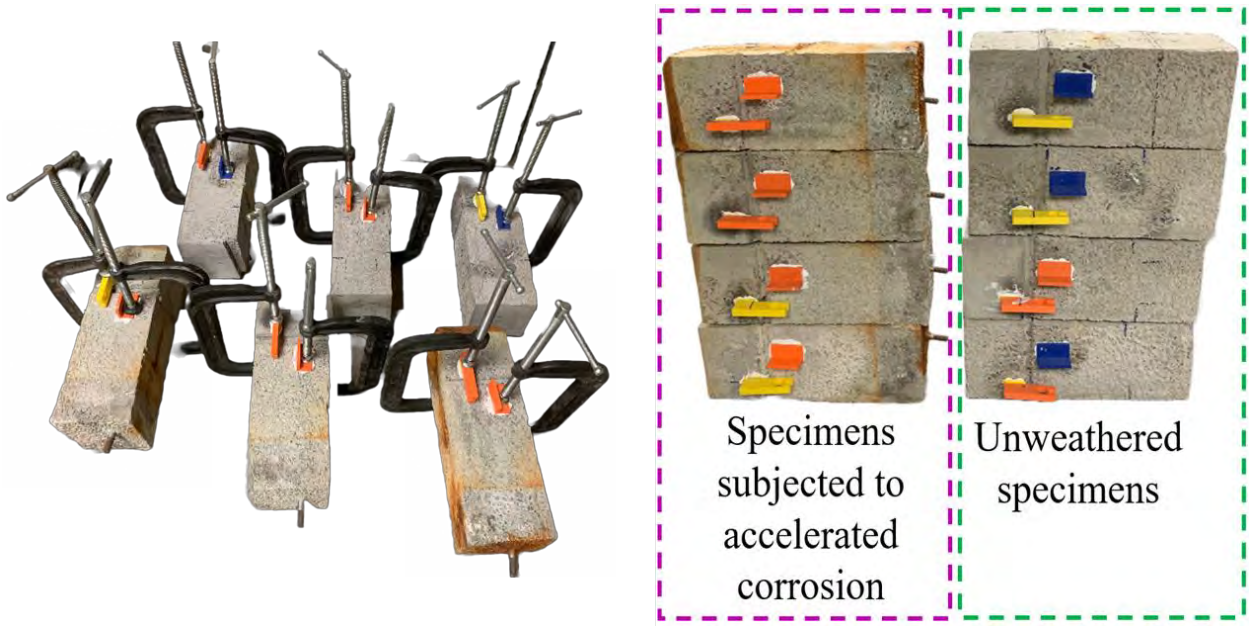

a) b)

Fig. 5.17 a) Installation of the 3D printed LVDT fixtures to the side of the concrete specimens, b) elevation of stacked concrete specimens after the installation of the 3D printed LVDT fixtures

Specimens subject to accelerated corrosion

Reinforced concrete prisms were subjected to direct shear testing after being exposed to accelerated corrosion to quantify the direct shear strength of the reinforced interface and any impact the corroded bars in the existing deck may have on this strength. The specimen reinforcement details are identical with those used for the direct shear testing of un-weathered specimens with the exception that there is a straight steel bar, which protrudes at the end and which is contact spliced with the U-shaped bars in the host part of the repaired specimen. This protruding bar provides a way to induce electrical current to the reinforcement and induce accelerated corrosion. The portion of the protruding bar that is 1 in. beyond the end of the concrete prism and 1 in. within it was covered with duct tape to prevent localized failure due to corrosion in this critical area.

The accelerated corrosion setup was similar to that used by Amleh and Mirza (1999) and Deb (2012). The reinforced prisms were placed in a plastic container filled with a 5% sodium chloride (NaCl) electrolytic solution. The top of the specimens protruded 3 in. above the electrolytic solution. Fig. 5.18 shows a photograph of the control and repaired specimens subjected to accelerated corrosion, the accelerated corrosion test setup, an illustration of periodic half-cell potential measurements, and the portion of the specimen that protruded past the electrolytic

solution. The direction of the current was arranged such that the bare steel bar acted as the cathode, and the embedded bars in concrete prisms acted as the anode. Before providing an electrical connection to the reinforcing bars, the surface of the bars was cleaned with a steel brush to ensure a good electrical connection. A parallel connection circuit system was created to supply the same voltage to all specimens by connecting the positive terminal to the reinforcement (protruding bar) (anode) and the negative terminal to the steel rod (cathode). A voltage of 5v was applied to the system. The electrolytic solution was changed on a weekly basis to eliminate any change in the concentration of NaCl.

The voltage and current were monitored daily in the first week and every two days thereafter using a multimeter capable of reporting voltage and current. The specimens were inspected daily the first week and every two days thereafter to detect any signs of cracking and note other relevant observations.

Half-cell potential measurements were taken to compare the level of induced corrosion to that measured during field testing described in the previous chapters. To conduct half-cell potential measurements, the specimens were removed from the plastic container with the electrolytic solution daily in the first week and once every two days thereafter. When conducting half-cell potential measurements, the specimens were placed in a location away from the rest of the specimens to ensure that the measurements were not affected by nearby specimens. Half-cell potential measurements were taken at three locations for the host specimen: at the left, middle, and right. Similarly, half-cell potential measurements were taken at four locations for the repaired specimens: at the repaired side, interface, middle of host, and right of host. In both cases, the average measurement was reported for each specimen. The surface of the specimens where half-cell potential measurements were taken was wetted using an electrical contact solution as stated in ASTM C876 (ASTM 2022). The impudence of the voltmeter was adjusted such that there is little to no fluctuations in the measurements, and varied from 10 mΩ to 80 mΩ. Once the half-cell potential measurements were taken, the specimens were inspected for signs of cracking and color change.

Accelerated corrosion testing continued for a minimum of 14 days and until periodic half-cell potential measurements on reinforced concrete prisms matched those recorded during field testing.

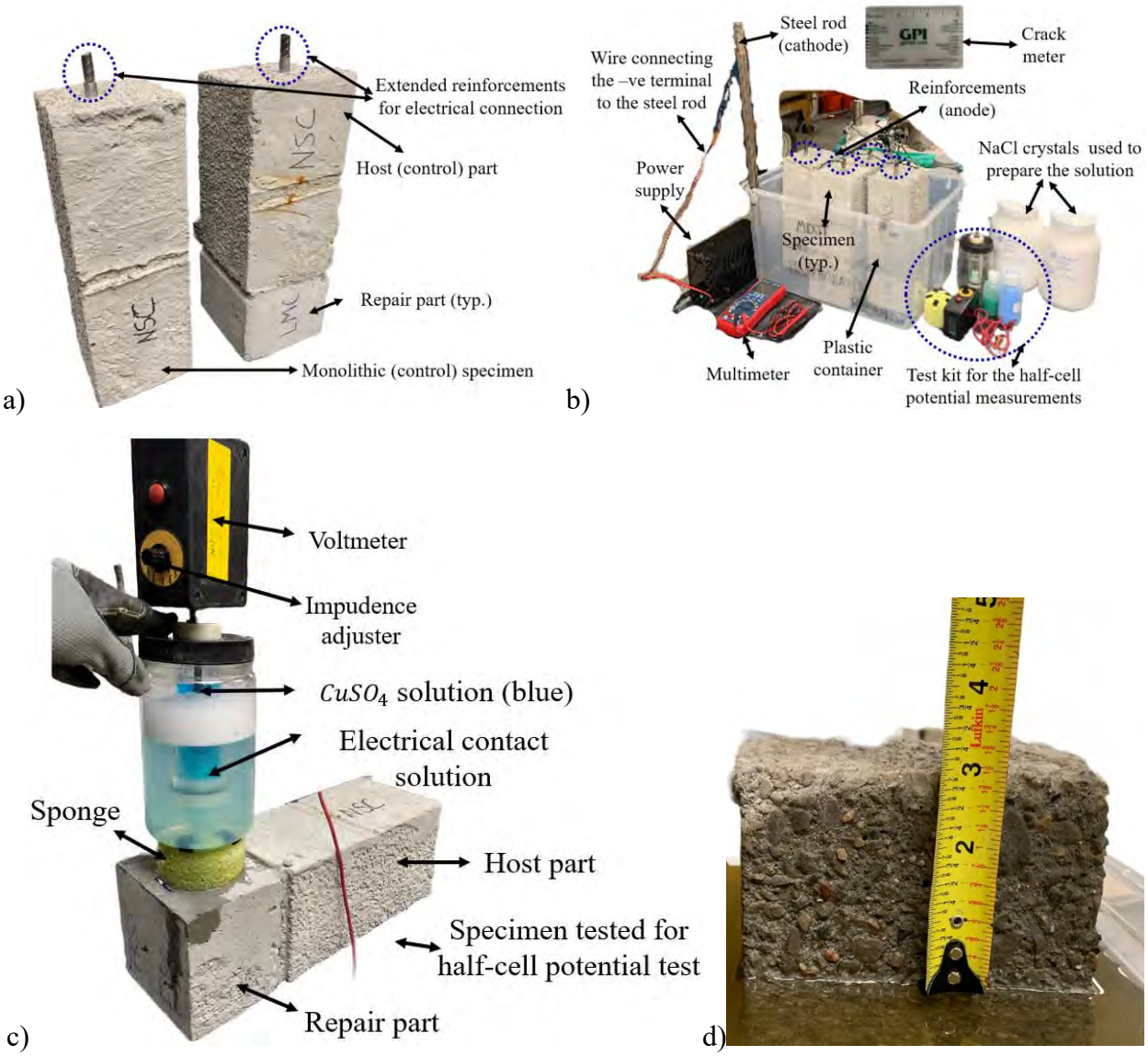

Fig. 5.18 a) Photograph of control and repaired specimens subjected to accelerated corrosion; b) accelerated corrosion test setup; c) periodic half-cell potential measurements; d) portion of the specimen that protrudes above the electrolytic solution

5.2 Results of Small-scale Testing

5.2.1 Material Characterization

Plastic Properties

The plastic properties for all concrete mixtures with exception of the FRC mixture are provided in Table 5.5.

Slump

Slump for the non-self consolidating concrete mixtures (Control, LMC, and FRC) varied from 4.75 in. to 7.0 in. These values represent placeable and workable concrete. Fig. 5.19 illustrates the slump for the control, LMC, and FRC mixtures.

a) b) c)

Fig. 5.19 Slump for: a) control, b) latex modified concrete, and c) fiber reinforced concrete

For the SCC mixture, once the concrete stopped flowing, the largest diameter was measured in two orthogonal directions and the average of these measurements was calculated as 24 in. The slump flow for SCC varies from 18 in. to 30 in. (ACI 2007). The measured slump flow of 24 in. suggests that the mixture has good free flow characteristics in the absence of obstructions. A slump flow of 22-26 in. is appropriate for: a) any reinforcement level (low, medium, high), b) any element depth low and medium element shape intricacy, c) low and medium surface finish importance (multiple discharge points can address cases of high surface finish importance), d) low and medium element length (see discharge points comment), e) any coarse aggregate content, and f) medium and high placement strategy. No evidence of segregation was detected. In addition, no mortar halo or aggregate pile in the slump flow spread was observed. Therefore, the visual stability index was noted as 0-1 due to the lack of halo and segregation and due to the uniformity of the spread. A visual stability index of 0-1 means that the mix is stable to highly stable. The recorded time for the T_{50} test was 6.11 seconds. A T_{50} time of 2 seconds or less characterizes a mix with low viscosity, and a T_{50} time of greater than 5 seconds generally characterizes a mix with high viscosity (ACI 2007). This indicates that the mix has high viscosity. Both, high viscosity and low viscosity mixes are viable options. High viscosity mixes may reduce placeability and require multiple discharge points – not an issue for deck fascia repair as multiple discharge points can be made available. Similar tests were conducted with a J-ring to determine the passing ability. The T_{50j}

time was measured as 10.6 seconds and the average diameter of the flow using the J-ring was measured as 23.5 in. The passing ability was calculated as 0.5 in. (the difference in the slump flow diameters without and with the J-ring). According to ACI 207R-07 (ACI 2007) a difference of less than 1 in. indicates good passing ability, while a difference greater than 2 in. indicates poor passing ability. Hence the mix had good passing ability. It should be noted that these are relative qualifications, and a mix with a difference of greater than 2.0 in. between the slump flow and J-ring flow may still be quite placeable, especially when the slump flow suggests that the mix is self-consolidating.

For the FRSCC mixture, slump flow without and with the J-ring was measured as 24 in. and 20.75 in., respectively (Fig. 5.20c-d), leading to a difference of 3.75 in. This suggests a lower passing ability compared to SCC. It should be noted that a lower passing ability while exhibiting stable properties as suggested by the visual stability index may require more discharge points, which as indicated above is not a concern for deck fascia repair. The visual stability index was noted as 0-1 due to the lack of halo and segregation suggesting a stable to highly stable mixture. There was no evidence of segregation in the slump flow spread (Fig. 5.20c-d). The T_{50} and T_{50j} times were measured as 4.34 seconds and 7.64 seconds, respectively.

a)  b) 

c)  d) 

Fig. 5.20 a) SCC: Slump flow test; b) SCC: J-ring test, c) FRSCC: Slump flow test, d) FRSCC: J-ring test

Air Content

The air content varied from 1.9% to 8%. The air content for the control mix was calculated with and without the aggregate correction factor. The air content for the other mixes was calculated without the aggregate correction factor. For the control mix, an aggregate correction factor of 0.2 was used, which was obtained from the mix design information provided by MDOT. This leads to $A_s = A_1 - G = 6.2 - 0.2 = 6.0\%$, where A_s is the air content including the aggregate correction factor, A_1 is the air content without the aggregate correction factor, and G is the aggregate correction factor. The air content for the repair concrete materials is smaller than what would

normally be specified for a concrete deck mixture although these mixtures offer higher densities, improved mechanical properties. The higher density reduces permeability and the improved tensile strength increases the resistance of these repair material to expansive forces that may be developed due to freeze-thaw or existing corrosion.

Concrete Temperature

Concrete temperature during placement varied from 74.5ºF to 79.6ºF.

Concrete Density

Concrete density varied from 141.8 lbs/ft^3 to 151.7 lbs/ft^3 with the host mix featuring the lowest density. As noted earlier, the repair concrete mixtures featured larger densities suggesting that they are potentially less permeable.

Table 5.5 Plastic Properties

Metric	ASTM Standard	Mix ID				
		Host Mix	LMC	SCC	FRC	FRSCC
Slump (in.)	C143 (ASTM 2020)	7.0	4.75	NA	5.6	NA
Slump Flow (in.)	C1611 (ASTM 2021)	NA	NA	24	NA	24
J-ring Flow (in.)	C1621 (ASTM 2017)	NA	NA	23.5	NA	20.25
Passing ability[1] (in.)	C1621 (ASTM 2017)	NA	NA	0.5	NA	3.75
Visual Stability Index[2]	C1611 (ASTM 2021)	NA	NA	0-1	NA	0-1
T_{50} (seconds)	C1611 (ASTM 2021)	NA	NA	0.5	NA	4.34
T_{50J} (seconds)	C1611 (ASTM 2021)	NA	NA	6.11	NA	7.64
Density (pcf)	C138 (ASTM 2023)	141.8	145.3	151.7	143.0	145.3
Temperature (ºF)	C1064 (ASTM 2017)	74.5	79.1	78.2	79.6	76.4
Air Content (%)	C231 (ASTM 2022)	6.2	2.9	1.9	8.0	3.1

1. Passing ability is the difference between Slump flow and J-ring flow.
2. Based on Daczko and Kurtz (2001).

Hardened Properties

Detailed hardened concrete mechanical properties are summarized in Table 5.6 and a summary of them is provided in Table 5.7. The specimens constructed with the FRC mixtures performed poorly and were excluded from consideration. Beginning with the removal of plastic molds, the specimens that featured the FRC mixture exhibited signs of disintegration with fragments or concrete separating from the cylinders or prisms upon mold removal. At the end of curing, when benchmark measurements were taken in the concrete prisms for freeze-thaw testing, prior to insertion in the environmental chamber, rebound measurements indicated a zero rebound associated with a dent

in the surface of concrete, suggesting low stiffness concrete. In addition, the average 28 days compressive strength of FRC cylinders was 487 psi, and the average splitting tensile strength was 69 psi.

Compressive Strength

All other repair concrete materials featured compressive strengths higher than the host material and greater than the minimums identified in the previous chapters. The compressive strength at 28 days, f_c' varied from 6.3 ksi to 11.6 ksi. The highest f_c' was exhibited by the SCC followed by FRSCC, LMC, and the control mix. The compressive failure mode for the SCC mixture was explosive in nature due to the high strength and the immediate release of stored strain energy (Fig. 5.21a). The failure mode of LMC and NSC (control mix) was also relatively brittle. The failure mode of FRSCC was ductile and restrained thanks to the fibers as evinced by the more gradual post-peak reduction in strength exhibited by the descending branch of the stress versus time relationship. COV varied from 1.5% to 5.5% suggesting good consistency.

Tensile Strength

The splitting tensile strength f_{st} varied from 401 psi 1007 psi. The COV varied from 3.9%-7.3% for Control, LMC, and FRSCC. The SCC mix exhibited a COV of 24%, suggesting higher variability than the other mixtures. The FRSCC mixture featured the highest tensile strength. The failure mode of FRSCC cylinders tested in compression and tension was gradual – i.e. a controlled and desired behavior – due to the presence of fibers. The failure mode of the FRSCC mixture in splitting tensile strength tests was characterized by the formation of a critical crack parallel with the applied load and a gradual increase of that crack up until the test was terminated when the load reduced to 90% of the peak load. The FRSCC cylinder remained in one piece providing further evidence that the FRSCC is a good candidate for the repair of deteriorated deck fascia due to its ability retain broken fragments of concrete.

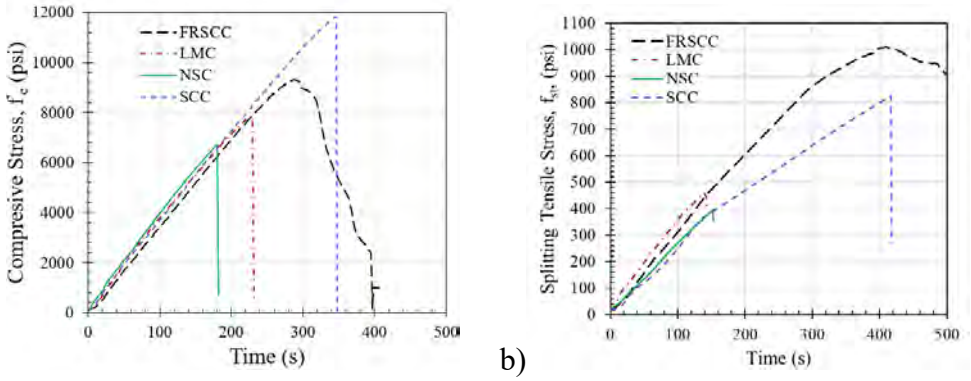

a) b)

Fig. 5.21 a) Concrete compressive stress versus time; b) concrete splitting tensile stress versus time

Modulus of Elasticity and Poisson's ratio

Modulus of elasticity varied from 4324 ksi to 5125 ksi. The Poisson's ratio for all concrete mixtures varied from 0.17 to 0.21, which is an expected range for concrete. The COV for modulus of elasticity and Poisson's ratio were no greater than 4.6% and 8.8%, respectively, suggesting good consistency.

Shrinkage

Fig. 5.22 shows the variation of shrinkage strain (in terms of microstrain) for the considered concrete mixtures. The unrestrained shrinkage of LMC, SCC, and FRSCC mixtures varied from 630 με to 830 με. Ultimately, the FRSCC mix and SCC mix exhibited virtually identical shrinkage strains. The LMC mix exhibited the lowest ultimate shrinkage strain. Although, a mix with low free shrinkage is desired, the FRSCC features good sustained tensile strength and should be able to accommodate and dissipate any tensile stresses developed due to free shrinkage.

Table 5.6 Hardened concrete material properties at 28 days

Cylinder No.	f_c' (ksi)	f_{st} (psi)	E_c (ksi)	μ
NSC-Host				
1	6.3	376.0	4570.6	0.20
2	6.0	433.6	4507.2	0.22
3	6.7	394.2	4403.4	0.21
Average	6.3	401.3	4493.7	0.21
St. Dev.	0.4	29.4	84.4	0.01
COV (%)	5.5	7.3	1.9	4.8
LMC				
1	7.6	429.6	4587.2	0.19
2	7.8	458.6	4697.8	0.18
3	7.8	461.7	4799.1	0.19
Average	7.8	450.0	4694.7	0.19
St. Dev.	0.1	17.7	106.0	0.01
COV (%)	1.5	3.9	2.3	3.1
SCC				
1	11.9	503.7	5262.3	0.20
2	11.0	663.5	5088.9	0.20
3	11.8	824.9	5022.9	0.18
Average	11.6	664.0	5124.7	0.19
St. Dev.	0.5	160.6	123.6	0.01
COV (%)	4.1	24.2	2.4	6.0
FRSCC				
1	9.1	940.5	4185.7	0.16
2	9.4	1069.9	4550.4	0.19
3	9.3	1009.1	4236.2	0.17
Average	9.3	1006.5	4324.1	0.17
St. Dev.	0.1	64.7	197.6	0.02
COV (%)	1.6	6.4	4.6	8.8

Table 5.7 Summary of hardened concrete material properties at 28 days

Mix	f_c' (ksi)	f_{st} (psi)	E_c (ksi)	μ
NSC-Host	6.3	401.3	4493.7	0.21
LMC	7.8	450.0	4694.7	0.19
SCC	11.6	664.0	5124.7	0.19
FRSCC	9.3	1006.5	4324.1	0.17

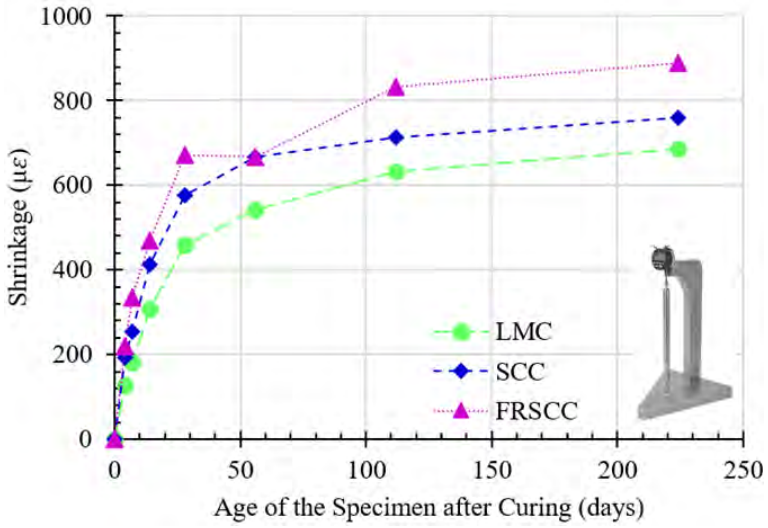

Fig. 5.22 Variation of shrinkage strain for considered concrete mixtures

5.2.2 Relative Durability

The results of freeze-thaw testing are shown in Fig. 5.23 in terms of the dynamic modulus of elasticity (Fig. 5.23a (left)), specimen weight (Fig. 5.23b (left)), and rebound number as a function of time (Fig. 5.23c (left)). Fig. 5.23 also shows the percent difference with respect to the initial measurements for all these parameters (Fig. 5.23a-c (right)). All concrete specimens showed a slight increase in the dynamic modulus with time as opposed to a decrease. The control specimens featuring deck concrete exhibited a 3% increase in the dynamic modulus, whereas the prisms representing the repair concrete material exhibited 4.5-5.5% increases in the dynamic moduli. All specimens featuring repair concrete mixtures exhibited higher dynamic moduli compared to the specimen that featured the host deck concrete material. The specimen that featured SCC exhibited the higher dynamic modulus of elasticity. The specimens that featured FRSCC and LMC exhibited almost identical dynamic moduli of elasticity. All specimens showed good stability to rapid freezing and thawing in water in terms of the dynamic modulus of elasticity.

The mass of the specimens remained relatively constant with some marginal increases, which could be attributed to slight changes in the moisture content at the time of measurement despite the fact that all specimens were towel dried prior to measurement. Increases in mass were no greater than 0.5%. Specimen mass stability corroborates the relative stability and slight increase in the dynamic modulus.

There was no strong trend with respect to the surface hardness as characterized by the rebound number, although a linear curve fit to the measured data suggests a slight decrease in

surface hardness with time. The SCC specimen exhibited the highest surface hardness as corroborated by static and dynamic moduli measurements. The FRSCC and LMC specimens exhibited a similar behavior in terms of surface hardness, which is consistent with the dynamic moduli measurements. The control specimen featuring deck concrete exhibited the lowest surface hardness. The surface hardness of the SCC specimen reduced with time to values that were comparable to those exhibited by the FRSCC and LMC.

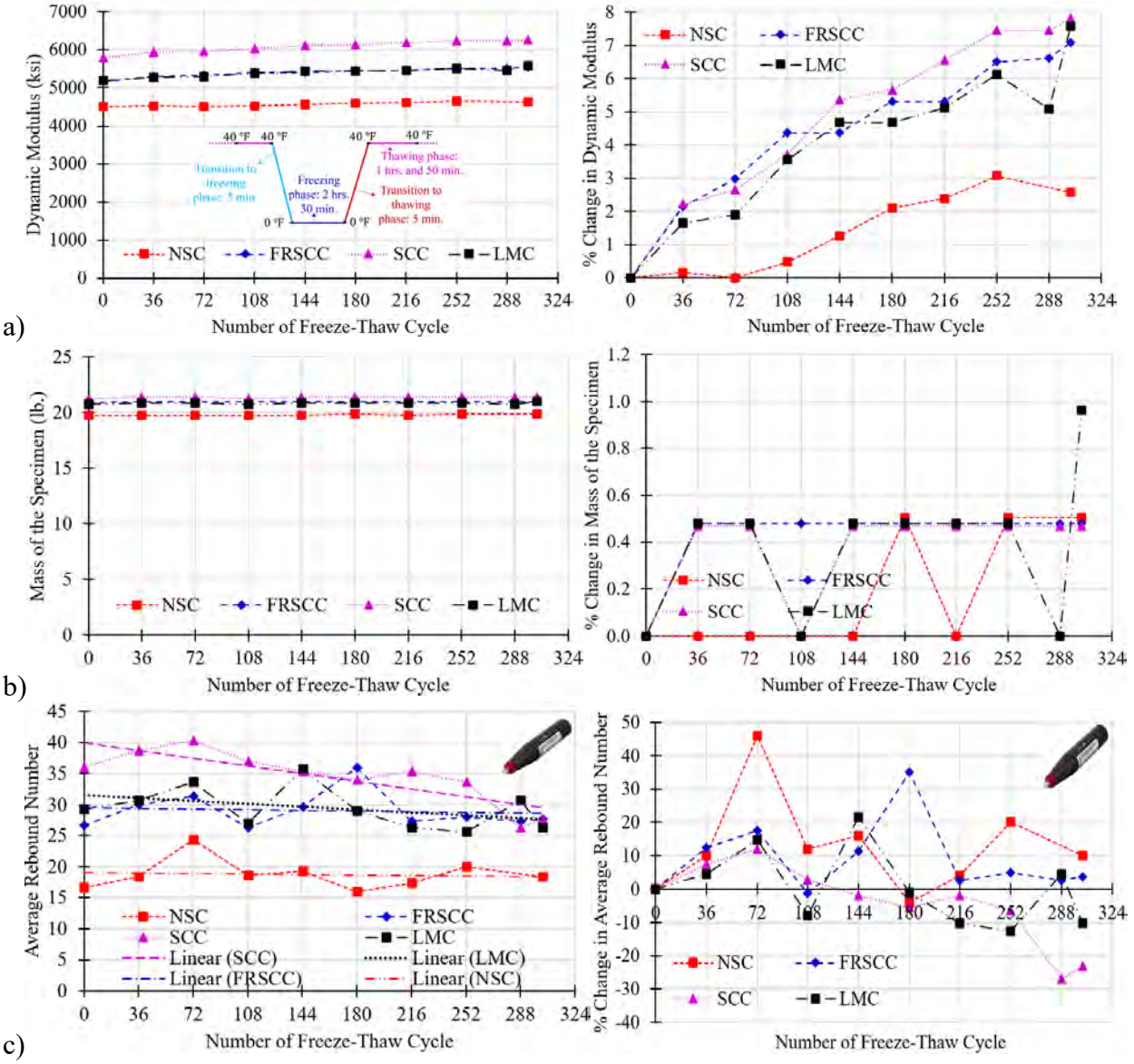

Fig. 5.23 Results of freeze-thaw durability testing: a) variation of the dynamic modulus (left) and % change in the dynamic modulus as a function of number of cycles; b) variation of the mass of the specimens (left) and % change in the mass as a function of number of cycles; and c) variation of the rebound number (left) and % change in the rebound number as a function of number of cycles

5.2.3 Reinforced Interface Shear Strength

Specimens Subject to Accelerated Corrosion

Fig. 5.24 shows the periodic measurements obtained during the corrosion test in terms of the average electrical potential (half-cell potential), and measured current. Fig. 5.25 illustrates the debris accumulated in the container during corrosion test, and the condition of the specimens during testing. Initial (benchmark) half-cell potential measurements suggest that there is a greater than 90% probability of no corrosion in the specimens constructed with the repair materials. During the first week, corrosion activity was observed at the locations where wood pieces are placed for reinforcement cover. This is supported by subsequent half-cell potential readings. At day 8, a color change near the extended reinforcement was observed for the SCC specimen, together with some NaCl deposits accumulated at the top. Similar observations were made for the NSC specimen at day 10. At day 13, the level of the corrosion at the top of the specimens increased (Fig. 5.25d). At day 17, the test was terminated since the corrosion level for the SCC and NSC specimens was visually notable. In addition, while the half-cell potential measurements fluctuated (recall that half-cell potential measurements were taken at various points and the average was reported – see methodology), on average, half-cell potential measurements suggest a greater than 90% probability of corrosion. It should be noted that the purpose of this test was to determine the impact that existing corrosion on the deck concrete can have on the repaired interface. The conditions of the specimens just before the termination of the test can be seen in Fig. 5.25f.

The current in all specimens was virtually identical. This is attributed to the fact that wooden supports were provided underneath the reinforcement to provide the necessary cover and the regions where these wooden supports were provided may have provided a direct avenue to close the electrical circuit and induce identical levels of corrosion in the host part of the repaired prismatic specimen. This normalization of current supply provided an avenue to examine the performance of the various repaired specimens when subject to a direct shear force, when the reinforcement in the host side exhibits identical levels of corrosion.

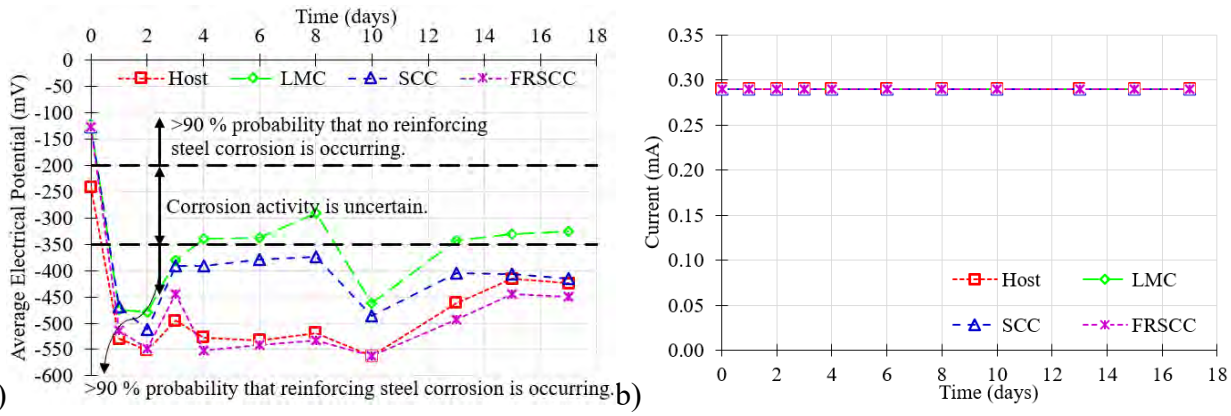

Fig. 5.24 Periodic measurements obtained during the corrosion test: a) average electrical potential; and b) measured current

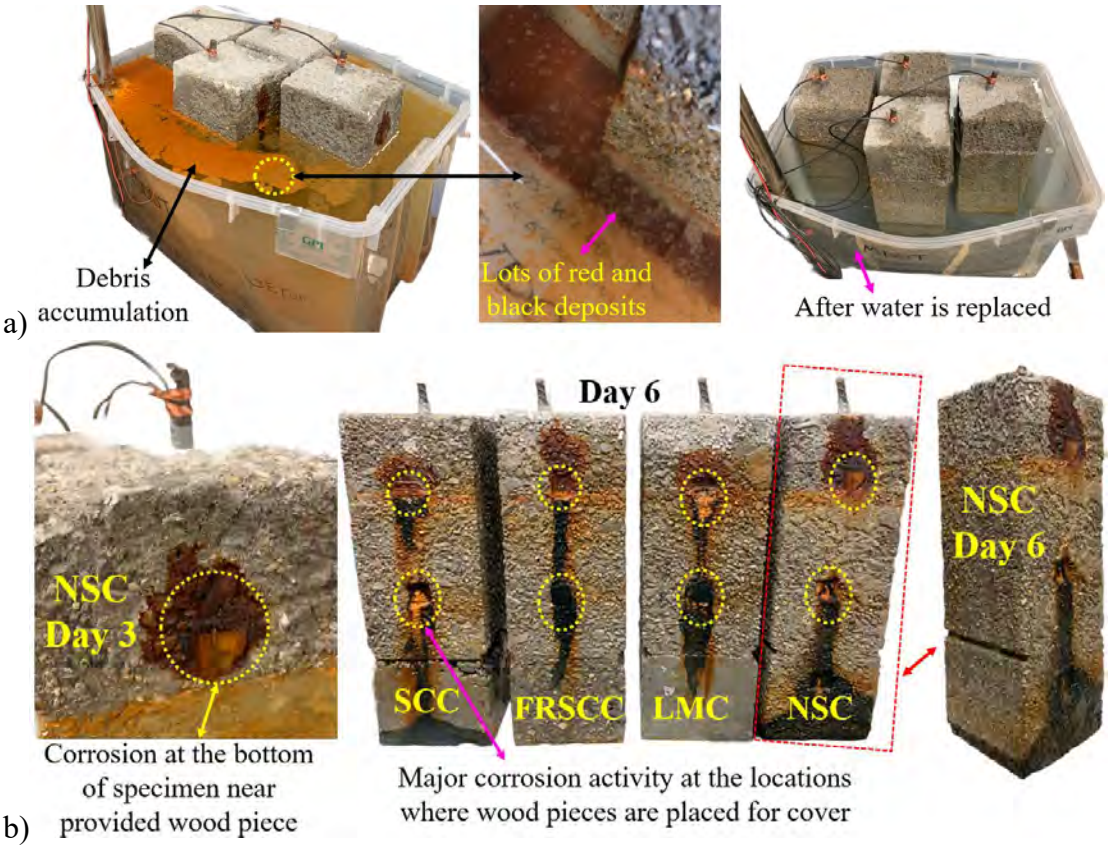

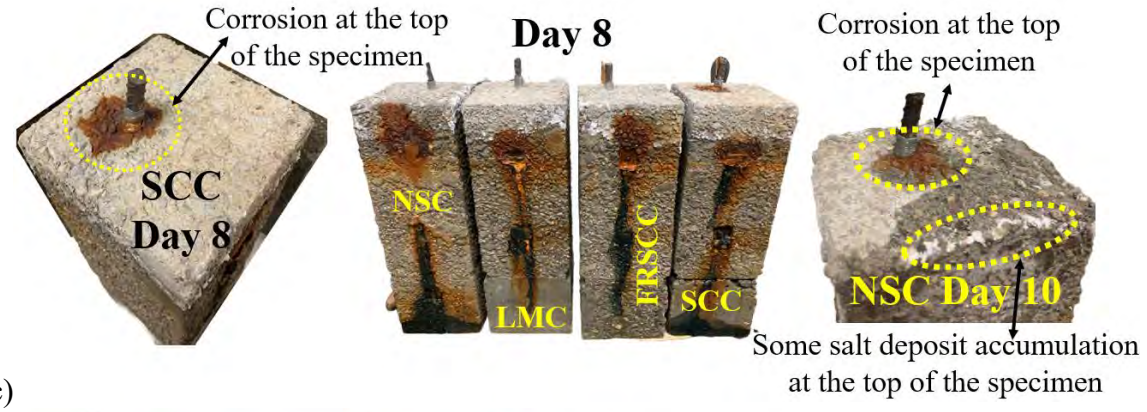

c)

d)

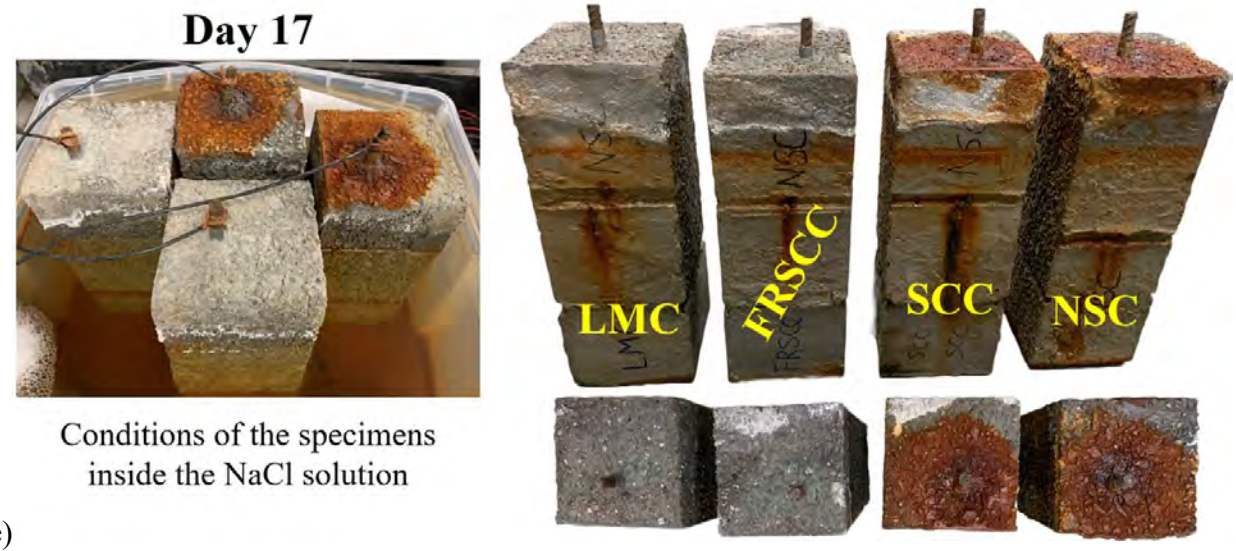

Conditions of the specimens inside the NaCl solution

e)

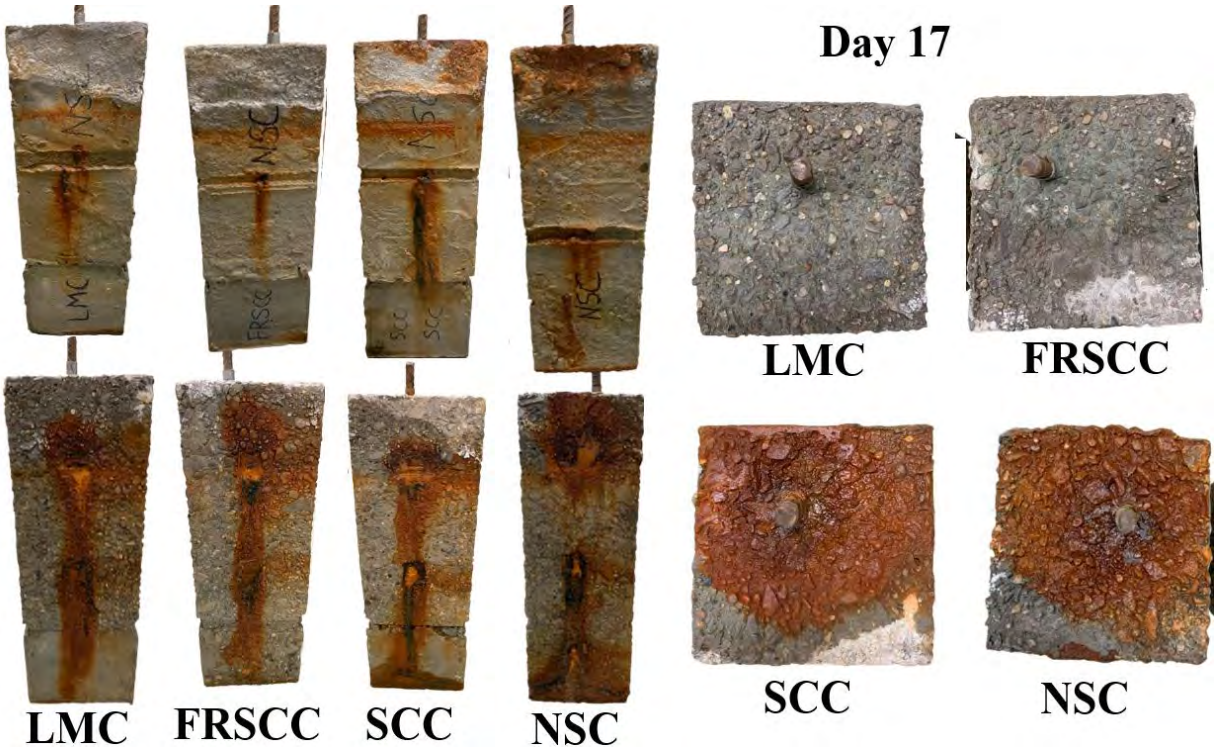

Fig. 5.25 a) Illustration of debris accumulation in the container during corrosion test; b-f) Conditions of the specimen throughout the corrosion test

Interface Shear Strength Testing

Fig. 5.26 shows the relationship between the applied force and interface slip for reinforced concrete prismatic specimens tested for interface shear strength. In each figure there are two curves. The curve with the solid line represents the response of the weathered (W) specimens to direct shear loading (i.e. the specimens subject to accelerated corrosion). The dashed line represents the response of the un-weathered (UW) specimens to direct shear loading. The markers shown in each graph illustrate the likely initiation of cracking, and are determined based on shear stiffness changes as determined by the load versus slip response Fig. 5.26a shows the response of the control specimen. Recall that in this specimen there was no joint between dissimilar materials. The plane where a direct shear failure was desired to be induced was weakened by reducing the specimen cross-section as explained in the methodology section. Fig. 5.26b-d show the response of the repaired specimens.

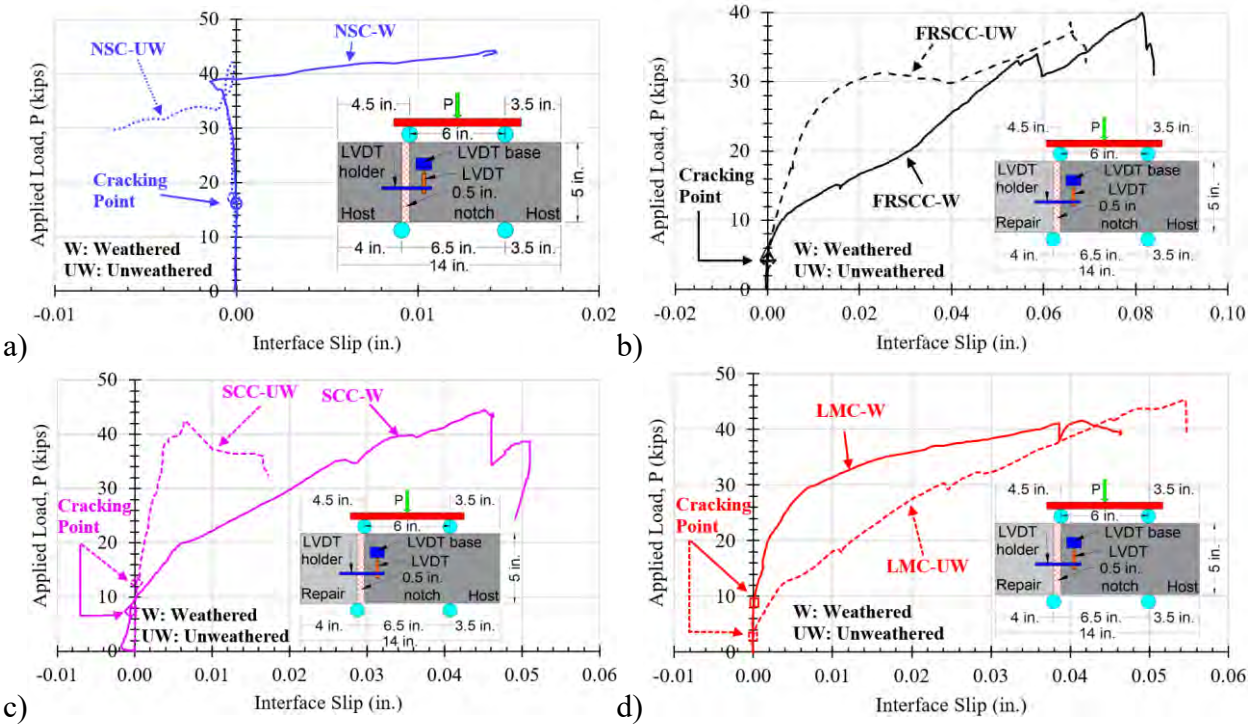

Fig. 5.26 Applied load (P) versus interface slip relationship for the reinforced concrete prismatic specimens: a) NSC; b) FRSCC; c) SCC; and d) LMC

Fig. 5.27 illustrates the relationship between applied load versus interface slip (a); and strain energy versus interface slip (b). This allows a direct comparison of all tested specimens in terms of their response to direct shear loading. In Fig. 5.27a, connection stiffness to direct shear loading, maximum recorded loads, incurred slip for a given load, and connection ductility can be directly compared among the tested specimens.

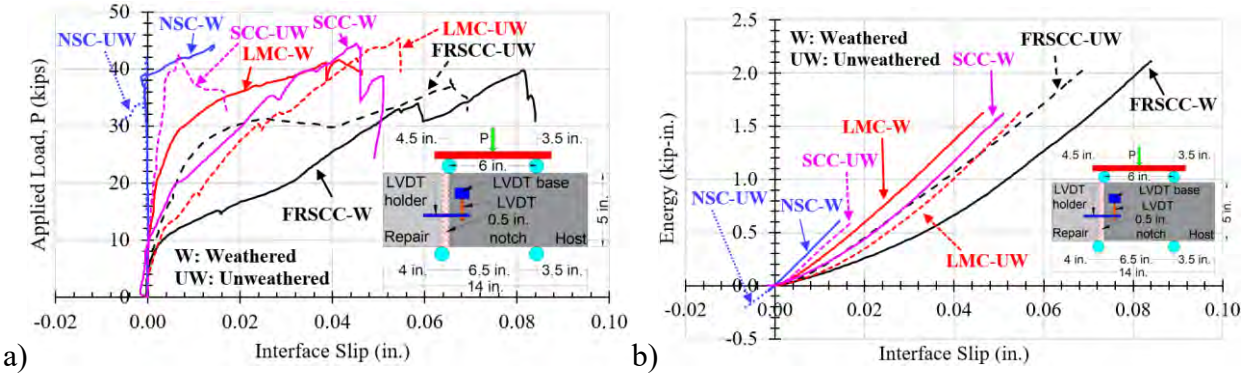

Fig. 5.27 a) Applied load (P) versus interface slip; and b) strain energy versus interface slip

In addition, Table 5.8 shows the result of direct shear testing in terms of the load at first cracking, P_{cr} , the interface slip at first cracking, $\Delta_{P_{cr}}$, maximum recorded load, P_{max}, interface slip at maximum recorded load, and dissipated energy (area under the complete load-slip curve),

which is used to characterize ductility. In addition, Table 5.8 shows the ratio of maximum load to load at first crack, P_{max}/P_{cr}.The ratio of peak load to load at first crack is an indication of the hardening behavior when this ratio is greater than 1.0 and softening behavior when the ratio is smaller than 1.0. Finally, the last column in Table 5.8 represents the failure mode of the specimens. The intended failure mode was a direct shear failure at the weakened interface unless this interface performed better than predicted. Fig. 5.28 illustrates the failure mode for all tested specimens.

Table 5.8 Results of direct shear testing

Specimen ID[λ]	At Cracking[ξ]		At Peak			Ratio	Failure Mode*
	P_{cr} (kip)	$\Delta_{P_{cr}}$ (in.)	P_{max} (kips)	$\Delta_{P_{max}}$ (in.)	E_{max}[ε] (kip-in.)	$\frac{P_{max}}{P_{cr}}$	
FRSCC-UW	4.2	8.0E-05	38.5	0.066	2.05	9.2	SPc
FRSCC-W	5.2	-1.0E-05	39.9	0.081	2.11	7.7	SPc
LMC -UW	2.8	-4.0E-05	45.4	0.054	1.63	16.2	SPc
LMC-W	9.0	8.0E-05	41.6	0.041	1.63	4.6	SPc
NSC-UW	17.0	-1.4E-04	42.1	-2.4E-4	-0.21	2.5	SPc
NSC-W	16.0	2.0E-05	44.2	0.014	0.61	2.8	S
SCC-UW	12.6	2.2E-04	42.5	0.007	0.60	3.4	S+SPc
SCC-W	7.3	-5.5E-04	44.4	0.045	1.62	6.1	SPc

[λ]UW: Unweathered; W: Weathered; [ξ]Cracking point is determined based on the load versus interface slip response of the specimens; [ε]Stored energy, the area under $P-\Delta$ curve, is numerically calculated using trapezoidal rule; *S: Sudden shear failure at the interface; SPc: Slipping of the interface followed by splitting and bond failure at the opposite support. P_{cr}: Cracking load; $\Delta_{P_{cr}}$: Slip at the interface at cracking load; E_{cr}: Stored energy at the instant of cracking; P_{max}: Maximum load; $\Delta_{P_{max}}$: Slip at the interface at maximum load; E_{max}: Total stored energy

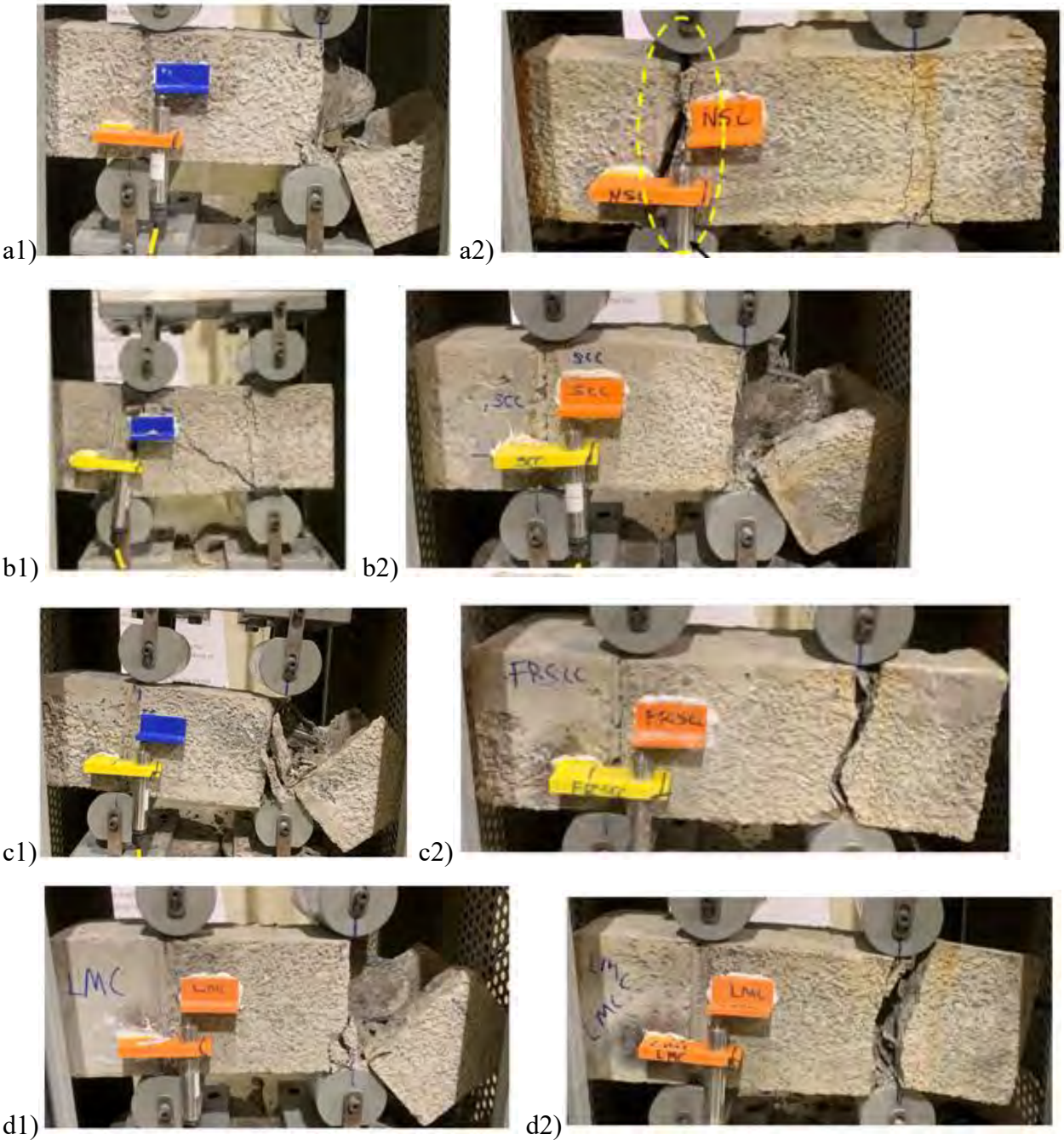

Fig. 5.28 Failure mode: a) Control NSC specimens: shear failure at the right support in un-weathered specimen (a1), shear failure in the left support in weathered specimen (a2); b) Repaired SCC specimen: shear failure near left support in un-weathered specimen (b1), splitting failure at right support in weathered specimen (b2); c) Repaired FRSCC specimen: splitting failure at right support with interface crack at left support in un-weathered specimen (c1), splitting failure at right support in weathered specimen (c2); d) Repaired LMC specimen: splitting failure at right support in un-weathered specimen (d1), splitting failure at right support in weathered specimen (d2).

Load at first crack: Load at first crack is provided in Table 5.8 as well as in Fig. 5.26, which as indicated earlier was based on shear stiffness changes as determined by the load versus slip response. First cracking loads vary from 2.8 kips to 17 kips. The first cracking load represents the loss of cohesion and engagement of dowel action. The repaired specimens exhibited lower loads at first cracking compared to the control specimen suggesting that the repaired interface cannot provide the same level of cohesion provided by the monolithic interface. However, ultimate loads were on par with the control specimen as further explained below.

Connection stiffness: Connection stiffness is represented by the slope of the applied load versus incurred interface slip. The overall connection stiffness is characterized by the initial elastic stiffness exhibited prior to interface slip, and inelastic stiffness exhibited after the loss of cohesion. The control specimen exhibited little slip at the weakened interface prior to failure suggesting a stiff monolithic response. The attainment of peak load was accompanied by a sudden increase in slip. All repaired specimens incurred slip at the host concrete repaired concrete interface, followed by a reduction in connection stiffness and ultimate failure. The repaired specimens exhibited overall lower stiffnesses compared to the control specimens. It should be noted here that connection stiffness is of little interest in terms of behavior at service because the main function of the barrier is to sustain the impact during a collision event and incurred slip or displacements are generally not of interest. What is of importance is that the connection is able to provide comparable ultimate capacities with those provided by the monolithic connection despite incurred larger slips. Connection stiffness may become relevant in cases where a nonlinear finite element analysis of the barrier to deck connection assembly is conducted to evaluate the performance of this assembly to a given impact. In this case, the correct modeling of the connection including its stiffness is important in terms of characterizing the incurred likely damage and overall response.

Maximum Load and Failure Mode: It is interesting to note how the maximum recorded load for all specimens is rather similar and ranged from 38.5 kips to 44.4 kips suggesting that the repaired specimens exhibited similar ultimate capacities in direct shear with the control specimens. All but one specimen exhibited positive slip at the host-repair interface suggesting the initiation of a direct shear failure as intended. The exhibition of positive slip is an indication of loss of cohesion at the interface and engagement of dowel action. The dowel action is effective if the specimens are able

to sustain loads that are equal to or higher than those incurred at first crack. This was the case for all specimens, which featured a ratio of maximum load to load at first cracking greater than 2.0. This is also an indication of an effective repair since the drilled and epoxied dowels were able to deliver a hardening response after the precipitation of the first crack. The un-weathered specimen exhibited negative slip after the ultimate load was attained. This is attributed to a rigid body counterclockwise rotation exhibited by the portion of the specimen that is on the right of the weakened interface once failure occurred at the right support. A flexural crack at the weakened interface was noted during testing, which allowed the rigid body rotation of the right portion of the specimen about the centroid of the compression region. Because of this, the distance between the LVDT holder and reference 3D printed angle increased.

The ultimate mode of failure was such that a direct shear failure was incurred in the control weathered specimens at the weakened plane as expected accompanied by a splitting failure in the support when the applied load and reaction were aligned. An interface shear failure was also observed in the un-weathered SCC repaired specimen in the vicinity of the weakened plane. The control un-weathered specimen and the repaired un-weathered FRSCC specimen exhibited an interface crack during loading but ultimately failed in splitting failure near the supports where the applied load and reaction aligned. This is an indication that the interface performed better than predicted and that the interface in the repaired specimens was able to resist ultimate shear stresses that were either comparable or higher than those resisted by the control specimens.

Connection Ductility: The supplied ductility of the repaired connection is best described by the stored strain energy as characterized by the area under the load-interface slip curve when the maximum load is attained. All repaired specimens were able to dissipate more strain energy than the control specimens. Connection ductility is important when conducting dynamic analysis for a given impact and when the analyst is interested how a given repaired barrier to deck connection redirects the vehicle in the event of a collision.

Effect of Weathering: The control un-weathered and weathered specimens exhibited maximum loads of 42.1 and 44.2, respectively, suggesting that the accelerated corrosion did not weaken the ultimate strength of the specimens in direct shear. Similar observations were made for the repaired specimens. However, the repaired weathered specimens that featured FRSCC and SCC exhibited

larger interface slips for a given load despite the fact that their ultimate loads were similar. In fact, the weathered repaired specimens that featured FRSCC and SCC exhibited slightly larger ultimate loads than their un-weathered counterparts. This means that for two of the repaired specimens while the induced corrosion may have weakened the interface such the contribution of cohesion to interface shear strength is lessened, the eventual and subsequent contribution of dowel action was able to deliver direct shear capacities that are on par with those exhibited by the un-weathered specimens. Unlike the FRSCC and SCC specimens, the repaired and weathered specimens that featured LMC exhibited a stiffer load-interface slip response compared to the un-weathered counterparts. This suggests that any expansive forces present in the existing uncoated deck reinforcement were not high enough to compromise the cohesion between the host and repair materials. This implies that if the level of corrosion in uncoated bars in existing bridge decks or those that feature repaired deck fascias as recommended in this report is such that no cracking has taken place, then the structural integrity of the interface remains intact.

5.3 Conclusions from Small-scale Testing

A series of small-scale laboratory tests were conducted to select the most promising repair concrete material for potential use in the repair of bridge deck fascias. The following conclusions are drawn:

1. All repair concrete mixtures with the exception of the FRC mixture performed well. The FRC specimens started to disintegrate once the molds were removed and featured low compressive strength. This mix was removed from consideration.
2. The remaining three repair concrete materials, LMC, SCC, and FRSCC featured compressive strengths and tensile strengths that exceed those of the host material. The FRSCC mix featured the highest tensile strength followed by the SCC mix. The FRSCC mix exhibited an ability to sustain compressive and tensile loads after crack initiation suggesting an ability to retain broken concrete fragments – a key ability for a bridge deck fascia repair or for a new bridge if this mix is selected for the deck concrete.
3. The SCC and FRSCC featured self-consolidating properties and are good candidates for the repair of bridge deck fascias as they facilitate placement in tight spaces.
4. The LMC, SCC, and FRSCC showed good stability in terms of specimen mass and dynamic modulus of elasticity during freeze-thaw testing suggesting resilience against weathering.

5. The FRSCC and SCC mixtures showed virtually identical ultimate shrinkage strains. The LMC exhibited the lowest shrinkage strains. While a concrete mixture with low shrinkage is desired in terms of reducing the magnitude of differential shrinkage induced tensile stress, the ability of the concrete mixture to resist and sustain tensile stresses is considered of higher importance in terms of retaining broken concrete fragments that may form due to tensile stresses created as a result of other phenomena such as corrosion or freezing and thawing.
6. In summary, the FRSCC is deemed as the most appropriate mixture as it possesses self-consolidating properties, which facilitate placement, and good tensile strength. A second candidate is the SCC mixture, which offered the second highest tensile strength and facilitates placement in tight spaces. Although, once cracking occurs this mixture does not have the ability to retain broken concrete fragments.

Chapter 6: Full Scale Sub-assemblage Testing

Chapter 6: Full Scale Sub-assemblage Testing

6.1 Methodology

6.1.1 Test Matrix, Test Setup, Specimen Design, and Specimens Details

Test Matrix and Test Setup

A total of three full-scale sub-assemblage specimens were subject to proof-of-concept testing under monotonic loading where a pseudo-static lateral load was applied to the barrier to simulate vehicular impact. The test matrix is provided in Table 6.1 and the test setup is shown in Fig. 6.1. The purpose of these tests was to demonstrate that the repair details and repair materials are viable at full-scale and provide sufficient strength to resist required barrier loads. The latter is critical, as one of the main functions of the deck overhang is to provide sufficient support for the barrier in case of a vehicle impact. The first specimen represents the control specimen in which there is no deterioration in the deck fascia. The second and third specimens represent existing decks with deteriorated deck fascias, which are repaired using the best performing repair concrete materials selected during the small-scale experimental investigation. These two repair concrete materials are the fiber reinforced self-consolidating concrete (FRSCC) mixture, and the self-consolidating concrete (SCC) mixture. Therefore, the second specimen features FRSCC and the third features SCC. Both specimens with deteriorated deck fascias feature drilled and epoxied dowels followed by the placement of repair concrete material. The drilled and epoxied dowels are epoxy coated to provide corrosion protection. To account for natural variations in specimen strength, the self-contained test setup allows the testing of two identical connections simultaneously. The depth of the deck facia, h, is 12 in. The deck is supported at two points, which represent locations of fascia beams. The distance from the center of the support to the deck edge is shown as 30 in. The width of the specimens is 2 ft to provide stability during testing while remaining within the lifting capabilities in the laboratory. This test setup is intended to emulate the presence of shear forces and bending moments in the barrier and tension, and bending moments in the deck overhang.

Table 6.1 Test matrix for full-scale sub-assemblage testing

Specimen ID	Deck		Barrier		Repair	
	Concrete[1] f_c' (psi)	Reinf.[2] f_y (ksi)	Concrete[1] f_c' (psi)	Reinf.[2] f_y (ksi)	Concrete f_c' (psi)	Reinf.[3] f_y (ksi)
S1 - Control	4,500	60	4,500	60	NA	NA
S2 – FRSCC[4]	4,500	60	4,500	60	>4,500	60
S3- SCC[5]	4,500	60	4,500	60	>4,500	60

[1]Control concrete mix used by MDOT for decks; [2]ASTM A615 – Uncoated (ASTM 2020); [3]ASTM A615 – Epoxy Coated (ASTM 2020); [4]Fiber Reinforced Self-Consolidating Concrete; [5]Self-consolidating concrete.

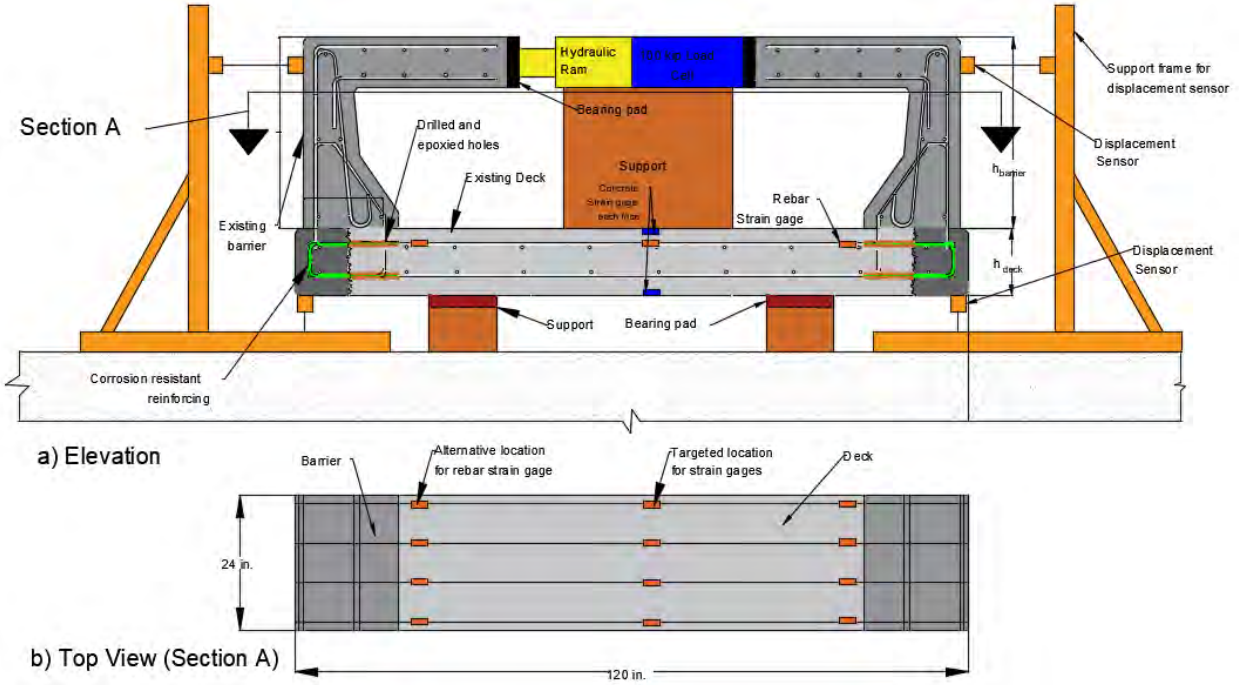

Fig. 6.1 Test setup to validate barrier crashworthiness after deck fascia repair: a) elevation, b) top view

Specimen Details

Specimen No. 1 – Control (S1 – Control)

Specimen details and reinforcement are shown in Fig. 6.2. Cover for top transverse deck reinforcement is specified as 3 in. based on MDOT BDG Detail 6.41.02. Cover for bottom transverse deck reinforcement is specified as 1.5 in. based on MDOT BDG Detail 6.41.02. The deck overhang length is selected as 30 in., which is within the range specified in MDOT BDG Detail 6.41.02. The top and bottom transverse deck reinforcement are selected as #5 at 7 in. o.c. based on the table provided in MDOT BDG Detail 6.41.01 considering the densest reinforcement layout. A 2 in. clear cover is specified from the face of the fascia to the transverse deck

reinforcement. Temperature and shrinkage reinforcements also known as distribution steel is selected as #4 at 10 in. o.c. based on the formula provided in AASHTO LRFD (AASTHO 2020). The reinforcement layout, and cover in the barrier are selected based on the Type IV barrier design in Bridge Design Guide (MDOT 2019) section 6.29.09. Size and spacing were determined such that the weakest section is in the deck to ensure a complete force transfer from the top of the barrier to the deck. Deck and barrier concrete has a compressive strength of f_c'=4,500 psi and is based on an MDOT approved deck mix design. Reinforcing in the deck and barrier is Grade 60 ksi steel (ASTM A615 2020) uncoated.

Specimen No. 2 – FRSCC Repair (S2 – FRSCC)

The drilled and epoxied length for the epoxy coated reinforcement is selected as 10 in. based on the guidance provides by Hilti for No. 5 bars. According to Hilti, for No. 5 rebar, the effective embedment should be in between 3.125 in. and 12.5 in. A 10 in. embedment was selected to increase lap length with existing deck steel. Minimum required concrete thickness is h_{min}=10+2∗5/8=11.25 in. For the specimen in question, the deck fascia thickness is 12 in. which satisfies this requirement. A minimum edge distance of 1.75 in. is permitted provided the rebar remains un-torqued, which is the case for the repair specimens in question. The selected concrete cover satisfies this recommendation. Epoxy coated bars are installed at 7 in. o.c. Minimum anchor spacing is given as 3.125 in., which is smaller than the selected 7 in. spacing. Deck and barrier concrete are the same with that used in the control specimen. Repair concrete is FRSCC as described in the previous chapter. Reinforcing in the deck and barrier is Grade 60 ksi steel (ASTM A615 2020) uncoated. Drilled and epoxied reinforcing is Grade 60 ksi (ASTM A615 2020) epoxy coated reinforcing. The straight extension of the 180° EC rebars denoted as l_{ext} in ACI 318-19 (ACI 2019) Table 25.3.1 is selected as 2.5 in. The minimum bend diameter is $6d_b$=3.75 in, where d_b is the diameter of the bent bar. Therefore, the total length of the extension of the EC rebars is calculated as 3.75/2+2.5=4.5 in. Providing a 2 in. cover from the edge of rebar to the face of the fascia, the repair length is determined as 2+4.5=6.5 in.

Specimen No. 3 – SCC Repair (S3- SCC)

Specimen No. 3 is identical to Specimen No. 2 with the exception of the repair concrete material, which is SCC as described in the previous chapter.

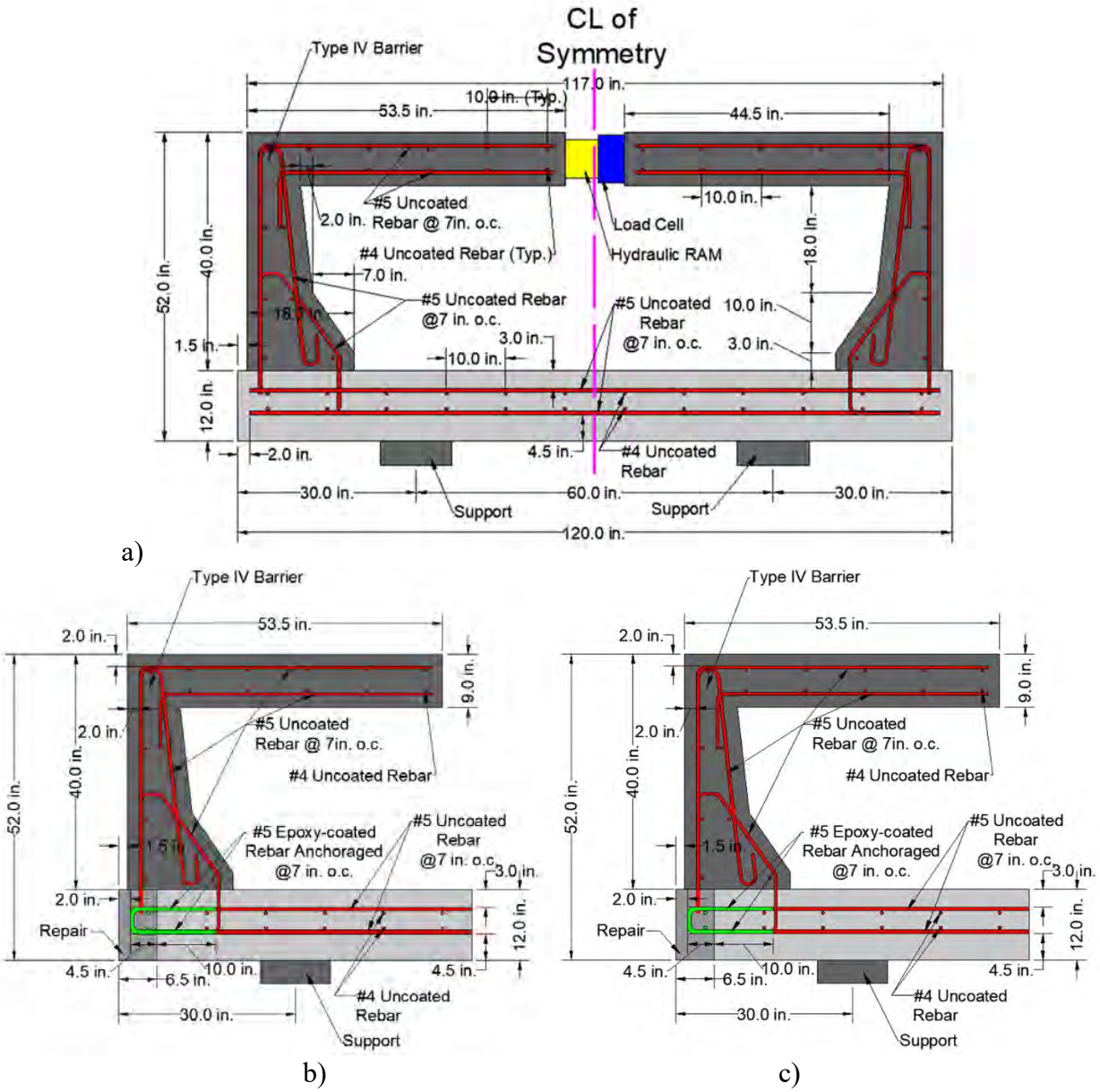

Fig. 6.2 Specimen details and reinforcement: a) S1- Control specimen complete elevation, b) S2 – FRSCC partial elevation, c) S3 - SCC partial elevation

Specimen Design

The success of the repair was evaluated using two metrics: 1) the failure load is higher than that mandated by AASHTO LRFD Specifications (2020) for the deck width in question, or 2) the failure mode is outside of the repaired region. The second criterion ensures that the axial tension

force and moment capacity of the connection is similar to that away from the connection. The relative behavior of the control and repaired specimens was compared in terms of the load versus horizontal displacement at the top of the barrier and vertical displacement at the bottom of the barrier. These relationships characterize the stiffness as well as the ultimate strength of the connection.

The failure mode was expected to be in the deck in the region outside of the repair, assuming that the proposed repair will restore the original capacity of the deck overhang-barrier connection. In a full scale bridge the failure mode is expected to be contained in the barrier through the formation of yield lines. However, in the proposed test setup, the width of the specimens is 2 feet and the moment capacity of the barrier is higher than that of the deck on a per foot basis. To determine whether the proposed connection meets the AASHTO LRFD specifications (2020) for a TL-4 barrier, the F_t = 54 kip equivalent static load demand was divided by $L_c + 2h_{barrier}$ (effective deck width) and multiplied by 2 ft (specimen width), where L_c is the critical length of yield line failure pattern and $h_{barrier}$ is the height of the barrier. According to AASHTO LRFD (2020) Table A13.2.-1, the impact force, F_t, is distributed horizontally over a length of $L_t = 3.5$ ft. If the F_t is transferred to the deck following a distribution based on a 45° angle, the effective deck width is $L_{tdist} = 3.5 + (40 + 12/2) * 2/12 = 11.2$ ft. Therefore, the load demand on the deck on a per foot basis is $w_{dist} = 54/11.2 = 4.84$ k/ft. In the presented test setup, the width of the test specimens is 2 ft. Therefore, the target load is $F_{target} = 4.84 * 2 = 9.7$ kips. This load represents the target load to meet the specifications for a TL-4 rating. Achievement of this load during the test was an indication of a successful repair.

Several cross-sections in the barrier and deck portions of the test specimens were evaluated for their strength to ensure that the target load is transferred from the point of load application to the mid-width of deck. These sections are shown in Fig. 6.3a. In addition, Fig. 6.3b shows the extent of the B-regions and D-regions in the test specimen where B-regions represent “beam” regions where the Euler-Bernoulli beam theory and the assumption of section planarity for predicting member response applies, and D-regions represent disturbed or discontinuity regions where the assumption of section planarity does not apply. The extent of these regions informed the determination of the location for installing surface mounted concrete strain gages. For example, concrete strain gages were installed in the blue region near deck mid-width. Fig. 6.4 shows the

axial force shear and moment diagrams in the test specimen when subject to the prescribed lateral loading. These diagrams are expressed in terms of the applied horizontal load P.

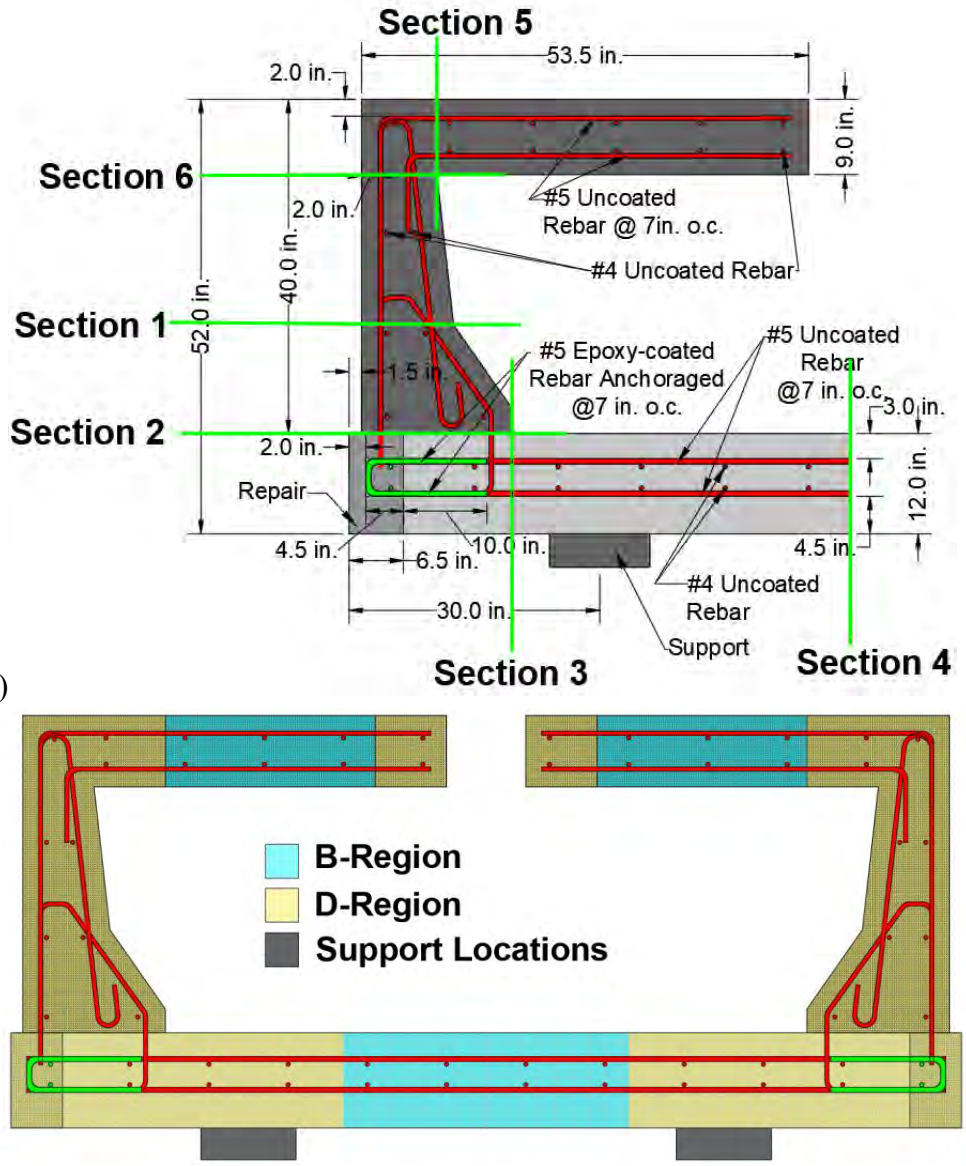

Fig. 6.3 a) Labelling of the critical sections; and b) location of B and D regions

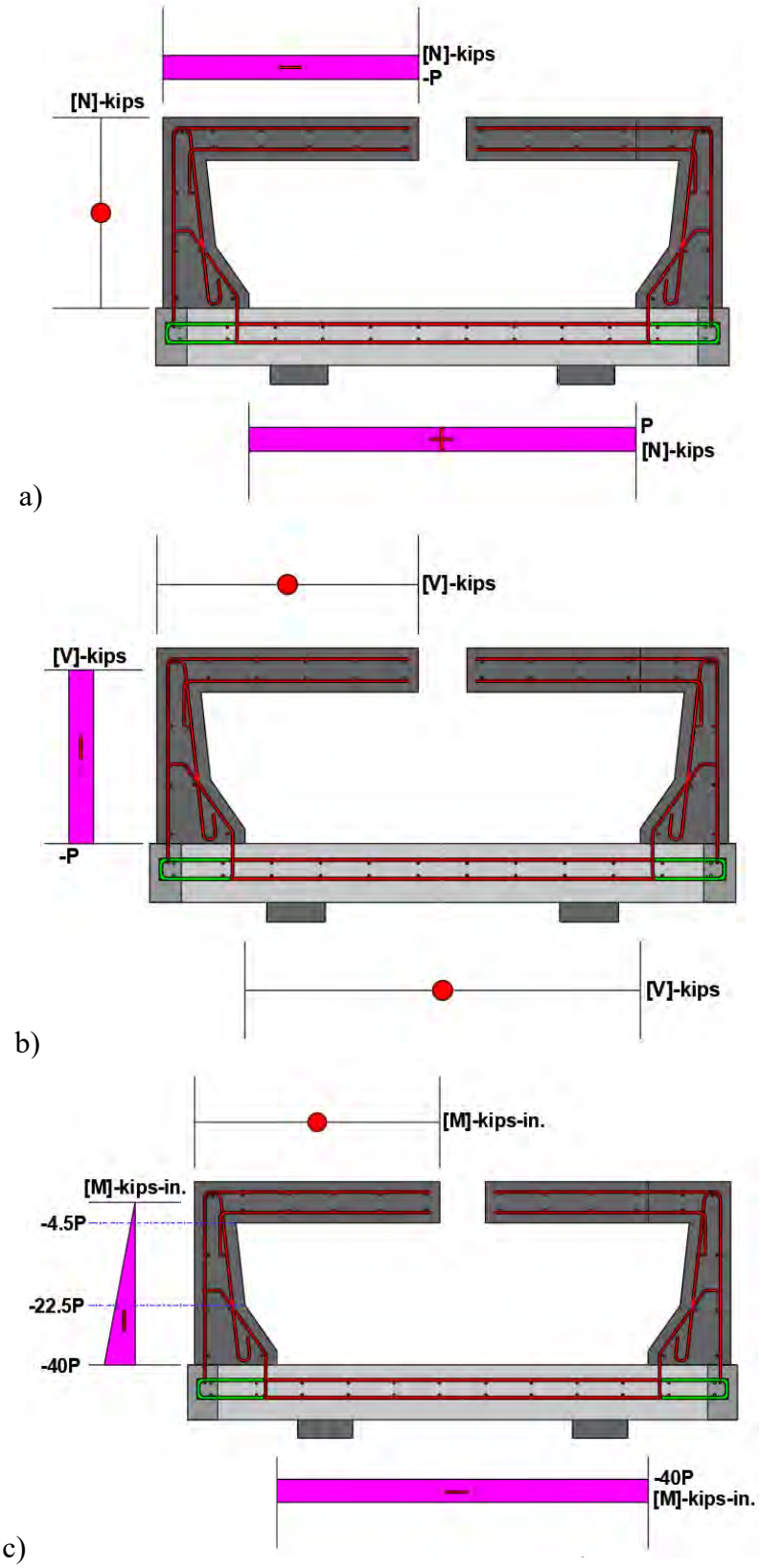

Fig. 6.4 a) Axial force; b) shear force; and c) bending moment diagrams for the barrier test setup

The summary of the selected cross-section analysis is shown in Table 6.2. The first column shows the section numbers, the second shows the applied moment and applied axial force in terms of the applied load *P* for each section, the third shows the calculated nominal moment capacity for each section, the fourth column shows the maximum applied horizontal load that each section can sustain, the fifth column shows the target horizontal load to provide a TL-4 level of protection against vehicle impact, and the last column shows the ratio of the maximum horizontal load and target horizontal load for each section. As can be seen, the controlling cross-sections are sections 3 and 4. This analysis was conducted assuming that the repaired connection is able to transfer the forces from Section 2 to Section 3 and 4 in the sense that the repaired connection was deemed to have the same strength as a new barrier to deck connection. In other words, the repaired interface as well as the overall repair were considered sound enough to preclude the introduction of a new failure path or failure mode. The moment capacity of Section 3 and 4 was determined using the computer software Midas Civil (2022) based on a moment-curvature analysis considering the presence of the axial tension force. Alternatively, the nominal moment capacity of these two sections could be determined using a column interaction diagram. The rest of nominal moment capacities were determined using manual calculations based on AASHTO LRFD (2020).

Table 6.2 Summary of the section analysis

Section	**Applied Moment (neglecting SW)**	M_n **(k-in.)**	P_{max} **(kips)**	F_{target} **(kips)**	P_{max}/F_{target}
1	22.5P	604	26.8	9.7	2.8
2	40P	1092	27.3	9.7	2.8
3	40P+P(Axial T)	619 (with 15.5 kips T)	15.5	9.7	1.6
4	40P+P(Axial T)	619 (with 15.5 kips T)	15.5	9.7	1.6
5	18 k-in. - P (Axial C)	162 (Cracking Moment) 530 (Ultimate Moment)	NA	9.7	NA
6	4.5P	493	20.5 (Shear G.)	9.7	2.1

Section 6 is the most critical section for shear. The shear strength of this section was determined based on AASHTO LRFD (2020) provisions for reinforced concrete members to ensure that it is greater than the controlling target horizontal load of 15.5 kips. This evaluation was conducted by relying on the shear strength provided by concrete alone since there are no stirrups present. The shear capacity of Section 6 was found to be satisfactory based on the provided specimen details.

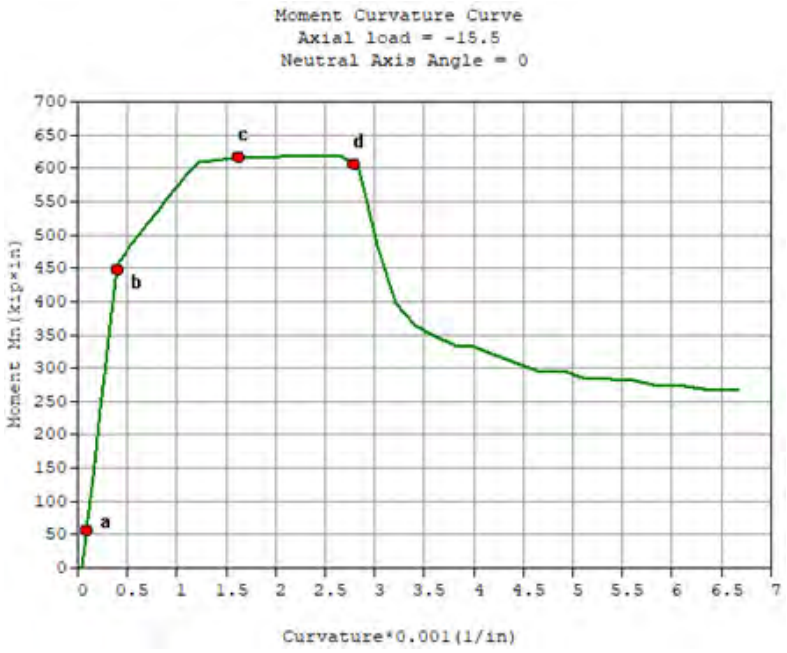

Fig. 6.5 Moment-curvature response of Sections 3 and 4 when subject to an axial tension force of 15.5 kips

Rationale for Layout of Sensors

Electrical resistance strain gages (ERSG) were installed in the reinforcing bars in the deck. Yielding of these bars was an indication of successful force transfer from the barrier to the deck and thus an indication of a successful repair. The description of these strain gauges and their location is illustrated in Fig. 6.8 and Table 6.3. This description is provided separately for the control and repair specimens. It should be noted that the strain gauges summarized in Table 6.3 include rebar strain gages and concrete strain gauges, which will be discussed later. As illustrated in Fig. 6.1, rebar strain gauges were installed on the top deck reinforcement near the inside face of the barrier, which is an area of stress concentration as it is the location where the cross-sectional geometry of the sub-assemblage test specimen changes and forces from the barrier are transferred to the deck. Rebar strain gages were also installed on the top deck reinforcement near midspan as before and after this section some of the top deck rebars were curtailed and therefore this section was critical.

Strain Gages:

Control Specimen: The control specimen featured hooked and straight top deck rebars. This reflects current practice as the straight rebars reflect the typical top deck reinforcement that is used

to resist negative bending moments due to permanent and transient loads. The hooked top deck rebars represent additional steel that is added to resist axial tension forces and bending moments in the deck due to vehicle impact. Two strain gages were installed on the top deck straight rebars and two on the top deck hooked rebars. This provided an opportunity to measure the efficiency of force transfer through the barrier to deck connection. For example, if both straight and hooked rebars yield it means that force transfer can be facilitated by straight rebars as well as hooked rebars. Calculations conducted based on AASHTO LRFD (2020) development length requirements suggest that only the hooked rebars are able to develop their full yield stress when subject to a concentrated moment and tension at the end of the deck fascia. The plane of force transfer is assumed to be a plane that aligns with the vertical reinforcement in the inside face of the barrier and is perpendicular to the plane of the deck. Strain gages on top deck rebars were installed on both barrier to deck connections thus providing some redundancy in data collection in case some of the strain sensors were to malfunction. At midspan, strain gages were installed on the middle left and right rebars.

Repair Specimens: In the repair specimens the top deck reinforcement featured all straight rebars at the barrier to deck connection and at midspan it featured only 50% of the top rebars since some of the top rebars were curtailed prior to midspan. This is consistent with the approach that some additional hooked bars are typically added at the deck fascia to resist vehicle impact induced forces and are curtailed at some distance past the exterior girder. Strain gauges were installed on both continuous straight and curtailed straight top deck rebars at the barrier to deck connection on both sides. An examination of strain readings during the test provided insights in terms of efficient force transfer during a vehicle impact. It should be noted that the reason why in the repair specimens all bars were straight as opposed to some straight and some hooked as in the control specimen is that in bridges that feature deteriorated deck fascias, it is assumed that the corrosion has attained the point at which any exposed rebars need to be cut to prevent additional corrosion from taking place. As a result, drilled and epoxied epoxy coated dowels are installed to facilitate force transfer between the deck and barrier. A relative comparison of strain gage readings in the top deck rebars at the barrier to deck connection as well as at deck midspan between the control specimen and repair specimens provided insights into the efficiency of the repaired detail.

6.1.2 Specimen Fabrication

The fabrication of the specimens was conducted using the following steps:

Step 1: Fabricate formwork for deck for all three specimens (Fig. 6.6a). The formwork for the control and repair specimens were different because the repair specimens featured a roughened edge at the ends. In addition, the formwork for the repair specimens was 13 in. shorter than the control formwork to represent a 6.5 in. deck fascia deterioration on each side. The creation of the roughened edge was intended to represent the roughness of the surface in a deteriorated deck fascia. To remain consistent in the emulation of this condition, 1 in. by 1 in. foam strips were adhered to the formwork as shown in Fig. 6.6b-c. A total of three foam strips were used, which were spaced at 3 in. on center thus creating a 1.5 in. distance from the center of the foam strip with respect to the top and bottom of the deck.

Step 2: Install the reinforcement for the deck including dowels for the barrier. The completion of this step is illustrated in Fig. 6.7.

Step 3: Install strain gages in the top deck reinforcement. A total of 28 rebar strain gauges, 10 for the control specimen; and 9 for each repair specimen were installed. The description of the installed strain gauges and their location is illustrated in Fig. 6.8 and Table 6.3. The installation of strain gauges included three steps: a) surface preparation, b) strain gauge installation, and c) application of environmental protection kit (for rebar strain gages). These steps are summarized below and were based on guidance provided by the strain gage supplier Vishay Micro-measurement. Fig. 6.9 illustrates some of the key steps for the strain gauge installation procedure.

a- Surface Preparation:

1- Determine the location of the rebar strain gauges.
2- Machine grind the surface of the rebar where the strain gauge is going be installed.
3- Clean the grinded surface with CSM-3 and gauze sponges to eliminate grease on the rebar.
4- Dry abrade the rebar surface using a 320 grit carbon silicone abrasive paper to remove gross particles and eliminate possible surface corrosion.
5- Wet abrade the rebar surface using a 320 grit carbon silicone abrasive paper together with Conditioner A chemical, and clean with a single wiping motion by using a gauze sponge.

6- Wet abrade the rebar surface more by using a 400 grit carbon silicone abrasive paper and Conditioner A. Clean the rebar surface with a single wiping motion and with a gauze sponge.
7- Remove remaining contaminants from the rebar surface by using a cotton tipped applicator together with Conditioner A. Clean the surface with a clean dry gauze sponge.
8- Clean the rebar surface with neutralizer 5A with a cotton tipped applicator to reduce the pH of the surface. Clean the surface with a dry clean gauze sponge.

b- Strain Gauge Installation:

1- Use a strip of plexiglass to align the strain gauge in the intended direction. Clean the surface of the plexiglass using Neutralizer 5A and gauze sponges.
2- Position the gauge on the glass plate using PCT-2M tape. Place the tape on the gauge transverse to the long axis of the gage.
3- Transfer the gauge to the reinforcing rebar by holding it from the edge of the tape. Position the longitudinal axis of the gauge along the longitudinal direction of the rebar.
4- Remove one side of the tape to expose the rebar area where the adhesive will be installed. The strain gauge should be attached to the tape at this point.
5- Apply catalyst C on the bonding surface allow it to air dry for 60 seconds.
6- Apply 1 or 2 drops of M-Bond 200 bonding adhesive on the surface of the gauge, and realign the gauge on the rebar surface by using the edge of the tape. Apply thumb pressure for 1 minute. Allow for an additional two minutes to finalize the catalyzation process.
7- Remove the gauge handling tape carefully, and visually check the strain gauge to see if the gauge appears to be bonded accurately.
8- Provide a strip of PCT-2M tape on the lead wire to prevent possible damage on the gauge.

c- Application of Environmental Protection:

1- Apply M-Coat JA protective coating to protect the strain gauges from the surrounding concrete and potential damage during concrete placement process:
2- Prepare the mix based on the guidelines provided by Vishay Micro-measurements.
3- Apply a relatively thin coat in the vicinity of the strain gauge. Allow the surface to air cure up to placement of concrete.

a)

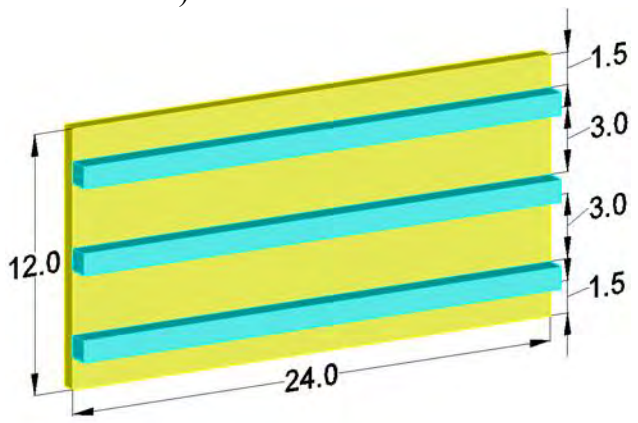

b)

c)

Fig. 6.6 a) Deck formwork for all three specimens, b) simulation of end deck formwork for the repair specimens showing location of foam strips to create a roughened surface, and c) actual end deck formwork with the foam strips to create a roughened surface for the repair specimens

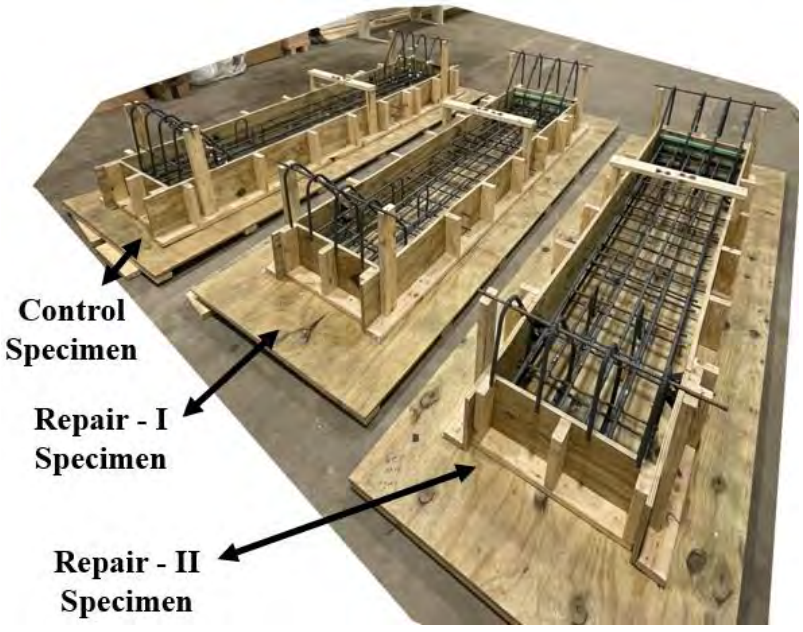

Fig. 6.7 Installed reinforcement for the deck and dowels for the barrier

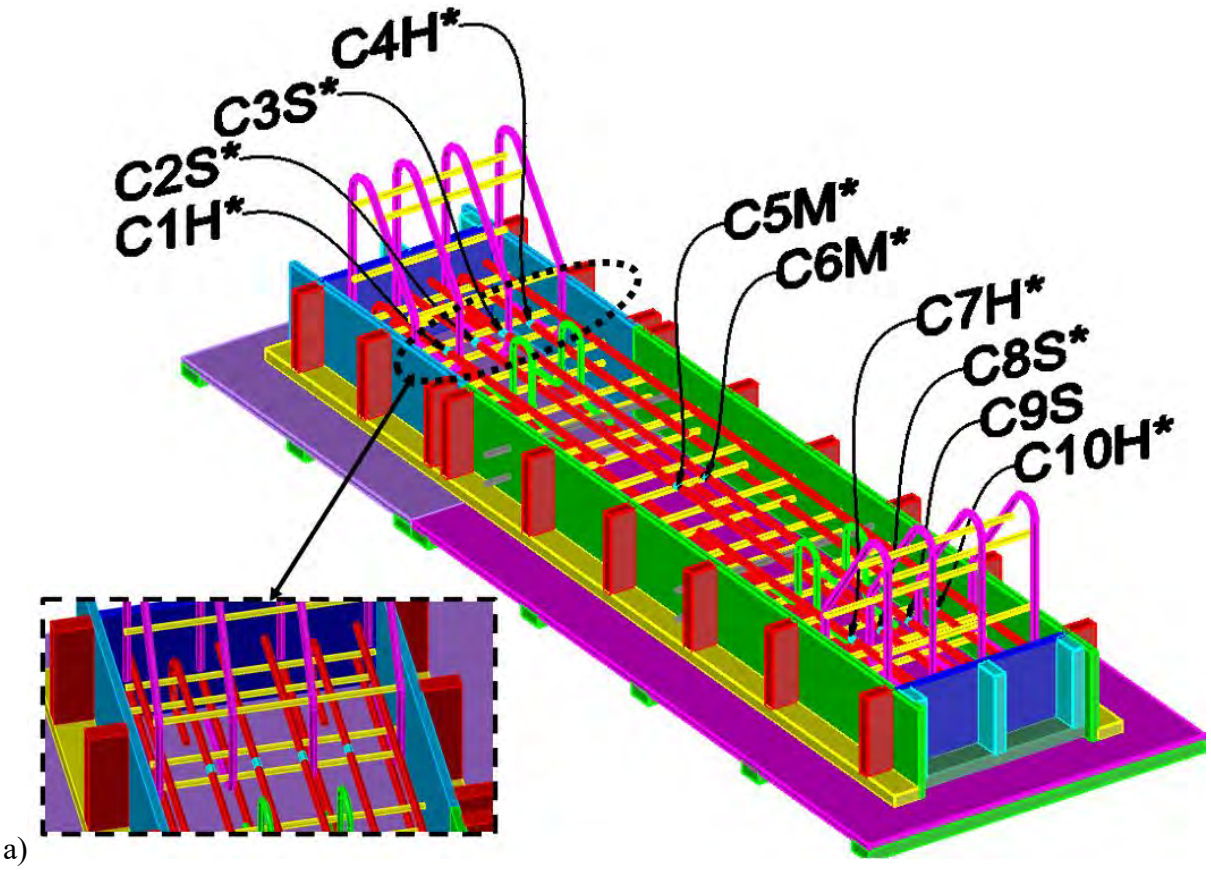

a)

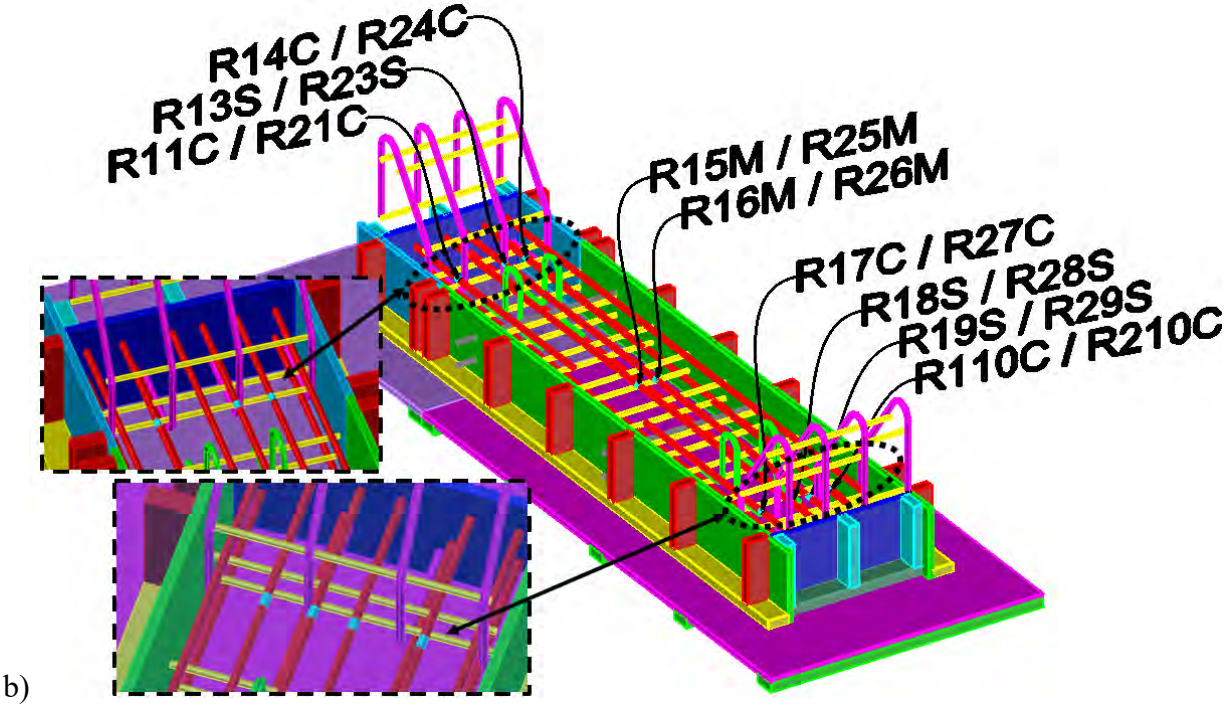

b)

Fig. 6.8 Location of installed rebar strain gauges on: a) Control specimen; and b) Repair I & II specimens

Table 6.3 Labelling and positioning of concrete and rebar strain gauges

Rebar Strain Gauge ID	Position
Control Specimen – 10 Rebar Strain Gauges (4+2+4) & 4 Concrete Strain Gauges	
C1H*	Deck-barrier connection – Mounted on hooked rebar
C2S*	Deck-barrier connection – Mounted on straight rebar
C3S*	Deck-barrier connection – Mounted on straight rebar
C4H*	Deck-barrier connection – Mounted on hooked rebar
C5M*	Midspan – Mounted on left middle rebar
C6M*	Midspan – Mounted on right middle rebar
C7H*	Deck-barrier connection – Mounted on hooked rebar
C8S*	Deck-barrier connection – Mounted on straight rebar
C9S	Deck-barrier connection – Mounted on straight rebar
C10H*	Deck-barrier connection – Mounted on hooked rebar
CTL	Midspan – Mounted on the top left on deck concrete
CTR	Midspan – Mounted on the top right on deck concrete
CBL	Midspan – Mounted on the bottom left on deck concrete
CBR	Midspan – Mounted on the bottom right on deck concrete
Repair I & II Specimens – 9 Rebar Strain Gauges for Each (3+2+4) & 4 Concrete Strain Gauges	
R11C / R21C	Deck-barrier connection – Mounted on cut rebar
R13S / R23S	Deck-barrier connection – Mounted on straight rebar
R14C / R24C	Deck-barrier connection – Mounted on cut rebar
R15M / R25M	Midspan – Mounted on left middle rebar
R16M / R26M	Midspan – Mounted on right middle rebar
R17C / R27C	Deck-barrier connection – Mounted on cut rebar
R18S / R28S	Deck-barrier connection – Mounted on straight rebar
R19S / R29S	Deck-barrier connection – Mounted on straight rebar
R110C / R220C	Deck-barrier connection – Mounted on cut rebar
R1TL / R2TL	Midspan – Mounted on the top left on deck concrete
R1TR / R2TR	Midspan – Mounted on the top right on deck concrete
R1BL / R2BL	Midspan – Mounted on the bottom left on deck concrete
R1BR / R2BR	Midspan – Mounted on the bottom right on deck concrete

*C4A-06-060SL-350-39P is used. For all other rebar gauges, C4A-06-125SL-350-39P is used. For the concrete strain gauges, N2A-06-40CBY-350/P is used.

Note: All rebar strain gauges are installed on the top reinforcements.

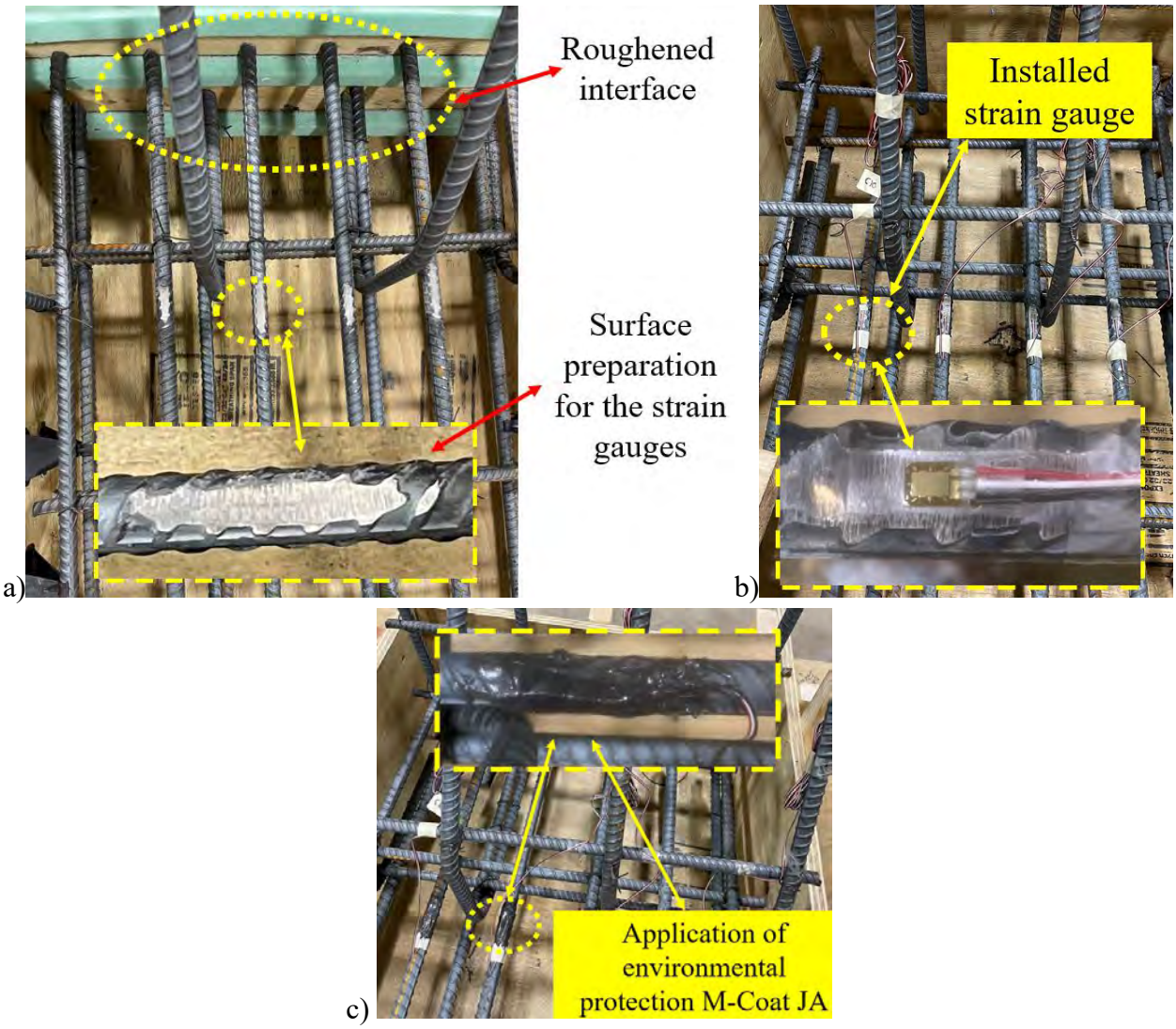

Fig. 6.9 Strain gauge installation: a) surface preparation (grinding, cleaning, neutralizing etc.); b) strain gauge mounting using M-Bond 200 and Catalyst C; and c) application of environmental protection using M-Coat JA

Step 4: Cast concrete for the deck for all three specimens. Activities related to concrete deck placement are illustrated in Fig. 6.10 including the condition of the specimens during deck placement, after the completion of finishing operations, and after the removal of the formwork the next day. A shear key was created underneath the footprint of the barrier to emulate current practice. The deck specimens were then moist cured for seven days. The moist curing process included the application of plastic sheets to contain moisture after deck placement, application and wetting of burlaps the day following the concrete placement, and the covering of wet burlaps with

plastic sheets to contain moisture after the burlap wetting process was completed. The burlaps were wetted every day for the duration of the 7-day moist curing period. Prior to the daily wetting of the burlaps it was observed that the burlaps were in the wet state suggesting good containment of moisture provided by the plastic sheets.

Table 6.4 Concrete mix design for the deck and barrier (1 cu. yd.)

Ingredients	**Source Name**	**MDOT Source No. & Series Class**	**Specific Gravity (Bulk Dry)**	**Absorption**	**Mass (lb.)**
Coarse Aggregate – 1	Calcite	71-3 & 6AA	2.53	1.5	1429
Coarse Aggregate – 2	Port Inland	75-5 & Int.	2.67	0.58	300
Fine Aggregate	Stoneco-Burmeister	81-093 & 2NS	2.61	NA	1088
Portland Cement Type IL	Ash Groove (Mississauga)	NA	3.12	NA	428
GGBFS	Ash Groove (Detroit)	NA	2.90	NA	230
Water	NA	NA	1.00	NA	265
Air Entrainment 0AE-PCA Premiere ConAir-X	NA	NA	NA	NA	1 oz/cwt
Water Reducer 0MR50-PCA Premiere OptiFlo-50	NA	NA	NA	NA	5-6 oz/cwt
Specified properties: Slump = 5 in.; Air content = 6.5%; $f_c' = 4500$ psi					

a) 

b) 

c) 

d) 

e) 

Fig. 6.10 a) Casting of concrete for the deck, b) creation of shear key in the deck underneath the footprint of the barrier, c) deck specimens after concrete placement – concrete is in plastic state, d) deck specimens after removal of formwork the day after concrete placement – concrete is in hardened state, e) creation of water stop (shear key) that emulates current practice in which the water stop is created manually

a)

b)

c)

d)

Fig. 6.11 Moist curing of concrete deck specimens: a) covering of deck specimen with plastic sheets after concrete placement, b) covering the specimens with burlap the day after concrete placement and after formwork removal, c) wetting the burlaps, and d) covering the wet burlap with plastic sheets

Step 5: Install formwork and reinforcement for the barrier for all three specimens. This included several steps as the barrier consists of the actual barrier and the horizontal arms, which were fabricated to apply the horizontal load.

a) *Install barrier reinforcements:* This includes the installation of vertical and horizontal reinforcement in the barrier and is illustrated in Fig. 6.12a.

b) *Install formwork for the barrier:* This includes the installation of formwork for the barrier itself as well as that for the cantilevered arms and is illustrated in Fig. 6.12b-d. This was done in several steps and was combined with the installation of the barrier reinforcement as the installation of barrier reinforcement required access. To provide this access the barrier formwork was constructed such that the bottom formwork for the horizontal wings was constructed first, followed by the side formwork, and concluding with the end formwork.

c) *Install reinforcement for the horizontal wings:* The installation of the reinforcement for the horizontal wings was conducted after the installation of bottom formwork for the horizontal wings and the side formwork for the barrier.

Fig. 6.12 a) Installation of barrier reinforcement, b-c) installation of bottom formwork for the horizontal wings and side formwork for the barrier, d) installation of the reinforcement for the horizontal wings, e-g) views of installed formwork and reinforcement for the barrier

Step 6: Cast concrete for the barrier and cantilever arms for all three specimens. Plastic property tests were conducted during barrier concrete placement and included slump (Fig. 6.13a-b), unit weight, and air content. Concrete was placed using a concrete pump Fig. 6.14c since the top of the barrier was 5 ft above the floor level and the specimens were 10 ft long. Finishing operations were conducted after the placement of concrete Fig. 6.14d. The specimens were then covered with plastic sheets to initiate moist curing (Fig. 6.14e). The next day the side and end formwork were removed (Fig. 6.14a) and the specimens were covered with wet burlap (Fig. 6.14b) and plastic sheets (Fig. 6.14c) to moist cure them for 7 days. A view of the specimens after the curing process was completed is shown in Fig. 6.14d.

Step 7: Drill and epoxy dowels for the repaired specimens. This task was completed in several steps. Initially the foam strips were removed. Then the holes were drilled at the designated location using a drilling machine. After the drilling process, the inside of the holes was cleaned using a towel, a brush, and an air sucker. Then the epoxy mortar was prepared and injected into the holes using a nozzle extension. The dowels were then installed and left to cure.

Step 8: Install formwork for casting the repair concrete material.

Step 9: Install repair FRSCC for Specimen No. 2 (use the mix described in the previous chapter). Moist cure for 7 days. Install repair SCC for Specimen No. 3 (use the mix described in the previous chapter). Moist cure for 7 days.

Fig. 6.13 a-b) Slump test during barrier concrete placement, c) placement of concrete using a concrete pump, d) finished top surface of the specimens, e) specimens covered with plastic sheets after concrete placement

a)  b) 

c)  d) 

Fig. 6.14 a) Test specimens after partial formwork removal, b) covering the specimens with wet burlap, c) covering the specimens with plastic sheets, d) specimens after curing and complete formwork removal

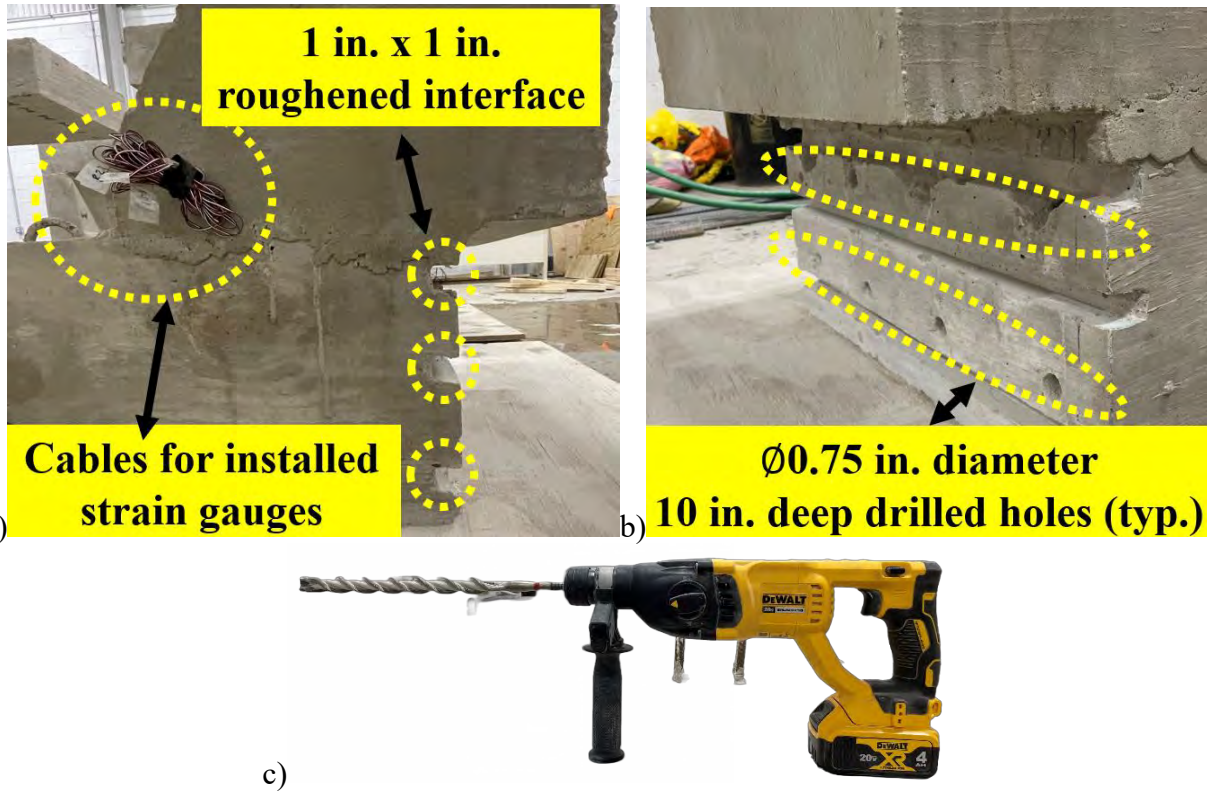

a) b) c)

Fig. 6.15 a) Roughened surface after foam strip removal, b) outline of the drilled holes, c) drilling machine used to drill the holes (Hilti drill bit 10 in. long and 0.75 in. in diameter)

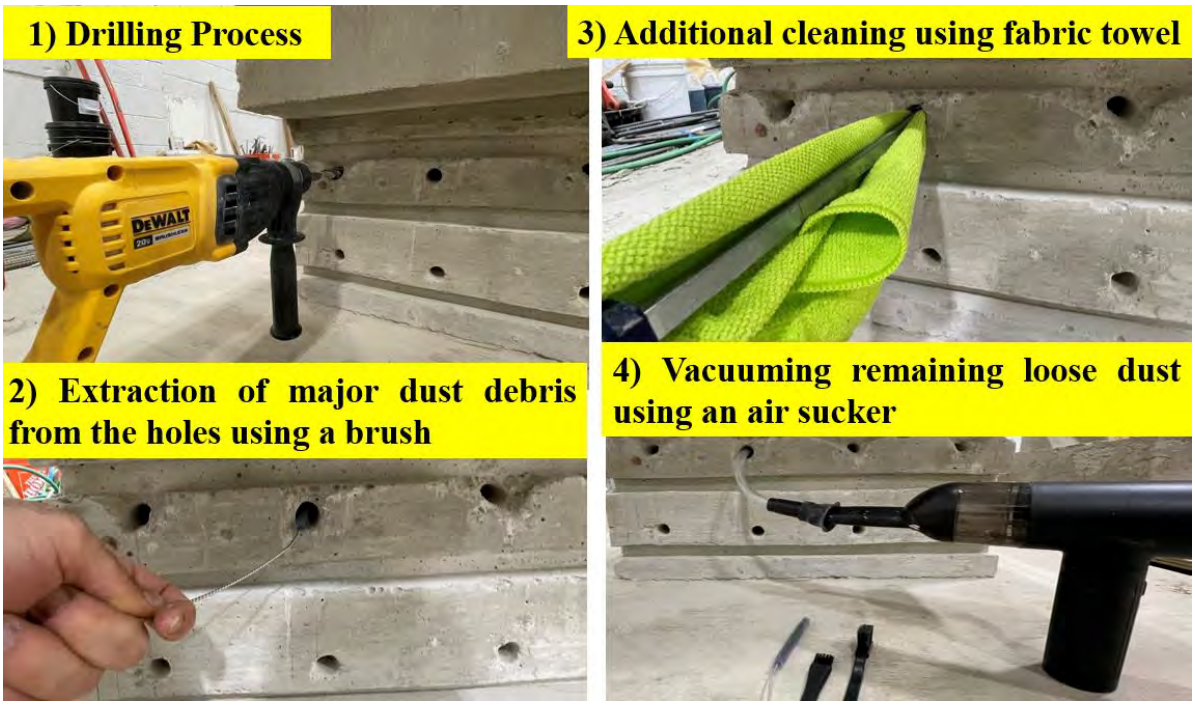

Fig. 6.16 Summary of procedure followed to drill the holes: 1) drilling process, 2) removal of dust, 3) additional cleaning, and 4) removing any remaining dust using an air sucker

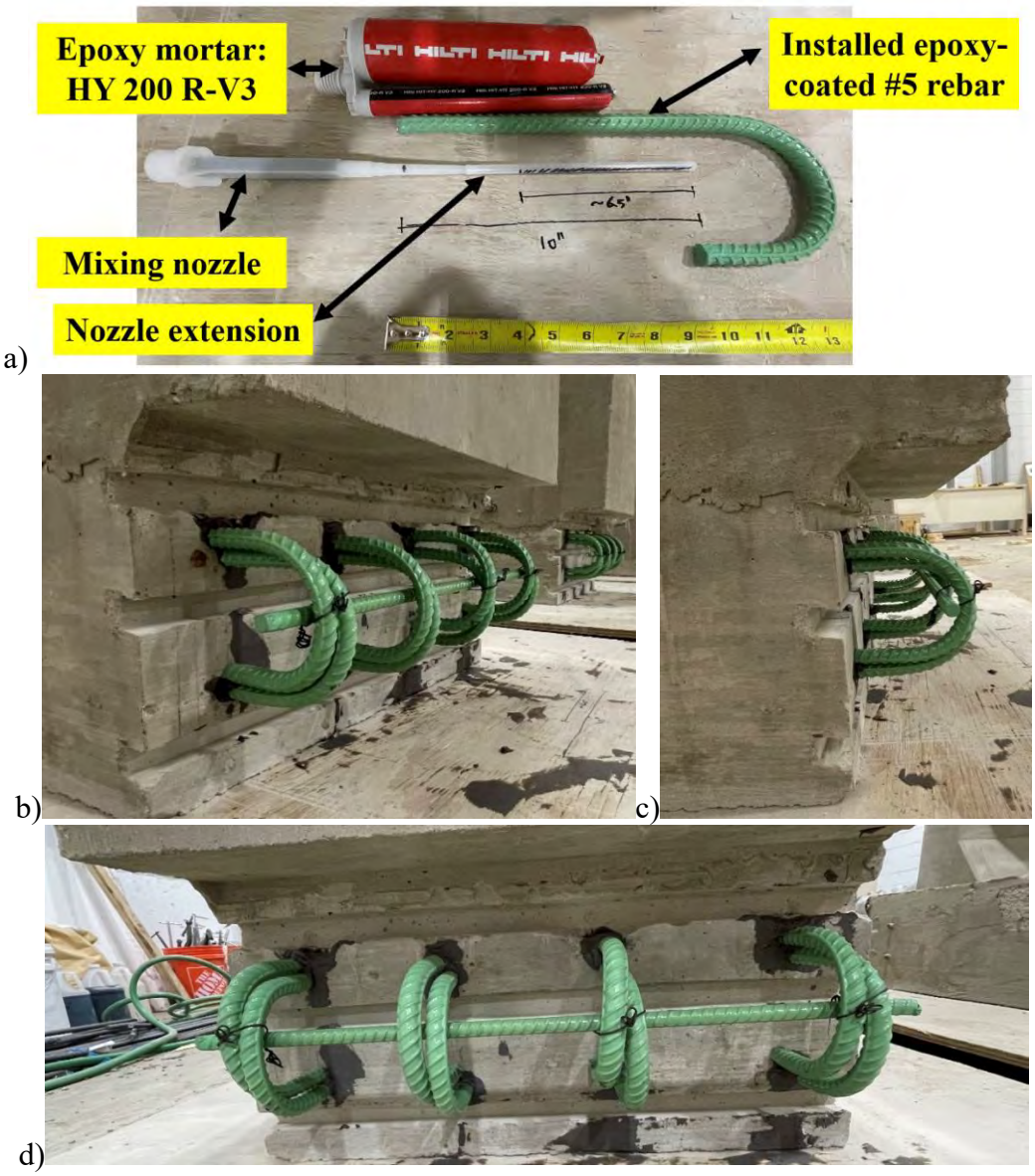

Fig. 6.17 a) Tools to install the epoxy coated dowels, b-d) views of epoxy coated dowels

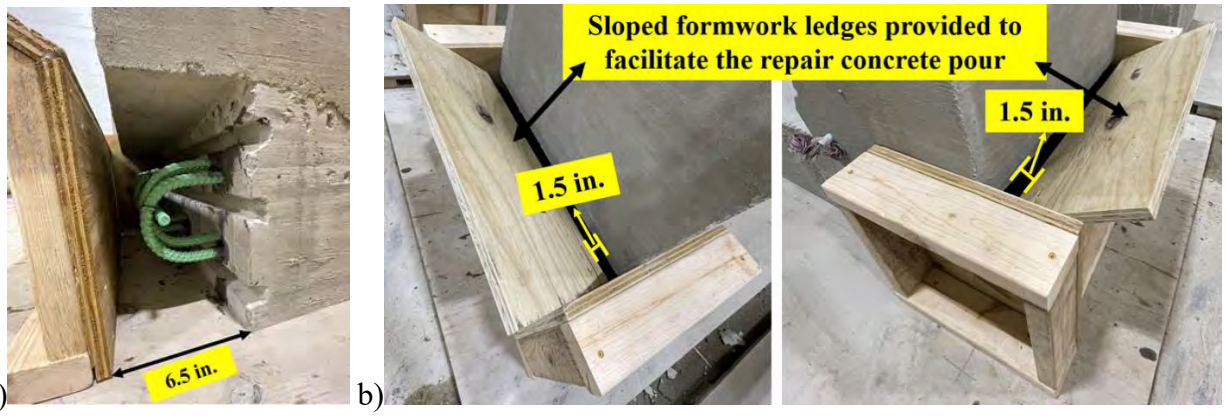

a) b)

Fig. 6.18 Installation of formwork for the repair concrete materials: a) side view of formwork, b-c) other views

Table 6.5 Repair concrete mix design

Ingredient	Repair Material (lbs/yd^3 – unless otherwise noted)	
	SCC	FRSCC
Portland Cement (PC) (Type IL)	589	610
Fly Ash (Class F)	193	254
Fine Agg. (Type 2NS)	1236	1367
Coarse Agg. (29A)	1649	1252
Water	292	354
HRWRA (UltarFlo 2000)	19.54 oz/cwt (9.55 lbs/yd^3)	7.39 oz/cwt (3.99 lbs/yd^3)
WRA (Optiflo 500)	3.93 fl oz/cwt (1.92 lbs/yd^3)	-
VMA	2.58 fl oz/cwt (1.26 lbs/yd^3)	0.40 oz/cwt (0.215 lbs/yd^3)
Air Ent. Ad. (Eucon AEA-92)	-	0.08 oz/cwt (0.042 lbs/yd^3)
Steel Fibers	-	131.1 (1 % by volume)
w/cm	0.37	0.41
Specific gravities were taken from a JMF supplied by MDOT for the mix #92MR-C and Job #128585 and Control section #09035 considering bulk-dry condition: PC=3.15; Fly-ash=2.59; Fine agg.=2.60; Coarse agg.=2.56; Steel fiber=7.85; Admixtures=1.0 (assumed).		

6.1.3 Install External Strain Gauges

Concrete strain gages were installed at midspan at the top and bottom concrete fibers on each side of the test specimens. The length of strain gages was 4 in., which is equal to 4 times the maximum aggregate size (i.e. the maximum aggregate size being 1 in.). This complies with the recommendations of the strain gage supplier (Vishay Micro-measurements), which indicate that the strain gage size should be 3-5 times the maximum aggregate size. The installation of concrete strain gages included several steps, which are outlined below, and which were based on the recommendations of the strain gage manufacturer.

a- Surface Preparation:

1- Determine the location of the concrete strain gauges.
2- Machine grind the surface of the concrete where the strain gauge is going be installed.
3- Clean the grinded surface with a steel brush to remove any residual debris.
4- Apply pressurized air on the grinded & brushed concrete surface.
5- Dry abrade the concrete surface using 220 grit carbon silicone abrasive papers, to remove large particles.
6- Wet-abrade the concrete surface using a 220 grit paper together with Conditioner A chemical. Clean with a single wiping motion using a gauze sponge together with Conditioner A.
7- Wet-abrade the concrete surface again by using 400 grit carbon silicone abrasive paper and Conditioner A. Clean the surface with a single wiping motion with a gauze sponge.
8- To reduce the pH of the surface, apply Neutralizer 5A with a cotton tipped applicator on the concrete surface. Clean the surface with a dry clean gauze sponge.
9- Mix the epoxy resin with the curing agent for 5 minutes. Apply the mixture on the surface to provide a smooth surface before the installation of the strain gauge.
10- Apply a strip of tape on the surface where the strain gauge is going to be installed, and allow it to cure overnight.
11- After curing, the tape is removed, and the resin is dry abraded using 220 and 400 grit abrasive papers. Then the surface is cleaned using Neutralizer 5A and gauze sponges.

b- Strain Gauge Installation:

1- Just before the gauge installation, the surface is cleaned using a single swiping motion using a gauze pad with GC-6 isopropyl alcohol.
2- A piece of plexiglass is used to align the strain gauge in intended direction. The surface of the plexiglass is cleaned using Neutralizer 5A and gauze sponges.
3- Apply a strip of tape on the gauge while the gauge is resting on the plexiglass
4- Then the gauge is positioned on the designated place by holding it from the edge of the tape and by applying the tape on the concrete surface.
5- Remove one side of the tape and expose the back surface of the gauge. The previously prepared AE-10 resin is applied on the back of the gauge. Similarly, a thin layer of epoxy

resin is applied on the concrete surface for proper bond between the strain gauge and concrete.

6- The gauge is realigned on the concrete surface by using the edge of the tape. To ensure that there is no gap between the surface of the concrete and strain gauge, a piece of gauze pad is used to rub over the surface of the strain gauge.
7- For the curing process, it is recommended to have 10-20 psf uniform pressure applied on the strain gauges. To accomplish this, the setups shown in Fig. 6.20b-c were used. The curing continued overnight until the next day.
8- After the curing ends, the clamps or weights are removed. The pressure pad and tape are removed from the surface of the strain gauges carefully.

a)

b)

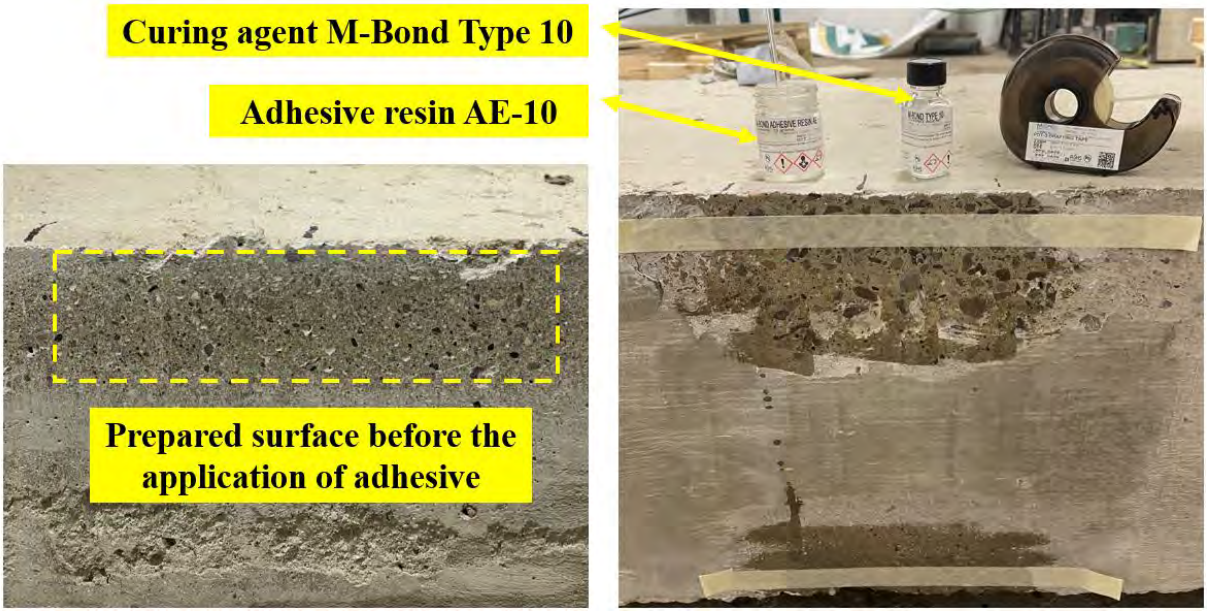

Fig. 6.19 a) Surface preparation for the installation of concrete strain gauges; b) prepared surface (left) and application of AE-10 adhesive to fill the holes on the surface of concrete

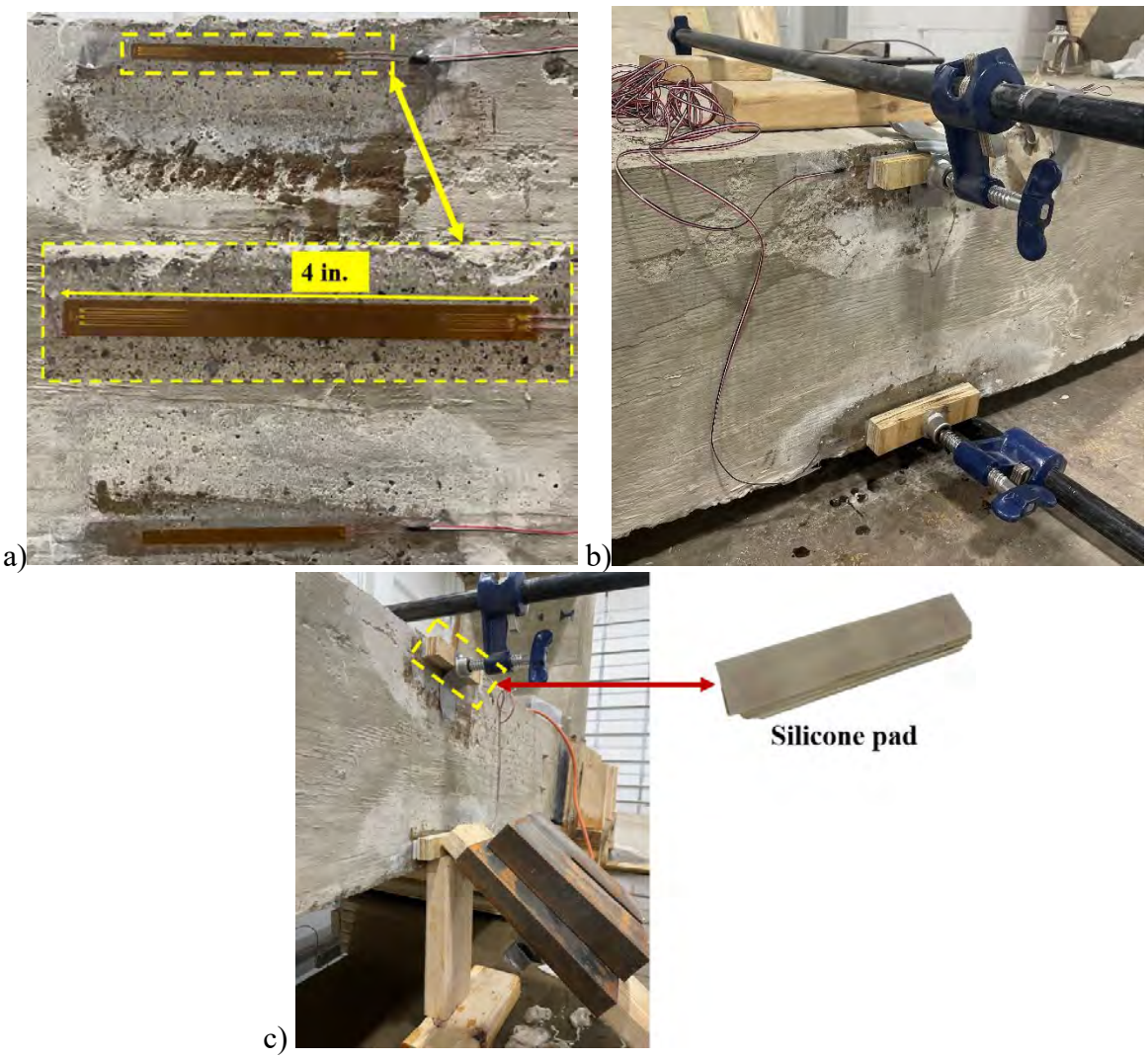

Fig. 6.20 a) Installed 4 in. concrete strain gauge; and b-c) methods to apply pressure on the strain gauges during curing process

6.1.4 Specimen Testing

Step 1: Induce accelerated corrosion. Prior to testing, the full-scale sub-assemblage specimens featuring repaired connections were subjected to accelerated corrosion using a similar procedure to that used for the small-scale specimens described in the previous chapter. The control specimen remained un-weathered to provide a benchmark for the capacity of the connection in a newly constructed bridge (i.e. undeteriorated). The test setup for accelerated weathering is shown in Fig. 6.21 and features forms for containing a 5% NaCl electrolytic solution (sodium chloride crystal supplied by Lab Alley). The setup exposes the sides and the bottom of the deck fascia to the 5% NaCl electrolytic solution to emulate exposure conditions that promote a higher moisture content in the vicinity of the deck fascia. The length of the deck perpendicular to the deck fascia that was

exposed to the electrolytic solution is 30 in. The electrolytic solution was contained using the water tanks illustrated in Fig. 6.21b These water tanks were constructed with plywood forms and featured a plexiglass layer on the inside to prevent leakage. The edges of the plexiglass received strips of silicon to provide water tightness. Initially, depth wise, the entire deck fascia was submerged in the electrolytic solution. Despite extensive efforts to prevent leakage, the electrolytic solution leaked on both sides of the specimen repaired with SCC and one side of the specimen repaired with FRSCC. The depth of the 5% NaCl solution was 3 in. – 1.5 in. extended below the bottom of the deck thus exposing the entire bottom deck portion for a length of 30 in. from the deck fascia to the solution. The other 1.5 in. of the 5% NaCl solution applied above the bottom of the deck thus keeping all three sides of deck fascia subject to the solution. The deck fascia on the side of the FRSCC repaired specimen that did not leak was fully submerged in the electrolytic solution. A current is applied from the positive end of the power supply to the hooked bars in the deck (anode), which are connected to the deck reinforcement thus being able to transmit electric current. A corrosion resistant steel rod is positioned vertically in the containers to serve as the cathode and is connected to the negative end of the power supply thus completing the electric circuit. Instead of 5V, which is the voltage applied to the small-scale specimens based on Amleh and Mirza (1999), this time, the applied voltage was 10V to further accelerate the corrosion process.

Before the electric current was applied to the system, half-cell potential benchmark readings were recorded. The recorded data included half-cell potential values and current values. Accelerated corrosion testing continued until the day of testing.

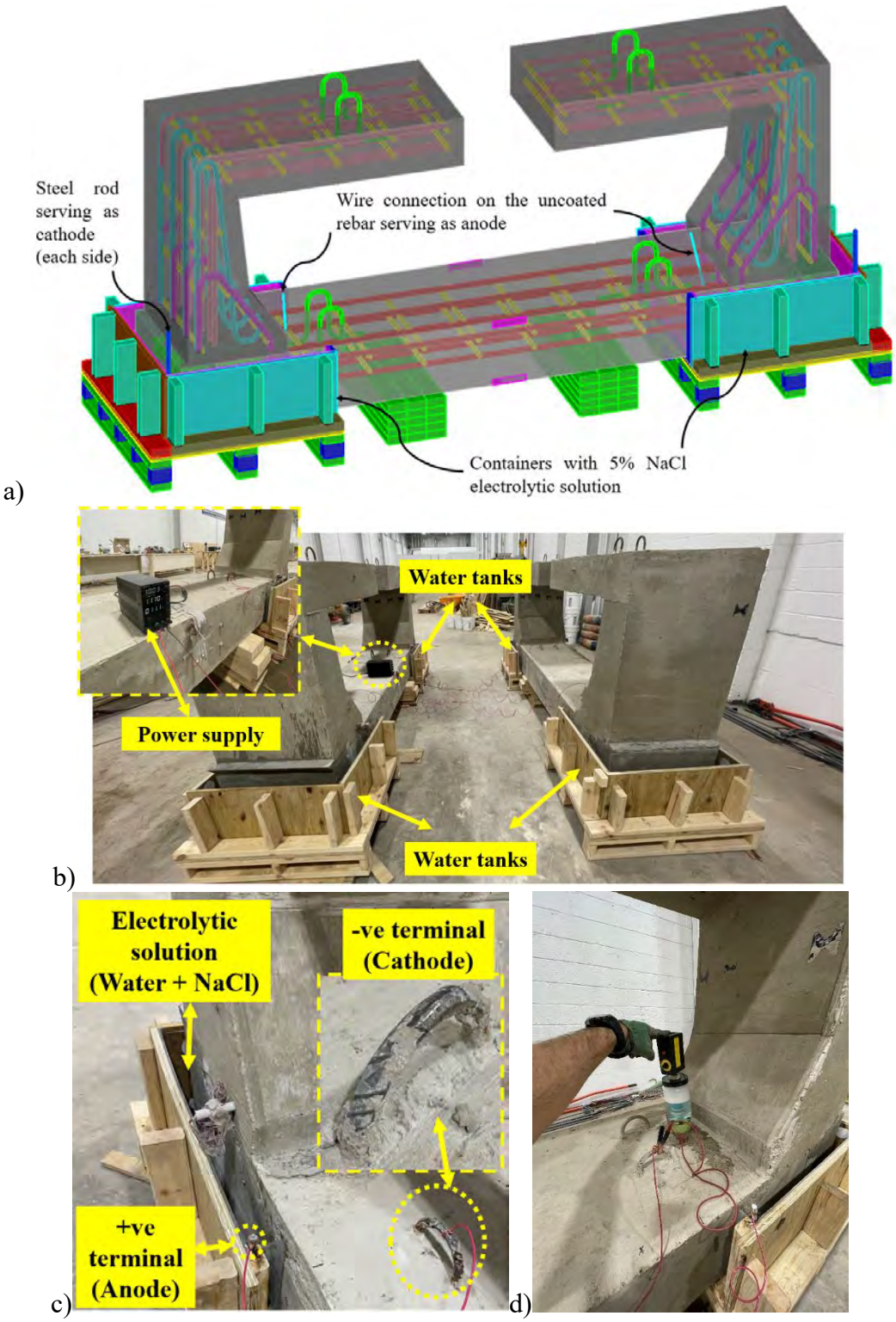

Fig. 6.21 a) Rendering of test setup for accelerated corrosion, b) actual test setup for accelerated corrosion, c) description of components of accelerated corrosion test, d) location of hall-cell potential measurements

Step 2: All three specimens were elevated from the ground using wooden supports and a wooden framework was installed for securing the LVDTs (Fig. 6.22). All LVDTs were installed followed by the installation of surface mounted concrete strain gages. Horizontal displacement sensors (LVDTs) were placed at the top of the barrier to help characterize the stiffness of various connections throughout the entire range of loading. Vertical LVDTs were placed at the bottom of the deck fascia to measure the vertical displacement during loading and to determine whether these vertical displacements are as predicted and consistent with the control specimen or different. For example, a failed connection would exhibit large vertical displacement as the load is transferred through the connection. Concrete strain gages were installed at the extreme fibers at mid-width of the specimen to compare the induced level of strain to that anticipated. For example, if the connection performs as intended (that is, the force is transferred successfully from the barrier to the deck), the failure is anticipated to be at section 4 described earlier, where the strain gages are located. If the failure occurs at the anticipated load level and the strain measurements confirm this then the connection is satisfactory.

Step 3: Install load cell, ram, and relevant support. Connect all sensors to the data acquisition system and conduct a trial test to ensure sensors are working.

Step 4: Conduct testing for all specimens in a sequential manner and record data. The specimens were loaded monotonically to failure. Since the anticipated failure load was 15.5 kips, the specimens were loaded in increments of 2.0 kips. Data from the LVDTs, strain gages, and load cell were measured using a mobile data acquisition system (purchased from BDI Inc.) at a frequency of 2 Hz (every 0.5 seconds). The loading was paused at increments of 2.0 kips to allow the research team to mark crack patterns. The cracks were marked with a black marker on the side of the cracks. At the end of the crack the load at which that particular cracks occurred was noted. Subsequent cracks, in subsequent load levels, were marked in a similar manner. This allowed the research team to distinguish between cracks that formed at different times and provided an opportunity to characterize the response of the specimens as a function of cracks patterns. The loading of the specimens continued until the hydraulic ram reached its maximum stroke. In all specimens this corresponded with load levels that were well beyond the maximum load capacity of the specimen.

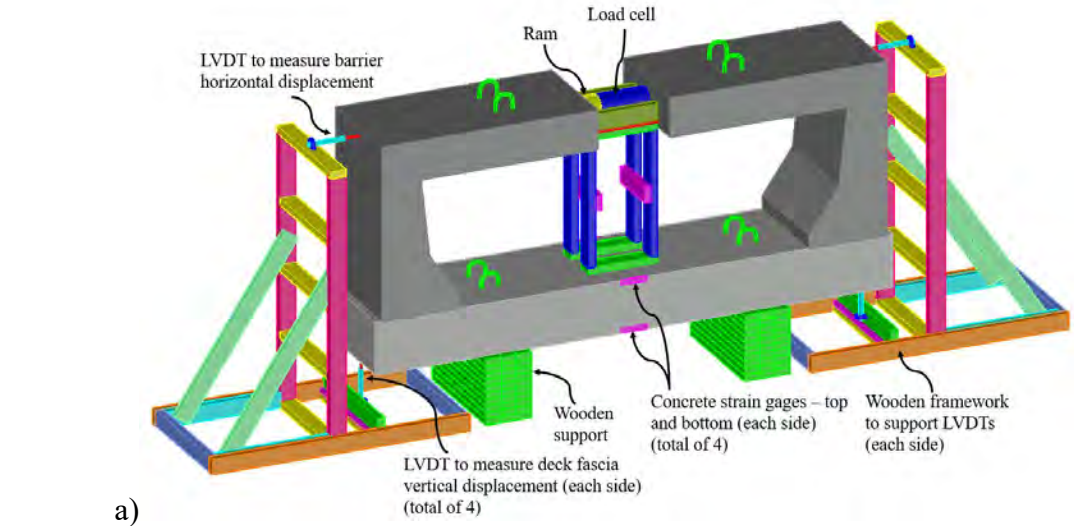

a)

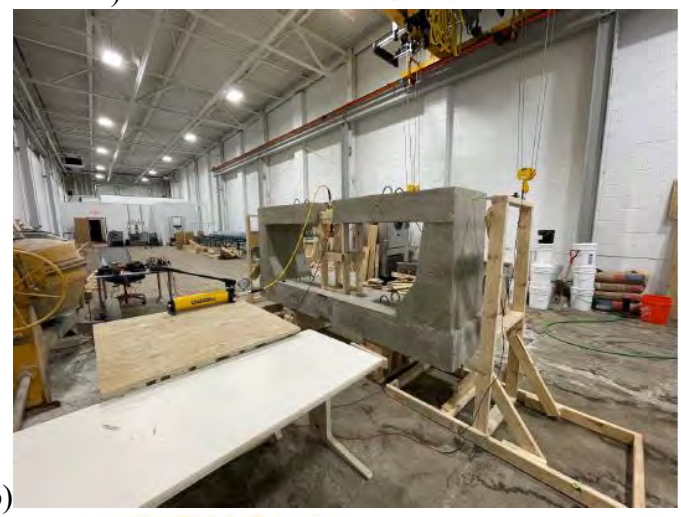

b)

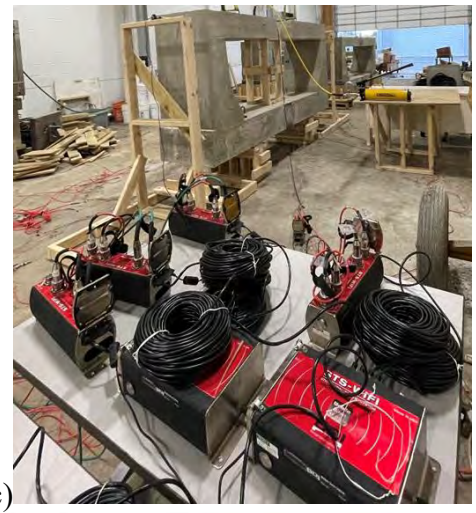

c)

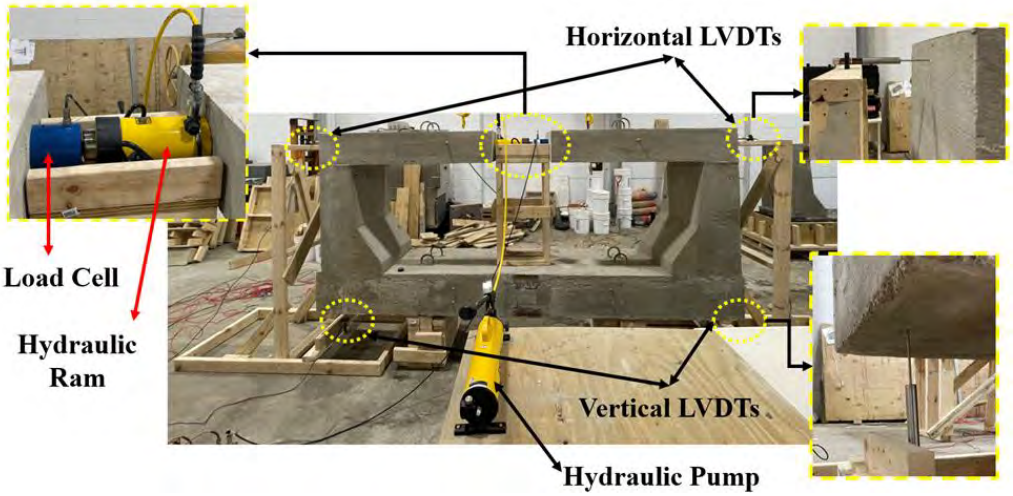

d)

Fig. 6.22 a) Rendering of test setup, b) angled view of the test setup, c) other angled view of the test setup showing components of the data acquisition system (nodes and main stations), d) front view of the test setup

6.2 Results of Sub-assemblage Testing

6.2.1 Plastic Properties of Concrete

Table 6.6 summarizes the plastic properties of deck, barrier, and repair concrete material. These properties include slump, density, and air content for deck and barrier concrete. For the repair concrete material, the plastic properties include slump, J-Ring Flow, passing ability, visual stability index (VSI) determined according to Daczko and Kurtz (2001), T_{50} and T_{50j}, density, and air content. It should be noted that the deck and barrier concrete were nominally the same mix. As can be seen from Table 6.6 and Table 6.7, the plastic properties are different. The unit weight of the barrier concrete was lower and air content was higher. These correlate to a lower concrete compressive strength as shown in Table 6.7 and Table 6.8. Since the as-supplied mix design was the same no explanation can be provided for the difference in the material properties other than noting that the actual delivered concrete must have been different to produce such notable differences in plastic and hardened properties. These differences go beyond those expected due to the inherent variability in concrete material properties. Deck concrete performed within expected parameters. Barrier concrete deviated from expected parameters. As the focus was on the deck and the connection this was deemed acceptable for the purpose of the test.

6.2.2 Hardened Properties of Concrete

The measured hardened properties include the compressive strength at 28 days and at the day of testing, modulus of elasticity, and Poisson's ratio.

At 28 days:

The deck concrete featured the highest compressive strength followed by FRSCC, SCC, and barrier concrete. FRSCC exhibited the highest tensile strength followed by SCC, barrier concrete, and deck concrete. Interestingly, barrier concrete featured a higher tensile strength than the deck concrete despite a notable difference in the compressive strengths. FRSCC was expected to feature the highest tensile strength due to the presence of fibers. SCC featured the second highest tensile strength despite the fact that the compressive strength of deck concrete was higher. Poisson's ratio varied from 0.18 to 0.24.

At Day of Testing:

At the day of testing, repair concrete materials exhibited either higher or comparable compressive strength with the deck concrete material. There was a notable difference between the 28 day and test day (47 day) strength for SCC (f_c' increased from 5.0 to 7.6 ksi). Deck concrete met the specified strength whereas barrier concrete did not. This did not affect results as the focus was on the deck.

Table 6.6 Plastic properties of deck, barrier, and repair concrete material

Concrete	Metric	ASTM Reference	Value
Deck Concrete Cast on Feb 6, 2023	Slump (in.)	C143 (ASTM 2020)	5.5
	Density (pcf)	C138 (ASTM 2023)	143.3
	Air Content (%)[1]	C231 (ASTM 2022)	5.7 / 5.5
Barrier Concrete Cast on Feb 20, 2023	Slump (in.)	C143 (ASTM 2020)	6.5
	Density (pcf)	C138 (ASTM 2023)	136.9
	Air Content (%)[1]	C231 (ASTM 2022)	9.0 / 8.8
Repair I – SCC Cast on March 2, 2023	Slump Flow (in.)	C1611 (ASTM 2021)	22.3
	J-Ring Flow (in.)	C1621 (ASTM 2017)	19.5
	Passing Ability (in.)[2]	C1621 (ASTM 2017)	2.8
	VSI[3]	C1611 (ASTM 2021)	2
	T_{50} & T_{50j} (sec)	C1611 (ASTM 2021)	4.7 & 7.6
	Density (pcf)	C138 (ASTM 2023)	147.1
	Air Content (%)	C231 (ASTM 2022)	5.8
Repair II – FRSCC Cast on March 4, 2023	Slump Flow (in.)	C1611 (ASTM 2021)	24.0
	J-Ring Flow (in.)	C1621 (ASTM 2017)	19.5
	Passing Ability (in.)[2]	C1621 (ASTM 2017)	4.5
	VSI[3]	C1611 (ASTM 2021)	Between 1 and 2
	T_{50} & T_{50j} (sec)	C1611 (ASTM 2021)	2.7 & 8.6
	Density (pcf)	C138 (ASTM 2023)	144.3
	Air Content (%)	C231 (ASTM 2022)	3.9

[1]According to ASTM C231 (ASTM 2022), the measured air content value should be calculated considering the aggregate correction factor (G): $A_s = A_1 - G$. The mix design submittal indicated that the aggregate correction factor is 0.2. Air content values are presented with and without consideration this factor, respectively.
[2]Passing ability is the difference in between Slump flow and J-ring flow.
[3]Based on Daczko and Kurtz (2001) for rating of SCC mixtures.

Table 6.7 Detailed hardened concrete material properties at 28 days

Cylinder No.	f'_c (ksi) ASTM C39 (ASTM 2021)	f_{st} (psi) ASTM C496 (ASTM 2017)	E_c (ksi) ASTM C469 (ASTM 2022)	μ
Deck Concrete – Cast on Feb 6, 2023				
1	6.4	315.2	3858.6	0.21
2	6.6	320.1	3963.6	0.21
3	6.3	345.7	4162.5	0.22
Average	**6.4**	**327.0**	**3994.9**	**0.21**
St. Dev.	0.15	16.42	154.35	0.01
COV (%)	2.3	5.0	3.9	2.8
Barrier Concrete – Cast on Feb 20, 2023				
1	4.4	430.3	3260.2	0.24
2	4.2	286.6	3498.6	0.25
3	4.2	478.9	3290.1	0.22
Average	**4.3**	**398.6**	**3349.7**	**0.24**
St. Dev.	0.12	99.99	129.89	0.01
COV (%)	2.7	25.1	3.9	6.0
Repair I – SCC – Cast on March 2, 2023				
1	4.0	435.6	3676.4	0.19
2	6.3	367.9	4170.0	0.18
3	4.7	513.6	3673.4	0.17
Average	**5.0**	**439.0**	**3839.9**	**0.18**
St. Dev.	1.13	72.87	285.89	0.01
COV (%)	22.6	16.6	7.4	6.8
Repair II – FRSCC – Cast on March 4, 2023				
1	5.9	858.1	3312.9	0.19
2	6.2	858.1	3420.3	0.18
3	6.4	739.6	3659.7	0.16
Average	**6.2**	**818.6**	**3464.3**	**0.18**
St. Dev.	0.22	68.43	177.57	0.01
COV (%)	3.6	8.4	5.1	8.2

Table 6.8 Summary of hardened concrete material properties

Mix	Time	f'_c (ksi)	f_{st} (psi)	E_c (ksi)	μ
Deck Concrete Cast on Feb. 6, 2023 Tested on April 18, 2023	28 days	6.4	327.0	3994.9	0.21
	At the day of testing (71 days)*	6.7	373.8	3889.5	0.19
Barrier Concrete Cast on Feb. 20, 2023 Tested on April 18, 2023	28 days	4.3	398.6	3349.7	0.24
	At the day of testing (54 days)*	4.3	331.6	3606.8	0.21
Repair I – SCC Cast on March 2, 2023 Tested on April 18, 2023	28 days	5.0	439.0	3839.9	0.18
	At the day of testing (47 days)	7.6	434.1	4093.8	0.19
Repair II – FRSCC Cast on March 4, 2023 Tested on April 22, 2023	28 days	6.2	818.6	3464.3	0.18
	At the day of testing (49 days)	6.4	764.4	3618.4	0.18
*Barrier and Deck concrete cylinders were tested at the same day when Repair 1 – SCC specimen was tested.					

6.2.3 Accelerated Corrosion Test Results

Fig. 6.23 shows the measurements obtained from the corrosion test in terms of the average electrical potential (half-cell potential measurements) (Fig. 6.23a) and current (Fig. 6.23b) as a function of time. The average current was measured periodically and was stable at 0.8 mA. The average values for half-cell potential were calculated using the individual readings that were taken at multiple points on each side of the specimen. These points are designated as 1-12 in Fig. 6.24 with points 1-3 being on the right side on the deck, point 4 being on the right side on the repair part, points 5-8 being on the end of the specimen on the repair portion, point 9 being on the left side on the repair portion, and points 10-12 being on the left side on the deck portion. For each repair specimen two curves are presented – one for each repaired end designated as I and II. The accelerated corrosion test lasted for 18 days, however, measurements continued to be taken for an additional 9 days after the termination of the test, thus providing data for a total of 27 days. On average, the research team could not obtain half-cell potential readings that would suggest >90% probability that reinforcing steel corrosion had occurred. This is attributed to the limited amount of sodium chloride solution present around the deck fascia on three out of four sides. On the side where the deck fascia was subject to larger amounts of sodium chloride solution higher half-cell potential readings were obtained.

Fig. 6.24 shows half-cell potential measurements at different points around the deck fascia at three different points in time: a) just after the termination of test (18 days), b) 2 days after the termination of test (20 days), and c) 9 days after the termination of test (27 days). Recall that only side I of FRSCC was completely submerged in the sodium chloride solution. The other side of FRSCC and the two sides of SCC were subjected only to 3 in. of standing sodium chloride solution due to leakage problems. Therefore, the half-cell potential measurements suggest that either corrosion activity is uncertain or there is 90% probability or greater that there is no corrosion of reinforcement in the test specimen that was repaired with SCC and one of the sides of the test specimen that was repaired with FRSCC. In FRSCC specimen side I, the half-cell potential readings suggest that there is >90% probability that reinforcing steel corrosion had occurred. There was also one measurement in the test specimen that was repaired with the SCC that suggested a > 90% probability that reinforcement corrosion had occurred. The differences in the likelihood of corrosion within the specimen as well as between the specimens provided an opportunity to determine the impact that any existing corrosion in the deck may have on the crashworthiness of

the barrier after the deck fascia has been repaired. Depending on the severity of the level of corrosion, potential deterioration mechanisms could include expansion of deck rebars near the repaired interface, which could compromise the bond and consequently the strength of the repair.

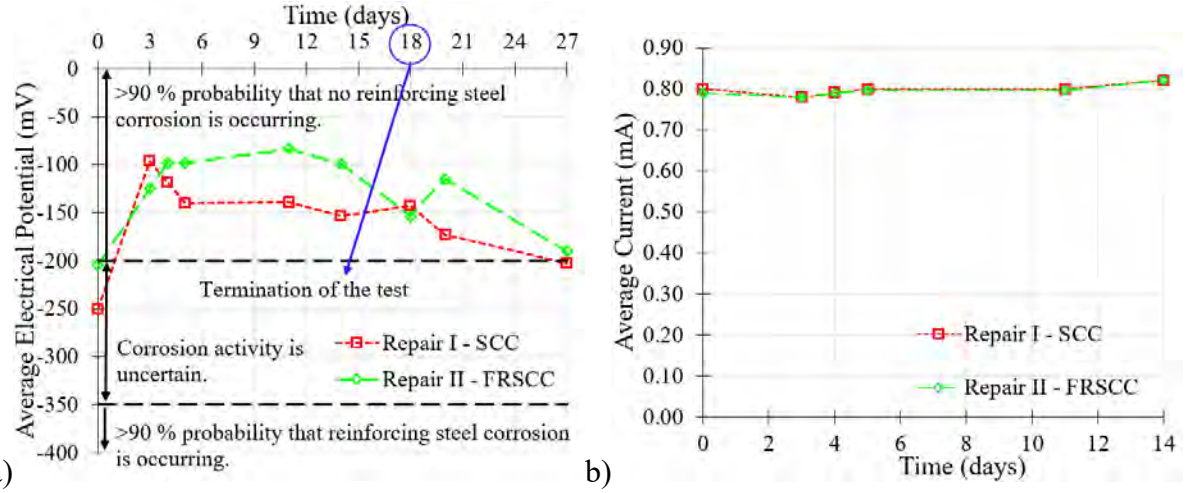

a) b)

Fig. 6.23 Average half-cell potential measurements on the surface of the deck for repair specimens; and b) average current measurements

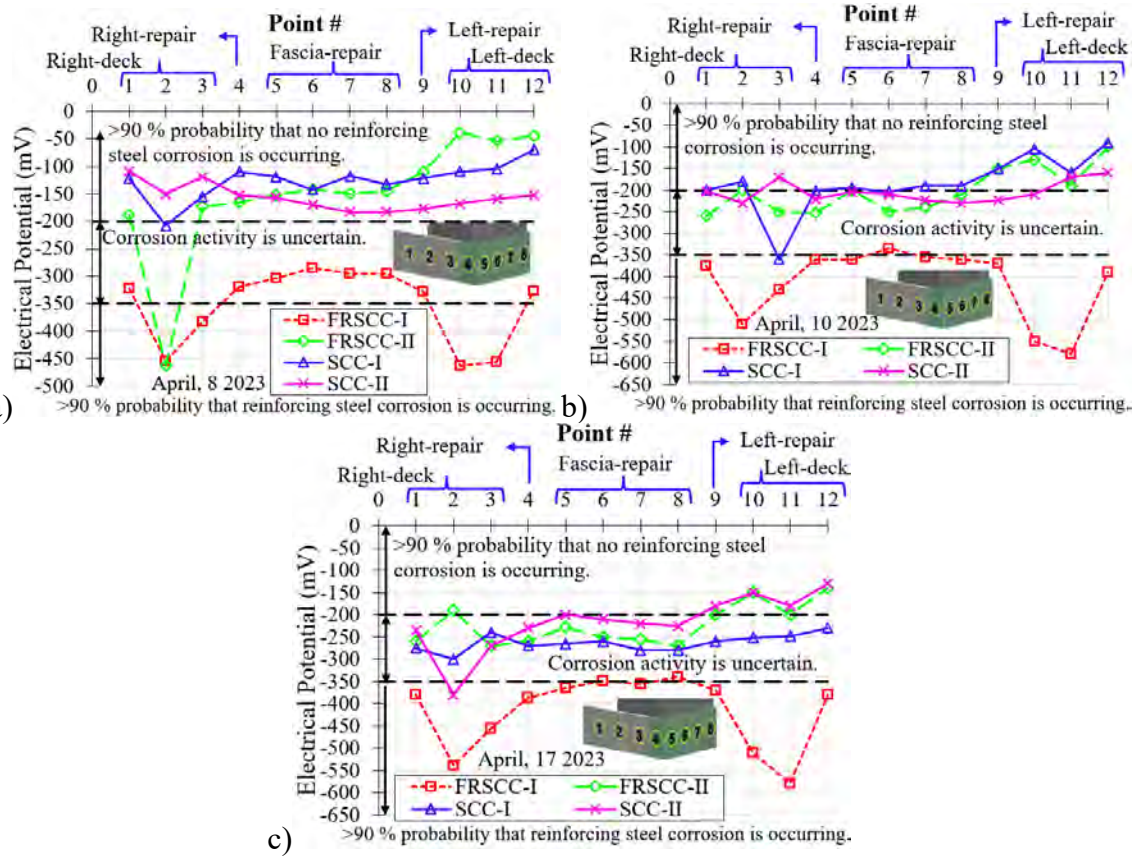

a) b) c)

Fig. 6.24 Half-cell potential measurements around the fascia taken from the repair specimens: a) on April 8, 2023 (just after the termination of the test); b) on April 10, 2023 (2 days after termination of the test); and c) on April 17, 2023 (9 days after the termination of the test)

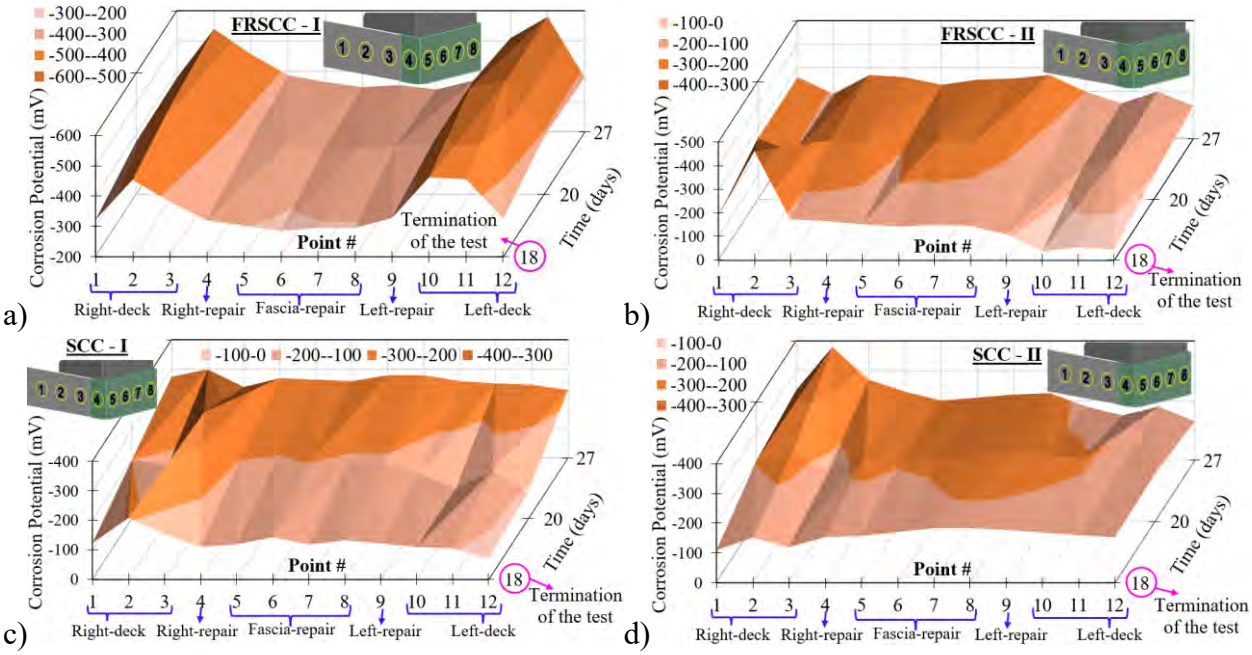

Fig. 6.25 3D surface plots for the half-cell potential measurements taken from the repair specimens after the test is terminated: a) measurements around the fascia side I on FRSCC specimen; b) measurements around the fascia side II on FRSCC specimen; c) measurements around the fascia side I on SCC specimen; and d) measurements around the fascia side II on SCC specimen

6.2.4 Pseudo-static Test Results

The results of the pseudo-static tests are presented first as a summary of the first cracking loads and ultimate lateral loads and then in terms of the load versus barrier displacement, and load versus strain relationships. As previously discussed, the type of displacements that were measured were horizontal displacements at the top of the barrier, and vertical displacements at the bottom of the barrier. The measured strains feature those measured at the rebars and concrete. Top deck rebar strains were measured at the barrier to deck connection, as well as at midspan. Concrete normal strains were measured at midspan near the most extreme compression and tension fibers.

Summary of First Cracking Loads and Ultimate Lateral Load Capacities

Table 6.8 provides a summary of first cracking loads and ultimate lateral loads recorded for each specimen. As can be seen, the proposed repair details have the ability to restore barrier crashworthiness (recall that the target load for TL-4 is 9.7 kips) since they attained lateral load capacities of 12.8 kips and 14.2 kips for deck fascias repaired with SCC and FRSCC, respectively. In addition, the measured lateral load capacities were within 21% of the predicted lateral load capacities using the sectional analysis approach. First cracking loads were 4.5 kips, 4.7 kips, and

3.0 kips for control, SCC, and FRSCC specimens, respectively. It should be noted that the first cracking loads were based on the first visible cracks. Since vehicle impact is an extreme event, cracking is not a concern. Recall that the goal of the barrier is to sustain the impact and redirect the vehicle in a controlled manner.

Table 6.8 Summary of first cracking loads and ultimate lateral loads

Specimen	At Cracking Load	At Ultimate Load
	F_{cr} (kips)	F_u (kips)
Control	4.5	16.0
Repair I – SCC	4.7	12.8
Repair II – FRSCC	3.0	14.2

Load versus Displacement Relationship

The average load versus lateral displacement response is reported in Fig. 6.26a. Recall that there were two horizontal LVDTs in each specimen (one on each side). To report the average response the average measurements from each horizontally placed LVDT were used. The horizontal dashed red line represents the load capacity of the specimen that is equivalent to a TL-4 barrier crashworthiness in a full-scale bridge. The load versus lateral displacement response was such that in the initial stages there was an increase in load with no measurable lateral displacement (i.e. the induced lateral displacements were outside the sensitivity range of the LVDTs). This is attributed to the large uncracked flexural stiffness of the barrier to deck assembly. Once cracking occurred and the flexural stiffness reduced, the horizontally placed LVDTs started to report measurable lateral displacements. The overall response could be characterized by a linear elastic response of the uncracked subassembly, vertical cracking of the deck caused by bending moments and axial tension, formation of additional vertical cracks in the deck including one near the inside face of the barrier, yielding of the reinforcement, formation of a critical diagonal crack, which intercepted the vertical crack near the inside face of the barrier, attainment of a maximum lateral load capacity, and provision of notable post-peak lateral load capacity. The test specimen that featured the FRSCC repair performed rather similarly with control specimen. Fig. 6.26a suggests that the FRSCC repair resulted in a stiffer response compared to the test specimen that featured the SCC repair. Side I (corroded side) in FRSCC specimen performed better than side II (uncorroded side) despite featuring higher half-cell potential readings as illustrated in Fig. 6.27a.

The load versus vertical displacement relationship was in general similar to the load versus horizontal displacement relationship in the sense that initially there was an increase in load accompanied by presumably immeasurable vertical displacements, formation of first cracking in the deck, creation of additional deck cracking, yielding of deck steel, attainment of maximum lateral load capacity, and a steeper post-peak load versus vertical displacement relationship compared to the post-peak load versus horizontal displacement curve. As expected, the horizontal displacements were larger than the vertical displacements due to the larger cantilever arm in the barrier compared to the deck. In addition, the presence of an axial tension force in the deck induces a self-straightening effect thus further reducing any downward displacements caused by the bending moment in the deck. Load versus vertical displacement relationship underneath the deck fascia was rather similar for both repair specimens and their response was less stiff than that of the control specimen (Fig. 6.26b). Some partial interface cracking was observed during the tests. However, these did not compromise the crashworthiness of the barrier. The primary crack patterns crossed the interface.

Side I (corroded side) performed similarly and better than side II (uncorroded side) (Fig. 6.26b). Therefore, the induced accelerated corrosion did not undermine the stiffness or capacity of the barrier deck assembly.

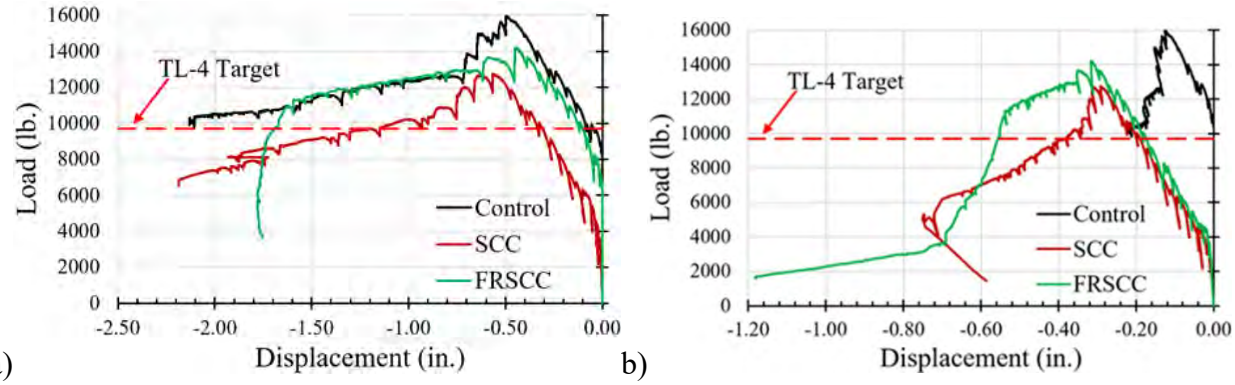

Fig. 6.26 Measured load versus a) average horizontal displacement (at the top of the barrier), and b) vertical displacement relationship (at the bottom of the barrier)

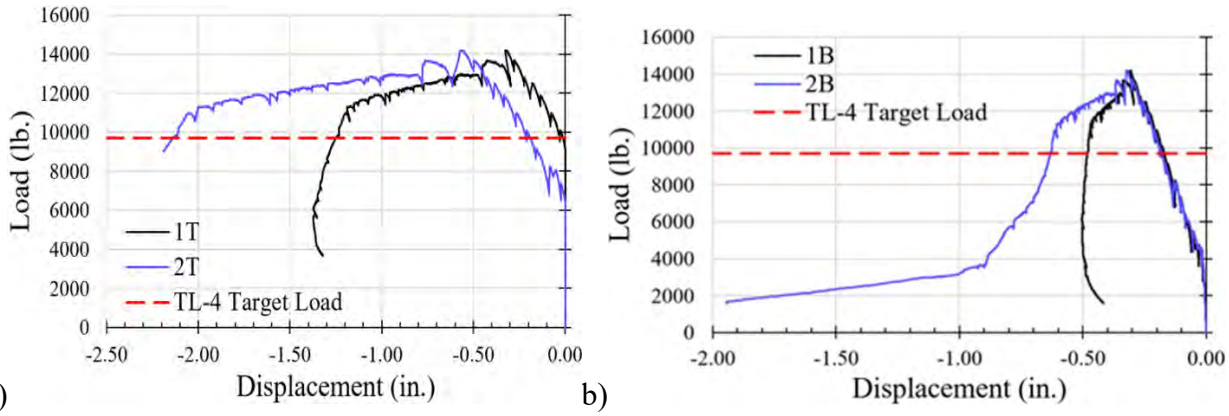

Fig. 6.27 Measured load versus a) horizontal (at the top of the barrier), and b) vertical displacement (at the bottom of the barrier) relationship for FRSCC – side I (1T/1B) versus side II (2T/2B)

Crack Pattern

Ultimate cracks patterns for all tested specimens were overall similar and are illustrated in Fig. 6.28. All cracks occurred in the deck. No cracks were observed in the barrier suggesting hinging behavior at the deck to barrier interface. Since the deck portion between the barriers is subject to constant tension and moment, the first cracks precipitated in the deck between the barrier in no particular order with respect to their location. That is, the first crack occurred in the region that provided the least tensile resistance considering the heterogeneity of deck concrete. These cracks were vertical flexural and axial tension cracks as would be expected since the principal tensile stress trajectories in the tensile deck region are horizontal. As the load intensified, the axial tension and flexural cracks, which started at the top of the deck, propagated towards the bottom of the deck. In all specimens, there was a vertical crack in the deck in the vicinity of the inside face of the barrier. This crack was later intercepted by a critical diagonal crack that precipitated failure. This critical diagonal crack aligns with the principle compressive stress trajectories – recall that there is a concentrated moment and tension force at each end of the deck. This critical diagonal crack crossed the repaired interface in the repair specimens suggesting comparable performance to the control specimen. In addition, the presence of the repair interface did not appear to affect the crack pattern. Crack patterns in the deck were also similar in all three specimens suggesting no change in the transfer of load from the barrier to the deck despite the repaired connections. Fig. 6.29 illustrates the condition of the tested specimen after failure. Links are also provided for accelerated test videos.

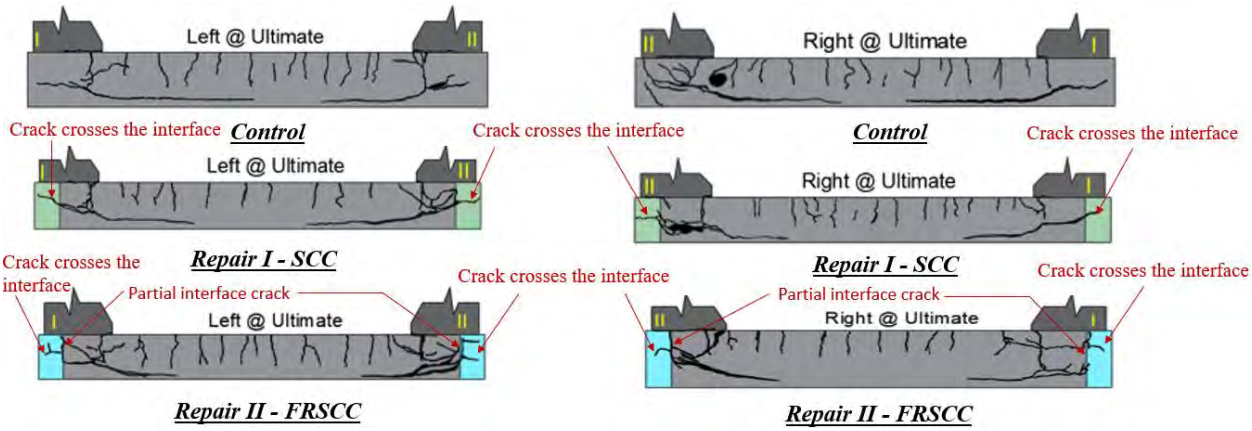

a)

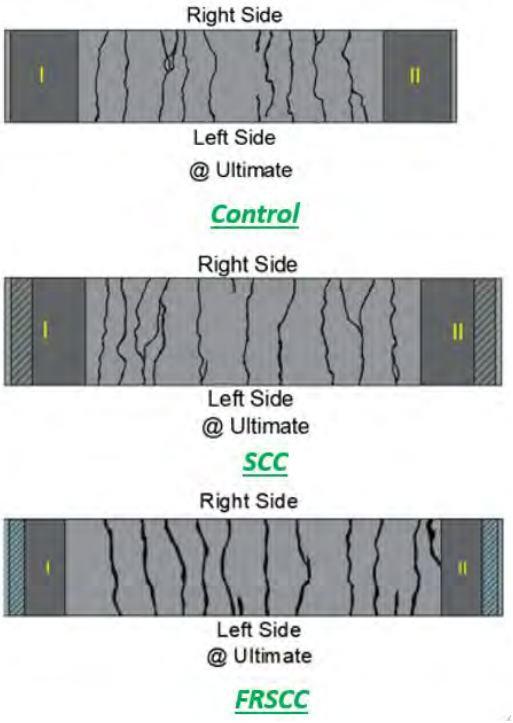

b)

Fig. 6.28 Crack pattern on: a) left and right sides at the ultimate condition for all tested specimens, b) top of deck

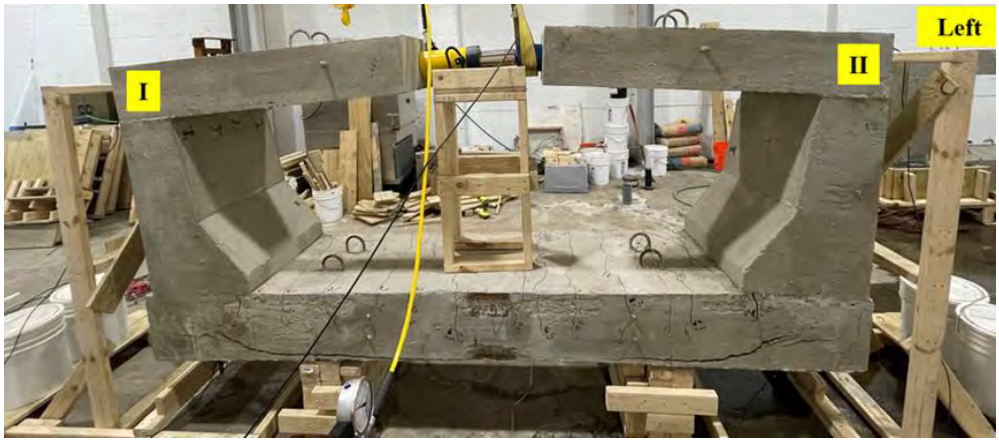

a) Control - https://www.youtube.com/watch?v=D1ovPcvyanQ

a) SCC - https://www.youtube.com/watch?v=Powy7D-WWKY

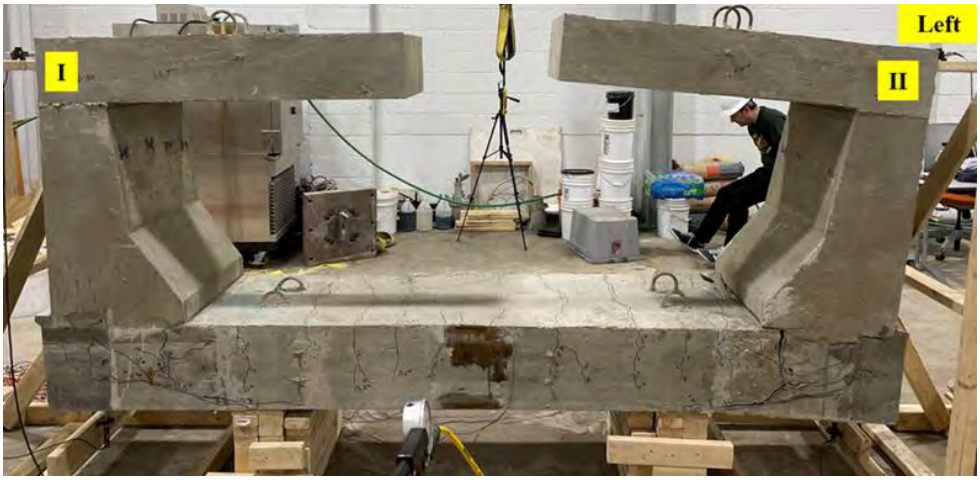

c) FRSCC - https://www.youtube.com/watch?v=GRd23ros0hY

Fig. 6.29 Photographs and video links for all three tested specimens – photographs are taken after failure: a) Control, b) SCC, c) FRSCC

Load versus Top Deck Reinforcement Strain Relationship

The average load versus rebar strain relationship is illustrated in Fig. 6.30. The sign convention is such that positive strain values indicate tension and negative strain values indicate compression. The vertical line represents the yield strain for Grade 60 rebars, which is 2000 με (or 0.002). The horizontal line represents the load capacity of the specimen that is equivalent to a TL-4 barrier crashworthiness in a full-scale bridge. Fig. 6.30a shows the load versus hooked/cut top deck reinforcement strain relationship in the deck fascia. The control specimen featured hooked and straight reinforcement in the deck fascia. The load versus hooked rebar strain relationship was averaged for all hooked bars with strain gages and the average response is shown in Fig. 6.30a. The repaired specimen featured all straight top deck reinforcement in the deck fascia. Some of this reinforcement is intended to represent the cut deck bars, which were originally hooked while the rest is intended to represent the originally straight bars, which would also be cut during the repair except that in Fig. 6.30b they are labeled as "edge-straight" bars. The cutting of the bars in a real bridge would occur due to severe reinforcement corrosion.

As noted earlier, the purpose of installing strain gages on the hooked and straight bars was to measure the level of engagement in each bar. It was expected that the only bars that would yield would be the hooked bars since it was only the hooked bars and not the straight bars that featured the required development length to allow the bars to yield. Fig. 6.30 suggests that for the control specimen both hooked and straight bars yielded despite the fact that the straight bars featured an available length that was equal to 67% of the required development length according to AASHTO LRFD (2020). As explained earlier, in a deck overhang the straight rebars represent the typical top deck rebars that are used elsewhere for negative bending moments in the deck. The hooked rebars are added to ensure barrier crashworthiness. Fig. 6.30 suggests the engagement of both hooked and straight rebars may be based on their yield stress when evaluating barrier crashworthiness. This is due to the fact that these bars yielded well before the attainment of peak load. This information can be especially useful when evaluating the crashworthiness of an existing barrier as many times the crashworthiness depends on the efficiency of the barrier to deck connection to transfer impact forces.

Another point of interest was whether the cut top deck rebars in the repaired specimen together with the noncontact lap splices provided through the drilled and epoxied dowels would be able to provide a reliable load transfer mechanism to ensure barrier crashworthiness. Fig. 6.30

suggests that the proposed repair detail is capable of ensuring barrier crashworthiness, as both the originally hooked and straight rebars which in the test specimens were represented by cut and straight rebars yielded before the attainment of peak load. In the case of the repair specimens all top deck rebars featured available length that were equal to 46% of the required development length according to AASHTO LRFD (2020). Therefore, the engagement of all cut deck top bars may be based on their yield stress during vehicle impact despite their shorter than required development lengths.

Finally, top deck rebars at midspan yielded – suggesting successful load transfer past the barrier to deck connection (Fig. 6.30c). For example, if the noncontact lap length of 10 in. between the drilled and epoxied bars and existing deck bars were insufficient, the connection would exhibit a bond failure and the top deck bars at midspan would not be strained. This is clearly not the case as shown in Fig. 6.30c, which suggests that the top deck bars in the repair specimens have yielded.

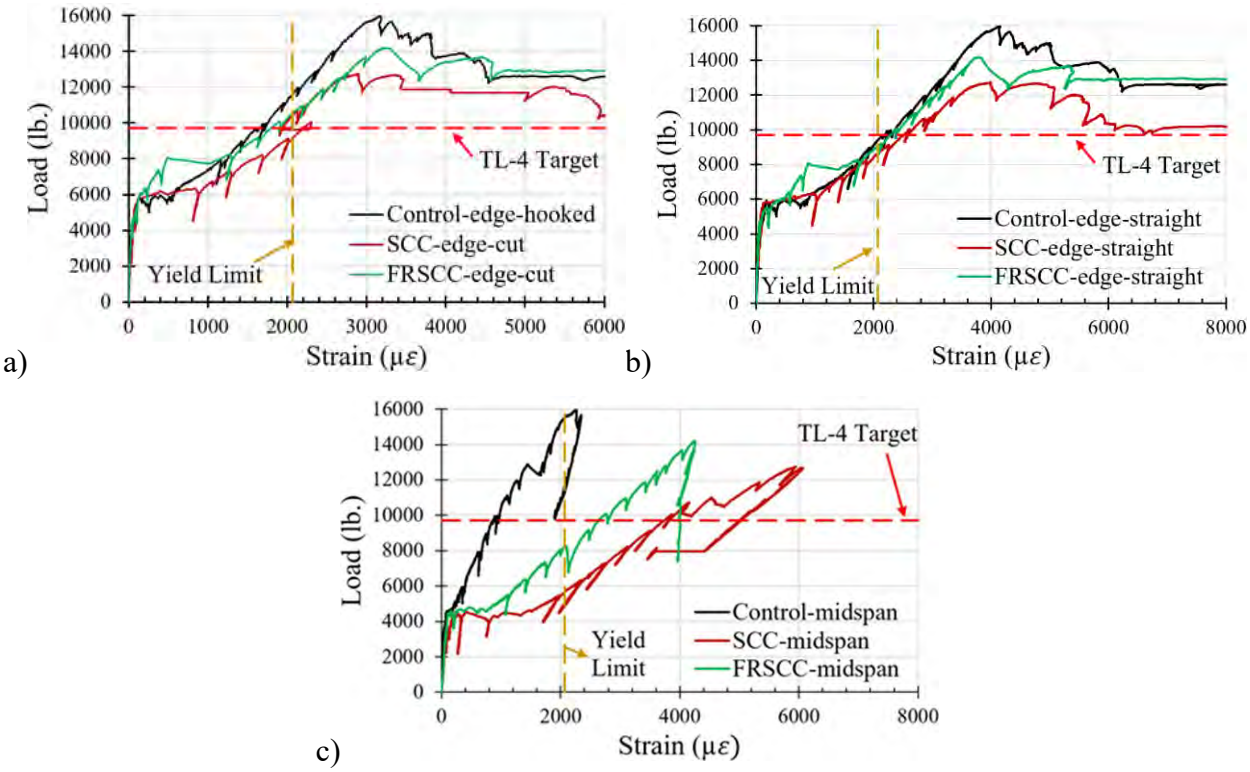

Fig. 6.30 Load versus strain at top deck rebars: a) in the deck fascia – hooked/cut bars, b) in the deck fascia – straight bars, c) at midspan

Load versus Concrete Strain Relationship

The load versus concrete strain relationship is provided in Fig. 6.31. As noted earlier, concrete strains were measured at midspan near the most extreme compressive and tensile fibers. Considering that the deck is subjected to a negative bending moment in addition to an axial force the most extreme tensile fiber is at the top of the deck and the most extreme compression fiber is at the bottom of the deck. The load versus compressive strain relationship illustrated in Fig. 6.31a is similar for all test specimens. In all cases, the maximum measured strain is smaller than 0.0012, which is smaller than the typical value of 0.003 representing the crushing of concrete. This is explained by the presence of the axial tension force in the deck, which reduces compressive strain caused by the bending moment. The overall load versus concrete compressive strain relationship further corroborates the observations presented earlier regarding the overall response of the subassembly, which can be characterized by a linear elastic response up until the first crack, cracking at the top of the deck, which causes a reduction in the slope of the load-strain relationship, and eventual attainment of maximum lateral load capacity.

Fig. 6.31b shows the load versus concrete tensile strain relationship. This response is different in each test specimen. This difference is attributed to the location of the strain gage with respect to the cracks. For the control specimen it is evident that the strain gages were located between the cracks as no notable tensile strain was measured. For the repaired specimens the cracks either intercepted the strain gage or were close enough to lead to notable measurements.

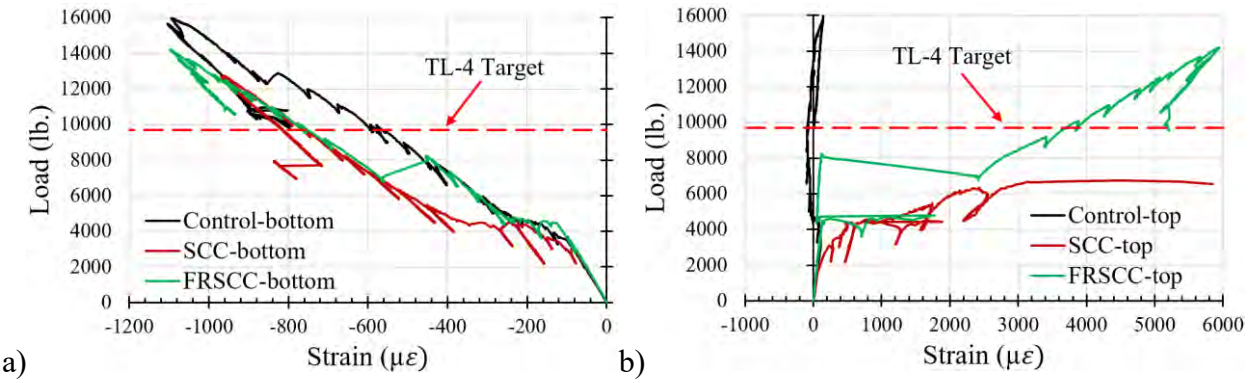

Fig. 6.31 Average strain measurements on surface of the concrete for all specimens: a) at the bottom fiber; and b) at the top fiber

Repeatability of Test Results

Since the test setup allowed the testing of two connections simultaneously there was an opportunity to measure the repeatability of the test results as it pertains to the load displacement and load strain relationships. Observations on the repeatability of results are presented for each test specimen.

Control Specimen

The load versus reinforcement strain relatinship on the same straight top deck reinforcement on each side is shown in Fig. 6.32 for the control specimen. The response is virtually identical suggesting repetable response in both sides throughout the duration of the test. The legend for rebar strain on each side is based on the nomenclature presented in Fig. 6.32a. As noted earlier, the straight top deck rebar reinforcement featured available lengths that were 67% of the required development lengths according to AASHTO LRFD (2020). Despite this deficit in the available length, straight top deck reinforcement exhbited tensile strains that exceeded the yield strain denoted with the the vertical dashed blue line. The length of the straight top deck bars past the point where its intersects with the hooked barrier dowel is 15 in. The required development length based on AASHTO LRFD (2020) is 22.4 in.

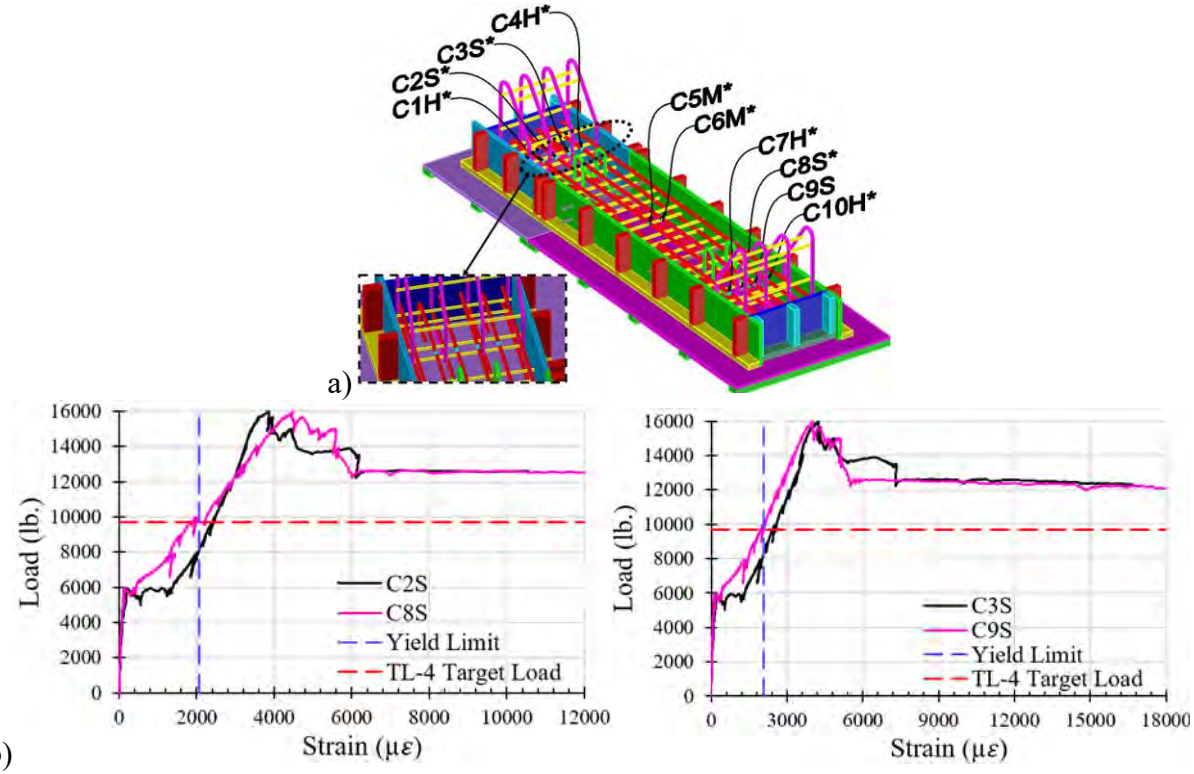

Fig. 6.32 a) Reference figure for strain gages, b) strain measurements on the same rebars at sides I and II for control specimen

The load versus concrete strain response on each side is essentially identical throughout the duration of the test when the bottom concrete strains are considered, which measure the compressive strains (Fig. 6.33a). When the tensile strains are considered, while the overall response is similar the measured strains on each side as a function of load are different (Fig. 6.33b). The overall response was characterized by: 1) initial tensile strains as the specimen was loaded, 2) a relief of these strains and incurrence of compressive strains as additional cracks formed thus reliving the initial tensile strains at the strain gages location, 3) a re-creation of tensile strains as perhaps new cracks formed in the vicinity of the gages, and 4) a relief of these strains as the load was released. The primary reason for the difference between the two curves is that the measured tensile strains are greatly affected by the proximity of the strain gages to the nearest crack. As the strain field in the concrete varies greatly between cracks, this can lead to the measurement of different concrete strain depending on how close the strain gage is to the crack.

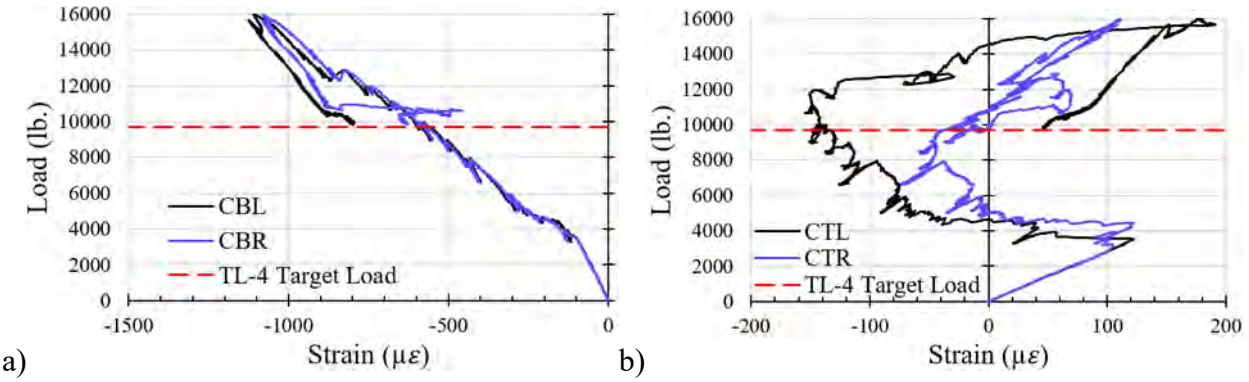

Fig. 6.33 Strain measurements on surface of the concrete for the control specimen on both sides: a) at the bottom fiber; and b) at the top fiber

The repeatability of test results when the behavior of one side is compared to that of the other side is best evaluated when the load versus lateral and vertical displacement relationships are evaluated as these two displacement sensors reflect the overall global response of the subassembly. The load versus horizontal and vertical displacement relationship was virtually identical throughout the duration of the test as illustrated in Fig. 6.34. The horizontal displacements were measured at the top of the barrier and the vertical displacements were measured at the bottom of the barrier. Overall, the response of each barrier to deck assembly in the control specimen was similar as further corroborated by the observed crack pattern presented earlier.

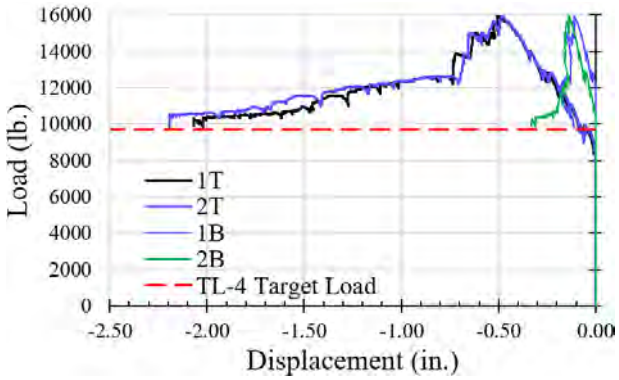

Fig. 6.34 Measured load versus displacement relationship obtained from displacement sensors on each side of the control specimen

SCC Specimen

The load versus reinforcement strain relationship on the same bar on each side is shown in Fig. 6.35 for the SCC specimen. It should be noted that all top deck bars in the repair specimens were straight and identical in length. Fig. 6.35 suggests that while all top deck bars in the deck fascia region with strain gages on them yielded either prior to the attainment of peak load or when the peak load was attained the load versus rebar strain relationship was not identical on both sides throughout the entire range of loading. Fig. 6.35a suggests that this relationship was virtually identical up until the yielding of the bars and then became different afterwards. This difference may be attributed to a potential bond failure for this particular rebar on one side of the test specimen. Similarly, Fig. 6.35b suggests that the same rebar was engaged more effectively on one side compared to the other side. Except that for this rebar, the side that engaged it more efficiently was the opposite side of that which exhibited a more efficient engagement for the bar shown in Fig. 6.35a.

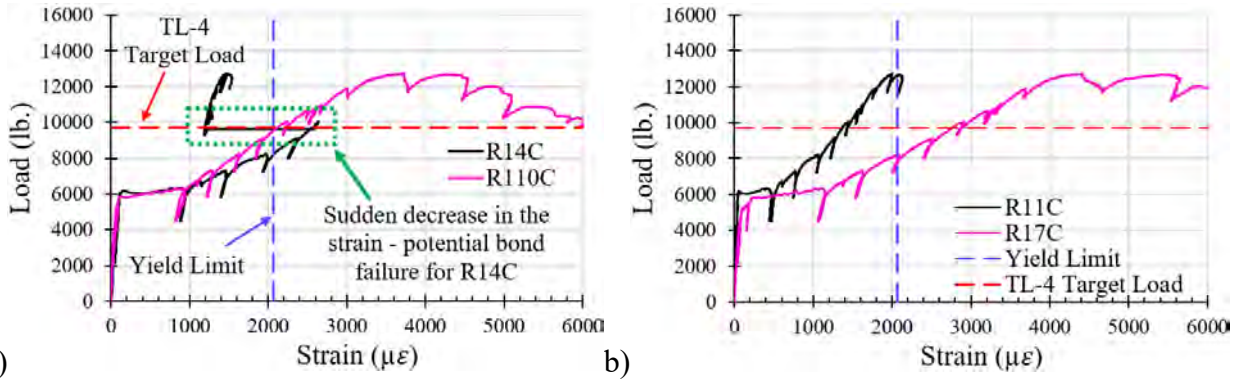

Fig. 6.35 a-b) Strain measurements on the rebars that are positioned at same location at sides I and II for Repair-1 SCC specimen

When the load versus concrete strain relationship is considered, it can be seen that overall the response measured on both sides was similar with some differences as expected due to the location of the strain gages with respect to the cracks and the propagation of it which affects both the tensile and compressive strain fields.

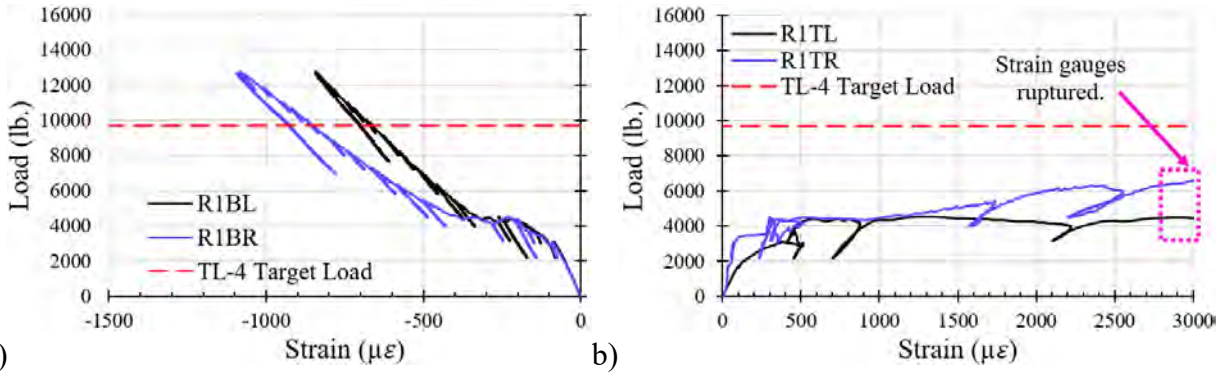

Fig. 6.36 Strain measurements on surface of the concrete for Repair-1 SCC specimen: a) at the bottom fiber; and b) at the top fiber

When the load versus lateral displacement relationship is considered, some differences are noted with one side exhibiting a less stiff response compared to the other. However, when the load versus vertical displacement relationship is examined, the response is almost identical. The measured and observed response of this test specimen was such that certain cracks such as the vertical flexural crack in the deck near the inside face of the barrier formed first on one side then in the other. Similarly, the critical diagonal cracks formed first on one side and then the other. However, the important observation is that one side was not notably weaker than the other as some differences in behavior are expected. This increases the level of fidelity in the proposed repair detail as the desired restoration of barrier crashworthiness was demonstrated indirectly twice for each repair concrete material using the presented test setup.

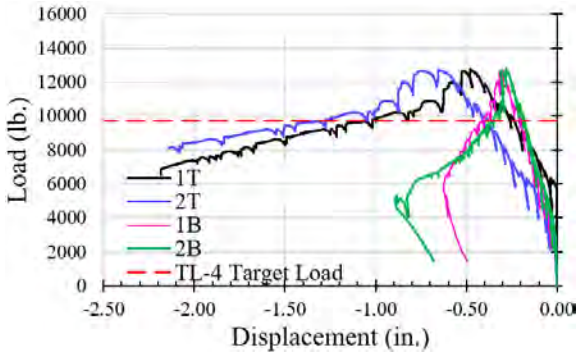

Fig. 6.37 Measured load versus vertical (1T and 2T) and horizontal (1B and 2B) displacements for Repair-1 SCC specimen (the numbers represent the side at which displacements were measured)

FRSCC Specimen

The measured load versus top deck rebar strain response on each side of the FRSCC specimen was generally similar as illustrated in Fig. 6.38 with some differences observed at different levels of loads.

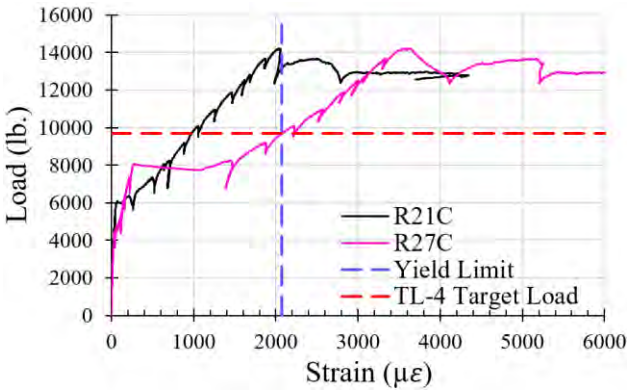

Fig. 6.38 Strain measurements on the rebars that are positioned at same location at sides I and II for Repair-2 FRSCC specimen

A similar observation is presented for the load versus compressive strain relationship in concrete in the sense that the response measured on each side was similar. With respect to the load versus tensile strain relationship, different responses were measured on each side as the top deck cracks in the vicinity of strain gages deviated from straightness. As such, the top deck cracks ruptured one of the strain gages on each side but not the other.

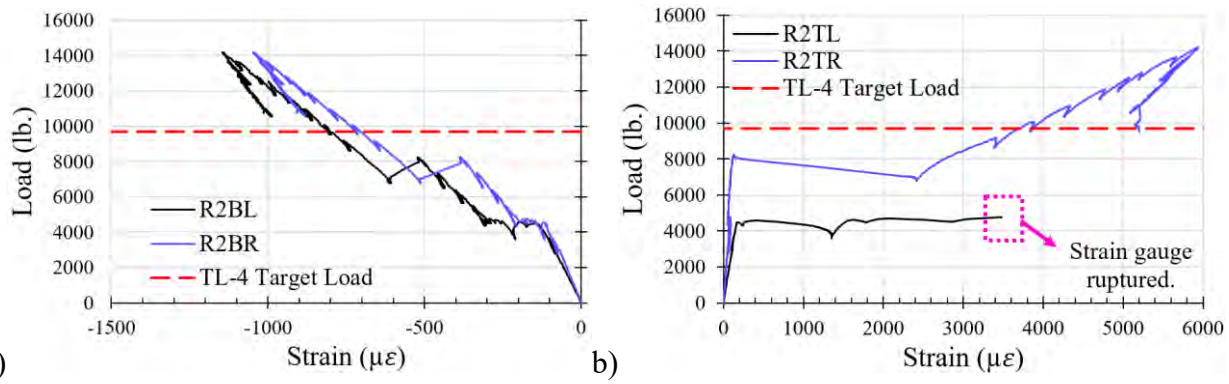

Fig. 6.39 Strain measurements on surface of the concrete for Repair-2 FRSCC specimen: a) at the bottom fiber; and b) at the top fiber

Similar to the behavior observed in the SCC specimen the load versus lateral displacement relationship was such that it suggests a slightly less stiff response on one side compared to the other. Although the load versus vertical displacement relationship suggests virtually identical behavior on both sides. Overall, the response of this repair specimen too was similar in both sides further increasing the fidelity of the proposed repair details. It should be noted that the described differences in behavior between each side are important in terms of understanding what caused them. However, the ultimate goal was to achieve the equivalent of a TL-4 level of crashworthiness on both sides, and this goal was clearly attained.

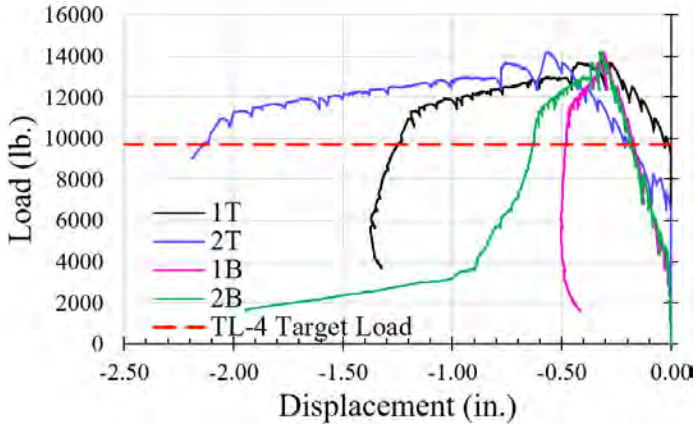

Fig. 6.40 Measured load versus vertical (1T and 2T) and horizontal (1B and 2B) displacements for Repair-2 FRSCC specimen (the numbers represent the side at which displacements were measured)

6.3 Conclusions from Sub-assemblage Testing

1) The proposed repair detail using both repair cementitious materials was able to restore the crashworthiness of the barrier providing strength against vehicle impact that is greater than that required for a TL-4.

2) The repair specimen that featured FRSCC exhibited a load versus horizontal displacement relationship that was almost coincidental with the control specimen.

3) The repair specimen that featured FRSCC exhibited a stiffer response than that exhibited by the repair specimen that featured SCC.

4) FRSCC is the recommended Option 1 for repair as FRSCC provides sustained tensile strength after cracking, which is critical in terms of preventing cracked deck fascia concrete from falling down.

5) The strain in the straight rebars in the deck fascia in the control specimen exceeded the yield strain suggesting that these rebars are capable of transferring forces despite their limited development length – this information may be used during barrier strength evaluation.

6) The existing cut top deck rebars in the repaired specimens yielded, suggesting a successful load transfer during vehicle impact from the barrier to the deck.

Chapter 7: Evaluation of Barrier Crashworthiness

Chapter 7: Evaluation of Barrier Crashworthiness

7.1 Introduction

The goal of this chapter is to introduce an analytical tool that can be used to evaluate the crashworthiness of solid bridge barriers that feature deteriorated deck fascias. Fig. 7.1 presents an overview of the proposed approach for the evaluation of existing bridge deck fascias. This starts with a visual inspection of the bridge deck fascia, followed by a characterization of the deterioration in terms of length and width. The deteriorated length and width are then idealized in terms of an average deteriorated length and width. This information is then entered into a computer program called MDOT Barrier, which is used to evaluate the crashworthiness of the barrier. The MDOT Barrier program can be downloaded using the guidance provided in Appendix E. If the crashworthiness or the barrier is undermined, then intervention in the form of a repair or replacement is required if it is desired to restore the crashworthiness of the barrier. If the crashworthiness of the barrier is not undermined, then the only intervention that may be required could be the scaling of the deck fascia to prevent concrete fragments from falling down or the scaling of the deck fascia and application of a protective coating such as polyurea to prevent further deterioration. As such, the determination of whether the crashworthiness of the barrier is undermined is critical. The reference used when developing the MDOT Barrier program is the example presented for the design of bridge barriers in the book titled "Design of Highway Bridges – An LRFD Approach" by Barker and Puckett (2013), Third Edition, Section 15.2.

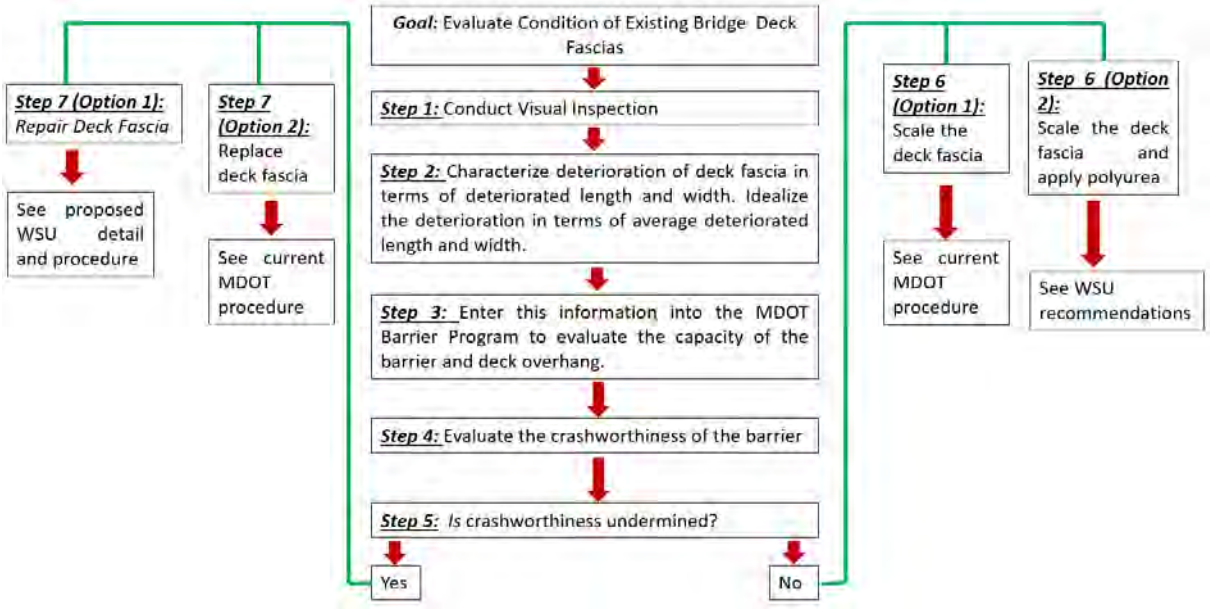

Fig. 7.1 Overview of proposed approach for the evaluation of existing bridge deck fascias

This chapter is organized such that the fundamental principles used to develop the MDOT Barrier program are presented first followed by an overview of the MDOT Barrier program. An example problem is provided in Appendix H. The MDOT Barrier program allows the analyst to investigate barrier Types 4-7 for crashworthiness. The following discussion pertains to barrier Types 4-5 unless specific discussions are provided for barrier Types 6-7.

7.2 Barrier Transverse Resistance to Vehicle Impact

The transverse capacity of a barrier is determined based on Eq. 7.1, where L_c is the critical length of yield line failure pattern (ft) (Eq. 7.2), M_b is the additional flexural resistance provide by a beam at the top of the barrier, if any, in addition to M_w, L_t is the length of distribution of impact force F_t (ft) (this is specified in AASHTO LRFD 2020), M_w is the flexural resistance of the barrier about its vertical axis (k-ft), M_c is the flexural resistance of the barrier about an axis parallel to the longitudinal axis of the bridge (k-ft/ft). Fig. 7.2 illustrates the yield line formation and analysis in a concrete bridge barrier for impact within the barrier segment. Equation references presented on the left correspond with those provided in AASHTO LRFD (2020).

[A13.3.1-1] $$R_w = \left(\frac{2}{2L_c - L_t}\right)\left(8M_b + 8M_w + \frac{M_c L_c^2}{H}\right) \quad \text{(Eq. 7.1)}$$

[A13.3.1-2] $$L_c = \frac{L_t}{2} + \sqrt{\left(\frac{L_t}{2}\right)^2 + \frac{8H(M_b + M_w)}{M_c}} \quad \text{(Eq. 7.2)}$$

$$R_w > F_t \quad \text{(Eq. 7.3)}$$

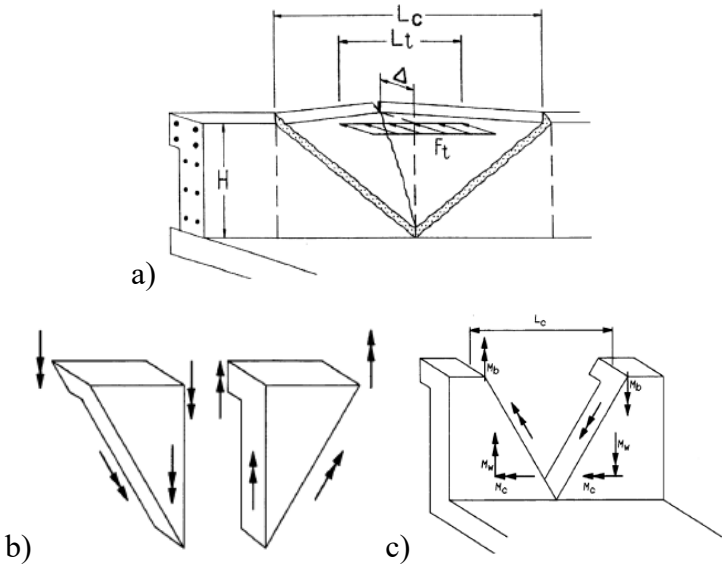

Fig. 7.2 Illustration of yield line formation and analysis in a concrete bridge barrier for impact within the barrier segment (adopted after AASHTO LRFD (2020) Article CA13.3.1-1)

The barriers considered as part of this research do not include a beam at the top. Therefore, M_b is set equal to zero. Both R_w and L_c are a function of M_w and M_c, the calculation of which is explained in the subsequent sections. For the barrier to satisfy the desired level of crashworthiness, Eq. 7.3 must be satisfied.

7.2.1 Flexural Resistance of the Barrier about Vertical Axis, M_w

The flexural resistance of the barrier about its vertical axis, M_w, is calculated using an equivalent constant thickness barrier (Fig. 7.3). This equivalent thickness is determined such that the area of the non-prismatic barrier and constant thickness barrier is the same (Eqs. 7.4-7.6). This constant thickness barrier is used when determining moment capacities. When calculating moment capacities only the reinforcement that is located on the tension side is considered. Flexural capacity if calculated using classical principles for reinforced concrete design as summarized in AASHTO LRFD (2020) and presented in Eqs. 7.7-7.13 for convenience. The stress block factors α_1 and β_1 can be determined based on Fig. 7.4. It should be noted that the deterioration of the deck fascia does not affect M_w, therefore, calculations for a deteriorated barrier and an undeteriorated one are identical.

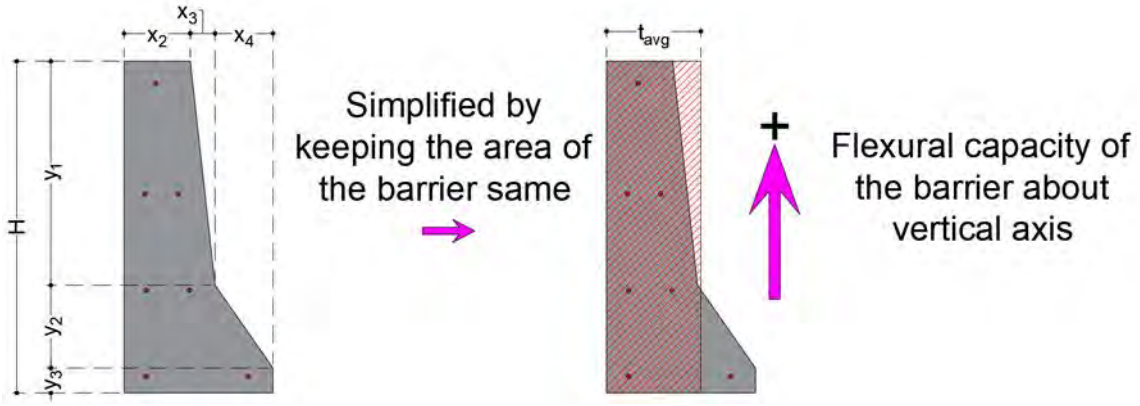

Fig. 7.3 Simplification of barrier geometry to calculate flexural capacity about the vertical axis

$$H_{barrier} = y_1 + y_2 + y_3 \quad \text{(Eq. 7.4)}$$

$$A_{barrier} = \frac{y_1(x_2 + x_2 + x_3) + y_2(x_2 + x_3 + x_2 + x_3 + x_4)}{2} + y_3(x_2 + x_3 + x_4) \quad \text{(Eq. 7.5)}$$

$$t_{avg} = \frac{A_{barrier}}{H_{barrier}} \quad \text{(Eq. 7.6)}$$

$$\sum C = \alpha_1 f'_{cb} b \beta_1 c \quad \text{(Eq. 7.7)}$$

$$\sum T = A_s f_y \quad \text{(Eq. 7.8)}$$

$$\sum C = \sum T \quad \text{(Eq. 7.9)}$$

$$c = \frac{A_s f_y}{\alpha_1 f'_{cb} b \beta_1} \quad \text{(Eq. 7.10)}$$

$$a_1 = \beta_1 c \quad \text{(Eq. 7.11)}$$

$$\varepsilon_t = \frac{0.003(d_s - c)}{c} \quad \text{(Eq. 7.12)}$$

$$M_n = A_s f_y \left(d_s - \frac{a}{2}\right) \quad \text{(Eq. 7.13)}$$

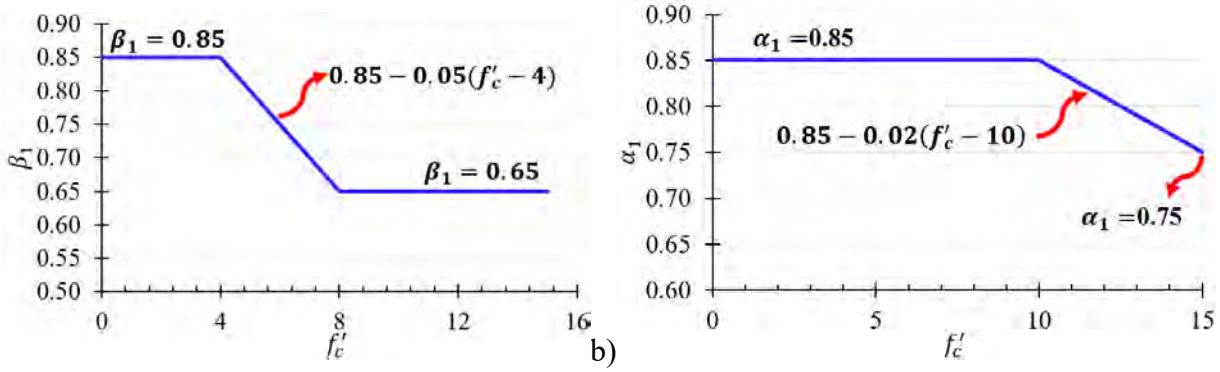

Fig. 7.4 Stress block factors: a) β_1, and b) α_1

7.2.2 Flexural Resistance of the Barrier about Horizontal Axis, M_c

When calculating the flexural resistance of an undeteriorated barrier about its horizontal axis the barrier is divided into several segments (Fig. 7.5). When analyzing barriers Type 4 and 5 the barrier is divided into three segments (Fig. 7.5a), and when analyzing barriers Type 6 and 7 the barrier is divided into two segments (Fig. 7.5b). Each non-prismatic segment is then further simplified into segments of constant thickness such that the area of each segment remains the same. When considering barrier Types 4 and 5, for segment I, only the barrier reinforcement denoted with the blue color is considered in the calculations. For segments II and III, only the dowels denoted in red are considered when calculating moment capacities for these segments. The development length of the dowel connecting the barrier to the deck is evaluated when determining the moment capacity of segment III. It is assumed that the yield stress of the dowel is fully developed on the barrier side and that only the development on the deck side is evaluated. Similarly, when considering barrier Types 6 and 7, only the dowels are considered in the flexural resistance about the horizontal axis in segment II. The evaluation of development length is conducted by comparing the available length (Eq. 7.17) with the development length using Eqs. 7.14-7.15, where:

- l_{hb} is the basic hook development length;
- d_b is the diameter of the rebar;

- f_y is the yield strength of the rebar; and
- f_c' concrete compressive strength;
- l_{dh} is the modified development length for a standard hook in tension;
- λ is concrete density modification factor: taken 1.0 for normal weight concrete and is calculated using Eq. 7.16 for light weight concrete where w_c is the unit weight of concrete, assumed 0.125 kcf;
- λ_{rc} is reinforcement confinement factor. If the cover on the bar extension beyond hook is greater than 2.0 in., it is taken as 0.8 (Fig. 7.6a). Otherwise, it is taken as 1.0.
- λ_{er} is excess reinforcement factor, taken as 1.0 as this is considered explicitly by adjusting the yield strength of steel.
- λ_{cw} is the coating factor, taken as 1.0 and 1.2 for uncoated, and epoxy coated reinforcement, respectively.

If the available length is smaller than the development length, the stress in the bars is proportioned as shown in Eq. 7.18. Finally, the weighted average of the flexural capacities of each segment is used to determine the flexural capacity of the barrier about its horizontal axis (Eq. 7.19). The ϕ factors in Eq. 7.19 are taken as unity as vehicle impact is considered an extreme event.

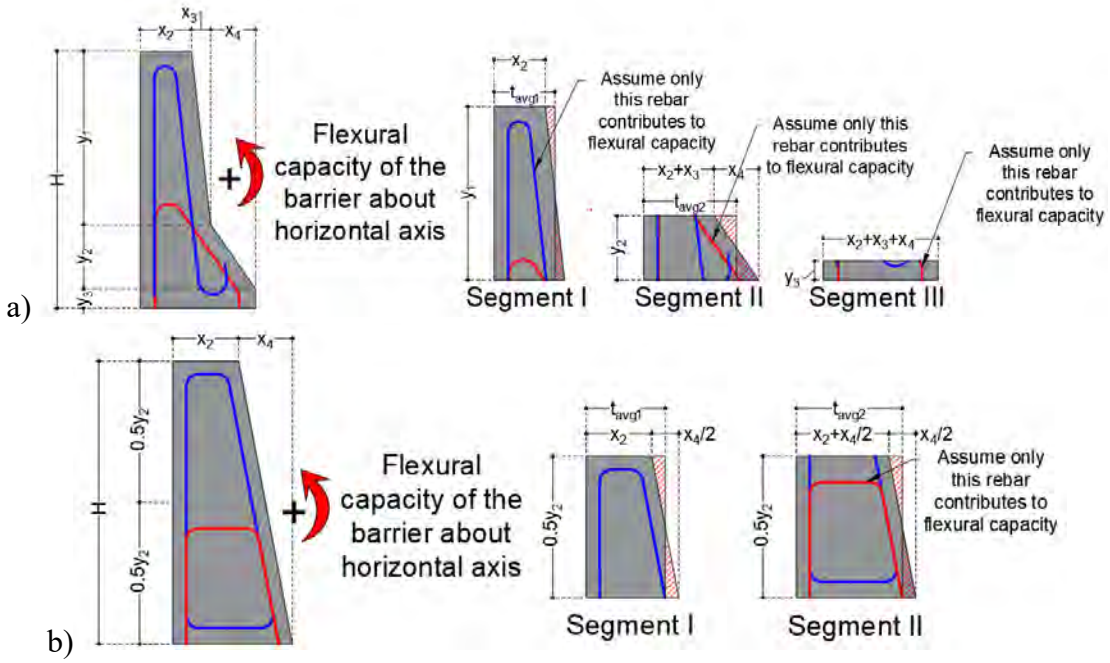

Fig. 7.5 Approach for calculating barrier flexural about horizontal axis in an undeteriorated barrier: a) barrier Types 4-5, and b) barrier Types 6-7

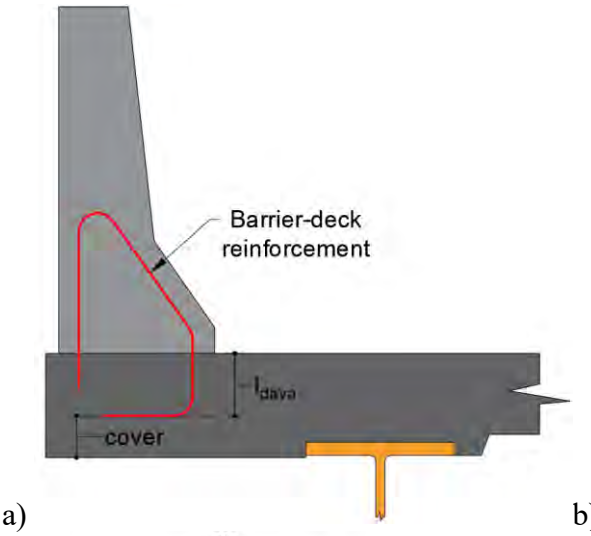

a)

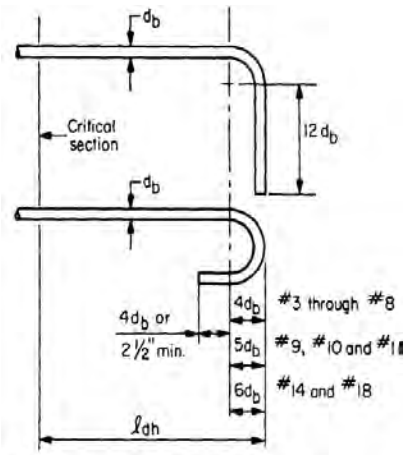

Figure C5.10.8.2.4a-1—Hooked Bar Details for Development of Standard Hooks (ACI Committee 318 2011)

b)

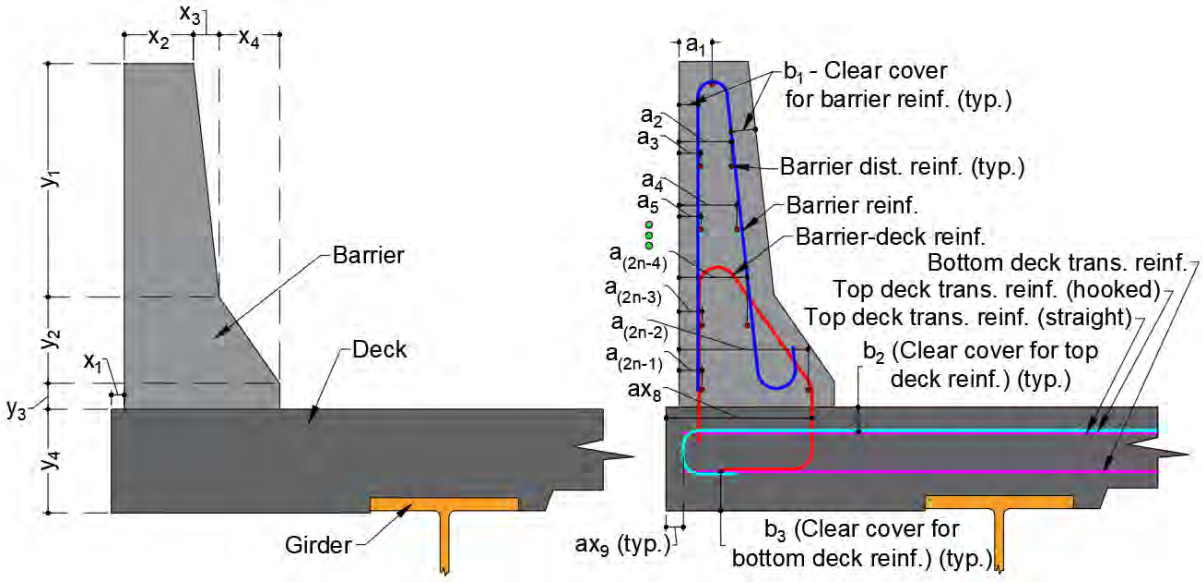

c)

Fig. 7.6 Barrier Types 4-5: a) dowel connecting barrier and deck, b) development length terminology (adapted from AASHTO LRFD (2020) Fig. C5.100.8.2.4a-1), c) illustration of input parameters required to conduct barrier crashworthiness analysis

[5.10.8.2.4a-1]
$$l_{dh} = \max\left[l_{hb}\left(\frac{\lambda_{rc}\lambda_{cw}\lambda_{er}}{\lambda}\right), 8d_b, 6\ in.\right] \quad \text{(Eq. 7.14)}$$

[5.10.8.2.4a-2]
$$l_{hb} = \frac{38d_b}{60}\left(\frac{f_y}{\sqrt{f_c'}}\right) \quad \text{(Eq. 7.15)}$$

[5.4.2.8-2]
$$0.75 \le \lambda = 7.5w_c \le 1.0 \quad \text{(Eq. 7.16)}$$

$$l_{dava} = y_4 - b_2 \quad \text{(Eq. 7.17)}$$

$$f_{yadj} = \frac{l_{dava}}{l_{dh}} f_y \quad \text{(Eq. 7.18)}$$

$$M_c = \frac{\phi M_{n1} y_1 + \phi M_{n2} y_2 + \phi M_{n3} y_3}{y_1 + y_2 + y_3} \quad \text{(Eq. 7.19)}$$

When calculating the flexural resistance of a deteriorated barrier about its horizontal axis the same approach of dividing the barrier into several segments is used. The deterioration of the deck fascia affects the flexural capacity of the barrier about the horizontal axis. This is considered by ignoring the portion of the barrier that overlaps with the deteriorated width (Fig. 7.7). The flexural capacity of each segment is affected by this reduction in barrier cross-section. Two scenarios can exist: 1) the deteriorated length L_d is greater than $L_{cdisttodeckcenterdet}$, and 2) L_d is smaller than $L_{cdisttodeckcenterdet}$. The calculation of moment capacity of the barrier with a deteriorated deck fascia about the horizontal axis can be conducted using Eqs. 7.20-7.23 where: $L_{cdisttodeckcenterdet} = L_{cdet} + 2(H_b + 0.5t_d)$, L_{undet} is the undeteriorated length of the deck fascia within $L_{cdisttodeckcenterdet}$, L_d is the deteriorated length, which the analyst provides as an input, M_c is the moment capacity of the barrier about the horizontal axis in the undeteriorated portion, and M_{cdet} is the moment capacity of the barrier about the horizontal axis along the deteriorated portion. Furthermore, L_{cdet} is the critical yield line failure pattern based on the flexural capacity of the barrier about horizontal axis considering deterioration, M_{cdet}. This critical length can be calculated using Eq. 7.2 by replacing M_c with M_{cdet}. The example in Appendix H provides additional details.

$$L_{undet} = L_{cdisttodeckcenterdet} - L_d \quad \text{(Eq. 7.20)}$$

If $L_{cdisttodeckcenterdet} \geq L_d$

$$M_{cdetadj} = \frac{M_c L_{undet} + M_{cdet} L_d}{L_{cdisttodeckcenterdet}} \quad \text{(Eq. 7.21)}$$

If $L_{cdisttodeckcenterdet} < L_d$

$$L_{undet} = 0 \quad \text{(Eq. 7.22)}$$

$$M_{cdetadj} = M_{cdet} \quad \text{(Eq. 7.23)}$$

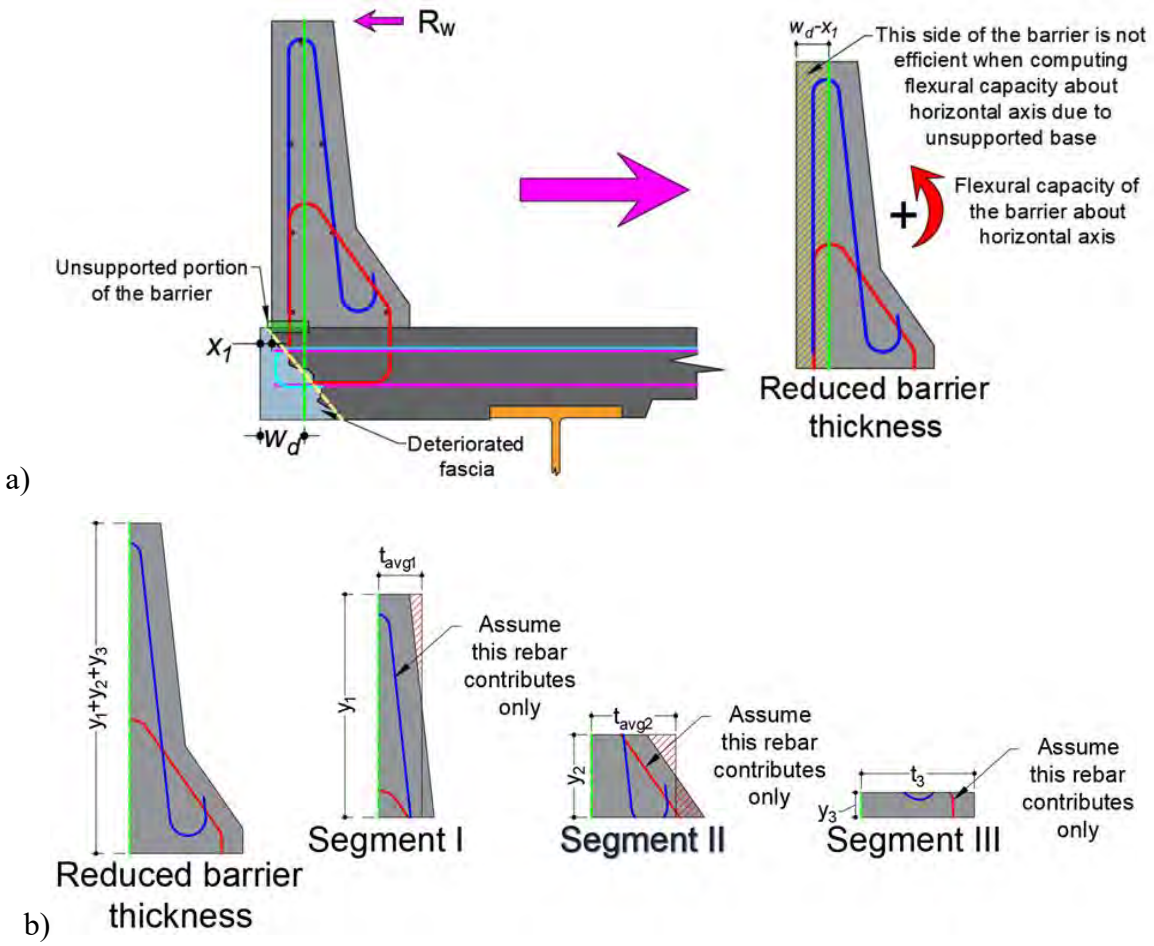

Fig. 7.7 Barrier Types 4-5: approach for calculating the flexural capacity of the barrier about horizontal axis: a) overall approach, and b) decomposition of barrier into several segments

7.3 Interface Shear Transfer Between Barrier and Deck

The evaluation of shear transfer between the barrier and deck can be determined by considering the distribution of the impact force. The shear force caused by the impact on a per foot basis can be determined using Eq. 7.24 where H is the same as H_b shown in Fig. 7.8. It should be noted that here a capacity design approach is used in the sense that it is the transverse barrier capacity, R_w, that is considered as the load that needs to be transferred to the deck rather than the impact force, F_t, for a particular Test Level. This ensures that if a failure were to occur, that failure would be limited to the barrier.

$$V_{ui} = V_{CT} = T = \frac{R_w}{L_c + 2H} \qquad \text{(Eq. 7.24)}$$

The factored interface shear resistance, V_{ri}, is calculated using Eq. 7.25. The shear capacity of the interface should be such that Eq. 7.26 is satisfied. The ϕ is taken unity as the vehicle collision is considered as an extreme event. In this case, $V_{ui} = V_{CT}$.

[5.7.4.3-1] $$V_{ri} = \phi V_{ni} \quad \text{(Eq. 7.25)}$$

[5.7.4.3-2] $$V_{ri} \geq V_{ui} \quad \text{(Eq. 7.26)}$$

The nominal shear resistance of the interface, V_{ni}, is calculated using Eq. 7.27, where c is the cohesion factor (Table 7.1), A_{cv} is the area engaged in shear transfer, μ is the friction factor, A_{vf} is the area of reinforcement crossing the interface, f_y is the yield stress of the reinforcement, and P_c is the normal force. The horizontal shear capacity, V_{ni} should be smaller than the value calculated from Eqs. 7.28 and 7.29 where K_1 and K_2 are factors provided in Table 7.1, and f_c' is the compressive strength of concrete.

[5.7.4.3-3] $$V_{ni} = cA_{cv} + \mu\left(A_{vf}f_y + P_c\right) \quad \text{(Eq. 7.27)}$$

[5.7.4.3-4] $$V_{ni} \leq K_1 f_c' A_{cv} \quad \text{(Eq. 7.28)}$$

[5.7.4.3-5] $$V_{ni} \leq K_2 A_{cv} \quad \text{(Eq. 7.29)}$$

[5.7.4.3-6] $$A_{cv} = b_{vi}L_{vi} \quad \text{(Eq. 7.30)}$$

According to Article 5.7.4.2 in AASHTO LRFD (2020), the area of shear reinforcement, A_{vf}, crossing the area engaged in shear transfer, A_{cv}, should satisfy the criteria given in Eq. 7.31.

[5.7.4.2-1] $$A_{vf_{min}} \geq \frac{0.05A_{cv}}{f_y} \quad \text{(Eq. 7.31)}$$

The minimum interface shear reinforcement, A_{vf}, need not exceed the lesser of the amount determined using Eq. 7.31 and the amount needed to resist $1.33V_{ui}/\phi$ as determined using Eq. 7.32. If friction between the base of the barrier and deck is sufficient alone to resist $1.33V_{CT}$, then no interface reinforcement is necessary.

$$A_{vf\_min2} = \frac{1}{f_y}\left[\frac{1.33V_{CT} - cA_{cv}}{\mu} - P_c\right] \geq 0 \quad \text{(Eq. 7.32)}$$

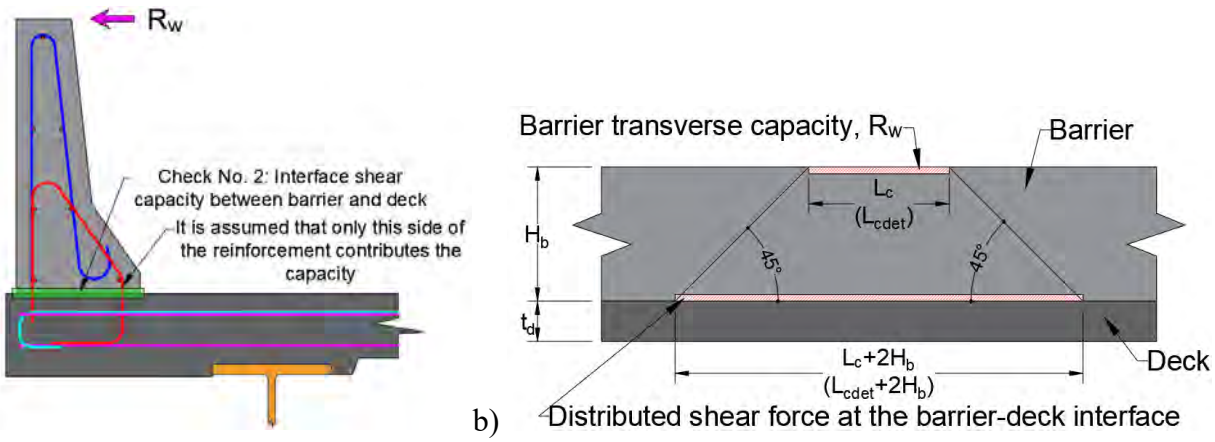

Fig. 7.8 a) Barrier subject to a transverse horizontal load emulating vehicle impact, b) distribution of the impact force, R_w, at the base of the barrier (top of the deck) using 1:1 slope (45° angle)

Table 7.1 Cohesion and Friction Factors (section 5.7.4.4 in AASHTO LRFD (2020))

Condition	Parameter	Value
For a cast-in-place concrete slab on clean concrete girder surfaces, free of laitance with surface roughened to an amplitude of 0.25 in.	c	0.28
	μ	1.0
	K_1	0.3
	K_2	1.8 ksi for nw. concrete 1.3 ksi for lw. concrete
For normal weight concrete placed monolithically	c	0.40
	μ	1.4
	K_1	0.25
	K_2	1.5
For lightweight concrete placed monolithically, or placed against a clean concrete surface, free of laitance with surface intentionally roughened to an amplitude of 0.25 in. (Type-1 in MDOTBarrier Program)	c	0.24
	μ	1.0
	K_1	0.25
	K_2	1.0 ksi
For normal weight concrete placed against a clean concrete surface, free of laitance, with surface intentionally roughened to an amplitude of 0.25 in. (Type-2 in MDOTBarrier Program)	c	0.24
	μ	1.0
	K_1	0.25
	K_2	1.5
For concrete placed against a clean concrete surface, free of laitance, but not intentionally roughened (Type-3 in MDOTBarrier Program)	c	0.075
	μ	0.6
	K_1	0.2
	K_2	0.8 ksi
For concrete anchored to as-rolled structural steel by headed studs or by reinforcing bars where all steel in contact with concrete is clean and free of paint	c	0.025
	μ	0.7
	K_1	0.2
	K_2	0.8 ksi
Highlighted condition represents the cases applicable in this project.		

The deterioration of the bridge deck fascia affects the shear transfer between the barrier and deck through the reduction of the area engaged in shear transfer. Two scenarios can exist: 1) $w_d > x_1$, and 2) $w_d \leq x_1$ where w_d is the average deteriorated width, and x_1 is the distance from the exterior face of the barrier to the exterior face of the fascia (Fig. 7.9a). For each case the area engaged in shear transfer per unit width can be calculated as shown in Eqs. 7.33-7.34 (Fig. 7.9). This can then be combined with the deteriorated length to calculate the total effective area engaged in shear transfer as described in Eqs. 7.35-7.38 where A_{cvdet} is the effective area engaged in shear transfer affected by the deterioration, A_{cv} is the area engaged in shear transfer for the portion of the interface that is outside the limits of the deterioration length, L_{undet2} the length of the undeteriorated interface, and L_d is the deteriorated length.

If $w_d > x_1$ $$A_{cvdet} = 12[(x_2 + x_3 + x_4) - (w_d - x_1)] \quad \text{(Eq. 7.33)}$$

If $w_d \leq x_1$ $$A_{cv} = 12(x_2 + x_3 + x_4) \quad \text{(Eq. 7.34)}$$

$$L_{undet2} = (L_{cdet} + 2H) - L_d \quad \text{(Eq. 7.35)}$$

If $L_{cdet} + 2H < L_d$ $$A_{cvdetadj} = \frac{A_{cv}L_{undet2} + A_{cvdet}L_d}{(L_{cdet} + 2H)} \quad \text{(Eq. 7.36)}$$

If $L_{cdet} + 2H \geq L_d$ $$L_{undet2} = 0 \quad \text{(Eq. 7.37)}$$

$$A_{cvdetadj} = A_{cvdet} \quad \text{(Eq. 7.38)}$$

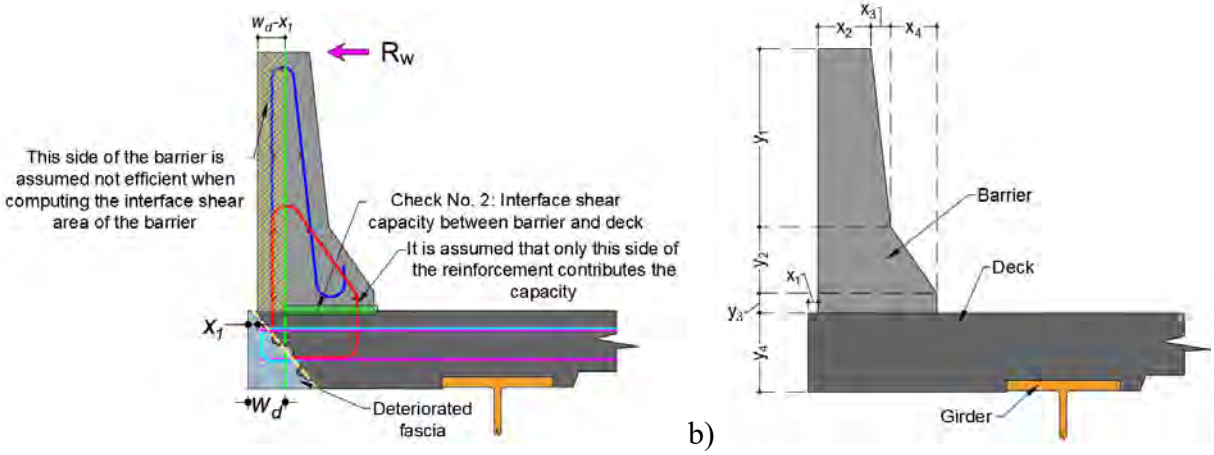

Fig. 7.9 a) Illustration of how the deterioration of the deck fascia affects the area engaged in shear transfer, b) illustration of other geometrical parameters used to calculate the effective area engaged in shear transfer

7.4 Axial Force and Moment Transfer from Barrier to Deck

Finally, the deck is evaluated for whether it has sufficient strength to resist the tension force and bending moment created by vehicle impact. The tension force per unit width can be calculated using Eq. 7.39 and the bending moment per unit width can be calculated using Eq. 7.40. Here again, a capacity design approach is used in the sense that it is the transverse capacity of the barrier, R_w, rather than the specified impact force, F_t, that is used to determine the axial tension force and bending moment demand in the deck. The critical section is considered to be at the intersection of the dowels and top deck reinforcement. This again ensures that in the event of failure, the damage is contained in the barrier facilitating the restoration of barrier crashworthiness by replacing only the barrier and barrier to deck connection. Both the tension force and bending moment are calculated assuming that the impact force will distribute at a 45-degree angle from the line of impact to the mid-depth of the deck. When computing the flexural capacity of the deck, only the top deck reinforcement is considered. When calculating the tensile capacity of the deck, both the top and bottom deck reinforcement are considered.

$$T = \frac{R_w}{L_c + 2(H_b + 0.5t_d)} \qquad \text{(Eq. 7.39)}$$

$$M = \frac{R_w(H_b + 0.5t_d)}{L_c + 2(H_b + 0.5t_d)} \qquad \text{(Eq. 7.40)}$$

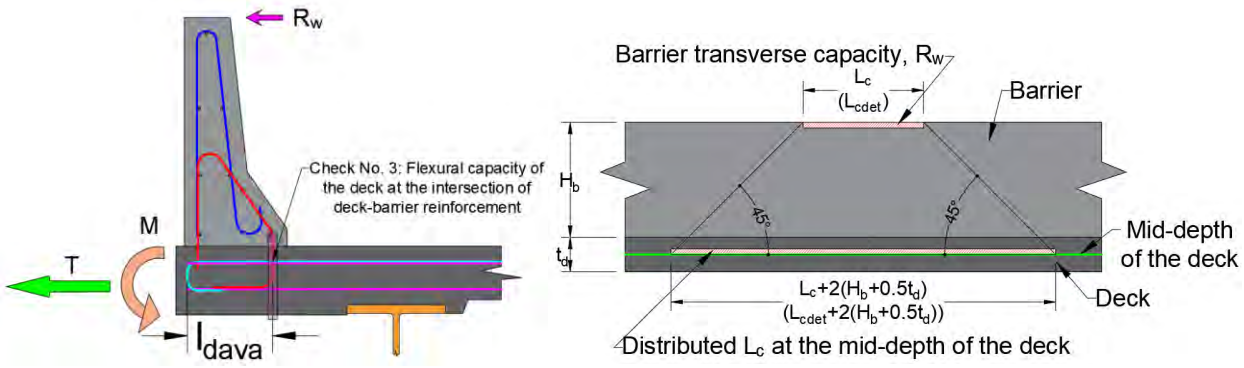

Fig. 7.10 a) Transfer of tension axial force and bending moment caused by vehicle impact from the barrier to the deck, b) distribution of impact load

It is assumed that the top deck reinforcement may feature straight and hooked bars and the bottom deck reinforcement may feature only straight bars. Since both layers of deck bars are used in the axial force and bending moment transfer, their development on the left-hand side of the

dowel top deck bar intersection is evaluated using AASHTO LRFD (2020) provisions. The equations for the development length of hooked bars were presented earlier. Those for the development length of straight bars are provided in Eqs. 7.41-7.47. If the available length for any of the bars is smaller than the development length, the stress for that particular bar is proportioned as described earlier.

5.10.8.2.1a-1 $$l_d = \max\left(l_{db}\left(\frac{\lambda_{rl}\lambda_{cf}\lambda_{cf}\lambda_{er}}{\lambda}\right), 12\right)$$ (Eq. 7.41)

5.10.8.2.1a-2 $$l_{db} = 2.4 d_b \frac{f_y}{\sqrt{f_c'}}$$ (Eq. 7.42)

$$\lambda_{rl}\lambda_{cf} \leq 1.7$$ (Eq. 7.43)

5.10.8.2.1c-1 $$0.4 \leq \lambda_{rc} \leq 1.0$$ (Eq. 7.44)

5.10.8.2.1c-2 $$\lambda_{rc} = \frac{d_b}{c_b + k_{tr}}$$ (Eq. 7.45)

$$c_b = \min(clear\ cover; spacing/2)$$ (Eq. 7.46)

5.10.8.2.1c-3 $k_{tr} = 40A_{tr}/sn$ (taken 0 in this project) (Eq. 7.47)

The axial capacity of the deck is then determined using Eq. 7.48, where P_n is the axial capacity, A_{s4} is the area of straight top bars, A_{s5} is the area of hooked top bars, A_{s6} is the area of straight bottom bars, f_{yadj4} is the stress in the straight top bars, f_{yadj5} is the stress in the hooked top bars, and f_{yadj6} is the stress in the straight bottom bars.

$$P_n = A_{s4}f_{yadj4} + A_{s5}f_{yadj5} + A_{s6}f_{yadj6}$$ (Eq. 7.48)

A linear interaction is assumed to account for the interaction between the axial tension force and bending moment as shown in Eq. 7.49 where M_{nint} is the moment capacity of the deck considering the presence of axial tension, M_n is the moment capacity of the deck without any axial force present, T_{CT} is the axial force demand, and P_n is the axial capacity of the deck without any bending moment present.

$$M_{nint} = M_n\left(1 - \frac{T_{CT}}{P_n}\right)$$ (Eq. 7.49)

In a bridge with a deteriorated fascia the moment capacity of the deck considering the presence of the axial force can be calculated using Eqs. 7.50-7.53, where $L_{cdetadj}$ is the adjusted critical length of the yield line failure pattern calculated based on $M_{cdetadj}$, L_{undet3} is the undeteriorated length of the bridge deck fascia as calculated by Eq. 7.50, L_d is the deteriorated

length provided as an input, $M_{nintdetadj}$ is the average moment capacity of the deck considering deterioration and the presence of axial tension, M_{nint} is the moment capacity of the deck in the undeteriorated portion considering the presence of axial tension, $M_{nintdet}$ is the moment capacity of the deck in the deteriorated portion considering the presence of axial tension.

$$L_{undet3} = (L_{cdetadj} + 2(H_b + 0.5t_d)) - L_d \quad \text{(Eq. 7.50)}$$

If $L_{cdetadj} + 2(H_b + 0.5t_d) \geq L_d$

$$M_{nintdetadj} = \frac{M_{nint}L_{undet3} + M_{nintdet}L_d}{L_{cdetadj} + 2(H_b + 0.5t_d)} \quad \text{(Eq. 7.51)}$$

If $L_{cdetadj} + 2(H_b + 0.5t_d) < L_d$

$$L_{undet3} = 0 \quad \text{(Eq. 7.52)}$$

$$M_{nintdetadj} = M_{nint} \quad \text{(Eq. 7.53)}$$

7.5 Overview of the MDOT Barrier Computer Program

The preceding sections provided an explanation of the fundamental principles used in the preparation of the MDOT Barrier Program. This section describes how the MDOT Barrier program can be used including figures that illustrate the graphical user interface. The MDOT Barrier program was written in Matlab. The graphical user interface consists of a total of five tabs named: Introduction, Inputs, Results Summary, Original Design, and After Deterioration. While the naming of each tab is self-explanatory and the graphical user interface is intuitive, a short description of the purpose and functions of each tab is provided.

In the “Introduction” tab the analyst provides general information about the project. The “i” button here and in every tab provides general information about that particular tab or that section of a given tab. In the introduction tab, the “i” button provides an overall description of what the program does. There is an opportunity to load a previously saved input file through the “Project Data” button.

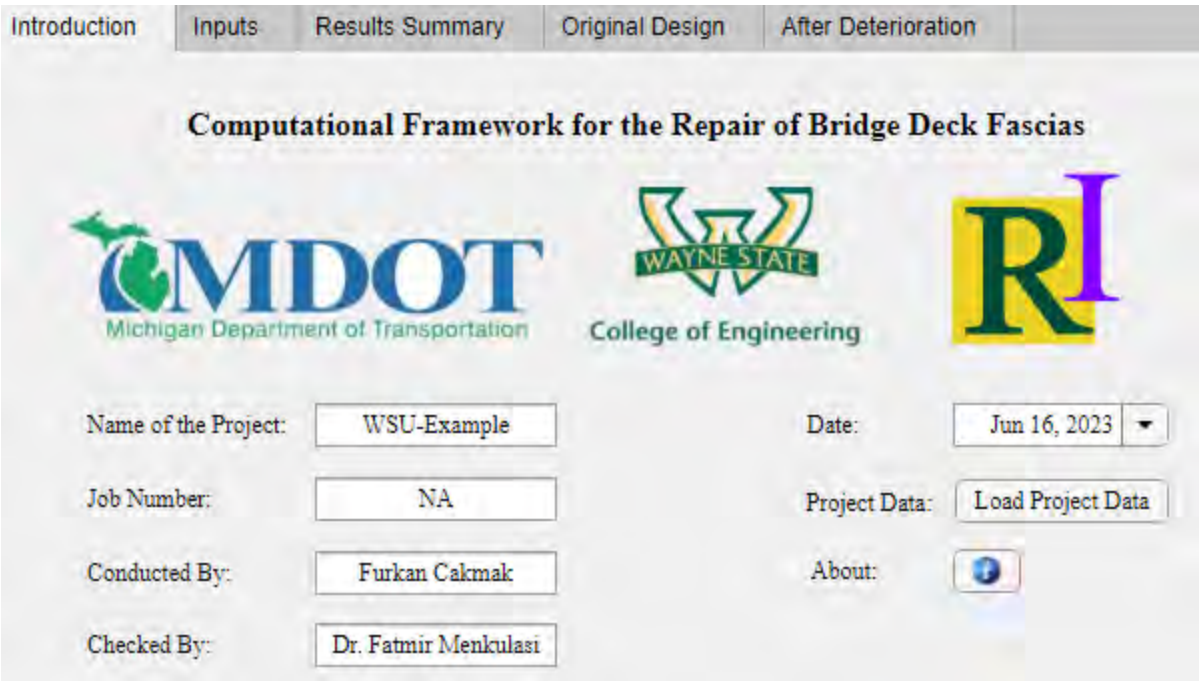

Fig. 7.11 Illustration of the introduction tab

Fig. 7.12 shows the input required to evaluate barrier crashworthiness. This includes the description of barrier and deck overhang geometry and reinforcement. The specification of barrier and deck geometry is required in terms of defining the width and depth of various cross-sections in the barrier and deck. This information is then used when determining the moment capacity of the barrier about vertical and horizontal axis, and the moment capacity of the deck. The specification of reinforcement geometry includes the specification of the location of the reinforcement with respect to the barrier and deck surfaces. This is used to determine effective depths when calculating moment capacities. In addition, the user must specify the grade of reinforcement, which represents the yield stress, the type of reinforcement whether it is uncoated or epoxy coated – this affects development length calculations, as well as the size and spacing of the reinforcement. The user can specify the Test Level for which the barrier is to be evaluated. The available Test Levels that the user can select vary from Test Level 1 to Test Level 6. In addition, the user can select the type of connection between the barrier and deck. The type of connection is characterized by a set of cohesion and friction factors, which depend on the type of interface between the barrier and deck. This information is used when checking shear transfer between the barrier and deck in the event of vehicle collision. This set of cohesion factors is a function of whether the barrier and deck concrete are normal weight or light weight. This information can be

specified in the input tab under deck concrete type and barrier concrete type. The user then needs to specify the deterioration width (thickness), w_d, and deterioration length, L_d, both of which are illustrated in Fig. 7.13. In this particular example, the deteriorated width is 6.5 in. and the deteriorated length is 180 in. (quite severe deterioration).

After all required input has been provided, the user can click on the "Calculate" button to initiate barrier analysis. During the analysis, three limit states are evaluated: 1) capacity of the barrier to resist a specified level of impact, 2) shear capacity of the barrier to deck connection, and 3) moment transfer from barrier to deck. The deck fascia deterioration affects all three limit states as explained in the previous sections. For example, a deteriorated fascia results in a smaller effective barrier cross-section when calculating barrier moment capacity about the horizontal axis. This affects the capacity of the barrier as determined using closed form equations obtained from yield line analysis presented in AASHTO LRFD (2020) Article 13.3.1-1. A deteriorated fascia also affects the shear transfer between the barrier and deck in case of a vehicle impact because the width of the effective interface is reduced. This means that the contribution of cohesion in shear transfer is reduced because the area engaged in shear transfer is reduced. Finally, to facilitate axial force and moment transfer between the barrier and deck, the top reinforcement in the deck should have sufficient development length. The deterioration of the deck fascia reduces the available space for developing the yield stress of the top deck reinforcement. From this discussion, it becomes clear that the deteriorated width of the deck fascia is a key parameter when evaluating the crashworthiness of the barrier. The deteriorated length is also an important parameter. For example, a large deteriorated width that applies only for a limited length will have limited impact on the ability of the barrier-deck overhang subassembly to resist vehicle impact loads. A weighted average approach was taken when developing the MDOT Barrier program to account for the influence of deteriorated length.

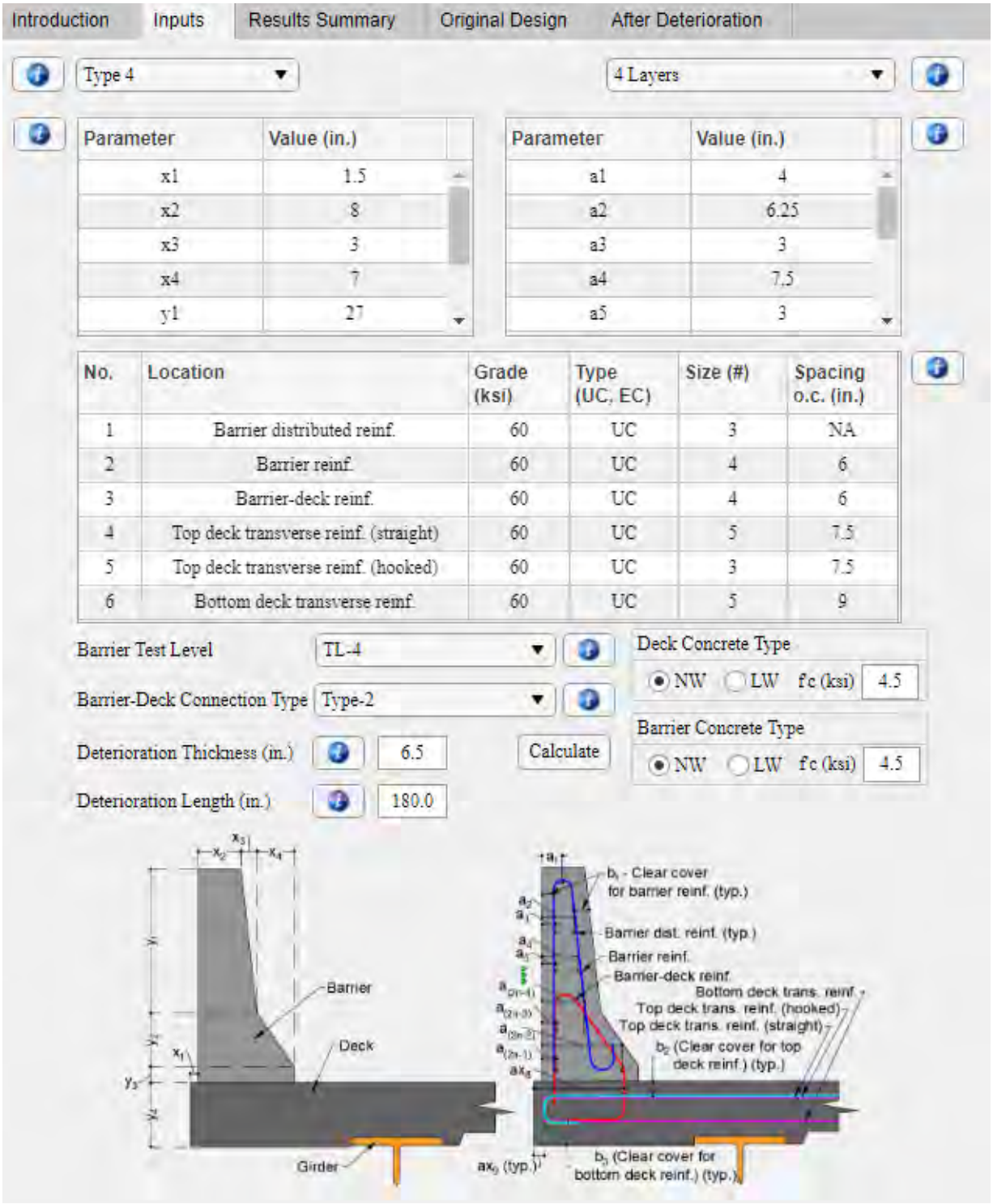

Fig. 7.12 Input for the MDOT Barrier computer program

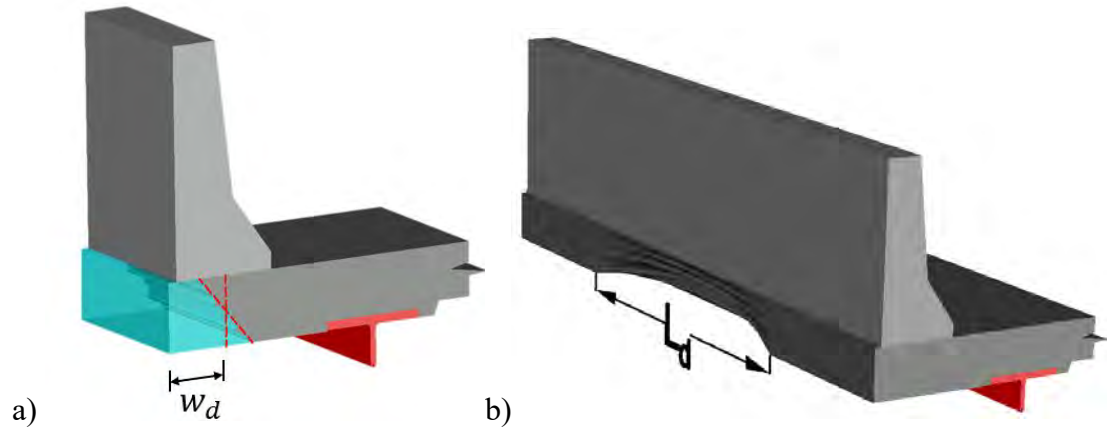

Fig. 7.13 Illustration of: a) deterioration width (thickness), w_d, and b) deterioration length, L_d

Fig. 7.14 shows the summary of the results, which can be seen from the "Results Summary" tab. In this example, the specified deteriorated width and length is such that it affects the crashworthiness of the barrier by reducing its transverse capacity from 76.74 kips to 50.25 kips. The 50.25 kips is smaller than TL-4 level crashworthiness. In the "Demand" columns there are two values for the shear transfer and moment transfer while there is only one value for the barrier transverse capacity. The required barrier transverse capacity is a singular value based on the selected Test Level specified in the input tap. This is based on AASHTO LRFD (2020). As noted earlier, the demand for shear and moment transfer is based on a capacity design approach and as such, two values are provided: the first represents the shear and moment transfer demand based on the undeteriorated fascia, and the second represent the corresponding values based on the deteriorated fascia. Two columns are provided for capacity: one based on the original design, and the other after deterioration. Here, the analyst can clearly see the impact of the deck fascia deterioration on barrier crashworthiness. In this case, the crashworthiness is undermined since the capacity after deterioration (50.25 kips) is smaller than F_t = 54 kips. It should be noted that on the one hand the specified deterioration was rather large, and on the other hand the original design presents a notable safety margin. If the original design would be such that the original capacity is close to the specified demand, then a combination of a smaller deterioration width and length would result in the undermining of the barrier crashworthiness.

Under the "Original Design" tab the analyst can find detailed information about the crashworthiness of the barrier based on the original design (i.e. undeteriorated deck fascia). In the

"After Deterioration" tab, the analyst can find detailed information about the crashworthiness of the barrier after deck fascia deterioration.

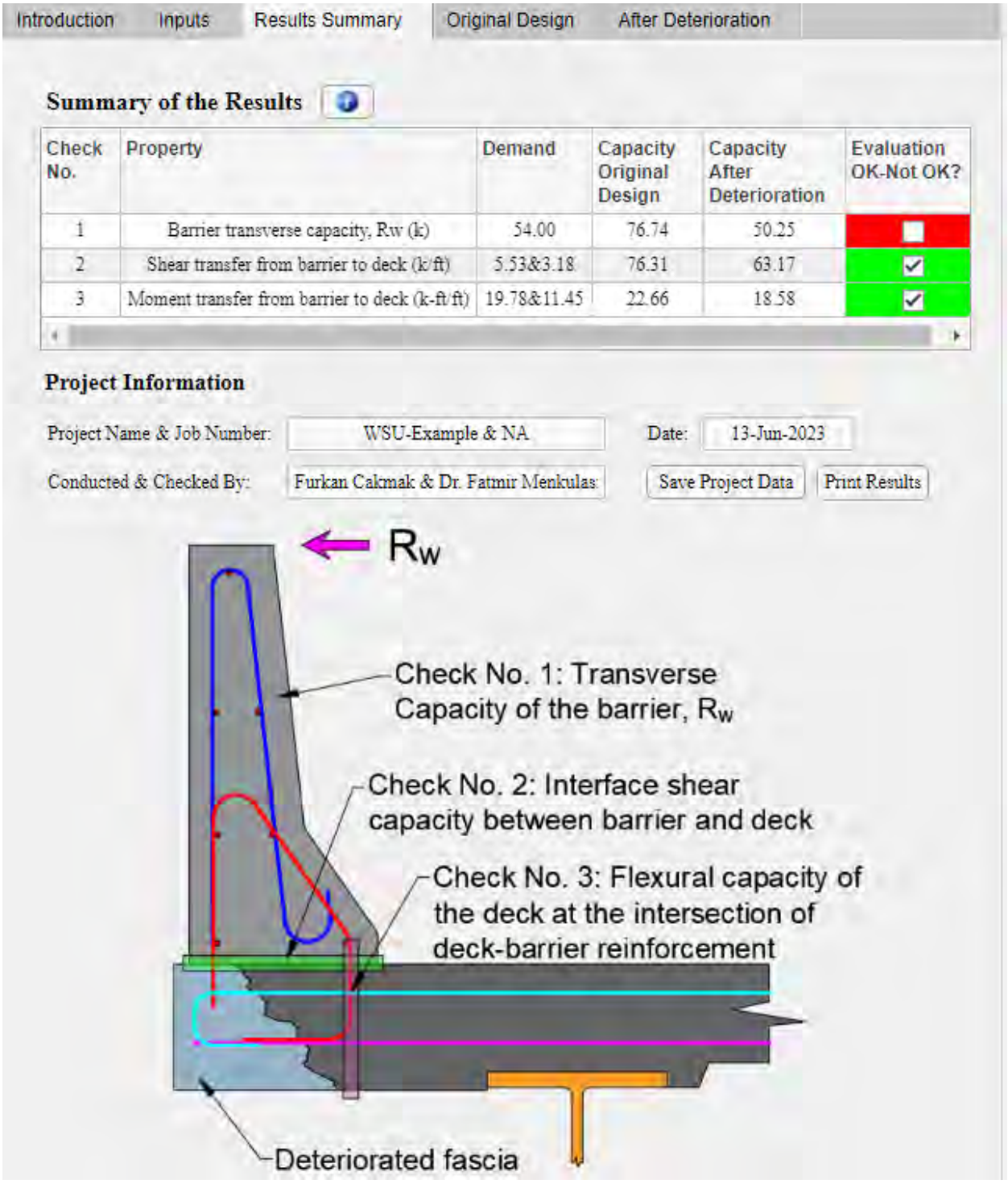

Fig. 7.14 Results summary

.

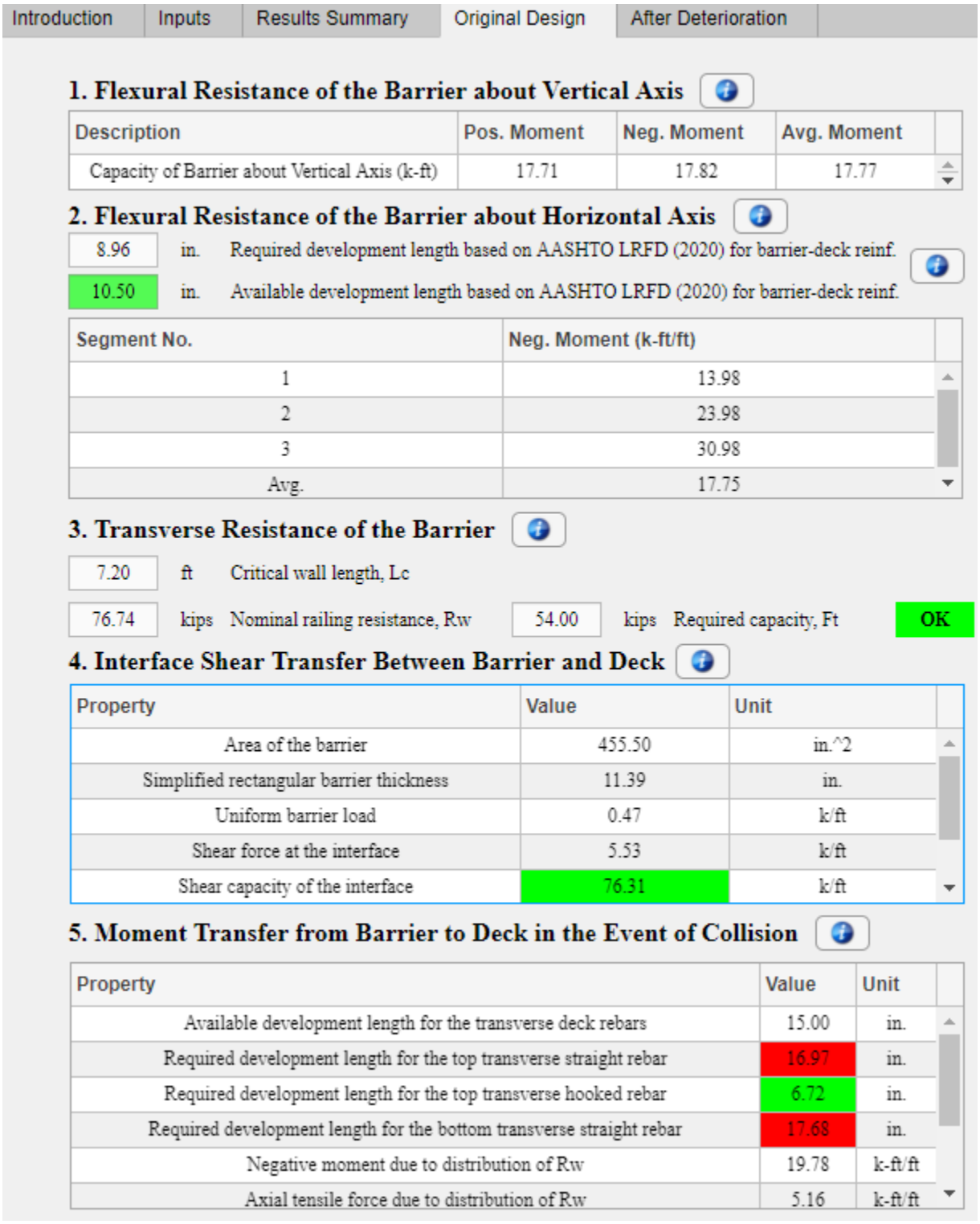

Fig. 7.15 Details about the crashworthiness of the barrier based on the original design

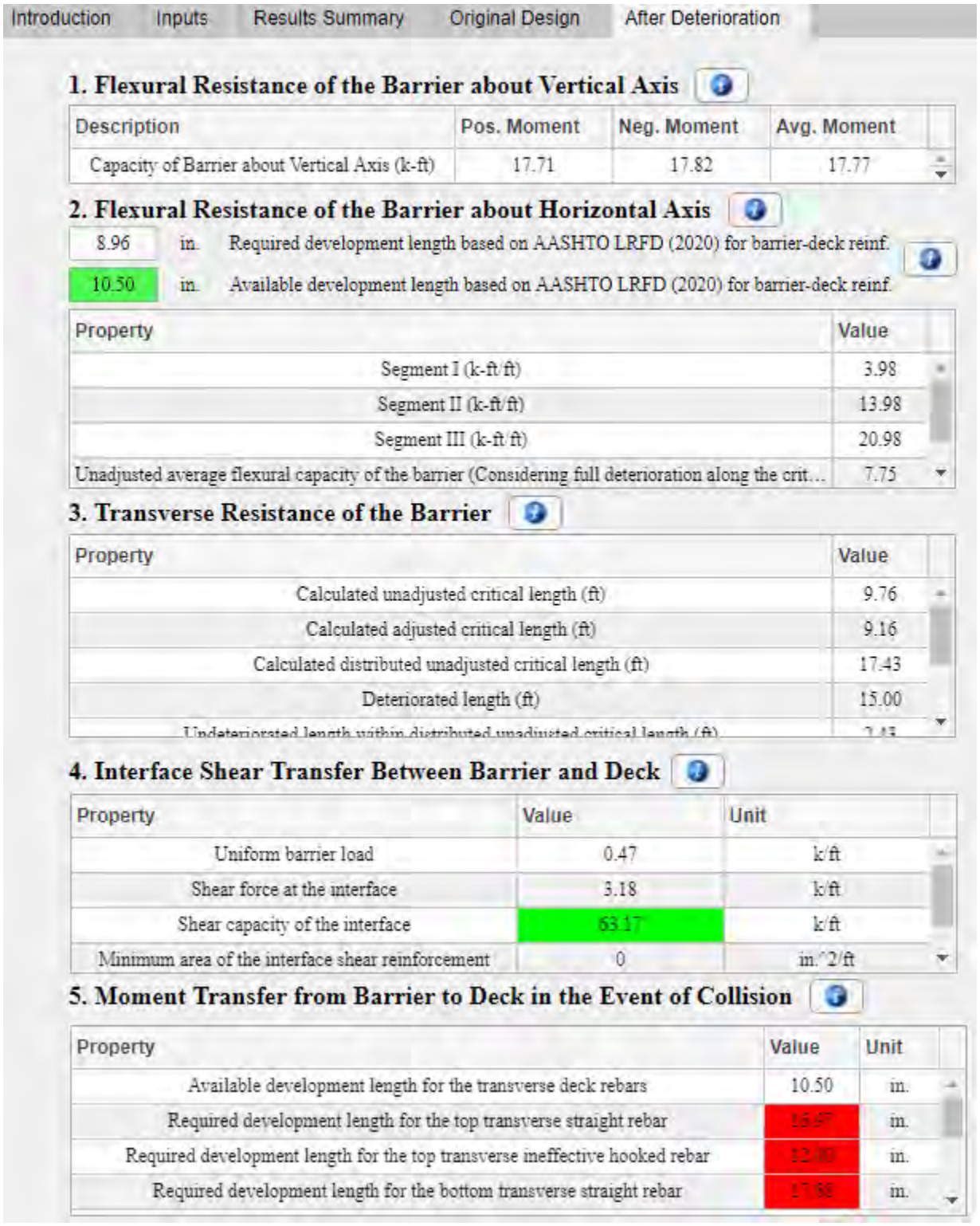

Fig. 7.16 Details about the crashworthiness of the barrier after deck fascia deterioration

Chapter 8: Develop Guidelines for Designing and Detailing Future Repair Details and New Barrier to Deck Overhang Connection

Chapter 8: Develop Guidelines for Designing and Detailing Future Repair Details and New Barrier to Deck Overhang Connections

The goal of this chapter is to present guidelines for designing and detailing future repair details and new barrier to deck overhang connections. A Special Provision for the Repair of Bridge Deck Fascias is provided in Appendix F and an Implementation Plan is provided in Appendix G. The chapter is organized in three main sections. The first section presents construction details that are intended to reduce moisture content in deck fascia in new bridges with the goal of preventing deck fascia deterioration. The second section addresses bridges that have exhibited moderate deck fascia deterioration. Here, guidelines for how to maintain the current geometry of the deck facia and prevent further deterioration are presented. Finally, the last section addresses bridges that have exhibited severe deck fascia deterioration. Here, repair details are presented with the goal of restoring the original geometry of the deck fascia such that the original crashworthiness of the barrier is re-instated.

8.1 Proposed Barrier to Deck Overhang Connections for New Bridges

The proposed barrier to deck connection details that are intended to reduce moisture content in the deck fascia and enhance durability are divided in to three categories: 1) Sloped Top Deck Surface Connections; 2) Elevated Shear Key Connections; 3) Suppressed Shear Key Connections; and 4) Deck Fascias with fiber reinforced self-consolidating concrete (FRSCC). It should be noted that these details are intended for bridges that feature solid barriers. Field evidence suggested a strong correlation between the deck fascia deterioration and the open barriers. One option for bridges that feature open barriers is the specification of a higher performing deck concrete ideally with sustained tensile strength after the first crack. This is addressed in section 8.1.4.

8.1.1 Sloped Top Deck Surface Connections

Fig. 8.1 shows a barrier to deck connection that features a sloped deck surface underneath the footprint of the barrier. The sloping of the top deck surface is done with the purpose of directing moisture away from the deck fascia. The creation of the sloped top deck surface can be achieved by using a relatively low slump concrete. The slump range typically specified for the deck concrete is believed to be sufficient to create this slope, thus no changes in the concrete mix design for the deck are needed to create the sloped surface. The slope may be created by hand after the placement of the deck concrete. No constructability issues were reported from the states that use similar

details. A ¾ in. drip notch is specified 4 in. away from the edge of the deck overhang to interrupt any moisture that may travel through surface tension. The sloped top deck surface is unfinished thus providing a naturally roughened surface. Alternatively, efforts may be put forth to create some desired amplitude in the roughened surface to further slow the progression of moisture. The 10º slope (1:6 slope) is used to determine the depth of the deck fascia. In this detail as well as in other details presented in this section, the top deck reinforcement consists of some straight bars and some hooked bars. The straight bars are provided as a continuation of the deck bars that provide negative moment resistance over the girder supports. The hooked bars are additional bars provided solely in the deck overhang regions and which extend a certain amount past the fascia girder as dictated by analysis. These bars are provided to ensure barrier crashworthiness. That is, the deck overhang is responsible for supporting its self-weight, the weight of the barrier, any applicable live loads, and forces transferred from the barrier in the event of a vehicle impact. The hooks are provided to facilitate force transfer from the barrier to the deck in the event of a vehicle impact, since the available space to facilitate this force transfer is limited. A 1.5 in. minimum ledge is provided between the deck fascia and exterior face of the barrier. It is important to have this ledge from the perspective of protecting the crashworthiness of the barrier. This ledge has several positive effects on the crashworthiness of the barrier: 1) it increases the available length for the top bars in the deck to transfer forces from the barrier to the deck in the event of vehicle impact, 2) if the deterioration of the barrier is less than the width of the ledge, the capacity of the flexural capacity of the barrier as determined from yield line analysis is not affected, and 3) if the deterioration of the barrier is less than the width of the ledge, shear transfer between the barrier and deck is also not affected. In general, the ledge provides some redundancy in terms of the ramifications of deck fascia deterioration to barrier crashworthiness.

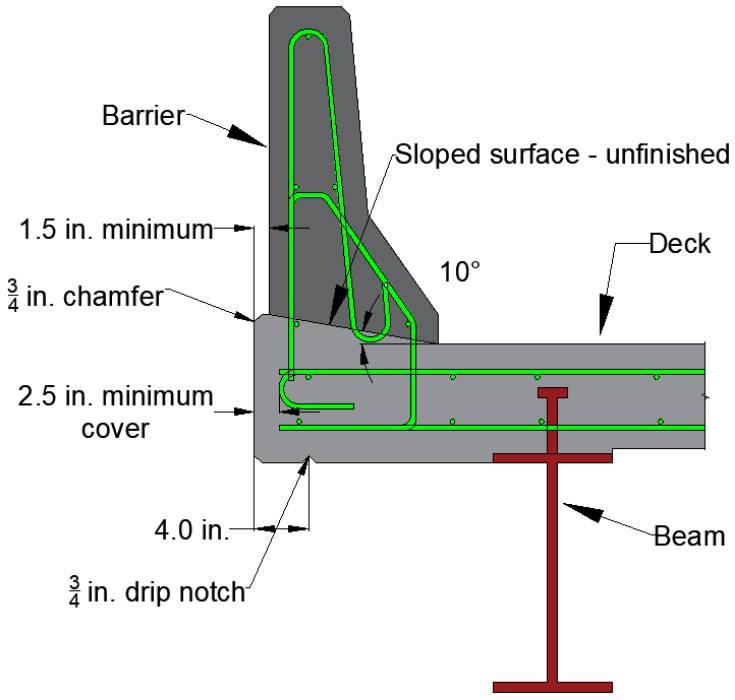

Fig. 8.1 Sloped top deck surface connection detail

8.1.2 Elevated Shear Key Connections

Fig. 8.2 shows an elevated shear key detail intended to prevent moisture migration from the deck surface to the deck fascia. The depth of the shear key is determined such that it can be formed using nominal 2 in. by 4 in. wooden studs oriented such that the nominal 4 in. dimension is in the vertical direction. The wooden stud is removed once the deck concrete has hardened. The width of the shear key is determined such that the elevated portion possesses sufficient integrity against any forces that it may incur during construction. The advantage of this detail compared to an elevated shear key placed in the middle of the barrier footprint is that it can be formed more easily. As noted, on the right-hand side a nominal 2x4 in. wooden stud turned vertically may be used. On the left-hand side, the traditional deck fascia formwork may be extended to create the elevated shear key. Discrete wooden studs may be used in the transverse direction connected to the top of the longitudinal 2x4 studs and the fascia formwork to provide formwork stability. This detail is provided as an alternative to the existing MDOT detail in which an isolated and elevated shear key, which either has a nominal semicircular shape or a trapezoidal shape, but in reality has a random shape as it is formed by hand. The proposed detail provides more control over the shape of the shear key.

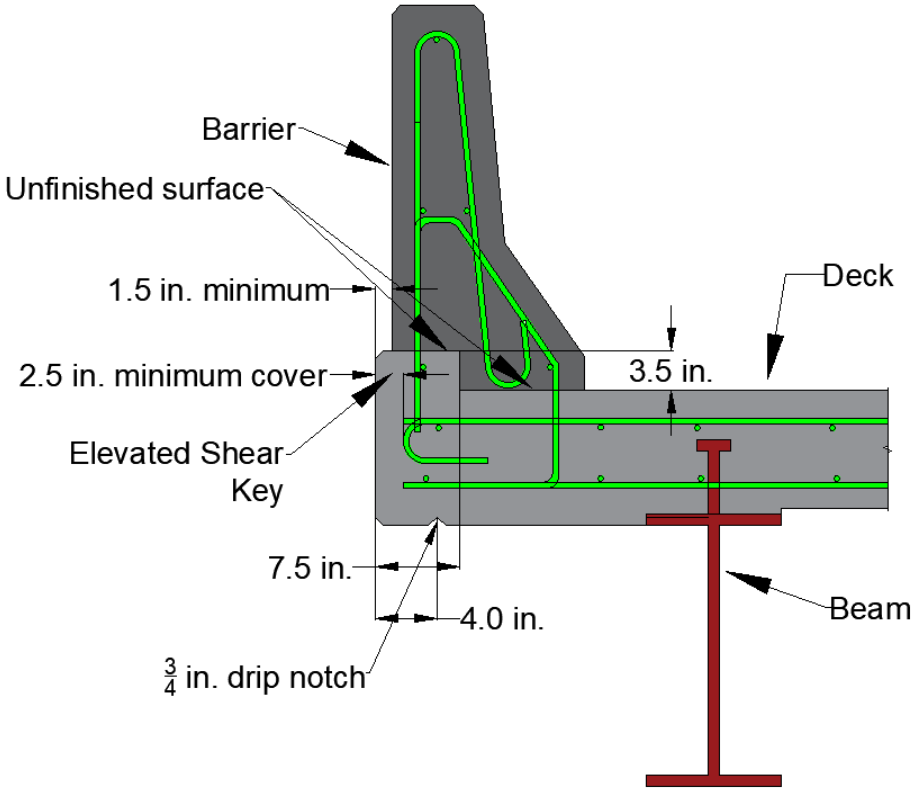

Fig. 8.2 Elevated shear key detail

8.1.3 Supposed shear key detail

Fig. 8.3 shows a suppressed shear key detail. The advantage of this detail is the ease of forming. A nominal 2x6 in. wooden stud may be used to create the shear key when the deck concrete is placed. As the wooden stud is pressed in the plastic concrete during deck concrete placement, no further support is required. The 2x6 wooden stud is removed once the concrete has hardened.

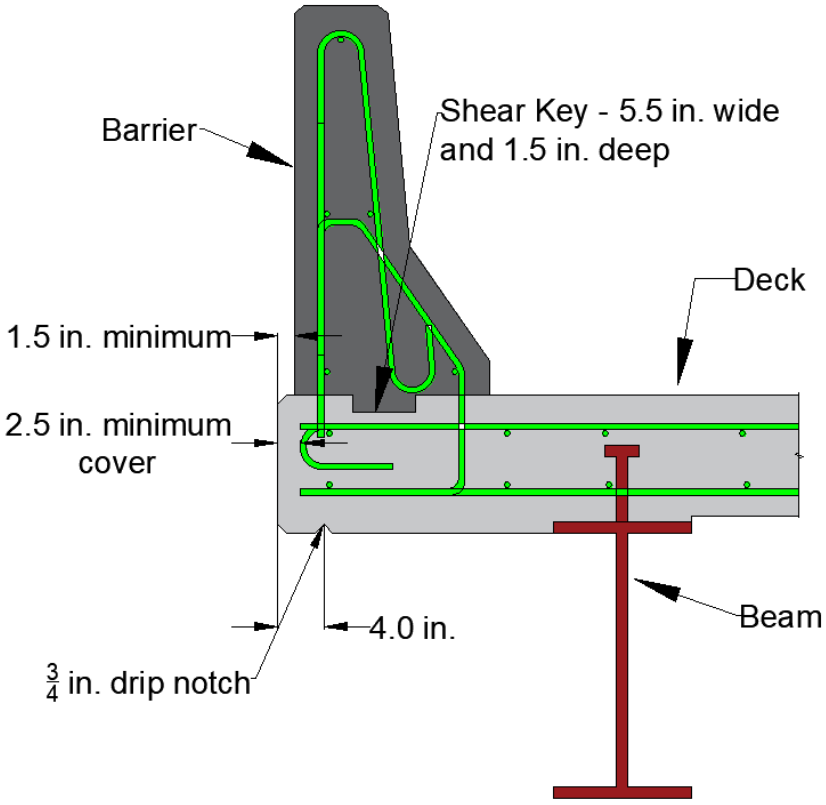

Fig. 8.3 Suppressed shear key detail

8.1.4 Self-consolidating concrete deck fascia detail

Fig. 8.4 shows a detail in which a higher performing concrete mixture is used for the deck fascia. The width of this strip may be chosen by the designer although some guidance is provided in terms of the location of the shear key with respect to fascia girder. The rationale for the specified 6 in. minimum distance between the fascia girder and the shear key is that in the event of leakage through the shear key, the fascia girder is protected. This detail has the disadvantage that it requires two deck placements; one for the majority of the deck and another for the deck fascia. This requires the creation of the shear key, which may provide an avenue for water and deicing chemicals. However, if the shear key performs well and no leakage is observed, this detail provides enhanced protection in one of the most vulnerable portions of the deck – i.e. the deck fascia. The same concept can be applied to the expansion joints, if they are specified in new bridges. Compare this proposed detail with that used in a deck overhang and expansion joint replacement project. The concept is the same. In lieu of removing the deteriorated deck overhang and a portion of the deck concrete near the expansion joint, here, a higher performing concrete mixture is used to prevent

that problem from occurring in the first place. A fiber reinforced self-consolidating concrete mixture is recommended primarily due to the ease of placement and the sustained tensile strength after cracking. The latter is important in terms of keeping the cracked concrete fragments from falling down in the event that such cracking and spalling precipitates in the future. A higher performing concrete mixture may be used for the barrier too, since during the winter months in Michigan, the snow in the deck is pushed towards the barriers to facilitate travel. This subjects the barriers to a high amount of moisture and deicing chemicals, which accelerates their deterioration.

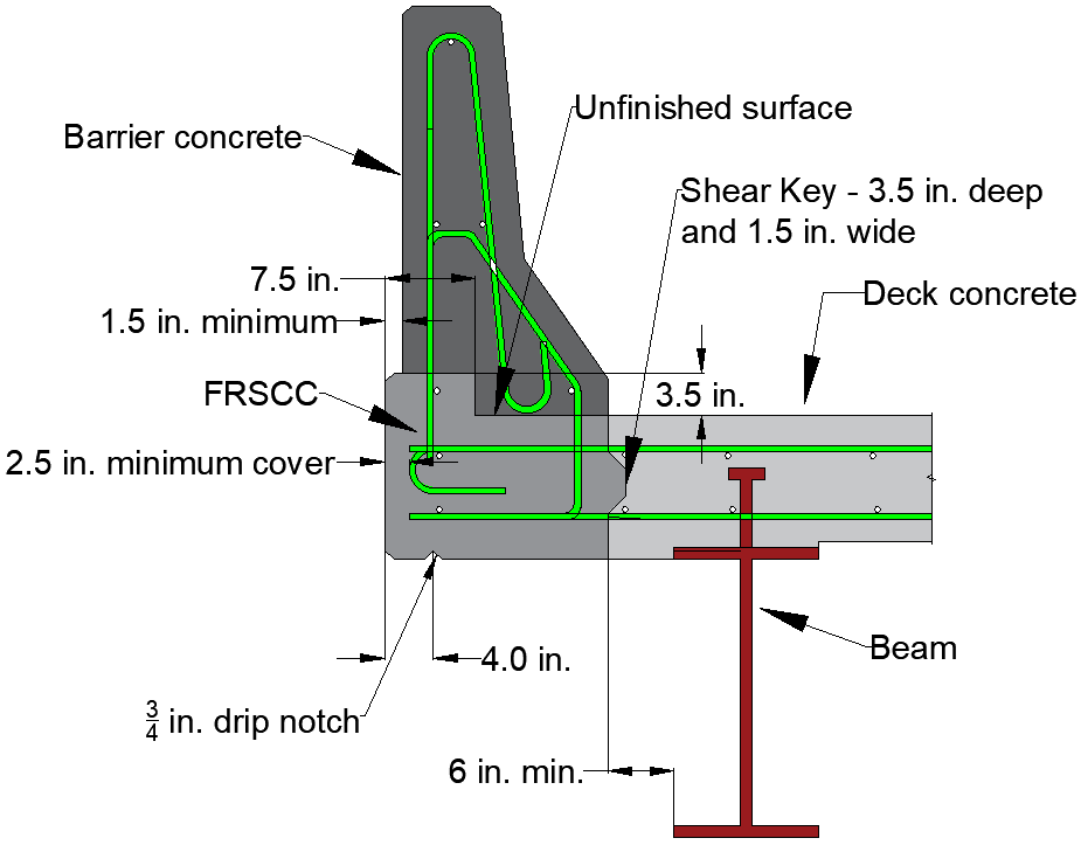

Fig. 8.4 Fiber reinforced self-consolidating concrete deck fascia detail

8.2 Proposed Deck Fascia Repair Details for Existing Bridges

The focus of the previous section was the prevention of the deck fascia deterioration in new bridges. The focus of this section is the repair and maintenance of bridges with deteriorated deck fascias.

Fig. 8.1 provides an overview of the proposed approach for the evaluation of existing bridge deck fascias, which have exhibited signs of deterioration. The approach is described in a step by step fashion. Each step is discussed below:

Step 1: Conduct Visual Inspection

Step 2: Characterize deterioration

The goal of this step is to characterize the deterioration of the deck fascia in terms of the deteriorated length and width. Here the term length aligns with the longitudinal direction of the bridge (i.e. the direction of traffic), and the term width aligns with the transverse direction of the bridge (i.e. perpendicular to traffic). It is expected that the deteriorated width will vary for a given deteriorated length. As such, an idealization of the deteriorated length and width is required. This can be done by presenting the average deteriorated width for a given length. Measurements of the deteriorated width at various discrete locations along the deteriorate length could be conducted or the average deteriorated width could be determined using visual means.

Step 3: Enter the idealized deteriorated length and width as an input in the MDOT Barrier computer program (see Chapter 7).

Step 4: Evaluate the crashworthiness of the barrier using the MDOT Barrier computer program.

This can be conducted using the analytical tool referenced above.

Step 5: Determine if the crashworthiness of the barrier is undermined

If the crashworthiness of the barrier is not undermined then go to Step 6. Otherwise go to Step 7.

Step 6 – Option 1: Scale the deck fascia

This option presents the current practice of MDOT where the deteriorated fascia is scaled to remove unsound concrete to prevent it from falling down.

Step 6 – Option 2: Scale the deck fascia and apply polyurea

This option provides future protection by applying polyurea after the deteriorated deck fascia has been scaled (see section 8.2.1)

Step 7 – Option 1: Repair the deck fascia

If this option is pursued, then the repair detail developed as part of this project may be used (see section 8.2.2).

Step 7 – Option 2: Replace the deck fascia

If this option is pursued then the current practice of MDOT for replacing the deteriorated deck overhang and barrier is used.

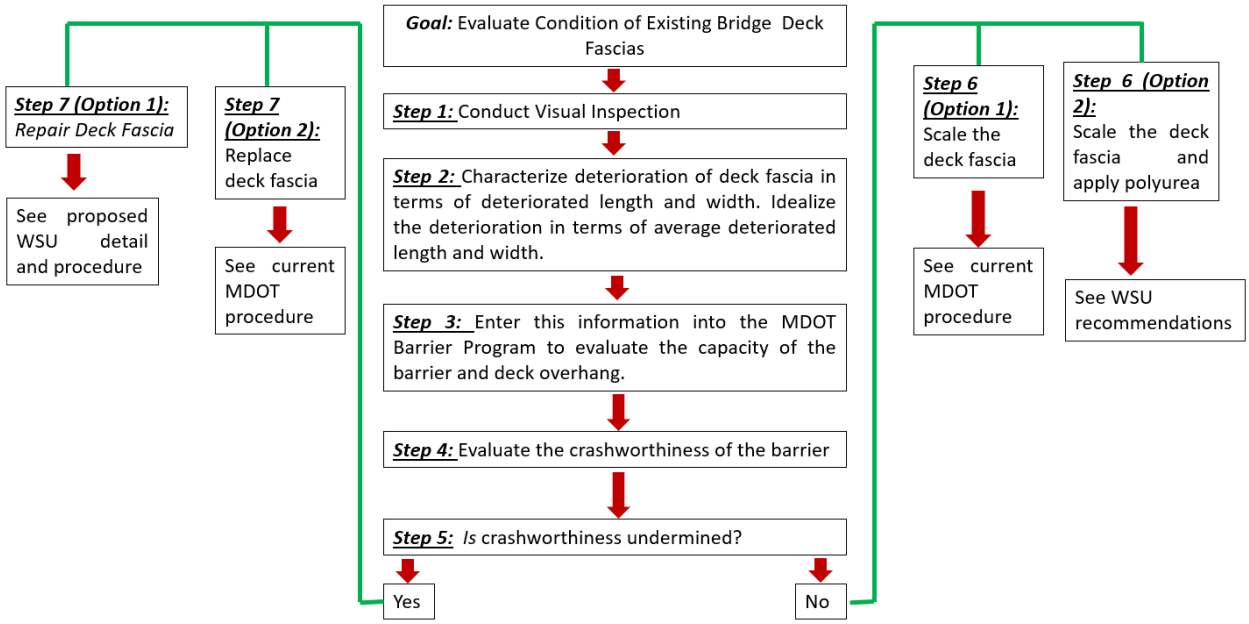

Fig. 8.1 Overview of Proposed Approach for the Evaluation of Existing Bridge Deck Fascias

8.2.1 Guidance for Maintaining Current Geometry and Preventing Further Deterioration

If it is determined that the deterioration of the fascia is moderate, the crashworthiness of the barrier is not undermined, and if it is desired to provide protection against future deterioration, then the application of polyurea is one option for doing so. It should be noted that the use of polyurea as a coating for providing protection was identified during the literature review process and its use for deck fascias is recommended based on research conducted by Miller et al. (2017; 2020) for bridge barriers. It is believed that the deterioration of bridge barriers and deck fascia is affected by similar mechanisms and a successful use of the polyurea for bridge barriers suggests a potential successful use for deck fascias. Polyurea products are supplied by various manufacturers which include: 1) Citadel Floor Finishing Systems, 2) Creative Material Technologies, Ltd., 3) Mirabel Coatings and 4) VersaFlex, Inc. The selected manufacturer's instructions should be followed when applying this product. Polyurea acts as a reinforcement layer to retain broken fragments of concrete. There are two types of polyurea, which are a function of the shape of the molecule: 1) Aromatic polyureas, and 2) Aliphatic polyureas. The aromatic option is easier to apply, while the aliphatic option is more durable against ultraviolet light. A combination of both is certainly possible. The polyureas set relatively fast. According to the study conducted by Miller et al. (2017) on bridge barriers, the

installed material cost varies from $3-$7.5 per square foot, compared to $1-$2 per square foot for epoxies. Special equipment is needed for installation and the cost of the machine for the spray on option may vary from $20,000-$40,000. If the material is installed using a cold spray approach and joint filling equipment utilizing static mixers, then the cost of equipment may vary from $5,000-$15,000. Skilled labor is required for installation, and a 10-day training is provided by the manufacturer. Protective equipment is required during installation. The material can be sprayed on, brushed on, or rolled on a surface. The typical thickness of the coat may vary from 0.02-0.1 in., although it can be as thick as ½ in. The study conducted by Miller et al. (2017) distinguished polyureas from the rest of protective sealants due to their ability to provide:

1) Abrasion resistance
2) Good bond to concrete and steel
3) Good resistance to many chemicals including chloride as well as to changes in humidity and temperature
4) Good sealing capability including cracks up to 1/8 in. due to their high level of elasticity
5) Reinforcement capabilities with some manufactures providing blast resistant formulas (Davidson et al. 2004; 2005)
6) A repairable material
7) Freeze-thaw and salt fogging resistance
8) A flexible repair option, which can be applied over a wide range of temperatures (-30^{o}F to 140^{o}F)
9) Colored as well as clear options

Miller et al. (2020) evaluated various polyurea products supplied by various manufacturers: 1) Citadel Floor Finishing Systems, 2) Creative Material Technologies, Ltd., 3) Mirabel Coatings and 4) VersaFlex, Inc. The types of tests conducted include field testing and laboratory testing. The field testing included V-notch tests, and impact tests. Laboratory testing included pull-off testing, flexural testing, and rapid freeze-thaw testing. All evaluated products were deemed acceptable for the purpose of sealing the surface and restraining small concrete fragments from falling off the surface.

8.2.2 Guidance for Implementing the Proposed Repair Detail

Fig. 8.5 shows the proposed repair detail. This detail is appropriate for deck fascias that have exhibited severe deterioration and for which analysis suggests that the crashworthiness of the barrier is undermined. This detail is intended to be less invasive than the complete deck overhang and barrier replacement option.

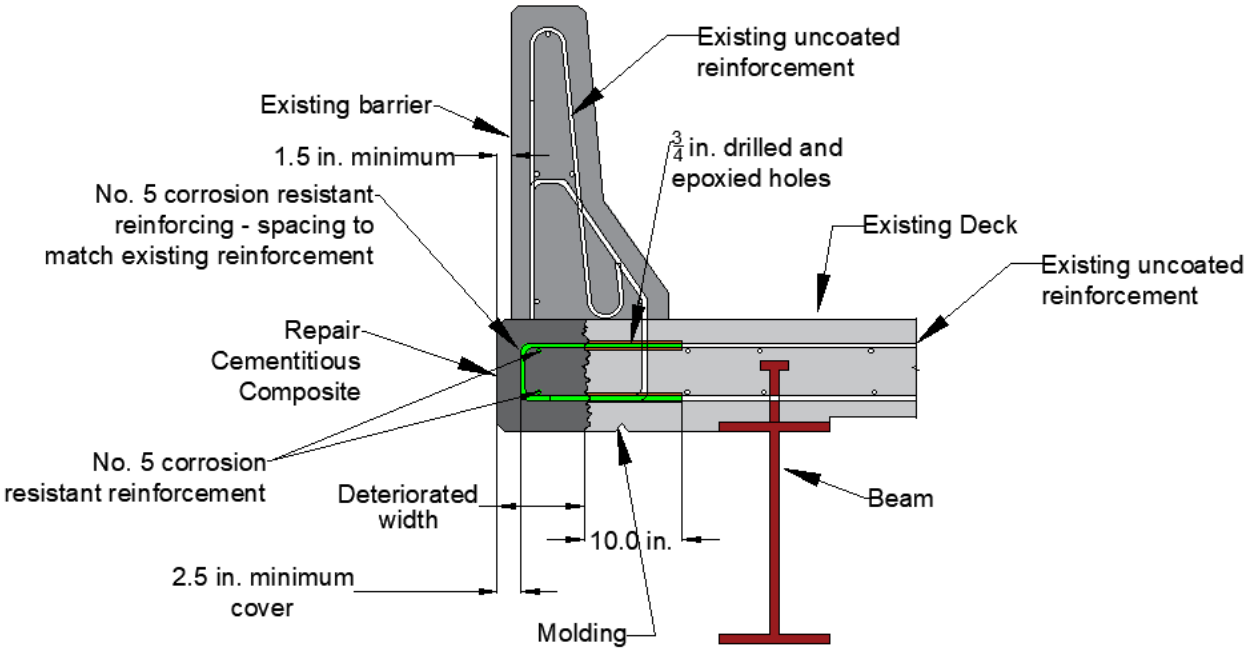

Fig. 8.5 Proposed repair detail

The following steps should be followed to implement the proposed repair detail.

Step 1: Scale the deteriorated deck fascia to remove all unsound concrete

Step 2: Cut all corroded reinforcement flush with the scaled deck fascia

Step 3: Drill and epoxy corrosion resistant dowels compliant with ASTM A615 (ASTM 2020). This includes several sub steps, which are outlined below.

- Drill ¾ in. diameter holes top and bottom at the same spacing as the existing deck reinforcement. The elevation of the holes should match that of existing top and bottom deck reinforcement. The horizontal offset should not be more than 2.0 in. The cut reinforcing steel can be used as a refence point to provide the 2 in. maximum horizontal offset. The ¾ in. diameter hole was determined as appropriate for No. 5 dowels. Consult

the epoxy mortar manufacturer's literature for hole sizes appropriate for smaller or larger dowels.

- Clean the holes using a steel brush followed by additional cleaning using a fabric towel. Finalize the cleaning using a vacuum pump. The first two steps may be eliminated if the vacuum pump is robust enough to provide a thorough cleaning
- Discharge the epoxy mortar using a nozzle extension. In the laboratory tests a Hilti epoxy mortar HY 200 R-V3 was used.
- Insert the epoxy coated dowels or other corrosion resistant dowels
- Allow the epoxy to cure. Follow manufacturer's recommendations for curing and working time.

Step 4: Install formwork for casting the repair concrete material. The details for this are left to the discretion of the contractor conducting the work. The provision of a sloping surface for discharging the repair concrete materials was found useful during laboratory testing.

Step 5: Discharge the repair cementitious material. It is recommended that fiber reinforced self-consolidating concrete be used for the repair due to its self-consolidating nature, sustained tensile strength after cracking, and good performance as suggested by small-scale and large-scale laboratory testing. The mix design used in laboratory testing is provided below. However, it is recommended that trial mixtures be prepared prior to placement of the repair concrete material to ensure that the desired plastic properties are obtained. This is due to the fact that FRSCC is rather sensitive to small changes in the high range water reducing admixture (HRWRA). As such, it is recommended that this ingredient be supplied incrementally to obtain the desired plastic properties. The specifications for the plastic and hardened properties of FRSCC are provided in Table 8.2.

Step 6: Remove the formwork no sooner than 24 hours.

Step 7: Moist cure the repair concrete for 7 days.

Table 8.1 Fiber reinforced self-consolidating concrete (FRSCC) mix design for repair of bridge deck fascias

Ingredient	Amount (lbs/yd^3 – unless otherwise noted)
Portland Cement (PC) (Type IL)	610
Fly Ash (Class F)	254
Fine Agg. (Type 2NS)	1367
Coarse Agg. (29A)	1252
Water	354
HRWRA (UltarFlo 2000)	7.39 oz/cwt (3.99 lbs/yd^3)
WRA (Optiflo 500)	-
VMA	0.40 oz/cwt (0.215 lbs/yd^3)
Air Ent. Ad. (Eucon AEA-92)	0.08 oz/cwt (0.042 lbs/yd^3)
Steel Fibers	131.1 (1 % by volume)
w/cm	0.41
Specific gravities were taken from a JMF supplied by MDOT for the mix #92MR-C and Job #128585 and Control section #09035 considering bulk-dry condition: PC=3.15; Fly-ash=2.59; Fine agg.= 2.60; Coarse agg.=2.56; Steel fiber=7.85; Admixtures=1.0 (assumed).	

Table 8.2 Specifications for the plastic properties of FRSCC

Concrete	**Metric**	**ASTM Reference**	**Value**
FRSCC	Plastic Properties		
	Slump Flow (in.)	C1611 (ASTM 2021)	22-26
	J-Ring Flow (in.)	C1621 (ASTM 2017)	17-26
	Passing Ability (in.)[1]	C1621 (ASTM 2017)	< 5.0
	VSI[2]	C1611 (ASTM 2021)	Between 1 and 2
	T_{50} & T_{50j} (sec)	C1611 (ASTM 2021)	<3.0 & <9
	Density (pcf)	C138 (ASTM 2023)	142-147
	Air Content (%)	C231 (ASTM 2022)	4-6
	Hardened Properties		
	f'_c (ksi)	C39 (ASTM 2021)	> 9 ksi
	f_t (ksi)[3]	C496 (ASTM 2017)	> 1 ksi
[1]Passing ability is the difference in between Slump flow and J-ring flow. [2]Based on Daczko and Kurtz (2001) for rating of SCC mixtures. [3]Tensile strength after cracking			

Chapter 9: Summary and Conclusions

Chapter 9: Summary and Conclusions

The objectives of this research project were to: 1) Identify the main cause of deck fascia deterioration; 2) Develop maintenance alternatives to scaling deck fascias; 3) Identify current design details contributing to fascia deterioration and develop corrective measures; 4) Develop best practices for long-term repair options of deteriorated fascias without removing the traffic barrier; and 5) Develop best practices in design, construction, and preventive maintenance to prevent deck fascia deterioration from occurring. The findings and conclusions are summarized based on each research objective as follows.

1) Identify the main cause of deck fascia deterioration

A literature review related to the deterioration of bridge deck fascias was conducted. A survey intended to determine the nation-wide current practice on the subject matter was prepared and distributed to all states. A total of 20 bridges were identified for field investigation. Twenty additional bridges were considered to expand the database considered for identifying trends and correlations pertaining to the deterioration of deck fascias. Field investigations and nondestructive testing were conducted on six bridges located in six regions in the lower peninsula. The non-destructive testing included half-cell potential measurements, concrete cover determination, moisture content tests, and rebound hammer tests. The causes of deck fascia deterioration as informed by the literature review, nationwide survey, and as determined by the examination of bridges that exhibited this phenomenon are summarized below:

1) Low Grade Concrete: The majority of the bridges that featured deteriorated deck fascias consisted of low-grade deck concrete with an f'_c=3000 psi at 28 days. This is below the ACI 318-19 (ACI 2019) requirements for concrete used in severe environments, which refer to a concrete with an f'_c= 5000 psi or greater. The current specification in Michigan, regarding deck concrete refer to a high performing mix with an f'_c = 4,500. This is a significant improvement from past practice. However, it is still 500 psi lower than that required by ACI 318-19 (ACI 2019). Since none of the investigated bridges contained deck concrete with f'_c = 4,500 psi, it is not clear whether this 500 psi difference is another cause for the deterioration of deck fascias. Naturally, a higher performing mix will lead to better future performance and longevity in terms of better durability

against freeze-thaw deterioration since permeability is reduced, better resistance to corrosion induced spalling since the tensile strength of concrete is higher, etc.

2) Increased Moisture Content: It was observed that a large number of bridges that featured deck fascia deterioration contained fencing, open barriers, and sidewalks. The presence of fencing results in an increased moisture content in the deck fascia due to moisture traveling down the deck fascia from the fencing. The open barriers and elevated sidewalks also lead to increased moisture content in the deck fascia. There was clear evidence of standing water near the barrier, or higher moisture content after a precipitation event for many of the bridges investigated in the field. Moisture content recorded during many of the field investigations was higher along the deck fascia compared to the rest of the deck surface. Efflorescence was noted in many of the field investigations, providing further evidence for higher moisture content along the deck fascia. Improved drainage is one option for reducing the moisture content along the deck fascia. Several approaches for how to reduce moisture content in the deck fascia were presented.

3) Corrosion of reinforcement: Almost all identified bridges with deteriorated deck fascias featured uncoated corroded deck reinforcement, and were built prior to the 1980 mandate to use corrosion resistant reinforcement. The 1980 mandate appears to have addressed the corrosion issue since only a few bridges with deteriorated facias contained corrosion resistant steel. For the investigated bridges, active corrosion was found through visual inspection, reinforcement section loss, and half-cell potential tests along the fascia as well as in the deck near the fascia region. Field investigations were conducted for a total of six bridges. In all bridges, half-cell potential measurements lower than -350 mV were recorded suggesting a 90% or higher probability of active corrosion in the area in question at the time of testing. Areas of highest corrosion activity were generally noted near the deck fascia. It is recommended that the practice of using epoxy coated reinforcement or other types of corrosion resistant reinforcement be continued.

4) Inconsistencies in concrete clear cover: For the investigated bridges, inconsistencies in clear cover were observed. Measured clear cover was in some locations smaller than what is recommended for concrete exposed to deicing salts in AASHTO LRFD (2020). In addition, for many of the investigated bridges, the recorded clear cover along the deck fascia was lower than

that recorded on the deck surface and lower than the minimum specified in AASHTO LRFD (2020). A lower than specified clear cover may accelerate the process of corrosion and shorten the life of the bridge. While all new bridge decks are constructed with epoxy coated reinforcement or corrosion resistant reinforcement, damages in the epoxy coating during construction combined with low clear cover may provide avenues for moisture and deicing chemicals to reach the surface of reinforcement and initiate the corrosion process. This can be resolved by ensuring that the specified clear cover is implemented and any damages to the epoxy coating are addressed.

5) Alkali-Silica-Reaction (ASR): The presence of ASR is considered likely based on field data. Broken concrete fragments were obtained from a total of six bridges. These samples were subjected to ASR testing using an ASR detection kit (Guthrie and Carey 1999). The kit is based on a geochemical method for staining various products of the alkali-silica reaction. This issue appears to have been addressed. In approximately 2012, MDOT implemented specifications to avoid ASR. Examples include:

- Special Provision for Alkali Silica Reactivity of Fine Aggregate Used in Portland Cement Concrete
- Special Provision for Quality Control and Acceptance of Portland Cement Concrete (For Local Agency Projects Only)
- Construction Specifications: Section 1003. Quality Assurance (Acceptance) for Concrete
- Construction Specifications: Section 902. Aggregates

The majority of bridges exhibiting deck fascia deterioration and considered as part of this research were constructed prior to the 1980s.

6) Slope of the Deck: The slope of the deck is a contributing factor to the deterioration of deck fascias. The lower side of the deck features typically higher deterioration.

7) Traffic Volume: Traffic volume on or below the bridge appears to be related to deck fascia deterioration (i.e. the higher the traffic the higher the deterioration). Most bridges with deteriorated fascias were located on or above an interstate/state highway.

2) Develop maintenance alternatives to scaling deck fascias

In addition to scaling unsound concrete, deck fascias with low to moderate deterioration may be protected against future deterioration by applying polyurea – a protective coating. The application of this coating requires specialized training. Additional information is provided in Chapter 8. The concept behind this maintenance alternative is that the polyurea coating serves as a reinforcement layer thus providing to the concrete what it needs the most – an ability to sustain tensile stresses that exceed its tensile strength. It should be noted that the application of polyurea may be used as a preventive maintenance technique in new bridges where the deck fascia may receive such coating.

3) Identify current design details contributing to fascia deterioration and develop corrective measures

It should be noted that most bridges which exhibited deck fascia deterioration were built prior to 1980, a period which reflects a different set of construction practices. As such, the deterioration of deck fascia may not be necessarily attributed to current practices but instead to past practices many of which have been corrected. Examples of such correction include:

a) The 1980 mandate for using epoxy coated reinforcement in bridge decks. Currently, deck and barrier reinforcement features epoxy coated bars or alternative corrosion resistant reinforcement. Therefore, reinforcement corrosion, a prevailing problem in the order bridges appears to have been addressed as virtually none of the bridges constructed after 1980 exhibited signs of corrosion;

b) The use of higher performing materials for deck and barrier concrete. Recall that in the past, deck and barrier concrete featured an f'_c=3,000 psi, whereas currently the specified concrete compressive strength is f'_c=4,500 psi. In addition, the current mix is labeled as high performance (HP) and additional specifications are put in place to ensure such high performance.

There was conceptual concern about the effectiveness of the elevated shear key used at the barrier to deck connection based on anecdotal evidence, which suggests that the key is constructed manually by creating a dam of concrete while it is still in its plastic state. The lack of forming for

this key raised concern about its effectiveness. A variety of details were presented in Chapter 8 where this key may be formed thus addressing these concerns.

4) Develop best practices for long-term repair options of deteriorated fascias without removing the traffic barrier

Evaluation

Before a repair is conducted, an evaluation must be made that justifies the intervention. The repair may be conducted because the level of deterioration in the deck fascia has reached the point where it undermines the crashworthiness of the barrier, to prevent further deterioration and provide a long-term repair option, or for aesthetic purposes. A computer program called MDOT Barrier was developed to evaluate barrier crashworthiness. This program allows the analyst to enter a deteriorated deck fascia length and width and determine whether the crashworthiness of the barrier has been undermined.

Repair

A deck fascia repair detail was proposed. It should be noted that the proposed repair detail features a repair cementitious material, which was tested for durability and its ability to restore the crashworthiness of the barrier using small-scale and large-scale testing. The repair detail also features corrosion resistant drilled and epoxied dowels. The guidance provided in the Special Provisions for Repair of Bridge Deck fascias as well as the recommendations presented in Chapter 8 should be followed. The recommendations for the repair detail were based on small-scale testing presented in Chapter 5 and the large-scale testing presented in Chapter 6. The evaluation of the proposed repair detail was conducted using the following metrics: 1) material characterization, 2) relative durability, 3) un-weathered reinforced interface shear strength, and 5) weathered reinforced interface shear strength. A total of four repair concrete materials were tested and include a: 1) Fiber Reinforced Concrete; 2) Latex Modified Concrete; 3) Self Consolidating Concrete; and 4) Fiber Reinforced Self Consolidating Concrete. The material characterization testing included testing for mechanical properties such as compressive strength, tensile strength, modulus of elasticity, and shrinkage. Plastic properties were also measured to characterize the plastic state of the repair concrete material. This is important because the repair concrete material should have good flowability and the capability to be placed in tight spaces. Measured plastic properties

included: slump, air content, temperature, and unit weight. Relative durability testing included freeze-thaw testing during which periodic measurements of the dynamic modulus, weight, and rebound hammer readings for each tested repair concrete material were taken. Small-scale testing was conducted to evaluate the interface shear strength of the repaired samples each featuring a different repair concrete material. In all cases, epoxy coated reinforcement was used. The following conclusions were drawn:

1. All repair concrete mixtures with the exception of the FRC mixture performed well. The FRC specimens started to disintegrate once the molds were removed and featured low compressive strength. This mix was removed from consideration.
2. The remaining three repair concrete materials, LMC, SCC, and FRSCC featured compressive strengths and tensile strengths that exceed those of the host material. The FRSCC mix featured the highest tensile strength followed by the SCC mix. The FRSCC mix exhibited an ability to sustain compressive and tensile loads after crack initiation suggesting an ability to retain broken concrete fragments-a key ability for a bridge deck fascia repair or for a new bridge if this mix is selected for the deck concrete.
3. The SCC and FRSCC featured self-consolidating properties and are good candidates for the repair of bridge deck fascias as they facilitate placement in tight spaces.
4. The LMC, SCC, and FRSCC showed good stability in terms of specimen mass and dynamic modulus of elasticity during freeze-thaw testing suggesting resilience against weathering.
5. The FRSCC and SCC mixtures showed virtually identical ultimate shrinkage strains. The LMC exhibited the lowest shrinkage strains. While a concrete mixture with low shrinkage is desired in terms of reducing the magnitude of differential shrinkage induced tensile stress, the ability of the concrete mixture to resist and sustain tensile stresses is considered of higher importance in terms of retaining broken concrete fragments that may form due to tensile stresses created as a result of other phenomena such as corrosion or freezing and thawing.
6. In summary, the FRSCC is deemed as the most appropriate mixture as it possesses self-consolidating properties, which facilitate placement, and good tensile strength. A second candidate is the SCC mixture, which offered the second highest tensile strength and facilitates placement in tight spaces. Although, once cracking occurs this mixture does not have the ability to retain broken concrete fragments.

A total of three full-scale sub-assemblage specimens featuring the best two performing repair concrete materials (FRSCC and SCC) as well as a control specimen were subject to proof-of-concept testing under monotonic loading where a pseudo-static lateral load was applied to the barrier to simulate vehicular impact. The purpose of these tests was to demonstrate that the repair details and repair materials are viable at full-scale as well as provide sufficient strength to resist required barrier loads. The latter is critical, as one of the main functions of the deck overhang is to provide sufficient support for the barrier in case of a vehicle impact. The following conclusions were drawn:

1. The proposed repair detail using both repair cementitious materials (FRSCC and SCC) was able to restore the crashworthiness of the barrier providing strength against vehicle impact that is greater than that required for a TL-4.
2. The repair specimen that featured FRSCC exhibited a load versus horizontal displacement relationship that was almost coincidental with the control specimen.
3. The repair specimen that featured FRSCC exhibited a stiffer response than that exhibited by the repair specimen that featured SCC.
4. FRSCC is the recommended Option 1 for repair as FRSCC provides sustained tensile strength after cracking, which is critical in terms of retaining broken fragments of deck fascia concrete from falling down.
5. The strain in the straight rebars in the deck fascia in the control specimen exceeded the yield strain suggesting that these rebars are capable of transferring forces despite their limited development length – this information may be used during barrier strength evaluation.
6. The existing cut top deck rebars in repaired specimens yielded, suggesting a successful load transfer during vehicle impact from the barrier to the deck.

5) Develop best practices in design, construction, and preventive maintenance to prevent deck fascia deterioration from occurring

The deterioration of bridge deck fascias appears to be largely unexamined. In general, moisture reduction, good quality concrete, corrosion resistant reinforcement, and appropriate construction practices appear to be the first line of defense for all concrete elements subject to severe

environmental effects. The recommendations presented herein are intended for new bridges. For the repair of existing bridges see item 4 above.

Design

Connection configuration: Specify one of the proposed barrier to deck connection details (Chapter 8), which are intended to reduce the moisture content in the deck fascia and increase its durability against weathering. Many of the proposed details were developed with the goal of reducing moisture content in the deck fascia. One was developed with the goal of reducing moisture content and increasing the durability of the deck fascia by specifying self-consolidating fiber reinforced concrete for a portion of the deck overhang. In fact, the use of fiber reinforced concrete or a higher performing concrete is recommended for all areas most vulnerable to deterioration. This includes deck fascias, and expansion joints. Engineers familiar with barrier and deck overhang replacement projects will recall that the replaced portions of the bridge are the areas near the expansion joints and deck overhangs. The use of fiber reinforced concrete is recommended due to its ability to supply sustained tensile strength after cracking thus keeping the fragments of concrete from falling down. This is not to say that the case of falling concrete is eliminated altogether because freeze-thaw deterioration can cause concrete to fall from the bottom of the deck as well. However, field evidence suggest that the most deteriorated areas are those near the expansion joints and deck fascias due to the increased moisture content. This of course would require the introduction of a vertical joint between the main deck portion and the deck fascias as well as another joint between the main deck and the concrete used near the expansion joints if the proposed approach is followed.

Mix design for the deck concrete: If the connection detail that does not feature FRSCC are pursued, either continue using the current specifications for deck concrete or consider further improving them such that $f'_c \geq 5{,}000$ psi while satisfying other durability related requirements to comply with ACI 318-19 (ACI 2019) for concrete subject to severe environments. However, freeze-thaw durability testing of concrete samples featuring the current MDOT mix design for deck concrete suggests that this mix performed very well thus not providing a reason for change. If the detail that features FRSCC is pursued, sample mix designs for the FRSCC are provided in this report in Chapter 8.

Deck Reinforcement: Continue specifying epoxy coated reinforcement or other corrosion resistant reinforcement for the deck and barrier concrete

Cover: Comply with minimum cover requirements specified in AASHTO LRFD (2020).

Vehicle impact: Ensure that the deck overhang and barrier are designed for vehicle impact. The MDOT Barrier program may be used for this purpose.

Construction

Ensure that the specified detail is constructed as intended and that concrete in the deck fascia region is consolidated properly thus ensuring low permeability.

Preventive Maintenance

Continue scaling deck fascia to remove unsound concrete. If the budget allows, consider applying polyurea as a protective coating to prevent further deterioration. This option should be used for bridges where deck fascia deterioration is low to moderate and analysis conducted using the MDOT Barrier program shows that the crashworthiness of the barrier has not been compromised.

References

Aaleti, S., Petersen, B., Sritharan, S. (2013). Design guide for precast UHPC waffle deck panel system, including connections (No. FHWA-HIF-13-032). United States. Federal Highway Administration.

ACI Committee 201. (2016). "*Guide to Durable Concrete"*, ACI PRC-201.2-16, American Concrete Institute, Farmington Hills, MI.

ACI Committee 228. (2013). "*Report on Nondestructive Test Methods for Evaluation of Concrete in Structures"*, ACI 228.2R-13, American Concrete Institute, Farmington Hills, MI.

ACI Committee 544 (2008), "Guide for Specifying, Proportioning, and Production of Fiber-Reinforced Concrete (ACI 544.3R-08)", Farmington Hills, Mich., American Concrete Institute.

Aktan, H., & Attanayake, U. (2004). *Causes and cures for cracking of concrete barriers* (No. Research Report RC-1448, CSD-2003-01). Wayne State University. College of Engineering.

American Association of State Highway and Transportation Officials (AASHTO). (2002). Standard specifications for highway bridges, 17th Ed., Washington, D.C.

American Association of State Highway and Transportation Officials (AASHTO). (2017). Load and resistance factor design (LRFD) bridge design specifications, 8th Ed., Washington, D.C.

American Association of State Highway and Transportation Officials (AASHTO). (2020). Load and resistance factor design (LRFD) bridge design specifications, 9th Ed., Washington, D.C.

American Concrete Institute (ACI). (2019). ACI 318-19: Building Code Requirements for Structural Concrete and Commentary; American Concrete Institute: Farmington Hills, MI, USA.

American Concrete Institute (ACI). (2004). Concrete Repair Guide. ACI 546R-04. American Concrete Institute, Farmington Hills, MI.

American Concrete Institute (ACI) PRC-237-07 (2007). Self-Consolidating Concrete. American Concrete Institute, Farmington Hills, MI.

Amleh, L., & Mirza, S. (1999). Corrosion influence on bond between steel and concrete. Structural Journal, 96(3), 415-423.

ASTM A615 / A615M-20. (2020). Standard Specification for Deformed and Plain Carbon-Steel Bars for Concrete Reinforcement, ASTM International, West Conshohocken, PA, 2020, www.astm.org

ASTM C39 / C39M-21. (2021). Standard Test Method for Compressive Strength of Cylindrical Concrete Specimens, ASTM International, West Conshohocken, PA, 2021, www.astm.org

ASTM C42 / C42M-20. (2020). Standard Test Method for Obtaining and Testing Drilled Cores and Sawed Beams of Concrete, ASTM International, West Conshohocken, PA, 2020, www.astm.org

ASTM C138/C138M-23. (2023). Standard Test Method for Density (Unit Weight), Yield, and Air Content (Gravimetric) of Concrete, ASTM International, West Conshohocken, PA, 2023, www.astm.org

ASTM C143/C143M-20. (2020). Standard Test Method for Slump of Hydraulic-Cement Concrete, ASTM International, West Conshohocken, PA, 2020, www.astm.org

ASTM C157/C157M-17. (2017). Standard Test Method for Length Change of Hardened Hydraulic-Cement Mortar and Concrete, ASTM International, West Conshohocken, PA, 2017, www.astm.org

ASTM C192/C192M-19. (2019). Standard Practice for Making and Curing Concrete Test Specimens in the Laboratory, ASTM International, West Conshohocken, PA, 2019, www.astm.org

ASTM C215-19. (2019). Standard Test Method for Fundamental Transverse, Longitudinal, and Torsional Resonant Frequencies of Concrete Specimens, ASTM International, West Conshohocken, PA, 2019, www.astm.org

ASTM C231/C231M-22. (2022). Standard Test Method for Air Content of Freshly Mixed Concrete by the Pressure Method, ASTM International, West Conshohocken, PA, 2022, www.astm.org

ASTM C496 / C496M-17. (2017). Standard Test Method for Splitting Tensile Strength of Cylindrical Concrete Specimens, ASTM International, West Conshohocken, PA, 2017, www.astm.org

ASTM C469/C469M-22. (2022). Standard Test Method for Static Modulus of Elasticity and Poisson's Ratio of Concrete in Compression, ASTM International, West Conshohocken, PA, 2022, www.astm.org

ASTM C666 / C666M-15. (2015). Standard Test Method for Resistance of Concrete to Rapid Freezing and Thawing, ASTM International, West Conshohocken, PA, 2015, www.astm.org

ASTM C805/C805M-18. (2018). Standard Test Method for Rebound Number of Hardened Concrete, ASTM International, West Conshohocken, PA, 2018, www.astm.org

ASTM C876-22b. (2022). Standard Test Method for Corrosion Potentials of Uncoated. Reinforcing Steel in Concrete, ASTM International, West Conshohocken, PA, 2022, www.astm.org

ASTM C1064/C1064M-17. (2017). Standard Test Method for Temperature of Freshly Mixed Hydraulic-Cement Concrete, ASTM International, West Conshohocken, PA, 2017, www.astm.org

ASTM C1611-21. (2021). Standard Test Method for Slump Flow of Self-Consolidating Concrete, ASTM International, West Conshohocken, PA, 2021, www.astm.org

ASTM C1621/C1621M-17. (2017). Standard Test Method for Passing Ability of Self-Consolidating Concrete by J-Ring, ASTM International, West Conshohocken, PA, 2017, www.astm.org

ASTM F2659-23. (2023). Standard Guide for Preliminary Evaluation of Comparative Moisture Condition of Concrete, Gypsum Cement and Other Floor Slabs and Screeds Using a Non-Destructive Electronic Moisture Meter, ASTM International, West Conshohocken, PA, 2018, www.astm.org

Araujo, D. D. L., Nunes, F. G. T., Toledo Filho, R. D., & Andrade, M. A. S. D. (2014). Shear strength of steel fiber-reinforced concrete beams.

Attanayaka, U., Ng, S. Y. C., & Aktan, H. (2002). *Criteria and benefits of penetrating sealants for concrete bridge decks*. Michigan Department of Transportation, Lansing, MI.

Attanayake, U., Liang, X., Ng, S., & Aktan, H. (2006). Penetrating sealants for concrete bridge decks—selection procedure. *Journal of Bridge Engineering*, *11*(5), 533-540.

Barker, R., & Puckett, J. (2013). Loads. *Design of highway bridges: An LRFD*.

Banthia, N., & Bindiganavile, V. (2001). Repairing with hybrid-fiber-reinforced concrete. *Concrete International*, *23*(6), 29-32.

Bazzo, J., Delatte, N., & Kalabon, A. (2013). *Uncontrolled concrete bridge parapet cracking* (No. FHWA/OH-2012/15). Ohio. Dept. of Transportation. Office of Research and Development.

Bertolini, L., Elsener, B., Pedeferri, P., Redaelli, E., & Polder, R. B. (2013). *Corrosion of steel in concrete: prevention, diagnosis, repair*. John Wiley & Sons.

Boatman, B. (2010). Epoxy coated rebar bridge decks: expected service life. *Michigan Department of Transportation, MI*.

Bush, A. J. (2008). *Concrete barrier distress in La Grande, Oregon* (No. OR-RD-08-09). Oregon. Dept. of Transportation. Research Unit.

Christodoulou, C., Goodier, C. I., Austin, S. A., Webb, J., & Glass, G. K. (2013). Long-term performance of surface impregnation of reinforced concrete structures with silane. *Construction and Building Materials*, *48*, 708-716.

Clear, K. C., & Chollar, B. H. (1978). *Styrene-butadiene latex modifiers for bridge deck overlay concrete. Washington DC, Department of Transportation*. FHWA-RD-78-35, p 117.

Daczko, J. A., & Kurtz, M. A. (2001). Development of high volume coarse aggregate self-compacting concrete. In *Proceedings of 2nd international RILEM symposium on self-compacting concrete, Tokyo* (pp. 403-412).

Davidson, J. S., Porter, J. R., Dinan, R. J., Hammons, M. I., & Connell, J. D. (2004). Explosive testing of polymer retrofit masonry walls. *Journal of Performance of Constructed Facilities*, *18*(2), 100-106.

Davidson, J. S., Fisher, J. W., Hammons, M. I., Porter, J. R., & Dinan, R. J. (2005). Failure mechanisms of polymer-reinforced concrete masonry walls subjected to blast. *Journal of Structural Engineering*, *131*(8), 1194-1205.

Deb, S. (2012). Accelerated short-term techniques to evaluate corrosion in reinforced concrete structures. *The Master Builder*, 248-255.

Deitz, D. H., Harik, I. E., Gesund, H., & Zatar, W. A. (2004). Barrier wall impact simulation of reinforced concrete decks with steel and glass fiber reinforced polymer bars. Journal of Composites for Construction, 8(4), 369-373.

Delatte, N. (Ed.). (2009). *Failure, distress and repair of concrete structures*. Elsevier.

ElBatanouny, M. K., Nadelman, E. I., Kurth, J. C., & SE, P. (2017). Use of polymer overlays or sealers on New Bridges. The Iowa Highway Research Board.

El-Hacha, R., Mirmiran, A., Cook, A., & Rizkalla, S. (2011). Effectiveness of surface-applied corrosion inhibitors for concrete bridges. *Journal of materials in civil engineering*, *23*(3), 271-280.

El-Tawil, S., Tai, Y-S., Belcher, J. A., Rogers, D. (2020), "Open-Recipe Ultrahigh 1161 Performance Concrete (UHPC): Busting the Cost Myth," Concrete International, American Concrete Institute, Farmington Hills, MI, June 2020, pp. 33-28. https://www.concrete.org/publications/getarticle.aspx?m=icap&pubID=51725915

Emmons, P. H. (1993) Concrete Repair and Maintenance Illustrated, R.S. Means

Fay, K. V. (2015). Guide to Concrete Repair. 2nd Edition. U.S. Department of the Interior Bureau of Reclamation Technical Service Center.

Federal Highway Administration (1998); Corrosion Protection – Concrete Bridges; Publication No. FHWA-RD-98-088; (no authors listed); http://www.fhwa.dot.gov/publications/research/infrastructure/structures/98088/index.cfm#toc.

Federal Highway Administration (2001); Long-Term Performance of Corrosion Inhibitors Used in Repair of Reinforced Concrete Bridge Components; Publication No. FHWA-RD-01-097; (no authors listed); https://www.fhwa.dot.gov/publications/research/infrastructure/pavements/ltpp/reports/01097/pdf/01097.pdf

Grace, N., & Jensen, E. (2012). *Investigating causes and determine repair needs to mitigate falling concrete from bridge decks* (No. RC-1567). Michigan. Dept. of Transportation. Office of Research and Best Practices.

Graybeal, B. (2014). Design and construction of field-cast UHPC connections (No. FHWA HRT-14-084; HRDI-40/10-14 (750) E). United States. Federal Highway Administration.

Guthrie Jr, G. D., & Carey, J. W. (1999). Geochemical method for identifying alkali-silica-reaction gel. *Transportation research record*, *1668*(1), 68-71.

Haber, Z. B., Graybeal, B. A. (2019). Advancing Bridge Repair and Preservation Using Ultra High-Performance Concrete, Aspire, Spring 2019.

Haber, Z. B., Munoz, J. F., De la Varga, I., Graybeal, B. A. (2018). Bond characterization of UHPC overlays for concrete bridge decks: Laboratory and field testing. Construction and Building Materials, 190, 1056-1068.

Howell, B., Hopwood, I. I., & Palle, S. (2015). *Evaluation of deterioration of structural concrete due to chloride intrusion and other damaging mechanisms* (No. KTC-14-03/SPR10-406-1F). Kentucky. Transportation Cabinet.

Islam, M. (2003). *Long-term performance of corrosion inhibitors used in repair of reinforced concrete bridge components*. FHWA-RD-01-097.

JSCE SF6 (1990) Method of test for shear strength of steel fiber reinforced concrete (SFRC). Japan Society of Civil Engineers, Tokyo

Johnson, K., Schultz, A. E., French, C., & Reneson, J. (2009). Crack and concrete deck sealant performance.

Kalabon, A. E. (2014). *Implementation and Field Testing of Improved Bridge Parapet Designs* (Doctoral dissertation, Cleveland State University).

Kamaitis, Z. (2006). Deterioration of bridge deck roadway members. Part I: site investigations. *The Baltic Journal of Road and Bridge Engineering*, *1*(4), 177-184.

Kassimi, F., El-Sayed, A. K., & Khayat, K. H. (2014). Performance of fiber-reinforced self-consolidating concrete for repair of reinforced concrete beams. *ACI Structural Journal*, *111*(6), 1277-1286.

Kerkhoff, B. (2007). *Effects of substances on concrete and guide to protective treatments*. Skokie, IL: Portland Cement Association.

Khayat, K. H., Kassimi, F., & Ghoddousi, P. (2014). Mixture design and testing of fiber-reinforced self-consolidating concrete. *ACI Materials Journal*, *111*(2), 143.

Khodayari, A., Mantawy, I. M., Azizinamini, A. (2021). Introducing a New Connection Detail for Connecting Prefabricated Barrier to Concrete Deck Using UHPC (No. TRBAM-21-03857).

King, P. L. (1993). *Waterproofing sealers for concrete structures* (No. FHWA-GA-93-8905). Georgia. Dept. of Transportation.

Knight, M. and Huddleston, J. (2016); Use of Thin Overlays on Tennessee Bridges; presentation; http://midcon2016.engr.wisc.edu/wp-uploads/2016/11/5-C-Knight.pdf

Kosmatka, M., & Wilson, S. (2016). Design and Control of Concrete Mixtures, Chapter 5: Aggregates for Concrete. *Portland Cement Association*.v

Lahdensivu, J. (2012). Durability properties and actual deterioration of Finnish concrete facades and balconies.

Lahdensivu, J., Mäkelä, H., Pirinen, P. (2013). Durability properties and deterioration of concrete balconies of inadequate frost resistance. International Journal of Sustainable Building Technology and Urban Development, 4(2), 160-169.

Liang, Y. C., Gallaher, B., & Xi, Y. (2014). *Evaluation of bridge deck sealers* (No. CDOT-2014-6). Colorado. Dept. of Transportation. Applied Research and Innovation Branch.

Liao, W. C., Chao, S. H., Park, S. Y., & Naaman, A. E. (2006). Self-Consolidating High Performance Fiber Reinforced Concrete (SCHPFRC)–Preliminary Investigation. *Report No. UMCEE 06*, *2*.

Maheu, J., Bakht, B. (1994). A new connection between concrete barrier walls and bridge decks. In Proceedings of the CSCE Annual Conference (Vol. 2, pp. 224-229).

Manning, D. G. (1995). Waterproofing membranes for concrete bridge decks (Vol. 220). Transportation Research Board, National Cooperative Highway Research Program, National Academies Press, Washington D.C.

Marusin, S. L. (1985). Repairs of Concrete Columns, Spandrels, and Balconies on a High-Rise Housing Complex in Chicago. Special Publication, 85, 157-174.

Matta, F., Nanni, A. (2009). Connection of concrete railing post and bridge deck with internal FRP reinforcement. Journal of Bridge Engineering, 14(1), 66-76.

Michigan Bridge Design Manual. (2020a). [Accessed March 2021], Michigan Department of Transportation, Lansing, MI.

MDOT. (2020b). Standard Specifications for Construction, The Michigan Department of Transportation, Lansing, Michigan.

MDOT. (2019). Bridge Design Guides, The Michigan Department of Transportation, Lansing, Michigan.

Miller, R., Delatte, N., Deshpande, A., Hartell, J. A., Mullins, S., & Karunaratne, E. (2020). *Evaluation of Maintenance Procedures for Bridge Spalling on Parapet Walls: Phase II-Final report* (No. FHWA/OH-2020-13).

Miller, R., Delatte, N., Deshpande, A., Hartell, J. A., Mullins, S., & Karunaratne, E. (2017). *Evaluation of Maintenance Procedures for Bridge Spalling on Parapet Walls-Final report* (No. FHWA/OH-2017-15).

Mirsayah, A. A., & Banthia, N. (2002). Shear strength of steel fiber-reinforced concrete. *Materials Journal*, *99*(5), 473-479.

Moen, C. D., & Sharp, S. R. (2016). Bond properties between concrete and corrosion-resistant reinforcing steels. ACI Structural Journal, 113(2), 383.

Morse, K. L. (2009). *Effectiveness of Concrete Deck Sealers and Laminates for Chloride Protection of New and In Situ Reinforced Bridge Decks in Illinois*. Illinois Department of Transportation, Bureau of Materials and Physical Research.

McMullen, K. F., & Zaghi, A. E. (2020). Experimental evaluation of full-scale corroded steel plate girders repaired with UHPC. *Journal of Bridge Engineering*, *25*(4), 04020011.

Occupational Safety and Health Administration (OSHA). (2017).

Oman, M. S. (2014). *Concrete Bridge Deck Crack Sealant Evaluation and Implementation* (No. MN/RC 2014-34).

Palle, S., & Hopwood II, T. (2006). Coatings, Sealants, and Fillers to Address Bridge Concrete Deterioration and Aesthetics-Phase 1.

Pfeifer, D. W., & Scali, M. J. (1981). Concrete sealers for protection of bridge structures. *NCHRP report*, (244).

Pincheira, J. A., & Dorshorst, M. A. (2005). *Evaluation of concrete deck and crack sealers*. Wisconsin Highway Research Program.

Russell, H. G. (2004). Concrete bridge deck performance (Vol. 333). Transportation Research Board, National Cooperative Highway Research Program, National Academies Press, Washington D.C.

Russell, H. G. (2012). Waterproofing membranes for concrete bridge decks (Vol. 425). Transportation Research Board, National Cooperative Highway Research Program, National Academies Press, Washington D.C.

Russell, H. G., Graybeal, B. A., & Russell, H. G. (2013). Ultra-high performance concrete: A state-of-the-art report for the bridge community (No. FHWA-HRT-13-060). United States. Federal Highway Administration. Office of Infrastructure Research and Development.

Safiuddin, M. (2017). Concrete damage in field conditions and protective sealer and coating systems. *Coatings*, *7*(7), 90.

Shahriari, V., Prabhakar, P., & Pincheira, J. A. (2021). *Evaluation of Roadway Concrete Barriers and Materials* (No. WHRP 0092-19-03).

Shearrer, A. J., Riding, K. A., & Peterman, R. J. (2015). Effects of Concrete Moisture on Polymer Overlay Bond Over New Concrete (No. K-TRAN: KSU-13-3). Kansas. Dept. of Transportation. Bureau of Materials & Research.

Smith, M. D. (1986). *Silane chemical protection of bridge decks* (No. FHWA/OK 86 (4)).

Sohanghpurwala, A. A., Scannell, W. T., & Hartt, W. H. (2002). *Repair and Rehabilitation of Bridge Components Containing Epoxy-Coated Reinforcement*. Transportation Research Board, National Research Council.

Staton, J. F., & Knauff, J. (2007). *Performance of Michigan's concrete barriers* (Vol. 1498). Michigan. Dept. of Transportation. Construction and Technology Division.

Susetyo, J. (2009). *Fibre reinforcement for shrinkage crack control in prestressed, precast segmental bridges* (Doctoral dissertation, University of Toronto).

Svensson, O., Fagerlund, G., Petersons, N. (1980). Repair of concrete balcony slabs. In advances in Concrete Slab Technology (pp. 649-662). Pergamon.

Tan, Y. (2019). Long term bond strength and chloride resistance of epoxy and concrete overlays.

Transportation Research Board. (1979). Durability of Concrete Bridge Decks. National Cooperative Highway Research Program Synthesis of Highway Practice 57, National Research Council, Washington D.C.

Trejo, D., Aguiniga, F., Buth, E. C., James, R. W., Keating, P. B. (2001). Pendulum impact tests on bridge deck sections. Rep. No. FHWA-01/1520, 1.

Vaysburd, A. M., & Emmons, P. H. (2000). How to make today's repairs durable for tomorrow—corrosion protection in concrete repair. *Construction and building materials*, *14*(4), 189-197.

Vaysburd, A. M., & Emmons, P. H. (2004). Corrosion inhibitors and other protective systems in concrete repair: concepts or misconcepts. *Cement and Concrete Composites*, *26*(3), 255-263.

Virmani, Y. P., & Clemena, G. G. (1998). *Corrosion protection: Concrete bridges* (No. FHWA-RD-98-088). United States. Federal Highway Administration.

Wenzlick, J. D. (2007). *Bridge deck concrete sealers* (No. OR07-009).

Zhang, R., Castel, A., & François, R. (2012). Concrete cracking due to chloride-induced reinforcement corrosion–influence of steel–concrete interface defects due to the 'top-bar effect'. *European Journal of Environmental and Civil Engineering*, *16*(3-4), 402-413.

Zmetra, K. M., McMullen, K. F., Zaghi, A. E., & Wille, K. (2017). Experimental study of UHPC repair for corrosion-damaged steel girder ends. *Journal of Bridge Engineering*, 22(8), 04017037

Appendix A: Survey Results – Part I

Deck Fascia Deterioration and Repair Questionnaire

Introduction

The following message was sent to the state DOTs together with the survey questions listed in the next page.

"The Michigan Department of Transportation (MDOT) needs your input to complete a research project in collaboration with Wayne State University. The main objectives of the project are to identify the primary cause of deck fascia deterioration and to develop design and maintenance strategies to address this issue. To help our team gain a better understanding of the current state of practice for preventive maintenance and repair of bridge deck fascias, we would greatly appreciate it if you could tell us about your State's experiences on this subject. In order to do so please respond to the survey questions listed below and attach any pertinent information that may be helpful."

This appendix provides the responses received from the state DOTs that responded to the survey.

Questions	
1. How prevalent or frequent is the deterioration of bridge deck fascias in your state? **2.** Have you conducted or sponsored research related to the deterioration of bridge deck fascias? If so, please provide a reference to the report, if possible, and indicate whether the results have been implemented. **3.** In your experience, what causes the deterioration of bridge deck fascias (e.g. freeze-thaw, corrosion, poor construction, poor drainage, etc.)? **4.** What reinforcement type do you use typically in bridge deck construction (i.e. uncoated steel, epoxy coated, or another type)? **5.** Are there any design details and notes that you follow during design to specifically prevent the deterioration of deck fascias? If so, please specify. **6.** Are there any special provisions that you follow during construction to specifically prevent the deterioration of deck fascias? If so, please specify. **7.** Are there any relevant specifications related to the mix design of deck concrete that your state uses to prevent the deterioration of bridge deck fascias (such as w/cm ratio, type of alternative cementitious materials, specified concrete compressive strength, air entrainment, etc.)? If so, please specify. **8.** Are there any preventive maintenance techniques that you follow to prevent the deterioration of bridge deck fascias? If so, please specify. **9.** Do you use protectants or sealants as a means to prevent the deterioration of deck fascias or prevent its exacerbation? If so, please specify type and frequency of application. **10.** How do you repair or address deteriorated bridge deck fascias? **11.** If you choose to remove the unsound concrete to prevent fall-off, which method do you choose to conduct the removal of concrete in bridge deck fascias? After removal of concrete do you apply a sealant and if so what type? **12.** If you choose to remove unsound concrete to prevent fall-off, is there a specific deterioration width in the horizontal transverse direction beyond which the removal of unsound concrete is stopped and alternative repair techniques are pursued? If so, please specify the width and the alternative repair technique.	
Alabama	
1	Very infrequent.
2	No
3	N/A
4	Uncoated
5	None
6	None
7	None
8	None
9	None
10	No issues with deterioration. We have had damaged fascias and repaired them by removing and replacing.
11	Mechanical removal.
12	None
Alaska	
1	Not common as we typically use precast prestressed decked bulb-tee girders with only 6” edge flange exposed. Steel bridges usually get precast deck panels, so CIP decks are not common due to our short construction season. As precast elements, they are higher strength with better quality control (steam curing is typical), so we don’t see deterioration issues as are common with CIP concrete.
2	No
3	For us, it would be poor construction, e.g., poor concrete due to haul distances, working late in season with cold weather, poor curing. Freeze-thaw is not a huge issue in Alaska, as things freeze and stay frozen throughout the winter (i.e., one cycle).
4	Decked bulb-tees use epoxy and for deck rehabs have used low carbon chromium (ASTM A1035 CM Grade 100). We would ideally use something other than epoxy coated if the price were to come down a little more.
5	No
6	No
7	No
8	No
9	No
10	If it occurred, we would probably specify a standard off-the-shelf high-strength cementitious patch material.

11	It would fall under the typical concrete removal spec is our Standard Specifications, shown below. A sealant is usually not required. **501-3.16 REMOVING CONCRETE.** Do not damage other portions of the structure remaining in place when removing concrete. Determine and delineate the extent of removal area. Outline the area with a 3/4-inch deep saw cut to form faces perpendicular to the surface prior to the removal of concrete. Do not cut or damage existing reinforcing steel or prestressing steel. During the course of removal, the Engineer may suspend removal or may require additional removal and outline saw cut. Use any combination of mechanical methods, water-blast cleaning, or abrasive-blast cleaning to remove coarse or broken concrete until a dense, uniform surface of concrete exposing solid coarse aggregate is obtained. When using mechanical methods for removal of concrete, meet the following: 1. Use impact tools weighing less than 15 lbs. 2. Operate impact tools at an angle less than 45 degrees relative to the surface of the concrete being removed. 3. Use hand tools such as hammers and chisels or small air chisels, water blast cleaning, or abrasive blast cleaning to remove final particles of unsound concrete. During the removal operation do not damage existing reinforcing steel, prestressing steel, or concrete to remain in place. Before applying the repair material, clean the surface according to ASTM D4258 within 24 hours of applying the repair material. Use water meeting the requirements of Subsection 712-2.01 for removal operations.
12	N/A
Arizona	
1	Not very prevalent but in the northern are of the state where plowing or deicing chemicals are used we have had older construction exhibit deterioration on the bridge deck fascias.
2	No
3	All of the above noted in the question. Older bridges with open rail bridge barrier with curb have exhibited deterioration on the deck fascia, where plows can deposit snow against the area and have snow remain for some time.
4	We use epoxy coated rebar in elevations above 3000 ft, where this is more prevalent.
5	No
6	No
7	No
8	No
9	No. However we do place seals on concrete barrier fascias in the higher elevations where dicing chemicals and plowing occur.
10	Patch or epoxy inject if deterioration is bad enough to be a concern.
11	We would apply a bonding agent and corrosion inhibitor coating to exposed reinforcement before patching.
12	No specific width
Delaware	
1	It is really dependent on the bridge drainage system configuration. We typically see more deterioration on bridges where scuppers are built into the concrete bridge railing/parapets. Sometimes there is sort of a “deflector shield” that will transport the water out away from the face of the bridge fascia through the scupper, but most times there isn’t such a feature and the roadway/bridge runoff travels through the scupper and down the bridge fascias. I would say except for a few bridges that have extensive deterioration along the fascia, the problem is typically minor in nature.
2	Delaware has not conducted or sponsored research related to this topic.
3	Poor drainage is the number one culprit.
4	Delaware predominantly uses epoxy coated. The bridges that typically have deterioration along the fascias are older and contain uncoated rebar

5	We have gotten away from incorporating scuppers or other drainage details that are problematic. We also use epoxy coated rebar which helps to protect against corrosion.
6	No
7	Nothing that is specific only to the bridge fascias.
8	Paint the concrete with an acrylic paint system.
9	We sometimes paint the outside face of the bridge railing and deck fascias.
10	Depends on the magnitude of the problem and size of the bridge. If the deterioration is such that the connection of the bridge railing/parapet to the deck is questionable, then a full deck replacement may be utilized if there are issues with the overall deck. If the overall deck is in fairly good shape, we may just remove and replace a 4'-6' strip along the fascia which includes the bridge rail and the supporting deck. If the bridge is a much smaller structure, such as a 25' concrete slab bridge, we would remove the deteriorated concrete back until sound concrete is reached – this is usually in the 8"-15" range. We would then tie in some new rebar to the existing bridge railing (if we're able to keep the existing rail) or to tie into a rebuilt bridge rail. If the deterioration is such that concrete is starting to fall off/spall and it could fall over traffic or areas of pedestrian activity, we will have inspectors remove during the routine inspection. This is a temporary activity until a permanent repair can be made.
11	Refer to question above for the first part of this question. We don't typically apply a sealant.
12	No specific width.
Kansas	
1	We haven't quantified it. Not uncommon, perhaps 10%-20% of span bridges have some.
2	No
3	Drainage over the side combined with insufficient cover. Exacerbated by lack of control of cover during construction.
4	Currently- epoxy. Most trouble is with older bridges with black steel.
5	We've added an inch of cover to the exterior soffit of girder bridges. Increased bottom cover to 1.5" on all bridges.
6	No
7	No
8	No
9	No
10	On girder bridges - remove and repair to original lines. On structural slab bridge with deeper slabs and where the very bottom corner bar is not critical - remove and reform to neat lines.
11	Hand tools, no sealant-typically
12	This is on a case by case basis
Louisiana	
1	I haven't seen such deterioration.
2	Not to my knowledge.
3	I have no experience to share on this.
4	Uncoated steel is used in the majority of our inventory. Epoxy coated steel is in many existing bridges in the north part of the state, but we no longer specify epoxy coated steel for bridges.
5	We occasionally specify water stops for bridge railing/barrier openings located between expansion joints, but this is done to prevent staining.
6	None that I am aware of.
7	None that I am aware of.
8	None that I am aware of.
9	Our deck fascia receives a Class 3 finish (coating), which protects against the growth of mildew, fungus, algae, etc.
10	Not applicable.
11	Not applicable.
12	Not applicable.
Maryland	
1	This is an uncommon issue in Maryland on our modern bridges, but older bridges built before 1960 we have seen some issues. Many have deterioration of deck facia due to water and chemical intrusion at the deck-to-barrier interface (see example picture 1). Other in-service bridges include those with spill through scuppers that have deck facia and soffit defects at the scuppers due to prolonged water and chemical exposure and fiberglass scupper defects. We also have similar issues for older in-service bridges that were originally constructed with curbs. These

	bridges have been paved to the point the curb is no longer a curb but a means to retain the HMA (see example picture 2).   Picture 1 Picture 2
2	No research has been conducted.
3	Drainage (ponding and debris accumulation); water and chemical intrusion at the deck-to-barrier interface
4	Epoxy coated reinforcement since late 1970s; older decks have uncoated reinforcements
5	None to report
6	None to report
7	None to report; typically 4,500 psi concrete is used for bridge decks.
8	We request district maintenance to remove debris from the curb/barrier lines and address ponding. This is simply an effort to prevent deterioration of the barrier joint and intrusion.
9	None
10	For bridges with these defects, repairs would include localized repairs or even a complete repair or replacement of the facia, curb or barrier. For localized areas, the deteriorated concrete is removed, the existing rebar is cleaned and coated with epoxy, and new concrete is cast. For bridges with more extensive defects or concerns with the impact resistance of the barrier, we would perform the same repair as mentioned previously but may also include a barrier or curb replacement. In addition, we would also pursue a deck condition survey to evaluate the chloride contamination in deck – particularly near the edge of the barrier or curb. If the chloride contamination, soffit, and deck deterioration is too great, we would consider installing precast barrier in the shoulder areas and program the bridge for either a deck replacement or total replacement.
11	Concrete would be removed with hand-held pneumatic chipping hammers for localized areas. For greater quantities, the contractor would use either hand-held pneumatic chipping hammers or hoe ram. However, we do not specify the means and methods in our construction contracts and the tools are decided by the contractor.
12	For localized repairs, we typically specify the removal to be limited to sound concrete. As a design and then preconstruction activity, both the engineer, inspector, and contractor would sound the area in question to determine approximate limits. These approximate limits help to determine the cost, MOT needs, design considerations, and public impacts. For bridges with more extensive defects, we would sound the areas and likely also perform a deck condition survey. These activities are an attempt to determine the limits of removal, design parameters, impacts, and program determination (i.e. permanent repairs, holding actions, deck replacement, or total replacement).
Minnesota	
1	This is fairly common for several situations: 1) 40+ year old decks with one line concrete barriers that allowed chlorides to leach over the coping and overhang; 2) Bridges with sidewalks and fencing that allowed chlorides to drain over the coping for example on chain link fence; 3) Twin bridges with a barrier separating the decks that allows chlorides in gap between barriers and at expansion joints; 4) Bridges parallel to each other with wider gap between barriers that chlorides are plowed onto the coping/beam area; 5) Bridges with poor quality construction copings/overhangs with poor consolidation or cover that causes premature deterioration.
2	No research. We generally know what causes so we try to prevent situations.
3	Increased exposure to chlorides from examples 1-4 in first question that causes corrosion. Poor construction cover/consolidation.
4	Current standard is epoxy coated rebar to typical bridges. Expensive/critical bridges will use stainless steel.
5	We detail a drip strip on the bottom of all overhangs to prevent water from leaching underside of overhang.

6	No
7	We don't design our deck mixes to specifically address overhang/coping issues. Our main focus is reducing deck cracking as much as possible.
8	No. We flush the bearing areas, strip seals glands and steel painted beams but nothing on overhang.
9	We paint all copings/overhangs with a concrete special surface finish that has protective qualities. Main reason is aesthetic, but products have some chloride permeability and silane properties. See link for APL.
10	For repair projects, we routinely do shotcrete on delaminated/spalled areas on substructure and overhangs. If overhangs are in poor condition, occasionally we will recast overhang.
11	Delaminated areas are chipped away by bridge maintenance crews with impact hammers. No sealant is applied.
12	No. Whatever width needs to be removed is done by chipping.
Missouri	
1	It is prevalent on older structures with curb outlets.
2	No
3	Mostly freeze-thaw and corrosion on structures with curb outlets.
4	New decks are typically epoxy coated. Old decks may be uncoated. We plan to use more Galvabar in the future.
5	New decks now have slab drains the drop drainage below the bottom of the exterior girders.
6	We just use slab drains now.
7	Section 501 of our Specification Book. (Link)
8	On rehabilitations we often do protective coatings after removing delaminated concrete.
9	Yes. Typically, only when a structure is being rehabilitated.
10	In some instances, we replace the slab cantilever. (Link)
11	Typically, removal of unsound concrete is with hand tools and the surface is sand blasted and coated with epoxy protective coating.
12	See Standard Specification Section 704. (Link) 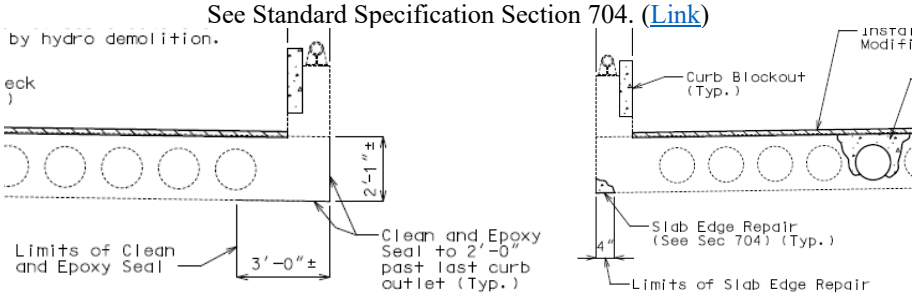
Montana	
1	Deck cracking is fairly common, which leads to deterioration of deck fascias. But we have not specifically noticed any significant problem with deck fascia deterioration in particular.
2	No
3	Deck cracking, corrosion, poor drainage, anti-icing chemical usage on the roadway.
4	Epoxy coated or corrosion resistant high chromium rebar.
5	No
6	No
7	No
8	No
9	No
10	Usually a full depth deck repair.
11	Full depth deck repair using typical removal methods (sawcut perimeter, lightweight jackhammer to remove unsound concrete, clean and prepare surfaces, place new low shrink concrete).
12	No
New York	
1	Frequent in older (30 to 40+ year) structures where the fascia is exposed to roadway runoff or salt spray. However, this specific type of deterioration is not currently tracked on a state-wide level.
2	Not aware of any research specifically addressing fascia deterioration in NYS.

<table>
<tr><td>3</td><td>The predominant cause of fascia deterioration is the exposure to chloride laden water from the roadway. Curbless details allowing roadway runoff to drain over the fascia is a major cause of deterioration. Lack of drip edge in older bridges also contributes to this deterioration.</td></tr>
<tr><td>4</td><td>NYSDOT policy is to use reinforcement having corrosion protection of epoxy-coating or better in bridge decks. Dual-coated, galvanized, chromium alloyed, and stainless-steel are options available for use. Stainless-steel deck reinforcement is used for high traffic volume applications. Uncoated rebar was used in older bridges, this is no longer the practice.</td></tr>
<tr><td>5</td><td>The use of curbs or barrier to prevent roadway runoff from reaching the fascia. Curb or barrier is required on NHS roadway bridges, bridges over railroads and recommended for all other bridges.</td></tr>
<tr><td>6</td><td>No special provisions. Maintaining specified cover and the repair of rebar coatings if damaged during handling is required.</td></tr>
<tr><td>7</td><td>NYSDOT Typical Deck Concrete Mixture
<table>
<tr><th>Concrete Class</th><th>T.C.M.5 Content (lb/cy)</th><th>Sand % Total Agg. (solid volume)</th><th>Water/ cementitious mat’ls (by weight)</th><th>Air Content % desired (Range)</th><th>Slump Range (in)</th><th>Type of Coarse Aggregate Gradation</th><th>Primary Use</th></tr>
<tr><td>HP</td><td>675</td><td>40.0</td><td>0.40</td><td>6.5 (5.0 - 8.0)</td><td>3 - 5</td><td>CA 2</td><td>pumping, structural slabs, approach slabs, substructures exposed to chlorides</td></tr>
</table>
Note: Class HP require the replacement of portland cement with 20% pozzolan and 6% microsilica and the addition of a water reducing admixture and / or water- reducing and retarding admixture.</td></tr>
<tr><td>8</td><td>Maintenance techniques vary state-wide. Bridge washing and protective sealing are used to some extent to prevent deterioration.</td></tr>
<tr><td>9</td><td>On new bridge decks, a protective penetrating silane sealer is specified for the top surface of the deck and wrapping around the fascia to the drip groove on the underside. Some Regional Offices apply protective sealer at regular intervals after construction.</td></tr>
<tr><td>10</td><td>Typical repair would include sound entire fascia, remove and repair deteriorated concrete as needed. During removal, any existing rebar that is corroded is sandblasted if there is minimal section loss. If there is significant section loss to existing bar, a new bar is added. Inspect anchorages for railing posts, remove and replace if necessary.</td></tr>
<tr><td>11</td><td>Sound entire fascia to map out unsound concrete. Use chipping hammers and light weight jackhammers to remove deteriorated concrete. Once repairs are done apply protective sealer.</td></tr>
<tr><td>12</td><td>For typical composite steel girders, if removal beyond the first row of stud shear connectors is expected, alternate repair (including analysis of the overhang if necessary) is recommended.</td></tr>
<tr><td colspan="2">North Carolina</td></tr>
<tr><td>1</td><td>Not frequent</td></tr>
<tr><td>2</td><td>No</td></tr>
<tr><td>3</td><td>NA</td></tr>
<tr><td>4</td><td>Epoxy coated steel in top mat and uncoated steel in bottom mat</td></tr>
<tr><td>5</td><td>No</td></tr>
<tr><td>6</td><td>No</td></tr>
<tr><td>7</td><td>No</td></tr>
<tr><td>8</td><td>No</td></tr>
<tr><td>9</td><td>Not specifically, it is included when applying sealant to deck and barrier rail.</td></tr>
<tr><td>10</td><td>Not standard practice; dependent on situation</td></tr>
<tr><td>11</td><td>Saw-cut concrete 2 inches beyond unsound concrete. If steel is exposed, remove concrete 1 inch beyond. Replace with shotcrete and smooth to match existing surrounding surface.</td></tr>
<tr><td>12</td><td>Dependent on the situation</td></tr>
<tr><td colspan="2">Oklahoma</td></tr>
<tr><td>1</td><td>The fascia on our more recent bridge decks is holding up really well. When we put epoxy reinforcing steel in the top layer only, we had trouble with corrosion on the south sides of bridges (at least in NW OK) where the parapet cast piled snow in shadow, slowing the melting process.</td></tr>
<tr><td>2</td><td>No</td></tr>
</table>

3	Corrosion appears to be the main cause of deterioration in our State especially for uncoated reinforcing steel (black steel).
4	Epoxy steel for On-System bridges and black steel for Off-System bridges.
5	Yes. In order to ensure drainage, we typically put our bridges on a vertical curve.
6	None at this time.
7	Reference is made to the Oklahoma Department of Transportation 2019 Standard Specifications Section 701, Class AA concrete link. Refer to Table 701:1 Concrete Classes.

Table 701:1 Concrete Classes

Class of Concrete	Minimum Cement Content, *lb/yd³ [kg/m³]*	Air Content, *%*	Water/Cement Ratio[a], *lb/lb [kg/kg]*	Slump[b], *in [mm]*	Minimum 28-day Compressive Strength[c], *psi [MPa]*
AA	564 [335]	6.5 ±1.5	0.25 – 0.44	2 ±1 [50 ±25]	4,000 [27.6]
A	517 [307]	6 ±1.5	0.25 – 0.48	2 ±1 [50 ±25]	3,000 [20.7]
AP	470 [279]	6 ±1.5	0.25 – 0.48	2 ±1 [50 ±25]	3,000 [20.7]
C	395 [234]	6 ±1.5	0.25 – 0.62	3 ±1 [75 ±25]	2,400 [16.5]
P	564 [335]	5 ±1.5	0.25 – 0.44	3 ±1 [75 ±25]	As required by the Contract

8	We use 2 ½" of cover and epoxy reinforcing steel. The summer after a bridge is constructed, we seal the cracks and apply silane sealers to the bridge deck.
9	Yes. We typically apply a silane or siloxane sealant the summer after construction in a District wide secondary project. This is a one-time application and in our environment, research indicates that it will last 12 years or more.
10	Usually with deck patching and/or overlays (latex overlay, thin bonded polymer overlays, etc.)
11	Removal is typically done with hammers, but we provide adequate traffic control to ensure the safety of the driving public. We do not apply sealants after we remove the concrete.
12	No
Pennsylvania	
1	Somewhat "Frequent". The deterioration degree varies in each of our eleven Engineering Districts.
2	No research has been conducted by PennDOT regarding bridge deck fascia deterioration.
3	Poor construction practices, anti-icing chemicals, and poor drainage (i.e. no deck curbing allowing water to flow freely over the fascia face of the concrete bridge deck). Also cracking in the deck overhang allows water to penetrate through the crack to the underside of the deck overhang.
4	The majority of PennDOT bridge deck reinforcement is epoxy coated. PennDOT does utilize some galvanized deck reinforcement.
5	A drip notch is provided to prevent water from wicking along the deck overhang. Additionally the underside of the deck overhang is constructed on a slope.
6	No
7	Yes. PennDOT does specify minimum deck compressive strength, W/C ratios, and maximum / minimum air entrainment for bridge decks. PennDOT Publication 408.

Class of Concrete	Use	Cement Factor[2][4] (lbs./cu. yd.)		Maximum Water Cement Ratio[6] (lbs./lbs.)	Minimum Mix[1,7] Design Compressive Strength (psi)				28-Day Structural Design Compressive Strength (psi)
					Days				
		Min.	Max.		3	7	28[8]	56[8]	
AAAP	Bridge Deck	560	640	0.45	—	3,000	4,000	—	4,000
AAA[3]	Other	634	752	0.43	—	3,600	4,500	—	4,000
AAAP LW	Bridge Deck	600	730	0.45	---	3,000	4,000	---	4,000
AA	Slip Form Paving	587	752	0.47	—	3,000	3,750	—	3,500
AA	Paving	587	752	0.47	—	3,000	3,750	—	3,500
AA	Accelerated[5]	587	800	0.47	—	—	3,750	—	3,500
AA	Structures and Misc.	587	752	0.47	—	3,000	3,750	—	3,500
AA LW		587	752	0.47	---	3,000	3,750	---	3,000
ASC[9]		587	846	0.47	---	---	4,000	---	4,000
A		564	752	0.50	—	2,750	3,300	—	3,000
C		394	658	0.66	—	1,500	2,000	—	2,000
HES		752	846	0.40	3,000	—	3,750	—	3,500

8	Proper vibration of the concrete deck to eliminate or reduce honeycombing and voiding of the deck fascia face concrete. Installation of curbing or parapet barrier to eliminate water or anti-icing chemical exposure to the fascia deck face. Install Protective Coatings in accordance with PennDOT Publication 408, Section 1019 – Protective Coatings for Reinforced Concrete Surfaces.
9	We do not apply a sealer to the underside of the deck fascia overhang. We do apply sealers to the top of the deck. PennDOT specifications for the following items are available in PennDOT Publication 408; Section 704 – Cement Concrete, Section 706 – Concrete Bonding Agents, Section 1019 – Protective Coatings for Reinforced Concrete Surfaces, Section 1040 – Concrete Bridge Deck Repair, and Section 1045 – Protective Coating for Concrete Surfaces. (Please see PennDOT Publication 408 – Highway Construction Specifications).
10	Apply concrete bonding agents (epoxy, cementious patching materials (Set-45, Pavement VR, etc.), partial deck slab replacements.
11	Physical hammering of unsound material. Yes, please see previous answer.
12	Yes. If the unsound fascia concrete affects, extends or penetrates the reinforced concrete bridge barrier system or parapet; or if the unsound concrete is past the first longitudinal deck reinforcement bar from the deck fascia vertical face, removal of the unsound concrete through partial deck replacement is applicable. For the alternative repair technique, partial deck slab or strip replacements is suggested.
South Carolina	
1	No significant frequency
2	No
3	No experience with this issue
4	Uncoated steel
5	Nothing other than 2” clear concrete cover. Most of our issues are with tops or bottoms of decks depending on environment.
6	No
7	No
8	No
9	Not as a typical practice
10	No specific procedures
11	No specific procedures for fascias
12	No specific procedures for fascias
Washington	
1	Infrequent, to the point of being almost non-existent
2	No research conducted
3	We have almost no deterioration in our deck fascias.
4	Epoxy coated, both top and bottom mats and the barrier bars.
5	We use drip groves (two of them) at our fascias to help prevent water from running fully underneath the overhang. Here is a typical detail: 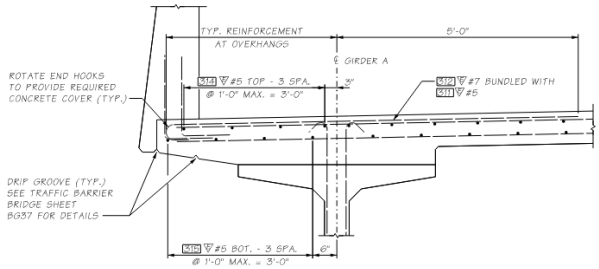 BRIDGE DECK REINFORCEMENT SECTION AT OVERHANG
6	No
7	Not really. We do use a performance-based concrete mix design, but it was implemented to address deck cracking. Even prior to introducing this mix, our deck fascias were never a problem.
8	No, nothing specific.
9	No, not specifically. Occasionally we will seal decks with methyl methacrylate, silane sealer or similar, but this is done for deck issues, not fascia issues.
10	We have not had to repair deck fascias.

11	N/A
12	N/A
West Virginia	
1	Not very prevalent.
2	No research has been conducted.
3	Chlorides and efflorescence leaking from joints in parapets above.
4	Epoxy coated reinforcing.
5	No
6	No
7	We have specified Class H Concrete for our bridge decks over the last decade.
8	We have washed, cleaned, and sealed our bridge decks as preventative maintenance as time and resources have allowed.
9	Linseed oil, epoxy-based sealant, and crystalline sealant have all been used in the past to seal bridge decks. Frequency of application has varied based on product being used and resources available.
10	Remove any/all unsound concrete, clean exposed reinforcing, install additional reinforcing if necessary, and perform concrete repair.
11	Removal is normally accomplished with a hammer, chisel, or jackhammer based on the size and quantity of removal. We have not applied a sealant after removal, but it would be a good idea to do so.
12	Determined on a case-by-case basis by thickness in addition to width and depth.
Wisconsin	
1	On bridges that utilize open railing systems, edge of deck/fascia deterioration is very prevalent. The frequency that fascia deterioration occurs with open railings above depends on the reinforcing steel detailing that was used (i.e., age of deck, black steel vs. epoxy coated, location of rebar with respect to drip grooves, etc.).
2	No
3	All of the items listed can contribute to the deterioration of edges of decks. Additionally, lack of clear cover to the reinforcing steel exacerbates the situation.
4	On current decks, we utilize epoxy coated reinforcing steel for both the top and bottom mats of rebar. Historically, depending on the vintage, we've utilized ECR top/black steel on bottom or all black steel.
5	We've done some outreach with designers to try to locate the bottom mat rebar as far away from drip grooves as possible to alleviate the lack of concrete cover issue at the edge of deck. Our Standard 17.02 (Link) shows the drip groove located 5" from the edge of deck, which should end up being located between the first and second bar above. That being said, this location can/should be modified by the EOR for project specific locations. Additionally, we have created a Standard Detail 17.03 (Link) which shows a flashing member included to try to prevent this edge of deck deterioration. These details are used based on the preference of the Region office and locals in the area of the bridges in question as some areas prefer this detail and others don't want it because it can become something else to inspect/maintain over the life of the bridge.
6	No
7	No
8	See response to question 5 above.
9	Yes. WisDOT projects utilize "Protective Surface Treatment" at the exterior edges of our decks in addition to what was referenced in the response to question 5 above. This PST can be seen in the details on the right side of Standard 17.02 (Link) and the bid item specifications can be found in Standard Spec 502.3.13.2 (Link).
10	The repair depends on the severity of the spalling. Concrete surface repairs, repairs using mechanical connections, addition of flashing, and potentially removing/repouring edges of deck are common occurrences to repair these issues.
11	The removal methods aren't dictated by the Department to the contractor unless full edge of deck removal/replacement is required. To simply remove unsound concrete, contractors typically use hand chippers for the removal methods. Typically, if removals are completed, we will then reform the edge of deck and use some type of positive, mechanical connection to engage the patch material.
12	No, these decisions are on a case-by-case basis.

Appendix B: Survey Results – Part II

Introduction

Several barrier to deck connection details were identified as promising in terms of reducing the moisture content along the bridge deck fascia. These details were identified from bridge design manuals and other resources posted by the state DOTs. Staff from the state DOTs who responded to the first phase of the survey, were contacted to obtain additional information in terms of how the identified details were constructed and how they performed. The messages sent to the selected state DOTs are provided below together with the responses.

Minnesota DOT Feedback

The following message was sent to Minnesota DOT staff:

"Thanks for responding to the survey on the deterioration of bridge deck fascias. We have identified the following detail as a promising detail from MnDOT in terms of reducing the moisture content along the bridge deck fascia. The detail features a sloped top deck surface. We believe that enhanced moisture content combined with freezing and thawing in the winter is one of the reasons for the deterioration of bridge deck fascias. The sloped deck surface as shown in the detail below could be an efficient mechanism for reducing moisture content along the deck fascia. We are interested in learning from your experience with this detail especially in terms of its constructability. If you could respond to the following questions we would greatly appreciate it."

Responses are provided in blue below.

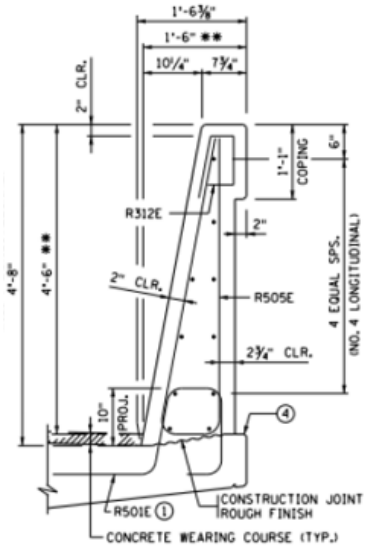

Fig. 1 Barrier to deck connection intended to reduce moisture migration from the deck to the fascia using a **sloped top deck surface**

Question 1: Do you specify any limits on slump to ensure that such a sloped top deck surface could be constructed?

The standard spec calls for 2 to 5 inches of slump for deck concrete. No specific slump is used for the sloped top deck surface under the barrier.

The primary requirements for Bridge Deck Concrete Mix are shown in the table below:

Table
2401.2-4
High Performance Bridge Deck Concrete Mix Design Requirements

Concrete Grade	Mix Number*	Intended Use	W/C Ratio	Target Air Content	Maximum percent SCM (Fly Ash/Slag/ Silica Fume/ Ternary) ‖	Slump Range†, inches	Minimum Compressive Strength, f'c (28 Calendar Day)	3137, "Coarse Aggregate for Portland Cement Concrete"
HPC	3YHPC-M	Bridge Deck – Monolithic	0.42-0.45	6.5 percent	30/35/5/40	2 - 5	4000 psi	2.D.2
	3YHPC-S	Bridge – Structural Slab						

* Provide a Job Mix Formula in accordance with 2401.2K.8, "Job Mix Formula." Use any good standard practice to develop a job mix formula and gradation working range by using procedures such as but not limited to 8-18, 8-20 gradation control, Shilstone process, FHWA 0.45 power chart, or any other performance related gradation control to produce a workable and pumpable concrete mixture meeting all the requirements of the Contract.
‖ The individual limits of each SCM shall apply to ternary mixtures.
† Keep the consistency of the concrete uniform during entire placement.

Question 2: A rough finish is specified in this detail. How is this rough finish constructed provided that there is barrier reinforcement present when the deck concrete is placed?

Essentially by hand with the concrete staying more or less the way it was placed without excessive working to make it too flat, the aggregate provides the rough surface. Generally done by the person who is finishing the gutters on the deck (smooth area in front of barriers). Here is the relevant section from our Specification Section 2401:

F.3.c(6) Bridge Slab Finish Under Curbs, Concrete Barriers, Sidewalks, and Medians

Float the top surface of the Bridge Slab under curbs, concrete barriers, Sidewalks, and narrow medians producing a rough surface with the coarse Aggregate embedded in mortar. Provide a smooth finished strip 2 inches wide at the edge of the slab and under the Roadway face of curbs, concrete barriers, Sidewalks, and narrow medians.

Question 3: In general, how do the contractors construct such a sloped deck surface and have they encountered any difficulties? Any photographs that may illustrate this would be very helpful.

As noted above finisher working on gutter area will usually do this and creates an approximate slope by hand in between the bars. How the concrete is initially placed can help too. There has been no significant negative feedback from contractors on this.

I have had a hard time finding any photos of this specific operation, but have included the one below. I have also put out a request for pictures to some of our Construction personnel and will follow up if I receive anything that shows this better.

The worker on the far right (circled) is doing finishing along the gutter line of a median and this would be similar to how it would be done at a barrier. Depending on how the contractor wants to work, equipment they are using etc. this could be anyone following behind the main finishing operation on a work bridge etc.

Question 4: It appears that the bottom of the deck overhang is also sloped away from the deck fascia. What is the reason for this? Is it done to reduce moisture content along the deck fascia? Have you noticed any deterioration in the fascia beam since the moisture at the bottom of the deck may travel towards the fascia beam?

This detail is not intended to keep moisture away from the deck fascia. Although it is not shown very clearly in the detail above, there is a drip strip /drip cap cast into the bottom of the overhang that intercepts runoff and acts as a barrier that prevents water from running along the bottom of the deck to the beam. Basically, just a strip tacked onto the forms to create a v shaped groove in the concrete. This has been very effective and runoff from the deck is not usually a significant source of deterioration in the fascia beam. See photo below.

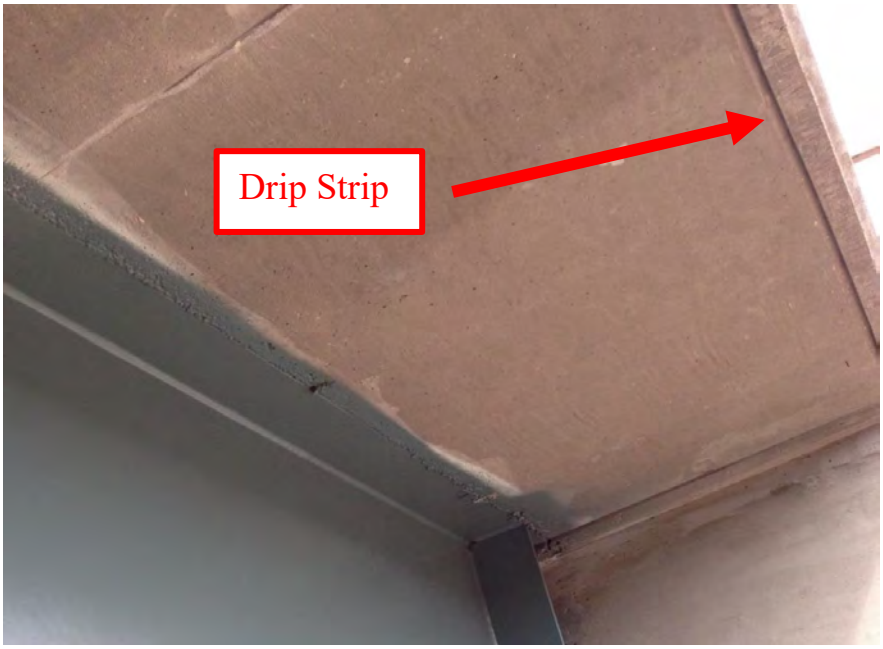

Question 5: In bridges where this detail has been implemented, have you observed any deterioration in the bridge deck fascia?

In general deterioration in the bridge deck fascia has not been an issue where "solid" type barriers have been placed. Bridges with older types of barrier such as a "one-line" barrier will show more deterioration as well as bridges that have been retro-fit with a new barrier, but previously had a more open barrier. (examples below) While this detail certainly helps, moisture seepage through the barrier/deck interface has not been a major issue on solid barriers that were originally placed on top of a flat deck surface.

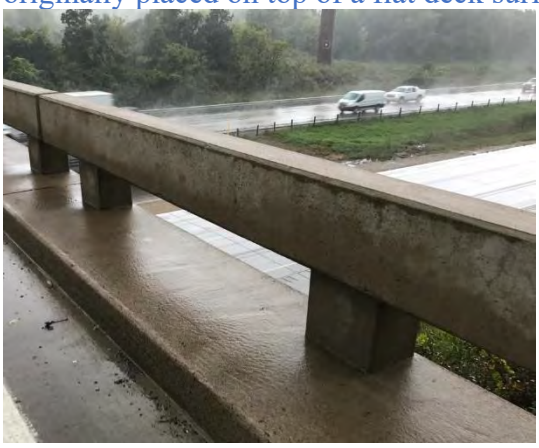

"One Line" Type Barrier

"Solid" type barrier retro-fit onto old one-line type barrier

Question 6: Do you have any other comments regarding the efficiency of the identified detail to reduce moisture content along the deck fascia and its constructability?

In general, this detail can only help with moisture content and seepage and has not been difficult to implement. Given lack of any significant contractor pushback, constructability has not been an issue in MnDOT experience.

NYS DOT Feedback

The following message was sent to NYS DOT staff:

"Thanks for responding to the survey on the deterioration of bridge deck fascias. We have identified the following details as promising details from NYS DOT in terms of reducing the moisture content along the bridge deck fascia. The details feature a sloped top deck surface and an elevated shear key connection. We believe that enhanced moisture content combined with freezing and thawing in the winter is one of the reasons for the deterioration of bridge deck fascias. The sloped deck surface and elevated shear key connection as shown in the details below could be efficient mechanisms for reducing moisture content along the deck fascia. We are interested in learning from your experience with these details especially in terms of their constructability. If you could respond to the following questions we would greatly appreciate it."

Responses are provided in blue below.

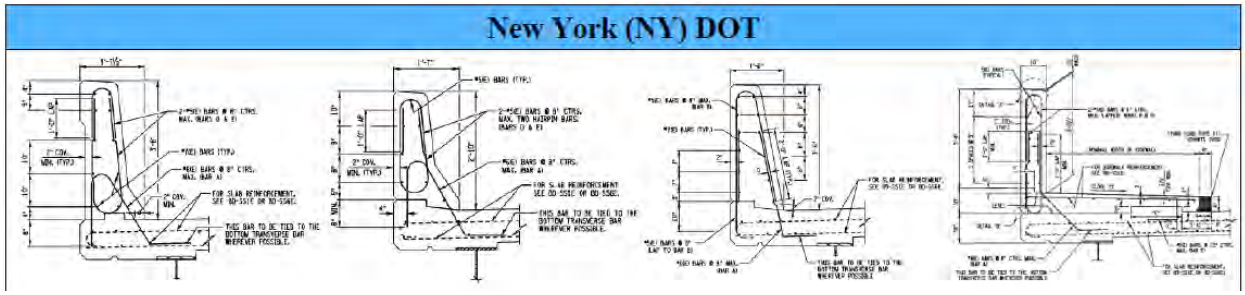

Fig. 1 Barrier to deck connections intended to reduce moisture migration from the deck to the fascia using a sloped top deck surface and elevated shear key connection

Question 1: Do you specify any limits on slump to ensure that such a sloped top deck surface could be constructed?

- Slump range for deck concrete (Class HP) is defined in the concrete specification and is 3" - 5".

Question 2: In general, how do the contractors construct such a sloped top deck surface and elevated shear key connection and have they encountered any difficulties? Any photographs that may illustrate this would be very helpful.

- Typically, wood is used to form the key. (See picture below). The sloped surface is generally troweled in with varied success.

Question 3: In bridges where these details have been implemented, have you observed any deterioration in the bridge deck fascia?

- I am unaware of any deterioration caused by leakage at the cold joint between decks and barriers. These details have been used for decades; changes would have likely been made if problems were reported.

Question 4: Is there any reason why both a sloped top deck surface as well as an elevated shear key connection is used? Is the specification of either a sloped top deck surface or elevated shear key connection considered insufficient to reduce moisture content along the deck fascia?

- It is assumed that the sloped surface prevents the collection of moisture under the barrier. However, some details do not provide the slopped surface in front of the key, and there are no reported problems. A key near the front face of the barrier seems more likely to prevent moisture than only specifying a sloped surface.

Question 5: Various details are shown in Fig. 1. What is the rationale for specifying each detail?

- The F-Shape and Jersy Shape barriers (first two details) are no longer used in NYS, but not due to the key details. While the rational for the differing details is unknown (due to how long they've been used), it is likely due to barrier dimensions and rebar location.

Question 6: Do you have any other comments regarding the efficiency of the identified details to reduce moisture content along the deck fascia and their constructability?

- None.

Wisconsin DOT Feedback

The following message was sent to Wisconsin DOT staff:

"Thanks for responding to the survey on the deterioration of bridge deck fascias. We have identified the following details as promising details from Wisconsin DOT in terms of reducing the moisture content along the bridge deck fascia. The details feature a sloped top deck surface. We believe that enhanced moisture content combined with freezing and thawing in the winter is one of the reasons for the deterioration of bridge deck fascias. The sloped deck surface as shown in the details below could be an efficient mechanism for reducing moisture content along the deck fascia. We are interested in learning from your experience with these details especially in terms of their constructability. If you could respond to the following questions we would greatly appreciate it."

Responses are provided in red below.

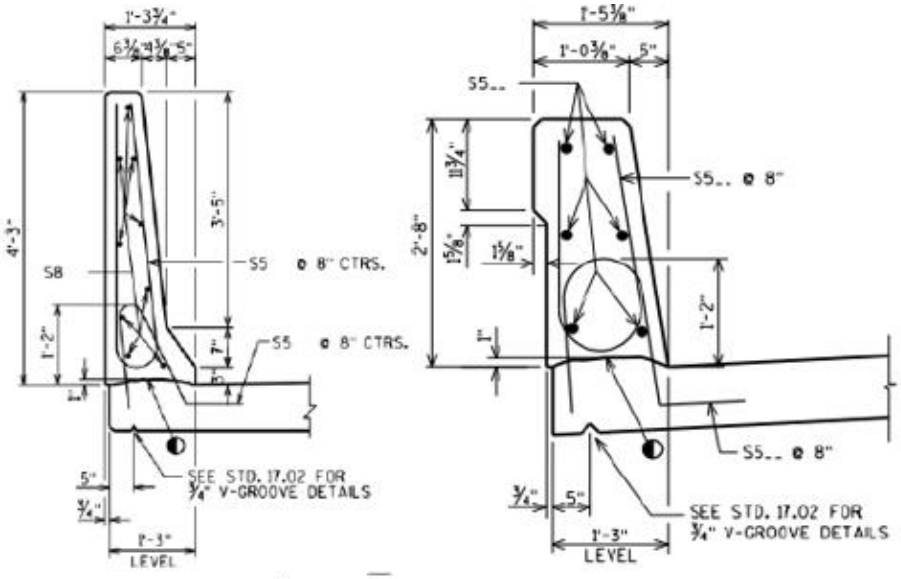

Fig. 1 Barrier to deck connections intended to reduce moisture migration from the deck to the fascia using a **sloped top deck surface**. When you state "sloped top deck surface", I am assuming that you are speaking to the area directly below the parapet that is noted by the half-filled-in circle symbol in the images above. If this is incorrect, please get back to me.

Question 1: Do you specify any limits on slump to ensure that such a sloped top deck surface could be constructed? We do not specify any different limits for this area of the deck when compared to the remaining concrete in the deck. Our concrete mix designs are specified in standard spec 501 (link here).

Question 2: In general, how do the contractors construct such a sloped deck surface and have they encountered any difficulties? Specifically, how is the curved top deck surface underneath the barrier constructed? Any photographs that may illustrate this would be very helpful. I don't have any specific pictures that I can quickly obtain, but I'd be happy to reach out to our field staff to get some if desired. We haven't had any issues with the constructability of this detail to my knowledge as it has been standard for well over a decade in Wisconsin. Basically, from personal viewing of

deck placements on our projects, the contractor roughens this area of the deck below the parapets (i.e., they don't finish it smooth like the remaining deck) and do the best they can to provide some 'amplitude' in this roughened area.

Question 3: In the detail on the left the bottom of the deck overhang appears to be flat whereas in the detail on the right the bottom of the deck is sloping towards the deck fascia. What is the rationale behind specifying each detail and which detail has resulted in better performing deck fascias in terms of deterioration? The details shown above may not be truly indicative of the "typical" edge of deck detailing practice on WisDOT projects. The vast majority of our deck overhangs slope downwards from the edge of deck towards the exterior girder. This can be seen in the Chapter 17 and Chapter 19 Standard Details. I'm not sure where the details above were pulled from, but I'd say they are definitely the outliers compared to the conventional practices shown in the linked Standards.

Question 4: In bridges where these details have been implemented, have you observed any deterioration in the bridge deck fascia? As stated previously, the details where the deck slopes down from the exterior girder to the edge of deck is not commonplace in Wisconsin. That being the case, I can't really speak to the viability of how these details would perform.

Question 5: Do you have any other comments regarding the efficiency of the identified details to reduce moisture content along the deck fascia and their constructability? Generally speaking, WisDOT doesn't see significant edge of deck deterioration on bridges that have solid concrete parapets. Our detail to include the roughened surface below the parapet, in conjunction with locating the "v-groove" in the edge of deck between the locations of the bottom longitudinal rebar (i.e., move the v-groove so that it is not located directly below a longitudinal bar which lessens the concrete between), seems to work well. WisDOT does see significant edge of deck/fascia deterioration when we utilize open steel railings on bridges. In these cases, some of the Regions have gone to installing a metal flashing element with the initial construction (these details are included in the Chapter 17 Standards referenced above) to try to hold back the edge of deck deterioration timeline. However, this detail isn't perfect either and adds another element to the bridge that has to be maintained.

Delaware DOT Feedback

The following message was sent to Delaware DOT staff:

"Thanks for responding to the survey on the deterioration of bridge deck fascias. We have identified the following details as promising details from Delaware DOT in terms of reducing the moisture content along the bridge deck fascia. The first detail features a sloped top deck surface, while the second detail features a suppressed shear key. We believe that enhanced moisture content combined with freezing and thawing in the winter is one of the reasons for the deterioration of bridge deck fascias. The sloped deck surface and suppressed shear keys as shown in the details below could be efficient mechanisms for reducing moisture content along the deck fascia. We are interested in learning from your experience with these details especially in terms of their constructability. If you could respond to the following questions we would greatly appreciate it."

Responses are provided below in red.

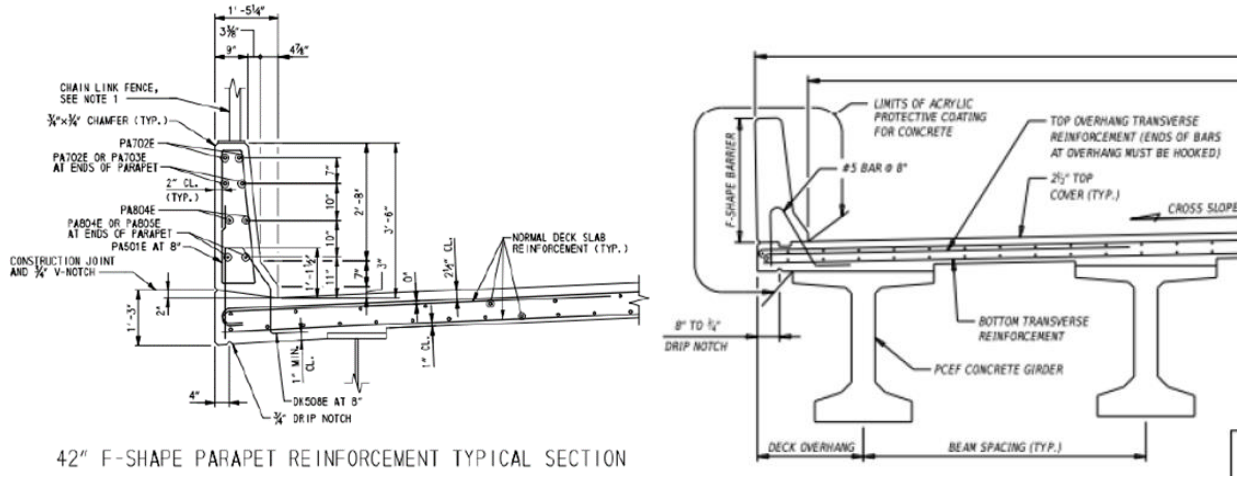

a) b)

Fig. 1 Barrier to deck connection intended to reduce moisture migration from the deck to the fascia using: a) a **sloped top deck surface**, and b) **suppressed shear key**

Question 1: Sloped top deck surface connection: Do you specify any limits on slump to ensure that such a sloped top deck surface could be constructed? DelDOT does not currently use the sloped surface detail shown as a) (left picture). Our standard barrier to deck connection would utilize a shear key as shown in b) (right). A similar detail to b) is what is shown in DelDOT's Bride Design Manual.

Question 2: Sloped top deck surface connection: In general, how do the contractors construct such a sloped deck surface and have they encountered any difficulties? Any photographs that may illustrate this would be very helpful. I am not aware of any bridge barrier to deck connections that have been constructed using this detail. Most, if not all of our bridge decks are poured with a shear key as shown in detail b.

Question 3: Sloped top deck surface connection: In this detail the bottom of the deck is sloped towards the deck fascia. Have you seen any correlation between this and deck fascia

deterioration? Is the deck fascia deterioration better or worse compared to a detail when the bottom of the deck overhang is flat? N/A as we don't have any bridges with this particular detail.

Question 4: Suppressed shear key connection: In general, how do the contractors construct such a suppressed shear key and have they encountered any difficulties? Any photographs that may illustrate this would be very helpful. Depending on the contractor performing the work, some will simply press a 2"X4" into the freshly poured concrete after the Bidwell has passed to create the shear key or some will use a square channel tool and create the shear key by hand following behind the Bidwell. Either method is simple to perform, and I am not aware of contractors have any issues with this process to date. I have attached a couple of photos below for reference.

Question 5: Suppressed shear key connection: In this detail an acrylic protective coating is specified. Have you seen a correlation between the specification of this coating and improvement in deck fascia deterioration? Sort of a tricky question to answer as the acrylic protective coating requirement is a more recent requirement (25-35 years). The trickiness is that for the past 30-35 years, we have been using epoxy coated rebar in our decks as well. So, it is hard to say for certain that our bridge deck fascias are holding up better because of the acrylic coating or holding up better because we use epoxy coated rebar. I do believe that the acrylic coating helps extend the life of the deck fascia by protecting it from deicing/salt spray that is lifted up by vehicular traffic and from moisture/rain in general. To further complicate things, we are less likely to include open scuppers in the base of our concrete bridge rail. Open scuppers in the concrete rail have been a problem for some of our older bridge inventory (35-65 years old). That's not to say that we never use open scuppers it now, but it is not as prevalent as from what we did during the interstate bridge construction era.

Question 6: In general, what is the rationale for specifying a sloping top deck surface versus a suppressed shear key detail? In DelDOT's Bridge Design Manual, we do not use or provide a sloping top deck surface detail. The suppressed shear key detail is what is most commonly used and detailed in the BDM.

Question 7: In bridges where these details have been implemented, have you observed any deterioration in the bridge deck fascia? N/A as we don't have any bridges with this particular detail.

Question 8: Do you have any other comments regarding the efficiency of the identified details to reduce moisture content along the deck fascia and their constructability? Regarding the shear key detail that we current specify and use – we are pretty satisfied with the performance overall and issues that we do have – are more related to problematic drainage details, lack of drainage maintenance, or failing expansion joints.

General View of Bidwell with rebar tying deck up into future concrete bridge rail.

Close-up of shear key at concrete deck/rail base interface.

Close-up of shear key at concrete deck/rail base interface.

Maryland DOT Feedback

The following message was sent to Maryland DOT staff:

"Thanks for responding to the survey on the deterioration of bridge deck fascias. We have identified the following details as promising details from Maryland DOT in terms of reducing the moisture content along the bridge deck fascia. The details feature a suppressed shear key connection. We believe that enhanced moisture content combined with freezing and thawing in the winter is one of the reasons for the deterioration of bridge deck fascias. The suppressed shear key connection as shown in the details below could be an efficient mechanism for reducing moisture content along the deck fascia. We are interested in learning from your experience with these details especially in terms of their constructability. If you could respond to the following questions we would greatly appreciate it."

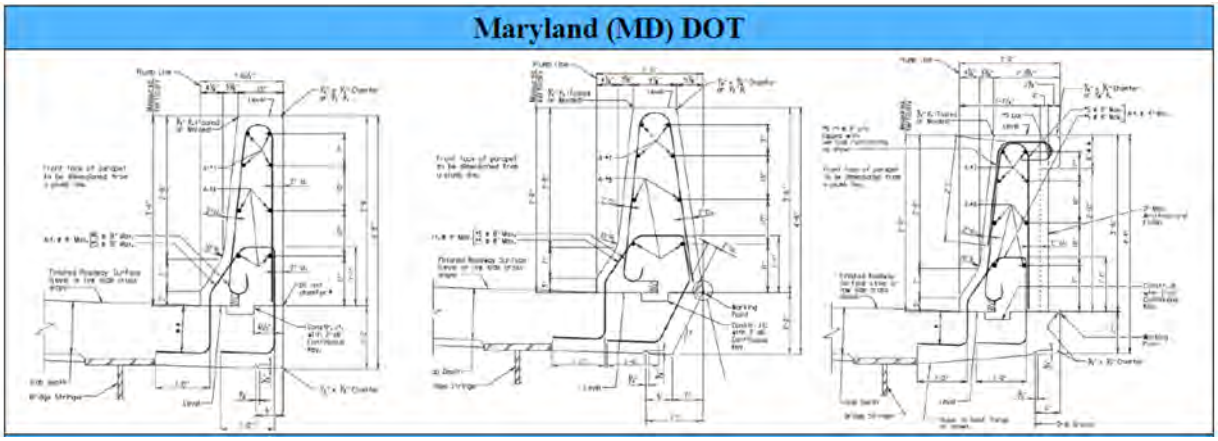

Fig. 1 Barrier to deck connections intended to reduce moisture migration from the deck to the fascia using a suppressed shear key connection

Question 1: In general, how do the contractors construct such a suppressed shear key connection and have they encountered any difficulties? Any photographs that may illustrate this would be very helpful. The shear key is nominal size and the contractor simply use a 2"x4" timber for creation of the key. It is very simple and there have been no problems to note. I do not happen to have any pictures of this.

Question 2: In bridges where these details have been implemented, have you observed any deterioration in the bridge deck fascia? Yes, I have been informed that we still do have this problem on some of our bridges (see attached picture). This being a cold joint between the parapet and deck, water does make its way through. If the key was reversed and went up, this possibly could help slow down the migration of water seepage. Also, not sure how good a job contractors are doing at putting the bonding agent along this joint before they pour which could be another contributing factor.

Question 3: Do you have any other comments regarding the efficiency of the identified details to reduce moisture content along the deck fascia and their constructability? It appears to slow the process, but water still finds its way through.

Appendix C: State DOT's Barrier Practices

Note: All illustrations including figures and details were obtained from literature published by the state DOTs.

Alabama (AL) DOT

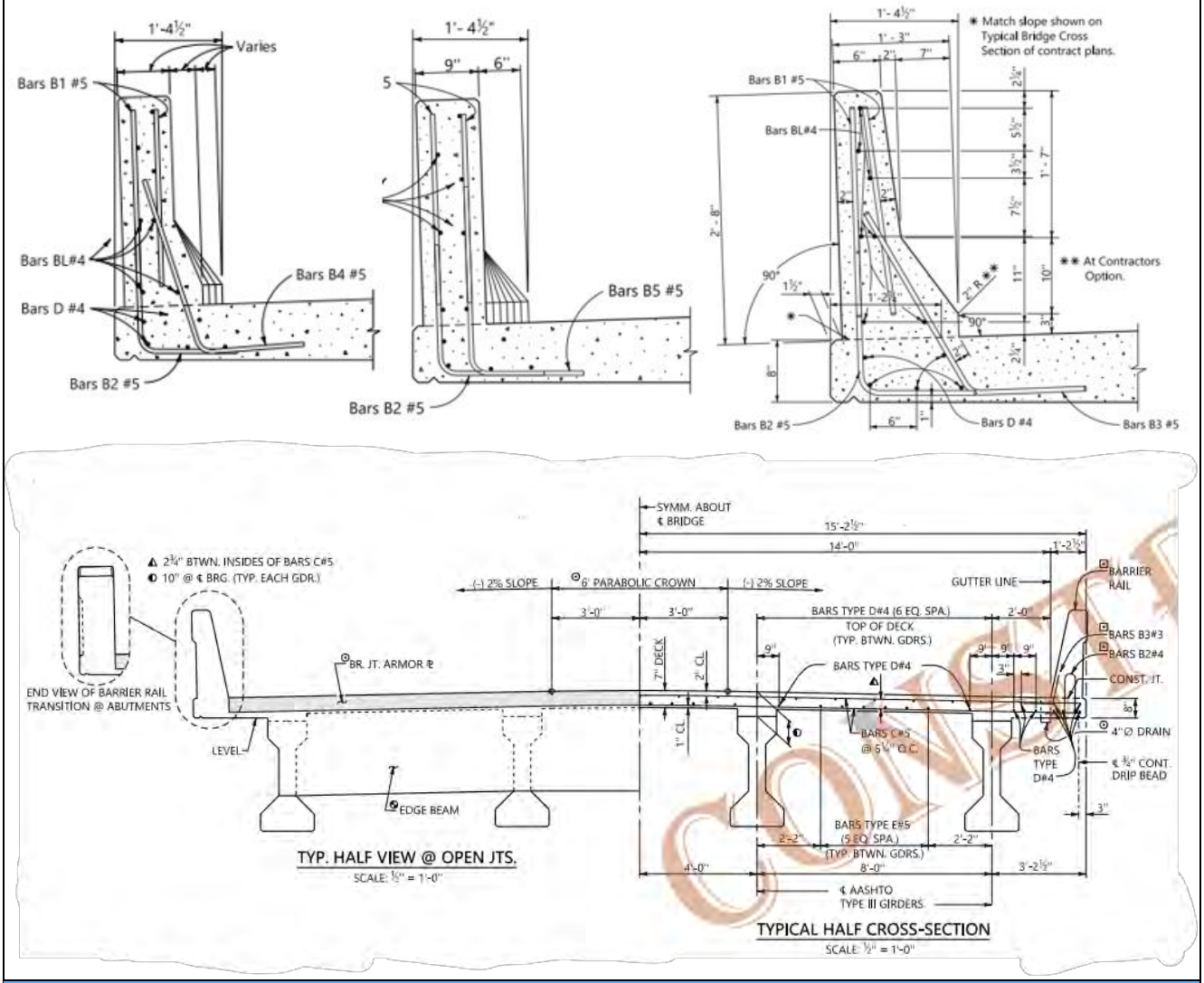

Alaska (AK) DOT

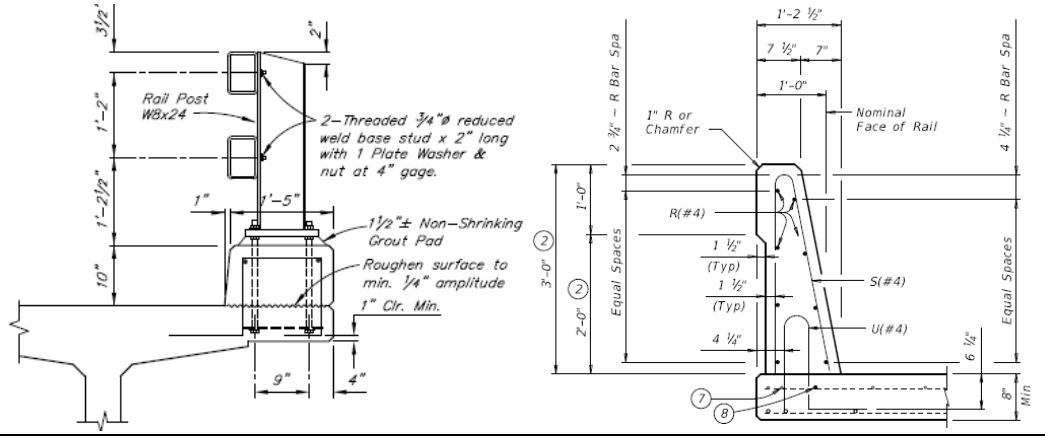

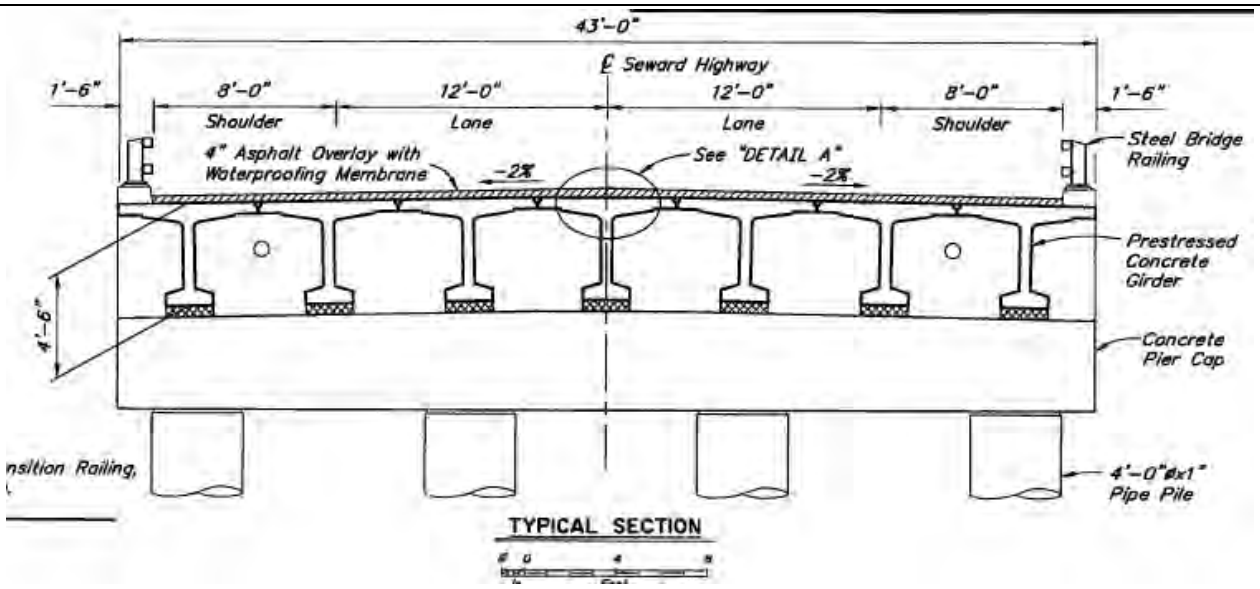

Arizona (AZ) DOT

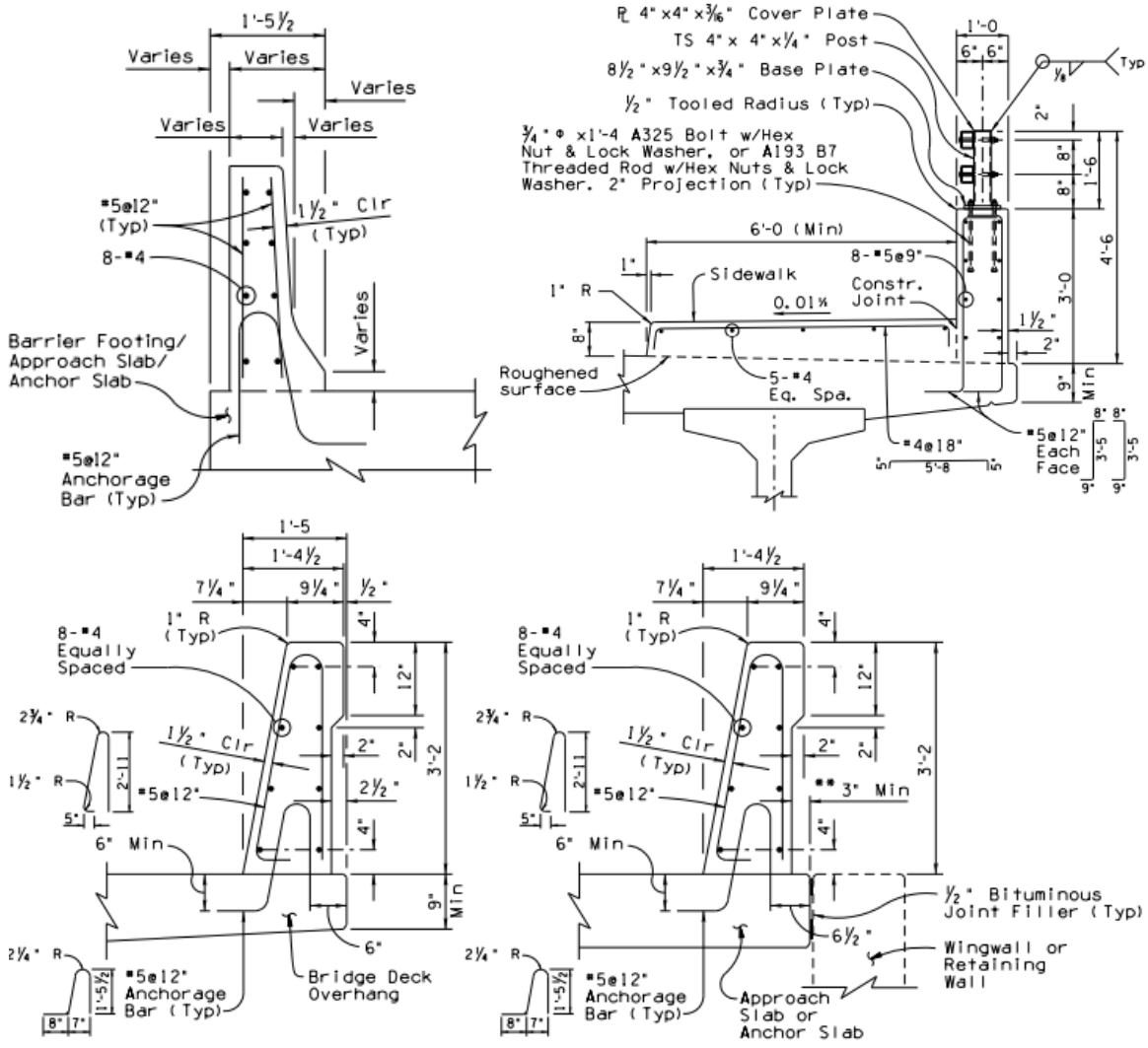

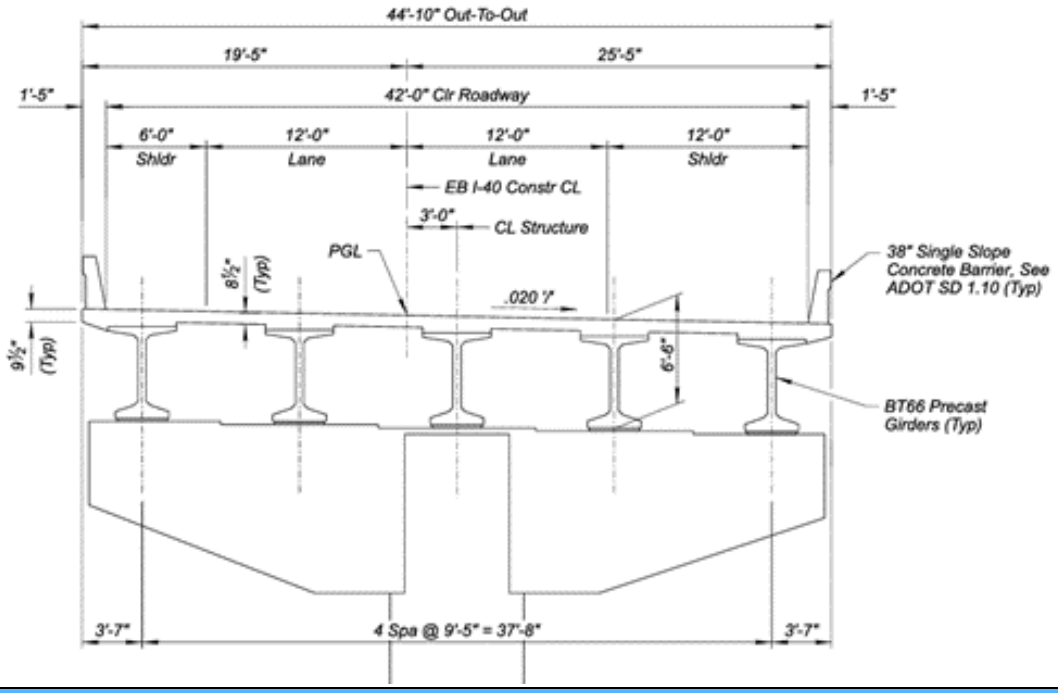

Arkansas (AR) DOT

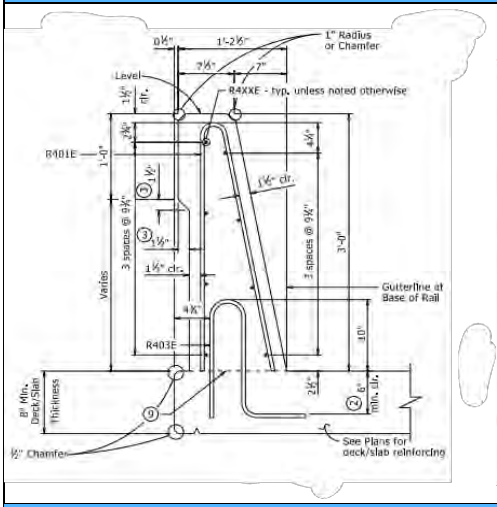

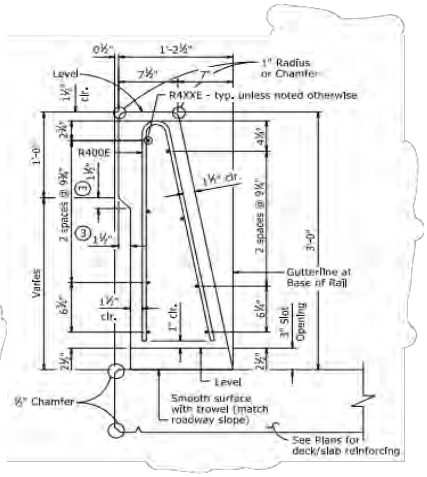

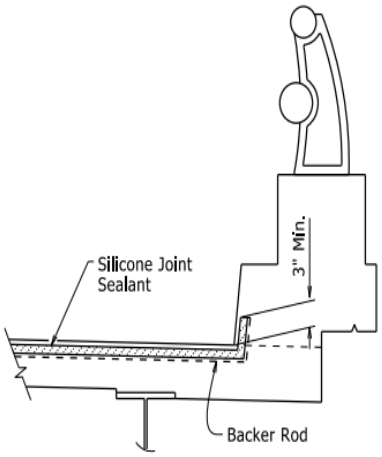

California (CA) DOT

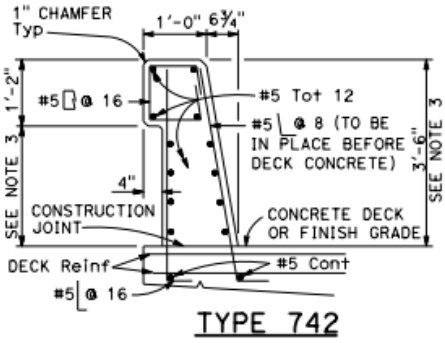

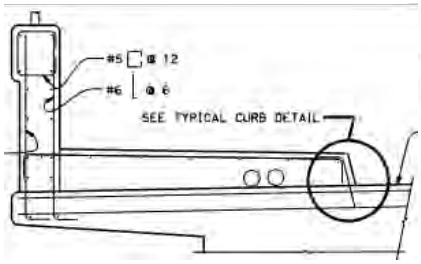

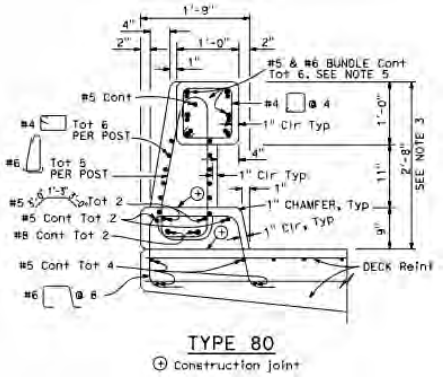

Colorado (CO) DOT

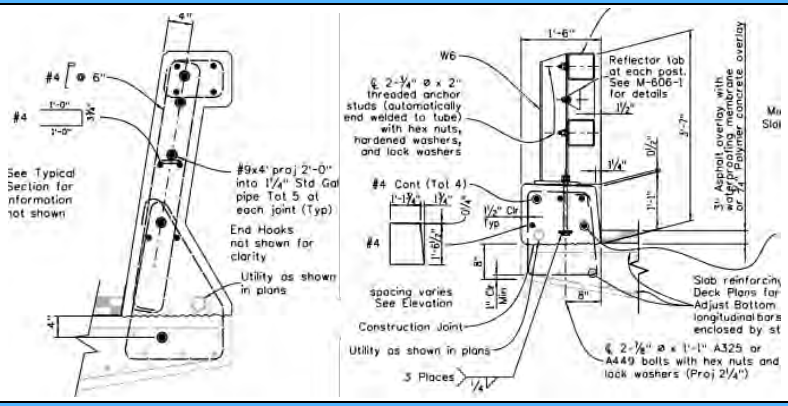

Connecticut (CT) DOT

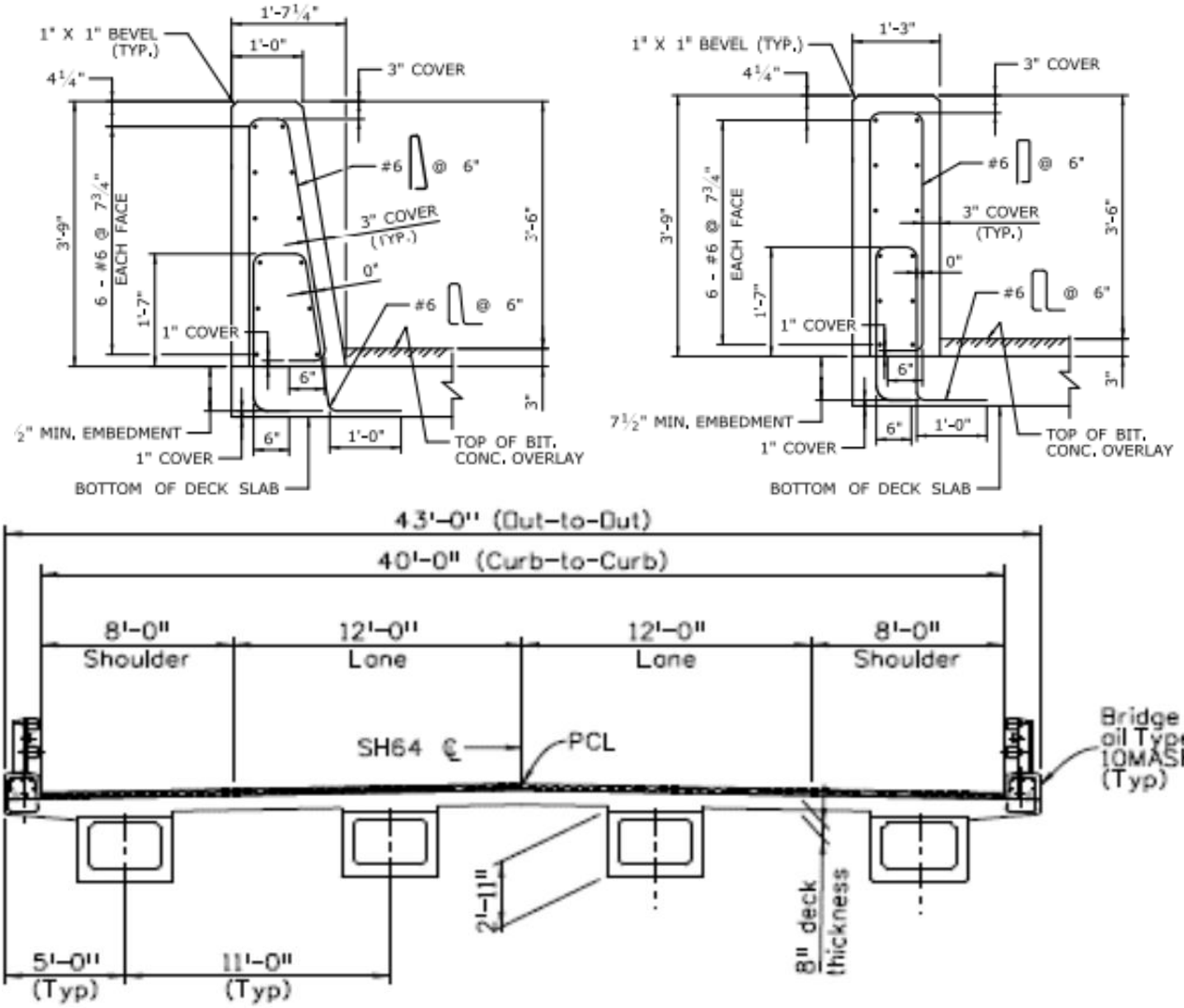

Delaware (DE) DOT

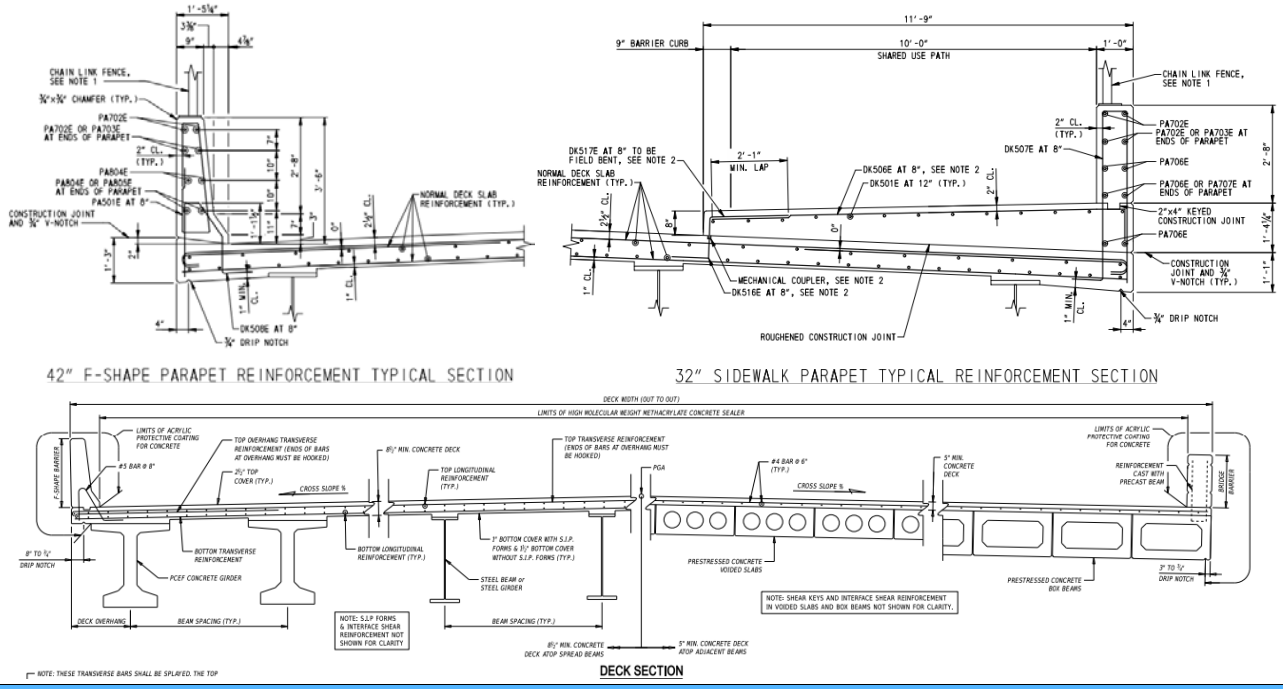

Florida (FL) DOT

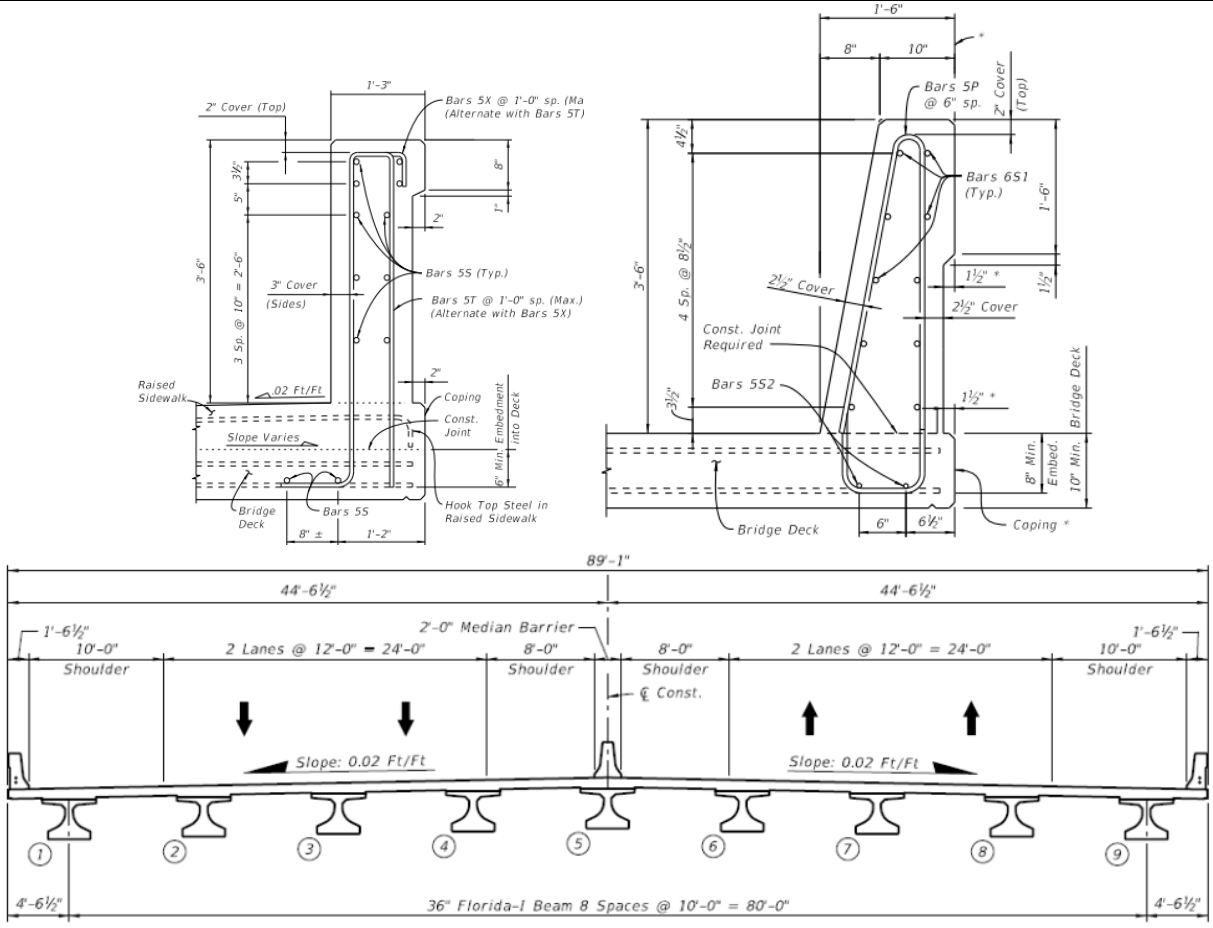

Georgia (GA) DOT

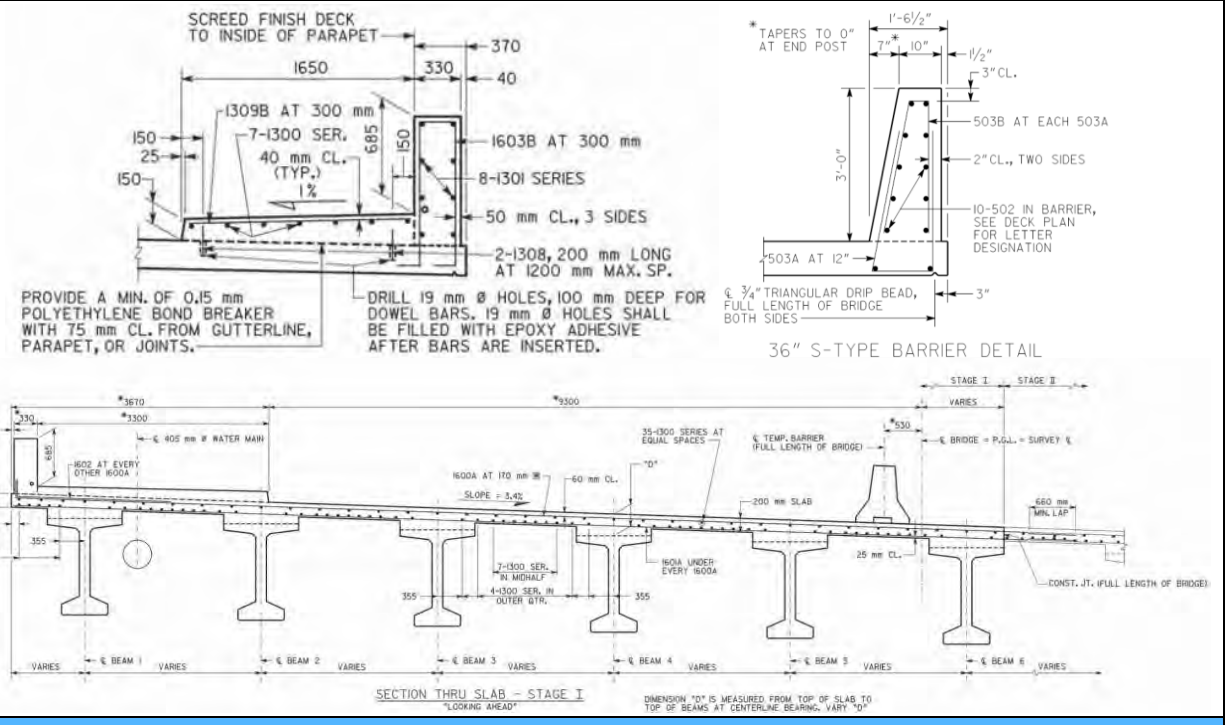

Hawaii (HI) DOT

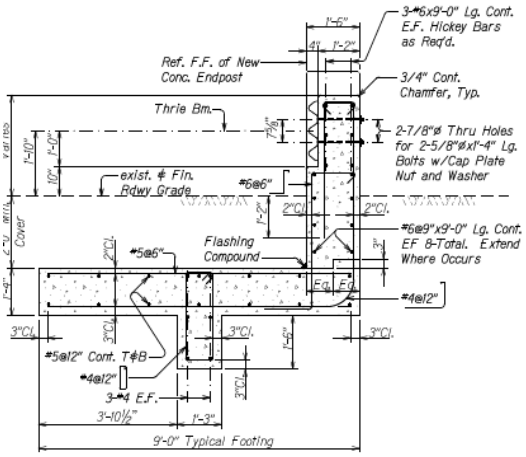

Idaho (ID) DOT

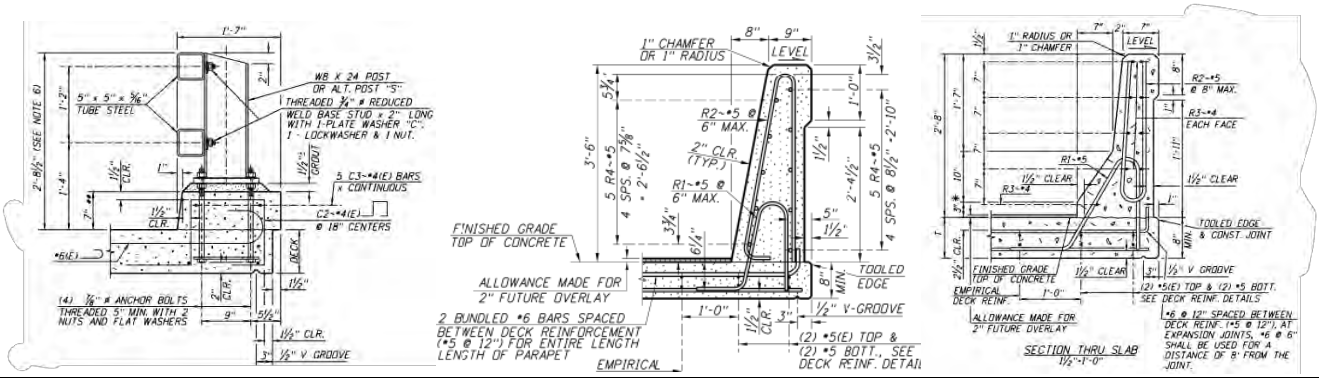

Illinois (IL) DOT

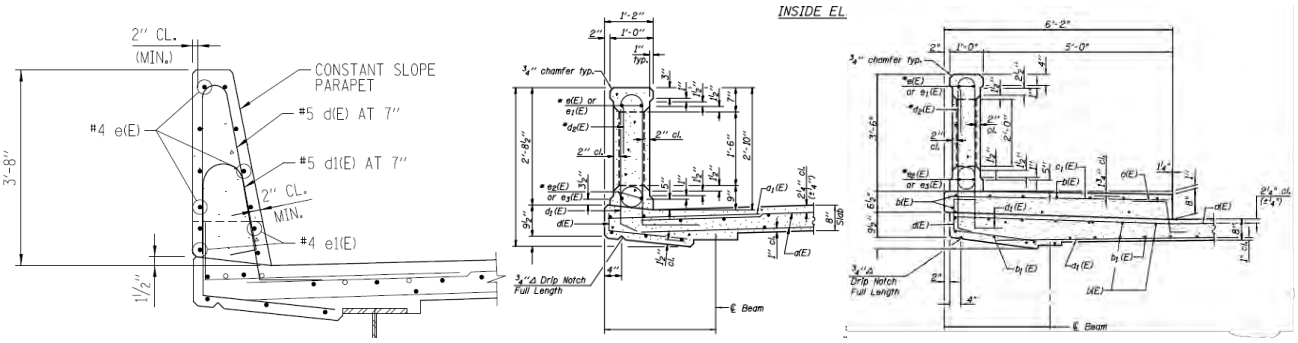

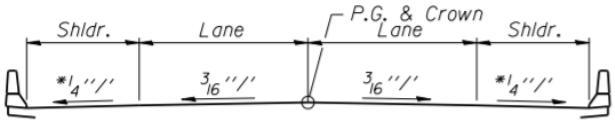

2 LANE HIGHWAY

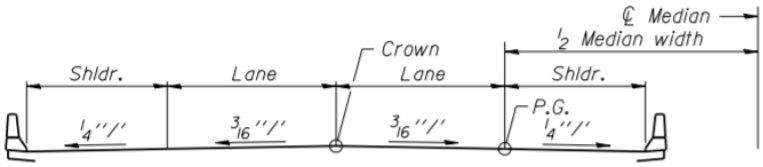

4 LANE DIVIDED HIGHWAY

Note:
A crown configuration shall be depicted on the deck cross-section on all T.S.&L. plans. The following sketches show the formation of the crown for typical template configurations.

* For structures 32' wide or less which utilize P.P.C. Box beams, the cross slope may be formed, by a plane having a constant slope of 3/16"/'.

Indiana (IN) DOT

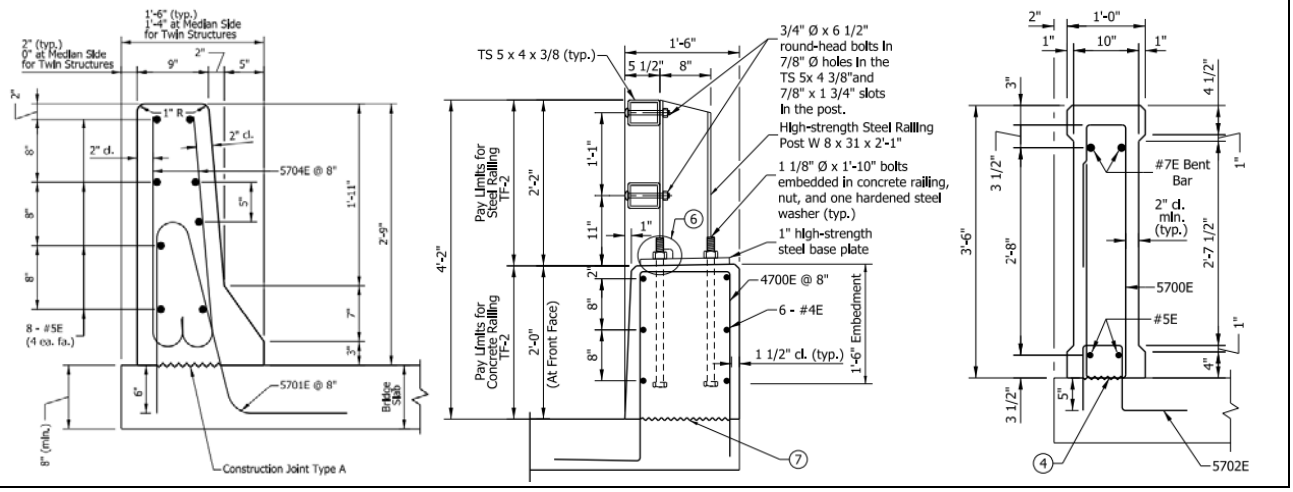

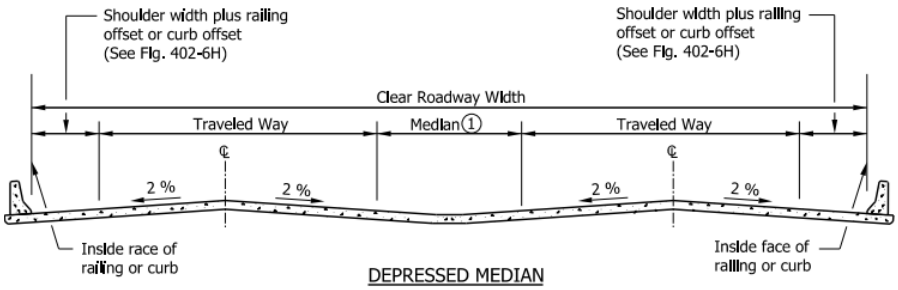

DEPRESSED MEDIAN

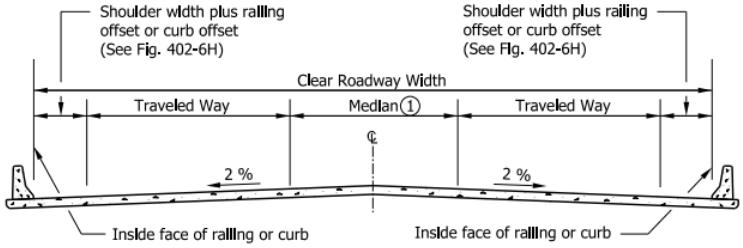

FLUSH MEDIAN

① *A raised island or CMB may be warranted. See Chapter 55 for criteria on median width for a single structure.*

Iowa (IA) DOT

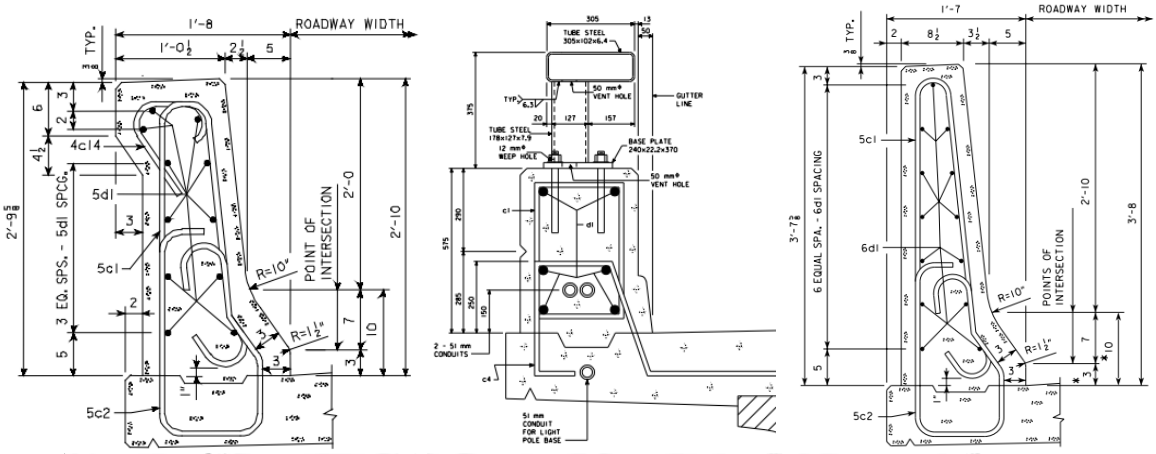

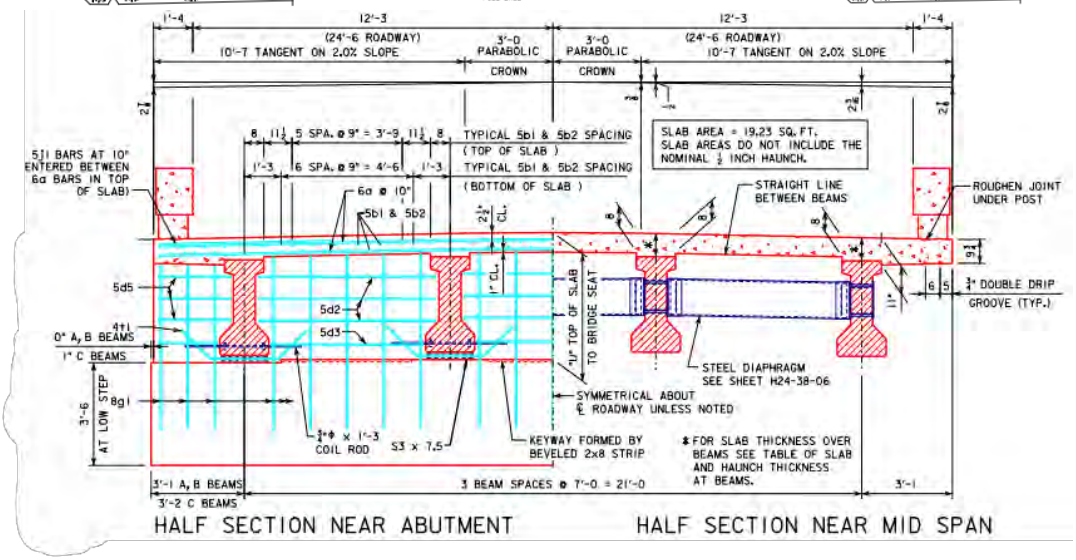

Kansas (KS) DOT

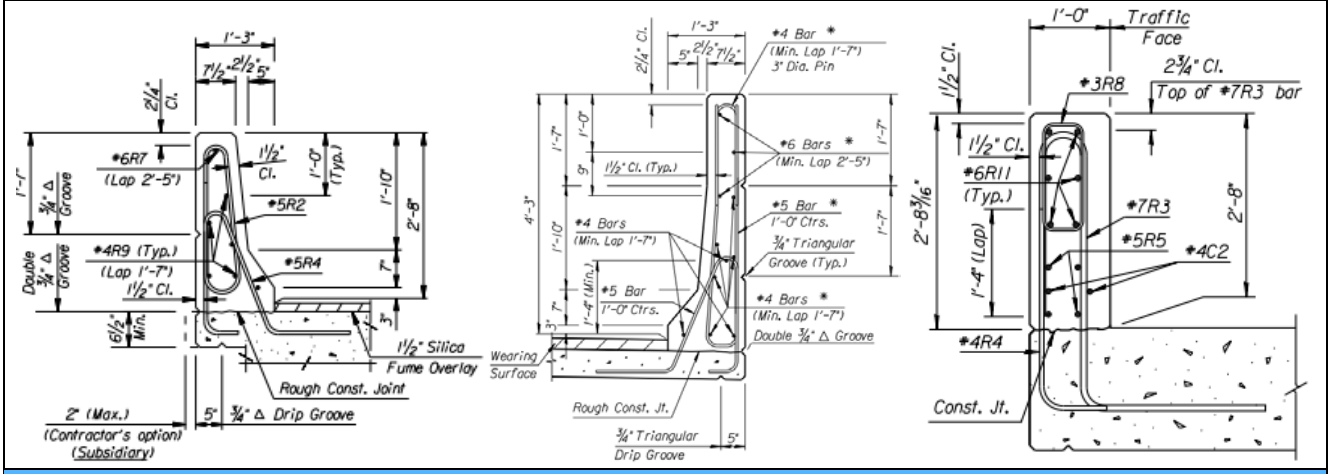

Kentucky (KY) DOT

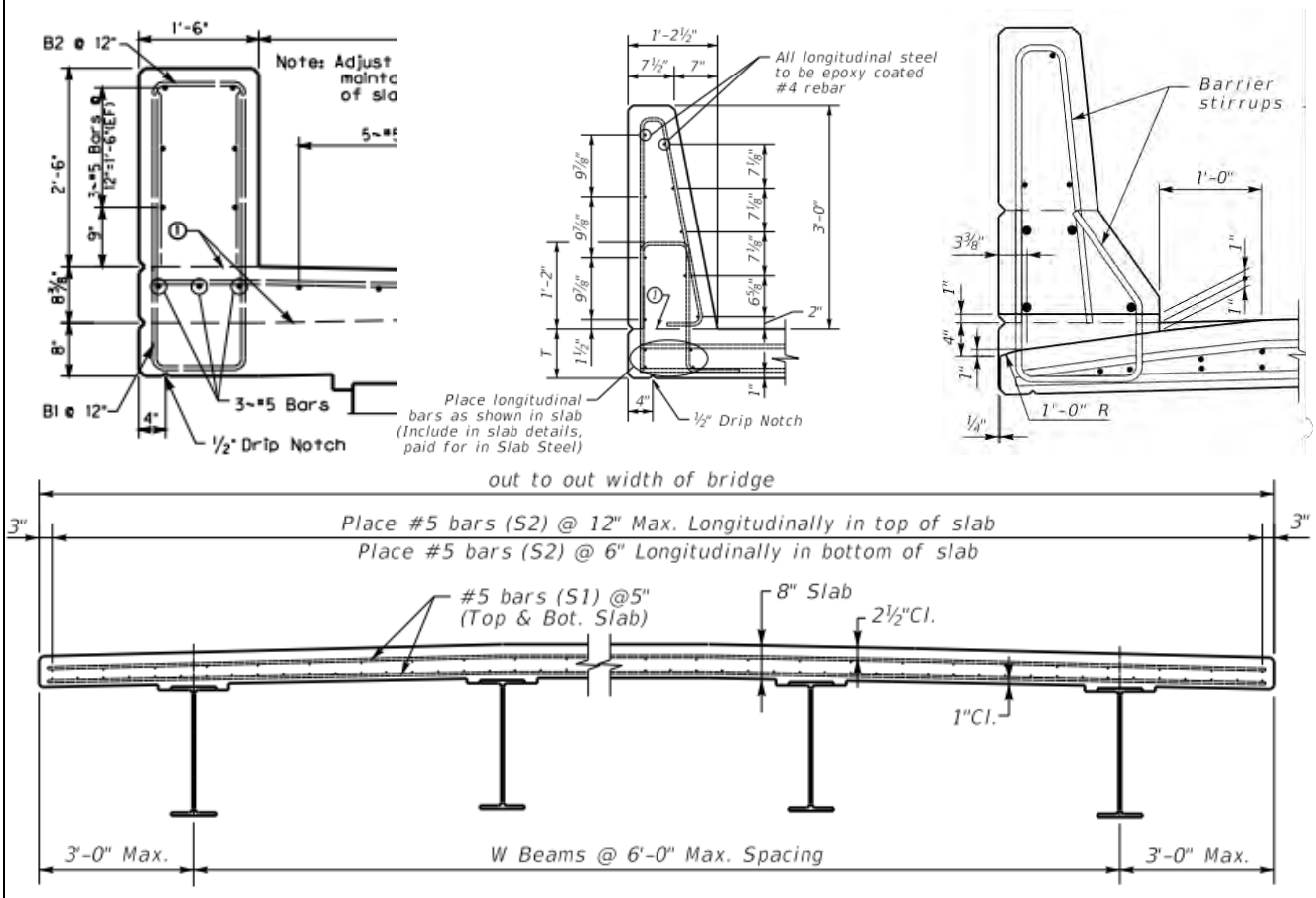

TYPICAL SECTION

Louisiana (LA) DOT

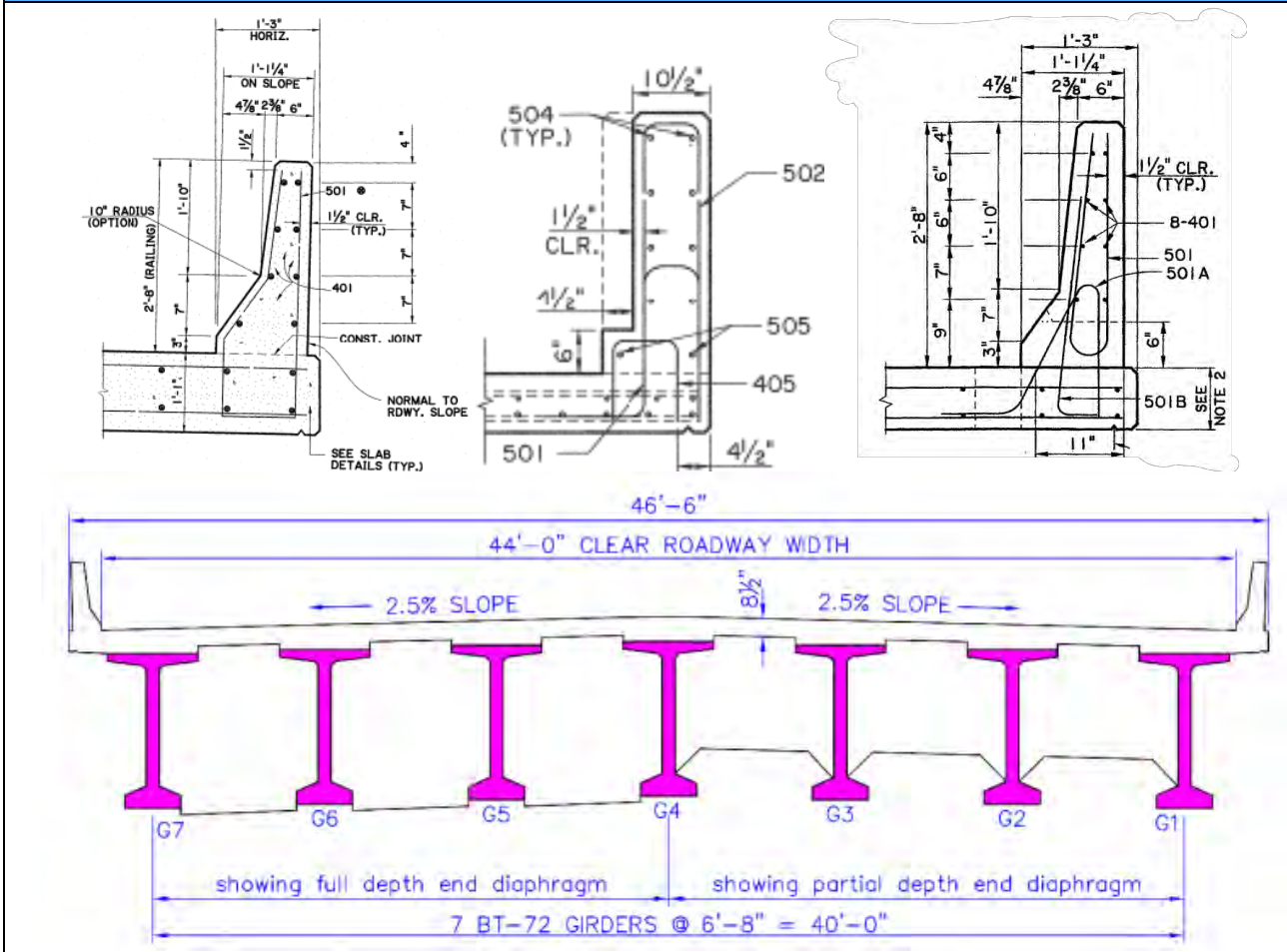

Maine (ME) DOT

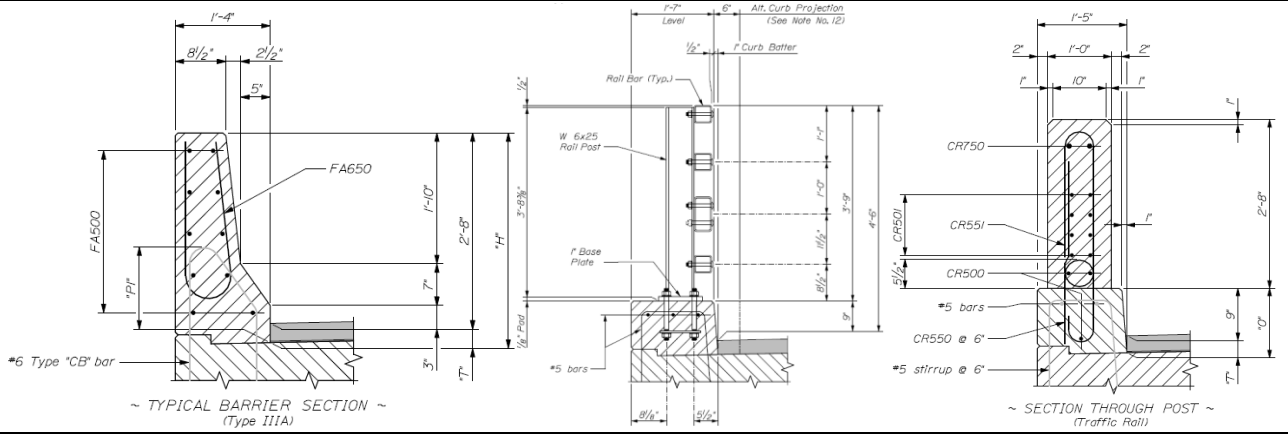

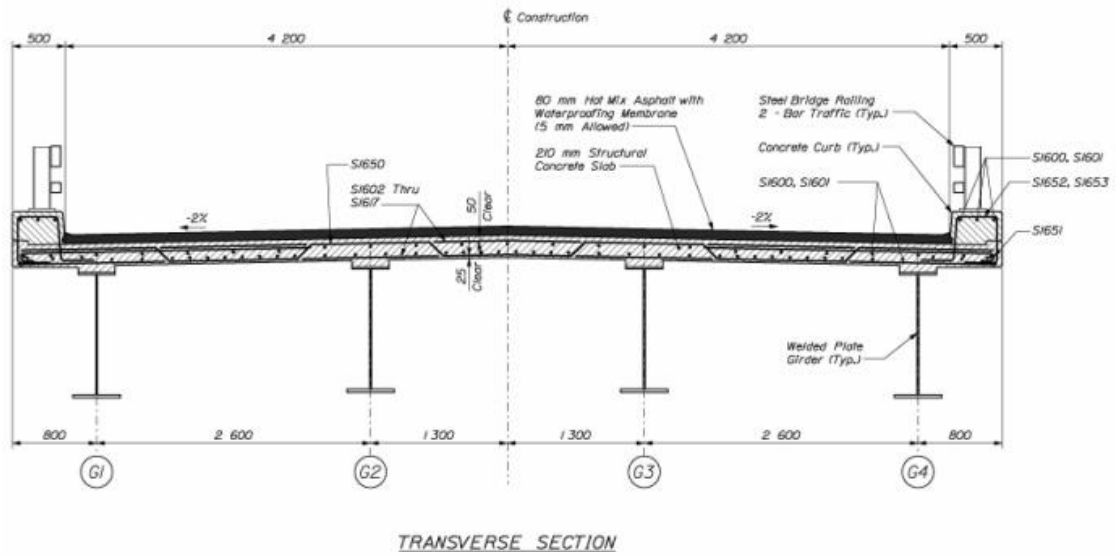

TRANSVERSE SECTION

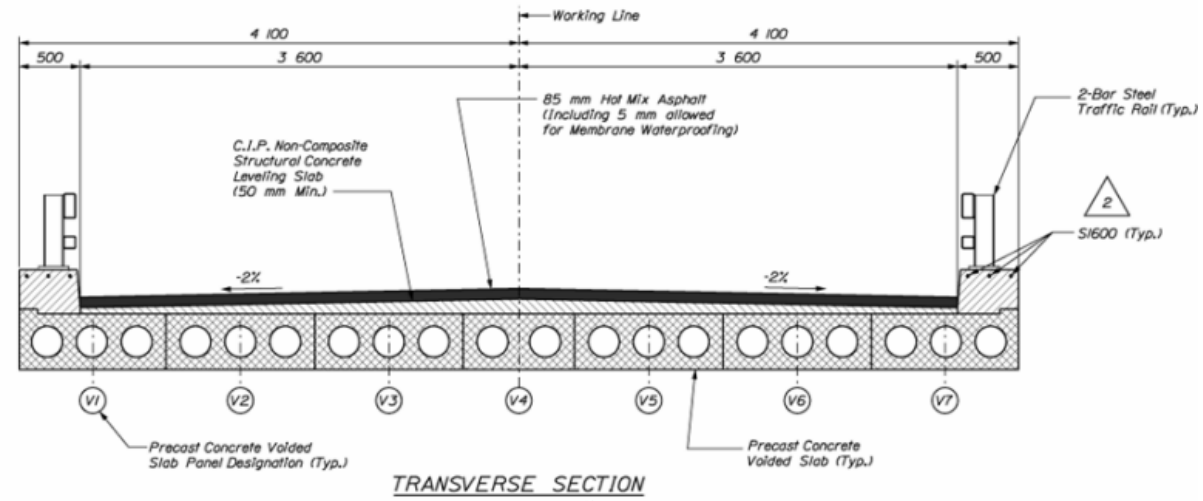

TRANSVERSE SECTION

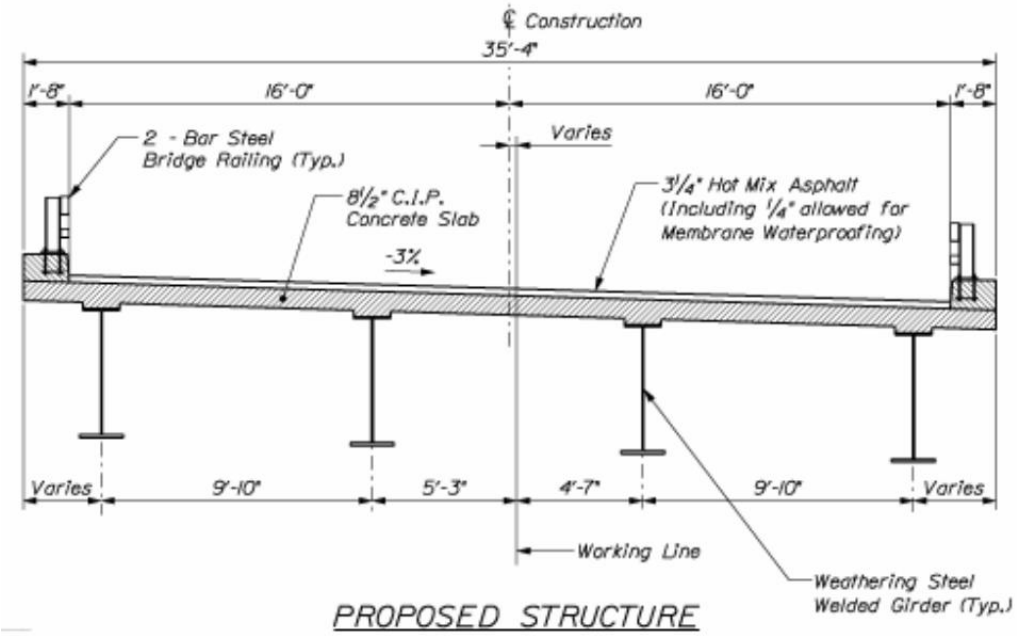

PROPOSED STRUCTURE

Maryland (MD) DOT

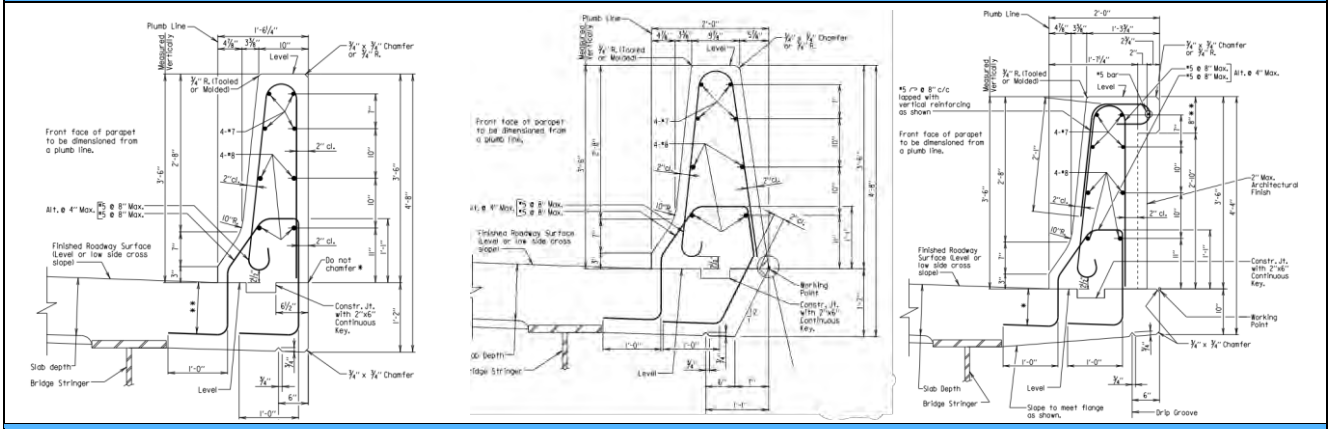

Massachusetts (MA) DOT

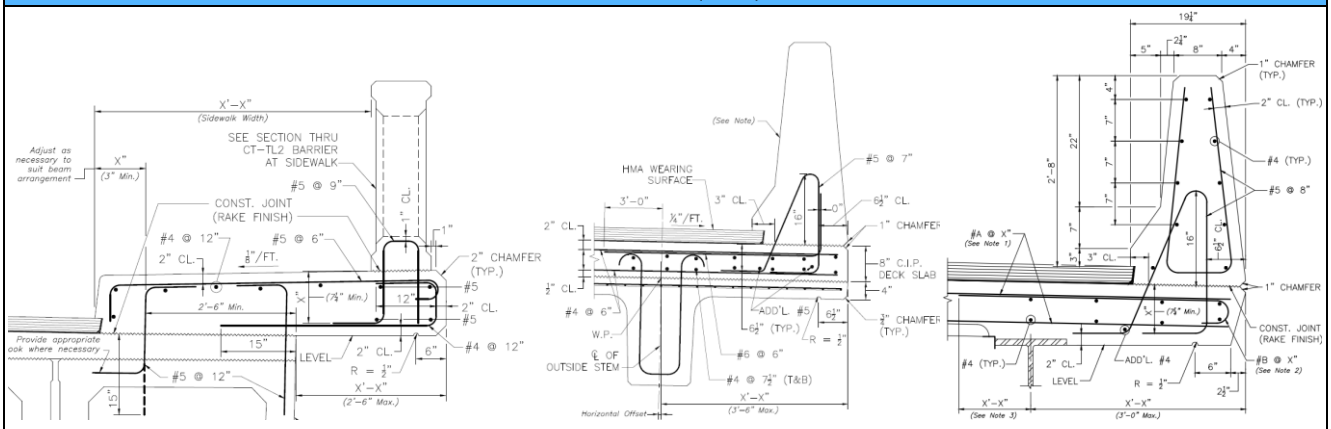

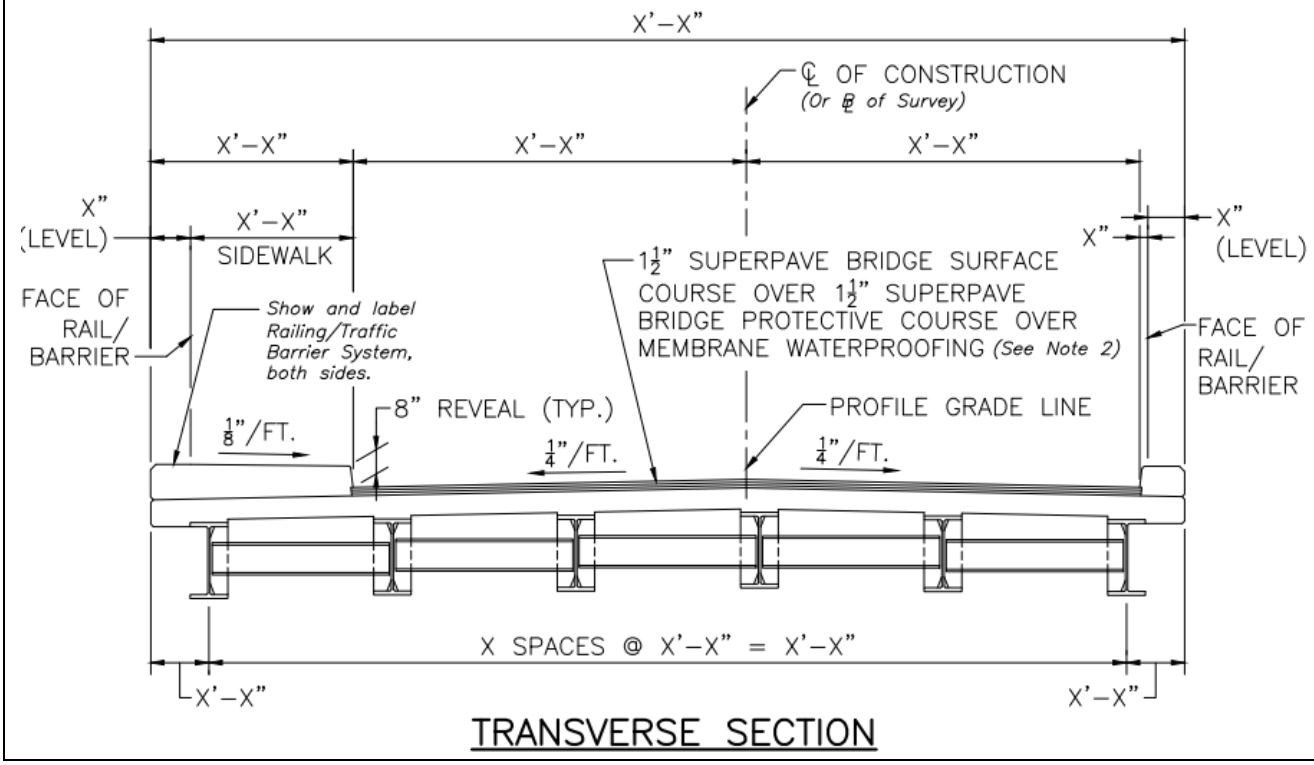

Michigan (MI) DOT

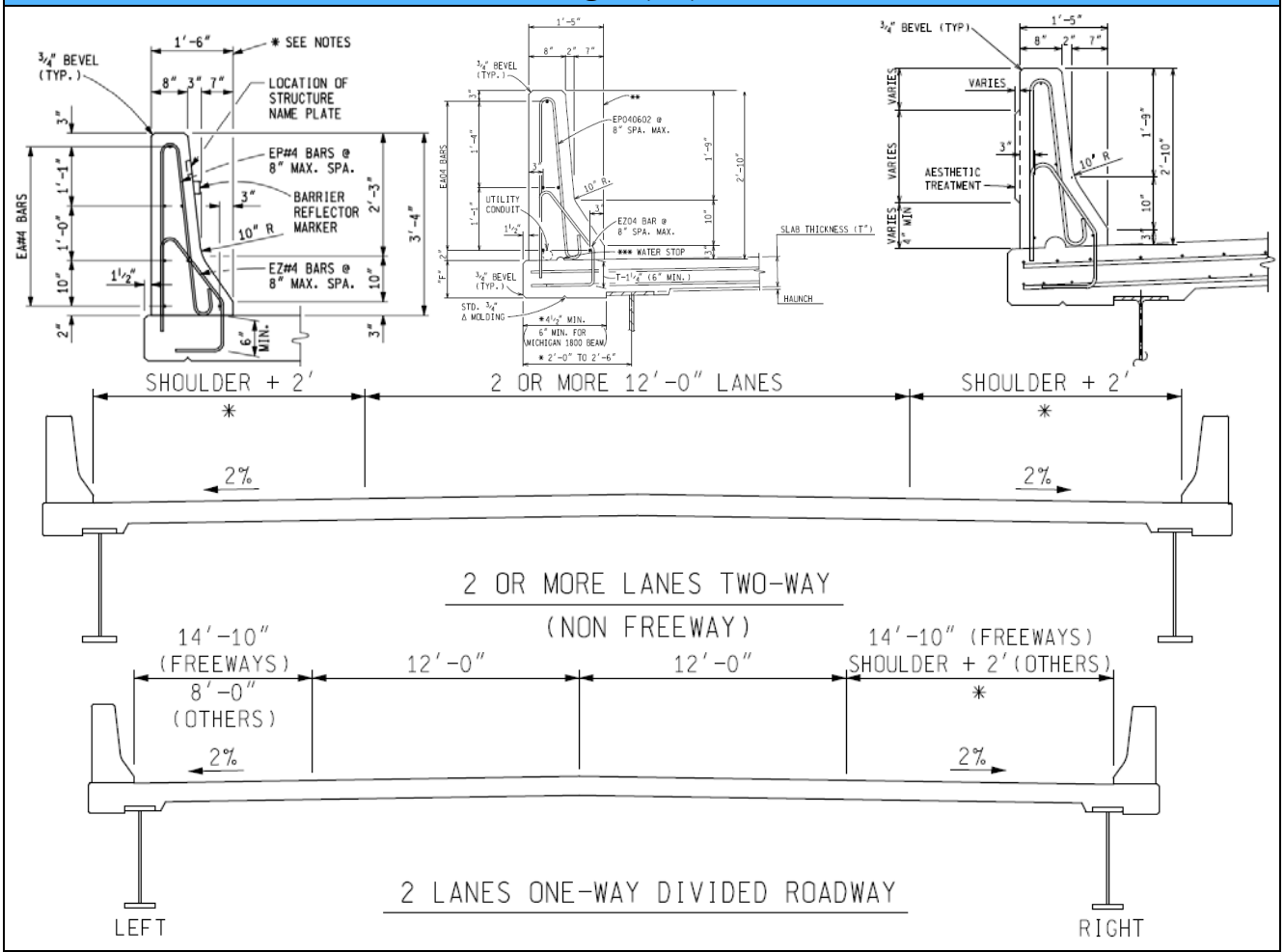

Minnesota (MN) DOT

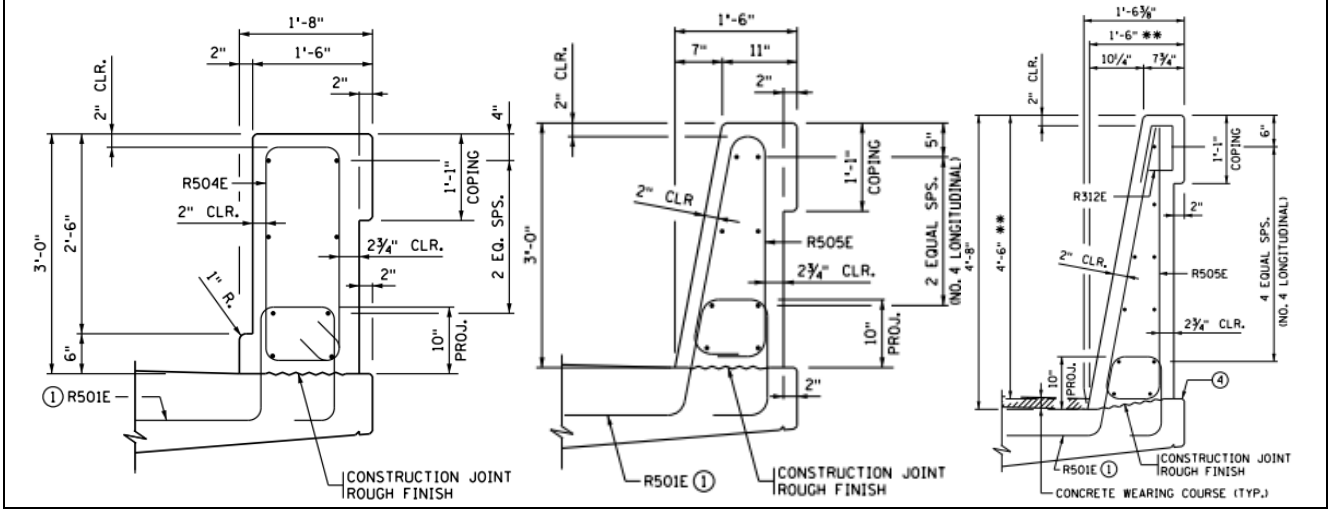

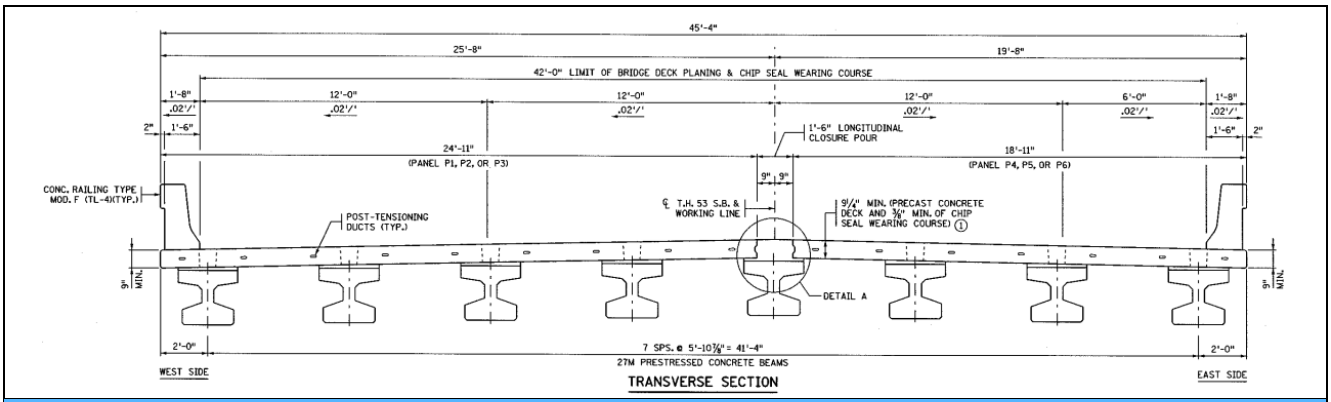

Mississippi (MS) DOT

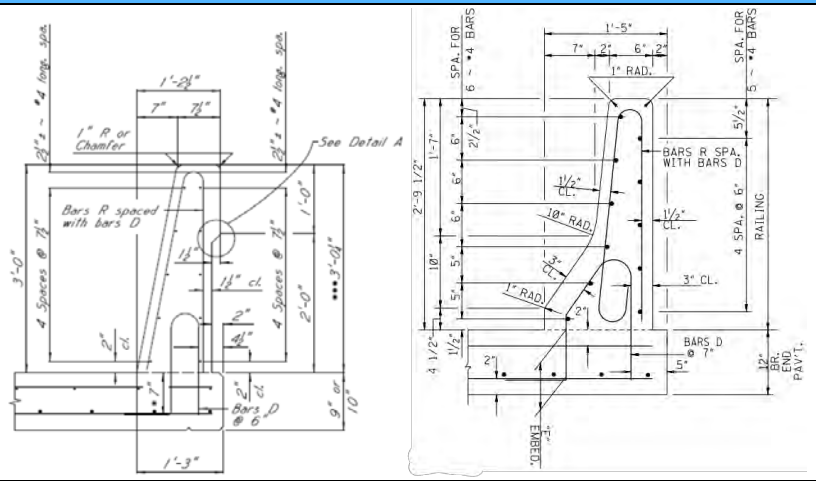

Missouri (MO) DOT

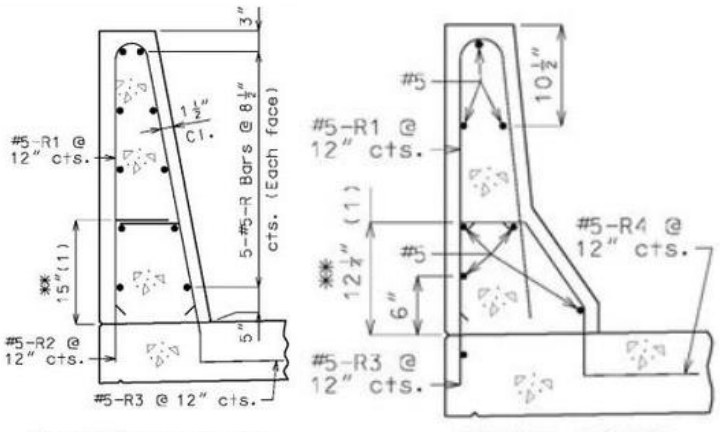

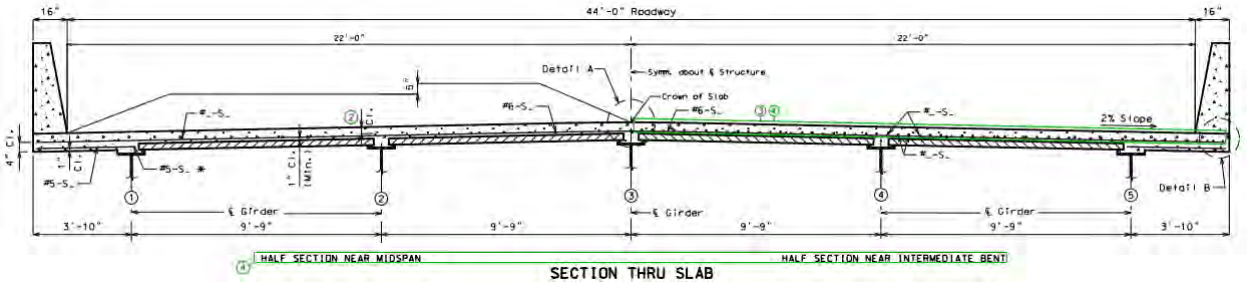

Montana (MT) DOT

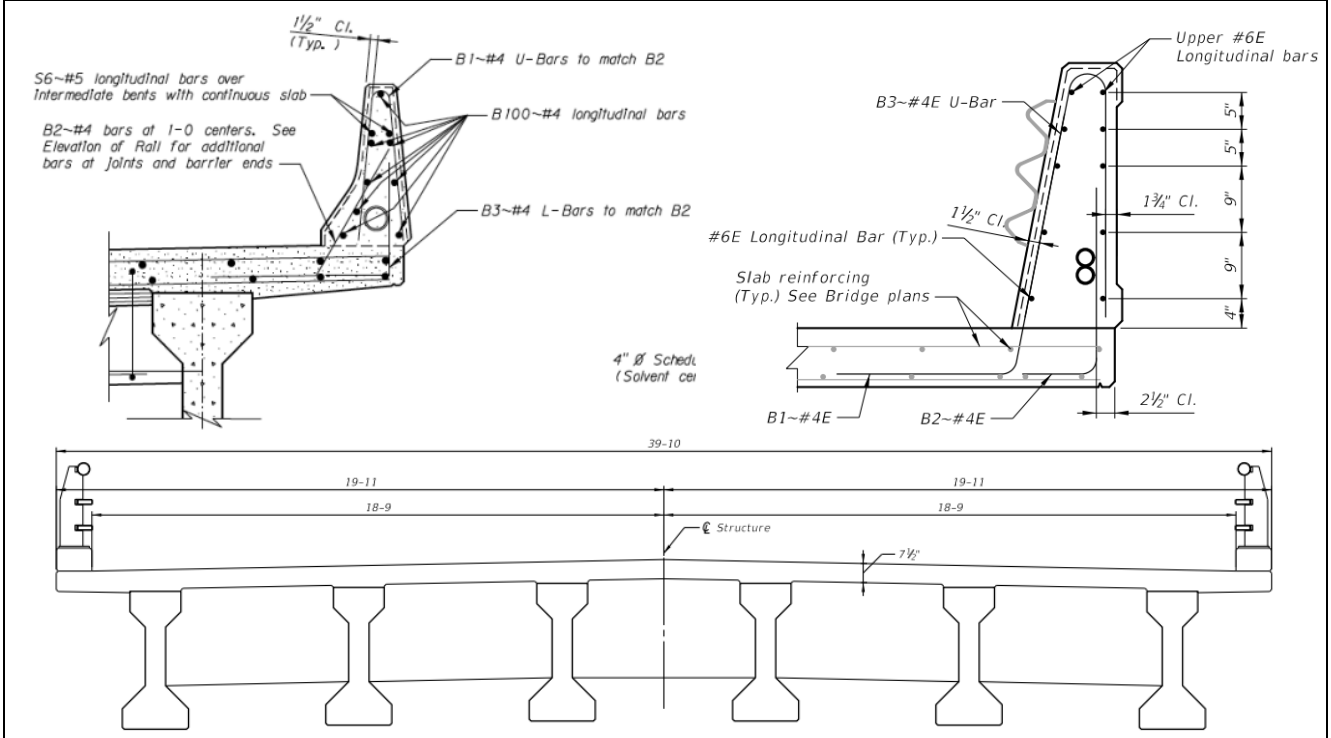

Nebraska (NE) DOT

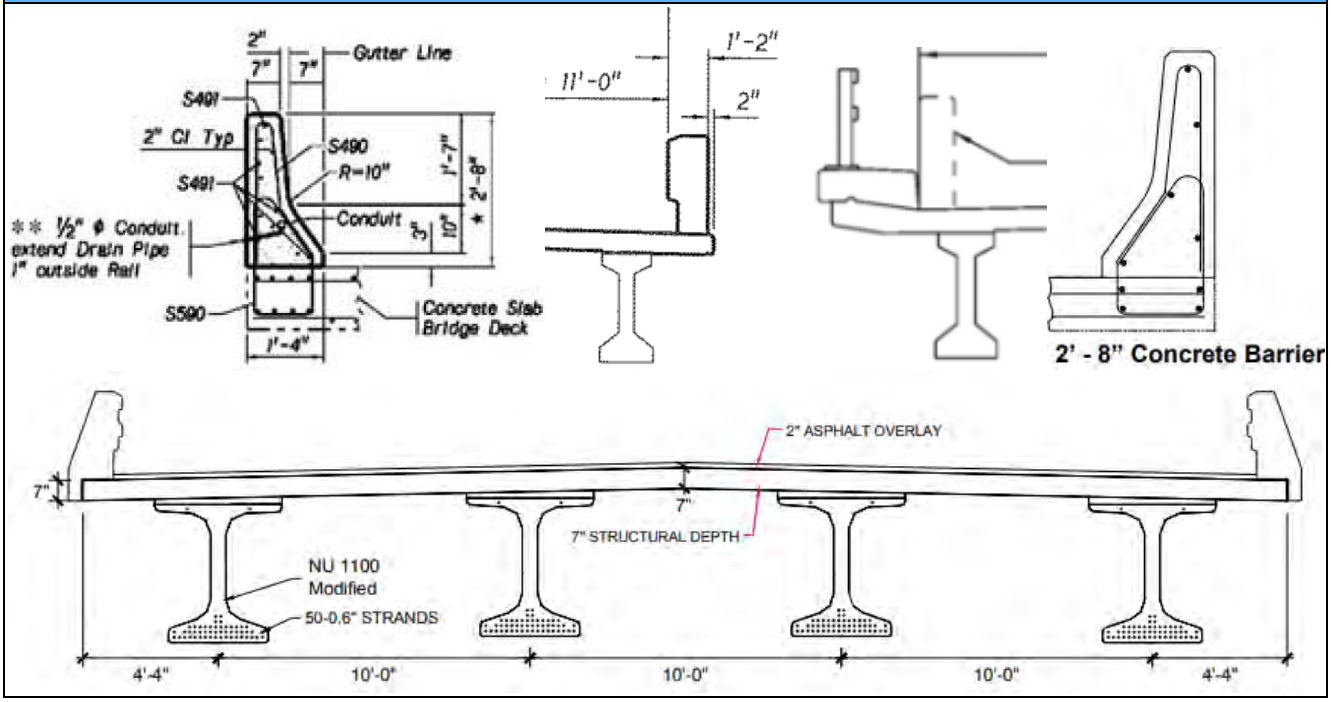

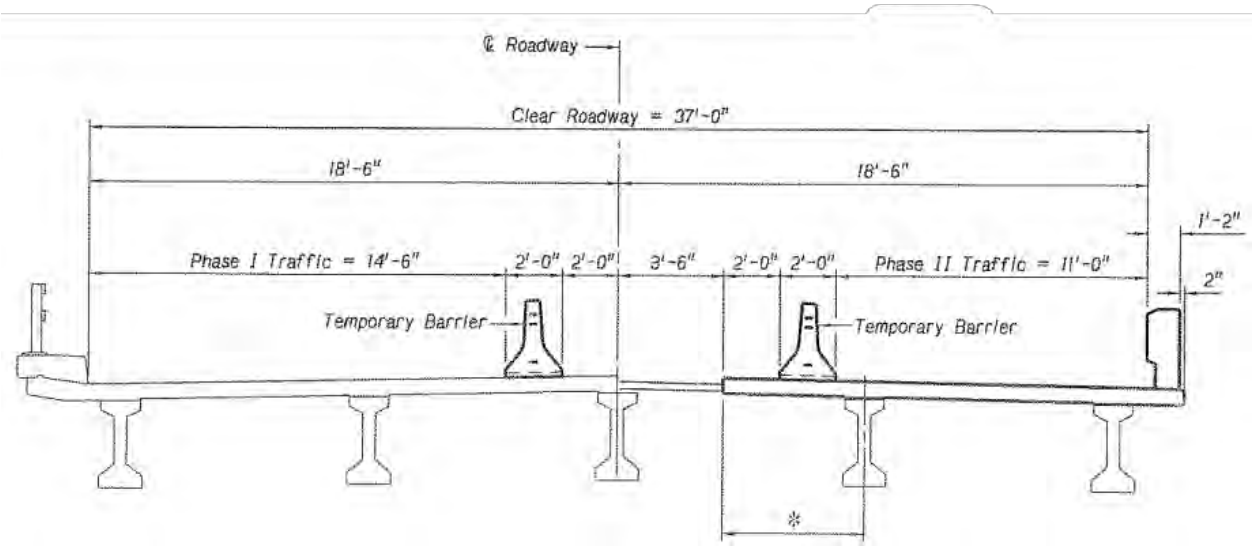

Nevada (NV) DOT

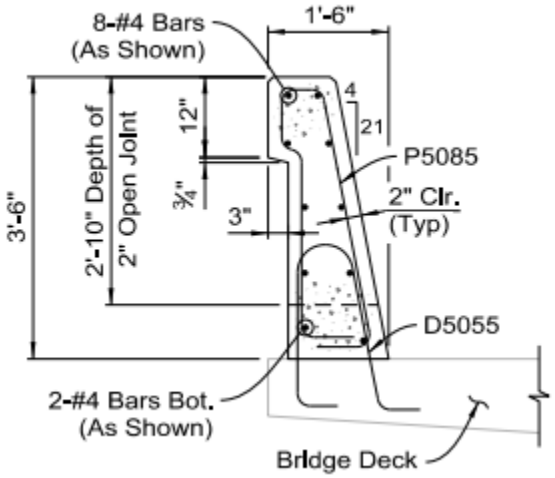

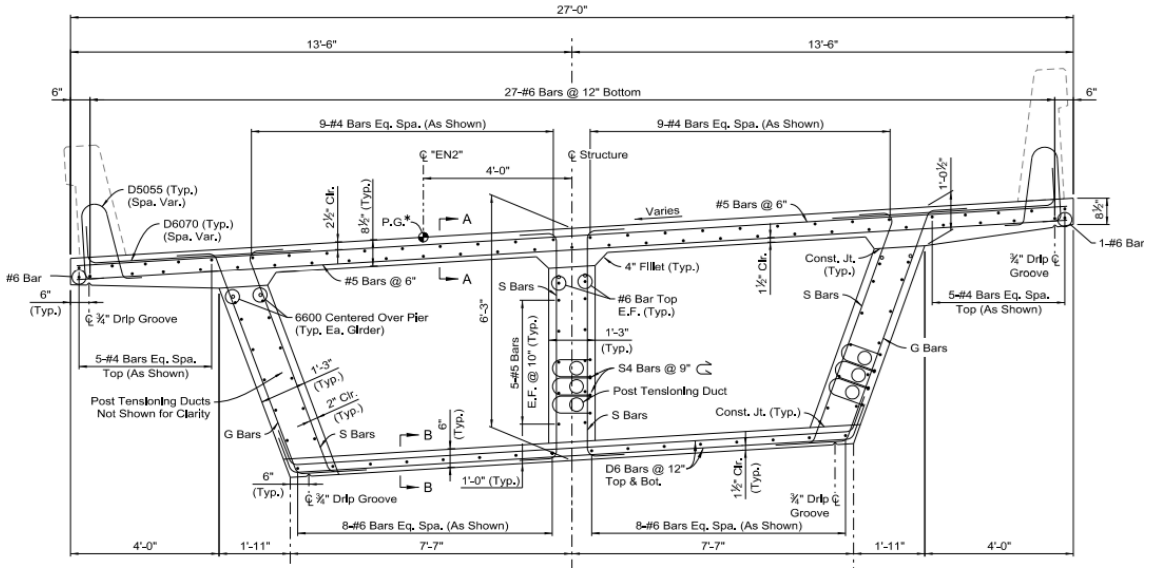

New Hampshire (NH) DOT

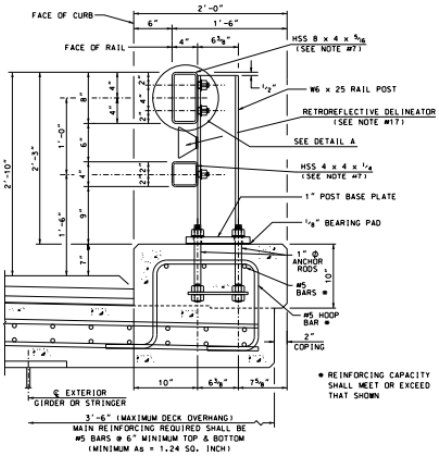

New Jersey (NJ) DOT

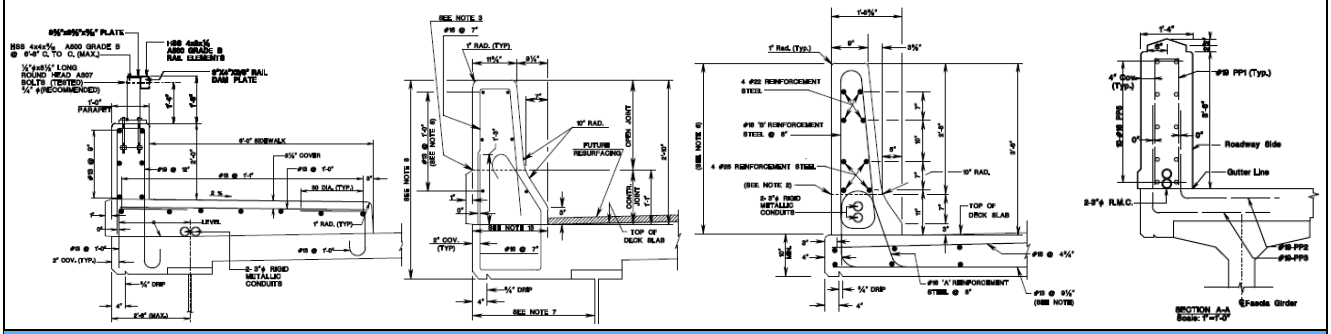

New Mexico (NM) DOT

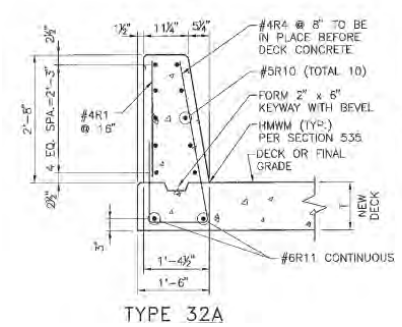

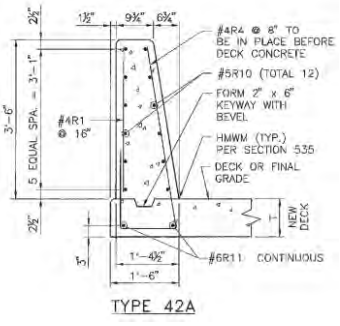

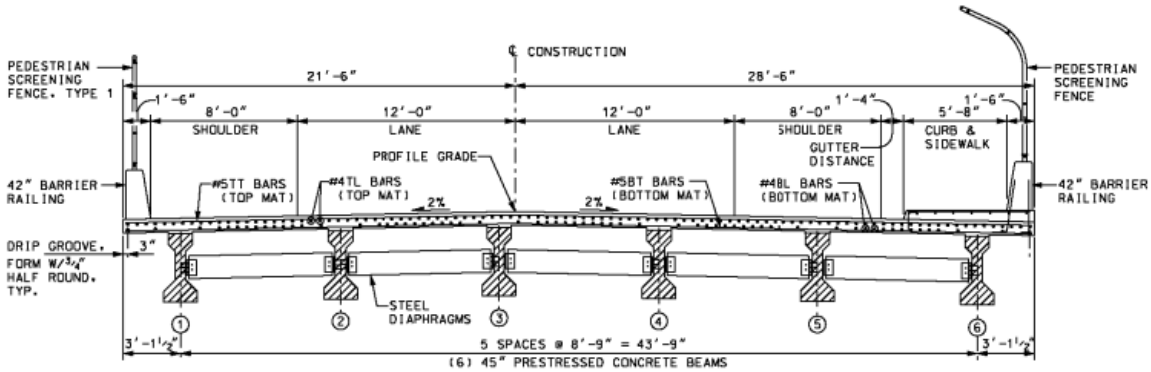

TRANSVERSE SECTION

New York (NY) DOT

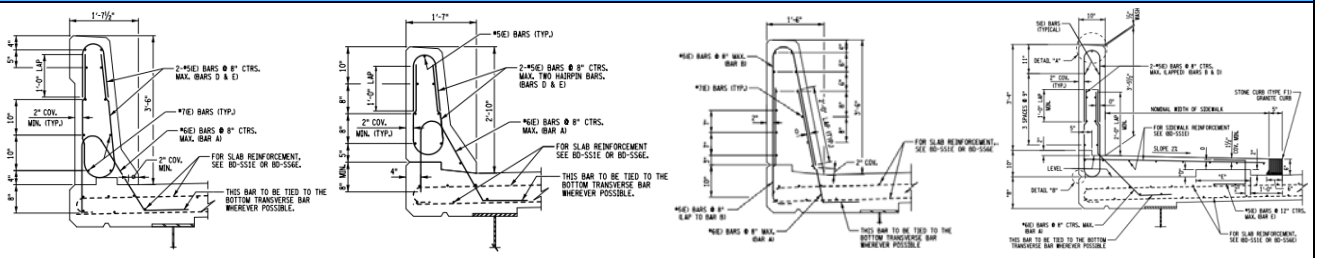

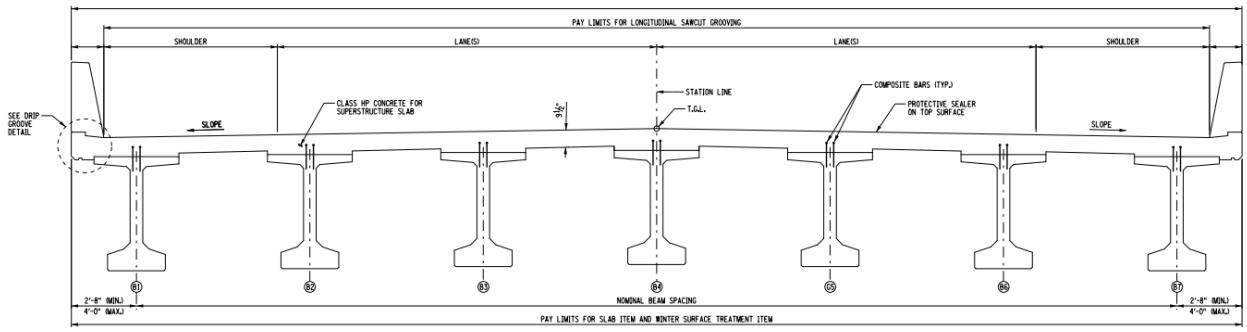

NEBT/PCFF TRANSVERSE SECTION

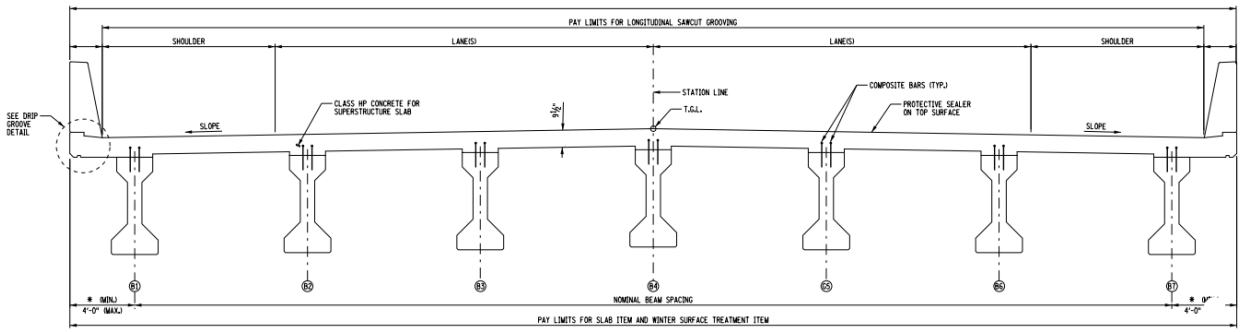

AASHTO I-BEAM TRANSVERSE SECTION

North Carolina (NC) DOT

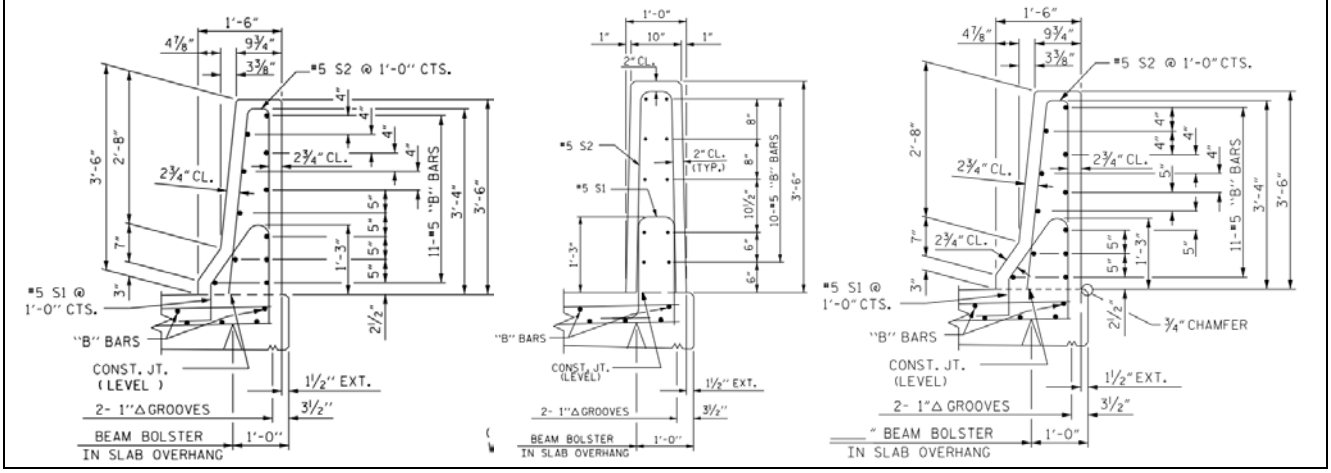

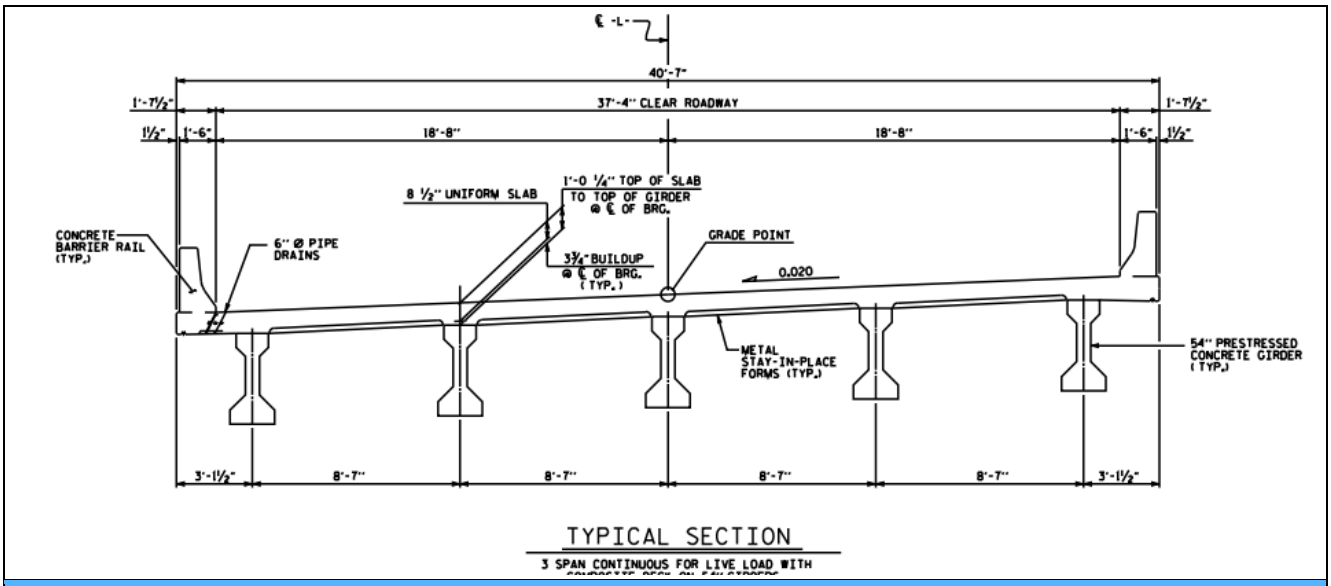

TYPICAL SECTION

3 SPAN CONTINUOUS FOR LIVE LOAD WITH

North Dakota (ND) DOT

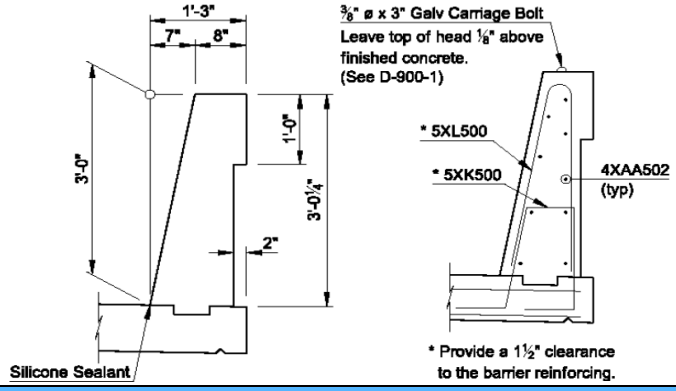

Ohio (OH) DOT

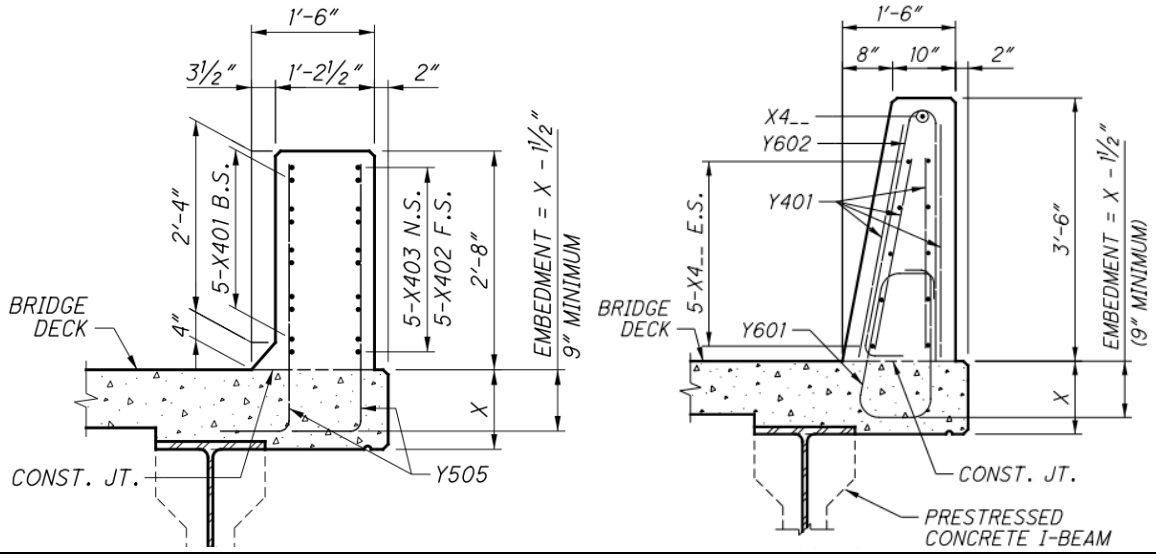

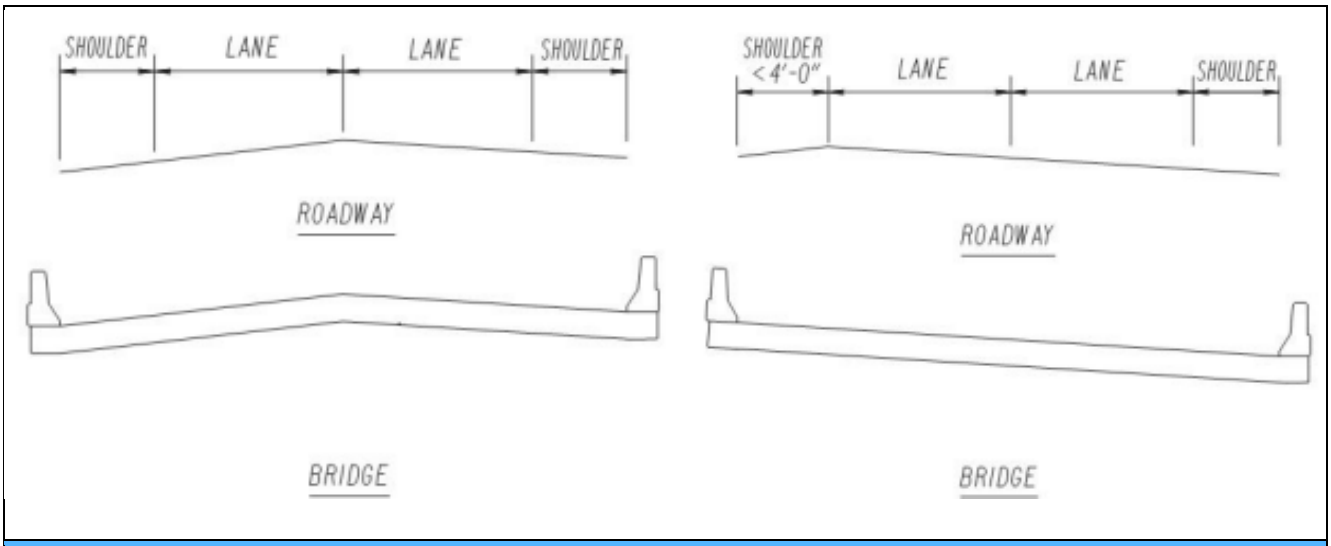

Oklahoma (OK) DOT

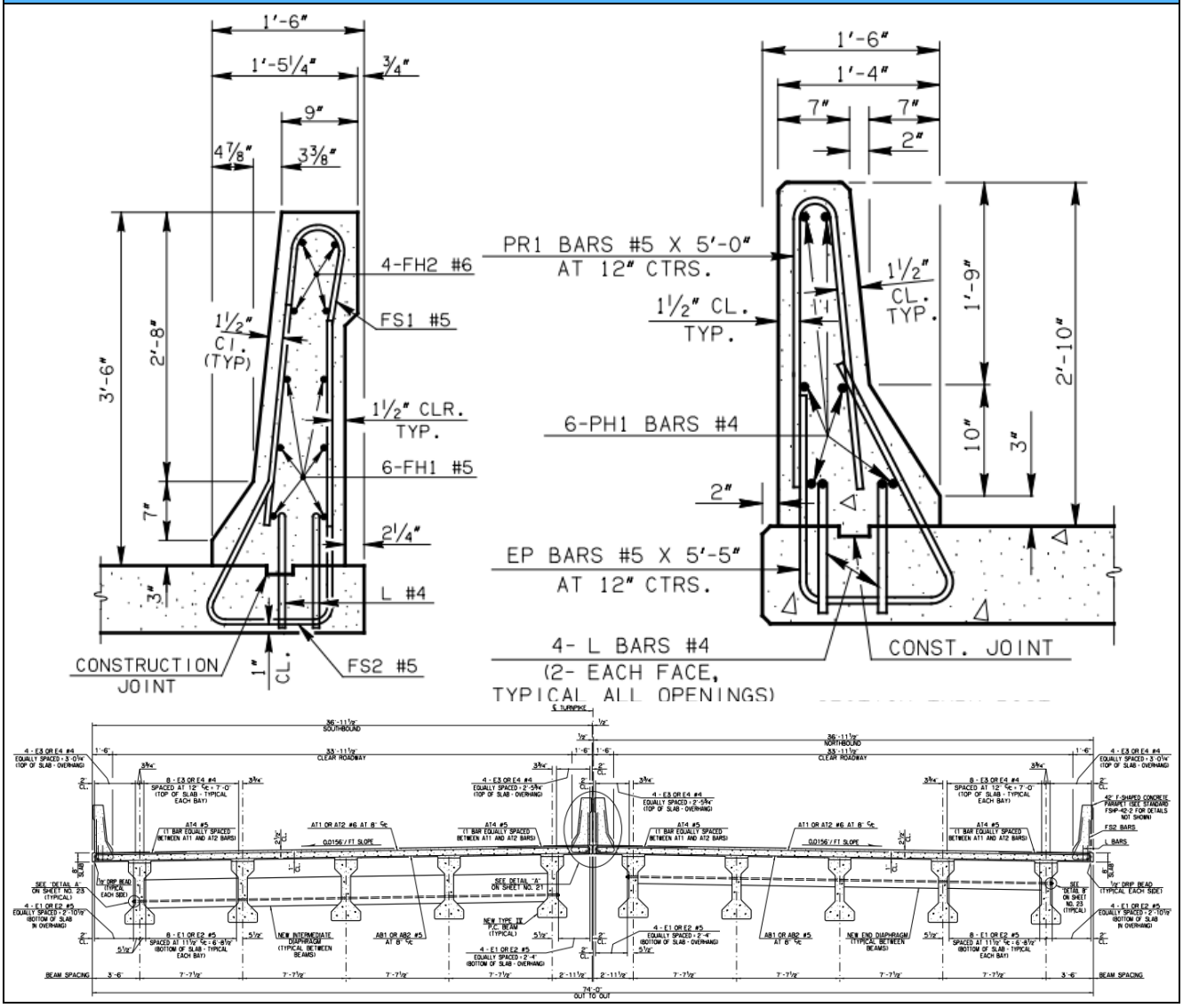

Oregon (OR) DOT

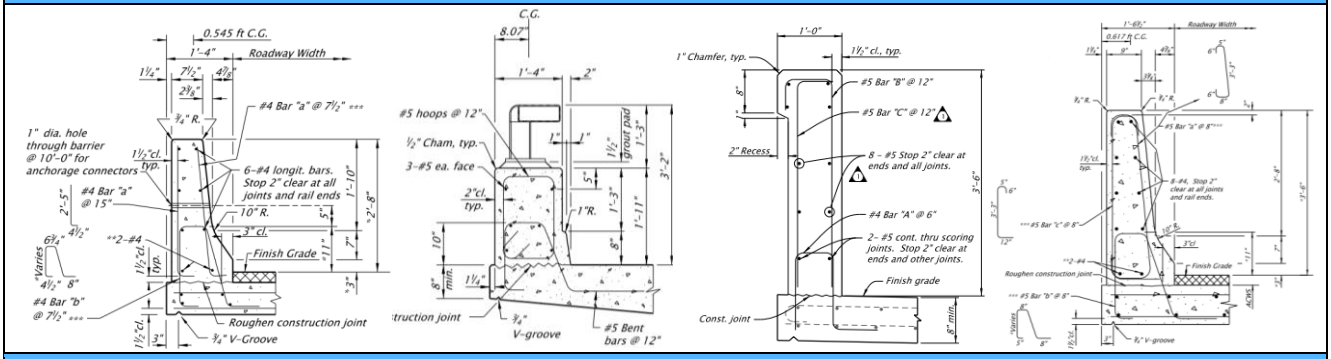

Pennsylvania (PA) DOT

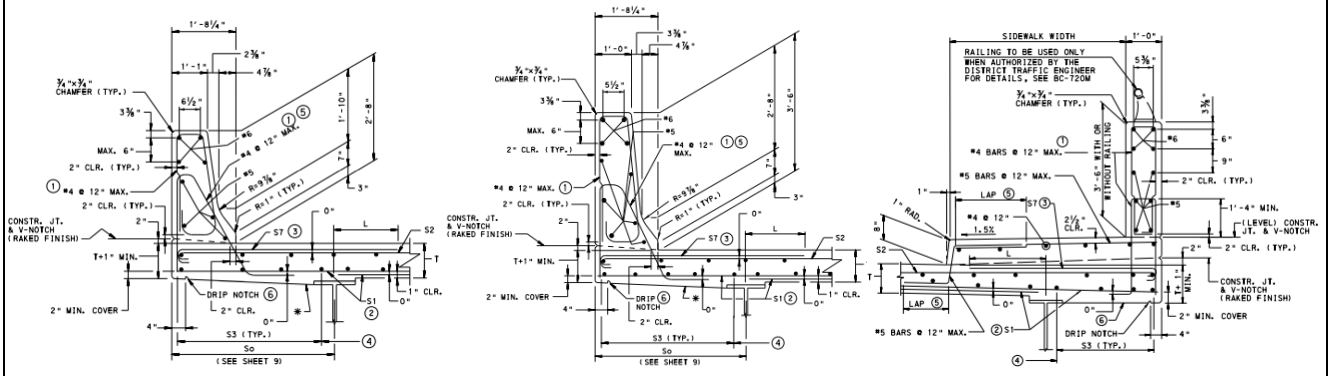

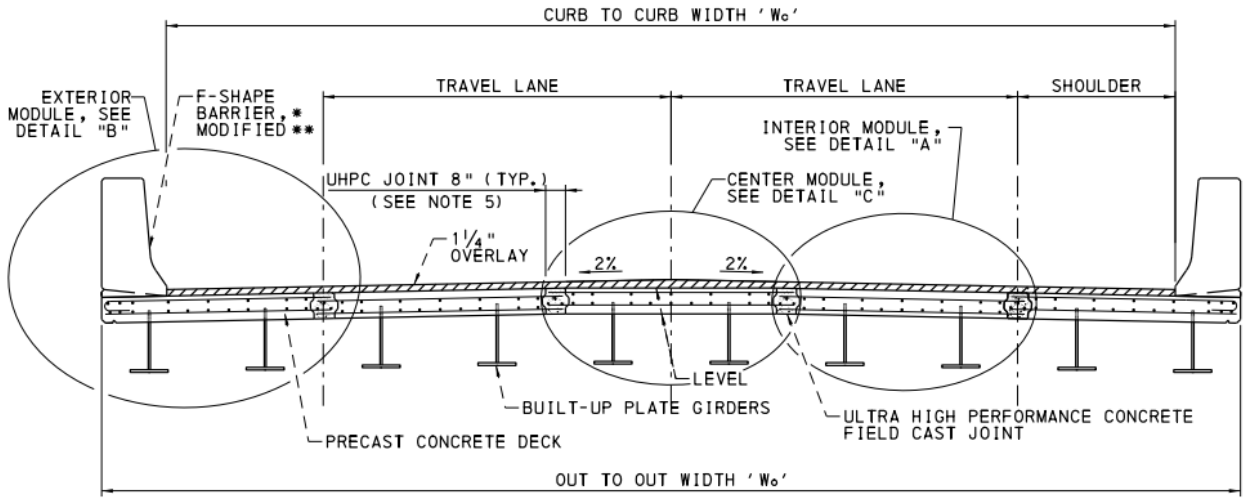

TYPICAL DECK SECTION - DOUBLE MODULE (ODD NUMBER OF MODULES)

Rhode Island (RI) DOT

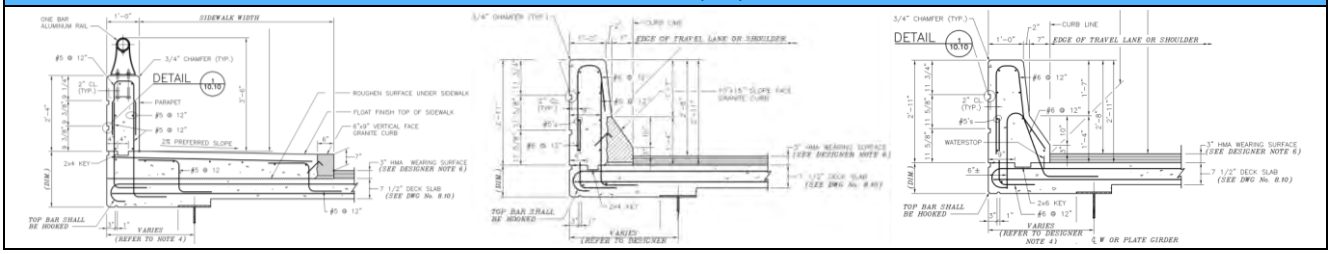

South Carolina (SC) DOT

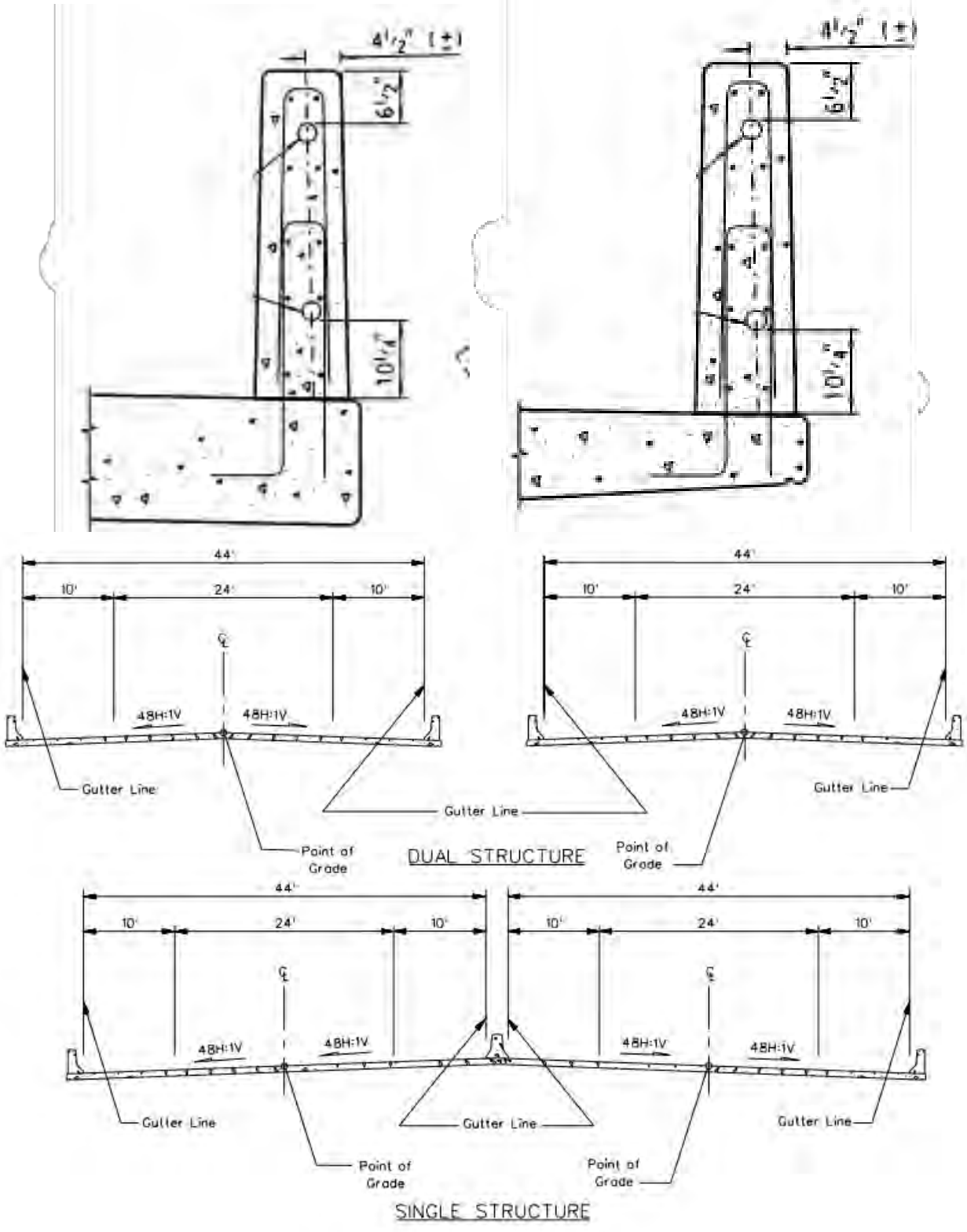

BRIDGE CROSS SECTION

South Dakota (SD) DOT

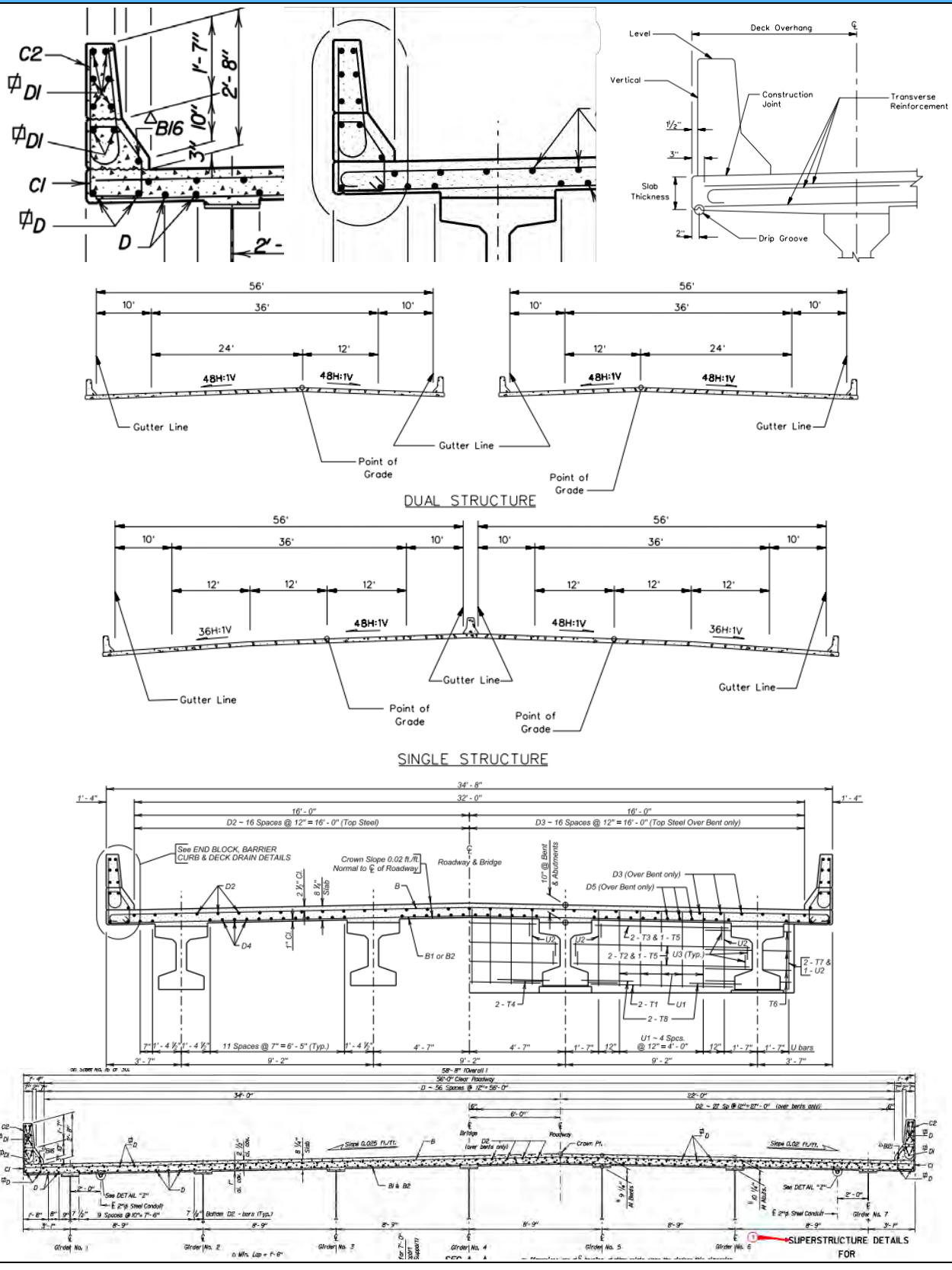

Tennessee (TN) DOT

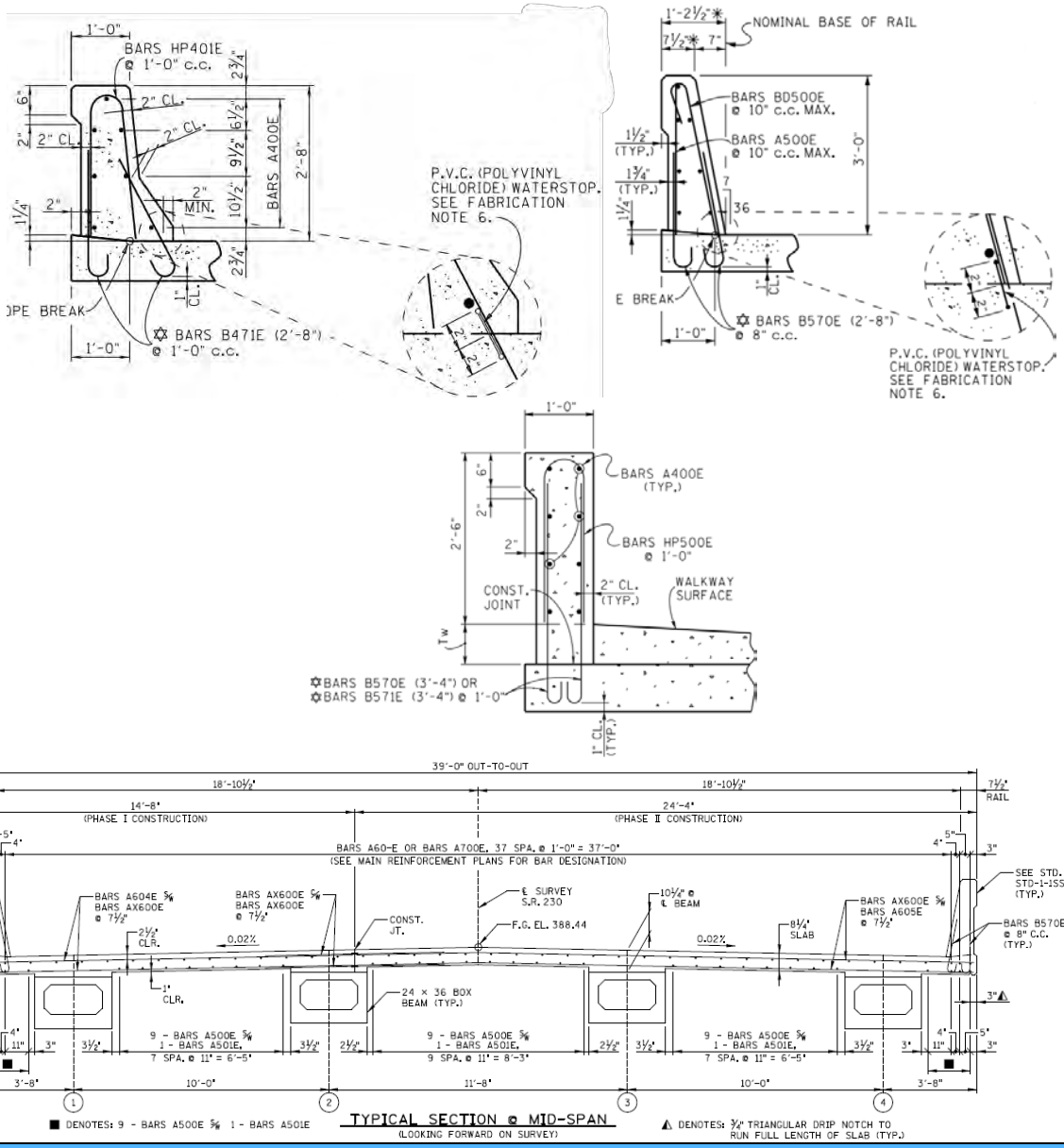

Texas (TX) DOT

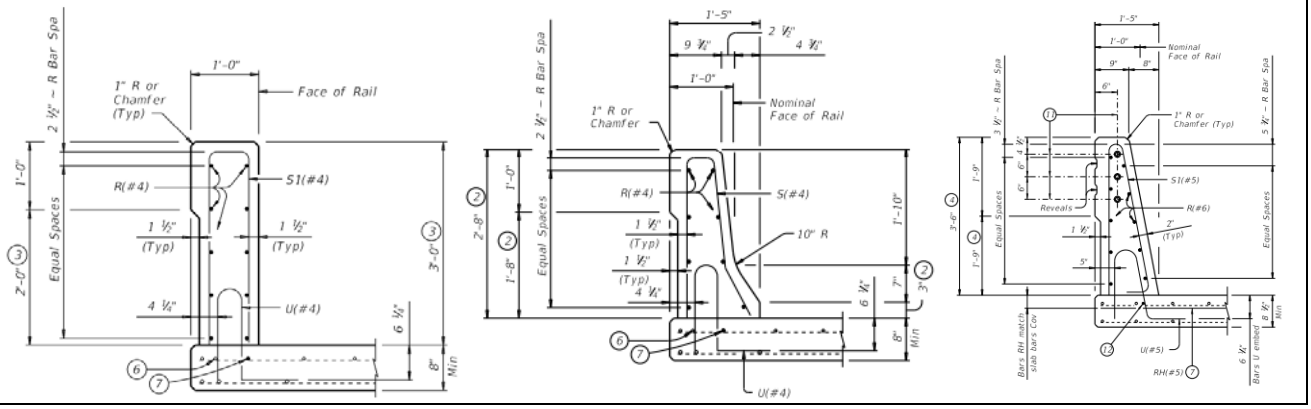

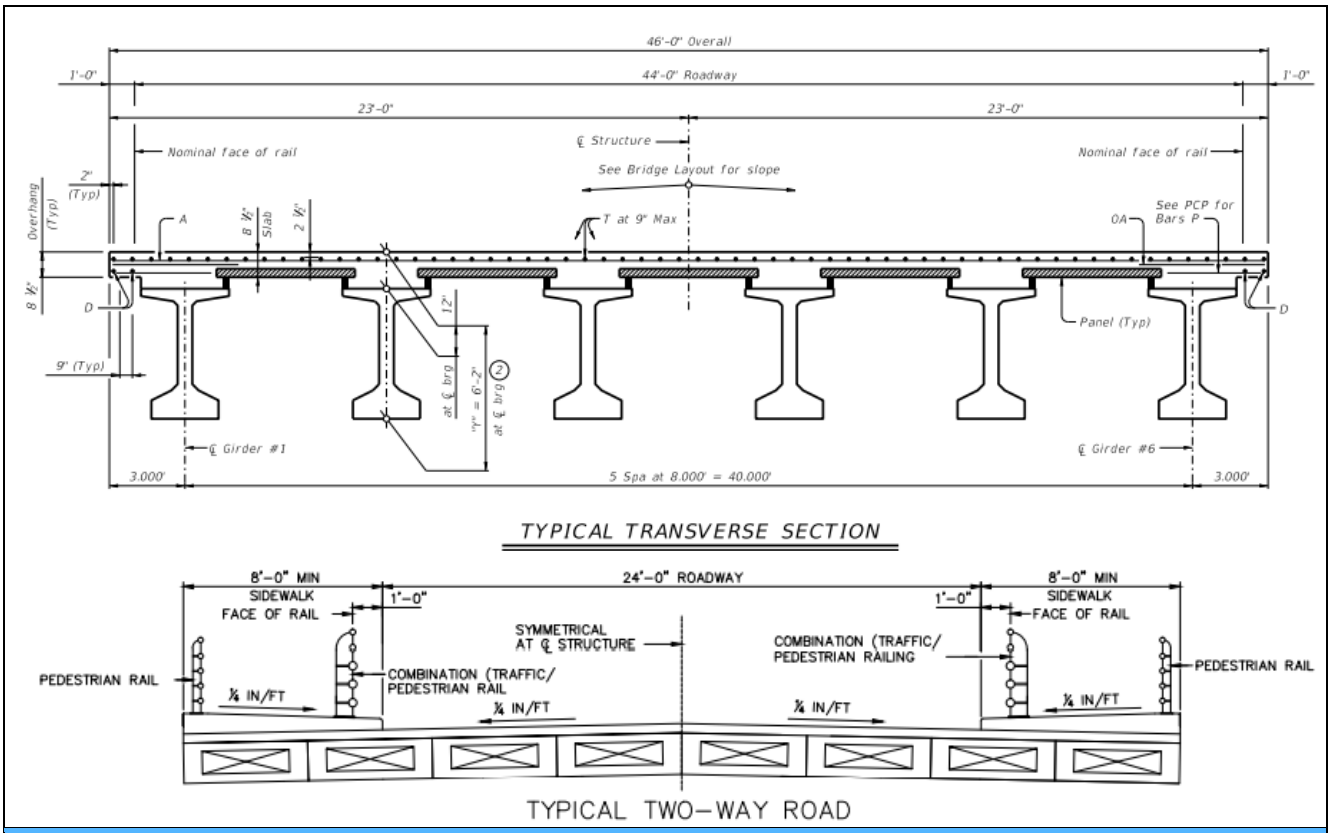
46'-0" Overall
1'-0"
44'-0" Roadway
1'-0"
23'-0"
23'-0"
Nominal face of rail
℄ Structure
See Bridge Layout for slope
Nominal face of rail
2" (Typ)
Overhang (Typ)
A
8 ½" Slab
2 ½"
T at 9" Max
See PCP for Bars P
0A
8 ½"
D
12"
"Y" = 6'-2"
at ℄ brg
at ℄ brg
Panel (Typ)
D
9" (Typ)
℄ Girder #1
℄ Girder #6
3.000'
5 Spa at 8.000' = 40.000'
3.000'
TYPICAL TRANSVERSE SECTION
8'-0" MIN SIDEWALK FACE OF RAIL
1'-0"
24'-0" ROADWAY
1'-0"
8'-0" MIN SIDEWALK FACE OF RAIL
SYMMETRICAL AT ℄ STRUCTURE
PEDESTRIAN RAIL
¼ IN/FT
COMBINATION (TRAFFIC/ PEDESTRIAN RAIL
¼ IN/FT
¼ IN/FT
COMBINATION (TRAFFIC/ PEDESTRIAN RAILING
¼ IN/FT
PEDESTRIAN RAIL
TYPICAL TWO-WAY ROAD

Utah (UT) DOT

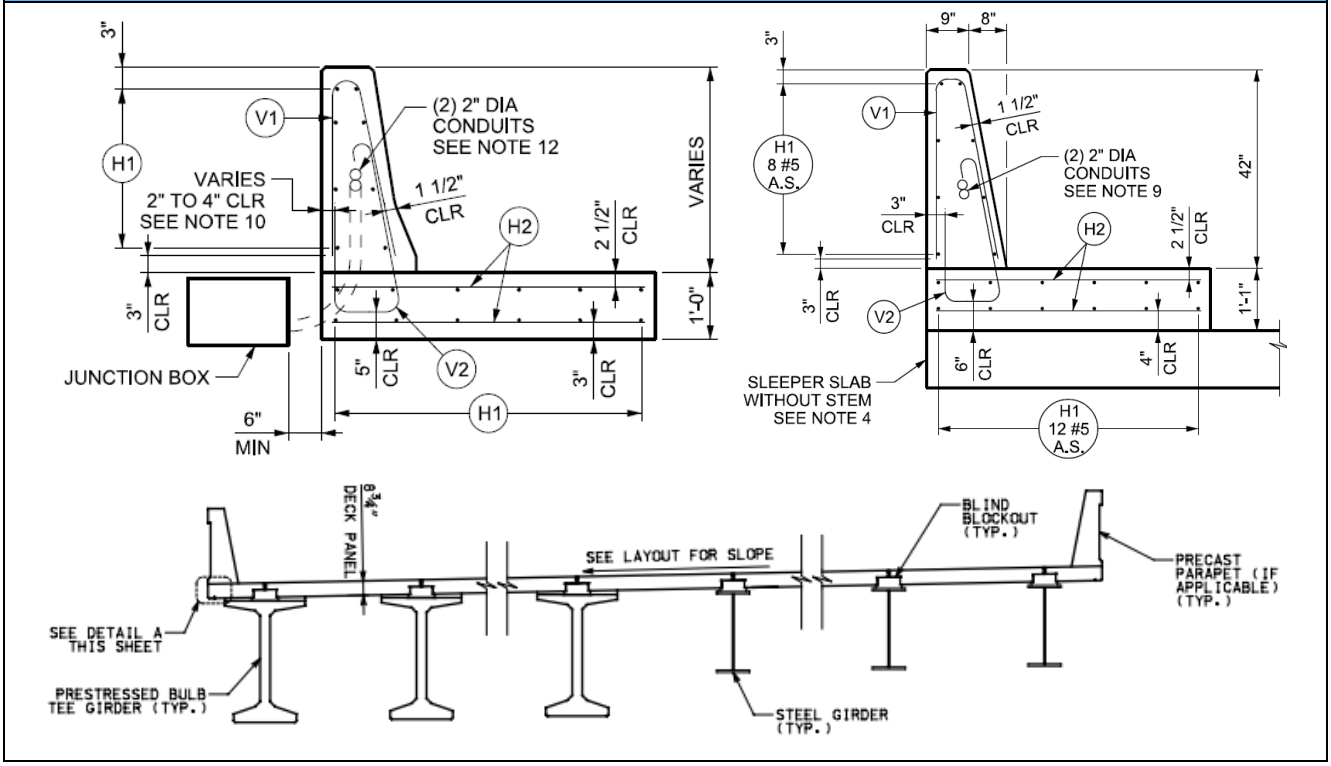
3"
V1
H1
VARIES 2" TO 4" CLR SEE NOTE 10
(2) 2" DIA CONDUITS SEE NOTE 12
1 1/2" CLR
H2
2 1/2" CLR
VARIES
1'-0"
3" CLR
JUNCTION BOX
5" CLR
V2
3" CLR
H1
6" MIN
9"
8"
3"
V1
1 1/2" CLR
H1 8 #5 A.S.
(2) 2" DIA CONDUITS SEE NOTE 9
42"
3" CLR
H2
2 1/2" CLR
1'-1"
3" CLR
V2
6" CLR
4" CLR
SLEEPER SLAB WITHOUT STEM SEE NOTE 4
H1 12 #5 A.S.
8¾" DECK PANEL
SEE LAYOUT FOR SLOPE
BLIND BLOCKOUT (TYP.)
PRECAST PARAPET (IF APPLICABLE) (TYP.)
SEE DETAIL A THIS SHEET
PRESTRESSED BULB TEE GIRDER (TYP.)
STEEL GIRDER (TYP.)

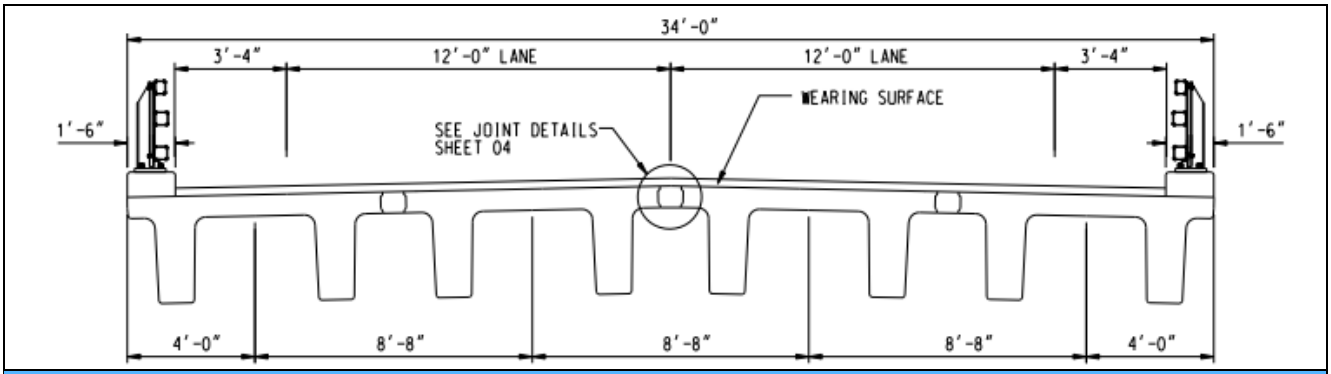

Vermont (VT) DOT

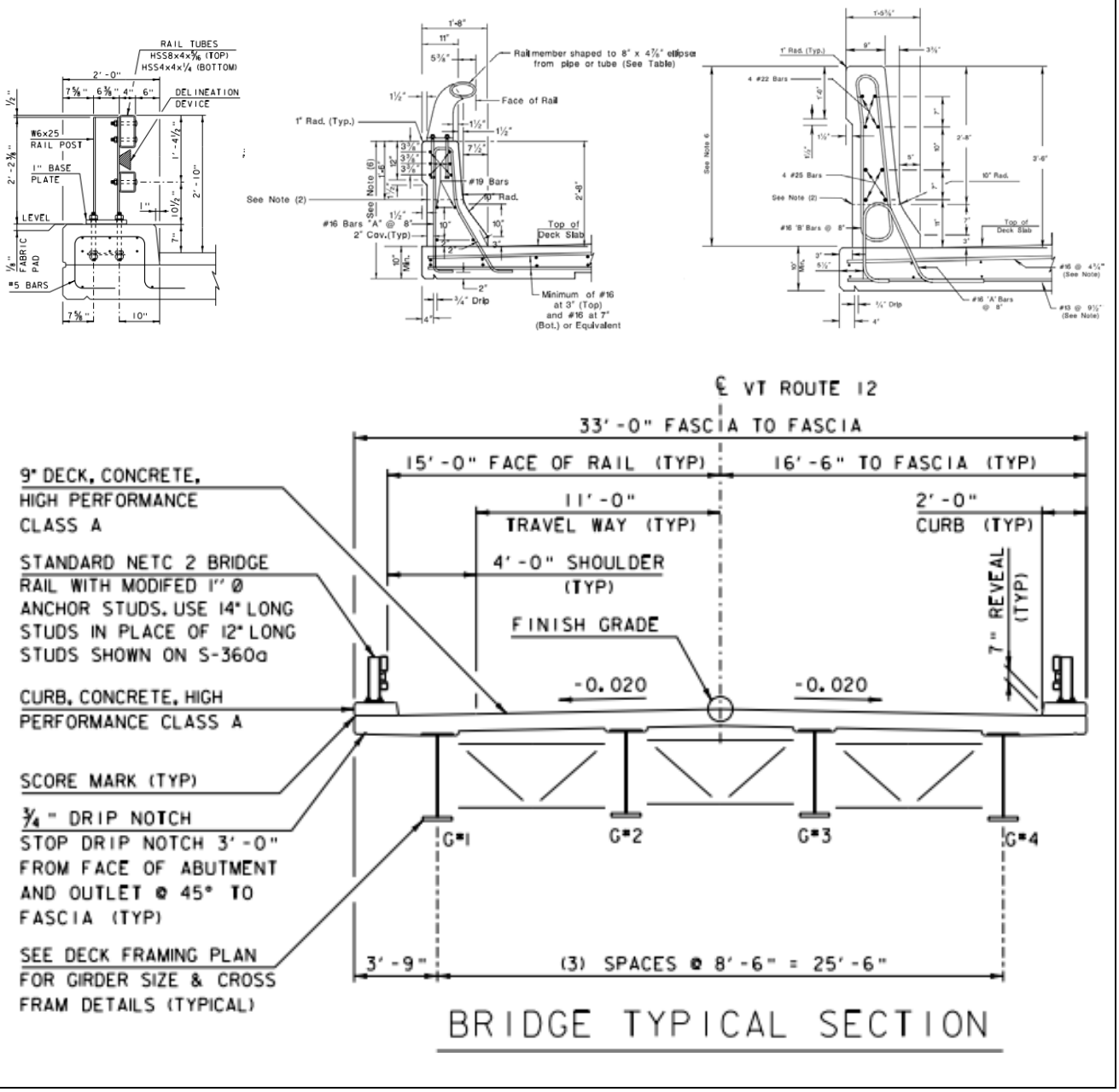

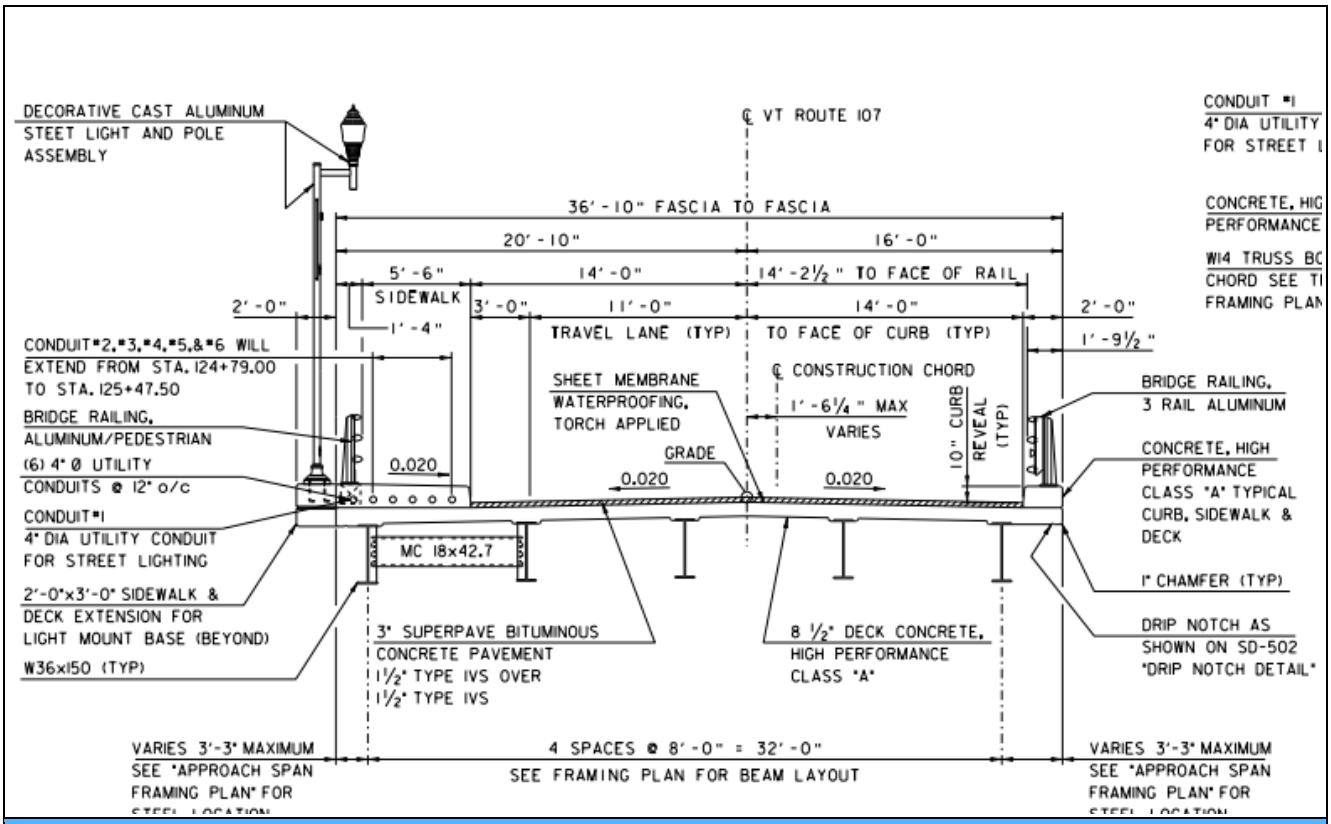

Virginia (VA) DOT

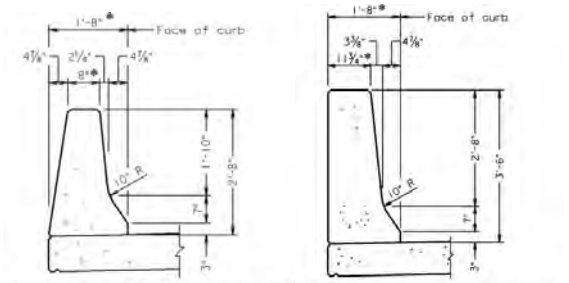

32" - CONCRETE PARAPET (F-SHAPE) BPB-3A, BPB-3B, BPB3C AND BPB-3D

42" - CONCRETE PARAPET (F-SHAPE) BPB-4

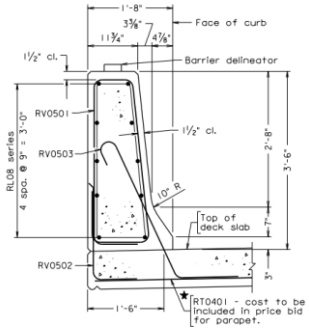

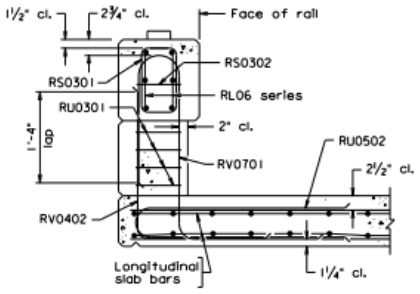

DECK SLABS

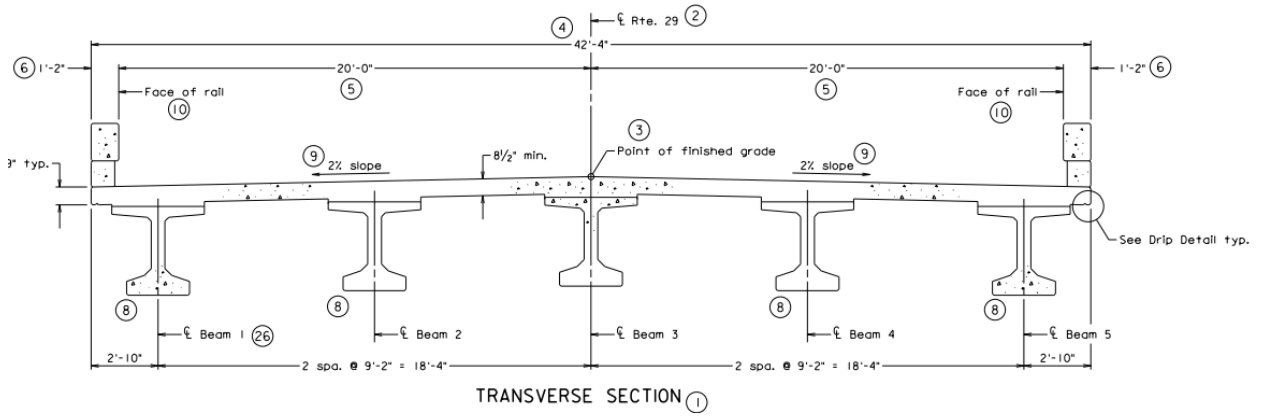

TRANSVERSE SECTION (1)

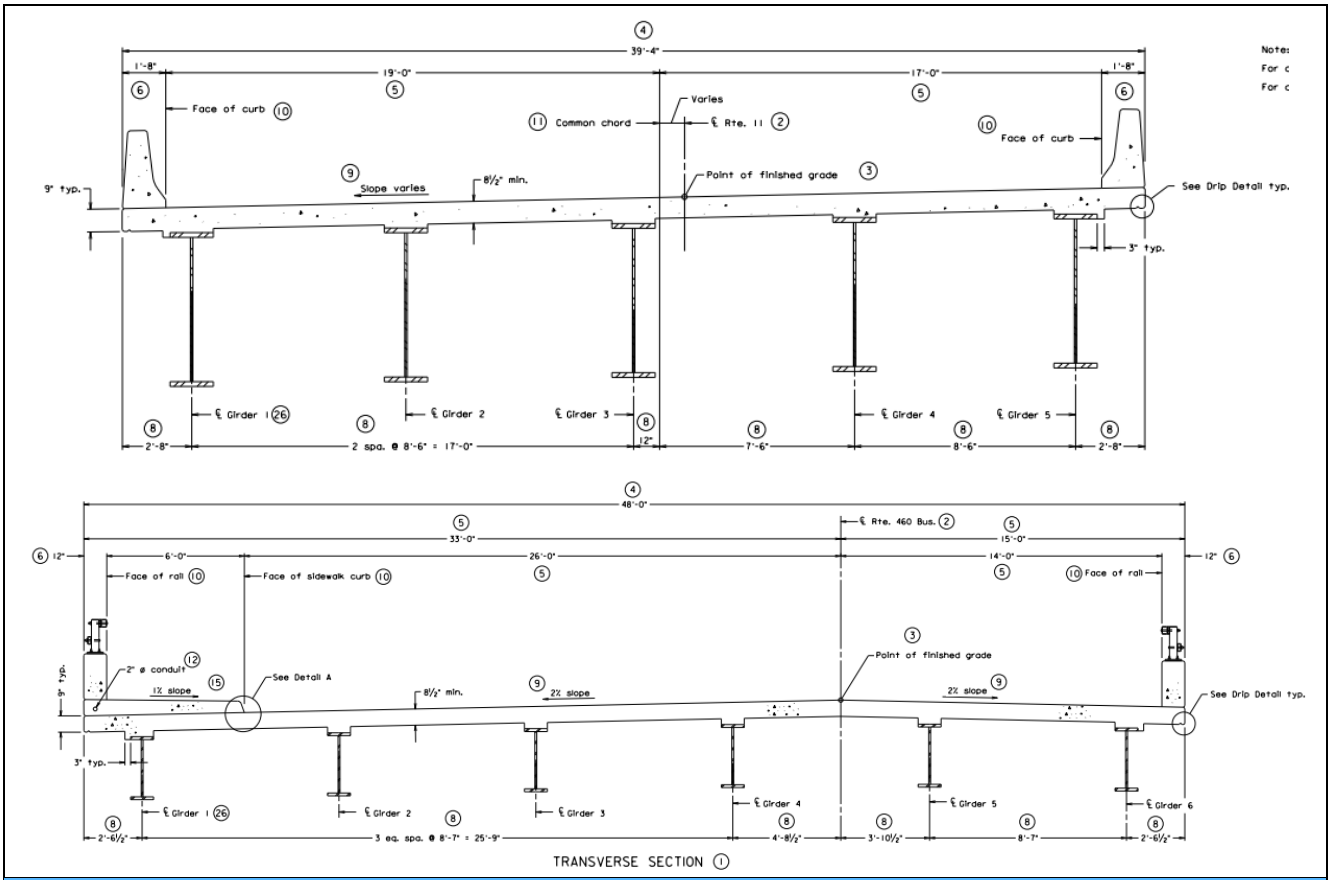

TRANSVERSE SECTION ①

Washington (WA) DOT

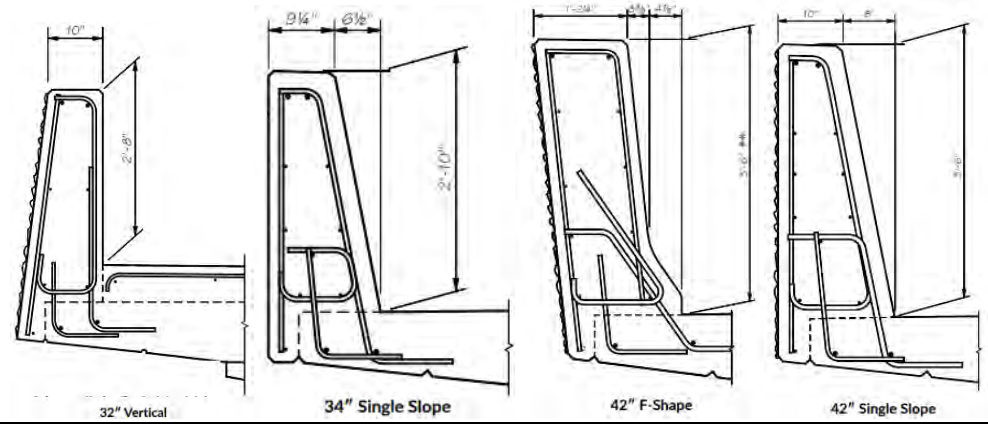

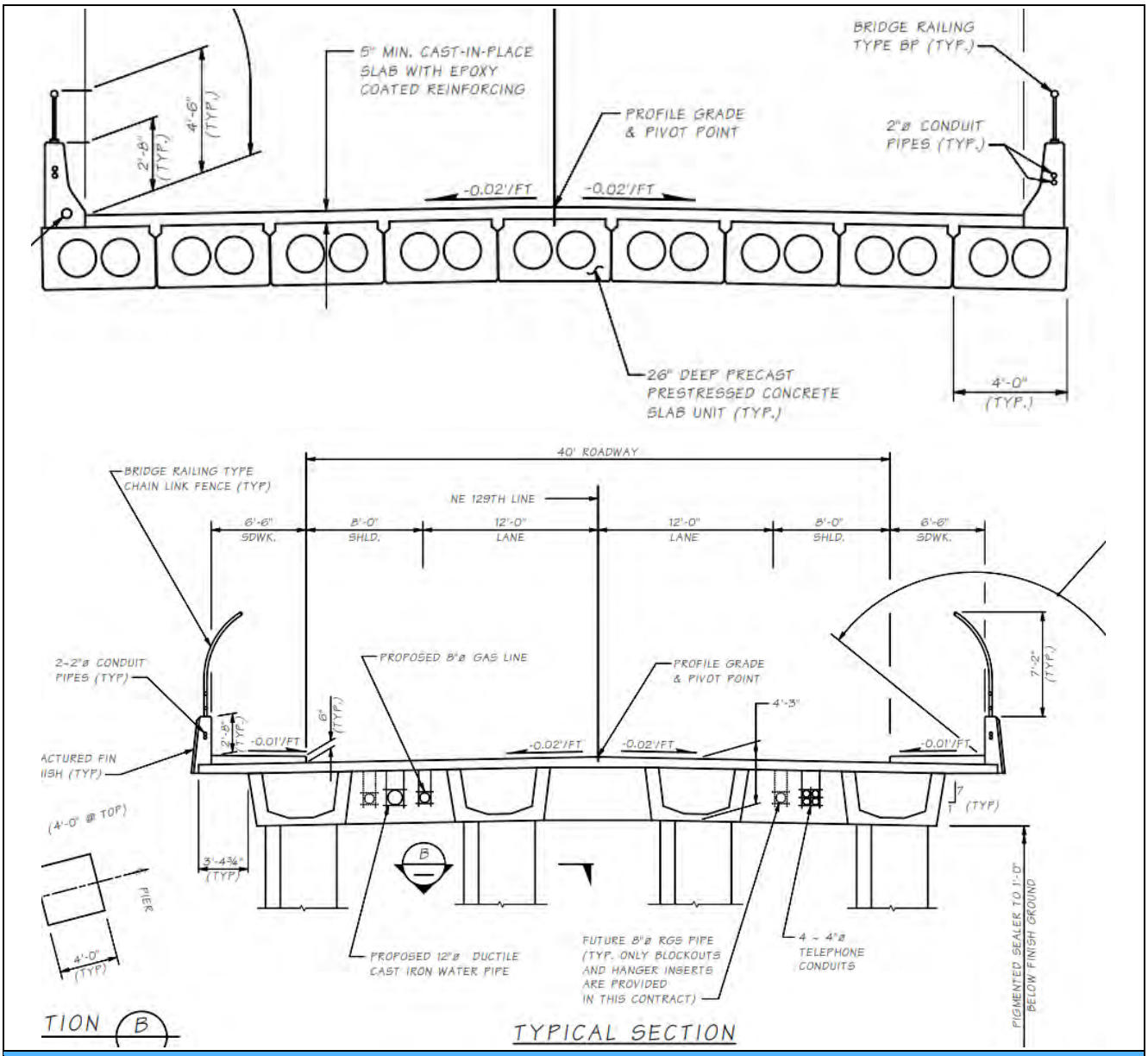

West Virginia (WV) DOT

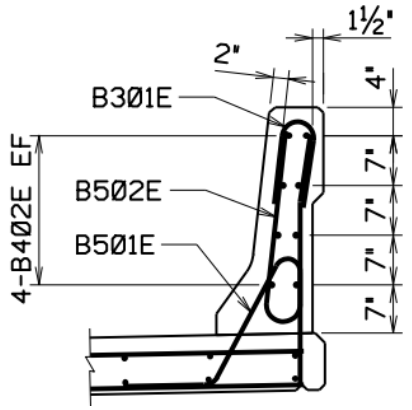

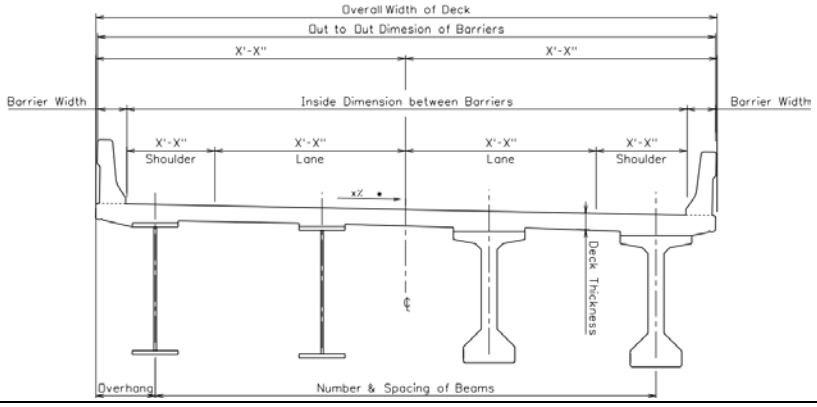

Wisconsin (WI) DOT

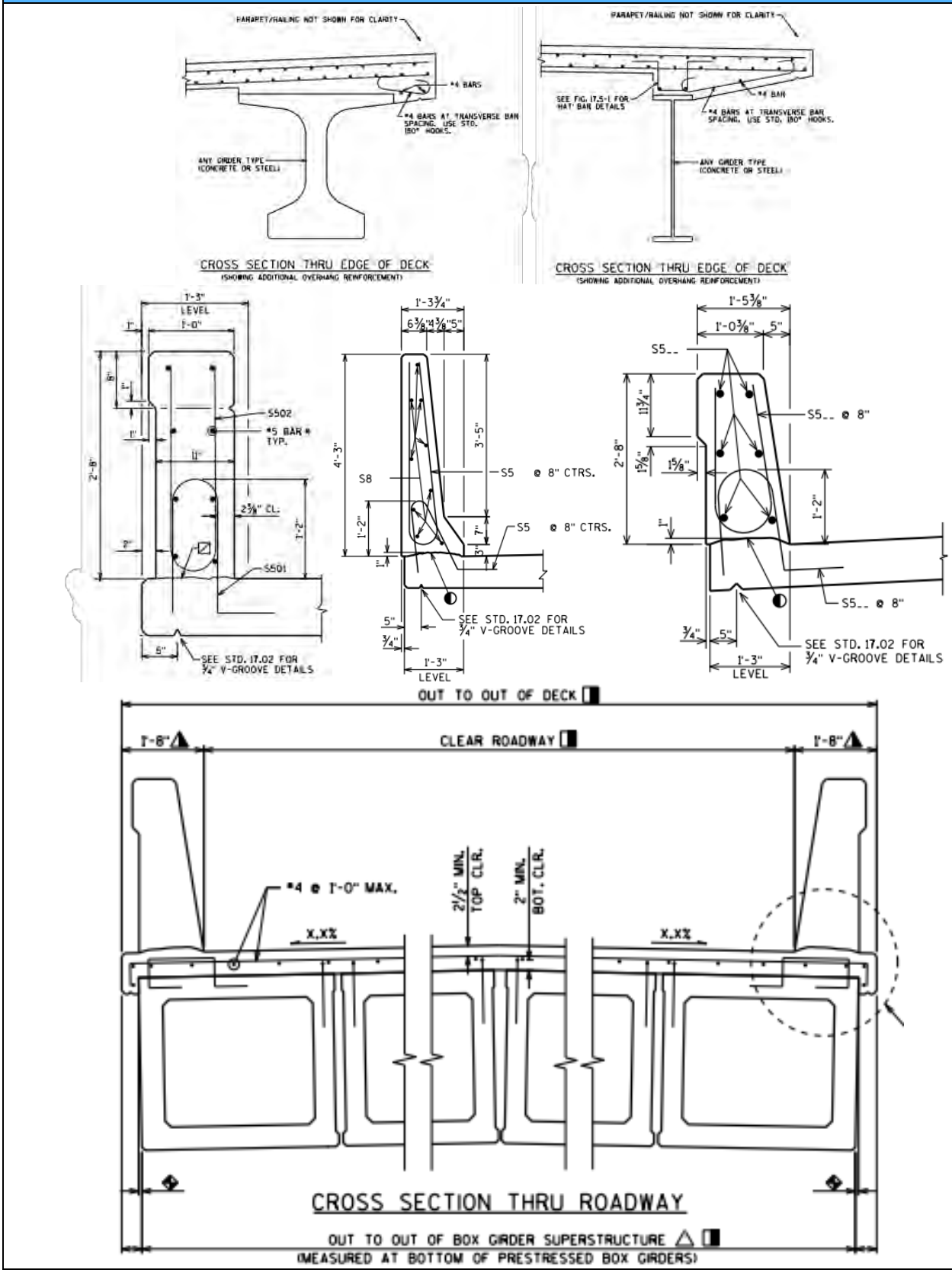

Wyoming (WY) DOT

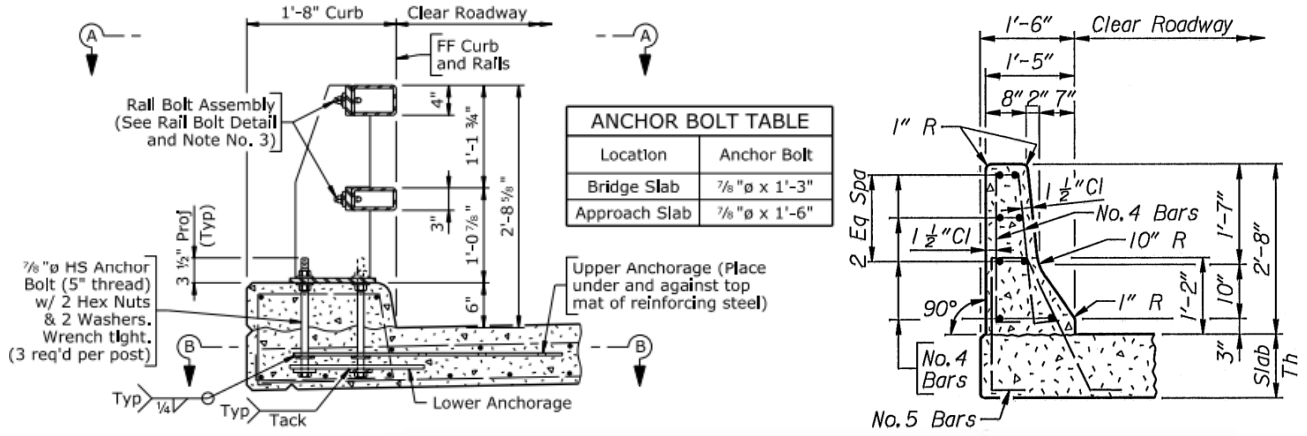

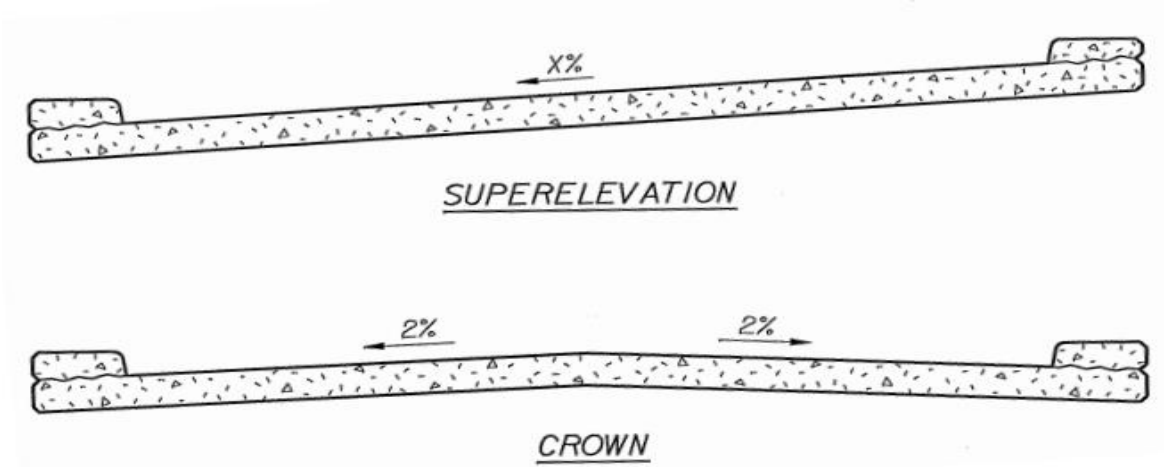

Appendix D: Bridges with Deteriorated Deck Fascia

Note: All figures provided in this appendix are obtained from either Google Maps or relevant MDOT Bridge Design Inspection Reports uploaded to MiBridge database.

D.1. Bridges Identified by MDOT

a)

b)

c)

Fig. D.1 I-96 EB over M-99: a-b) lower side; c) upper side

a)

b)

c)  d) 

Fig. D.2 I-496 WB Ramp over CSX Railroad: a-b) lower side; c-d) upper side (obtained from MDOT inspection report conducted on 3/19/2021)

a)  b) 

c)  d) 

Fig. D.3 I-75 NB over Lake State Railroad: a-b) lower side; c-d) upper side (obtained from MDOT inspection report conducted on 09/27/2021)

a)

b)

c)

Fig. D.4 US-31 SB US-31 Business Route: a) lower side; b-c) upper side

a)

b)

c)

d)

Fig. D.5 M-43 WB (Grand River) over US-127: a-b) lower side; c-d) upper side

a)

b)

c)

d)

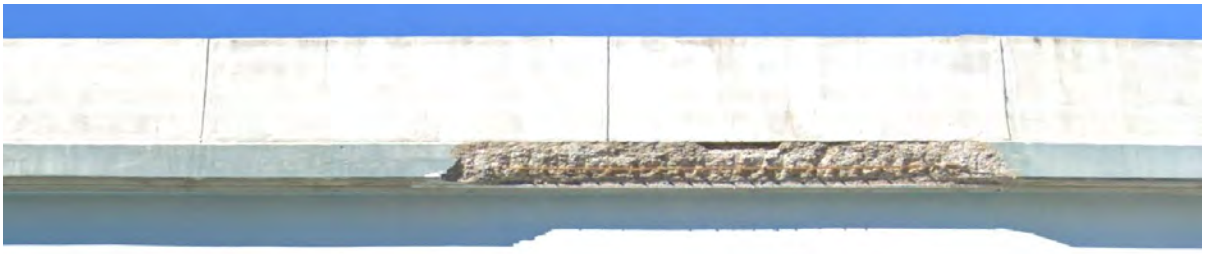

e)

Fig. D.6 Webster Rd. over I-69: a-c) lower side; d-e) upper side

a)

b)

c)

d)

Fig. D.7 County Rd. 612 over I-75 SB: a) lower side; b-d) upper side

a)

b)

c)

d)

e)

Fig. D.8 US-127 NB over Kalamazoo St.: a-b) lower side; c-e) upper side

a)

b)

c)

d)

e)

f)

Fig. D.9 I-496 WB over CSX Railroad & Trowbridge Ramp: a-b) lower side; c-f) upper side

Fig. D.10 Luther Rd. over US-131: a-c) lower side; d-f) upper side

a)


b)


c)


d)


e)


Fig. D.11 M-59 / I-96 Bl. over I-96: a-c) lower side; d-e) upper side

a)

b)

c)

d)

e)

Fig. D.12 I-96 WB over M-99: a-b) lower side; c-e) upper side

a)

b)

c)

d)

e)

Fig. D.13 Milwaukee Rd. over US-23: a-b) lower side; c-e) upper side

a)

b)

c)

d)

e)

Fig. D.14 I-496 EB over CSX Railroad & Trowbridge Ramp: a-c) lower side; d-e) upper side

a)

b)

c)

d)

e)

Fig. D.15 I-296 WB connector over I-96 EB: a-b) lower side; c-e) upper side

a)

b)

c)

d)

Fig. D.16 I-75 NB over Charles Brink: a-c) lower side; d) upper side

a)

b)

c)

e)

Fig. D.17 I-496 WB over US-127 SB Ramp: a) lower side; b-e) upper side

a)

b)

c)

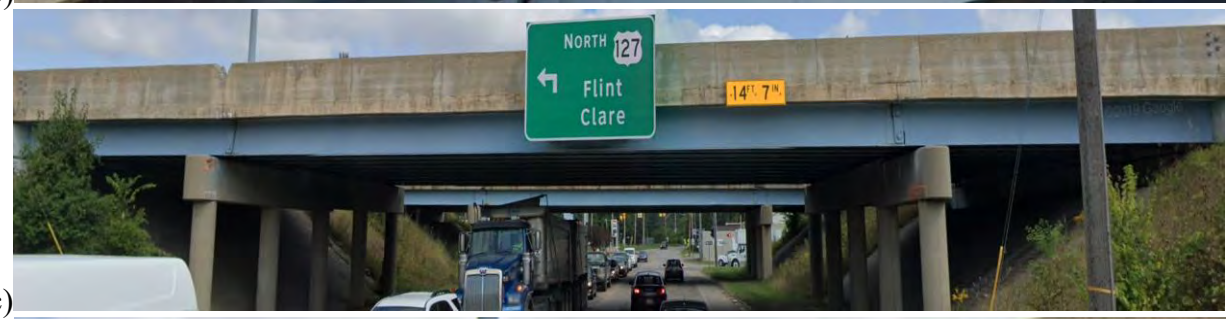

d)

Fig. D.18 US-127 SB over Kalamazoo St.: a-b) lower side; c-d) upper side

a)

b)

Fig. D.19 I-296WB / US-131 over Ann St.: a) lower side; b) upper side

a)

b)

Fig. D.20 Leroy Rd. over US-131: a) lower side; b) upper side

D.2. Bridges Identified by WSU

a)

b)

c)

d)

Fig. D.21 McGraw Ave. over I-96 in Detroit: a-b) lower side; c-d) upper side

a)

b)

c)

d)

Fig. D.22 Brush St. over I-75: a-b) lower side; c-d) upper side

a)

b)

c)

d)

Fig. D.23 Larned St. over I-375: a-b) lower side; c-d) upper side

a)

b)

c)

Fig. D.24 Junction Ave. over I-75: a) lower side; b-c) upper side

a)

b)

c)

d)

Fig. D.25 Dragoon St. over I-75: a-b) lower side; c-d) upper side

a)

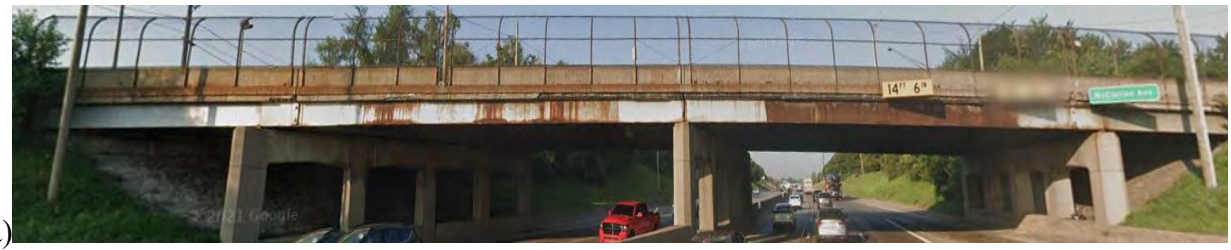

b)

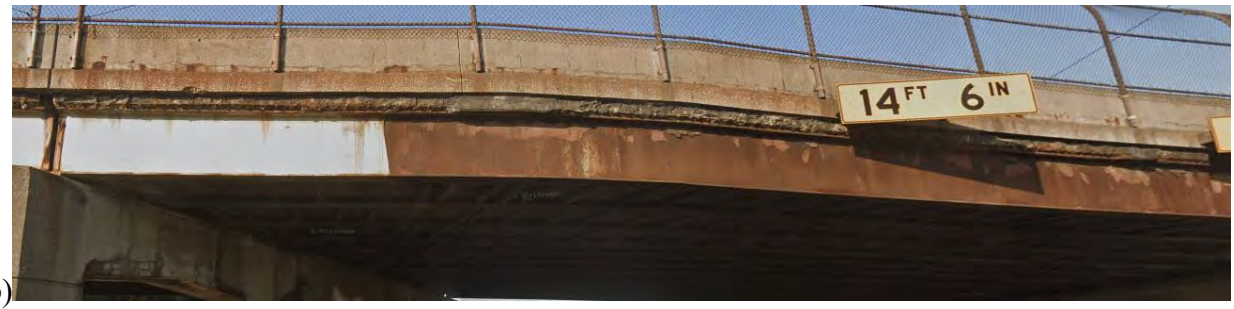

c)

d)

Fig. D.26 McClellan Ave. over I-94: a-b) lower side; c-d) upper side

a)

b)

c)

Fig. D.27 Holbrook Ave. over I-75: a) lower side; b-c) upper side

a)

b)

c)

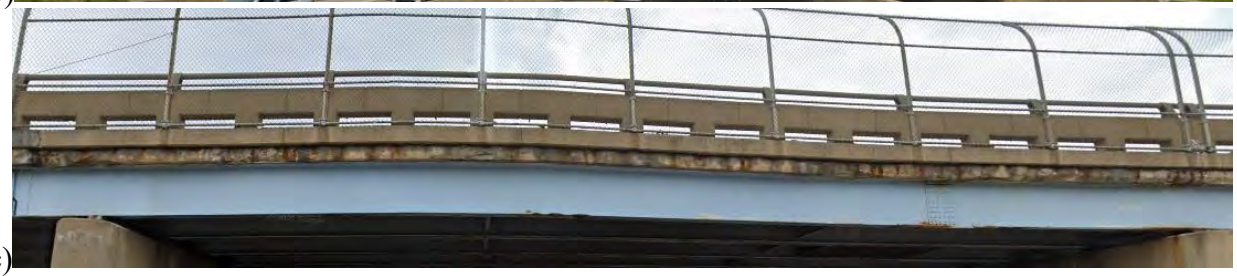

Fig. D.28 Rosa Parks Blvd. over I-75: a) lower side; b-c) upper side

a)

b)

c)

d)

Fig. D.29 Fullerton Ave. over I -96: a-b) lower side; c-d) upper side

a)

b)

c)

Fig. D.30 Schaefer Rd. over I-96: a-b) lower side; c-d) upper side

a)

b)

c)

d)

e)

Fig. D.31 Green Ave. Over I-75: a-c) lower side; d-e) upper side

a)

b)

c)

Fig. D.32 E Jefferson Ave. over I-375: a-b) lower side; c) upper side

a)

b)

c)

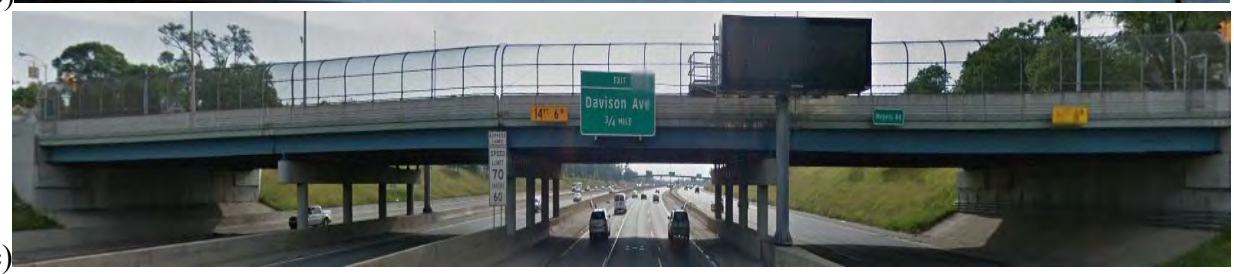

Fig. D.33 Meyers Rd. over I-96: a-b) lower side; c-d) upper side

Fig. D.34 Chrysler Dr. over I-375: a-b) lower side; c-d) upper side

a)

b)

c)

Fig. D.35 Hubbell Ave. over I-96: a-b) lower side; c) upper side

a)

b)

c)

d)

Fig. D.36 Waldon Rd. over I-75: a-c) lower side; d) upper side

a)

b)

c)

d)

Fig. D.37 Scotten Ave. over I-96: a-b) lower side; c-d) upper side

a)

b)

c)

d)

Fig. D.38 Belanger Ave. over I-696: a-b) lower side; c-d) upper side

a)
b)
c)

Fig. D.39 M-5 Grand River Ave. over I-96: a) lower side; b-c) upper side

a)
b)
c)
d)

Fig. D.40 Wyoming Ave. over I-96: a-b) lower side; c-d) upper side

Appendix E: Installation Guidance for the MDOT Barrier Program

MDOTBarrier v1.1 Installation Manual

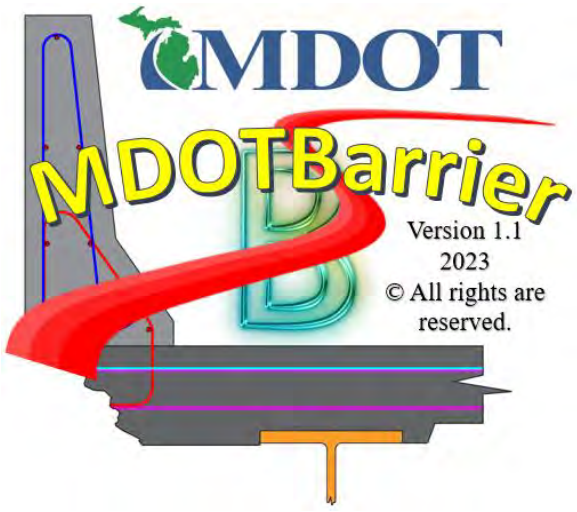

June 2023

MDOTBarrier v1.1 Installation Manual

- The executable file for the MDOTBarrier Computer program version v1.1 can be downloaded from this link.
- Click on the folder named "Installation (Executable) Files" (Fig. E.1a). You should see a total of three files (Fig. E.1b). Two of these files are executable files: 1) MDOTBarrier v1.1 (Runtime included).exe; and 2) MDOTBarrier v1.1 (Web Runtime). Since the program was developed in Matlab, it requires Matlab Runtime to run. The first executable file includes Matlab Runtime as part of the installation and does not require an internet connection. The second requires internet connection to download Matlab Runtime. Choose accordingly.
- Here the second option is selected for demonstration (Fig. E.2a). The downloaded file should have an icon similar to that shown in Fig. E.2b. Double click the selected executable file. A series of security warnings may appear. Click on "More Info" (Fig. E.3a), and then "Run anyway" (Fig. E.3b) buttons. If the user has an antivirus program or another firewall protection in his/her computer, this may prevent the installation of MDOT Barrier program. In this case, it is suggested to deactivate such virus protection programs temporarily until the MDOT Barrier program is installed. After you click on "Run anyway", the windows firewall defender may give a final warning as illustrated in Fig. E.3. By clicking the "Yes" button, you will initiate the installation of the MDOTBarrier program. Follow the prompts.
- Note that if you do not have Matlab Runtime installed in your computer this does not mean that you need a Matlab license to run the MDOT Barrier program. Matlab Runtime will be installed for free during the installation of the MDOT Barrier program if you choose the first option, or it will be downloaded for free from the internet if you choose the second option.
- Fig. E.4 shows likely prompts that may appear if Matlab Runtime is already installed in your computer.
- Fig. E.5 shows likely prompts if you do not have Matlab Runtime installed in your computer.

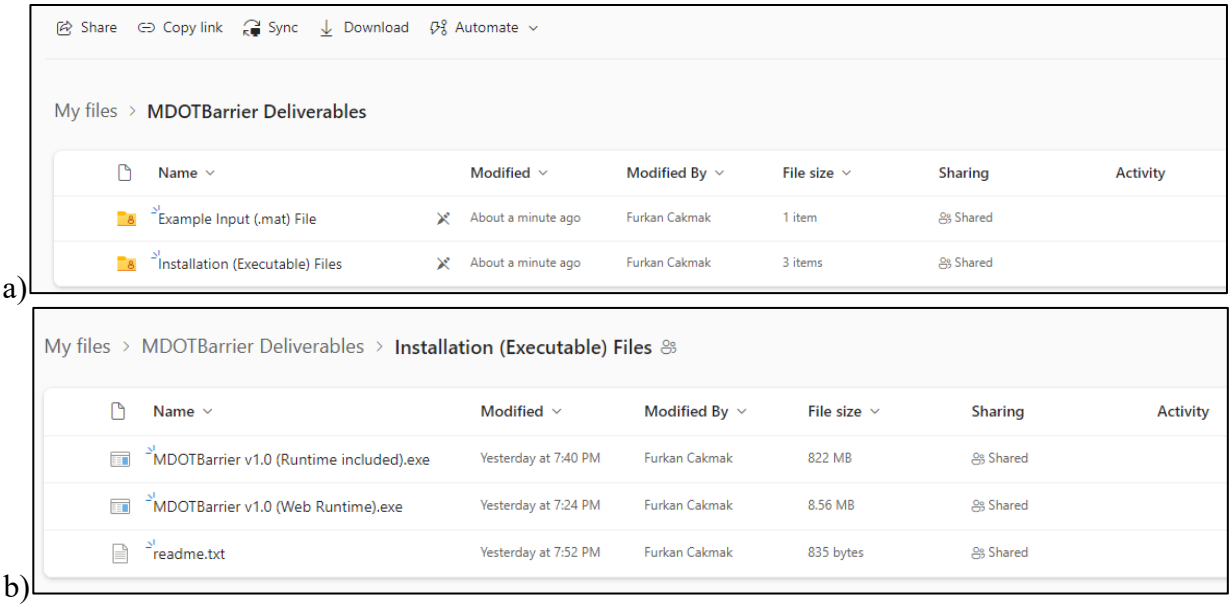

Fig. E.1 Downloading the executable file for the MDOTBarrier program

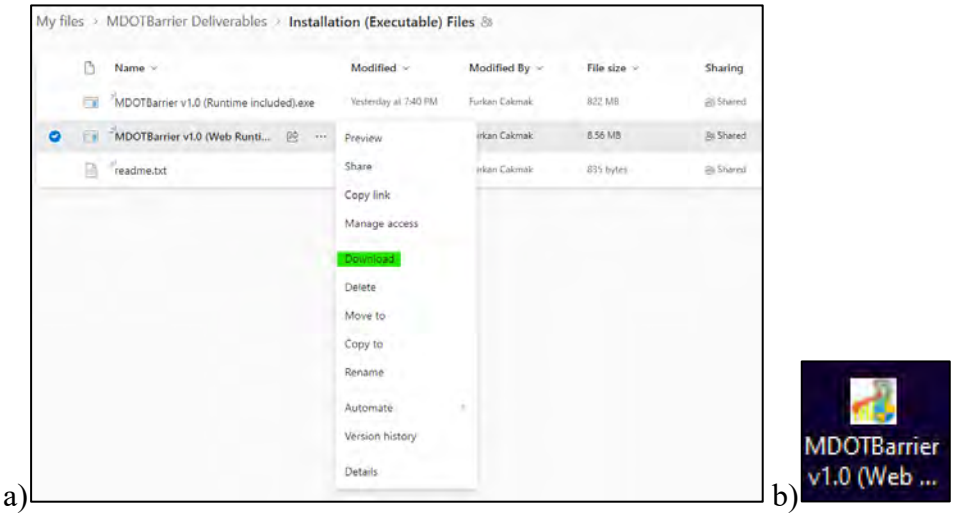

Fig. E.2 Running the executable file for the MDOTBarrier program

a) b) c)

Fig. E.3 Security warnings that may appear during installation due to .exe file extension

Fig. E.4 Prompts that may appear during the installation of the MDOT Barrier program if Matlab Runtime is already installed

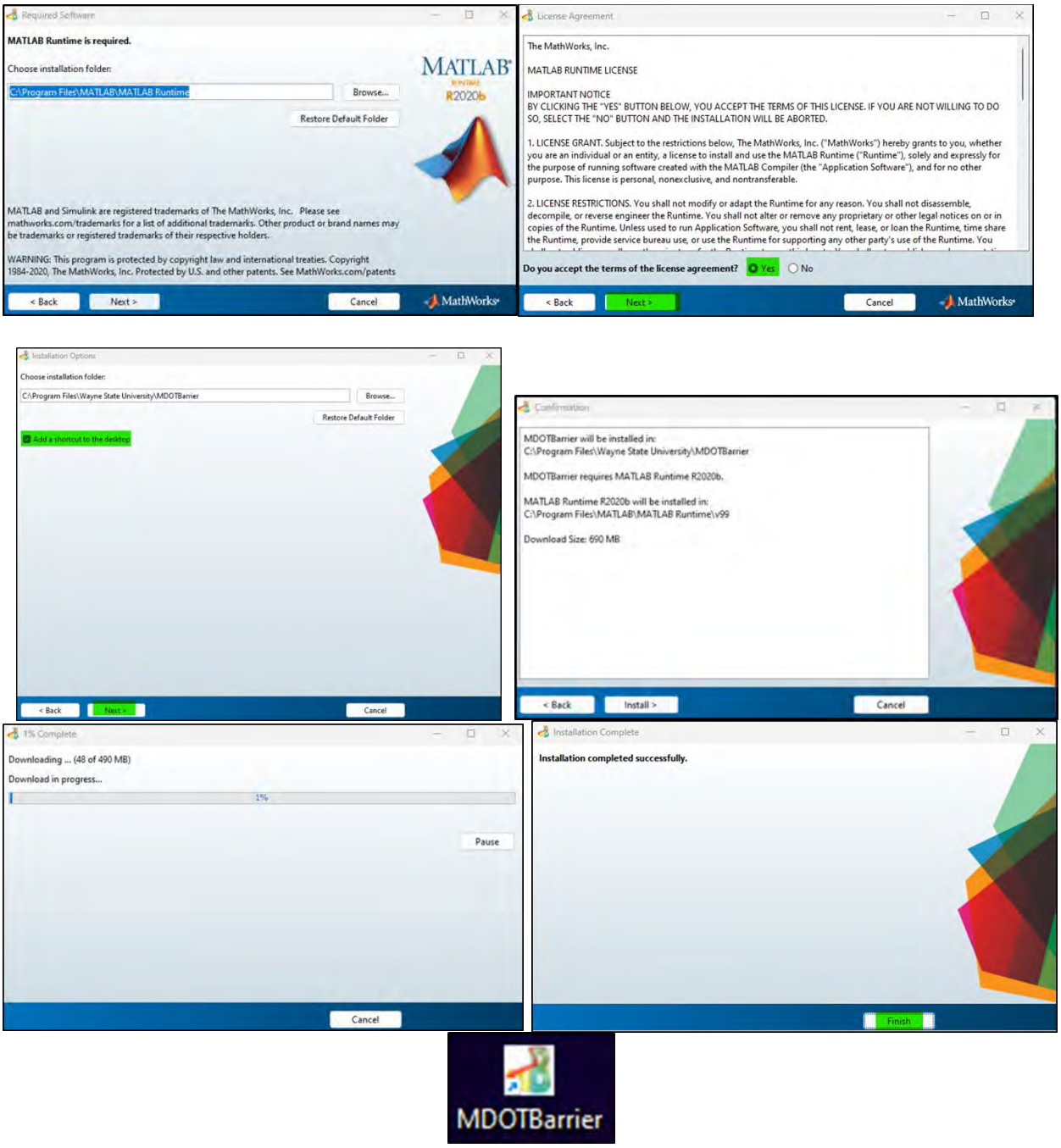

Fig. E.5 Prompts that may appear during the installation of the MDOT Barrier program if Matlab Runtime is not installed

Appendix F: Special Provisions for the Repair for Bridge Deck Fascias

MICHIGAN

DEPARTMENT OF TRASPORTATION

SPECIAL PROVISION

FOR

REPAIR OF BRIDGE DECK FASCIAS

a. Description. This work consists of drilling and epoxying reinforcement, forming, casting, finishing, and curing fiber reinforced self-consolidating concrete (FRSCC) where required by the contract documents to repair bridge deck fascias. The work described herein also includes the preparation of deck fascia surface where the repair will be conducted and incudes the removal of unsound concrete. The location and limits of the repair shall be specified in the contact documents. The repair work shall be conducted only if the Engineer has determined through analysis that intervention is required and that the deck fascia must be repaired.

b. Repair Detail. A sample repair detail in shown in Fig. F.1. This repair detail shall be modified to fit the application in question and to reflect the type of bridge girders used, barrier type, deck overhang region, and other applicable details. The width of the repair denoted as deteriorated width in Fig. F.1 as well as the length of the repair shall be as specified in the contract documents. If field evidence suggests that unsound concrete extends past the specified repair width and length, this information shall be submitted to the engineer for analysis and approval prior to the execution of the repair.

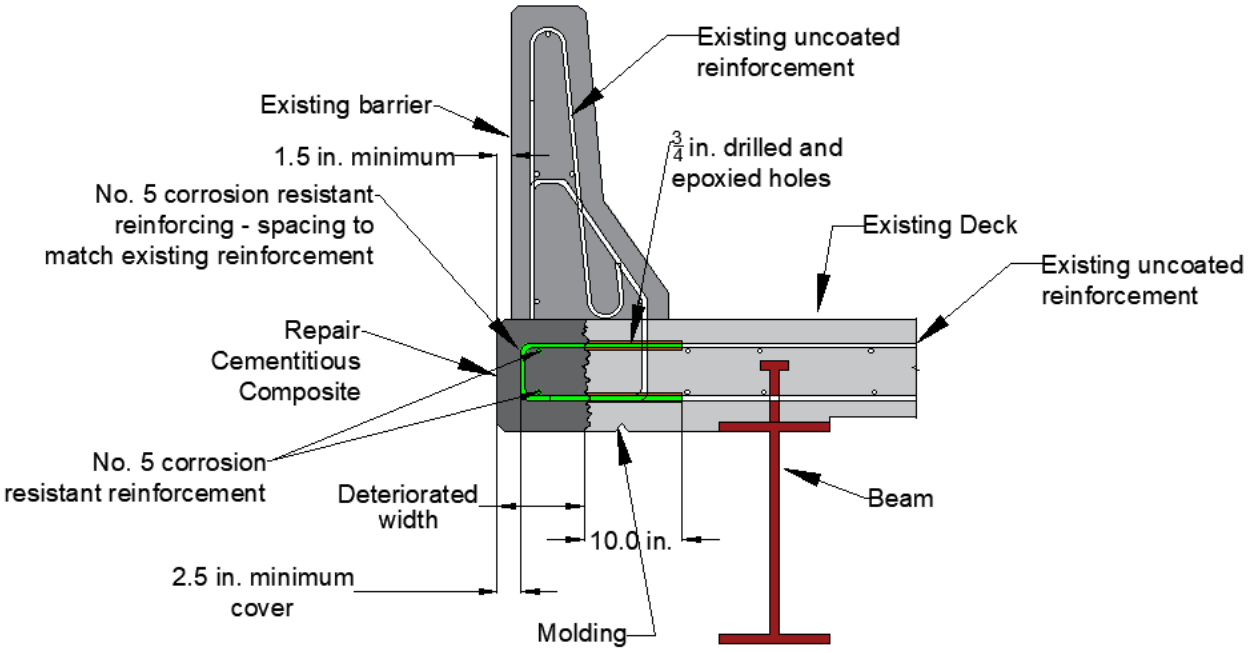

Fig. F.1 Bridge deck fascia repair detail

c. Materials. Epoxy coated dowels: The repair reinforcement shall be epoxy coated reinforcement complying with ASTM A615 (ASTM 2020) or other corrosion resistant reinforcement approved by the Engineer. The shape of the repair reinforcement shall be as shown in the contract documents. To supply the U-shaped repair reinforcement shown in Fig. F.1, the reinforcement can feature two distinct epoxy coated reinforcing bars each drilled at the top and bottom and each featuring a 180 degree hook.

FRSCC: A mix design that can be used as a starting point for finalizing the final mixture for FRSCC is shown in Table F.1. However, trial mixtures shall be prepared prior to placement of the repair concrete material to ensure that the desired plastic properties are obtained. This is due to the fact that FRSCC is rather sensitive to small changes in the high range water reducing admixture (HRWRA). As such, it is recommended that this ingredient be supplied incrementally to obtain the desired plastic properties as described in section i.5. The specifications for the plastic and hardened properties of FRSCC are provided in Table F.2 and Table F.3, respectively.

Table F.1. Fiber reinforced self-consolidating concrete (FRSCC) mix design for repair of bridge deck fascias

Ingredient	Amount[1] (lbs/yd^3 – unless otherwise noted)
Dry Ingredients	
Portland Cement (PC) (Type IL)	610
Fly Ash (Class F)	254
Fine Agg. (Type 2NS)	1367
Coarse Agg. (29A)	1252
Liquid Ingredients (introduce incrementally as outlined in section i.5)	
Water	≤354
HRWRA	≤7.39 oz/cwt (3.99 lbs/yd^3)
VMA	≤0.40 oz/cwt (0.215 lbs/yd^3)
Air Ent. Ad.	≤0.08 oz/cwt (0.042 lbs/yd^3)
Steel Fibers	
Steel Fibers	131.1 (1 % by volume)
w/cm	0.41

[1]When developing this mix design, specific gravities were taken from a JMF supplied by MDOT for the mix #92MR-C and Job #128585 and Control section #09035 considering bulk-dry condition: PC=3.15; Fly-ash=2.59; Fine agg.= 2.60; Coarse agg.=2.56; Steel fiber=7.85; Admixtures=1.0 (assumed). These specific gravities shall be verified for the selected ingredients, and adjustments shall be made to ensure that the specified ingredient weight yields to a volume 1 yd^3 of repair concrete material.

Table F.2 Specifications for the plastic properties of FRSCC

Concrete	Metric	ASTM Reference	Value
FRSCC	Slump Flow (in.)	C1611 (ASTM 2021)	22-26
	J-Ring Flow (in.)	C1621 (ASTM 2017)	17-26
	Passing Ability (in.)[1]	C1621 (ASTM 2017)	< 5.0
	VSI[2]	C1611 (ASTM 2021)	Between 1 and 2
	T_{50} & T_{50j} (sec)	C1611 (ASTM 2021)	<3.0 & <9
	Density (pcf)	C138 (ASTM 2023)	142-147
	Air Content (%)	C231 (ASTM 2022)	4-6

[1]Passing ability is the difference in between Slump flow and J-ring flow.
[2]Based on Daczko and Kurtz (2001) for rating of SCC mixtures.

Table F.3 Specifications for the hardened properties of FRSCC

Concrete	Metric	ASTM Reference	Value
FRSCC	f'_c (ksi)	C39 (ASTM 2021)	> 9 ksi
	f_t (ksi)	C496 (ASTM 2017)	> 1 ksi

d. Equipment. Pan or truck mixers can be used to mix FRSCC per the requirements of section f. If pan mixers are used, ensure paddle- or scraper-to-pan wall clearance is small enough to prevent the material being mixed from adhering to the sidewalls. Pumping FRSCC is prohibited.

e. Submittals.

Construction Work Plan.

A. Formwork.
   (1) Proposed formwork materials.
   (2) Proposed formwork for deck fascia repairs. Ensure methods for accommodating the different deteriorated conditions of the deck fascia are addressed.
   (3) Methods for bracing formwork.
   (4) Procedure for installing, sealing, and maintaining watertight formwork.
   (5) Removal of formwork including tools and access to underside of deck.
   (6) Anticipated production rate.
B. Surface Preparation
   (1) Procedure for surface preparation
   (2) Proposed debris shield and debris disposal method
C. Mixing
   (1) Storage plan for FRSCC ingredients.
   (2) Mixers and mixing setup including the type and number of mixers, mixing location, water source, and contingency plan if a mixer malfunctions.
   (3) Description of equipment for weighing FRSCC ingredients.
   (4) Procedure for controlling FRSCC mix temperatures including methods of storing ice.
   (5) Sample batch identification sheet to be used during FRSCC production.
D. Placement

(1) Placement sequence and schedule.
(2) Equipment for transportation and placement of FRSCC.
(3) Contingency plan if placement operations are interrupted by weather, equipment malfunctions or other issues.

E. Protection and Curing
(1) Procedure to protect FRSCC repairs during curing.
(2) Cold weather protection plan, if required.

F. Grinding
(1) Proposed equipment for finishing new FRSCC surfaces.
(2) Method of collecting and disposing of debris.

G. Trial Placement Plan
A trial placement plan outlining procedures to be followed and a dimensioned drawing showing the proposed FRSCC placement of a representative deck fascia.

H. Contractor QC.
(1) QC Plan, including equipment list, testing setup, sampling methods, frequency and types of tests at least 90 days in advance of the first placement of FRSCC.
(2) The name and location of the Contractor's proposed AASHTO accredited testing laboratory submitted at least 90 days in advance of the first placement of FRSCC.
(3) Submit reports of test results to the Engineer within 7 days of each test.

f. Pre-Pour Meeting. Prior to the initial placement of the FRSCC, arrange for an onsite meeting with the Engineer. The objective of the meeting will be to clearly outline the procedures for mixing, transporting, finishing and curing of the FRSCC, and to review the trial batch requirements.

g. Trial Placement. Construct a demonstration FRSCC bridge deck repair that represents a repetitive section of the actual repair. The cross-sectional size and scope of the repair should be similar and should reflect the components shown in Fig. F.1. The length of the repair shall be a minimum of 2 ft. The trial placement shall be executed using the approved mix design, at least 6 weeks prior to the placement of FRSCC for bridge deck fascia repairs. The intent of the sample FRSCC bridge deck fascia repair is to demonstrate the Contractor's ability to properly cast the FRSCC in accordance with the design plans and this special provision. Ensure the methods used for the trial placement, including materials, mixing equipment, formwork, bracing elements, and pouring methods are similar to those which will be utilized to perform the actual repair in the field. Additional bracing may be used on the right-hand side of Fig. F.1 to replicate bracing that is provided by the continuity of the deck as well as the torsional restraint provided by the superstructure as a whole to the fascia girder.

Perform a water tightness test at least 1 week prior to the placement of FRSCC, to ensure proper sealing of the formwork. Ensure the test is reviewed and approved by the Engineer prior to placement of FRSCC. Following placement and sufficient curing of the FRSCC, the trial placement will be visually inspected by the Engineer to ensure proper placement and fit with the host interface.

Perform flow tests in accordance with subsection i.6 of this special provision. Cast five sets of three 4 inch by 8 inch cylinders during trial placement for determination of compressive strength. Cure all cylinders using the same method of curing as outlined in the QC plan. Conduct the compressive strength tests in accordance with ASTM C39/C39M (ASTM 2021) at 2, 4, 7, 14, and 28 days. Submit test results to the Engineer for review and approval. The deck fascia repair trial specimen is the property of the Contractor. Ensure it is removed from the site prior to completion of construction activities.

h. Safety. Furnish FRSCC safety data sheets (SDS) to the Engineer. Conduct a safety briefing to all on-site personnel prior to FRSCC placement. Furnish required personal protective equipment (including, at a minimum, goggles, dust masks, and respirators) as required by the SDS based on proximity to specific operations.

h. Storage. Properly store dry premixed components, steel fibers and admixtures as recommended by the supplier and the following:
1. Store all dry premixed components on raised pallets, with vapor barrier between the pallets and the ground surface to prevent moisture ingress and cover thoroughly.
2. Store steel fibers with the same protection as the dry premixed components. Do not use rusted fibers.
3. Store liquid admixtures in sealed containers in above freezing temperatures and protected from direct sunlight.

i. Construction

1. Bridge Deck Fascia Surface Preparation: Remove all unsound concrete using the method specified by the Engineer. Such methods may include: saw cutting, hand chipping, scarifying, and hydrodemolition. The selection of the appropriate method will depend on the extend of the repair in the longitudinal direction of the bridge as well as in the transverse direction. Refer to Section 712 Bridge Rehabilitation – Concrete for additional details regarding the selected method of unsound concrete removal. If field evidence suggests that unsound concrete extends past the specified repair width and length, this information shall be submitted to the engineer for analysis and approval prior to the execution of the repair.

2. Cut all corroded reinforcement flush with the scaled deck fascia

3. Drill and Epoxy Reinforcement Dowels: The diameter and depth of holes shall be as specified in the contract documents and will depend on the selected epoxy material. The diameter and length of the drilling bit shall be chosen such that it can deliver the desired hole diameter and length. Consult the epoxy mortar manufacturer's literature for hole sizes appropriate for a given reinforcement size. The drilling and epoxying of reinforcement dowels should comply with the epoxy manufacturer's recommendations for installation. In addition, the following steps shall be taken:

- Drill holes top and bottom at the same spacing as the existing deck reinforcement. The elevation of the holes should match that of existing top and bottom deck reinforcement. A 2 in. maximum horizontal offset from the existing bars is considered sufficient. The cut

reinforcing steel can be used as a refence point to provide the 2 in. maximum horizontal offset.

- Clean the holes using a steel brush followed by additional cleaning using a fabric towel. Finalize the cleaning using a vacuum pump. The first two steps may be eliminated if the vacuum pump is robust enough to provide a thorough cleaning
- Discharge the epoxy mortar using a nozzle extension.
- Insert the epoxy coated dowels or other corrosion resistant dowels.
- Allow the epoxy to cure. Follow manufacturer's recommendations for curing and working time.

4. Install Formwork: Ensure the formwork is resistant to the hydraulic pressure of the mix and other applicable loads that may be present during construction. Ensure the forms are watertight and coated to prevent absorption of water. Perform a watertight test at least 1 week prior to pouring of the FRSCC to ensure proper sealing of the formwork. In the case that the formwork fails the watertight test, reseal the formwork and repeat the test. Formwork will be approved by the Engineer prior to the placement of the FRSCC. After the Contractor has proven their ability to properly install and seal the formwork, the watertight test may be waived as approved by the Engineer. Prior to placing the FRSCC, the bridge deck fascia and formwork will be visually inspected by the Engineer to ensure that there is no remaining water. Placement of FRSCC when there is visible ponded water is prohibited. Take the necessary measures to ensure that the repaired surface and formwork are dry prior to placement of FRSCC. Furnish the means to drain the formwork after the watertight test is performed. Formwork removal must not begin until a representative compressive test demonstrates that the compressive strength has reached $0.75f_c'$. A sloping surface may be used at the top of the formwork to discharge the repair FRSCC. A minimum width of 1.5 in. as specified in Fig. F.1 between the outside face of barrier and deck fascia (in this case the inside face of the formwork was found sufficient to discharge FRSCC.

5. Mixing Protocol:

- Prior to starting the mixing, prepare the correct amounts for each ingredient. In addition, prepare the premix liquid (Water+HRWRA+VMA+AEA). This premix liquid shall be added incrementally as outlined below to ensure that the desired slump flow, and visual stability index (VSI) are obtained. The acceptable range for the slump flow is between 18-30 in. (ACI 2007). The VSI shall be between 1-2 as outlined in ACI 237-07 (ACI 2007), which is indicative of a mix that stable to highly stable. The high range water reducing admixture is extremely effective and even small changes in its amount may cause notable changes in the plastic properties of the mix.
- Dry-mix the cement, fly-ash, and sand for 30 seconds.
- Add all coarse aggregates in the mixer and mix for 2 minutes,
- Pour 50% of the premix liquid into the mixer and mix for 1 minute.
- Pour 25% of the remaining fluid and mix for 1 minute.
- Slowly add all steel fibers in the mixer while the mixer is operating and mixing for about 3 minutes after all the fibers have been added.

- Check if the fibers are dispersed thoroughly and remix if necessary. It is recommended that a quick flow test be conducted at this point to measure the flow of the mix. If the mix is too stiff and does not meet the specifications for FRSCC then proceed to the next step.
- Pour 12.5% of liquid and mix for 1 minute. Redo the flow test and if the mix is still too stiff proceed with the next step.
- Pour 6.25% of liquid and mix for 1 minute. Redo the flow test and if the mix is still too stiff proceed with the next step.
- Pour all remaining liquid and mix for 1 minute.

6. Slump Flow Test: The filling ability test (slump flow test), T_{50}, and Visual Stability Index (VSI) shall be conducted based on ASTM C1611 (ASTM 1611). The acceptable range for the slump flow is between 18-30 in. (ACI 2007). The VSI shall be between 1-2 as outlined in ACI 237-07 (ACI 2007), which is indicative of a mix that is stable to highly stable.

7. Compression Testing Requirements: Make at least one set of compressive strength test samples for each FRSCC placement. Each set consists of at least three 4 inch by 8 inch cylinders. Make additional sets as required to justify formwork removal at a particular concrete age after placement. Cure all test samples using the same method of curing as outlined in the QC plan. Conduct the compressive strength tests on a minimum of three 4 inch by 8 inch cylindrical samples in accordance with ASTM C39/C39M (ASTM 2021).

j. Placement. Place FRSCC within the limits shown in the contract documents using the approved mix design. Ensure any changes in repair limits due to field conditions are submitted to the engineer for review and approval.

Prior to placing FRSCC, the Engineer will perform an inspection to determine the exact limits and locations of all areas to be repaired. Provide scaffolding or other access as required for the Engineer's inspection. Do not perform any repair work without prior approval of the Engineer for locations.

Construction loads applied to the bridge during the entire repair work are the responsibility of the Contractor. The Contractor must submit significant construction loads to the Engineer for review prior to the pre-placement meeting described herein.

k. Acceptance. The Engineer will sample the FRSCC and test it for 28 day compressive strength and slump flow. If the FRSCC achieves a minimum of 5 ksi at 28 days, the slump flow is within 18 to 30 inches, and FRSCC placement, segregation, and consolidation are acceptable, the FRSCC for each representative placement will be accepted.

l. Measurement and Payment. The completed work, as described, will be measured and paid for at the contract unit price using the following pay item:

Pay Item	Pay Unit
Conc, FRSCC	Cubic Foot

Conc, FRSCC will be measured in cubic feet based on plan quantities. Conc, FRSCC includes the first trial batching and placement, preparing and cleaning the existing deck fascia, forming, furnishing, testing, placing, finishing, and curing the concrete in accordance with this special provision. No additional compensation will be made for trial batches or trial placements that fail to meet the requirements of this special provision.

Furnishing and installing drilled and epoxied dowels will be paid for separately.

Appendix G: Implementation Plan for the Repair of Bridge Deck Fascias

Repair of Bridge Deck Fascias

Implementation Plan

1. Identify several bridges that feature severe deck fascia deterioration.

2. Conduct a virtual inspection of these bridges and identify one bridge that features the worst deck fascia deterioration.

3. Conduct a site visit and characterize the deterioration in terms of the variation of the deterioration width and length along the span of the bridge. This can be conducted by taking several discrete measurements along the deck fascia. At every measurement point record the location of measurement along the span and record the width of deterioration.

4. Idealize the deterioration of the bridge deck fascia such that the deterioration is expressed using an average deteriorated length and width for several segments along the bridge.

5. Use the MDOT Barrier Computer Program to demonstrate that intervention is required in terms of restoring the crashworthiness of the barrier.

6. Prepare drawings that define the scope of the repair work. These drawings together with the Special Provision for the Repair of Bridge Deck Fascias will define the scope of work.

7. Identify a contractor to conduct the repair work.

8. Follow the guidance provided in the drawings and Special Provision for the Repair of Bridge Deck Fascias to ensure that the work is executed as intended.

Appendix H: Evaluation of Bridges with Deteriorated Deck Fascias for Barrier Crashworthiness – Example Problem using MDOT Barrier Program

Evaluation of Bridges with Deteriorated Deck Fascias for Barrier Crashworthiness

Example Problem using MDOT Barrier Program

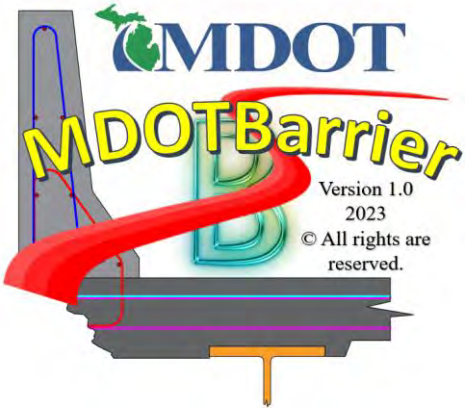

Table of Contents

List of Figures

List of Tables

1. Problem Statement

The bridge barrier shown in Fig. H.1.1 is to be evaluated whether it meets a TL-4 level of crashworthiness. The barrier performance criteria based on different test levels is illustrated in Table H.1.1. Fig. H.1.2 illustrates some of the parameters presented in Table H.1.1. For each test level, a definition is provided below Fig. H.1.2 that describes the level of barrier protection appropriate for that test level. The bridge is assumed to be an existing bridge built prior to the 1980 mandate in Michigan to use epoxy coated reinforcement in the deck and features a deteriorated deck fascia. An inspection of the bridge has been conducted and it has been determined that the average deteriorated width is w_d = 6.5 in. and the deteriorated length over which the average deteriorated width is calculated is L_d = 180 in. The specified concrete compressive strength for the barrier and deck is $f_c' = 4.5$ ksi. Deck and barrier reinforcement are uncoated. Top deck fascia transverse reinforcement consists of No. 5 straight bars at 7.5 in. on center and No. 3 hooked bars at 7.5 in. on center. The straight bars are extensions of top transverse deck steel used across the entire width of the bridge, whereas the No. 3 bars are added to the deck fascia to provide additional resistance to vehicle impact. Deck fascia transverse bottom reinforcement consist of No. 5 bars at 9 in. on center. Assume that the deck is constructed with normal weight cast-in-place concrete and the top surface of the deck where barrier is cast is free of laitance and roughened to an amplitude of 0.25 in. – this corresponds with a Type-2 connection type in MDOT Barrier program. Results obtained from hand calculations are compared with those obtained from the MDOT Barrier program. In the following analysis it is assumed that the barrier configuration meets geometric requirements for crashworthiness as presented in ASHTO LRFD (2020). Therefore, the goal of the analysis is to check barrier crashworthiness from a strength point of view. It is assumed that vehicle impact occurs within the solid barrier and not at the ends. A list of notations is provided at the end of the example for parameters not defined in the text.

Approach

The presented approach is such that barrier capacity to transversely applied loads that simulate vehicle impact is calculated one time assuming no deterioration in the deck fascia and another time considering the specified deck fascia deterioration. This is done for two reasons. The first reason is to quantify the impact of deck fascia deterioration on barrier transverse load capacity compared to the undeteriorated condition. The second reason is that the specified deterioration length may

be smaller than the critical yield line failure pattern and the effective deck width that is used to resist vehicle impact. In this scenario, the transverse load capacity of the barrier is computed by using a weighted average approach in which capacities related to the deteriorated and undeteriorated condition are considered. The contribution of reinforcement is determined such that their stress is taken equal to the yield stress or the stress than can be developed in the given configuration. The limit states of interface shear transfer and axial tension and moment transfer from the barrier to the deck are evaluated using a capacity-based approach in which the full barrier lateral load capacity is used as the demand rather than the specified level of crashworthiness. This capacity-based approach is used in the design of barriers with the goal of ensuring that in the event of a vehicle impact, the damage is contained to the barrier. This allows the stakeholders to restore barrier crashworthiness by replacing only the barrier and not the deck overhang.

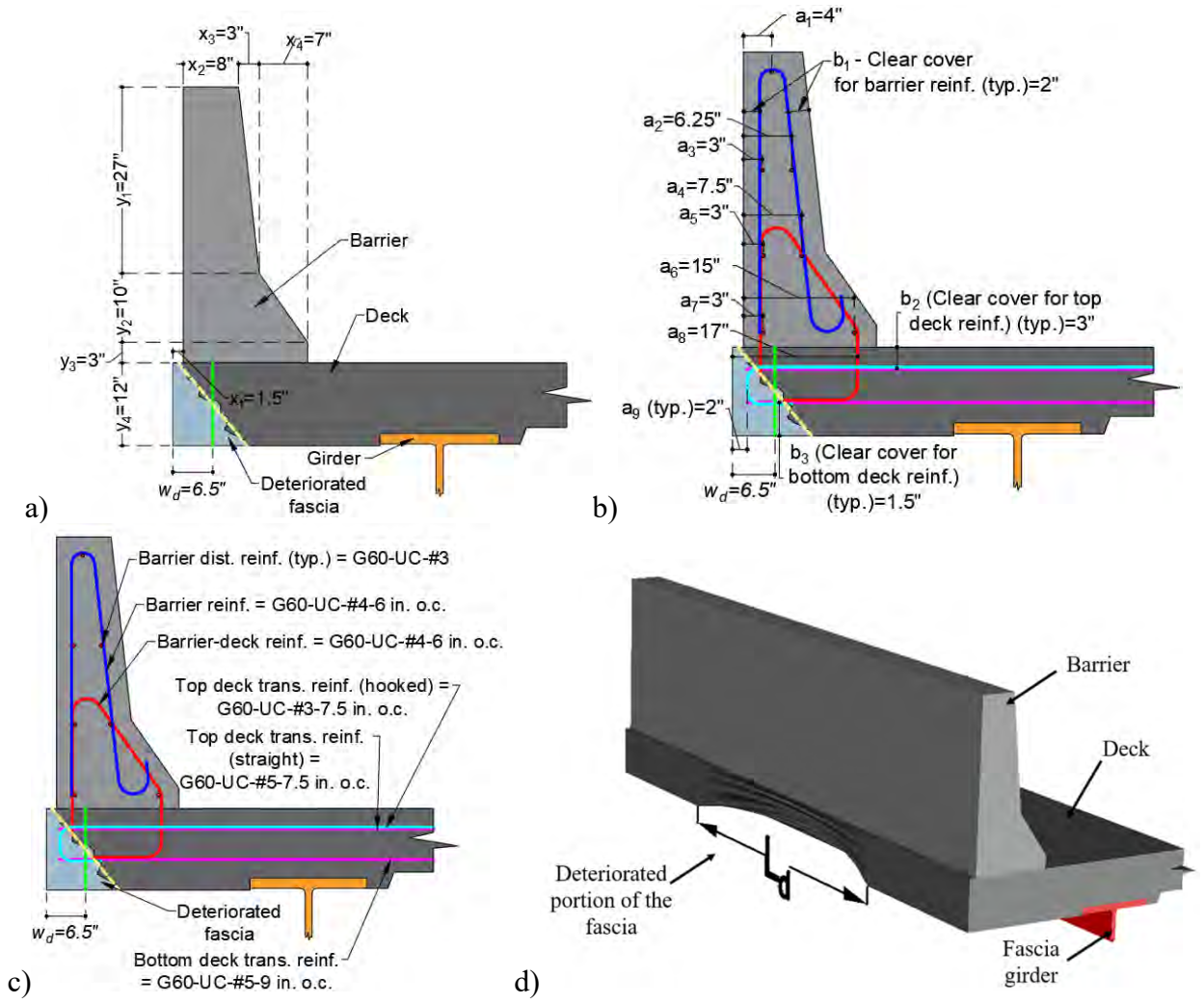

Fig. H.1.2. Bridge barrier with deteriorated deck fascia: a) cross-sectional dimensions; b) location of the reinforcements; c) reinforcement grade, type, size, and spacing, and d) deterioration length, L_d

Table H.1.1. Barrier performance criteria (Adapted from AASHTO LRFD 2020 Table A13.2.1)

Design Forces and Designations	**Railing Test Levels**					
	TL-1	TL-2	TL-3	TL-4	TL-5	TL-6
F_t Transverse (kips)	13.5	27.0	54.0	54.0	124.0	175.0
F_L Longitudinal (kips)	4.5	9.0	18.0	18.0	41.0	58.0
F_v Vertical (kips) Down	4.5	4.5	4.5	18.0	80.0	80.0
L_t and L_L (ft)	4.0	4.0	4.0	3.5	8.0	8.0
L_v (ft)	18.0	18.0	18.0	18.0	40.0	40.0
H_e (min) (in.)	18.0	20.0	24.0	32.0	42.0	56.0
Minimum H Height of Rail (in.)	27.0	27.0	27.0	32.0	42.0	90.0

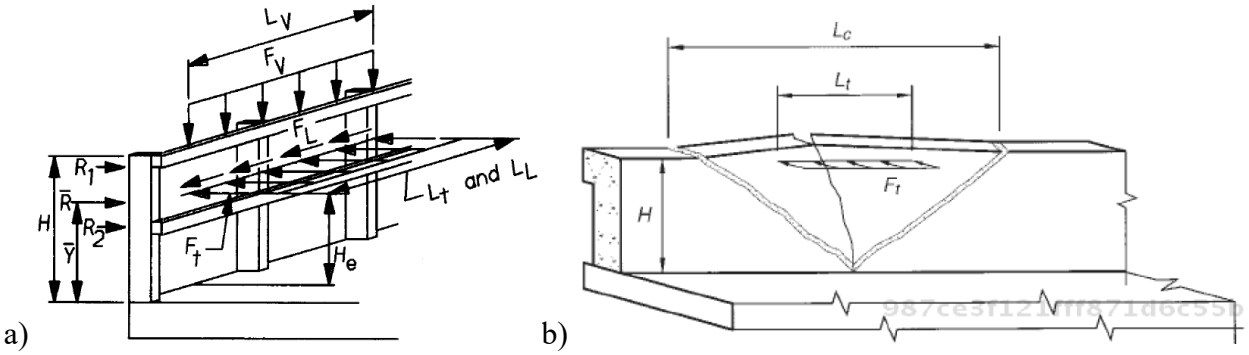

Fig. H.1.2. a) Bridge railing design forces, vertical location, and horizontal distribution length (adapted from AASHTO LRFD 2020 Figure A13.2-1); and b) loading and yield-line pattern for a concrete barrier (adapted from Barker and Puckett 2021)

- TL-1: Test Level One—taken to be generally acceptable for work zones with low posted speeds and very low-volume, low-speed local streets;
- TL-2: Test Level Two—taken to be generally acceptable for work zones and most local and collector roads with favorable site conditions as well as where a small number of heavy vehicles is expected and posted speeds are reduced;
- TL-3: Test Level Three—taken to be generally acceptable for a wide range of high-speed arterial highways with very low mixtures of heavy vehicles and with favorable site conditions;
- TL-4: Test Level Four—taken to be generally acceptable for the majority of applications on high-speed highways, freeways, expressways, and Interstate highways with a mixture of trucks and heavy vehicles;
- TL-5: Test Level Five—taken to be generally acceptable for the same applications as TL-4 and where large trucks make up a significant portion of the average daily traffic or when unfavorable site conditions justify a higher level of rail resistance; and
- TL-6: Test Level Six—taken to be generally acceptable for applications where tanker-type trucks or similar high center of gravity vehicles are anticipated, particularly along with unfavorable site conditions.

2. Solution

2.1. Required Barrier Transverse Lateral Load Capacity

The required transverse lateral load capacity for a bridge barrier with TL-4 level crashworthiness is F_t = 54 kips. The evaluation whether the barrier with the deteriorated deck fascia meets this level of crashworthiness will be conducted by first determining the lateral load capacity of the barrier using closed form equations derived from yield line theory and presented in AASHTO LRFD (2020) Article A13.3. The barrier lateral load capacity will be determined assuming that the barrier to deck connection is capable of transferring the shear force that corresponds with the controlling yield line mechanism in the barrier. It will also be assumed that the deck reinforcement has sufficient anchorage and development length to transfer the axial tension and bending moment created in the deck from vehicle impact. Both of these assumptions will be evaluated once the barrier lateral load capacity is determined. If these assumptions are found to be incorrect, the transverse capacity of the barrier will be re-calculated based on valid assumptions.

2.2. Barrier Transverse Resistance

The transverse resistance of the barrier is determined using Eqs. H2-1 – H2-3, where R_w is the total transverse resistance of the barrier, L_c is the critical length of yield line failure pattern, L_t longitudinal length of distribution of impact force, M_b is the additional flexural resistance of beam in addition to M_w, if any, at the top of the barrier, M_w is the flexural resistance of the barrier about its vertical axis, M_c, is the flexural resistance of the barrier about an axis parallel to the longitudinal axis of the bridge, and H is the height of the barrier measured from the top of the deck to the top of the barrier. The critical length of yield line failure pattern, L_c, may be determined from Eq. H2-2. The transverse resistance of the barrier must be greater than the required barrier transverse lateral load capacity (Eq. H2-3). Fig. H.2.1 illustrates the formation of the critical yield line pattern and some of the terms used in Eqs. H2-1 – H2-3. It is assumed that vehicle impact occurs within the barrier and not at the ends.

A13.3.1-1
For impacts within a wall segment

$$R_w = \left(\frac{2}{2L_c - L_t}\right)\left(8M_b + 8M_w + \frac{M_c L_c^2}{H}\right) \quad \text{H2-1}$$

A13.3.1-2
For impacts within a wall segment

$$L_c = \frac{L_t}{2} + \sqrt{\left(\frac{L_t}{2}\right)^2 + \frac{8H(M_b + M_w)}{M_c}} \quad \text{H2-2}$$

$$R_w > F_t \qquad \text{H2-3}$$

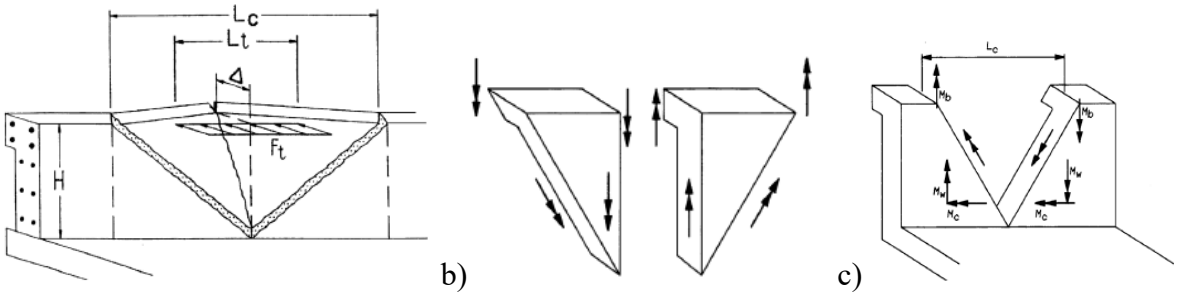

a) b) c)

Fig. H.2.1 Illustration of yield line formation and analysis in a concrete bridge barrier for impact within the barrier segment (adopted after AASHTO LRFD (2020) Article CA13.3.1-1)

2.2.1. Flexural Resistance of the Barrier about Vertical Axis (M_w)

The flexural resistance of the barrier about its vertical axis is determined by converting the non-prismatic barrier into an equivalent prismatic cross-section. This conversion is conducted ensuring that the equivalent thickness, t_{avg}, leads to a barrier area that is equal to the non-prismatic barrier area. In the derivation of the closed form equations in AASHTO LRFD (2020) Article A13.3, it is assumed that the positive and negative moment capacities are equal. Therefore, both positive and negative moment capacities will be calculated and the average will be used to represent the flexural resistance of the barrier about the vertical axis. A positive moment is one which creates tension on the outside face of the barrier and compression on the inside face of the barrier. A negative moment is one which creates tension in the inside face of the barrier and compression on the outside face of the barrier. While there are various layers of longitudinal reinforcement, only the layers that are closest to the tensile face are considered in the flexural capacity calculations. The other layers are conservatively ignored. It should be noted that the deterioration of the deck fascia does not affect the calculation of the flexural resistance of the barrier about the vertical axis. Therefore, the following calculations do not distinguish between a barrier with a deteriorated fascia and a barrier with no deterioration in the deck fascia. In the flexural capacity calculations, it is always assumed that the most extreme layer of tension steel yields. This assumption is validated by computing the strain in the most extreme layer of tension steel and comparing it to the yield strain. The strength reduction factor, ϕ, is always taken as 1.0 regardless of the limit state evaluated since vehicle impact is an extreme event.

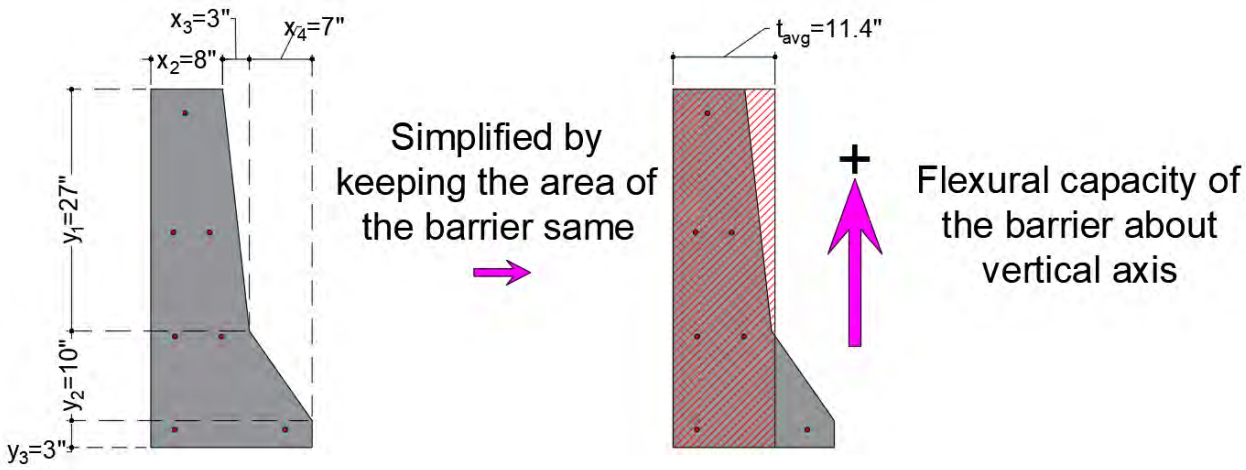

Fig. H.2.2. Assumed uniform barrier thickness for vertical axis moment resistance

The average thickness of the barrier is determined as follows:

$$H_{barrier} = y_1 + y_2 + y_3 \qquad \text{H2-4}$$

$$H_{barrier} = 27 + 10 + 3 = 40\ in.$$

$$A_{barrier} = \frac{y_1(x_2 + x_2 + x_3) + y_2(x_2 + x_3 + x_2 + x_3 + x_4)}{2} + y_3(x_2 + x_3 + x_4) \qquad \text{H2-5}$$

$$A_{barrier} = \frac{27(8 + 8 + 3) + 10(8 + 3 + 8 + 3 + 7)}{2} + 3(8 + 3 + 7) = 455.5\ in.^2$$

$$t_{avg} = \frac{A_{barrier}}{H_{barrier}} = \frac{455.5}{40} = 11.4\ in. \qquad \text{H2-6}$$

The compression stress block factors (Whitney's stress block) are determined as follows.

For $f_c' = 4.5$ ksi, $\beta_1 = 0.825$ and $\alpha_1 = 0.85$.

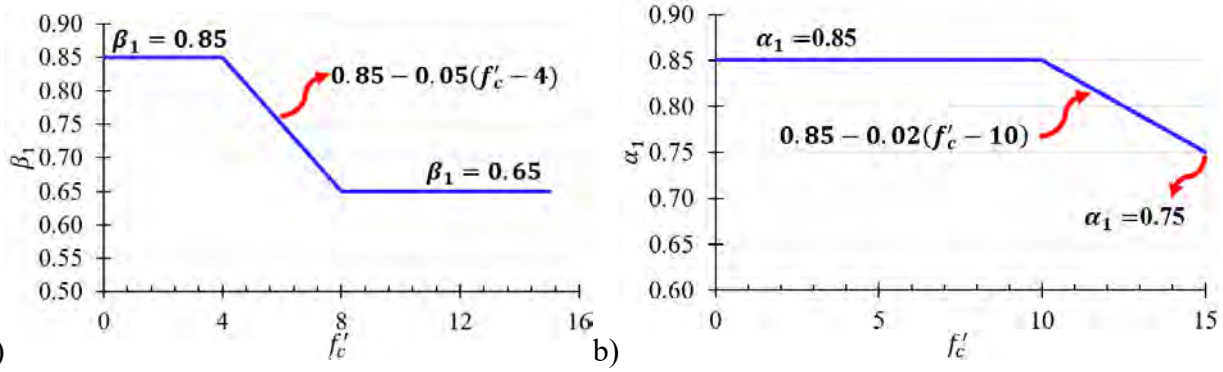

Fig. H.2.3. a) Stress block factor, β_1; and b) Compressive stress block factor, α_1

The area of a #3 rebar is $A_s = 0.11\ in.^2$ and the yield strain is $\varepsilon_{sy} = f_y/E_s$.

$$\varepsilon_{sy} = \frac{60}{29000} = 2.1 * 10^{-3}$$

Positive Moment (Tension at the Outer Edge)

When calculating the positive flexural resistance of the barrier an average effective depth, d_{sp}, needs to be calculated since the position of the reinforcement from the outside face of the barrier varies.

$$d_{sp} = 11.4 - \frac{4+3+3+3}{4} = 8.15\ in.$$

Resultant compressive and tension forces are calculated as follows assuming that the tension steel yields:

$$\sum C = 0.85 f'_{cb} b \beta_1 c \qquad \text{H2-7}$$

$$\sum T = A_s f_y \qquad \text{H2-8}$$

$$\sum C = 0.85(4.5)(40)(0.825)c = 126.2c$$

$$\sum T = 4(0.11)(60) = 26.4\ ksi$$

The depth of the neutral axis is calculated as follows by establishing equilibrium and equating the tension and compression forces:

$$\sum C = \sum T \qquad \text{H2-9}$$

$$c = \frac{A_s f_y}{0.85 f'_{cb} b \beta_1} \qquad \text{H2-10}$$

$$c = \frac{26.4}{126.2} = 0.21\ in.$$

The depth of the Whitney's stress block is calculated as follows:

$$a_1 = \beta_1 c \qquad \text{H2-11}$$

$$a = 0.825 * 0.21 = 0.173\ in.$$

The strain in the outer most layer of steel is calculated as follows and is compared to the yield strain to validate the assumption about steel yielding and to classify the member as a tension controlled, compression controlled, or a member in the transition zone. As can be seen, the steel strain is larger than the yield strain, which validates the assumption about tension steel yielding.

In addition, based on the steel tensile strain, the section is classified as tension controlled for which ϕ = 0.9. However, the strength reduction factor is always taken as ϕ = 1.0, regardless of which limit state is evaluated and regardless of the classification of the section as tension controlled, compression controlled, or member in the transition zone, because vehicle impact is an extreme event. However, there is assurance in determining that the section is tension controlled because the formation of the assumed yield line mechanism relies on the flexural ductility of the barrier.

$$\varepsilon_t = \frac{0.003(d_s - c)}{c} \qquad \text{H2-12}$$

$$\varepsilon_s = \frac{0.003(8.15 - 0.21)}{0.21} = 0.11 \gg \varepsilon_{sy} \rightarrow OK$$

$$M_n = A_s f_y \left(d_s - \frac{a}{2}\right) \qquad \text{H2-13}$$

$$M_n = 4(0.11)(60)\left(8.15 - \frac{0.173}{2}\right) = 212.9\ k - in$$

The positive flexural strength of the barrier about the vertical axis is:

$$\phi M_n = (1.0)\left(\frac{212.9}{12}\right) = 17.7\ k - ft$$

Negative Moment (Tension at the Inside Edge)

A similar approach is used to calculate the negative flexural resistance about the barrier vertical axis.

$$d_{sn} = \frac{4 + 6.25 + 7.5 + 15}{4} = 8.1875\ in.$$

Resultant compressive and tension forces are calculated as follows:

$$\sum C = 0.85(4.5)(40)(0.825)c = 126.2c$$

$$\sum T = 4(0.11)(60) = 26.4\ ksi$$

The depth of the neutral axis is calculated as follows:

$$c = \frac{26.4}{126.2} = 0.21\ in.$$

The depth of the Whitney's stress block is calculated as follows:

$$a = 0.825 * 0.21 = 0.173\ in.$$

The strain in the outer most layer of steel is calculated as follows and is compared to the yield strain. As can be seen, the steel strain is larger than the yield strain, which validates the assumption about tension steel yielding. In addition, based on the steel tensile strain, the section is classified as tension controlled for which ϕ = 0.9. However, the strength reduction factor is always taken as ϕ = 1.0, regardless of which limit state is evaluated and regardless of the classification of the section as tension controlled, compression controlled, or member in the transition zone, because vehicle impact is an extreme event. However, there is assurance in determining that the section is tension controlled because the formation of the assumed yield line mechanism relies on the flexural ductility of the barrier.

$$\varepsilon_s = \frac{0.003(8.1875 - 0.21)}{0.21} = 0.11 \gg \varepsilon_{sy} \rightarrow OK$$

The negative flexural strength of the barrier about the vertical axis is:

$$M_n = 4(0.11)(60)\left(8.1875 - \frac{0.173}{2}\right) = 213.9\ k - in$$

$$\phi M_n = (1.0)\left(\frac{213.9}{12}\right) = 17.8\ k - ft$$

The average of positive and negative moment resistances of the barrier about vertical axis is calculated as follows:

$$\phi M_n = M_w = \frac{17.7 + 17.8}{2} = 17.8\ k - ft$$

Similar results are obtained from the MDOT Barrier program as shown in Fig. H.2.4.

1. Flexural Resistance of the Barrier about Vertical Axis

Description	Pos. Moment	Neg. Moment	Avg. Moment
Capacity of Barrier about Vertical Axis (k-ft)	17.71	17.82	17.77

Fig. H.2.4. Program output for the flexural resistance of the barrier about vertical axis

2.2.2. Flexural Resistance of the Barrier about Horizontal Axis

The flexural resistance of the barrier about the horizontal axis is obtained by dividing the barrier into three segments (Fig. H.2.5). Each non-prismatic segment is then converted into a prismatic segment by calculating an average thickness. The total flexural resistance of the barrier is then obtained by using a weighted average approach based on segment length. Flexural resistances are

expressed considering a one foot strip in the longitudinal direction of the bridge. The impact of deck fascia deterioration is illustrated in Fig. H.2.6. A deteriorated deck fascia reduces the effective depth of each segment which reduces the flexural capacity of the barrier about horizontal axis and consequently the transverse resistance of the barrier.

It should be noted that the yield line mechanism that is precipitated by vehicle impact is such that bending about the horizontal axis creates compression on the outside face of the barrier and tension on the inside face of the barrier. This is different from the bending that takes place about the vertical axis of the barrier, which includes positive and negative bending moments that are consistent with the critical yield line mechanism.

The flexural resistance of Segments II and III about the horizontal axis is provided by the dowels that protrude from the deck into the barrier denoted in red in Fig. H.2.6. The flexural capacity of Segment I is calculated based on the reinforcement denoted in blue. The dowels are lapped with barrier reinforcement that is denoted in blue in Fig. H.2.6. The blue reinforcement in the barrier is the same size and spacing as the dowels. The dowels consist of No. 4 bars at 6 in. o.c. No. 4 bar diameter is $d_b = 0.5\ in$. The dowels have a 90° hook in the deck.

The calculations are organized such that the lateral load resistance of the barrier with an undeteriorated fascia is calculated first followed by the lateral load resistance of the barrier with deteriorated fascia. This way the reader may determine the impact of deck fascia deterioration on barrier crashworthiness by comparing lateral load capacities before and after deterioration. Another reason for calculating flexural capacities before and after deterioration is that the length of the critical yield line failure pattern may be smaller or greater than the deteriorated length. If the length of the critical yield line failure pattern is smaller than the deteriorated length, then the flexural resistance of the barrier about its horizontal axis will be determined entirely by considering the deteriorated width. If the length of the critical yield line failure pattern is greater than the deteriorated length, then the flexural resistance of the barrier about its horizontal axis will be determined partially by the undeteriorated deck fascia configuration and partially by the deteriorated configuration as outlined later in this example.

The adequacy of the anchorage length of the dowels that connect the deck to the barrier is evaluated first followed by flexural strength calculations about the horizontal axis of the barrier.

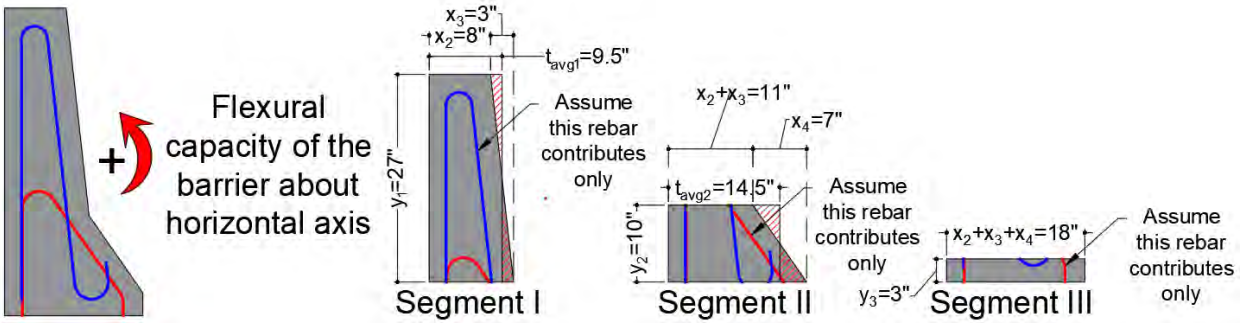

Fig. H.2.5. Simplification made when computing flexural resistance of the barrier about horizontal axis

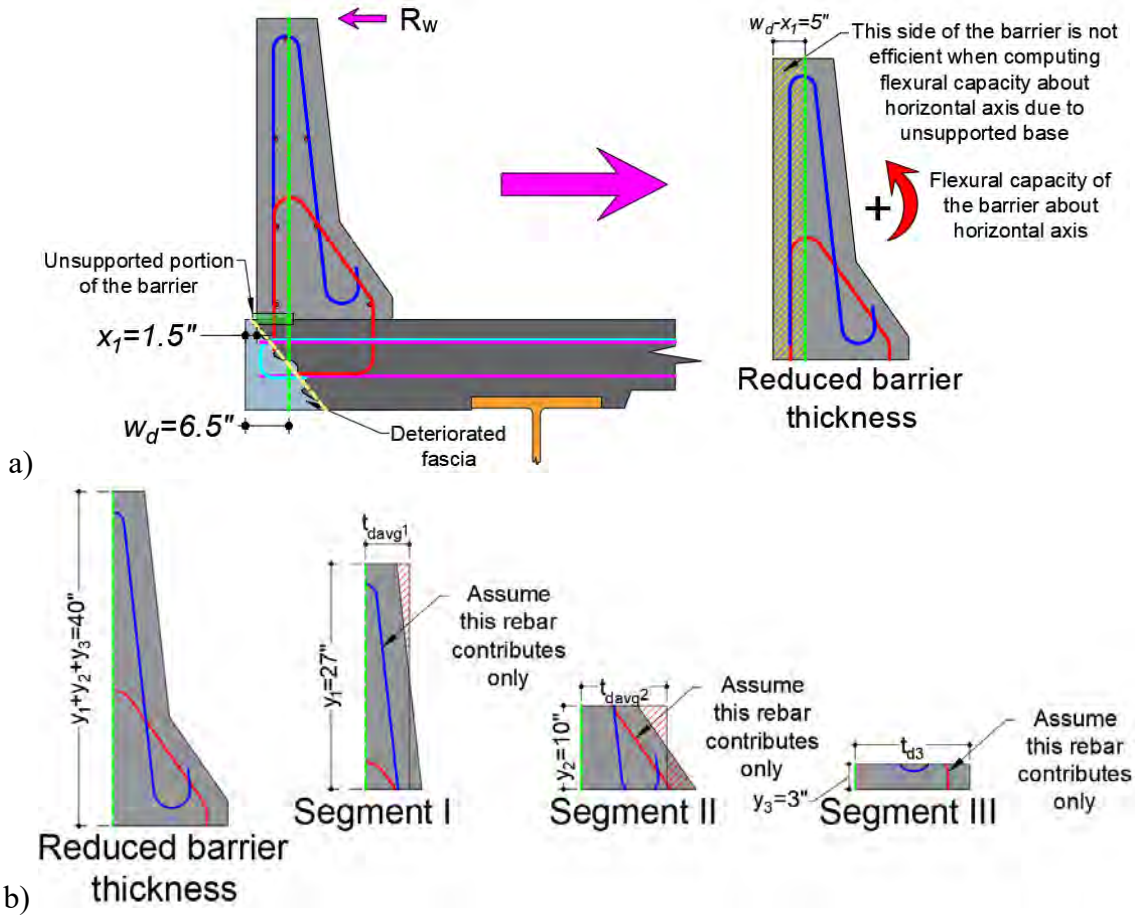

Fig. H.2.6. Consideration of deterioration when computing flexural resistance of the barrier about horizontal axis: a) reduced barrier thickness; and b) application of reduced barrier thickness for considered segments

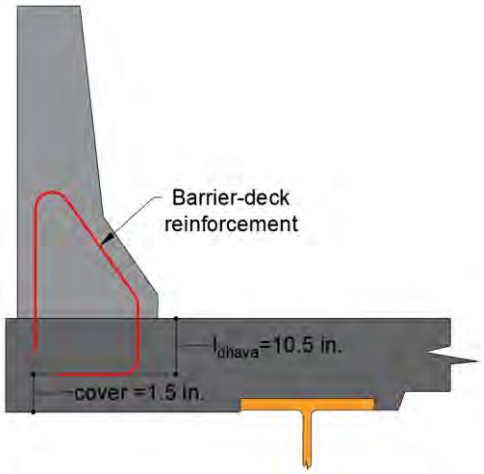

Fig. H.2.7. Available development length for the barrier-deck reinforcement

The available development length for the dowels is calculated as 10.5 in. (Fig. H.2.7).

$$l_{dhava} = y_4 - b_3 = 12 - 1.5 = 10.5\ in.$$

The development length for the dowels is calculated based on Eqs. H2-14 – H2-16, where d_b is the diameter of the rebar; f_y is the yield strength of the rebar; and f_c' concrete compressive strength.

- λ is concrete density modification factor: taken 1.0 for normal weight concrete and is calculated using Eq. H2-14 for light weight concrete where w_c is the unit weight of concrete, assumed 0.125 kcf.
- λ_{rc} is reinforcement confinement factor. If the cover on the bar extension beyond hook is greater than 2.0 in., it is taken 0.8 (Fig. H.2.6a). Otherwise, it is taken 1.0.
- λ_{er} is excess reinforcement factor, taken as 1.0 as this is considered explicitly by adjusting the yield strength of the steel.
- λ_{cw} is the coating factor, taken as 1.0 and 1.2 for uncoated, and epoxy-coated reinforcement, respectively.

5.4.2.8-2 $$0.75 \le \lambda = 7.5 w_c \le 1.0$$ H2-14

5.10.8.2.4a-1 $$l_{dh} = \max\left[l_{hb}\left(\frac{\lambda_{rc}\lambda_{cw}\lambda_{er}}{\lambda}\right), 8d_b, 6\ in.\right]$$ H2-15

5.10.8.2.4a-2 $$l_{hb} = \frac{38 d_b}{60}\left(\frac{f_y}{\sqrt{f_c'}}\right)$$ H2-16

The parameters specified in Eqs. H2-14 – H2-16 are determined as follows:

- Deck is normal-weight concrete, hence λ is taken 1.0;

- The cover beyond the 90° hook (b_3) is 1.5 $in. < 2$ $in.$, hence $\lambda_{rc} = 1.0$;
- λ_{er} is 1.0 as the lack of development is considered explicitly; and
- λ_{cw} is 1.0 for uncoated reinforcement.

$$l_{hb} = \frac{38(0.5)}{60}\left(\frac{60}{\sqrt{4.5}}\right) = 9.0\ in.$$

$$l_{dh} = \max\left[9\left[\frac{(1.0)(1.0)(1.0)}{(1.0)}\right], 8(0.5), 6\ in.\right] = 9\ in.$$

$$l_{dhava} = 10.5\ in. > l_{dh} = 9\ in. \rightarrow Fully\ develops$$

$$f_{yadj} = f_y = 60\ ksi$$

Fig. H.2.8 shows that the same results can be obtained using the MDOT Barrier program.

2. Flexural Resistance of the Barrier about Horizontal Axis

8.96	in.	Required development length based on AASHTO LRFD (2020) for barrier-deck reinf.
10.50	in.	Available development length based on AASHTO LRFD (2020) for barrier-deck reinf.

Fig. H.2.8. Required and available development lengths for the dowels as computed by the MDOT Barrier program

Flexural Capacity of the Barrier About Horizontal Axis prior to Deck Fascia Deterioration

Segment I Flexural Capacity About Horizontal Axis

The flexural capacity of Segment I about horizontal axis is calculated based on the following simplifications. An average thickness is calculated followed by the calculation of the equivalent effective depth. Only the bars denoted in blue in Fig. H.2.9 are considered. The reinforcement denoted in blue is assumed to develop its yield strength. Even though there are two layers of reinforcement, one near the inside face of the barrier and the other near the outside face of the barrier, only the reinforcement closest to the tension face (i.e. the inside face of barrier) is considered in the flexural strength calculations.

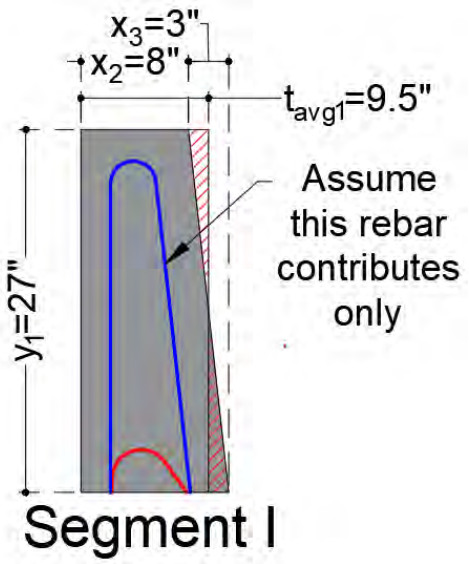

Fig. H.2.9. Flexural resistance for the segment I about horizontal axis

The average thickness is calculated as follows:

$$t_{avg1} = \frac{x_2 + x_2 + x_3}{2} = \frac{8 + 8 + 3}{2} = 9.5\ in.$$

$$h_1 = y_1 = 27\ in.$$

The effective depth is calculated as follows by subtracting the cover plus the radius of the bar from the average thickness.

$$d_s = t_{avg1} - \left(b_1 + \frac{d_b}{2}\right) = 9.5 - \left(2 + \frac{0.5}{2}\right) = 7.25\ in.$$

Area of steel on a per foot basis is:

$$A_s = 0.20 * \frac{12}{6} = 0.40\ in.^2/ft$$

The total compression and tension forces can be expressed as:

$$\sum C = 0.85(4.5)(12)(0.825)c = 37.9c$$

$$\sum T = 0.40(60) = 24.0\ kips/ft$$

The neutral axis depth can be computed as:

$$c = \frac{24.0}{37.9} = 0.633\ in./ft$$

The depth of the Whitney's stress block is:

$$a = 0.825(0.633) = 0.522\ in./ft$$

As can be seen, the steel strain is larger than the yield strain, which validates the assumption about tension steel yielding. In addition, based on the steel tensile strain, the section is classified as tension controlled for which ϕ = 0.9. However, the strength reduction factor is always taken as ϕ = 1.0, regardless of which limit state is evaluated and regardless of the classification of the section as tension controlled, compression controlled, or member in the transition zone, because vehicle impact is an extreme event. However, there is assurance in determining that the section is tension controlled because the formation of the assumed yield line mechanism relies on the flexural ductility of the barrier.

$$\varepsilon_s = \frac{0.003(7.5 - 0.633)}{0.633} = 0.03 \gg \varepsilon_{sy} \rightarrow OK$$

The flexural strength is:

$$M_{n1} = (0.40)(60)\left(7.25 - \frac{0.522}{2}\right) = 167.7\ kips - in./ft$$

$$\phi M_{n1} = (1.0)\left(\frac{167.7}{12}\right) = 14.0\ k - ft/ft$$

Segment II Flexural Capacity About Horizontal Axis

A similar approach is followed for Segment II. An average thickness is calculated followed by the determination of the effective depth. Only the dowels – i.e. the reinforcement denoted in red are considered when computing flexural resistance. The layers of reinforcements closest to the compression side are ignored. The blue reinforcement closest to the tension side is also ignored due to concerns about development length.

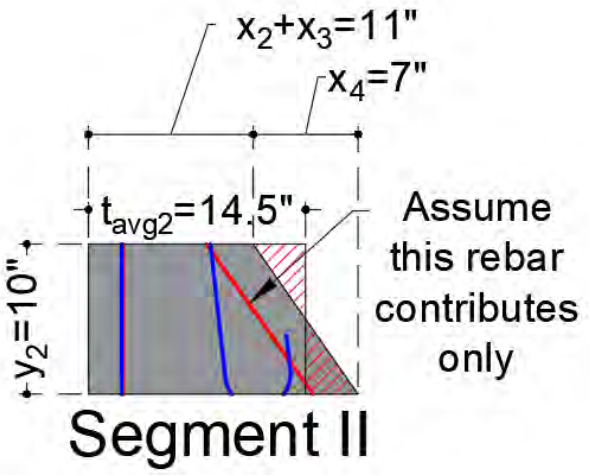

Fig. H.2.10. Flexural resistance for the segment II about horizontal axis

The average thickness is calculated as follows:

$$t_{avg2} = \frac{x_2 + x_3 + x_2 + x_3 + x_4}{2} = \frac{8 + 3 + 8 + 3 + 7}{2} = 14.5\ in.$$

$$h_2 = y_2 = 10\ in.$$

The effective depth of the reinforcement is calculated as follows by subtracting the cover plus the radius of the bar from the average thickness.

$$d_s = t_{avg2} - \left(b_1 + \frac{d_b}{2}\right) = 14.5 - \left(2 + \frac{0.5}{2}\right) = 12.25\ in.$$

The area of reinforcement on a per foot basis is:

$$A_s = 0.20 * \frac{12}{6} = 0.40\ in.^2/ft$$

The resultant compressive and tensile forces are:

$$\sum C = 0.85(4.5)(12)(0.825)c = 37.9c$$

$$\sum T = 0.40(60) = 24.0\ kips/ft$$

The depth of the neutral axis is:

$$c = \frac{24.0}{37.9} = 0.633\ in./ft$$

The depth of the Whitney's stress block is:

$$a = 0.825(0.633) = 0.522\ in./ft$$

As can be seen, the steel strain is larger than the yield strain, which validates the assumption about tension steel yielding. In addition, based on the tensile strain value in steel, the section is classified as tension controlled for which $\phi = 0.9$. However, the strength reduction factor is always taken as $\phi = 1.0$, regardless of which limit state is evaluated and regardless of the classification of the section as tension controlled, compression controlled, or member in the transition zone, because vehicle impact is an extreme event. However, there is assurance in determining that the section is tension controlled because the formation of the assumed yield line mechanism relies on the flexural ductility of the barrier.

$$\varepsilon_s = \frac{0.003(12.25 - 0.633)}{0.633} = 0.06 \gg \varepsilon_{sy} \rightarrow OK$$

The flexural strength is:

$$M_{n2} = (0.40)(60)\left(12.25 - \frac{0.522}{2}\right) = 287.7\ kips - in./ft$$

$$\phi M_{n2} = (1.0)\left(\frac{287.7}{12}\right) = 24.0\ k - ft/ft$$

Segment III Flexural Capacity About Horizontal Axis

Segment III is prismatic and therefore no cross-sectional simplification is needed. Only the dowels closest to the tension face are assumed to contribute to flexural resistance.

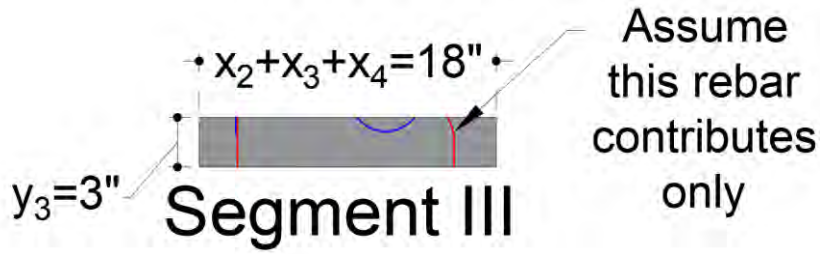

Fig. H.2.11. Flexural resistance for the segment III about horizontal axis

The total thickness is;

$$t_3 = x_2 + x_3 + x_4 = 8 + 3 + 7 = 18\ in.$$

$$h_3 = y_3 = 3\ in.$$

The effective depth is:

$$d_s = t_3 - \left(b_1 + \frac{d_b}{2}\right) = 18 - \left(2 + \frac{0.5}{2}\right) = 15.75\ in.$$

The area of steel on a per foot basis is:

$$A_s = 0.20 * \frac{12}{6} = 0.40\ in.^2/ft$$

The resultant compressive and tensile forces are:

$$\sum C = 0.85(4.5)(12)(0.825)c = 37.9c$$

$$\sum T = 0.40(60) = 24.0\ kips/ft$$

The depth to the neutral axis is:

$$c = \frac{24.0}{37.9} = 0.633\ in./ft$$

The depth to the Whitney's stress block is:

$$a = 0.825(0.633) = 0.522\ in./ft$$

As can be seen, the steel strain is larger than the yield strain, which validates the assumption about tension steel yielding. In addition, based on the steel tensile strain, the section is classified as tension controlled for which ϕ = 0.9. However, the strength reduction factor is always taken as ϕ = 1.0, regardless of which limit state is evaluated and regardless of the classification of the section as tension controlled, compression controlled, or member in the transition zone, because vehicle impact is an extreme event. However, there is assurance in determining that the section is tension controlled because the formation of the assumed yield line mechanism relies on the flexural ductility of the barrier.

$$\varepsilon_s = \frac{0.003(15.75 - 0.633)}{0.633} = 0.07 \gg \varepsilon_{sy} \rightarrow OK$$

The flexural strength is:

$$M_{n3} = (0.40)(60)\left(15.75 - \frac{0.522}{2}\right) = 371.7\ kips - in./ft$$

$$\phi M_{n3} = (1.0)\left(\frac{371.7}{12}\right) = 31.0\ k - ft/ft$$

The weighted average for the flexural strength considering flexural resistances from each segment and segment length is:

$$M_c = \frac{\phi M_{n1} y_1 + \phi M_{n2} y_2 + \phi M_{n3} y_3}{y_1 + y_2 + y_3} \qquad \text{H2-17}$$

$$M_c = \frac{14.0(27) + 24.0(10) + 31.0(3)}{27 + 10 + 3} = 17.8\ k - ft/ft$$

The calculated flexural strength for each segment as well as the average flexural strength are tabulated in Table H.2.1. A similar table is provided by the MDOT Barrier program yielding similar results.

Table H.2.1. Flexural resistance of the barrier about horizontal axis based on hand calculations

Segment No.	Parameter	Value	Unit
1	ϕM_{n1}	14.0	k-ft/ft
2	ϕM_{n2}	24.0	k-ft/ft
3	ϕM_{n3}	31.0	k-ft/ft
Average	M_c	17.8	k-ft/ft

Table H.2.2. Flexural resistance of the barrier about horizontal axis based on the MDOT Barrier program

Segment No.	Neg. Moment (k-ft/ft)
1	13.98
2	23.98
3	30.98
Avg.	17.75

The critical length of yield line failure pattern is calculated as follows. Since there is no beam at the top of the barrier $M_b = 0$.

[A13.3.1-2]
$$L_c = \frac{L_t}{2} + \sqrt{\left(\frac{L_t}{2}\right)^2 + \frac{8H(M_b + M_w)}{M_c}}$$

$$L_c = \frac{3.5}{2} + \sqrt{\left(\frac{3.5}{2}\right)^2 + \frac{8\left(\frac{40}{12}\right)(0 + 17.8)}{17.8}} = 7.2\ ft$$

Nominal resistance of the barrier to transversely applied loads, R_w, is:

$$R_w = \left(\frac{2}{2L_c - L_t}\right)\left(8M_b + 8M_w + \frac{M_c L_c^2}{H}\right)$$

$$R_w = \left(\frac{2}{2(7.2) - 3.5}\right)\left(8(0) + 8(17.8) + \frac{(17.8)(7.2)^2}{40/12}\right) = 76.9\ kips$$

This is larger than the required transverse load for TL-4.

$$R_w = 76.9\ kips > F_t = 54\ kips \rightarrow OK$$

As can be seen, for the original design i.e. undeteriorated deck fascia, the barrier meets the TL-4 requirements in terms of transverse load capacity.

Flexural Capacity of the Barrier About Horizontal Axis after Deck Fascia Deterioration

The deterioration of the deck fascia affects the flexural capacity of the barrier about the horizontal axis by reducing the effective depth of all three segments in the barrier as effective bearing on the deck fascia for the barrier is provided only past the remaining portion of the deck fascia. It should be noted that since the deck fascia extends past the outside face of the barrier, the impact of deterioration will manifest itself only if the deterioration extends past the outside face of barrier. In this example, the deterioration width that affects the barrier flexural capacity about its horizontal axis is $x_{adj} = w_d - x_1 = 6.5 - 1.5 = 5.0\ in.$ Flexural capacities for each segment are re-calculated based on this reduction on the width of the barrier.

Segment I Flexural Capacity About Horizontal Axis

The reduced thickness of segment I after deck fascia deterioration in shown in Fig. H.2.12.

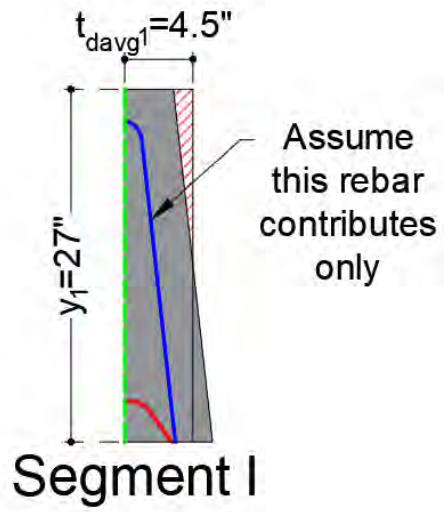

Fig. H.2.12. Flexural resistance for segment I about horizontal axis after deck fascia deterioration

The average thickness of segment I is:

$$t_{davg1} = t_{avg1} - x_{adj}$$

$$t_{davg1} = 9.5 - 5 = 4.5\ in.$$

$$h_1 = y_1 = 27\ in.$$

The effective depth is:

$$d_s = t_{davg1} - \left(b_1 + \frac{d_b}{2}\right) = 4.5 - \left(2 + \frac{0.5}{2}\right) = 2.25\ in.$$

The area of steel per foot is:

$$A_s = 0.20 * \frac{12}{6} = 0.40\ in.^2/ft$$

The resultant compressive and tensile forces are:

$$\sum C = 0.85(4.5)(12)(0.825)c = 37.9c$$

$$\sum T = 0.40(60) = 24.0\ kips/ft$$

The depth of the neutral axis is:

$$c = \frac{24.0}{37.9} = 0.633\ in./ft$$

The depth of the Whitney's stress block is:

$$a = 0.825(0.633) = 0.522\ in./ft$$

As can be seen, the steel strain is larger than the yield strain, which validates the assumption about tension steel yielding. In addition, based on the steel tensile strain, the section is classified as tension controlled for which ϕ = 0.9. However, the strength reduction factor is always taken as ϕ = 1.0, regardless of which limit state is evaluated and regardless of the classification of the section as tension controlled, compression controlled, or member in the transition zone, because vehicle impact is an extreme event. However, there is assurance in determining that the section is tension controlled because the formation of the assumed yield line mechanism relies on the flexural ductility of the barrier.

$$\varepsilon_s = \frac{0.003(2.25 - 0.633)}{0.633} = 7.66 * 10^{-3} \gg \varepsilon_{sy} \rightarrow OK$$

The flexural strength is:

$$M_{n1det} = (0.40)(60)\left(2.25 - \frac{0.522}{2}\right) = 47.7\ kips - in./ft$$

$$\phi M_{n1det} = (1.0)\left(\frac{47.7}{12}\right) = 4.0\ k - ft/ft$$

Segment II Flexural Capacity About Horizontal Axis

The reduced thickness of segment II after deck fascia deterioration in shown in Fig. H.2.13.

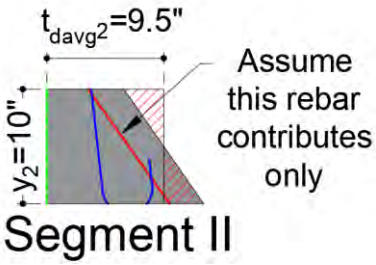

Fig. H.2.13. Flexural resistance for the segment II about horizontal axis after deterioration

The average thickness of segment II is:

$$t_{davg2} = t_{avg2} - x_{adj}$$

$$t_{davg2} = 14.5 - 5 = 9.5\ in.$$

$$h_2 = y_2 = 10\ in.$$

The effective depth is:

$$d_s = t_{davg2} - \left(b_1 + \frac{d_b}{2}\right) = 9.5 - \left(2 + \frac{0.5}{2}\right) = 7.25\ in.$$

The area of steel per foot is:

$$A_s = 0.20 * \frac{12}{6} = 0.40\ in.^2/ft$$

The resultant compressive and tensile forces are:

$$\sum C = 0.85(4.5)(12)(0.825)c = 37.9c$$

$$\sum T = 0.40(60) = 24.0\ kips/ft$$

The depth of the neutral axis is:

$$c = \frac{24.0}{37.9} = 0.633\ in./ft$$

The depth of the Whitney's stress block is:

$$a = 0.825(0.633) = 0.522\ in./ft$$

As can be seen, the steel strain is larger than the yield strain, which validates the assumption about tension steel yielding. In addition, based on the steel tensile strain, the section is classified as tension controlled for which $\phi = 0.9$. However, the strength reduction factor is always taken as

ϕ = 1.0, regardless of which limit state is evaluated and regardless of the classification of the section as tension controlled, compression controlled, or member in the transition zone, because vehicle impact is an extreme event. However, there is assurance in determining that the section is tension controlled because the formation of the assumed yield line mechanism relies on the flexural ductility of the barrier.

$$\varepsilon_s = \frac{0.003(7.25 - 0.633)}{0.633} = 0.03 \gg \varepsilon_{sy} \rightarrow OK$$

The flexural strength is:

$$M_{n2det} = (0.40)(60)\left(7.25 - \frac{0.522}{2}\right) = 167.7\ kips - in./ft$$

$$\phi M_{n2det} = (1.0)\left(\frac{167.7}{12}\right) = 14.0\ k - ft/ft$$

Segment III Flexural Capacity About Horizontal Axis

The reduced thickness of segment III after deck fascia deterioration in shown in Fig. H.2.14.

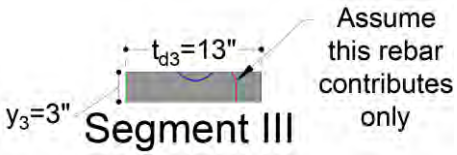

Fig. H.2.14. Flexural resistance for the segment III about horizontal axis after deterioration

The average thickness of segment III is:

$$t_{3davg} = t_3 - x_{adj}$$

$$t_{3davg} = 18 - 5 = 13\ in.$$

$$h_3 = y_3 = 3\ in.$$

The effective depth is:

$$d_s = t_{d3} - \left(b_1 + \frac{d_b}{2}\right) = 13 - \left(2 + \frac{0.5}{2}\right) = 10.75\ in.$$

The area of steel per foot is:

$$A_s = 0.20 * \frac{12}{6} = 0.40\ in.^2/ft$$

The resultant compressive and tensile forces are:

$$\sum C = 0.85(4.5)(12)(0.825)c = 37.9c$$

$$\sum T = 0.40(60) = 24.0\ kips/ft$$

The depth of the neutral axis is:

$$c = \frac{24.0}{37.9} = 0.633\ in./ft$$

The depth of the Whitney's stress block is:

$$a = 0.825(0.633) = 0.522\ in./ft$$

As can be seen, the steel strain is larger than the yield strain, which validates the assumption about tension steel yielding. In addition, based on the steel tensile strain, the section is classified as tension controlled for which ϕ = 0.9. However, the strength reduction factor is always taken as ϕ = 1.0, regardless of which limit state is evaluated and regardless of the classification of the section as tension controlled, compression controlled, or member in the transition zone, because vehicle impact is an extreme event. However, there is assurance in determining that the section is tension controlled because the formation of the assumed yield line mechanism relies on the flexural ductility of the barrier.

$$\varepsilon_s = \frac{0.003(10.75 - 0.633)}{0.633} = 0.05 \gg \varepsilon_{sy} \rightarrow OK$$

The flexural strength is:

$$M_{n3det} = (0.40)(60)\left(10.75 - \frac{0.522}{2}\right) = 251.7\ kips - in./ft$$

$$\phi M_{n3det} = (1.0)\left(\frac{251.7}{12}\right) = 21.0\ k - ft/ft$$

The weighted average of the flexural capacity of the barrier with a deteriorated deck fascia about its horizontal axis is:

$$M_{cdet} = \frac{4.0(27) + 14.0(10) + 21.0(3)}{27 + 10 + 3} = 7.8\ k - ft/ft$$

Table H.2.3 provides a summary of the calculated flexural resistances of the barrier with a deteriorated deck fascia about its horizontal using hand calculations. A similar summary is provided in Table H.2.4 for the computed flexural resistances obtained from the MDOT Barrier program. The results are rather similar.

Table H.2.3. Results for the flexural resistance of the barrier about horizontal axis after deterioration

Segment No.	Parameter	Value	Unit
1	ϕM_{n1det}	4.0	k-ft/ft
2	ϕM_{n2det}	14.0	k-ft/ft
3	ϕM_{n3det}	21.0	k-ft/ft
Average	M_{cdet}	7.8	k-ft/ft

Table H.2.4. Outputs obtained from MDOT Barrier program for the flexural resistance of the barrier about horizontal axis after deterioration

Property	Value
Segment I (k-ft/ft)	3.98
Segment II (k-ft/ft)	13.98
Segment III (k-ft/ft)	20.98
Unadjusted average flexural capacity of the barrier (Considering full deterioration along the crit…	7.75

The critical length for the yield line failure pattern is:

$$L_{cdet} = \frac{L_t}{2} + \sqrt{\left(\frac{L_t}{2}\right)^2 + \frac{8H(M_b + M_w)}{M_{cdet}}}$$

$$L_{cdet} = \frac{3.5}{2} + \sqrt{\left(\frac{3.5}{2}\right)^2 + \frac{8\left(\frac{40}{12}\right)(0 + 17.8)}{7.8}} = 9.76\ ft$$

The nominal resistance of the barrier with the deteriorated deck fascia to transversely applied loads, R_{wdet}, is:

$$R_{wdet} = \left(\frac{2}{2L_{cdet} - L_t}\right)\left(8M_b + 8M_w + \frac{M_{cdet}L_{cdet}^2}{H}\right)$$

$$R_{wdet} = \left(\frac{2}{2(9.76) - 3.5}\right)\left(8(0) + 8(17.8) + \frac{(7.8)(9.74)^2}{40/12}\right) = 45.4\ kips$$

This is significantly smaller than the lateral resistance of a barrier with no deterioration in the deck fascia. The length over which the applied vehicle impact is resisted by the deck, $L_{cdisttodeckcenterdet}$, is calculated 17.4 ft (209.1 in.).

$$L_{cdisttodeckcenterdet} = L_{cdet} + 2(H_b + 0.5t_d)$$

$$L_{cdisttodeckcenterdet} = 9.76 + 2\left(\frac{40}{12} + 0.5\left(\frac{12}{12}\right)\right) = 17.4\ ft$$

The adjusted flexural capacity of the barrier about the horizontal axis considering the deteriorated and undeteriorated portions of the deck fascia is calculated as follows:

If $L_{cdisttodeckcenterdet} \geq L_d$

$$L_{undet} = L_{cdisttodeckcenterdet} - L_d$$

$$M_{cdetadj} = \frac{M_c L_{undet} + M_{cdet} L_d}{L_{cdisttodeckcenterdet}}$$

If $L_{cdisttodeckcenterdet} < L_d$

$$L_{undet} = 0$$

$$M_{cdetadj} = M_{cdet}$$

Since $L_{cdisttodeckcenterdet}$ is greater than the specified deterioration length in the problem statement, $L_d = 180\ in.$, the effective width of the deck, $L_{cdisttodeckcenterdet}$, consists of deteriorated and undeteriorated portions for the deck fascia. This suggests that the flexural resistance of the barrier about the horizontal axis must be computed considering the deteriorated as well as the undeteriorated portions.

The undeteriorated length of the deck fascia within the $L_{cdisttodeckcenterdet}$ is calculated 29.12 in.

$$L_{undet} = L_{cdisttodeckcenterdet} - L_d$$

$$L_{undet} = 209.1 - 180 = 29.12\ in.$$

The flexural resistance of the barrier about the horizontal axis is:

$$M_{cdetadj} = \frac{M_c L_{undet} + M_{cdet} L_d}{L_{cdisttodeckcenterdet}}$$

$$M_{cdetadj} = \frac{(17.8)29.12 + (7.8)(180)}{209.1} = 9.19\ k - ft/ft$$

Similar results can be obtained from the MDOT Barrier program as shown Table H.2.5.

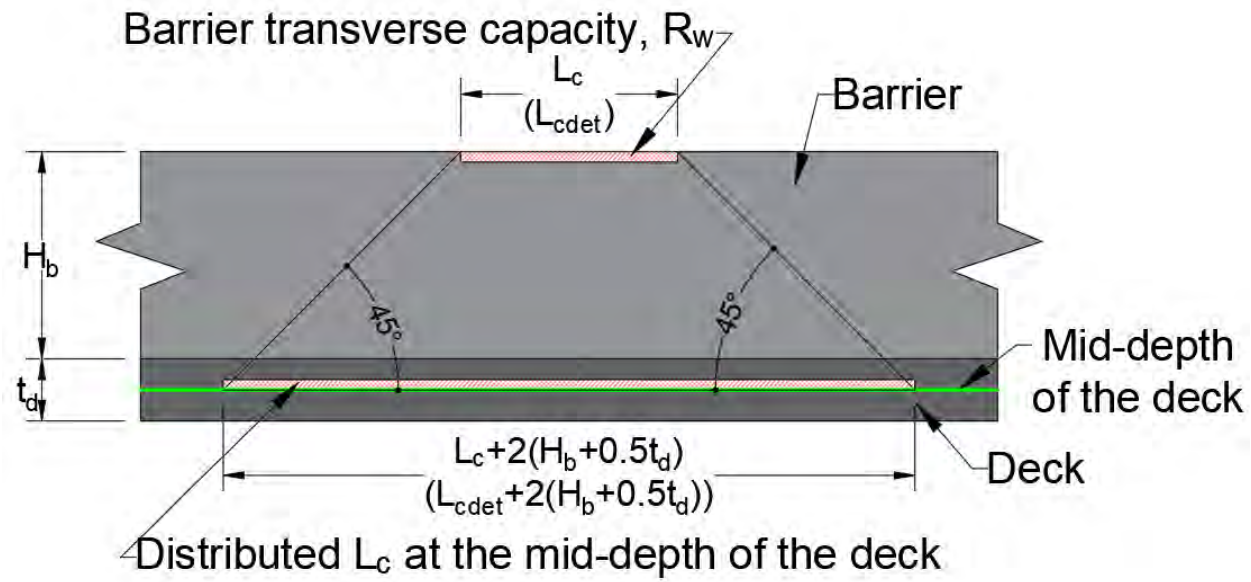

Fig. H.2.15. Distribution of critical wall length to the mid-depth of the deck

Table H.2.5. Adjusted deteriorated flexural resistance of the barrier about horizontal axis (obtained from MDOT Barrier)

Property	Value
Segment II (k-ft/ft)	13.98
Segment III (k-ft/ft)	20.98
Unadjusted average flexural capacity of the barrier (Considering full deterioration along the crit…	7.75
Adjusted average flexural capacity of the barrier (Considering adjusted deterioration length) (k-…	9.15

The adjusted flexural capacity is used to calculate the adjusted critical length of yield line failure pattern, $L_{cdetadj}$, as follows:

$$L_{cdetadj} = \frac{L_t}{2} + \sqrt{\left(\frac{L_t}{2}\right)^2 + \frac{8H(M_b + M_w)}{M_{cdetadj}}}$$

$$L_{cdetadj} = \frac{3.5}{2} + \sqrt{\left(\frac{3.5}{2}\right)^2 + \frac{8\left(\frac{40}{12}\right)(0 + 17.8)}{9.19}} = 9.15\ ft$$

This information is then used to calculate the adjusted lateral load capacity of the barrier considering both deteriorated and undeteriorated portions of the deck fascia.

$$R_{wdetadj} = \left(\frac{2}{2L_{cdetadj} - L_t}\right)\left(8M_b + 8M_w + \frac{M_{cdetadj}L_{cdetadj}^2}{H}\right)$$

$$R_{wdetadj} = \left(\frac{2}{2(9.15) - 3.5}\right)\left(8(0) + 8(17.8) + \frac{(9.19)(9.15)^2}{40/12}\right) = 50.4\ kips$$

$$R_{wadj} = 50.4\ kips < F_t = 54\ kips \rightarrow Not\ OK$$

As can be seen above, the deterioration of the deck fascia reduces the transverse load capacity of the barrier to 50.4 kips. This is lower than the required transverse load capacity for TL-4 level crashworthiness, which is 54 kips. The same conclusion is drawn by examining the results from the MDOT Barrier program (Table H.2.6).

Table H.2.6. Transverse resistance of the barrier after deterioration (obtained from MDOT Barrier)

3. Transverse Resistance of the Barrier

Property	Value
Undeteriorated length within distributed unadjusted critical length (ft)	2.43
Transverse capacity of the barrier with unadjusted critical length (kips)	45.40
Transverse capacity of the barrier with adjusted critical length (kips)	50.35
Required transverse capacity of the barrier (kips)	54.00

2.3. Interface Shear Transfer Between Barrier and Deck

The shear strength of the barrier deck interface is evaluated prior to the deck fascia deterioration and after the deterioration using shear friction theory as outlined in AASHTO LRFD (2020) Article 5.7.4.4. It should be noted that the deck fascia deterioration affects the area of the interface that is engaged in shear transfer illustrated by the green rectangle in Fig. H.2.16. Since a capacity design approach is implemented, the interface shear demand is determined based on the lateral load capacity of the barrier. Therefore, there will be two interface shear demands: one for the barrier with an undeteriorated fascia and another for the barrier with deteriorated fascia. Interface shear strength will be calculated for the undeteriorated deck fascia and for the deteriorated deck facia and will be compared to the corresponding demands. When determining the shear strength of the interface between the barrier and deck, only the dowel leg that is hooked in the deck overhang is considered in resistance calculations as the other leg is close to the deck edge, does not feature a 90-degree hook, and is not fully developed (Fig. H.2.16).

Before Deterioration

The full lateral load capacity of the undeteriorated barrier is distributed to the base of the barrier (top of the deck) as illustrated in Fig. H.2.17 and as expressed in Eqs. H2-18 – H2-19.

$$L_{cdisttodecktop} = L_c + 2H_b \quad \text{H2-18}$$

$$V_{CT} = \frac{R_w}{L_{cdisttodecktop}} \quad \text{H2-19}$$

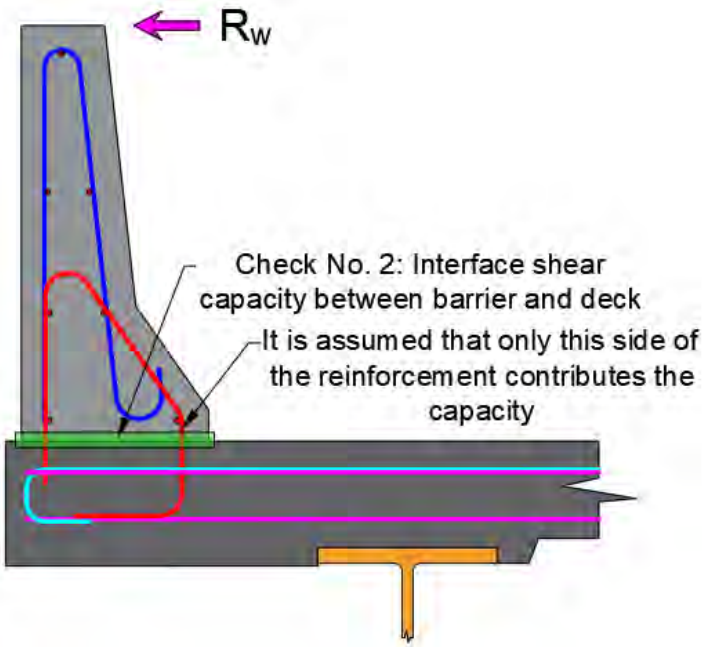

Fig. H.2.16. Barrier-deck interface shear capacity to transfer R_w from barrier to the deck

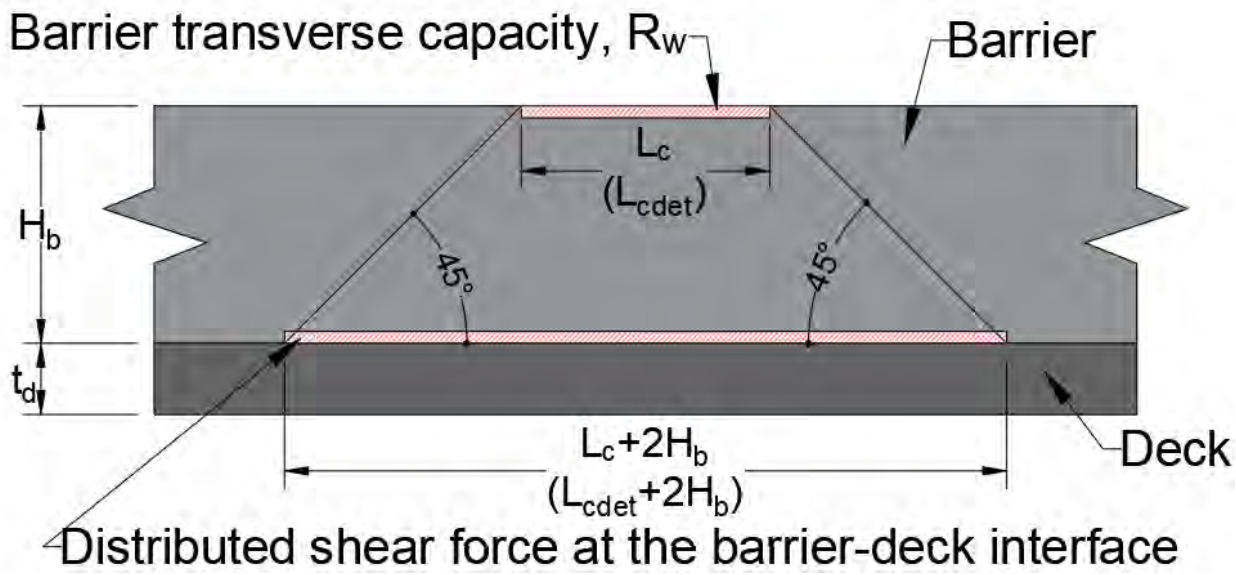

Fig. H.2.17. Distribution of critical wall length to the base of the barrier (top of the deck)

Based on Eq. H2-18 $L_{cdisttodecktop}$ is calculated as 13.87 ft.

$$L_{cdisttodecktop} = 7.2 + 2\left(\frac{40}{12}\right) = 13.87\ ft$$

The interface shear demand, V_{CT}, is calculated as $V_{CT} = 5.55\ k/ft$.

$$V_{CT} = \frac{76.9}{13.87} = 5.55\ k/ft$$

The shear resistance of the interface is determined using Eqs. H2-20 through H2-23.

5.7.4.3-3	$V_{ni} = cA_{cv} + \mu\left(A_{vf}f_y + P_c\right)$	H2-20
5.7.4.3-4	$V_{ni} \le K_1 f_c' A_{cv}$	H2-21
5.7.4.3-5	$V_{ni} \le K_2 A_{cv}$	H2-22
5.7.4.3-6	$A_{cv} = b_{vi}L_{vi}$	H2-23

The shear contact area, A_{cv}, per ft is calculated as 216 $in.^2/ft$.

$$A_{cv} = (x_2 + x_3 + x_4)12$$

$$A_{cv} = (8 + 3 + 7)12 = 216\ in.^2/ft$$

$$H_{barrier} = 40\ in.$$

$$A_{barrier} = 455.5\ in.^2$$

$$t_{avg} = 11.4\ in.$$

$$\gamma_{barrier} = 150\ pcf\ (5\ pcf\ for\ reinforcement\ weight, 145\ pcf\ for\ f_c' = 4.5\ ksi\ concrete)$$

$$w_{barrier} = A_{barrier}\gamma_{barrier}$$

$$w_{barrier} = \frac{(455.5)(150)}{1000 * 144} = 0.475\ kips/ft$$

$$P_c = w_{barrier} = 0.475\ k/ft$$

For the specified type of interface between the barrier and deck, cohesion factor, c, and friction factor, μ, are taken 0.24 and 1.0; and K_1 and K_2 are taken 0.25 and 1.5 ksi based on Table H.2.7.

$$c = 0.24\ \&\ \mu = 1.0$$

$$K_1 = 0.25\ \&\ K_2 = 1.5\ ksi$$

Table H.2.7. Cohesion and Friction Factors (section 5.7.4.4 in AASHTO LRFD 2020)

Condition	Parameter	Value
For a cast-in-place concrete slab on clean concrete girder surfaces, free of laitance with surface roughened to an amplitude of 0.25 in.	c	0.28
	μ	1.0
	K_1	0.3
	K_2	1.8 ksi for nw. concrete 1.3 ksi for lw. concrete
For normal weight concrete placed monolithically	c	0.40
	μ	1.4
	K_1	0.25
	K_2	1.5
For lightweight concrete placed monolithically, or placed against a clean concrete surface, free of laitance with surface intentionally roughened to an amplitude of 0.25 in. (Type-1 in MDOT Barrier Program)	c	0.24
	μ	1.0
	K_1	0.25
	K_2	1.0 ksi
For normal weight concrete placed against a clean concrete surface, free of laitance, with surface intentionally roughened to an amplitude of 0.25 in. (Type-2 in MDOT Barrier Program)	c	0.24
	μ	1.0
	K_1	0.25
	K_2	1.5
For concrete placed against a clean concrete surface, free of laitance, but not intentionally roughened (Type-3 in MDOT Barrier Program)	c	0.075
	μ	0.6
	K_1	0.2
	K_2	0.8 ksi
For concrete anchored to as-rolled structural steel by headed studs or by reinforcing bars where all steel in contact with concrete is clean and free of paint	c	0.025
	μ	0.7
	K_1	0.2
	K_2	0.8 ksi
Highlighted condition represents the cases applicable in this project.		

It has been shown that interface reinforcement can attain their yield stress, $f_y = 60$ ksi.

$$f_y = 60\ ksi$$

The area of interface shear reinforcement, A_{vf}, is calculated as 0.40 $in.^2/ft$.

$$A_{vf} = \frac{(0.20)12}{6} = 0.40\ in.^2/ft$$

The upper bounds on interface shear strength are calculated as:

$$K_1 f_c' A_{cv} = 0.25 * 4.5 * 216/12 = 243\ kips/ft$$

$$K_2 A_{cv} = 1.5 * 216 = 324\ kips/ft$$

For the calculation of interface shear strength, the weaker material between deck and barrier concrete is considered. Since they are both equal with an $f_c' = 4500$ psi, the calculations are not affected by this selection. The nominal interface shear resistance can be calculated using Eq. H2-20 as follows.

$$V_{ni} = 0.24(216) + 1.0(0.40 * 60 + 0.475) = 76.3\ kips/ft \leq \begin{matrix} 243\ kips/ft \\ 324\ kips/ft \end{matrix} \rightarrow OK$$

The ϕ factor is taken as 1.0 since vehicle impact is an extreme event. From Eqs. H2-20 – H2-23 the interface shear resistance, V_{ri}, is calculated as shown below.

$$V_{ri} = (1.0)(76.3) = 76.3\ kips/ft > 5.5\ kips/ft = V_{ui} \rightarrow OK$$

The provided capacity for the interface shear strength between the deck and barrier is greater than the demand, hence the original (undeteriorated) design is adequate in terms of interface shear strength. Requirements related to minimum interface shear reinforcement are evaluated as follows:

$$A_{vfprovided} = 0.40\ in.^2/ft$$

$$A_{vfmin} = \min\left(\begin{matrix} \dfrac{0.05 * 216}{60} \\ \dfrac{\left(\dfrac{1.33 * 5.50}{0.9} - 0.24 * 216\right)}{\dfrac{1.0}{60}} - 0.475 > 0 \end{matrix}\right) = 0$$

$$A_{vfprovided} = 0.40\ in.^2/ft > 0 = A_{vfmin} \rightarrow OK$$

Similar results are obtained from the MDOT Barrier program as shown Table H.2.8 (Original Design Tab – Section 4).

Table H.2.8. Interface shear strength as computed by the MDOT Barrier program

4. Interface Shear Transfer Between Barrier and Deck

Property	Value	Unit
Uniform barrier load	0.47	k/ft
Shear force at the interface	5.53	k/ft
Shear capacity of the interface	76.31	k/ft
Minimum area of the interface shear reinforcement	0	in.^2/ft
Provided area of the interface shear reinforcement	0.40	in.^2/ft

After Deterioration

Since the deck fascia deterioration extends 5 in. past the outside face of the barrier it affects the interface shear capacity by reducing the area engaged in interface shear transfer.

The deteriorated critical shear area, A_{cvdet}, is calculated as 156 $in.^2/ft$. It is assumed that the P_c term remains the same after deterioration.

$$A_{cvdet} = A_{cv} - 5 * 12 = 156\ in.^2/ft$$

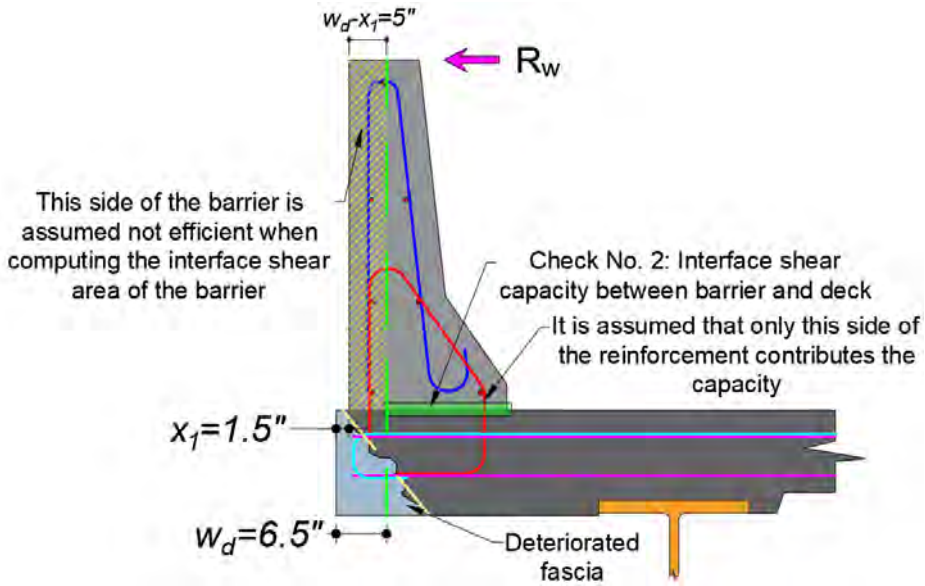

Fig. H.2.18. Consideration of deterioration when computing interface shear strength

Using A_{cvdet}, the nominal interface shear resistance can be calculated as follows:

$$V_{ni} = 0.24(156) + 1.0(0.40 * 60 + 0.475) = 61.9\ kips/ft \leq \begin{matrix} 175.5\ kips/ft \\ 234.0\ kips/ft \end{matrix} \rightarrow OK$$

The upper bounds specified above can be calculated as:

$$K_1 f_c' A_{cvdet} = 0.25 * 4.5 * 156 = 175.5\ kips/ft$$

$$K_2 A_{cvdet} = 1.5 * 156 = 234\ kips/ft$$

The interface shear demand is calculated by using the lateral load capacity of the barrier with a deteriorated fascia as calculated earlier and the corresponding effective deck width. The effective deck width is calculated using the adjusted critical yield line length obtained earlier and assuming a 45° distribution from the barrier to the deck.

$$L_{cdisttodecktopdet} = L_{cdetadj} + 2H_b$$

$$L_{cdisttodecktopdet} = 9.15 + 2\left(\frac{40}{12}\right) = 15.82\ ft$$

$$V_{CTdet} = \frac{R_{wdetadj}}{L_{cdisttodecktopdet}} = \frac{50.4}{15.82} = 3.18\ k/ft$$

The area engaged in shear transfer is calculated as follows:

If $L_{cdisttodecktopdet} \geq L_d$

$$L_{undet2} = L_{cdisttodecktopdet} - L_d \quad \text{H2-24}$$

$$A_{cvdetadj} = \frac{A_{cv}L_{undet2} + A_{cvdet}L_d}{L_{cdisttodecktopdet}} \quad \text{H2-25}$$

If $L_{cdisttodecktopdet} < L_d$

$$L_{undet2} = 0 \quad \text{H2-26}$$

$$A_{cvdetadj} = A_{cvdet} \quad \text{H2-27}$$

Since $L_d = 180\ in. < L_{cdisttodecktopdet} = 189.84\ in.$, then the interface shear strength is calculated using a weighted average approach as follows.

$$L_{undet2} = 189.84 - 180 = 9.84\ in.$$

$$A_{cvdetadj} = \frac{216(9.84) + 156(180)}{189.84} = 159.1\ in.^2/ft$$

Using $A_{cvdetadj}$, the nominal interface shear resistance can be calculated as follows:

$$K_1 f_c' A_{cvdetadj} = 0.25 * 4.5 * 159.1 = 179\ kips/ft$$

$$K_2 A_{cvdetadj} = 1.5 * 159.1 = 239\ kips/ft$$

$$V_{ni} = 0.24(159.1) + 1.0(0.40 * 60 + 0.475) = 62.7\ kips/ft \leq \begin{matrix} 179\ kips/ft \\ 239\ kips/ft \end{matrix} \rightarrow OK$$

The ϕ factor is taken 1.0 considering that vehicle impact is an extreme event.

$$V_{ri} = (1.0)(62.7) = 62.7\ kips/ft > 3.18\ kips/ft = V_{ui} \rightarrow OK$$

The interface shear strength is greater than the demand suggesting that the limit state of interface shear is not the controlling limit state. Checks for minimum interface shear reinforcement requirements are conducted as follows.

$$A_{vfprovided} = 0.40\ in.^2/ft$$

$$A_{vfmin} = \min\left(\begin{matrix} \frac{0.05 * 159.1}{60} \\ \frac{\left(\frac{1.33 * 3.18}{0.9} - 0.24 * 159.1\right)}{\frac{1.0}{60}} - 0.475 > 0 \end{matrix}\right) = 0$$

$$A_{vfprovided} = 0.40\ in.^2/ft > 0 = A_{vfmin} \rightarrow OK$$

Similar results are obtained from MDOT Barrier program as shown Table H.2.9 (After Deterioration Tab – Section 4).

Table H.2.9. Results for interface shear analysis considering deck fascia deterioration as computed by the MDOT Barrier computer program

4. Interface Shear Transfer Between Barrier and Deck

Property	Value	Unit
Shear force at the interface	3.18	k/ft
Shear capacity of the interface	62.66	k/ft
Minimum area of the interface shear reinforcement	0	in.^2/ft
Provided area of the interface shear reinforcement	0.40	in.^2/ft

2.4. Axial Tension Force and Moment Transfer from Barrier to Deck

The transfer of axial tension and bending moment created by vehicle impact from the barrier to the deck is evaluated for the barrier to deck connection prior to the deterioration of the deck fascia and after the deterioration. Here again the demand is based on the lateral load capacity of the barrier prior to the deterioration and after the deterioration. A linear interaction is assumed between the axial tension force and the moment as shown below where T_{CT} is the axial tensile force demand due to vehicle impact, M_{nint} is the flexural capacity of the deck overhang considering the presence of axial tension, M_n is the flexural capacity of the deck, and P_n is the axial tensile capacity of the deck overhang. Fig. H.2.19 illustrates the creation of axial tension and flexure in the deck overhang due to vehicle impact, and the critical section evaluated for axial tension force and moment transfer.

$$M_{nint} = M_n\left(1 - \frac{T_{CT}}{P_n}\right)$$

This means that for a given applied axial tension, the corresponding moment capacity is determined assuming a linear interaction diagram. Since a capacity design approach is followed, deck fascia deterioration may cause a reduction in the axial tension force which is equal to the lateral capacity of the deteriorated barrier. This reduction in the axial force demand will result in an increase in flexural moment capacity in the deck with the deteriorated fascia. This may seem counterintuitive as one would expect the moment capacity of the deck to reduce after the

deterioration, but it is because there is a larger moment capacity available due to the reduction in the axial force demand.

When determining the axial tension capacity of the deck both transverse layers of reinforcement are considered. When determining the flexural resistance of the deck, only the top most layer is considered. The deck transverse reinforcement features top straight bars and top hooked bars.

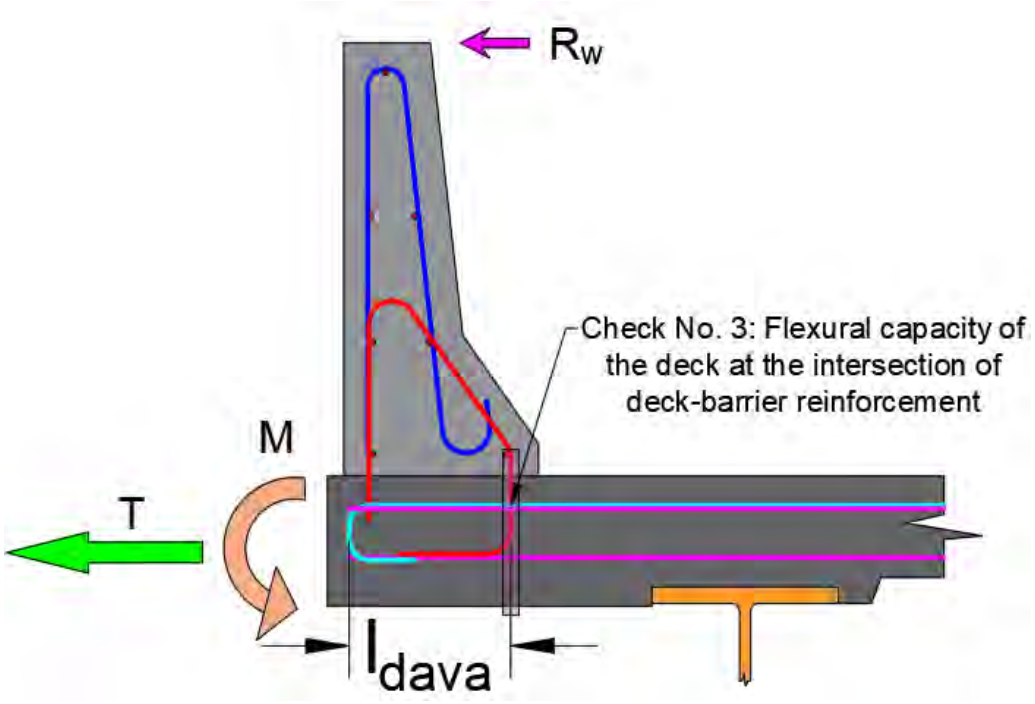

Fig. H.2.19. Illustration of critical section for flexural resistance calculation of the deck

Before Deterioration

The effective deck width over which axial tension and moment from vehicle impact can be transferred from the barrier to the deck is:

$$L_{cdisttodeckcenter} = 7.2 + 2\left(\frac{40}{12} + 0.5\left(\frac{12}{12}\right)\right) = 14.87\ ft$$

Moment demand is:

$$M_{CT} = \left(\frac{R_w}{L_{cdisttodeckcenter}}\right)(H_b + 0.5t_d)$$

$$M_{CT} = \left(\frac{76.9}{14.87}\right)\left(\frac{40}{12} + 0.5\left(\frac{12}{12}\right)\right) = 19.83\ k - ft/ft$$

Axial force demand is:

$$T_{CT} = \frac{R_w}{L_{cdisttodeckcenter}}$$

$$T_{CT} = \frac{76.9}{14.87} = 5.17\ k/ft$$

These results can also be retrieved from the MDOT Barrier program (Original Design Tab – Section 5) as shown in Table H.2.10.

Table H.2.10. Moment and axial force demands obtained from MDOT Barrier program for original (undeteriorated) design

5. Moment Transfer from Barrier to Deck in the Event of Collision

Property	Value	Unit
Required development length for the bottom transverse straight rebar	17.88	in.
Negative moment due to distribution of Rw	19.78	k-ft/ft
Axial tensile force due to distribution of Rw	5.16	k-ft/ft
Flexural moment capacity without interaction	24.88	k-ft/ft
Axial tension capacity	57.91	k-ft/ft
Flexural moment capacity with interaction	22.65	k-ft/ft

Before calculating the flexural resistance of the deck, it is necessary to determine if the transverse reinforcement can be fully developed. The available length for hooked and straight rebars is 15 in. as shown in Fig. H.2.20 and as calculated below.

$$l_{dava} = a_8 - a_9 = 17 - 2 = 15\ in.$$

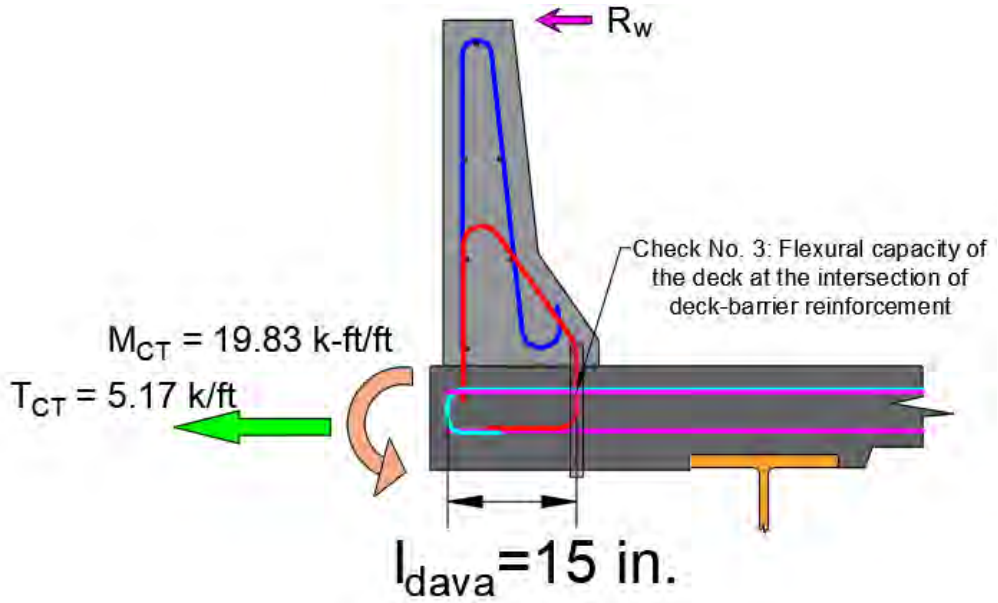

Fig. H.2.20. Available length for the deck transverse reinforcement at the critical section

2.4.1. Development Length Top Straight Transverse Deck Reinforcement

Development length for the straight rebars in tension can be calculated using the following set of equations.

5.10.8.2.1a-1 $$l_d = \max\left(l_{db}\left(\frac{\lambda_{rl}\lambda_{cf}\lambda_{cf}\lambda_{er}}{\lambda}\right), 12\right)$$ H2-28

5.10.8.2.1a-2 $$l_{db} = 2.4 d_b \frac{f_y}{\sqrt{f_c'}}$$ H2-29

$$\lambda_{rl}\lambda_{cf} \leq 1.7$$ H2-30

5.10.8.2.1c-1 $$0.4 \leq \lambda_{rc} \leq 1.0$$ H2-31

5.10.8.2.1c-2 $$\lambda_{rc} = \frac{d_b}{c_b + k_{tr}}$$ H2-32

$$c_b = \min(clear\ cover; spacing/2)$$ H2-33

5.10.8.2.1c-3 $k_{tr} = 40A_{tr}/sn$ (taken 0 in this project) H2-34

Modification factors are defined as follows:

- λ is concrete density modification factor: taken 1.0 for normal weight concrete and is calculated using Eq. H2-14 for light weight concrete where w_c is the unit weight of concrete, assumed 0.125 kcf.
- λ_{rl} is the reinforcement location factor. It is taken 1.3 if >12 in. concrete is placed is cast below the reinforcement. It can also be taken 1.3 if <12 in. concrete is placed below the reinforcement but $f_c' > 10$ ksi. Since in a typical deck fascia used in MI, it is not likely to have these situations, hence it might be taken 1.0. Although MDOT Barrier program checks these requirements in any case.
- λ_{rc} is reinforcement confinement factor. It is calculated using Eqs. H2-31 – H2-34.
- λ_{er} is excess reinforcement factor, taken as 1.0 as this is considered explicitly by adjusting the yield strength of the steel.
- λ_{cf} is the coating factor. It is taken 1.5 for epoxy-coated rebars with cover less than 3_{db} or with clear spacing between bars less than $6d_b$. For epoxy-coated reinforcement not covered in the previous statement, it is taken 1.2. For uncoated reinforcement, it is taken 1.0.

Using the information provided in the problem statement, the development length can be calculated as follows:

$$l_{db} = 2.4\left(\frac{5}{8}\right)\frac{60}{\sqrt{4.5}} = 42.4\ in.$$

The modification factors can be calculated as follows:

- $\lambda_{rl} = 1.0$ since $f'_{cd} < 10\ ksi$ and the concrete thickness below the reinforcement is smaller than 12 in.
- $\lambda_{cf} = 1.0$ since the rebars are uncoated.
- $\lambda_{rc} = \frac{d_b}{c_b + k_{tr}}$; $0.4 \le \lambda_{rc} \le 1.0$

$$k_{tr} = 0;$$

$$c_b = \min\left(b_2, \frac{spacing}{2}\right)$$

$$c_b = \min\left(3, \frac{7.5}{2}\right) = 3\ in.$$

$$\lambda_{rc} = \frac{5/8}{3+0} = 0.21 < 0.4 \rightarrow \lambda_{rc} = 0.4$$

- $\lambda_{er} = 1.0$ (inherently considered by adjusting the yield stress)
- $\lambda = 1.0$ for normal weight concrete

$$l_d = \max\left(42.4\left(\frac{1.0 * 1.0 * 0.4 * 1.0}{1.0}\right), 12\right) = 17.0\ in.$$

Since $l_{dava} = 15.0\ in. < l_d$, adjustment in the yield stress of the top deck transverse straight rebars is necessary.

$$f_{yadj} = f_y \frac{l_{dava}}{l_d}$$

$$f_{yadj} = 60\frac{15.0}{17.0} = 52.9\ ksi$$

2.4.2. Development Length for Bottom Straight Transverse Reinforcement

Development length for the straight rebars in tension can be calculated as follows.

$$l_{db} = 2.4\left(\frac{5}{8}\right)\frac{60}{\sqrt{4.5}} = 42.4\ in.$$

The modification factors can be calculated as follows:

- $\lambda_{rl} = 1.0$ since $f'_{cd} < 10\ ksi$ and the concrete thickness below the reinforcement is smaller than 12 in.
- $\lambda_{cf} = 1.0$ since the rebars are uncoated.
- $\lambda_{rc} = \frac{d_b}{c_b + k_{tr}}$; $0.4 \leq \lambda_{rc} \leq 1.0$

$$k_{tr} = 0;$$

$$c_b = \min\left(b_3, \frac{spacing}{2}\right)$$

$$c_b = \min\left(1.5, \frac{7.5}{2}\right) = 1.5\ in.$$

$$\lambda_{rc} = \frac{5/8}{1.5 + 0} = 0.42 > 0.4 \rightarrow \lambda_{rc} = 0.42$$

- $\lambda_{er} = 1.0$ (inherently considered by adjusting the yield stress)
- $\lambda = 1.0$ for normal weight concrete

$$l_d = \max\left(42.4\left(\frac{1.0 * 1.0 * 0.42 * 1.0}{1.0}\right), 12\right) = 17.8\ in.$$

Since $l_{dava} = 15.0\ in. < l_d$, adjustment in the yield stress of the top deck transverse straight rebar is necessary.

$$f_{yadj} = f_y \frac{l_{dava}}{l_d}$$

$$f_{yadj} = 60\frac{15.0}{17.8} = 50.6\ ksi$$

2.4.3. Development Length Check for the Top Hooked Transverse Deck Rebar

Development length for the hooked rebars in tension can be calculated using Eqs. H2-35 – H2-36.

5.10.8.2.4a-1 $$l_{dh} = \max\left[l_{hb}\left(\frac{\lambda_{rc}\lambda_{cw}\lambda_{er}}{\lambda}\right), 8d_b, 6\ in.\right]$$ H2-35

5.10.8.2.4a-2 $$l_{hb} = \frac{38d_b}{60}\left(\frac{f_y}{\sqrt{f'_c}}\right)$$ H2-36

$$l_{hb} = \frac{38(3/8)}{60}\left(\frac{60}{\sqrt{4.5}}\right) = 6.72\ in.$$

The modification factors are taken as follows:

- Deck is normal-weight concrete, hence λ is taken 1.0;
- The side cover normal to the plane of hook (a_9) is 2.0 $in.$ < 2.5 $in.$, hence $\lambda_{rc} = 1.0$;
- λ_{er} is 1.0 as the lack of development is considered explicitly; and
- λ_{cw} is 1.0 for uncoated reinforcement.

$$l_{dh} = \max\left[6.72\left(\frac{1.0 * 1.0 * 1.0 * 1.0}{1.0}\right), 8 * \frac{3}{8}, 6\ in.\right] = 6.72\ in.$$

Since $l_{dava} = 15.0\ in. > l_{dh}$, no adjustment in the yield stress of the top deck hooked transverse reinforcement is necessary.

$$f_{yadj} = f_y = 60\ ksi$$

Having performed the development length checks, the flexural resistance of the deck at critical section and the nominal axial tension capacity of the deck can be calculated as follows.

The nominal flexural moment capacity of the deck at critical section considering only top transverse reinforcement is:

$$\sum C = 0.85(4.5)(12)(0.825)c = 37.9c$$

$$\sum T = 0.31 * \frac{12}{7.5} * 52.9 + 0.11 * \frac{12}{7.5} * 60 = 36.8\ k/ft$$

$$c = \frac{36.8}{37.9} = 0.971\ in./ft$$

$$a = 0.825(0.971) = 0.801\ in./ft$$

$$\varepsilon_s = \frac{0.003\big((12 - 3 - 0.5(5 + 3)/16) - 0.971\big)}{0.971} = 0.02 \gg \varepsilon_{sy} \rightarrow OK$$

$$M_n = 36.8\left(8.75 - \frac{0.801}{2}\right) = 307.3\ k - in./ft$$

$$M_n = \frac{307.3}{12} = 25.6\ k - ft/ft$$

Axial tension capacity considering both layer of transverse deck reinforcement is:

$$P_n = A_{s4}f_{yadj4} + A_{s5}f_{yadj5} + A_{s6}f_{yadj6} \qquad \text{H2-37}$$

$$P_n = 0.31 * \frac{12}{7.5} * 52.9 + 0.11 * \frac{12}{7.5} * 60 + 0.31 * \frac{12}{9} * 50.6 = 57.7\ k/ft$$

Assuming a linear interaction between tension and moment, and considering the $\phi = 1.0$ for extreme event, the moment capacity of the overhang can be calculated as follows.

$$\phi M_{nint} = \phi M_n \left(1 - \frac{T_{CT}}{\phi P_n}\right)$$

$$\phi M_{nint} = (1.0)(25.6)\left(1 - \frac{5.17}{(1.0)(57.7)}\right) = 23.7\ k - ft/ft$$

$$\phi M_{nint} = 23.3\ k - ft/ft > M_{CT} = 19.83\ k - ft/ft \rightarrow OK$$

The flexural capacity of the undeteriorated deck is 23.3 k-ft/ft based on the linear axial tension bending moment interaction. Required flexural capacity due to vehicle impact is 19.83 k-ft/ft, which suggests that deck capacity is not the controlling limit state. Similar results can be obtained from the MDOT Barrier program as shown in Table H.2.11.

Table H.2.11. Flexural capacity of the deck with interaction obtained from MDOT Barrier program

5. Moment Transfer from Barrier to Deck in the Event of Collision

Property	Value	Unit
Required development length for the bottom transverse straight rebar	[illegible]	in.
Negative moment due to distribution of Rw	19.78	k-ft/ft
Axial tensile force due to distribution of Rw	5.16	k-ft/ft
Flexural moment capacity without interaction	25.65	k-ft/ft
Axial tension capacity	57.91	k-ft/ft
Flexural moment capacity with interaction	23.36	k-ft/ft

After Deterioration

The deterioration of the deck fascia reduces the available length of the transverse reinforcement thereby reducing axial tensile and flexural capacity of the deck. In addition, the deterioration in the case in question extends past the hook for the hooked bars thereby reducing anchorage effectiveness for hooked bars. For this reason, the hooked bars are considered as straight bars in the evaluation of the axial tension and moment capacity of the deck with a deteriorated deck fascia.

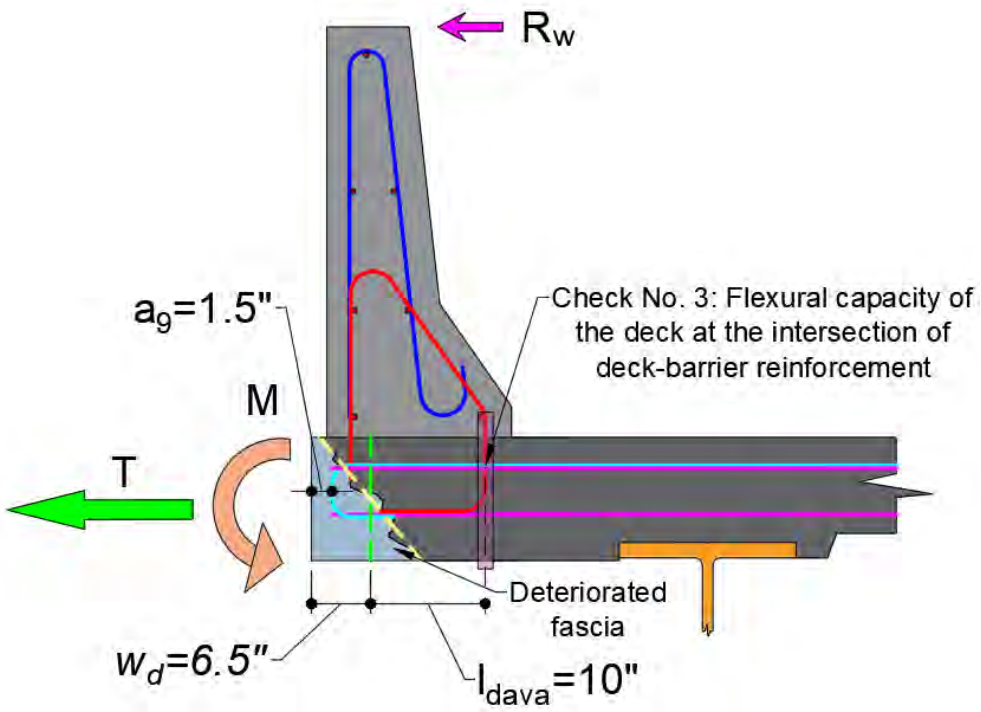

Fig. H.2.21. Available development length of the transverse rebars after deterioration

The development length for the hooked bars with ineffective hooks is identical with that of a straight bar and is calculated as follows:

$$l_{db} = 2.4\left(\frac{3}{8}\right)\frac{60}{\sqrt{4.5}} = 25.5\ in.$$

The modification factors can be calculated as follows:

- $\lambda_{rl} = 1.0$ since $f'_{cd} < 10\ ksi$ and the concrete thickness below the reinforcement is smaller than 12 in.
- $\lambda_{cf} = 1.0$ since the rebars are uncoated.
- $\lambda_{rc} = \frac{d_b}{c_b + k_{tr}}$; $0.4 \le \lambda_{rc} \le 1.0$

$$k_{tr} = 0;$$

$$c_b = \min\left(b_2, \frac{spacing}{2}\right)$$

$$c_b = \min\left(3, \frac{7.5}{2}\right) = 3\ in.$$

$$\lambda_{rc} = \frac{3/8}{3+0} = 0.125 < 0.4 \rightarrow \lambda_{rc} = 0.4$$

- $\lambda_{er} = 1.0$ (inherently considered by adjusting the yield stress)
- $\lambda = 1.0$ for normal weight concrete

$$l_d = \max\left(25.5\left(\frac{1.0 * 1.0 * 0.4 * 1.0}{1.0}\right), 12\right) = 12.0\ in.$$

Since $l_{dava} = 10.5\ in. < l_d = 12\ in.$, adjustment in the yield stress of the top deck transverse reinforcement with ineffective hooks is necessary.

$$f_{yadj} = f_y \frac{l_{dava}}{l_d}$$

$$f_{yadj} = 60\frac{10.5}{12} = 52.5\ ksi$$

The yield stress for the top and bottom straight rebars can be adjusted by reducing the available development length to 10.5 in.

$$Top\ straight\ rebar \rightarrow f_{yadj} = 60\frac{10.5}{17.0} = 37.1\ ksi$$

$$Bottom\ straight\ rebar \rightarrow f_{yadj} = 60\frac{10.5}{17.8} = 35.4\ ksi$$

Reinforcement development lengths after deck fascia deterioration occurs can be obtained from the MDOT Barrier program as shown in Table H.2.12.

Table H.2.12. Development length calculations for the transverse deck rebars after deterioration (Outputs obtained from MDOT Barrier program)

5. Moment Transfer from Barrier to Deck in the Event of Collision

Property	Value	Unit
Available development length for the transverse deck rebars	10.50	in.
Required development length for the top transverse straight rebar	[illegible]	in.
Required development length for the top transverse ineffective hooked rebar	[illegible]	in.
Required development length for the bottom transverse straight rebar	[illegible]	in.

As shown previously, $R_{wdetadj}$ and $L_{cdetadj}$ are used to determine the axial force and flexural demands on the deck by distributing $R_{wdetadj}$ at a 45° angle.

Effective deck width that can be used to provide resistance to vehicle impact is:

$$L_{cdisttodeckcenter2det} = 9.15 + 2\left(\frac{40}{12} + 0.5\left(\frac{12}{12}\right)\right) = 16.81\ ft$$

Flexural demand on the deck is:

$$M_{CTdet} = \frac{50.4}{16.81}\left(\frac{40}{12} + 0.5\left(\frac{12}{12}\right)\right) = 11.5\ k - ft/ft$$

Axial tensile force demand on the deck is:

$$T_{CTdet} = \frac{50.4}{16.81} = 3.0\ k/ft$$

The nominal axial tensile capacity of the deck after deterioration considering top and bottom transverse reinforcement is:

$$P_{ndet} = 0.31 * \frac{12}{7.5} * 37.1 + 0.11 * \frac{12}{7.5} * 52.5 + 0.31 * \frac{12}{9} * 35.4 = 42.3\ k/ft$$

The nominal flexural capacity of the deck at critical section after deterioration considering only top transverse reinforcement is:

$$\sum C = 0.85(4.5)(12)(0.825)c = 37.9c$$

$$\sum T = 0.31 * \frac{12}{7.5} * 37.1 + 0.11 * \frac{12}{7.5} * 52.5 = 27.64\ k/ft$$

$$c = \frac{29.64}{37.9} = 0.73\ in./ft$$

$$a = 0.825(0.73) = 0.602\ in./ft$$

$$\varepsilon_s = \frac{0.003\big((12 - 3 - 0.5(5+3)/16) - 0.73\big)}{0.73} = 0.03 \gg \varepsilon_{sy} \rightarrow OK$$

$$M_{ndet} = 27.64\left(8.75 - \frac{0.602}{2}\right) = 233.3\ k - in./ft$$

$$M_{ndet} = \frac{233.3}{12} = 19.46\ k - ft/ft$$

Assuming a linear interaction between axial tension and moment, and considering a $\phi = 1.0$ for extreme event, the moment capacity of the deck fascia is:

$$\phi M_{nintdet} = \phi M_{ndet}\left(1 - \frac{T_{CTdet}}{\phi P_{ndet}}\right)$$

$$\phi M_{nintdet} = (1.0)(19.46)\left(1 - \frac{3.0}{(1.0)(42.3)}\right) = 18.1\ k - ft/ft$$

$$\phi M_{nintdet} = 18.1\ k - ft/ft$$

This moment capacity is based on the assumption that the deterioration length is equal to infinity. Consideration must be given to the actual deterioration length and how that compares to

the effective width of the deck engaged in axial tension and moment transfer. The adjusted moment capacity considering the actual deterioration length is calculated as follows:

If $L_{cdisttodeckcenter2det} \geq L_d$

$$L_{undet3} = L_{cdisttodeckcenter2det} - L_d \quad \text{H2-38}$$

$$M_{nintdetadj} = \frac{M_{nint}L_{undet3} + M_{nintdet}L_d}{L_{cdisttodeckcenter2det}} \quad \text{H2-39}$$

If $L_{cdisttodeckcenter2det} < L_d$

$$L_{undet3} = 0 \quad \text{H2-40}$$

$$M_{nintdetadj} = M_{nint} \quad \text{H2-41}$$

Since the deterioration length, L_d, is smaller than $L_{cdisttodeckcenter2det} = 201.72\ in.$, an adjustment in the flexural resistance is necessary and is conducted as follows using a weighted average approach.

$$L_{undet3} = 201.7 - 180.0 = 21.7\ in.$$

$$M_{nintdetadj} = \frac{(23.3)21.7 + (18.1)180}{201.7} = 18.66\ k - ft/ft$$

$$M_{nintdetadj} = 18.7k - ft/ft > M_{CTdet} = 11.5\ k - ft/ft \rightarrow OK$$

As can be seen, after the adjustment is made, the deteriorated deck has sufficient capacity to resist the vehicle impact. Similar results can be obtained from the MDOT Barrier program as shown in Table H.2.13. (After Deterioration Tab – Section 5).

Table H.2.13. Flexural resistance of the deck after deterioration occurs – outputs obtained from MDOT Barrier program

5. Moment Transfer from Barrier to Deck in the Event of Collision

Property	Value	Unit
Axial force demand due to distribution of Rw	2.99	k-ft/ft
Flexural moment capacity without interaction (without consideration of Ld)	19.47	k-ft/ft
Axial tension capacity (without consideration of Ld)	42.38	k-ft/ft
Flexural moment capacity with interaction (with consideration of Ld)	18.67	k-ft/ft

3. Summary

A total of three main limit states were evaluated for a bridge barrier subjected to vehicle impact, which features a deteriorated deck fascia. The goal was to determine whether the bridge barrier with a deteriorated deck fascia meets a TL-4 level of crashworthiness. Results obtained using manual calculations outlined in the example were compared with those computed using the MDOT Barrier computer program. The MDOT Barrier computer program is an analytical tool that may be used to evaluate the crashworthiness of a variety of solid barriers with or without deck fascia deterioration. An overview of the program is provided in Chapter 7 and instructions for how to download it are provided in Appendix E. Since the MDOT Barrier program is based on the formulations used in the manual calculations, the results are similar with minor differences attributed to round off errors.

The crashworthiness of the barrier was evaluated prior to the deterioration of the deck fascia and after it to quantify the impact of deck fascia deterioration on barrier crashworthiness. The evaluated limit stated prior to and after the deck fascia deterioration included: 1) the lateral load capacity of the barrier as determined by the controlling yield line mechanism in the barrier; 2) shear strength of the interface between the barrier and deck; and 3) axial tension and flexural capacity of the deck overhang.

It was demonstrated that since the deterioration was too severe both in terms of length and width the bridge barrier does not meet the TL-4 level of crashworthiness. If there is no deterioration in the deck fascia, the lateral load capacity of the barrier exceeds the TL-4 requirements by a notable amount. While the specified level of deterioration was severe, the barrier was overdesigned in terms of its crashworthiness for a TL-4 level of protection. A more economically designed barrier would be more sensitive to deck fascia deterioration when the deterioration extends past the outside face of the barrier. Therefore, the likelihood of bridge deck fascia deterioration affecting the crashworthiness of the barrier depends on the level of conservatism used in the original design and whether or not the deterioration extends past the outside face of barrier. If the deterioration is limited to the portion of the deck fascia that extends past the outside face of barrier, crashworthiness is not affected.

A summary of the analysis results obtained from manual calculations and computed based on the MDOT Barrier program is provided in Table H.3.1 and Table H.3.2, respectively. These tables provide the demand and capacity for the three considered limit states. Capacities are

provided prior to the deck fascia deterioration and after the deterioration thus allowing the analyst to quickly examine the impact of the deterioration on barrier crashworthiness. The last column in both tables outlines whether the barrier with the deteriorated deck fascia meets the specified level of crashworthiness (TL-4 in this case). The controlling limit state for barrier lateral load capacity was the flexural capacity of the barrier as dictated by the assumed yield line pattern. A capacity design approach was then used to determine whether the calculated lateral capacity can be transferred to the deck by evaluating the interface shear strength and axial tension and flexural capacity of the deck. It was determined that both the interface shear strength and axial tension and flexural capacity of the deteriorated deck were sufficient to transfer the reduced lateral capacity of the barrier thereby suggesting that a further reduction in the level of crashworthiness is not required.

Since a capacity design approach is followed for evaluating the limit state of interface shear and deck overhang capacity, two numerical values are presented in the demand column for the second and third limit states. The first corresponds to the barrier transverse capacity prior to the deck fascia deterioration (original design) and the second to the barrier transverse capacity after deck fascia deterioration.

To restore the crashworthiness of the barrier in question to a TL-4 level of protection, the deck fascia must be repaired. A repair procedure validated using small scale and large-scale laboratory experiments is outlined in main body of this report.

Table H.3.1. Summary of the analysis results for the example problem

Check No.	Check	Demand	Capacity for Undeteriorated Bridge Deck Fascia	Capacity for Deteriorated Bridge Deck Fascia	Evaluation
1	Barrier's transverse load capacity, R_w (kips)	54.0	76.9	45.4	Not OK
2	Interface shear capacity (kips/ft)	5.5 & 3.2	76.3	62.7	OK
3	Flexural resistance of the deck at critical section (k-ft/ft)	19.8 & 11.5	23.3	18.7	OK

Table H.3.2. Summary of the analysis results for the example problem – Outputs obtained from MDOTBarrier program

Summary of the Results

Check No.	Property	Demand	Capacity Original Design	Capacity After Deterioration	Evaluati OK-Not
1	Barrier transverse capacity, Rw (k)	54.00	76.74	50.25	☐
2	Shear transfer from barrier to deck (k/ft)	5.53&3.18	76.31	62.66	☑
3	Moment transfer from barrier to deck (k-ft/ft)	19.78&11.45	23.36	18.67	☑

4. References

1. American Association of State Highway and Transportation Officials (AASHTO). 2020. AASHTO LRFD Bridge Design Specifications. 9th ed. Washington, DC: AASHTO.
2. Barker, R. M., & Puckett, J. A. (2021). *Design of highway bridges: An LRFD approach*. John wiley & sons.

5. Notations

a: depth of the Whitney's stress block factor, $\beta_1 c$
a_8, a_9: inputs required to calculate l_{dava}
$A_{barrier}$: area of the barrier
A_{cv}: area of concrete considered to be engaged in interface shear transfer
A_{cvmin}, A_{vf_min2}: minimum required area of concrete considered to be engaged in interface shear transfer
A_{cvdet}: deteriorated area of concrete considered to be engaged in interface shear transfer
$A_{cvdetadj}$: adjusted deteriorated area of concrete considered to be engaged in interface shear transfer
A_{vf}: area of interface shear reinforcement crossing the shear plane within the area
$A_{vfprovided}$: provided area of interface shear reinforcement crossing the shear plane within the area
A_{vfmax}: maximum area of interface shear reinforcement crossing the shear plane within the area
A_s: area of nonprestressed tension reinforcement
A_{s4}: area of the top deck straight transverse rebar
A_{s5}: area of the top hooked straight transverse rebar
A_{s6}: area of the bottom deck straight transverse rebar
A_{tr}: total cross-sectional area of all transverse reinforcement which is within the spacing s and which crosses the potential plane of splitting through the reinforcement being developed (taken zero in this project)
b: width of the compression face of the member; for a flange section in compression, the effective width of the flange
b_1: clear cover for the barrier reinforcement
b_2: clear cover for the top deck reinforcement
b_3: clear cover for the bottom deck reinforcement
b_{vi}: interface width considered to be engaged in shear transfer
c: cohesion factor
c: distance from the extreme compression fiber to the neutral axis
c_b: the smaller of the distance from center of bar or wire being developed to the nearest concrete surface and one-half the center-to-center spacing of the bars or wires being developed
d_s: distance from extreme compression fiber to the centroid of nonprestressed tensile reinforcement
d_{sp}: average effective depth for positive moment
d_{sn}: average effective depth for negative moment
d_b: bar diameter
d_{savg}: average effective thickness of the reinforcement
E_s: Modulus of elasticity of the mild steel
f'_c: concrete compressive strength
f'_{cd}: deck concrete compressive strength
f'_{cb}: barrier concrete compressive strength
f_y: yield strength of the mild reinforcement
M_c: ultimate flexural resistance of wall about horizontal axis
M_{cdet}: unadjusted deteriorated barrier's ultimate flexural resistance of wall about horizontal axis
$M_{cdetadj}$: adjusted deteriorated barrier's ultimate flexural resistance of wall about horizontal axis
M_n: nominal flexural resistance
M_{n1}: nominal flexural resistance of the barrier segment I about horizontal axis
M_{n2}: nominal flexural resistance of the barrier segment II about horizontal axis
M_{n3}: nominal flexural resistance of the barrier segment III about horizontal axis
M_{n1det}: nominal flexural resistance of the barrier segment I about horizontal axis after deterioration
M_{n2det}: nominal flexural resistance of the barrier segment II about horizontal axis after deterioration
M_{n3det}: nominal flexural resistance of the barrier segment III about horizontal axis after deterioration
M_{nint}: nominal flexural resistance with interaction
$M_{nintdet}$: deteriorated nominal flexural resistance with interaction
$M_{nintdetadj}$: adjusted deteriorated nominal flexural resistance with interaction
M_b: ultimate moment capacity of beam at top of wall (taken zero in this project)
M_w: ultimate flexural resistance of wall about vertical axis
V_{CT}: Shear force at the base of the barrier from the vehicle collision
M_{CT}: Moment force at the mid-depth of the deck due to the vehicle collision
n: number of bars or wires developed along plane of splitting
P_c: permanent net compressive force normal to the shear plane (only barrier's self-weight is considered in this project)
P_n: nominal axial tension resistance
P_{ndet}: nominal axial tension resistance after deterioration
R_w: total transverse resistance of the railing
R_{wdet}: unadjusted deteriorated total transverse resistance of the railing
$R_{wdetadj}$: adjusted deteriorated total transverse resistance of the railing
s: maximum center-to-center spacing of transverse reinforcement within l_d
t_3: thickness of the barrier segment III
t_{avg}: average barrier thickness
t_{avg1}: average thickness of the barrier segment I
t_{avg2}: average thickness of the barrier segment II
t_d: nominal deck thickness

f_{yadj}: adjusted yield strength of the reinforcement due to lack of development length
f_{yadj4}: adjusted yield strength of the top deck straight transverse rebar
f_{yadj5}: adjusted yield strength of the top hooked straight transverse rebar
f_{yadj6}: adjusted yield strength of the bottom deck straight transverse rebar
F_t: transverse vehicle impact force distributed over a length L_t at a height H_e above bridge deck
F_L: longitudinal friction force along rail
F_v: vertical force of vehicle laying on top of rail
E_s: modulus of elasticity of the steel
h_1: height of the barrier segment I
h_2: height of the barrier segment II
h_3: height of the barrier segment III
H_e: minimum barrier height from the base of barrier to impact level
H, $H_{barrier}$, H_b: height of the barrier
k_{tr}: transverse reinforcement index (taken 0 in this project)
K_1: fraction of concrete strength available to resist interface shear
K_2: limiting interface shear resistance
l_d: development length
l_{dava}, l_{dhava}: available development length
l_{dh}: development length of deformed bars in tension terminating in a standard hook
l_{db}: basic development length for straight reinforcement to which modification factors are applied to determine l_d
l_{hb}: basic development length of standard hook in tension
L_t: longitudinal length of distribution of impact force F_t along the railing located a height of the H_e above the deck
L_L: longitudinal length of distribution of friction force, F_L
L_v: longitudinal distribution of vertical force F_v on top of railing
L_{vi}: interface length considered to be engaged in shear transfer
L_c: critical length of wall failure
L_{cdet}: unadjusted deteriorated critical length of wall failure
$L_{cdetadj}$: adjusted deteriorated critical length of wall failure
$L_{cdisttodeckcenter}$, $L_{cdisttodeckcenter2}$: distributed critical length of wall failure to the mid-depth of the deck
: distributed critical length of wall failure to the mid-depth of the deck
$L_{cdisttodecktop}$: distributed critical length of wall failure to the top of the deck
t_{davg1}: average thickness of the barrier segment I after deterioration
t_{davg2}: average thickness of the barrier segment II after deterioration
t_{davg3}: average thickness of the barrier segment III after deterioration
T_{CT}, V_{CT}: tensile force per unit of deck length
V_{CTdet}: tensile force per unit length in the overhang due to vehicle hit after deterioration
V_{ni}: nominal interface shear resistance
V_{ri}: factored interface shear resistance
$w_{barrier}$: weight of the barrier
w_c: unit weight of concrete
w_d: deterioration thickness
x_{adj}: the deterioration width that affects the barrier flexural capacity about its horizontal axis
x_1: barrier offset measured from the edge of deck fascia to the toe of the barrier
x_2: top base of the barrier segment I
x_3: distance from the top base of the barrier segment I to bottom base of the barrier segment I
x_4: distance from the top base of the barrier segment II to bottom base of the barrier segment II
y_1: height of the barrier segment I
y_2: height of the barrier segment II
y_3: height of the barrier segment III
α_1: compressive stress block factor
β_1: stress block factor
$\gamma_{barrier}$: barrier concrete density
ε_t: net tensile strain in the extreme tension steel at nominal resistance
ε_s: strain the extreme tension steel
ε_{sy}: yield strain of steel
ϕ: resistance factor
μ: friction factor
λ_{rc}: reinforcement confinement factor
λ_{rl}: reinforcement location factor
λ_{cw}, λ_{cf}: coating factor
λ_{er}: excess reinforcement factor
λ: density modification factors, taken as unity for normal weight concrete
ΣC: total compressive forces in the cross-section in the compression zone
ΣT: total tensile forces in the cross-section in the tension zone

$L_{cdisttodeckcenterdet}, L_{cdisttodeckcenter2det}$: unadjusted deteriorated distributed critical length of wall failure to the mid-depth of the deck

$L_{cdisttodecktopdeck}$: unadjusted deteriorated distributed critical length of wall failure to the top of the deck

$L_{cdisttodeckcenterdetadj}$: adjusted deteriorated distributed critical length of wall failure to the mid-depth of the deck

$L_{cdisttodecktopdetadj}$: adjusted deteriorated distributed critical length of wall failure to the top of the deck

L_{undet}: undeteriorated length within the $L_{cdisttocenterdeckdet}$.

L_{undet2}: undeteriorated length within the $L_{cdisttodecktopdet}$.

L_{undet3}: undeteriorated length within the $L_{cdisttocenterdeck2det}$.

L_d: deterioration length